

**Gujarat
Technological
University**



International Innovative University

**2nd Multi-Disciplinary
International Conference**

**GTU
ICON
2022**

International Conference



**Emerging Trends &
Innovations *in*
Pharmaceutical Sciences**

**Gujarat
Technological
University**



International Innovative University

**2nd Multi-Disciplinary
International Conference**

**GTU
ICON
2022**

International Conference



**Emerging Trends &
Innovations *in*
Pharmaceutical Sciences**

First Published: 22 September 2022

Copyright © Graduate School of Pharmacy, Gandhinagar, Gujarat, India

“Emerging Trends and Innovations in Pharmaceutical Sciences”

Proceedings of Multi-Disciplinary International Conference (GTUICON2022)

Editors: Dr. Sanjay Chauhan, Dr. Manju Misra, Dr. Rajesh Patel

ISBN: 978-81-955306-5-6

All rights reserved. No part of this book may be reproduced or transmitted in any form by any means electronic or mechanic or mechanical, including photocopy, recording, or any other information storage and retrieval system, without permission in writing from the copy owners.

DISCLAIMER

The authors are solely responsible for the contents of the papers compiled in this volume.

The publishers or editors do not take any responsibility for the same in any manner.

Errors if any are purely unintentional and readers are requested to communicate such errors to the editors or publisher to avoid discrepancies in future.

Typeset by:

Graduate School of Pharmacy, Gandhinagar

GTU Gandhinagar Campus

Gujarat Technological University, Ahmedabad-383001 (Gujarat)

Printed in India by:

Graduate School of Pharmacy, Gandhinagar

GSP Campus, (Name of typist)

Gujarat Technological University, Ahmedabad-383001 (Gujarat)

डॉ. मनसुख मांडविया
DR. MANSUKH MANDAVIYA



स्वास्थ्य एवं परिवार कल्याण
व रसायन एवं उर्वरक मंत्री
भारत सरकार

Minister for Health & Family Welfare
and Chemicals & Fertilizers
Government of India

MESSAGE

I am glad to learn that the Gujarat Technical University is organizing a Multidisciplinary International Conference from 20th to 23rd September with Pharmacy Track as one of its topics of discussion.

India is a powerhouse of talent. Gathering academic experts from various parts of the country who will share their experiences and knowledge will help encourage research and innovation among young minds in the field of pharmaceutical sciences. Through innovation and research, we can bring a positive difference in the lives of the people of our country. Our government under the able leadership of Hon'ble Prime Minister Shri Narendra Modi is taking numerous steps to create an eco-system that furthers outstanding research, innovation and strides in technology in all fields including pharmaceuticals. India has already emerged as a key player in global pharma supply chains. With new innovation, research and technology, we can take our pharma sector to new heights & help in fulfilling the vision of an Aatmanirbhar Bharat.

I hope that the conference will be an occasion for experts and academicians to deliberate on enhancing and advancing the pharmaceutical sector. I convey my best wishes for the success of the conference.

(Dr. Mansukh Mandaviya)

15 September, 2022



Message from Vice Chancellor, GTU

I am very pleased to know that our Gujarat Technological University is organizing the GTUICON2022 International conference from 20th September 2022 to 23th September 2022. The conference, aptly called multidisciplinary, is a unique amalgamation of different domains of research work carried out at four schools of Gujarat technological university. The graduate school of pharmacy has the theme of “ Emerging Trends and Innovations in Pharmaceutical Sciences” which I feel is very suitable considering the need to keep oneself updated about the recent and emerging trends in drug discovery. With the rapid increase in use of the emerging technology trends like AI, MI , deep learning etc, it is high time that we incorporate these concepts in the field of pharmaceutical research .

The different sub themes of the conference namely Innovation in Pharmaceutical Formulation, Quality Assurance by Advanced Analytical Techniques, Innovation in Medicinal and Phytomedicinal chemistry, Novel Approaches in biological evaluation of Pharmaceuticals and Natural Products, Multidisciplinary approaches in Drug discovery and Development etc. will also add a unique flavour to the conference and foster multidisciplinary research. I congratulate all the authors who have given their valuable contribution in this conference in terms of their research and knowledge sharing. I also congratulate the organizers, technical session chairs and members of the review committee of this conference.

I am sure that the conference will provide a unique forum for people to interact, collaborate and form new joint alliances for taking this multidisciplinary research further to fulfill the vision and mission laid down by our new education policy.

I convey my warm regards to the Graduate School of pharmacy for a organizing such a conference. I am sure this proceeding will be helpful to all the stakeholders.


Prof. (Dr.) Navin Sheth
Vice Chancellor
Gujarat Technological University, Ahmedabad

Message from GSP-GTU Director



I am delighted to inform you that the Graduate school of Pharmacy - Gujarat technological Technology is organizing the conference on “Emerging Trends and Innovation in Pharmaceutical Science” from 20th September 2022 to 23th September 2022. The conference has several themes covering several topics like Innovation in Pharmaceutical Formulation, Quality Assurance by Advanced Analytical Techniques, Innovation in Medicinal and Phytomedicinal chemistry, Novel Approaches in biological evaluation of Pharmaceuticals and Natural Products, Multidisciplinary approaches in Drug discovery and Development, which will offer a great opportunity to all pharmacy students to showcase their research work. Further with experts and invited oral talk it will be good platform for researchers and academicians to foster newer collaboration and search for likeminded partners for joint research activity

I am sure that this conference will provide the much-needed impetus to research in the domain of drug discovery and development and forge better research ties amongst the stakeholders involved.

I wish all the dignitaries, delegates and participants of INTERNATIONAL CONFERENCE 2022 a grand and successful event.

A handwritten signature in blue ink, appearing to read 'Sanjay Chauhan'.

Prof Dr Sanjay Chauhan
Director Graduate school of pharmacy
Gujarat Technological University

CONTENTS

I	ABOUT GSP	x
II	ABOUT GTUICON 2022	x
III	ORGANIZING COMMITTEE	xi
IV	LOCAL ORGANIZING COMMITTEE	xii
V	LIST OF VOLUNTEERS	xiii
VI	SCIENTIFIC SCHEDULE AT A GLANCE	xiv
VII	PLENARY LECTURE	xiv
VIII	ABSTRACT	1

SR. NO.	TITLE	PAPER ID	Page No.
------------	-------	----------	-------------

SESSION 1 - INNOVATION IN PHARMACEUTICAL FORMULATION

1	SCREENING STUDIES FOR OPTIMIZATION OF CRITICAL QUALITY ATTRIBUTES OF NANOSPANLASTICS BASED DRUG DELIVERY SYSTEM Ashwini Patel, Dr. Prachi Pandey	PCP369	02
2	FORMULATION, OPTIMIZATION AND IN VIVO PHARMACOKINETIC ESTIMATIONS OF RIFAMPICIN-LOADED CHITOSAN NANOPARTICLES FOR PULMONARY TUBERCULOSIS Reena Avichal Ughreja	PCP373	11
3	DESIGN AND DEVELOPMENT OF FLOATING MICROSPHERE FOR LOCALIZED DRUG DELIVERY IN MANAGEMENT OF GASTRIC CANCER Komal Rahevar	PCP375	29
4	PHARMACEUTICAL 3-D PRINTING TECHNOLOGY AT A GLANCE Dr. Chetan H. Borkhataria, Mr. Jaydeep Mehta, Mr. Dhruv C. Sakhiya	PCP377	44
5	AUGMENTED REALITY AND VIRTUAL REALITY IN PHARMACEUTICAL INDUSTRY Ravin Malam, Dishita Parmar, Dr. D. M. Patel, Dr. Sanjay Chauhan	PCP394	60
6	FORMULATION AND EVALUATION OF FLOATING MICROBALLOONS OF ALLOPURINOL Prachi Gohil	PCP401	61
7	INSIGHTS OF MEDICAL DEVICE RULES 2017 AND ITS AMENDMENTS Hardi Patel, Bhumika Maheriya	PCP409	70
8	A MINI REVIEW ON PHAGE THERAPEUTICS AND FORMULATION STRATEGIES-SUPPLEMENTING THE MODERN MEDICINE SYSTEM Charmi Soni, Aajvi Jansari	PCP413	71
9	FORMULATION AND EVALUATION OF ORALLY DISINTEGRATING TABLETS OF BRIVARACETAM Jay Patel, Sejal Solanki, Nehang Raval	PCP415	82
10	SCREENING STUDY OF TRANSFERSOME FORMULATION OF RASAGILINE MESYLATE BY PLACKETT - BURMAN DESIGN Shivani M. Patel, Dr. Lalit Lata Jha	PCP425	102
11	COLOSTRUM ENRICHED READY-TO-SPRINKLE IMMUNOMODULATORY HEMATINIC NUTRACEUTICAL SUPPLEMENT FOR PAEDIATRIC SUBPOPULATION Jayvin Raval, Vivek Joshi, Dr. Manju Misra	PCP437	107
12	INTRODUCING DIGITAL PILL: A STEP AHEAD TO CONVENTIONAL DRUG FORMULATIONS	PCP450	108

Flora Pujara, Hetvi Prajapati

SESSION 2 - QUALITY ASSURANCE BY ADVANCE ANALYTICAL TECHNIQUES

- 13** **COMPARATIVE STUDY OF UV SPECTROSCOPIC AND RP-HPLC METHOD FOR THE ESTIMATION OF EFONIDIPINE HCL ETHANOLATE AND METOPROLOL SUCCINATE IN THEIR COMBINED DOSAGE FORM** **PCP372** **120**
Hitanshi Darji, Dr. Prasanna Pradhan
- 14** **RISK ASSESSMENT OF NITROSAMINES IN PHARMACEUTICALS: A LOOK AHEAD OF DRUG DEVELOPMENT** **PCP385** **130**
Mr. Ravi Patel, Mr. Ravisinh Solanki, Dr. Rajesh Patel, Mr. Shalin Parikh, Dr. Dignesh Khunt
- 15** **NITROSAMINE IMPURITIES AND LONG-TERM MEDICATION: THE NEED FOR INVESTIGATION IN GUJARAT REGION** **PCP392** **131**
Mr. Ravisinh Solanki, Mr. Ravi Patel, Dr. Rajesh Patel, Mr. Shalin Parikh, Mr. Bhavinkumar Gayakvad
- 16** **ISOLATION AND CHARACTERIZATION OF SELECTIVE HERBAL MARKERS FROM GARCINIA INDICA EXTRACT** **PCP410** **132**
Kankshi Pathak, Monika Sorathiya, Dr. Sanjay Chauhan
- 17** **STABILITY INDICATING HPLC METHOD DEVELOPMENT AND VALIDATION FOR SIMULTANEOUS ESTIMATION OF CELECOXIB AND TRAMADOL HYDROCHLORIDE IN COMBINATION** **PCP417** **133**
Harmish Asodariya, Dr. Hiral Panchal, Dr. Hiral Panchal, Nitya Patel
- 18** **CURRENT TRENDS IN GREEN CHEMISTRY BASED ON PHARMACEUTICAL APPROACH** **PCP418** **134**
Kartiksindh Solanki
- 19** **A REVIEW ON IMPURITY PROFILING IN PHARMACEUTICALS** **PCP429** **135**
Shraddha Patil, Dr. Rajesh Patel
- 20** **METABOLIC FINGERPRINTING WITH FTIR SPECTROSCOPY FOR ANTIBIOTIC SCREENING ASSAY** **PCP434** **136**
Shikha Sharma, Dr. Rajeshkumar Patel
- 21** **A NOVEL AND ROBUST STABILITY INDICATING RP-HPLC-DAD METHOD FOR SIMULTANEOUS ESTIMATION OF MONTELUKAST AND ACEBROPHYLLINE CONTAINING THEOPHYLLINE-7-ACETIC ACID AND AMBROXOL BASE IN ITS MARKETED TABLET** **PCP446** **137**
Janki Goswami, Ravisinh Solanki, Ravi Patel
- 22** **A REVIEW OF AZIDO IMPURITY IN DRUG SUBSTANCES AND ITS PRODUCTS** **PCP452** **151**
Kinnari Patel, Dr. Rajesh Patel
- 23** **RISK ASSESSMENT, ANALYSIS AND CONTROL OF GENOTOXIC IMPURITIES IN DRUG SUBSTANCES AND PRODUCTS** **PCP454** **152**
Jaitri Nayanbhai Mehta, Dr. Jayant B. Dave, Ami Sureshbhai Gadhiya
- SESSION 3 - DESIGN & INNOVATION IN MEDICINAL & PHYTOMEDICINAL CHEMISTRY**
- 24** **PREPARATION AND EVALUATION OF HERBAL LOZENGES FOR THE TREATMENT OF SORE THROAT** **PCP376** **168**
Ms. Kanchiben Pandya, Ms. Pooja Patel, Mr. Kaish Pathan, Ms. Pooja Goswami

25	DESIGN, SYNTHESIS AND EVALUATION OF SOME PIPERAZINE-ARYLAMIDE ANALOGUES AS ANTITUBERCULAR AGENTS Divya Teli, Palak Vadodariya, Mahesh Chhabria	PCP430	177
SESSION 4 - NOVEL APPROACHES IN BIOLOGICAL EVALUATION OF PHARMACEUTICALS & NATURAL PRODUCTS			
26	CURRENT UPDATES IN ANTISENSE THERAPY Dishita Parmar, Ravin Malam, Dr. D. M.Patel, Dr. Sanjay Chauhan	PCP389	190
27	CHROMATOGRAPHIC FINGERPRINTING AND ASSESSMENT OF ANTIINFLAMMATORY ACTIVITY OF CUMINUM CYMINUM AND ZINGIBER OFFICINALE EXTRACTS Hirvita Bhatt, Dr. Deepti K. Jani	PCP391	191
28	PRODUCING, PURIFYING, AND REGULATING BIOSIMILARS: A STEP-BY-STEP GUIDE Mr. Shalin Parikh, Mr. Ravi Patel, Mr. Ravisinh Solanki	PCP393	203
29	ASSESSMENT OF APHRODISIAC ACTIVITY USING A POLY HERBAL FORMULATION IN RATS Modhiya Raini, Goswami	PCP411	204
30	DESIGN OF EXPERIMENT (DoE) BASED APPROACH FOR FORMULATION AND OPTIMIZATION OF CURCUMIN TRANSFEROSOMES FOR WOUND HEALING Manisha Jadav, Dr. Vandana B. Patel, Dr. Lalit Lata Jha	PCP416	217
31	TO STUDY THE DEVELOPMENT OF PHYTOPHARMACEUTICAL MEDICATED JELLY FORMULATION OF CURCUMIN AND TULSI AND ITS REGULATORY ASPECTS IN INDIA Rutvi Tandel, Ms. Asmatbanu Pathan	PCP435	226
32	ESTIMATION OF HEAVY METALS AND MICROBIAL DETERMINATION IN SHATAVARI TABLETS Ms. Vanessa James, Dr. Hiral Panchal	PCP439	227
33	CEREBROPROTECTIVE EFFECT OF HYDRILLA VERTICILLATA ROYLE AGAINST CEREBRAL ISHCHEMIC REPERFUSION INJURY Rumana Patel, Naisargi Pathak, Dr. Jitendra Vaghasiya	PCP441	233
34	PREPARATION AND EVALUATION OF ANTIAECNE HERBALA CREAM OF TAGETES EECTA FLOWER PETALS Prachi Rathod	PCP443	242
35	EVALUATION OF THE NEUROPROTECTIVE EFFECT OF CURCUMIN-VITAMIN A-FORTIFIED YOGURT ON ALZHEIMERâ€™S DISEASE IN RATS Mehta Saloni K	PCP456	255
SESSION 5 - MULTIDISCIPLINARY APPROACHES IN DRUG DISCOVERY & DEVELOPMENT			
36	DEVELOPMENT AND VALIDATION OF QUESTIONNAIRE MEASURING QOL OF WOMEN DURING MENSTRUAL CYCLE. Ms. Priyanka R. Parmar, Dr. Shrikalp Deshpande	PCP378	272
37	ASSESSMENT OF THE EFFECT OF METHANOLIC EXTRACT OF VANDA TESSELLATA ROXB. AGAINST EXPERIMENTALLY INDUCED COLITIS IN ALBINO WISTAR RATS Ms. Pooja Goswami, Dr. Devang B. Sheth, Ms. Dharti Ribadiya, Dr. Ravi A. Manek	PCP382	279

38	TO STUDY PHYTOPHARMACEUTICAL REGULATORY PERSPECTIVES IN INDIA AND DEVELOPMENT OF OCIMUM SANCTUM Ms. Shital Singh Rajput Sujeet Singh, Ms. Asmatbanu M. Pathan	PCP404	291
39	REVIEW ON REGULATIONS FOR GENOTOXIC IMPURITIES IN PHARMACEUTICALS Krupali Rangani, Dr. Kashyap Thummar	PCP405	292
40	REGENERATIVE MEDICINES: REGULATORY COMPARISON IN INDIA AND US Divya Sharma, Ms. Hardi Joshi	PCP407	293
41	MEDICAL FOOD: OVERVIEW OF REGULATION IN INDIA, US AND EUROPE Shivani Patel, Mr. Ravisinh Solanki	PCP412	294
42	ASSESSMENT OF EFFICACY AND SAFETY OF TENELIGLIPTIN AS ADD ON THERAPY IN TYPE-2 INDIAN DIABETIC HYPERTENSIVE PATIENTS Vinendra Parmar	PCP414	295
43	NOVEL FOOD: COMPARATIVE REGULATION AND RISK ASSESSMENT Pooja Parmar, D, Rajesh Patel	PCP419	307
44	A COMPREHENSIVE REVIEW OF SARS-COV-2 VACCINES IN INDIA: COVISHIELD & COVAXIN Nidhi Hitesh Nayi, Ms. Bhumika Maheriya	PCP422	308
45	NUTRICOSMETICS Reena Makwana, Ms. Bhumika Maheriya	PCP426	309
46	CURRENT REGULATORY NORMS FOR CLINICAL RESEARCH IN INDIA Priti Modi, Ms. Bhumika Maheriya	PCP427	310
47	PROTECTIVE EFFECT OF 2-DEOXY-D GLUCOSE ON CHEMICALLY INDUCED ENDOMETRIAL CANCER IN MICE Disha Patel, Rishabh Malik, Dr. Jitendra Vaghasiya	PCP440	311
48	A STUDY ON REGISTRATION PROCESS OF MICRO INVASIVE GLAUCOMA SURGICAL DEVICE IN USA Mandeep Kaur Banth, Dhraastiben Bhatt, Dr. Sanjay Chauhan	PCP447	323
49	DIABETES MELLITUS: A REVIEW ON PATHOPHYSIOLOGY CURRENT STATUS OF ORAL MEDICATION AND FUTURE PERSPECTIVES Dr. D. B. Meshram, Parth Patel, Dr. Vaishali Sharma, Kauna Patel, Divya Varde	PCP448	324
50	NANOPARTICLES HOLD PROMISE IN COVID DIAGNOSIS, VACCINE DEVELOPMENT AND TREATMENT Ami Sureshbhai Gadhiya, Dr. Jayant B. Dave, Jaitri Nayanhbai Mehta	PCP453	339

ABOUT GSP-GTU

Graduate School of Pharmacy (GSP) is a constituent institute of Gujarat Technological University (GTU). It started its operations from the Academic Year 2017-18. It is established by Gujarat Technological University with a view to engage in M. Pharm and PhD level programs and to offer quality education at affordable cost. The institute is recognized by All India Council for Science and Technology (AICTE) as well as Pharmacy Council of India (PCI). Currently it offers M. Pharm (Pharmaceutical Regulatory Affairs), M. Pharm (Pharmaceutical Quality Assurance) and M. Pharm (Pharmaceutics) courses. GSP will be starting M. Pharm in Phytopharmacy and Phytomedicines form AY 2021-22.

ABOUT GTUICON

Health care is the second-fastest growing sector worldwide and it has the largest occupation within the industry. Many view quality health care as the overarching umbrella under which patient safety resides. The way to improve patient safety is to learn about causes of error and use this knowledge to design systems to provide Quality Medicine. The quality medicine system has emerged as central to the development of good healthcare, and requires acquisition of substantive knowledge and skills. The goal of this conference is to provide a platform for exchange of ideas related to different facts of quality medicine and how emerging technology trends could be incorporated to expedite the process of drug discovery. The Gujarat Technological University International Conference - 2022 (GTU ICON-2022) will focus on thought provoking discussion and knowledge sharing on different aspects of innovation in Pharmaceutical Formulation, Quality Assurance by Advanced Analytical Techniques, Innovation in Medicinal and Phytomedicinal chemistry, Novel Approaches in biological evaluation of Pharmaceuticals and Natural Products, Multidisciplinary approaches in Drug discovery and Development besides other related fields. The Annual GTU ICON conference is the gathering of pharma and healthcare professionals in India and across the globe for four days. The conference is the ideal venue for learning about the latest trends shaping the pharma industry & Pharmacy practice from pharma experts and researchers. By sharing global expertise and collating information the GTU ICON 2022 offers research opportunities and strengthens knowledge of the scale of the problem of poor-quality medicines and the most affected areas, and raises vital awareness among key stakeholders. This unique multidisciplinary conference will provide a unique forum to forge and develop new collaborations amongst the stakeholders and lead to better and faster outcomes.

ORGANIZING COMMITTEE

❖ Chief Patron

PROF. (DR.) NAVIN SHETH
Hon'ble Vice Chancellor,
GTU

❖ Patron

DR. K. N. KHER
Registrar, GTU

❖ Overall Convenor

DR. KEYUR DARJI
Director, GTU

❖ Overall Convenor

DR. SARIKA SRIVASTAVA
Assistant Professor,
GSMS, GTU

ADVISORY COMMITTEE

❖ **Dr. Sanjay Chauhan**

(Convenor for Pharmacy)
Director, GTU-GSP

❖ **Dr C. N. Patel**

Dean-Pharmacy, GTU &
Principal, Shri Sarvajanik
Pharmacy College

❖ **Dr. Mahesh Chabbariya**

Asso. Dean, GTU & Principal,
L.M. College of Pharmacy

❖ **Dr. Nehal Shah**

Asso. Dean, GTU & Principal,
Indubhai Patel College of
Pharmacy and Research Centre,
Dharmaj

❖ **Dr. Ashok B Patel**

Asso. Dean, GTU & Associate
Professor, B.K. Mody Govt.
Pharmacy College, Rajkot

❖ **Dr. Dhiren P. Shah**

Asso. Dean, GTU & Principal,
Shree Naranjibhai Lalbhai Patel
College of Pharmacy

LOCAL ORGANIZING COMMITTEE

Sr. No.	Committee	Name of Person	Committee Coordinator
1.	GTUICON 2022	Dr. Rajesh Patel	Coordinator
2.	Scientific & Oral Presentation	Dr. Manju Misra	Coordinator
		Mr Ravi Patel	Member
		Ms Vidhi Sheth	Member
		Ms Janki Goswami	Member
		Mr Pratik Siddhpura	Member
		Mr Hassan Harsoliya	Member
		Mr Jasvant Chaudhari	Member
		Ms Nila Kalwani	Member
		Ms Urmila Patel	Member
		Ms Himani Khandelwal	Member
3.	Registration	Mr Ravisinh Solanki	Coordinator
		Mr Bhavin Gayakwad	Member
		Mr Akash Rathod	Member
		Mr Raju Senma	Member
4.	Food & Hospitality	Dr D M Patel	Coordinator
		Dr Dignesh Khunt	Member
		Mr Devang Master	Member
		Mr Dinesh Senma	Member
5.	Printing, Media and Designing	Ms Bhumika Maheriya	Coordinator
		Ms Anjali patel	Member
		Ms Deepmala Senma	Member
6.	Stage Committee	Dr Kashyap Thummar	Coordinator
		Ms Hardi Joshi	Member
		Ms Asmat Pathan	Member
		Mr Sunilbhai	Member
7.	Advertisement	Mr Uday Vegad	Coordinator
		Dr Sanjay Chauhan	Member
		Dr D M Patel	Member
		Dr Rajesh Patel	Member
		Dr Kashyap Thummar	Member

LIST OF VOLUNTEERS

Sr. No.	Committee	Name of Volunteers
1.	Registration	Jahanvi Solanki
		Pooja Wadhvana
		Shraddha Patel
		Mihir Jesur
		Manil Patel
		Kankshi Pathak
		Mandeep Banth
		Nikhita Badiyavadara
2.	Food & Hospitality	Meet Shah
		Mansi Lakhatraiya
		Parth Narigara
		Urvik Zalavadiya
		Reeya Patel
		Dishita Parmar
		Pinal Patel
		Shraddha Patil
		Hardi Patel
		Krupali Rangani
3.	Stage Committee	Vishva Bhavsar
		Shivani Patel
		Rutvi Shah
		Shital Rajput
		Pooja Prajapati
		Pankaj Bhoje
		Sudhir Shukla
		Nitish Mandal
		Smit Nayi
		Anjali Patel
		Janki Kakkad
		Daneshwari Bhusara
		Nishant Tejpura
		Ravin Malam
		Dhruvil Shah
		Riti Patel
		Ritu Sharma
		Mansi Patel
Riya Makwana		
Chelsi Gadhavi		
Rutvi Tandel		

SCIENTIFIC SCHEDULE



Gujarat Technological University
Graduate School of Pharmacy
2nd Multidisciplinary International Conference (GTU ICON 2022)
Theme: Emerging Trends and Innovations in Pharmaceutical Sciences
Date: 22nd September, 2022 Time: 10:00 AM to 05:30 PM
Venue: B-0 Conference Hall, GTU Chandkheda Campus, Ahmedabad, India

Programme Schedule

Time	Event	Person
09:00 AM to 10:00 AM	Registration And Breakfast	
10:00 AM to 11:00 AM	Inaugural Session	
10:00 AM to 10:05 AM	Lamp Lighting and Prayer	
10:05 AM to 10:10 AM	GTU Song	
10:10 AM to 10:15 AM	Welcome & Felicitation of Dignitaries	Dr. Manju Misra
10:15 AM to 10:20 AM	Overview of the Conference	Dr. Sanjay Chauhan, Director, GSP-GTU
10:20 AM to 10:25 AM	Welcome Address	Dr. K. N. Kher, Registrar, GTU.
10:25 AM to 10:40 AM	Address by Chief Guest	Dr. J. M. Vyas Hon. Vice-Chancellor National Forensic Sciences University (NFSU), Gandhinagar.
10:40 AM to 10:50 AM	Presidential Address	Prof. (Dr.) Navin Sheth Hon'ble Vice Chancellor, GTU
10:50 AM to 11:00 AM	Vote of Thanks	Dr. D. M. Patel, Associate Professor, GSP
11:00 AM to 11:45 AM	PLENARY SESSION: 1	Key note Address by Dr. Rabinarayan Acharya, Director General Central Council for Research in Ayurvedic Sciences (CCRAS)
11:45 AM to 12:00 PM	Break	
12:00 PM to 12:45 PM	PLENARY SESSION: 2	Key note Address by Dr. Pulok Mukharji, Director, Institute of Bioresources and Sustainable Development (IBSD) Takyelpat, Imphal, India
12:45 PM to 01:30 PM	Lunch Break	
01:30 PM to 04:00 PM	Technical Session: Oral Presentation, In Respective Hall	
04:00 PM to 04:30 PM	High Tea	
04:30 PM to 05:30 PM	Valedictory Session	
04:30 PM to 04:35 PM	Welcome of Dignitaries	Dr. Manju Misra
04:35 PM to 04:40 PM	Summary of Conference	Dr. Rajesh Patel
04:50 PM to 05:00 PM	Declaration of Best Paper Award	Dr. Manju Misra
05:00 PM to 05:10 PM	Vote of Thanks	Dr. Kashyap Thummar
05:10 PM to 05:12 PM	National Anthem	
05:12 PM to 05:30 PM	Certificate Distribution	At Registration Desk

PLENARY LECTURES

Prof. Jyantkumar M. Vyas

*Vice Chancellor of National Forensic Sciences University,
Gandhinagar*



Dr. J. M. Vyas is the founder Vice Chancellor of a unique and highly specialized, National Forensic Sciences University (NFSU), Gandhinagar which has been recognized as an Institution of National Importance by the Government of India. He is holding this position from 1 st October, 2020. Besides this, Dr. Vyas is heading the Directorate of Forensic Science of Gujarat, Gandhinagar for past 28 years including the additional charge of its Director General since 9th November, 2020. As such, with his vast experience and 48 years long service, Dr. Vyas is the senior most serving Forensic Scientist of the country.

Dr. Vyas was instrumental in establishing NFSU's predecessor, the erstwhile Gujarat Forensic Sciences University (GFSU) as the first and so far, the only forensics university of the world. As the founder Director General of GFSU, Dr. Vyas started this, one of its kind institution of higher learning, in 2009 which has more than 5000 students undergoing 70 specialized Post Graduate Degree / Diploma courses being run in every possible branch of the forensic science and its allied subjects.

Besides launching academic courses, Dr. Vyas has laid special emphasis on undertaking training of officers from Police, Judiciary, Armed Forces, Bureaucrats, Banking, Vigilance, Customs, Immigration, and Forensic Science from India as well as abroad. As a result, the university has so far trained more than 25,000 officers which is a huge effort in capacity building of the country. Even bigger contribution is in capacity building for 70 friendly foreign countries as officers from these nations are being regularly imparted training which has been deeply appreciated.

Consultancy is yet another unique feature initiated by Dr. Vyas through which wide ranging expertise of NFSU is shared with different government agencies, private organizations and even foreign countries to overcome complex issues and setting up state-of-the-art facilities.

Continuing in a Mission Mode, Dr. Vyas has taken major strides once the university was mandated to set up campuses and centers across the country as well as abroad. Within one year of establishment of NFSU, Dr. Vyas has not only got its first campus running in New Delhi but also established from scratch campuses in Goa and Tripura and launched post graduate courses from the current academic year itself. Work is in progress to set up more campuses in other states and plans are afoot to establish centres abroad too.

Under his guidance, the NFSU has also progressed rapidly during past one year, with the establishment of a modern Centre of Excellence for NDPS with similar centers in other streams underway. With an aim to strengthen the criminal justice delivery system, Dr. Vyas has also established dedicated schools for Police Science & Security Studies, Law & Forensic Justice and Forensic Psychology.

Needless to mention that the vast experience and expertise of Dr. Vyas is being widely tapped, some of which is listed below:-

- (a) Appointed as a member of “Task Force” for Railway safety audits by the Ministry of Railways, Government of India.
- (b) Appointed as a consultant to C.B.I., New Delhi for the establishment of “International Centre of Excellence in Forensic Science” (ICEFS), Ghaziabad.
- (c) Appointed as a member of the Organizing Committee of INTERPOL for three consecutive terms i.e. from 2008 to 2016.
- (d) Appointed as a Member of the Governing Council of Association of Indian Universities (AIU), New Delhi.
- (e) Appointed as a member of Governing Council of International Institute of Digital Technology (IIDT), Tirupati which is headed by Hon’ble Chief Minister of Andhra Pradesh, to provide necessary advice in Academic and Administrative matters.
- (f) Appointed as a member of the Governing Council of Indian Council of World Affairs (ICWA), New Delhi which is headed by Hon’ble Vice President of India.
- (g) Invited by Parliamentary Standing Committee on Science & Technology, Environment, Forests & Climate Change, Rajya Sabha Secretariat, Parliament of India for giving his views and suggestions on various provisions of the DNA Technology (Use & Application) Regulation Bill, 2019.

Dr. J.M. Vyas is an internationally renowned forensic expert. He has large number of publications in various journals of national and international repute to his credit. During the long and illustrious career of Dr. J.M. Vyas, number of recognitions, and National and International awards have been bestowed upon him, some of which are mentioned below: -

International Recognition:

- (a) ‘Distinguished International Forensic Scientist Award’ in recognition of leadership and excellence in forensic science and education to the international community by The Henry C. Lee Institute of Forensic science, University of New Haven, West Haven, USA, in October, 2018.
- (b) ‘Lifetime Achievement Award’ for outstanding contribution in the field of Forensic and Investigative Sciences at the international level by the International Association of Police Academies (INTERPA), Turkey on 11th February, 2019.
- (c) ‘Humanitarian Forensic Award’ in recognition of exceptional services in the field of Humanitarian Forensics by the International Centre for Humanitarian Forensics (ICHF) on 5th September, 2019.

National Recognition:

- (a) ‘Padma Shri’, one of the highest civilian Awards, has been awarded, on the occasion of 73rd Republic Day (Year-2022), for his extraordinary, distinguished and commendable services in the field of Science and Engineering.
- (b) ‘Gujarat Nu Gaurav’ (Pride of Gujarat) Award received by Hon’ble Chief Minister of Gujarat on 28/04/2022.
- (c) ‘DRONA Education Excellence Awards – 2022’ received by Hon’ble Education Minister of Gujarat on 29/04/2022.
- (d) ‘Bharat Mata Award’ by Indian Institute of Oriental Heritage in 2014.
- (e) ‘Life time Achievement Award’ in the area of Forensic Chemistry by Amity University, Uttar Pradesh & All India Institute of Medical Sciences, New Delhi, in October 2008.
- (f) ‘Best Forensic Science Laboratory Director of the country’ in 2004.
- (g) ‘President's Police Medal’ for meritorious services on the eve of Republic Day, in the year 1997

Prof. Vaidya Rabinarayan Acharya

Director General

Central Council for research in Ayurvedic Science



TOIPC: AYURVED PHARMACEUTICS: CHALLENGES AND WAY FORWARD

The Central Council for Research in Ayurvedic Sciences (CCRAS) is an autonomous body under the Ministry of Ayush, Government of India. CCRAS boasts of a robust network of 30 peripheral units conducting scientific research activities in Ayurveda and allied disciplines. The council is governed by its Governing Body comprising of higher officials of Government of India. The council is currently headed by the Director General, Vaidya Rabinarayan Acharya. Born in village Nalibar Jagatsinghpur, Odisha, Professor Acharya is serving in the current position since 28th February 2022. He was a Professor of Dravyaguna (Ayurveda Pharmacology) at ITRA, Jamnagar where he has been a faculty since September 2007 to February 2022. He also served ITRA as HoD Dravyaguna and Dean. He started his career as faculty in SSN Ayurveda college, Paikmal and Government Ayurveda College Balangir, Odisha. Professor Acharya completed his PG in 1996, Ph.D. in 2002, from Gujarat Ayurved University, Jamnagar, and his undergraduate degrees, B.Sc.(Botany Hons.) in 1986 and BAMS in 1993, from Utkal University Bhubaneswar Odisha and PG Diploma in Bio ethics from IGNOU New Delhi in 2015. He is having more than 27 years of teaching and research experience in the various fields of drug research.

Prof. Acharya has published more than 325 research articles in peer-reviewed journals and have authored five books. He also has 10 book chapters to his credit. He has served IGNOU as a course writer and WHO as a temporary advisor. Dr. Acharya also provided his service to the Ministry of AYUSH, Government of India, at different capacities such as Chairman, Ayurvedic Pharmacopoeia Committee, member ASUDTAB, member Scientific Advisory Group for drug development CCRAS, Member project screening committee of NMPB, National Coordinator, National Pharmacovigilance programme for ASU drugs. Prof Acharya has worked as principal investigator in more than research grant projects and under his guidance 35 Ph.D., 51 Post Graduate theses/ dissertations in Dravyaguna, have been awarded. He represented India in five different countries, in various capacity, including the WHO meeting on herb-drug interaction at Beijing and Pharmacovigilance at Geneva. Prof Acharya is the recipient of the Best teacher award for drug Research Teaching and the Best research paper award on literary research, in the field of Ayurveda conferred by CCRAS, Ministry of Ayush, New Delhi, CCRAS, prestigious IASTAM Shri Gopaldas Parikh Award for Contributions to Drug Development and Late Shri Ram Krishna Pandey Memorial Service Excellence Award.

Prof. Pulok K Mukherjee (PhD, FIC, FRSC)

Director & Professor

School of Natural Product Studies

Dept. of Pharmaceutical Technology

Jadavpur University

Kolkata – 700 032

India

www.pulokmukherjee.in



Professor Pulok K. Mukherjee is working as the Director, School of Natural Product Studies, Jadavpur University, Kolkata, India. His research/academic works highlights on traditional medicine inspired drug discovery from Indian medicinal plants to make them available from 'Farm to Pharma'. He has made several innovative and outstanding contributions in academic and research in the area of natural product studies, Ethnopharmacology and evidence based validation of herbs used in AYUSH, India. His academic and research career has been outstanding, including globally acclaimed contributions on teaching and research on validation of medicinal plants from India systems of medicine, their formulation and standardization, which are useful bio-prospecting tools for the traditional medicine based drug discovery programme. He has to his credit more than 200 publications in peer reviewed impact journals, several patents and 5 books authored/edited and 16 book chapters. His research publications have cumulative Impact Factor of 233; h-Index- 54, i10-index - 226; which has been cited for over 14642 times.

Dr Mukherjee is a Fellow of the Royal Society of Chemistry (FRSC) and has been awarded with so many laurels from Govt. of India and abroad; to name a few: awarded with the prestigious Commonwealth Academic Staff Fellowship from Association of Commonwealth Universities [ACU], UK; TATA innovation fellowship, by Department of Biotechnology, Govt. of India; Outstanding Service Award from Drug Information association [DIA], USA; Career Award for Young Teacher from All India Council for Technical Education (AICTE), Govt. of India; Best Pharmaceutical Scientist of the Year, from the Association of Pharmaceutical Teachers' of India (APTI); IASTAM Award for Contributions to Development of Ayurvedic and Herbal Pharmaceutics by Indian Association for the Study of Traditional Asian Medicine (IASTAM) and many others.

Dr Mukherjee is serving as Associate Editor of the Journal of Ethnopharmacology, Elsevier Science. He is the member of the editorial board of several International journals including Phytomedicine, Life Science, Pharmaceutical analysis, Synergy; Phytochemical Analysis, World Journal of Traditional Chinese Medicine, India J Traditional Knowledge, J Pharma Education and Research and many others. He is associated as advisor/member to different organizations and administrative bodies of Government of India and abroad including the American Herbal Pharmacopoeia, Programme Advisory Committee (PAC) of Dept. of Science & Technology, Expert Group on translational research on MAP, NER Twinning R&D program in Medicinal, Aromatic Plants & Drug Development of Department of Biotechnology (DBT) Govt. of India; Advisory board of Ayurvedic, Siddha and Unani Drugs Technical Advisory Board (ASUDTAB), Ministry of AYUSH, Govt. of India, Scientific Advisory Committee of National Research Institute of Ayurveda for Drug Development (NRIADD), National Institute of Pharmaceutical Education & Research (NIPER), Kolkata and many others. He is the

Secretary of the Society for Ethnopharmacology, India (SFE India), working on dissemination of knowledge promotion and development of medicinal plant and Ethnopharmacology.

Abstract:

“EXPLORING BIOECONOMY FROM BIORESOURCES – DRUGS FROM NATURE AND OUR ANCESTORS”

Pulok K Mukherjee, Amit Kar

Institute of Bioresources and Sustainable Development, Takyelpat, Imphal, Manipur 795001 (India) www.pulokmukherjee.in

Bio economy involves understanding the rational use of bioresources from the viewpoint of social sciences, international institutions and policy makers in convergences between science and technology in the biosciences represented by biotechnology, genomics, proteomics, bioinformatics, bio-nanotechnology and stem cell research. Medicinal plants are very important natural resources which can help India to reshape its economy. Critical factor in product development for the bioeconomy is the establishment of Indigenous organizations, such as traditional knowledge-based enterprises, to lead the process and form institutions that reflect traditional values to guide such enterprises. Considering the bioeconomy of medicinal plants ethnopharmacology, ethnobotany has important role involving the indigenous people about biological resources (traditional knowledge) and acting as harvesters of raw materials at the bottom of the value chain. For bioeconomic development direct or indirect use of biological resources like medicinal plants including discoveries, and related products and services arising out of the bioscience. The ancient culture of India has worshipped and observed nature to develop high philosophies towards the liberation of humans. The ancient people used medicinal plants for the treatment and management of human wealth. This knowledge system has now been appreciated for their unique chemical and biological therapeutic potential in modern world. Thus, the importance of ethno-pharmacology and ethnomedicine has developed which depends on plant science, chemistry and pharmacology; along with the crucial involvement of different interdisciplinary scientific exploration of biologically active agents. Ethno-medicines are gaining global acceptance because of their less side effects and approach towards the treatment of diseases and also promote human health at large. In order to promote ethno-medicines in different form of finished/ marketed product with the intervention of modern state-of-the-art technologies for the development of healthcare products. This approach will contribute to develop of standardized, synergistic, safe and effective medicinal plant-based products with robust scientific evidence, which can be served as an effective new generation alternative therapeutics. Thus, sustainable health care alternatives can be developed by investigating medicinal plants and other therapeutic bioresources.

ABSTRACT

SESSION 1 - INNOVATION IN PHARMACEUTICAL FORMULATION

PCP369

SCREENING STUDIES FOR OPTIMIZATION OF CRITICAL QUALITY ATTRIBUTES OF NANOSPANLASTICS BASED DRUG DELIVERY SYSTEM

AP0336

Ashwini Patel

Assistant Professor

Krishna School Of Pharmacy & Research

patelashwini1987@gmail.com

AP0341

Dr. Prachi Pandey

Associate Professor

Krishna School Of Pharmacy & Research

prachipandey.ksp@kpgu.ac.in

Abstract:

Nanospanlastics are surfactant based elastic vesicular drug delivery system comprising of non-ionic surfactant and edge activator. Non-ionic surfactant being lipophilic nature assists in formation of vesicles due to presence of saturated alkyl chain. High HLB values of edge activator affords flexibility to the prepared vesicles and facilitates the penetration of drug through the biological membrane. The aim of the present study is screening of the effective process and formulation parameters as critical quality attributes (CQA) in the formulation of nanospanlastics vesicles for improving the drug penetration through mucosa. Six high risk variables obtained from the risk analysis and assessed their impact on the vesicles like drug entrapment, particle size and zeta potential. It was discovered that out of six variables, nanospanlastics vesicles prepared with ethanol injection method using Span 60 as a non-ionic surfactant and Tween 80 as an edge activator using chloroform: ethanol (3:2) as organic solvent demonstrated maximum drug entrapment efficiency above 50 % with minimum particle size below 200 nm. This allowed to use Central Composite Design for the further elucidation of relationship between the dependent and independent variables. Using this developed model, the design space for nanospanlastics preparation has been established based on desirability (maximum drug loading and minimum particle size). This finding illustrates robust nanospanlastics preparation, which could be time and cost saving to industrial formulation scientists.

Key words: Nanospanlastics, non-ionic surfactant, edge activator, critical quality attributes, Central Composite Design

1. INTRODUCTION:

The recent research studies are focused on use of nanoparticles for systemic and targeted drug delivery. Nanoparticles can act as a drug reservoir and modify the drug release patterns using different types of polymers. Shape, size and flexibility are essential physical parameters of nanoparticles influencing the stability, penetration and transportation across the biological membrane [1]. Nanospanlastics (NSLs) are modified form of niosomes that possess combine properties of vesicles and nanoparticles. NSLs are bilayer vesicles formed by non-ionic surfactant Span along with edge activators. NSLs have organized microscopic structure can entrap drug molecules by interior hydrophilic layer and exterior lipophilic layer. The arrangement of the Span, a Sorbitan alkyl esters, in the spanlastics which have concentric bilayer depending on the associated fatty acids. Span 60 shows more stability in the vesicles compare to other Span molecules. Being lipophilic in nature and containing saturated alkyl chain in Span 60 helps in the formation of unilaminar or multilaminar vesicles with greater sustainability compared to other members of class. The surface-active properties would be augmented by the presence of edge activators (EAs) like Tween 80 and ethanol. EAs improves the entrapping of drug molecules and decreasing the vesicles membrane thickness and ultimately reduce the particle size. Moreover, they destabilize the biological membrane and provide the elasticity and deformability of vesicles. Ethanol would provide stearic stabilization

by modifying the net charges on the surface[2,3]. One of the greater advantage of the NSLs is the elasticity facilitates the transmucosal penetration and improves drug absorption. Based on the evidence provided by many researchers, NSLs exhibit greater stability, flexibility and drug targeting at the target sites[4,5,6].

One of the obstacles/key challenges for the commercial development of vesicle drug delivery system is limited shelf lives. Lack of understanding of process and formulation parameters result in variability of product quality. Therefore, the objective/aim of present study is utilization of quality by design(QbD) approaches for designing the final product based on the critical quality attributes (CQAs) of process and formulation. QbD helps to understand the source of variability and assures the final product quality through implementation of the CQAs. In this study, Edaravone (EDR) was selected as a hydrophilic model drug for the preparation of NSLs. Accordingly, NSLs provide an excellent carrier for intracellular penetration and drug targeting and hence improving the drug therapeutic indexing. For this, the target profile of the intended EDR nanospanlastics are relatively high drug encapsulation (>40%), low particle size (<200 nm), sufficient storage (at 4 °C) and minimum variation in the particle size as well as drug entrapment.

This manuscript emphasizes on identification of CQAs and their variation to obtain consistent quality of drug product with the desired characteristics. An coherent approach for the optimization of the CQAs is necessary for minimizing the cost and time of formulation development. It is obvious that the amount of the Span 60 and surfactant are most significantly affecting the quality of the prepared vesicles. However, systemic investigation of the influence of variance in the parameters on the vesicle preparation have not been studied.

For this purpose, first preliminary studies have been performed to identify most critical parameters affecting the drug encapsulation. Next, Central Composite Design was employed in the surface response methodology for the understanding of the various variable factors on the dependent variables. After obtaining the response surface the optimum formulation and process variables identified and tested for the robustness and accuracy of the model.

2. OBJECTIVES:

First objective is identifying the CQAs for the preparation of NSLs and screening of variables on particle size and drug entrapment. Second, study of effect on variation in the most significant factors on dependent factors using response surface methodology by applying the central composite design.

3. LITERATURE REVIEW:

Asmaa Saleh et al formulated intranasal spanlastics of Zolmitriptan for direct brain delivery using quality by design approach. The spanlastics were designed based on central composite design and ethanol injection method. Prepared optimized batch showed the 117.5 nm particle size with 45.65% of entrapment efficiency. Moreover, 70% of drug was permeated via nasal membrane and complete permeation was observed within 2 hrs with steady state flux[7].

Ahmed M. Fatouh et al developed chitosan coated Ledipasvir spanlastic for targeting the liver. Prepared formulation was given orally and showed enhancement of liver bioavailability. Pharmacokinetic studies exhibited high C_{max}, prolonged half life and mean residence time[8].

Fatma Elzahraa Abdelrahman et al investigated the improvement of brain bioavailability of spanlastics vesicular preparation of risperidone via nasal route. The prepared optimized batch had low particle size, polydispersity index, high zeta potential and encapsulation efficiency. Moreover, they observed 2.16 fold increment in brain targeting efficiency with 1.43 folds improvement in the drug transport[9].

DCruz et al developed the nanosplanlastics for the buccal delivery of antihypertensive drug Lacidipine for improving the bioavailability. The prepared oral film possessed flexibility with mechanical strength, instant disintegration within 35 seconds, maximum drug release upto 92%. The prepared film was stable and with minimum barrier permeation, alleviate hepatic metabolism[10].

4. RESEARCH METHODOLOGY:

4.1 Material

Sorbitan based non-ionic surfactants Span 60 & 40, edge activators Tween 80 and PVA were purchased from Molychem, Vadodara. HPLC grade distilled water, methanol, ethanol and chloroform was also purchased from Molychem, Vadodara. EDR was obtained as a gift sample from the Sun Pharma Advanced Research Company (SPARC). All the other reagents were of an analytical grade.

4.2 Methods

4.2.1 Preparation of NSLs

Spanlastic vesicles were prepared by using ethanol injection method[11]. In this method, aqueous phase containing the edge activator was heated at 60 °C. The organic phase containing the non-ionic surfactant and EDR was injected at constant rate into the aqueous phase. Immediately vesicular formation was begun upon contacting of organic and aqueous phase. The resultant solution was stirred at a constant speed (800 RPM) on magnetic stirrer for 15 minutes followed by probe sonication for 5 min. The resultant suspension was kept in refrigeration till further evaluation.

4.2.2 Characterization of the vesicles:

4.2.2.1 Organoleptic Properties:

NSLs dispersions were characterized for visual appearance, color, and odor to confirm the presence of any residual solvent.

4.2.2.2 % Drug Entrapment efficiency:

0.2 ml of prepared NSLs were mixed with 25 ml of methanol and shook for 1 hr in the mechanical shaker. After rupturing of the all the vesicles, centrifuged the resultant solution in the ultra-centrifuge at 10,000 RPM for 30 min at 4 °C. The clear supernatant was analyzed using UV-spectrophotometer at λ_{max} 246 nm for determining the total drug concentration. The prepared NSLs were filter using the whatman filter paper where the unilaminar vesicles easily filter out while pure drugs were retained on the filter paper. Total entrapped drug was determined by treating 0.2 ml of filtrate with methanol and shook for 1 hr in mechanical shaker followed by centrifugation. The clear supernatant was analyzed by UV-spectrophotometer. The % entrapment efficiency was calculated by following equation.

$$\% EE = \frac{\text{entrapped drug}}{\text{total drug}} \times 100$$

4.2.2.3 Particle size:

Particle size of all the prepared batches were determined by using Malvern zetasizer. Samples were 50 times diluted with deionized water. Analysis was performed at 25 °C in the triplicate.

4.2.3 Experimental design:

Maximum drug loading with minimum particle size and appropriate zeta potential for preventing the aggregation of formed vesicles are influencing the drug targeting and penetration through mucosal membrane. Hence, they are selected as a CQAs. For the screening of the most significant process and formulation parameters on the CQAs Placket Burman design (PBD) was studied. On the bases of prior knowledge and extensive literature review, five significant parameters were identified and studied. The identified parameters were type of non-ionic surfactant (Span 60 & 40), type of edge activators (Tween 80 and PVA), hydration volume, hydration time and type of solvent. The actual and coded values of the independent variables are given in the table 1.

Design expert 11 software is used for the PBD studies and based on the software 12 different batches were prepared and analyzed for the CQAs. (Table 2)

Table:1 Independent and dependent variables used in PBD

Independent variables	High level	Low level
Type of Non-ionic surfactant (X_1)	Span 60	Span 40
Type of edge activators (X_2)	Tween 80	PVA
Hydration volume (X_3)	10 mL	20 mL
Hydration time (X_4)	60 min	180 min
Type of solvent (X_5)	Ethanol	Chloroform: Ethanol (3:2)
Dependent variables		
% Entrapment Efficiency		
Particle size		
Zeta potential		

Table 2: Plackett Burman design table and results

Batch No	X_1	X_2	X_3 (mL)	X_4 (min)	X_5	% EE	Particle size (nm)
PBD1	Span 60	Tween 80	20	180	Ethanol	65.93	325.6
PBD2	Span 40	Tween 80	10	180	Ethanol	40.21	123.1
PBD3	Span 60	PVA	10	60	Ethanol	45.93	93.5
PBD4	Span 60	Tween 80	10	60	Chloroform: Ethanol	55.39	145.7
PBD5	Span 60	Tween 80	20	60	Chloroform: Ethanol	49.12	165.6
PBD6	Span 60	PVA	20	60	Ethanol	50.32	541.8
PBD7	Span 60	PVA	20	60	Chloroform: Ethanol	42.46	654.4
PBD8	Span 60	Tween 80	20	180	Chloroform: Ethanol	62.31	653.7
PBD9	Span 60	PVA	10	180	Chloroform: Ethanol	40.19	107.3
PBD10	Span 60	Tween 80	10	60	Ethanol	39.51	256.6
PBD11	Span 60	PVA	10	180	Chloroform: Ethanol	44.39	432.4
PBD12	Span 60	PVA	20	180	Ethanol	44.92	345.5

Based on the screening studies, non-ionic surfactant Span 60, Edge activator Tween 80 and hydration volume were selected for the further studies as they were the most influencing factors. Further, relationship between the variation in the most significant factors and dependent factors were studied using response surface methodology. For this, central composite design using three independent factors at two different level was studied along with central points. (Table 3)

Design expert 11 was used for the study of CCD design. According to CCD matrix, total 20 batches were generated including eleven factorial points, four axial points and five replicas for the statistical assessment. of the using different level and evaluated for the particle size, and drug entrapment (Table 4). For the prediction of the suitable optimized formulation, the fitness

of model among the quadratic, linear and two factor interactions was studied based on the analysis of variance (p values < 0.005) and regression coefficients (R^2) values.

Table: 3 Independent and dependent variables for CCD

Independent variables	High level	Low level
Concentration of Span 60 (X_1)	160mg	200 mg
Concentration of Tween 80 (X_2)	10 mg	30 mg
Hydration volume (X_3)	10 ml	20 ml
Dependent variables		
% Entrapment efficiency (%)	Maximum	
Particle size (nm)	Minimum	

Two different check point batches were prepared according to desirability overlay plot and % relative error was calculated based on the predicted and actual values of dependent variables.

5. FINDINGS

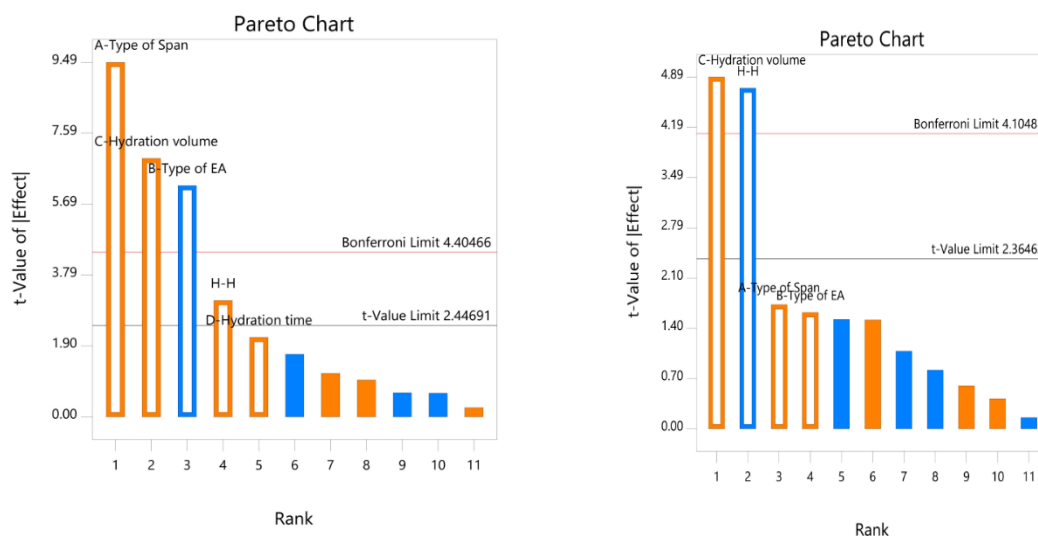
5.1 Screening of most influencing variables on the CQAs using PBD

Process and formulation parameters directly impacted on the CQAs of prepared nanospanlastic formulations. All Span have the same head group with different alkyl chain length. Non-ionic surfactant having HLB values between 3 to 8 are preferable for the formation of bilayer vesicles[12]. Mostly the entrapment of hydrophobic drug is associated with length of alkyl chain in the Span. From the demonstration of previous research work, to obtain greater entrapment efficiency into the vesicles, surfactants with alkyl chain length between C12 to C18 are most suitable as more stable and robust vesicles are formed[13]. Span 60 have alkyl chain length C18 showed more drug entrapment compared to Span 40. Moreover, Span 60 has glass transition temperature near about 60°C and HLB values 4.7, are other possible reasons for the greater drug entrapment[14]. Hence the Span 60 was selected as a most significant variables for the further study[15].

Another significant factor is co-surfactant Tween 80. Being non-ionic in nature, tween 80 helps the formation of prepared vesicles into spherical micellar form. This could be a key factor for the formation of unilaminar vesicles as compared to multilaminar vesicles[16]. The formed micelles are of in very narrow range and hence particle size of the prepared vesicles is controlled by the varying concentration of tween 80. Moreover, protection of the prepared vesicles from the coalesce is necessary for the stabilization of the formulation. Tween 80 shows optimum interfacial stabilization due to high HLB value 15 compared to PVA and hence affecting the particle size. So, Tween 80 was also considered the most significant variables in the NSLs formulation.

Hydration volume was also showing significant effect on the CQAs. As the increase in the hydration volume, decreases the viscosity of the dispersion medium leads to diffusion of the drug from the organic layer to aqueous layer improves the drug entrapment. Less viscosity helps in the application of high shear stress on the prepared vesicles. This leads to reduction in the vesicle size[17]. Pareto chart obtained by using PBD, also reveals the same results (Fig 1).

Fig 1: Pareto charts of the most influencing variables based on PBD studies (a) %EE; (b) Particlesize



From above finding of the PBD studies, indicates that nanospanlastics formulation is strongly influenced by Concentration of Span 60, Tween 80 and hydration volume hence further effects of variation in these responses on the characteristics of formulation, were studied by the central composite design (Table 4).

5.2 Statistical analysis of responses and formulation optimization using response surface methodology

For optimization of formulation using CCD design, Response surface Methodology was employed to validate the statistical model and determination of best possible combinations of influencing factors to achieve the target responses.

Quadratic model was found most fit compared to linear and 2 factor model as quadratic model had larger R² values for all the dependent variables (Table 5). Therefore, quadratic model interaction and quadric terms was selected for describing the possible effects of variables [18]. Moreover, the significance of the selected quadratic model for the effect of independent variables on dependent variables were analyzed based on analysis of variance (ANOVA). At the 95% confidence intervals, if the p-values less than 0.05 and the difference between R²_{pre} and R²_{adj} is close to <0.2 indicates the significance of the model. Effects of model term and associated p-values are given in the table 6. Based on the obtained p-values for Y₁ (p < 0.0001) and Y₂ (p < 0.0001), it can be said that the selected model is better for the understanding of the relationship between the variables.

Table 5: Regression values of the selected responses during optimization

Model	Y ₁ (% EE)		Y ₂ (Particle size)	
	Adjusted R ²	Predicted R ²	Adjusted R ²	Predicted R ²
Linear	0.6358	0.4665	0.5524	0.3937
2F	0.5942	0.3938	0.5308	0.1074
Quadratic	0.9381	0.7525	0.9692	0.8713

From the response surface methodology, the regression equation for all the dependent variables were obtained as per the following. (equation 1 & 2).

$$\begin{aligned} \% EE &= +59.11 + 6.64 X_1 + 3.53 X_2 - 1.32 X_3 - 0.991 X_1 X_2 - 1.3 X_1 X_3 + 1.22 X_2 X_3 \\ &\quad - 4.24 X_1^2 - 0.39824.24 X_2^2 + 0.81634.24 X_3^2 \\ Particle\ size &= +112.71 + 26.82 X_1 - 43.88 X_2 + 9.33 X_3 - 10.40 X_1 X_2 - 1.5 X_1 X_3 \\ &\quad - 17.55 X_2 X_3 + 18.47 X_1^2 + 31.87 X_2^2 + 0.8644.24 X_3^2 \end{aligned}$$

Table 6: ANOVA of optimized quadratic model.

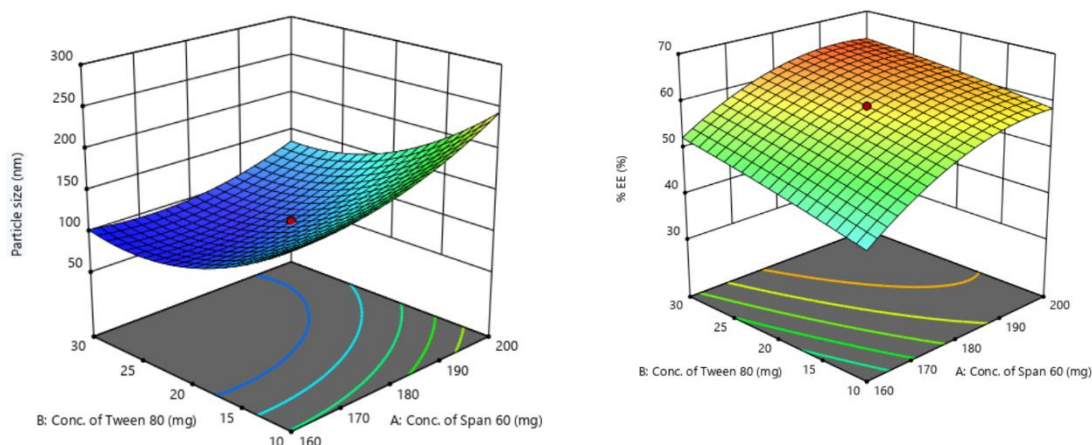
Parameters	Source	Degree of freedom	Sum of square	Mean of square	F value	p value
% EE	Model	9	1111.88	123.54	32.99	< 0.0001
	Residue	10	37.45	3.74		
	Lack of fit	5	37.45	7.49		
	Pure error					
Particle size	Model	9	58895.63	6543.96	67.33	< 0.0001
	Residue	10	971.95	97.19		
	Lack of fit	5	971.95	194.39		
	Pure error					

The values of coefficients and sign in the regression equation shows the impact of each variable on the dependent variables. The positive sign indicates the synergistic and negative sign indicates antagonistic relationship between the variables and response.

5.3 Three-dimensional (3D) plots

For the investigation of optimum combination and quadratic effect of the selected independent variables based on the desirable dependent variables, three-dimensional plots of RSM is used. It is also used for In the figure 2 the effect of amount of span 60 and tween 80, along with their interaction on the dependent variables particle size and % drug entrapment were graphically represented in 3D plots.

Fig 2: Response surface methodology showing the influence of concentration of Span 60 and tween 80 on (a) %EE; (b) Particle size



In this study, the attention was focused on the screening of the principle variables using the design space the laboratory level for the drug encapsulation and particle size since these are the most significant dependent variables for transporting the drug at the target site as well as the most difficult to predict and control them in the vesicular preparation. The particle size can be controlled by using prob sonication and the aggregation of the vesicles can be prevented by storing them at low temperature (4⁰ C).

5.4 Validation of model:

Based on the above findings, the criteria for dependent variables were set for model validation. The particle size was kept minimum and the % drug encapsulation was kept between 60-65%. From the design expert software and based on the desirability, the overlay plot was obtained

(fig 3). In the plot, the yellow region shows the desirability and was utilized for the selection of two check point batches. The batches were formulated based on the flag values given in the overlay plot and evaluated. The difference between the observed result and predicted results is less than 5% (Table 7). Hence, the selected model was validated and can be used for further studies.

Fig 3: Overlay plot for model validation

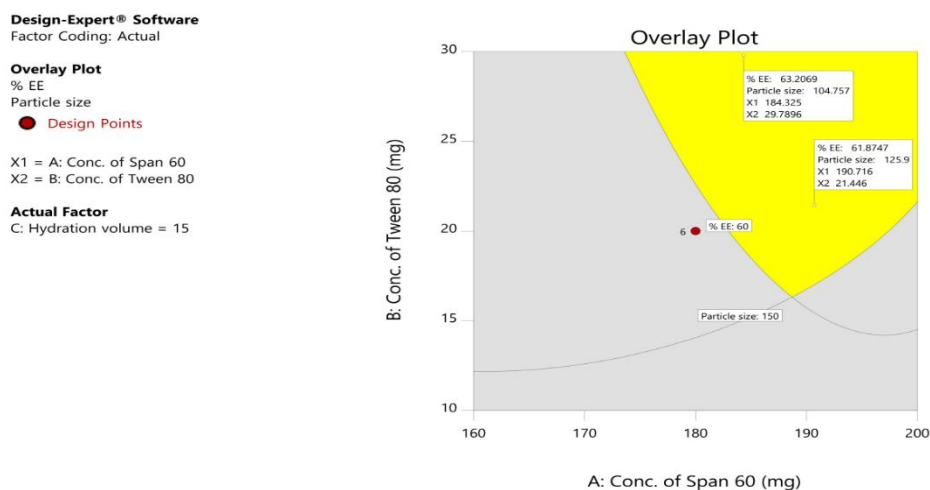


Table 7: Checkpoint batches

Batch No	Particle size (nm)			% Entrapment efficiency		
	Predicted	Experimental	% bias	Predicted	Experimental	% bias
Batch 1	104.757	102.9	1.857	63.2069	65.34	2.133
Batch 2	125.9	127.2	1.3	61.8747	62.67	0.7953

5.5 Selection of optimized batch

For easy penetration through biological membrane smaller particle size with maximum drug entrapment would be preferable. For the same, design expert software version 11 was utilized for the selection of optimized batch by applying the constraints like minimum particles size and maximum drug entrapment. The optimized batch having 184 mg Span 60, 30 mg Tween 80 and 15 ml hydration volume was formulated. The resulted formulation has particle size about 105 nm and % drug entrapment efficiency about 63%. The obtained result values are near about the predicted values and hence can be selected as an optimized batch for the further studies.

6. CONCLUSION

For improving the fundamental understanding, quality by design approach was utilized in the vesicular preparation. Fishpond diagram was constructed based on the preliminary studies for focusing on the critical quality attributes for identification of the critical process and formulation parameters. For this case study, Plackett-Burman and central composite design were utilized. These designs are highly predictive models and with minimum number of experiments, can be easily identified the critical attributes. This design provides the design space for the nanospanlastics formulation with minimum variability in quality of product. The results obtained based on experiments, the critical process and formulation variables are concentration of non-ionic (Span 60) surfactant, concentration of surfactant and hydration volume. These have the significant effect on the CQAs like particle size and % drug encapsulation. The experimental design and statistical analysis tools revealed a best possible composition of formulation consisting of Span 60 (184 mg), Tween 80 (30 mg) and hydration volume (15 ml) to achieve the target responses of size of 105 nm and entrapment efficiency of

63%. The studies done can act as milestones in future research on the formulation development of non-ionic surfactant based vesicles for the site-specific targeted drug delivery systems.

7. REFERENCE

- [1] Nowak, M., Brown, T. D., Graham, A., Helgeson, M. E., & Mitragotri, S. (2020). Size, shape, and flexibility influence nanoparticle transport across brain endothelium under flow. *Bioengineering & translational medicine*, 5(2), e10153.
- [2] Sharma, A., Pahwa, S., Bhati, S., & Kudeshia, P. (2020). Spanlastics: A modern approach for nanovesicular drug delivery. *Int. J. Pharm. Sci. Res*, 11, 1057-1065.
- [3] Ge, X., Wei, M., He, S., & Yuan, W. E. (2019). Advances of non-ionic surfactant vesicles (niosomes) and their application in drug delivery. *Pharmaceutics*, 11(2), 55.
- [4] Abdelrahman, F. E., Elsayed, I., Gad, M. K., Elshafeey, A. H., & Mohamed, M. I. (2017). Response surface optimization, ex vivo and in vivo investigation of nasal spanlastics for bioavailability enhancement and brain targeting of risperidone. *International Journal of Pharmaceutics*, 530(1-2), 1-11.
- [5] Saleh, A., Khalifa, M., Shawky, S., Bani-Ali, A., & Eassa, H. (2021). Zolmitriptan intranasal spanlastics for enhanced migraine treatment; formulation parameters optimized via quality by design approach. *Scientia Pharmaceutica*, 89(2), 24.
- [6] Zaki, R. M., Ibrahim, M. A., Alshora, D. H., & El Ela, A. E. S. A. (2022). Formulation and Evaluation of Transdermal Gel Containing Tacrolimus-Loaded Spanlastics: In Vitro, Ex Vivo and In Vivo Studies. *Polymers*, 14(8), 1528.
- [7] Saleh, A., Khalifa, M., Shawky, S., Bani-Ali, A., & Eassa, H. (2021). Zolmitriptan intranasal spanlastics for enhanced migraine treatment; formulation parameters optimized via quality by design approach. *Scientia Pharmaceutica*, 89(2), 24.
- [8] Fatouh, A. M., Elshafeey, A. H., & Abdelbary, A. (2022). Liver targeting of ledipasvir via galactosylated chitosan-coated spanlastics: chemical synthesis, statistical optimization, in vitro, and pharmacokinetic evaluation. *Drug Delivery and Translational Research*, 12(5), 1161-1174.
- [9] Abdelrahman, F. E., Elsayed, I., Gad, M. K., Elshafeey, A. H., & Mohamed, M. I. (2017). Response surface optimization, ex vivo and in vivo investigation of nasal spanlastics for bioavailability enhancement and brain targeting of risperidone. *International Journal of Pharmaceutics*, 530(1-2), 1-11.
- [10] DCruz, C. E. M., Bhide, P. J., Kumar, L., & Shirodkar, R. K. (2022). Novel nano spanlastic carrier system for buccal delivery of lacidipine. *Journal of Drug Delivery Science and Technology*, 68, 103061.
- [11] Abdelmonem, R., El Nabarawi, M., & Attia, A. (2018). Development of novel bioadhesive granisetron hydrochloride spanlastic gel and insert for brain targeting and study their effects on rats. *Drug Delivery*, 25(1), 70-77.
- [12] Moghassemi, S., & Hadjizadeh, A. (2014). Nano-niosomes as nanoscale drug delivery systems: an illustrated review. *Journal of controlled release*, 185, 22-36.
- [13] Shah, P., Goodyear, B., Haq, A., Puri, V., & Michniak-Kohn, B. (2020). Evaluations of quality by design (QbD) elements impact for developing niosomes as a promising topical drug delivery platform. *Pharmaceutics*, 12(3), 246.
- [14] Nasser, B. (2005). Effect of cholesterol and temperature on the elastic properties of niosomal membranes. *International journal of pharmaceutics*, 300(1-2), 95-101.
- [15] Jivrani, S. D., & Patel, V. K. (2014). Formulation, development and evaluation of niosomal drug delivery system for clindamycin phosphate. *Pharma Science Monitor*, 5.
- [16] Mkam Tsengam, I. K., Omarova, M., Kelley, E. G., McCormick, A., Bothun, G. D., Raghavan, S. R., & John, V. T. (2022). Transformation of Lipid Vesicles into Micelles by Adding Nonionic Surfactants: Elucidating the Structural Pathway and the Intermediate Structures. *The Journal of Physical Chemistry B*, 126(11), 2208-2216.
- [17] Ray, S., Mishra, A., Mandal, T. K., Sa, B., & Chakraborty, J. (2015). Optimization of the process parameters for the fabrication of a polymer coated layered double hydroxide-methotrexate nanohybrid for the possible treatment of osteosarcoma. *RSC advances*, 5(124), 102574-102592.
- [18] Verma, S., Lan, Y., Gokhale, R., & Burgess, D. J. (2009). Quality by design approach to understand the process of nanosuspension preparation. *International journal of pharmaceutics*, 377(1-2), 185-198.

PCP373

FORMULATION, OPTIMIZATION AND IN VIVO PHARMACOKINETIC ESTIMATIONS OF RIFAMPICIN- LOADED CHITOSAN NANOPARTICLES FOR PULMONARY TUBERCULOSIS

AP0357

Reena Avichal Ughreja
Research Scholar

B K Mody Government Pharmacy College
reena.ughreja@gmail.com

Abstract

The main aim of this study is to develop, evaluate and optimize the rifampicin loaded chitosan nanoparticles and to assess its bio-availability and bio-distribution for the effective treatment of tuberculosis through pulmonary administration. Rifampicin being the first line agent for tuberculosis treatment, its chitosan nanoparticles were formulated with the aim to deliver drug directly to lungs and thereby reduce drug associated side effects. Spray drying process variables (concentration of chitosan (X1), concentration of tripolyphosphate (X2) and polymer: drug ratio) were applied through 3² factorial designs for their effect on mean particles size (Y1), entrapment efficiency and cumulative drug release at 1 hr. (Y2) and at 24 hrs. (Y3). The statistical analysis revealed that both independent variables had a significant effect ($p < 0.05$) on dependent variables. The optimized formulation (D = 0.8145) had mass median aerodynamic diameter (MMAD) of 4.83 μm , indicating that the chitosan nanoparticles would be able to reach to deep lungs and could effectively deliver the drug to alveolar macrophage. The optimized formulation and pure rifampicin were pulmonary and orally administered in two rat groups respectively. HPLC-UV method was used for the assaying rifampicin in plasma and organ viz. lung, liver, spleen and kidney for the determination of maximum serum concentration (C_{max}), the time of maximal serum concentration (T_{max}), half-life ($t_{1/2}$), the area under the curve AUC_{0-t} , $AUC_{0-\infty}$, the mean residence time (MRT). Blood data (through pulmonary route) showed significant reduced rifampicin concentration thereby reducing drug interactions and its systemic toxicity. In lungs, improved pharmacokinetic parameters (through pulmonary route) indicated rifampicin's significant increased resident time as compared to oral. In liver, significant lower drug concentration (through pulmonary route) was obtained thus supporting reduced hepatotoxicity. Spleen pharmacokinetics data indicated reduced drug bio-distribution (through pulmonary route). In kidney, higher drug concentration (through pulmonary route) was achieved indicating its increased excretion with reduced enterohepatic circulation. From the collected data, these polymeric nanoparticles might constitute a clinically translatable therapy for treating pulmonary tuberculosis.

Keywords: Chitosan nanoparticles, tuberculosis, pulmonary delivery, biodistribution, pharmacokinetics

1 INTRODUCTION

Tuberculosis (TB) is a leading cause of mortality and a global health issue among several mycobacterial illnesses. Based on the World Health Organization's (WHO) annual TB report for 2021, around 9.9 million people are ill with TB, with an anticipated 1.3 million deaths. This necessitates the development of new medicines, as well as improved diagnostics and health-care coverage. The WHO internationally endorsed **Directly Observed Treatment Short Course Chemotherapy strategy, "DOTS,"** in 1970. It has been acknowledged as a highly efficient and cost-effective technique for tuberculosis control. (Global Tuberculosis Report2021, 2021).

Among all medications, rifampicin (RIF) was selected because it is a first-choice drug for tuberculosis treatment and resistance to RIF can develop rapidly (Son & McConville, 2011) (Agrawal et al., 2016). Thereby, there is a therapeutic rationale for delivering RIF, to passively target alveolar macrophages where a large number of tubercle bacilli harbour. This can be done by changing the route of administration and the dosage formulation.

Lungs being the primary gate for many respiratory diseases, this takes more attention for treatment of diseases through same pathway of entry. Pulmonary systems possess applicability and alternative for both oral and parenteral routes of administration (Kwatra et al., 2012) (Kim & De Jesus, 2022). It bypasses hepatic first pass metabolism thus reducing the administered doses which are reflected in side effect reduction and drug bioavailability enhancement (Shah et al., 2020)(Ahmed & Aljaeid, 2016). Thus, for the current research work pulmonary route was selected for further studies.

With respect to selection of dosage formulation, nanotechnology has various advantages in drug delivery through pulmonary route. This method enables uniform drug distribution within the lung and enhances absorption, resulting in a higher drug therapeutic index. (Dharmadhikari et al., 2013) (Nainwal et al., 2022). Also nanoparticles based drug delivery system of anti-tubercular drug shorten the sterility time and improves the patient compliance (Claire du Toit et al., 2006). For the development of therapeutic interventional techniques against alveolar tuberculosis, nanoparticle formulations have shown targeted and controlled drug distribution (Luna-Herrera et al., 2021). This targeted and controlled drug distribution can be achieved by appropriate selection of suitable polymer. Many factors influence the polymer under study to create polymeric nanoparticles. It includes size of the nanoparticles required, inherent qualities of the drug, surface features, biodegradability, biocompatibility, toxicity, and drug release desired profile. Keeping all this in mind and moving further it was found that chitosan, a natural polymer, is most extensively studied polysaccharide to develop polymeric nanoparticles because of its low toxicity, and anti-microbial & anti-bacterial properties (Divya & Jisha, 2018) (Ruiz & Corrales, 2017).

Because of their biodegradable and biocompatible characteristics, as well as enhanced encapsulation and targeting, chitosan nanoparticles have attracted substantial attention, particularly for pulmonary delivery of numerous therapeutic agents such as medicines, genes, and vaccinations (Garg et al., 2015) (Islam & Ferro, 2016) (Divya & Jisha, 2018). In inhalation therapy, the deposition of inhaled therapeutic agent in the respiratory airways is one of the crucial prerequisites to produce either their systemic or local therapeutic effects. Many parameters must be taken in consideration to ensure deep lung deposition such as aerosol particle diameter, mass median aerodynamic diameters (MMAD), shape, density, hygroscopicity and the respiratory system complexity (Agarwal et al., 2018). The respiratory deposition pattern and absorption profile are influenced by particle size of pulmonary drug delivery systems.

In the consideration of this, the current work was carried out to prepare rifampicin loaded chitosan nanoparticles which could deliver rifampicin directly to the host macrophage.

The following objectives were decided to be achieved

- Formulating nanoparticles with mean particle size less than 1000 nm.
- Achieving encapsulation efficiency of at least 80%.
- Minimizing the burst release and extending the drug release up to 24 hrs.
- To study the bio – distribution of rifampicin loaded chitosan nanoparticles in rats.

2 MATERIALS

Rifampicin was received as a gift sample from Torrent Pharmaceuticals Ahmedabad, Gujarat India. Chitosan 652 was purchased from Cadila Pharmaceuticals Limited, Ahmedabad, Gujarat, India. Sodium tripolyphosphate, glutaraldehyde (25%), Polyvinylpyrrolidone were purchased from S. D. Fine Chemicals Rajkot, Gujarat, India. Mannitol and L Valine were purchased from Chemdyes, Ahmedabad, Gujarat, India. Double distilled water was used throughout the study.

3 METHODS

3.1 Evaluation of drug excipients compatibility

Drug excipient compatibility was studied by performing Fourier transform infrared spectroscopy (FT-IR) (Fadlelmoula et al., 2022) and Differential scanning calorimetry (DSC) (Anjani et al., 2021) study.

An IR spectrum was taken for the drug and polymer. FT-IR spectra were recorded with Thermoscientific. The FT-IR spectrum of the obtained sample of the drug was compared with the standard FT-IR spectra of the pure drug. The samples were scanned in the range of 400-4000 cm^{-1} .

Thermal behaviour of drug and polymer was examined using thermal analyser. An accurately weighed sample was placed in sealed aluminium pans before heating under nitrogen flow (20 mL/min) at a scanning rate of 10 $^{\circ}\text{C min}^{-1}$ from 50 to 500 $^{\circ}\text{C}$. An empty aluminium pan was used as reference.

3.2 Spray drying of rifampicin nanoparticles

Rifampicin loaded chitosan nanoparticles were spray dried using Labultima-222 Advanced Spray-dryer (Labultima, Bangalore, India). Chitosan solution was prepared by dissolving chitosan in to 1 % v/v acetic acid with continuous stirring at 1000 rpm to get a clear solution. Later the cross-linking of the particles was induced by the dropwise addition of tripolyphosphate or 25 % v/v glutaraldehyde. After the addition of cross-linking agent, the clear solution turned opaque, which could be due to the cross linking of chitosan. To this crosslinked suspension, weighed amount of rifampicin was added. Various process parameters for spray drying such as temperature, aspirator setting, and feed rate were studied for their effect on mean particle size, percentage drug entrapment and in vitro dissolution studies (Pourshahab et al., 2011) (K et al., 2022). In the preliminary studies the suspension with a predetermined polymer: drug ratio along with other excipients was fed to the spray dryer. The inlet temperature was maintained from 120 $^{\circ}\text{C}$ to 140 $^{\circ}\text{C}$, the aspiration rate was maintained from 35 – 40 Nm^3/hr and the feed rate was varied from 1 – 5 ml/min (Ngan et al., 2014) as shown in Table 1. Finally, the spray dried nanoparticles were collected and stored in desiccator until further use.

Table 1 Formulation optimization

Batch no.	F3	F4	F5	F6
Formulation parameters				
Conc. of Chitosan % w/v	0.5	0.1	0.1	0.5
Conc. of Crosslinking agent (Glu./TPP) % w/v	0.5 Glu	0.1 TPP	0.1 TPP	0.5 TPP
Conc. of Drug(mg)	-	-	100	500
Spray-drying process parameters				
Inlet temperature (oc)	120	120	120	120
Aspiration rate ($\text{Nm}^3/\text{hr.}$)	37	37	37	37
Feed rate (ml/min)	3	3	3	3
Problem Observed				
	Particle size is too high	Particles obtained are in nano range	Good particle size and satisfactory yield	Good particle size and satisfactory yield

3.3 3² Full factorial design

A 3² full factorial design was used to optimize the formulation and process parameters for the preparation of chitosan nanoparticles (Shah et al., 2020). A total of nine experiments as generated by Minitab® 17.0 (trial version) were prepared and evaluated (D. Patel et al., 2008). Concentration of chitosan (X1) and polymer to drug ratio (X2) were selected as independent variables, while mean particle size (Y1), % entrapment efficiency (Y2), cumulative percentage drug release at 1 hr (Y3) and cumulative percentage drug release at 24 hr (Y4) were selected as dependent variables (Ughreja, R; Parikh, 2019). The design matrix is shown in Table 2.

Table 2 Layout and observed response of 3² full factorial design (Average ± Standard Deviation, n = 3)

Formulation	Independent variables				Dependent variables			
	Coded value		Decoded value		Y1 Particle size (nm)	Y2 %Entrapment Efficiency	Y3 CPR at 1 hr.	Y4 CPR at 24 hr.
	X1	X2	X1(%w/v)	X2				
F1	-1	-1	0.1%	1:1	878	65.80	77.06	94.98
F2	0	-1	0.3%	1:1	1184	42.15	53.93	91.84
F3	1	-1	0.5%	1:1	693	90.20	27.23	41.45
F4	-1	0	0.1%	1:1.5	856	89.24	41.28	75.13
F5	0	0	0.3%	1:1.5	1045	74.08	24.41	40.98
F6	1	0	0.5%	1:1.5	707	86.85	21.55	36.54
F7	-1	1	0.1%	1:2	762	85.08	38.43	82.44
F8	0	1	0.3%	1:2	866	46.94	27.41	45.68
F9	1	1	0.5%	1:2	724	89.39	23.51	47.41

3.4 Evaluation parameters

3.4.1 Particle size and particle size distribution

Mean particle size and particle size distribution of spray dried nanoparticles were determined using Zetatrac (Microtrac Inc., USA). Suspension samples were directly placed into cuvette and mean particle size and size distribution were measured and reported in triplicate.

3.4.2 Drug Content

Rifampicin content in chitosan nanoparticles was determined by weighing nanoparticles equivalent to 100 mgs of rifampicin and dissolving in 100 ml of methanol, followed by sonication using bath sonicator. The resultant solution was filtered through a 0.45µ membrane filter, diluted suitably and the absorbance was measured spectrophotometrically at 473 nm by the regression equation of standard curve developed in the same media in the linearity range of 0 – 40.0 µg/ml.

3.4.3 Percentage drug entrapment efficiency

The drug loaded nanoparticles were suspended in phosphate buffer pH 7.4 and centrifuged at 4000 rpm for 30 minutes to separate out unbound drug in the supernatant layer. The concentration of the drug in the supernatant layer was determined by measuring the absorbance

spectrophotometrically at 473 nm by the regression equation of standard curve developed in the same media in the linearity range of 0 – 40.0 µg/ml. The percentage entrapment efficiency was determined using the following equation (Rawal et al., 2017):

$$\% \text{ Drug Entrapment Efficiency} = \frac{\text{Total amount of drug added} - \text{amount of drug in supernatant}}{\text{Total amount of drug added}} \times 100$$

3.4.4 In- vitro dissolution studies

In vitro dissolution studies (Electrolab Dissolution Tester TDT-06P, USP) were carried out in USP Apparatus II using 100ml of simulated lung fluid at 100 rpm. The formulation equivalent to 100 mg of rifampicin was added to the dissolution medium and sampling was done at 60, 120, 180, 240, 360, 1440 min. at every interval. The samples were filtered with whatman filter paper (0.22µm) and finally the absorbance was measured at wavelength 473nm. The dissolution medium was replenished with equal amount of buffer at each time interval (Pai et al., 2016).

3.4.5 Determination of the Minimum Inhibitory Concentration (MIC) against *M. Tuberculosis*

Minimal inhibitory concentrations were determined by the broth microdilution method. The broth microdilution method was performed in 96-well microplates with u shaped wells. Wells were filled with 100 mL of M7H9 broth, supplemented with 10% OADC enrichment and 0.05% Tween 80. Firstly, the sample was diluted with distilled water; the following two-fold dilutions were performed with 0.1 mL of M7H9 (without Tween 80). The final concentration of *M. tuberculosis* was 5×10^4 CFU/mL. A sample without bacteria in the wells was used as a control to detect the auto-fluorescence of compounds. Plates were incubated at 37 °C. After 4 days of incubation, 20 µL of 10% alamar blue solution and 12.5 µL of 20% Tween 80 were added to either test wells (containing bacilli) or control wells (without bacilli), and plates were incubated at 37 °C. If a well containing bacterium became pink from blue by 24 hrs, reagent was added to the entire plate. If the well remained blue, additional bacteria was loaded and tested daily until the colour change occurred, in which the reagent was added to all the remaining wells. Then finally the plates were incubated at 37 °C, and results were recorded at 24 h after addition of reagent. MIC was defined as the lowest drug concentration that exhibited no growth by visual reading, that prevented a colour change (Rakhmawatie et al., 2019).

3.4.6 Short Term Accelerated Stability Study

Rifampicin chitosan nanoparticle were kept at 40 ± 2 °C and at $75 \pm 5\%$ RH and after 30 days, evaluated.

3.4.7 Animal Studies in Male Wistar rats

Male wistar rats were divided in 2 groups for the study. Group I was given rifampicin chitosan nanoparticles through pulmonary route while Group II was given rifampicin pure drug orally.

3.4.7.1 Development of bioanalytical method for estimation of rifampicin in male wistar rats

HPLC Model- SPD-M10AVP using a Phenomenex C18 column was used for development of bioanalytical method for estimation of rifampicin in male wistar rats (Swamy et al., 2019). After the preliminary trials following experimental condition were set,

Mobile phase – water (pH 2.27): acetonitrile (40:60)

Flow rate – 1 mL/min

Column temperature – 25 °C

Detector- Photo Diode Array (PDA)

λ_{max} - 333 nm.

3.4.7.2 Sample preparation for rifampicin analysis

Stock standard solutions of Rifampicin (100 µg/mL) were prepared by dissolving 10 mg of the Rifampicin in 100 ml of Acetonitrile (ACN) (containing 0.02% BHT). Standard solutions of RIF (concentrations ranging from 0.5 to 20 µg/ml) were obtained by diluting the stock solutions with ACN (0.02% BHT). The RIF standard solutions were stored protected from light at 4 °C.

3.4.7.3 Sample preparation from blood

1 ml of blood sample was withdrawn from retroorbital plexus at time intervals of 1, 2, 3, 4, 6 and 24 h after the dosage form was administered in animals from each group. Plasma was separated and filtered through a membrane filter (0.45 µm) and frozen immediately at -20°C until analysed. To a 100 µL rat plasma sample (ice cooled) 50 µL of ACN (0.02 %BHT) were

added. After vortex mixing (30 sec) 3 ml of dichloromethane/n-pentane (1:1) (0.02% BHT) were used for extraction of RIF by vortexing for 60 sec. The mixture was then centrifuged at 2406×g for 5 min (4°C) and the organic layer was transferred to a glass conical tube and evaporated to dryness in a vortex evaporator. The total residue obtained was reconstituted in 100 or 200 µl of ACN. Aliquots of these solutions (75 and 100 µL, respectively) were injected into the chromatograph after the Millipore Millex-HV filtration (0.45 µm).

3.4.7.4 Sample preparation for Bio-Distribution Study

For bio-distribution studies, various organs like lungs, liver, spleen and kidney were removed at fixed intervals of 1, 2, 3, 4, 6 and 24 h after blood sampling. To 0.5 gm rat organ sample, 2 ml of sodium phosphate buffer (pH-4.5) containing 10⁻³ M sodium ascorbate was added. The sample was homogenized by tissue homogenizer apparatus at 24,000 rpm for 3 min. An aliquot of the homogenate ie 300 µL was transferred to a glass conical tube, placed on ice, and 50 µL of ACN (BHT 0.02%) was added and vortex mixed for 30 sec. The mixture was extracted with 3 ml of dichloromethane/ n-pentane (1:1) (0.02% BHT) by vortexing for 60 sec. After centrifugation at 2406×g for 5 min 4°C, the supernatant was transferred to a glass conical tube and evaporated to dryness in a vortex evaporator. The total residue obtained was reconstituted in 100 or 200 µl of ACN. Aliquots of these solutions (75 and 100 µL, respectively) were injected into the chromatograph after Millipore Millex-HV filtration (0.45 µm) (del Carmen Domínguez et al., 2020).

3.4.7.5 Pharmacokinetic parameter data analysis

Pharmacokinetic parameters were determined by using, free Microsoft Excel add-in, “PKSolver 2.0”. The specifications of this program as well as validation were published in the January 2010 edition of Computer Methods and Programs in Biomedicine. Six parameters calculated were the maximal concentration (C_{max}), the time of maximal concentration (T_{max}), half-life (t_{1/2}), the area under the curve AUC_{0-t}, AUC_{0-∞} and the mean residence time (MRT). The Mean ± SD pharmacokinetics parameter estimated for standard was oral rifampicin and for test was rifampicin chitosan nanoparticle (CNP).

3.4.7.6 Statistical Analysis and Graphing

The plasma concentration and organ distribution graphs were plotted as mean±SEM values of data obtained from bioassay of rifampicin, the biodistribution data was plotted as mean±standard deviation values.

4 RESULTS AND DISCUSSION

Lung is the main site of entry for *Mycobacterium tuberculosis* (MTb) residing within alveolar macrophages. Therefore, the present study offers an effective delivery of rifampicin loaded chitosan nanoparticles for achieving the better targeting of lungs.

4.1 Evaluation of drug excipients compatibility

The drug and excipients compatibility studies were carried out by FTIR. As shown in Figure 1 the FTIR spectra of pure drug showed characteristic peaks at 3792 cm⁻¹, 3482 cm⁻¹, 1708 cm⁻¹, 1651 cm⁻¹, 1251 cm⁻¹, 1026 cm⁻¹ corresponding to secondary aromatic amine, hydroxyl group, furanone group, acetyl group and –CN stretching and –CH bonding frequency. As shown in in the FTIR spectra of drug and chitosan all the characteristic peaks were retained indicating that drug and chitosan were compatible with each other. Further DSC studies were employed to assess the compatibility of rifampicin and chitosan. As shown in

Figure 3 the pure drug showed endothermic peak at 205°C relating its melting point followed by its recrystallization at 248°C. As shown in **Error! Reference source not found.** the DSC curve of pure chitosan showed endothermic peak at 219°C and as seen from **Error! Reference source not found.** in the DSC spectra of drug and chitosan mixture, the peaks relating to pure drug were retained indicating that drug and polymer are compatible with each other (Rawal et al., 2017). Further studies were now conducted to prepare rifampicin loaded chitosan nanoparticles.

Figure 1: FTIR of pure drug rifampicin

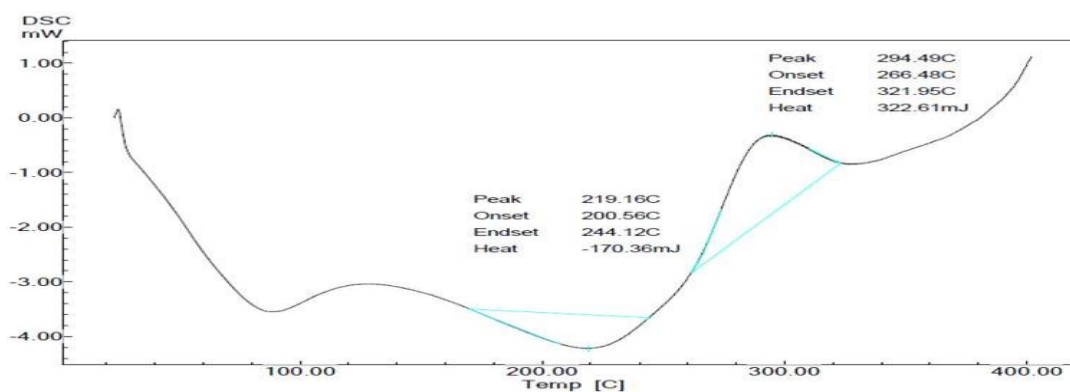


Figure 2: FTIR of pure drug rifampicin and chitosan

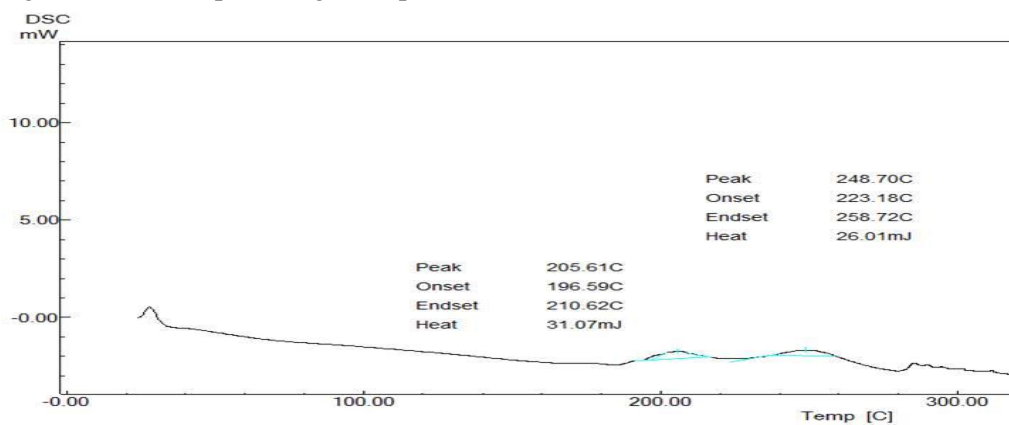


Figure 3: DSC of rifampicin

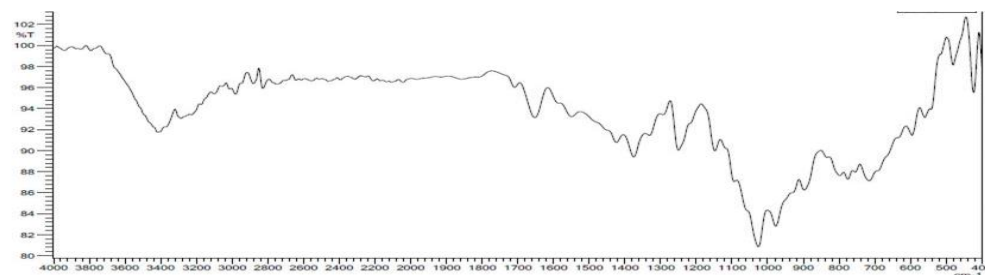


Figure 4 DSC of chitosan

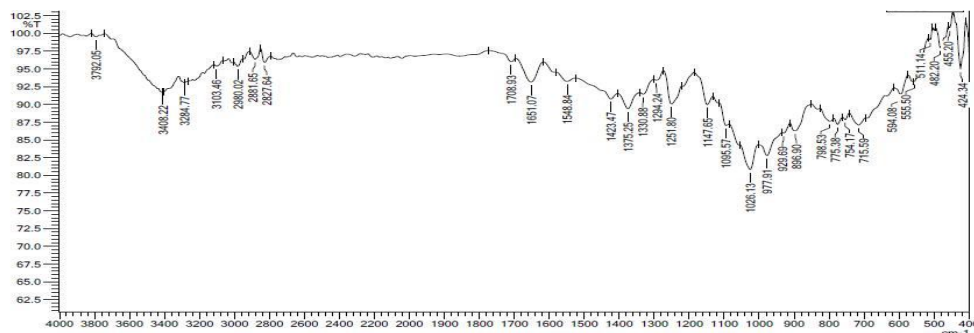
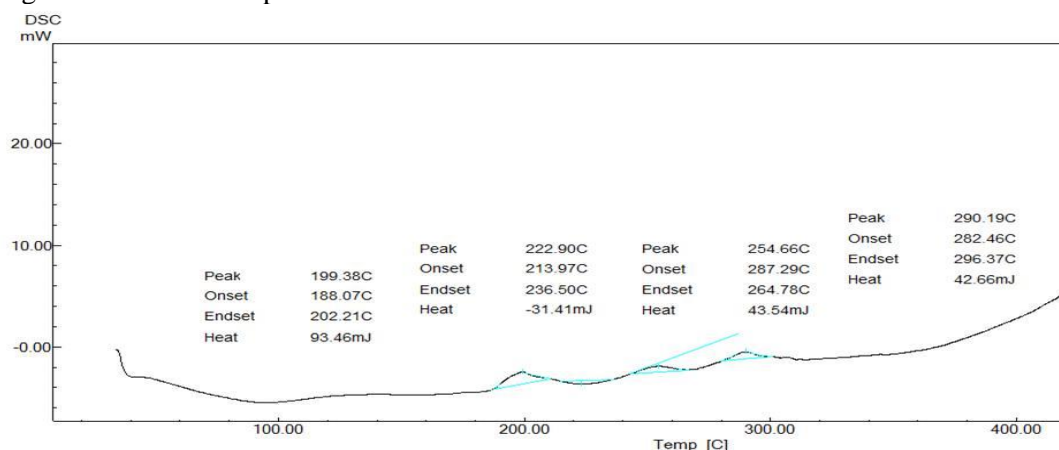


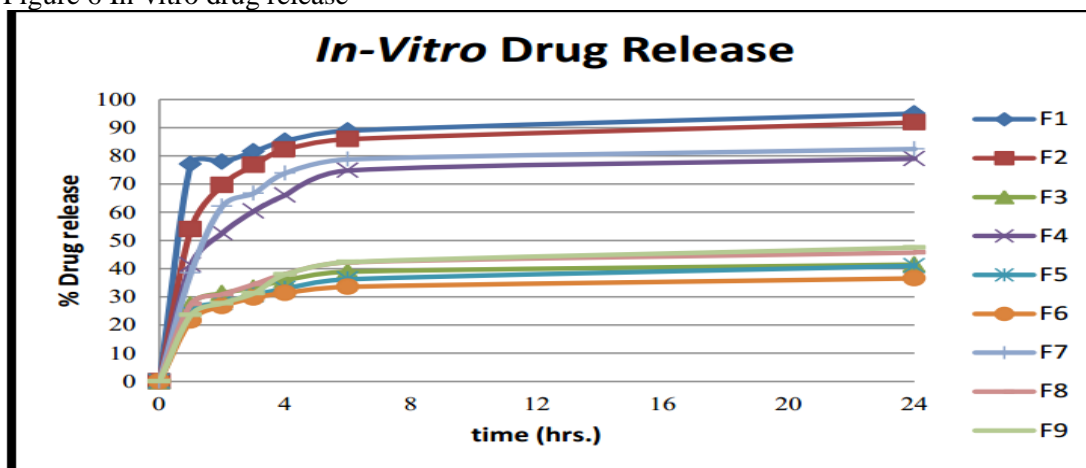
Figure 5 DSC of rifampicin and chitosan



4.2 Formulation and process development of rifampicin loaded chitosan nanoparticles

The preliminary studies were carried out to evaluate the effect of the process parameters on the size and % entrapment efficiency of chitosan nanoparticles. To study the process parameters, the concentration of chitosan solution and glutaraldehyde was kept constant at 0.1 % w/v. It was seen that when the inlet temperature was kept at 120°C and the outlet temperature was kept at 40°C at feed rate of 5 ml/min, higher particle size of 4000 nm was obtained, which could be due to the reason that a higher feed rate would lead to a higher droplet size which would again lead to a higher particle size. It was also seen that inlet temperature had minimal effect on mean particle size and in subsequent studies the inlet temperature was kept constant at 120°C and reducing the feed rate from 5 ml/min to 3 ml/min, produced the nanoparticles with mean particle size 1000 nm. Further studies were done to evaluate the formulation parameters at fixed process parameters viz., nozzle size, inlet temperature, aspiration rate and feed rate of 0.5 mm, 120°C, 40Nm³ and 3 ml/min respectively. As shown in Table 1 chitosan concentration at 0.5% w/v and 0.1% w/v was evaluated with two cross linking agent glutaraldehyde and tripolyphosphate at 0.1 % v/v and 0.5 v/v. It was seen that nanoparticles prepared with tripolyphosphate showed a smaller particle size compared to nanoparticles prepared with glutaraldehyde and hence TPP was selected for further studies (Rawal et al., 2018). Figure 6 shows the in vitro dissolution studies of formulations prepared with TPP. It was found that drug release profile of rifampicin loaded chitosan nanoparticles showed initial burst release within 1 hr. and was sustained for at least 24 hrs. However it was also seen that manoeuvring the process and formulation parameters, we were not able to achieve the set objectives (as discussed in the introduction section) and hence it was decided to employ a 3² full factorial design (J. Patel & Mori, 2020).

Figure 6 In-vitro drug release



4.3 3² Full factorial design

To study the combined effect of the amount of drug: polymer ratio and to study the concentration of chitosan a 3² full factorial design was employed. Table 2 shows the layout of full factorial design and it could be seen that there is a wide variation amongst the observed response, further indicating that the independent variables had significant effect on dependent variables. For further statistical analysis, the three responses were individually fitted to the second-order polynomial model and each model was validated by Analysis of Variance combined with the F test. As shown in Table 3 the independent variables had significant effect (p value < 0.05) for all the response variables. All of the regression models yielded a good fit with high determination coefficient and F value. The goodness of fit of the model was confirmed since the R² for one(Y3) of all the three responses was larger than 0.9, indicating that over 90% of the variation in the response could be explained by the model. The F-ratio was found to be far greater than the theoretical value for one regression model(Y3), indicating that the regression model is significant with a confidence level of 95%.

Table 3 Statical analysis of 3² full factorial design

Response	β_0	β_1	β_2	β_{11}	β_{22}	β_{12}	R ²	F
Y1 (Particle Size)	1043.77	-62	-	-	-	36.75	0.882	0.122
p value	0.0006	0.199	0.173	0.028	0.799	0.485		
Y2 (%Entrapment Efficiency)	63.36	4.38	3.87	30.03	-	-5.02	0.873	0.135
p value	0.004	0.398	0.448	0.030	0.179	0.425		
Y3 (CPR at 1 hr.)	26.55	-	-11.5	3.16	12.16	8.78	0.972	0.014
p value	0.005	0.005	0.010	0.432	0.040	0.030		
Y4 (CPR at 24 hr.)	50	-	-8.16	2	18.50	6.50	0.788	0.269
P value	0.036	0.048	0.358	0.888	0.252	0.532		

4.3.1 Effect of chitosan concentration and polymer to drug ratio on mean particle size

Response surface plots were generated to graphically represent the effect concentration of chitosan and drug to polymer ratio on mean particle size. As shown in Figure 8 at lower level of polymer to drug ratio when chitosan concentration was increased from -1 to 0 the mean particle size increased 693 nm to 878 nm and further increase in the level of chitosan concentration increased the particle size to 1184 nm. Such an observation could be ascribed to the fact that increasing the concentration of chitosan from 0.1 % w/v to 0.5 % w/v could result in a higher droplet size, which eventually would lead to higher particle size (Ughreja, R; Parikh, 2019). Similarly at lower level of concentration of chitosan, increasing the drug to polymer ratio from -1 to 0 and then 0 to +1, increased the particle size from 693 nm to 707 nm and then 707 nm to 724 nm respectively. This marginal increase in particle size could be attributed to the fact that increasing the polymer to drug ratio from 1:1 to 1:2, would increase the viscosity of solution and eventually would increase the droplet size as discussed above, and hence could increase the particle size. However, the magnitude of increase in particle size by changing the polymer to drug ratio is quite less as compared to changing the concentration of chitosan. This is also evident from the statistical analysis as shown in Table 3 that for deep lung delivery of chitosan nanoparticles, the size range below 1000 nm would be advantageous. From ANOVA test, it was found that independent variables (X1 and X2) showed insignificant (p value >0.05)

effect on dependent variables (Y1). However, it was found that the range of the independent variables were successful in preparation of chitosan particles of nano range. Further, the value of $R^2 = 0.882$ shows a linearity between the dependent and independent variables which is further depicted by the regression equation (Zhang et al., 2011).

The regression equation for particle size is shown below:

$$Y1 = 1043.77 - 62X1 - 67.16X2 - 261.66X1^2 - 18.16X2^2 + 36.75X1X2$$

Figure 8 Contour plot and Surface plot of Y1 (Particle Size)

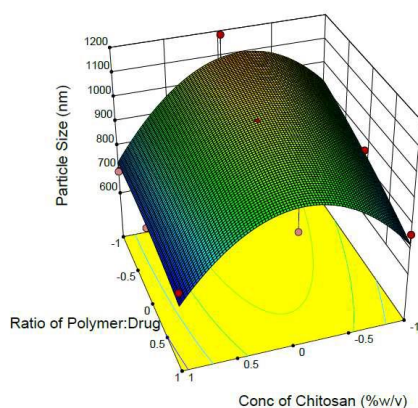
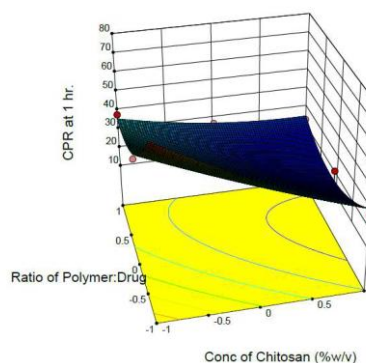


Figure 7 Contour plot and Surface plot of Y3 (CPR at 1 hr.)



4.3.2 Effect of chitosan concentration and polymer to drug ratio on % drug release

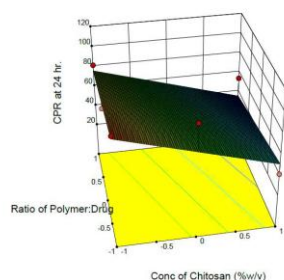
As shown in

and **Error! Reference source not found.** for all the levels of amount of polymer to drug ratio, increasing the level of chitosan concentration from -1 to +1 there was decrease in the drug release. At lower level of polymer to drug ratio increase in concentration of chitosan from -1 to +1 the percentage drug release at 1 hr decreased from 77.06 % to 27.23 % and the percentage drug release at 24 hr decreased from 94.98 % to 47.41%. The decrease in the drug release could be attributed to fact that increasing the concentration of chitosan, the diffusion of the rifampicin through the nanoparticle decreases and hence there is decrease in drug release (Shah et al., 2020). The adequacy and significance of model was justified by analysis of variance (ANOVA). The analysis of acquired data (Y3) showed that the F value of model is 21.37 which is significant with p value < 0.05 which indicated the model has significant capacity to explain variation in response variable Y3 (% CPR at 1 hr). However, both linear (effects of X1 and X2) and quadratic effects (effects of X22 and X12) are also significant. But interaction effect (effect of X1X2) is not significant. After all, $R^2 = 0.972$ implies that the model was successful in correlating independent variables (X1 and X2) with the dependent variables (Y3).

The regression equation for % drug release is shown below:

$$Y3 = 26.55 - 14.16X1 - 11.5X2 + 3.16X1^2 + 12.16X2^2 + 8.78X1X2$$

Figure 9 Contour plot and Surface plot of Y4 (CPR at 24 hr.)



4.3.3 Optimization

Optimization studies were carried out to prepare rifampicin loaded chitosan nanoparticles with set constraints. Based on the equation obtained from factorial design, the desirability function was applied using Minitab 17. The constraints set were to minimize response Y1, maximize Y2, Y3 targeted 30% and maximize response Y4. As shown in Figure 11, an optimum D of 0.8292 was obtained at respective levels of X1 (0.1% w/v chitosan) and X2 (polymer to drug ratio of 1:2). A final formulation was prepared according to the levels obtained from desirability function. As shown in Table 4 the model dependent release kinetics studies of optimized batch revealed that the drug release follows korsmeyer peppas model and the value of n more than 0.5 indicates fickian diffusion. The optimized batch was then evaluated to find out the mass median aerodynamic diameter and other parameters as shown in Table 5. The particle size of optimized batch is 750nm as shown in Figure 10. The MMAD was found to be 483 μm , indicating that the rifampicin nanoparticles would reach till deep lungs (Harris et al., 2013).

Table 4 Model fitting for optimized batch

Optimized batch	Zero order	First order	Higuchi	Korsmeyer peppas		Hixon crowell
	LSSR	LSSR	LSSR	LSSR	n	LSSR
F7	13093.54	530.37	3820.16	371.10	0.170	2784.22

Table 5 Evaluation parameters of optimized batch

Coded value		Decoded value
X1= -1		0.1% w/v
X2= +1		1:2
Sr. no.	Parameters	Value
1	Particle size	750 nm
2	%Entrapment efficiency	87.08
3	CPR at 1 hr.	33.43
4	CPR at 24 hr.	85.44
5	MMAD	4.54 μm

Figure 11 Desirability Profile for Response optimization

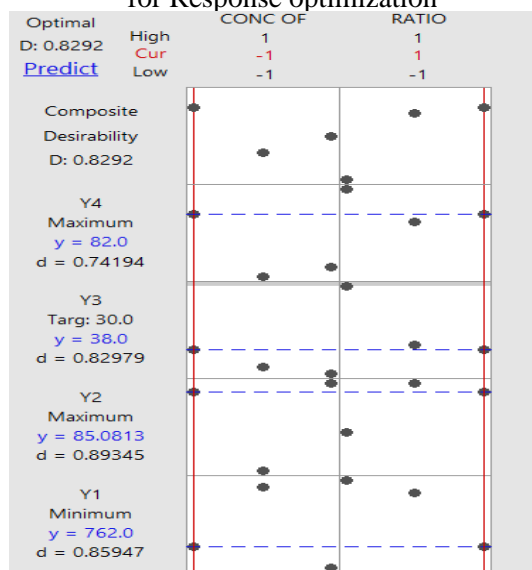
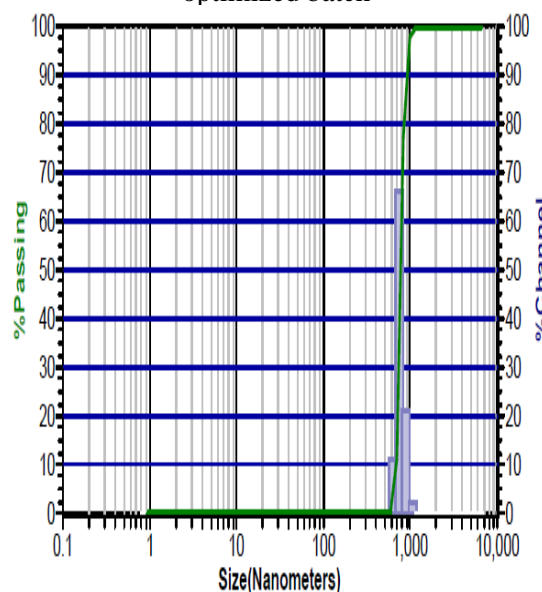


Figure 10 Particle size of optimized batch



Against *M. tuberculosis*

Rifampicin pure drug MIC was 0.4 µg/mL and rifampicin chitosan nanoparticle MIC was 0.07 µg/ml.

Here, Rifampicin loaded chitosan nanoparticle significantly decreased MIC concentration as compared to pure rifampicin drug (Figure 12).

Figure 12 Rifampicin and rifampicin-chitosan nanoparticle MIC against *M. tuberculosis*



4.5 Short Term Accelerated Stability Study

Evaluation showed that there was no significant change in rifampicin CNP characteristics and rifampicin CNP were stable during the time span. From the Table 6 % bias was within the limit and formulation was stable after short term Accelerated Stability period (Debnath et al., 2018).

Table 6 Short term accelerated stability study

Parameter Before Stability	Before Stability Study (0 day)	After Stability Study (30 days)	% Bias
Particle Size(nm)	759	764	-0.65
PDI	0.2	0.2	0.00
% CPR after 24 hrs.	81.69	80.96	0.90

4.6 Development of bioanalytical method for estimation of rifampicin in male wistar rats:

With respect to HPLC chromatogram of rifampicin, Figure 13 and Figure 14 depicts rifampicin's detection without any interference. Peak symmetry was good with minimum band spreading. Retention time of rifampicin was around 2.5 min. under the assay conditions.

4.7 Animal Studies in Male Wistar rats

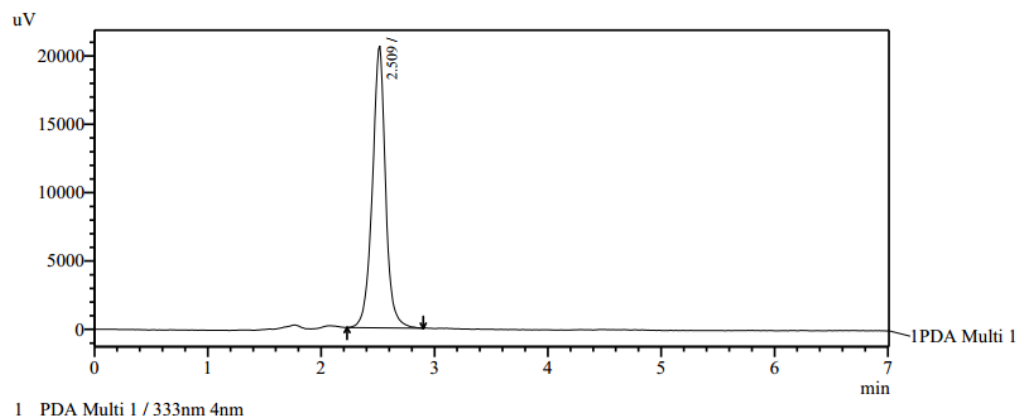
Equivalent dose of oral rifampicin and pulmonary rifampicin CNP has been calculated according to mean weight of rat ie 250 gm, where dose of RIF is 2.7 gm (Standard dose 12 mg/kg). Rifampicin CNP of 3.1 gm, which contained 2.7 gm actual rifampicin was administered by modified dry powder insufflator (Quenelle et al., 1999).

4.7.1 Pharmacokinetic Parameter Data Analysis

Rifampicin bio-availability and bio-distribution in different organ at respected time is obtained as shown in

Figure 15. Here initial high concentration followed by a decline in concentration of pulmonary rifampicin CNP showed a burst release pattern followed by a sustain release. Poor bioavailability and inability of 24 hours maintenance was observed with oral rifampicin.

Figure 13 HPLC Chromatograph of rifampicin



1 PDA Multi 1 / 333nm 4nm

PeakTable

Peak#	Name	Ret. Time	Area	Area %	Theoretical Plate#
1		2.509	166924	100.000	2019.040
Total			166924	100.000	

Figure 14 3D HPLC Chromatograph of rifampicin

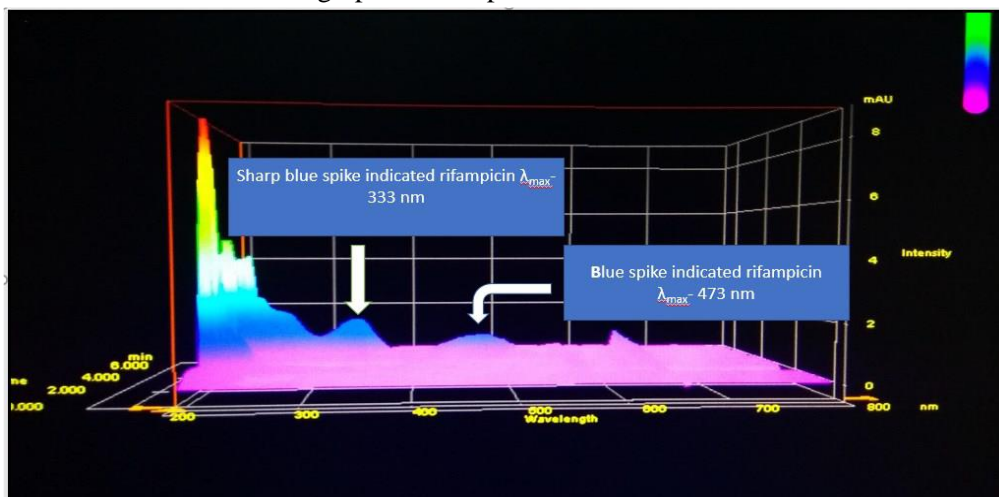
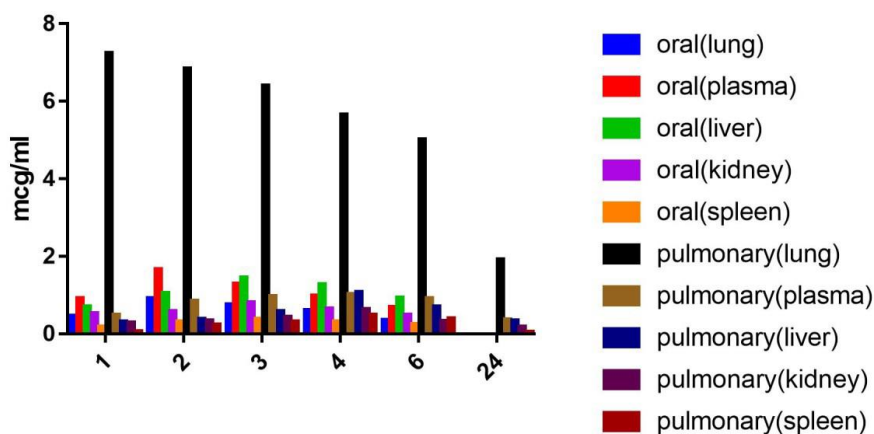


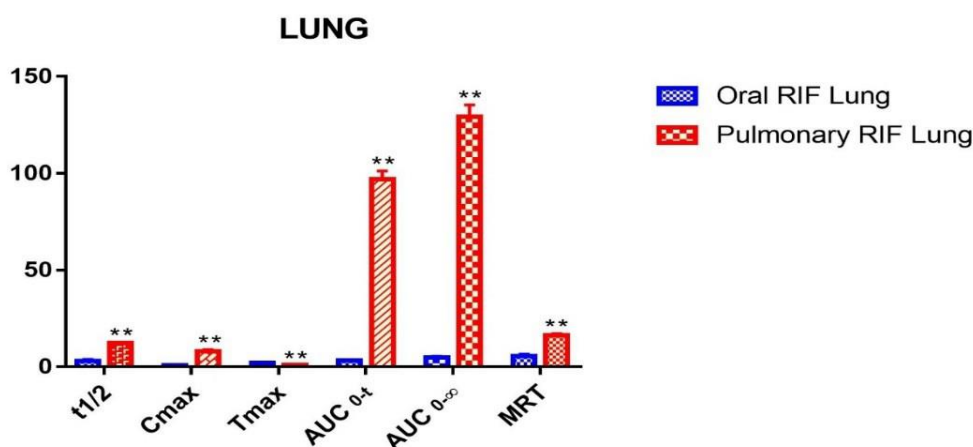
Figure 15 Rifampicin bio-availability and bio-distribution in different organ at respected time (hrs)



4.7.1.1 Rifampicin Bio-assay in lungs

Rifampicin concentrations were found to be 9-fold higher in the lungs as shown in Figure 16, which is significantly ($p < 0.0001$) higher and more quickly attained in rifampicin CNP as compared to oral drug. This finding may be related to controlled and localised drug delivery under the physiological conditions in the lung. Rifampicin CNP's T_{max} and MRT data revealed that the drug first had a burst release followed by a sustained release. When compared to oral rifampicin, the C_{max}/MIC ratio of rifampicin CNP was extremely high, which is important for the quick bactericidal effect and reduction of drug resistance (Patil et al., 2015).

Figure 16 Oral rifampicin and pulmonary RCN in lungs



4.7.1.2 Rifampicin Bio-assay in plasma

In the case of rifampicin CNP, lower C_{max} and greater T_{max} assured reduced systemic toxicity and high local drug concentration is retained in the lungs, resulting in improved clinical results, as shown in Figure 17. Oral rifampicin had a lower $t_{1/2}$ than pulmonary rifampicin CNP and a higher $AUC_{0-\infty}$ than rifampicin CNP, indicating that rifampicin CNP has a more sustained release effect and is more retained in the lungs. Rifampicin CNP has 305.52% relative bioavailability, indicating a decreased first pass metabolism (Khadka et al., 2021).

4.7.1.3 Rifampicin Bio-assay in liver

Figure 18 shows that with oral rifampicin delivery, MRT is lower with a higher C_{max} , indicating that the medication is metabolised faster by the liver than with pulmonary administration. Hepatic $t_{1/2}$ and $AUC_{0-\infty}$ results revealed that oral rifampicin was eliminated more quickly by the hepatic circulation than by the pulmonary circulation. Rifampicin CNP formulation is slowly removed and has a lower concentration in the liver. It could be of great assistance in reducing dose-induced hepatotoxicity and dose-related contraindications.

4.7.1.4 Rifampicin Bio-assay in spleen

Lower rifampicin CNP concentration (with higher MRT, longer $t_{1/2}$, higher $AUC_{0-\infty}$) indicated lower bio-distribution in spleen that means more drug is retained into lungs finally indicating sustain release of drug (Figure 19). MRT of 6.60 ± 0.37 hrs and 19.75 ± 1.17 hrs with oral rifampicin and pulmonary CNP respectively further confirmed sustained release pattern of drug.

Figure 17 Oral RIF and pulmonary RCN in plasma

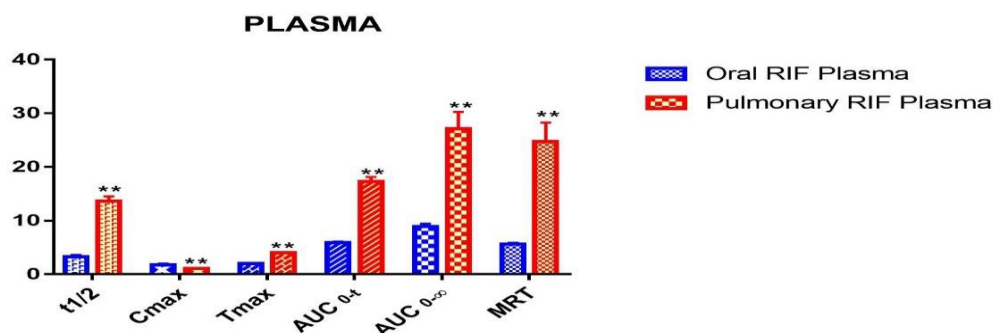


Figure 18 Oral RIF and pulmonary RCN in liver

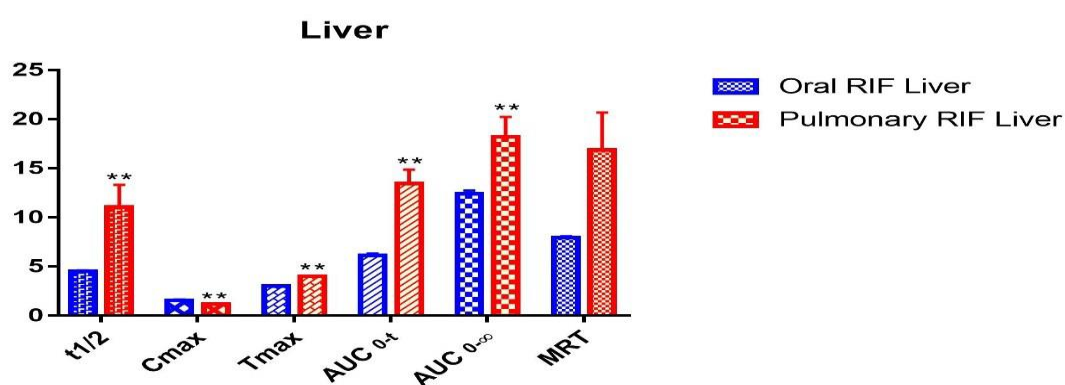


Figure 19 Oral RIF and pulmonary RCN in spleen

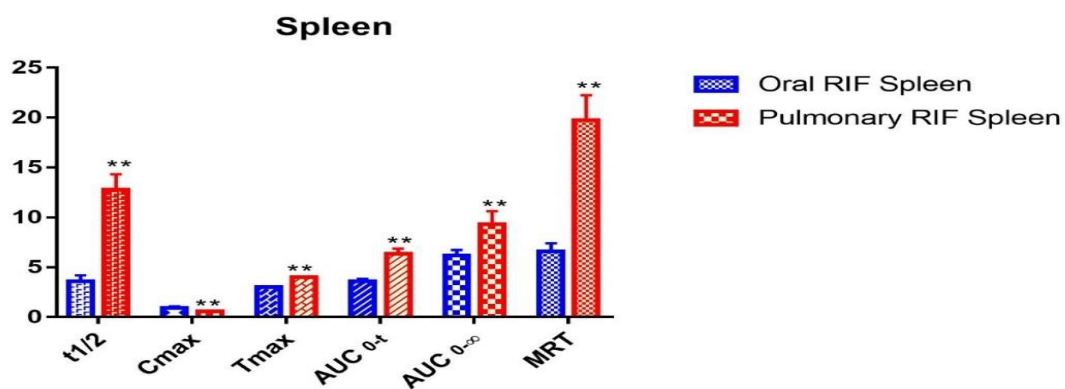
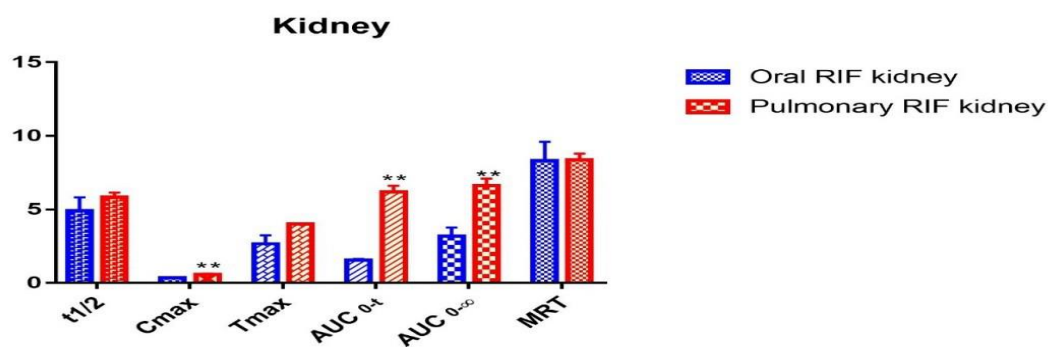


Figure 20 Oral RIF and pulmonary RCN in kidney



4.7.1.5 Rifampicin Bio-assay in kidney

The higher C_{max} (with pulmonary administered rifampicin CNP) in kidney clearly indicated more elimination of drug by kidney as shown in Figure 20. This might be due to reduced enterohepatic circulation as compared to oral rifampicin. T_{max} , $t_{1/2}$ and MRT are with less significant difference of rifampicin CNP and oral rifampicin. This can be because of rifampicin CNP's initial burst release which later followed sustained release.

5 Conclusion

Rifampicin loaded nanoparticles were prepared successfully using chitosan as carrier polymer by spray-drying method. From the preliminary studies it could be concluded that spray-drying process parameters i.e., inlet temperature 120°C, feed rate 3 ml/min. and aspiration rate 37 Nm³/hr showed desired particle size and entrapment efficiency hence it was explored for formulation optimization. The developed and optimized rifampicin chitosan nanoparticles showed $D=0.8292$ which released 33.43% drug at 1hr. and 85.44% drug at 24hr. with particle size of 750nm and entrapment efficiency 87%. Optimized formulation showed MMAD of 4.54µm which confirms the deep lung penetration of prepared nanoparticles. It showed sustained drug release pattern which could be beneficial for reducing drug dose hence helpful in improving patient compliance, which is correlated with *in-vivo* studies. *In-vivo* pharmacokinetics study comparison between oral rifampicin and pulmonary rifampicin CNP revealed that rifampicin CNP resides for more time in lungs than when given orally and systemic effect is seen with initial burst release followed by sustain release. It further helps in reducing the dosing frequency as compare to oral rifampicin. From *in-vivo* bio-distribution study of liver, data reflected reduced pulmonary rifampicin CNP concentration in liver. This might reduce the dose related hepatotoxicity and improve the drug related contraindication in patient of TB concomitant HIV infection. *In-vivo* bio-distribution study in spleen and kidney suggested sustain release with reduced drug concentration in spleen as compared to oral rifampicin. In kidney, drug's higher concentration indicated that drug is more eliminated by kidney and this might help reduce the enterohepatic circulation as compared to oral rifampicin. Finally, our findings by using chitosan nanoparticles for successful rifampicin administration open up new opportunities for developing therapeutic approaches for lung tuberculosis.

REFERENCES

1. Agarwal, R., Johnson, C. T., Imhoff, B. R., Donlan, R. M., McCarty, N. A., & García, A. J. (2018). Inhaled bacteriophage-loaded polymeric microparticles ameliorate acute lung infections. *Nature Biomedical Engineering*, 2(11), 841–849. <https://doi.org/10.1038/s41551-018-0263-5>
2. Agrawal, A., Agarwal, S., Kaleekal, T., & Gupta, Y. (2016). Rifampicin and anti-hypertensive drugs in chronic kidney disease: Pharmacokinetic interactions and their clinical impact. *Indian Journal of Nephrology*, 26(5), 322. <https://doi.org/10.4103/0971-4065.176145>
3. Ahmed, T. A., & Aljaeid, B. M. (2016). Preparation, characterization, and potential application of chitosan, chitosan derivatives, and chitosan metal nanoparticles in pharmaceutical drug delivery. *Drug Design, Development and Therapy*, 10, 483–507. <https://doi.org/10.2147/DDDT.S99651>
4. Anjani, Q. K., Domínguez-Robles, J., Utomo, E., Font, M., Martínez-Ohárriz, M. C., Permana, A. D., Cárcamo-Martínez, Á., Larrañeta, E., & Donnelly, R. F. (2021). Inclusion Complexes of Rifampicin with Native and Derivatized Cyclodextrins: In Silico Modeling, Formulation, and Characterization. *Pharmaceuticals*, 15(1), 20. <https://doi.org/10.3390/ph15010020>
5. Claire du Toit, L., Pillay, V., & Paul Danckwerts, M. (2006). *Tuberculosis chemotherapy: current drug delivery approaches*. <https://doi.org/10.1186/1465-9921-7-118>
6. Debnath, S. K., Saisivam, S., Debanth, M., & Omri, A. (2018). Development and evaluation of Chitosan nanoparticles based dry powder inhalation formulations of Prothionamide. *PLOS ONE*, 13(1), e0190976. <https://doi.org/10.1371/journal.pone.0190976>
7. del Carmen Domínguez, M., Cabrales, A., Lorenzo, N., Padrón, G., & Gonzalez, L. J. (2020). Biodistribution and pharmacokinetic profiles of an altered peptide ligand derived from heat-shock proteins 60 in Lewis rats. *Cell Stress & Chaperones*, 25(1), 133. <https://doi.org/10.1007/S12192-019-01054-3>
8. Dharmadhikari, A. S., Kabadi, M., Gerety, B., Hickey, A. J., Fourie, P. B., & Nardell, E. (2013). Phase I, single-dose, dose-escalating study of inhaled dry powder capreomycin: a new approach to

- therapy of drug-resistant tuberculosis. *Antimicrobial Agents and Chemotherapy*, 57(6), 2613–2619. <https://doi.org/10.1128/AAC.02346-12>
9. Divya, K., & Jisha, M. S. (2018). Chitosan nanoparticles preparation and applications. *Environmental Chemistry Letters*, 16(1), 101–112. <https://doi.org/10.1007/S10311-017-0670-Y>
 10. Fadlelmoula, A., Pinho, D., Carvalho, V. H., Catarino, S. O., & Minas, G. (2022). Fourier Transform Infrared (FTIR) Spectroscopy to Analyse Human Blood over the Last 20 Years: A Review towards Lab-on-a-Chip Devices. *Micromachines*, 13(2), 187. <https://doi.org/10.3390/mi13020187>
 11. Garg, T., Rath, G., & Goyal, A. K. (2015). Inhalable chitosan nanoparticles as antitubercular drug carriers for an effective treatment of tuberculosis. *Artificial Cells, Nanomedicine, and Biotechnology*, 44(3), 1–5. <https://doi.org/10.3109/21691401.2015.1008508>
 12. *Global Tuberculosis Report2021*. (2021).
 13. Harris, R., Acosta, N., & Heras, A. (2013). Chitosan and inhalers: a bioadhesive polymer for pulmonary drug delivery. In *Inhaler Devices* (pp. 77–93). Elsevier. <https://doi.org/10.1533/9780857098696.2.77>
 14. Islam, N., & Ferro, V. (2016). Recent advances in chitosan-based nanoparticulate pulmonary drug delivery. *Nanoscale*, 8(30), 14341–14358. <https://doi.org/10.1039/C6NR03256G>
 15. K, P. D., D, R. D., S, B., & B. Narayanan, V. H. (2022). In-vivo pharmacokinetic studies of Dolutegravir loaded spray dried Chitosan nanoparticles as milk admixture for paediatrics infected with HIV. *Scientific Reports*, 12(1), 13907. <https://doi.org/10.1038/s41598-022-18009-x>
 16. Khadka, P., Sinha, S., Tucker, I. G., Dummer, J., Hill, P. C., Katare, R., & Das, S. C. (2021). Pharmacokinetics of rifampicin after repeated intra-tracheal administration of amorphous and crystalline powder formulations to Sprague Dawley rats. *European Journal of Pharmaceutics and Biopharmaceutics*, 162, 1–11. <https://doi.org/10.1016/j.ejpb.2021.02.011>
 17. Kim, J., & De Jesus, O. (2022). Medication Routes of Administration. In *StatPearls*. StatPearls Publishing. <https://www.ncbi.nlm.nih.gov/books/NBK568677/>
 18. Kwatra, S., Taneja, G., & Nasa, N. (2012). Alternative Routes of Drug Administration- Transdermal, Pulmonary & Parenteral. *Indo Global Journal of Pharmaceutical Sciences*, 02(04), 409–426. <https://doi.org/10.35652/IGJPS.2012.47>
 19. Luna-Herrera, J., Pérez-Martínez, D. E., Barradas-Hernández, V. M., & Zenteno-Cuevas, R. (2021). Nanoparticles as drug transporters: A promising tool against tuberculosis. *Revista Peruana de Medicina Experimental y Salud Pública*, 38(1), 143–152. <https://doi.org/10.17843/rpmesp.2021.381.6156>
 20. Nainwal, N., Sharma, Y., & Jakhmola, V. (2022). Dry powder inhalers of antitubercular drugs. *Tuberculosis*, 135, 102228. <https://doi.org/10.1016/j.tube.2022.102228>
 21. Ngan, L. T. K., Wang, S.-L., Hiep, Đ. M., Luong, P. M., Vui, N. T., Đinh, T. M., & Dzung, N. A. (2014). Preparation of chitosan nanoparticles by spray drying, and their antibacterial activity. *Research on Chemical Intermediates*, 40(6), 2165–2175. <https://doi.org/10.1007/s11164-014-1594-9>
 22. Pai, R. V., Jain, R. R., Bannaliker, A. S., & Menon, M. D. (2016). Development and Evaluation of Chitosan Microparticles Based Dry Powder Inhalation Formulations of Rifampicin and Rifabutin. *Journal of Aerosol Medicine and Pulmonary Drug Delivery*, 29(2), 179–195. <https://doi.org/10.1089/jamp.2014.1187>
 23. Patel, D., Shah, M., Shah, S., Shah, T., & Amin, A. (2008). Design, development, and optimization of orally disintegrating tablets of etoricoxib using vacuum-drying approach. *PDA Journal of Pharmaceutical Science and Technology*, 62(3), 224–232. <http://www.ncbi.nlm.nih.gov/pubmed/18661871>
 24. Patel, J., & Mori, D. (2020). Application of 3 2 Full Factorial Design and Desirability Function for Optimizing The Manufacturing Process for Directly Compressible Multi-Functional Co-Processed Excipient. *Current Drug Delivery*, 17(6), 523–539. <https://doi.org/10.2174/1567201817666200508094743>
 25. Patil, J., Devi, Vk., Devi, K., & Sarasija, S. (2015). A novel approach for lung delivery of rifampicin-loaded liposomes in dry powder form for the treatment of tuberculosis. *Lung India*, 32(4), 331. <https://doi.org/10.4103/0970-2113.159559>
 26. Pourshahab, P. S., Gilani, K., Moazeni, E., Eslahi, H., Fazeli, M. R., & Jamalifar, H. (2011). Preparation and characterization of spray dried inhalable powders containing chitosan nanoparticles for pulmonary delivery of isoniazid. *Journal of Microencapsulation*, 28(7), 605–613. <https://doi.org/10.3109/02652048.2011.599437>
 27. Quenelle, D. C., Staas, J. K., Winchester, G. A., Barrow, E. L. W., & Barrow, W. W. (1999). Efficacy of Microencapsulated Rifampin in Mycobacterium tuberculosis -Infected Mice. *Antimicrobial Agents and Chemotherapy*, 43(5), 1144–1151. <https://doi.org/10.1128/AAC.43.5.1144>

28. Rakhmawatie, M. D., Wibawa, T., Lisdiyanti, P., Pratiwi, W. R., & Mustofa. (2019). Evaluation of crystal violet decolorization assay and resazurin microplate assay for antimycobacterial screening. *Heliyon*, 5(8), e02263. <https://doi.org/10.1016/j.heliyon.2019.e02263>
29. Rawal, T., Parmar, R., Tyagi, R. K., & Butani, S. (2017). Rifampicin loaded chitosan nanoparticle dry powder presents: An improved therapeutic approach for alveolar tuberculosis. *Colloids and Surfaces B: Biointerfaces*, 154, 321–330. <https://doi.org/10.1016/j.colsurfb.2017.03.044>
30. Rawal, T., Patel, S., & Butani, S. (2018). Chitosan nanoparticles as a promising approach for pulmonary delivery of bedaquiline. *European Journal of Pharmaceutical Sciences*, 124, 273–287. <https://doi.org/10.1016/j.ejps.2018.08.038>
31. Ruiz, G. A. M., & Corrales, H. F. Z. (2017). Chitosan, Chitosan Derivatives and their Biomedical Applications. In *Biological Activities and Application of Marine Polysaccharides*. InTech. <https://doi.org/10.5772/66527>
32. Shah, S., Christopher, D., Sharma, S., Soniwala, M., & Chavda, J. (2020). Inhalable linezolid loaded PLGA nanoparticles for treatment of tuberculosis: Design, development and in vitro evaluation. *Journal of Drug Delivery Science and Technology*, 60(April), 102013. <https://doi.org/10.1016/j.jddst.2020.102013>
33. Son, Y.-J., & McConville, J. T. (2011). A new respirable form of rifampicin. *European Journal of Pharmaceutics and Biopharmaceutics*, 78(3), 366–376. <https://doi.org/10.1016/j.ejpb.2011.02.004>
34. Swamy, N., Basavaiah, K., & Vamsikrishna, P. (2019). Stability-Indicating HPLC Determination of Rifampicin in Bulk Drug and Dosage Form. *Pharmaceutical Chemistry Journal*, 53(6), 580–588. <https://doi.org/10.1007/S11094-019-02041-9/FIGURES/5>
35. Ughreja, R.; Parikh, R. (2019). Optimization of Ethyl Cellulose Microspheres containing Satranidazole using 3² Factorial Design. *International Journal of Pharmaceutical Sciences and Nanotechnology*, 12(1).
36. Zhang, Y., Wei, W., Lv, P., Wang, L., & Ma, G. (2011). Preparation and evaluation of alginate–chitosan microspheres for oral delivery of insulin. *European Journal of Pharmaceutics and Biopharmaceutics*, 77(1), 11–19. <https://doi.org/10.1016/j.ejpb.2010.09.016>

PCP375

DESIGN AND DEVELOPMENT OF FLOATING MICROSPHERE FOR LOCALIZED DRUG DELIVERY IN MANAGEMENT OF GASTRIC CANCER

AP0361

Komal Rahevar
Research scholar,
Dharmsinh Desai University,
komalrahevar.kr@gmail.com

ABSTRACT

The current research aimed to formulate, evaluate and optimize gastro retentive drug delivery system of Trifluridine/Tipiracil HCl, in a ratio of 1:0.5 with increased bioavailability of Trifluridine for a prolonged period in the treatment of gastric cancer, which is benefited by preparing stomach specific drug delivery systems in the form of floating microspheres. The formulation was evaluated for physical and chemical incompatibility and stability using an FTIR study and found that there is no such interaction with drugs and excipients. The analytical methods of UV spectrophotometer were developed for the in vitro analysis of the drug. floating microsphere prepared by Double emulsion method using HPMC K 15M and Ethyl cellulose 45 as a polymer. The prepared microspheres were evaluated for their production yields, particle size distribution, morphology, entrapment efficiency, and in-vitro drug release. Box-Behnken design produced fifteen formulations containing specified amounts of the independent variables, HPMC 15: EC45 ratio (X1), DCM: Acetone (X2), and stirring rate (rpm) (X3), the dependent factors studied were entrapment efficiency % (Y1), % drug released after 6 hrs (Y2), % drug released after 12 hrs (Y3), 90% release (Y4) and particle size (Y5). The prepared microspheres were characterized for their micromeritic properties and drug loading, as well as by infrared spectroscopy (IR), differential scanning calorimetry (DSC), Transmission electron microscopy (TEM), scanning electron microscopy (SEM), and Gas chromatography (GC). The in vitro release studies were performed in 0.1 N HCl. Microspheres were spherical in shape and had a smooth surface. The results showed that the production yield of the prepared microspheres was found to be between 66 to 80%. The formulated microspheres exhibited acceptable entrapment efficiency % values in the range of 73 to 80%. The optimized batch shows the most promising controlled drug release pattern for the period of 12 hours and remained buoyant for > 12 hrs.

Keywords: Trifluridine, Tipiracil HCl, Microsphere, Gastric cancer, controlled release

1. INTRODUCTION

Oral controlled drug delivery is the most preferable route of drug delivery system is to achieve better bioavailability and release of drug. Gastro retentive dosage forms significantly extend for the period of time, over which drug may be released and thus prolong dosing intervals and increase patient compliance. Floating drug delivery systems or hydro dynamically balance systems have a bulk density lower than gastric fluids and thus remain buoyant in the stomach for a prolonged period of time without affecting the gastric emptying rate. Microspheres are small spherical particles, with diameters in the micrometer range (typically 1 μ m to 1000 μ m). Hollow microspheres are typically used as additives to lower the density of a material. Hollow microspheres, Microballoons or floating microparticles are terms used synonymously for floating microspheres. Floating microspheres are, in a strict sense, spherical empty particles without a core. These are free-flowing particles, with size ranging from 1 to 1000 μ m^{1,2}

Gastric cancer is cancer that starts anywhere inside the stomach or stomach wall. Advanced gastric cancer can be locally advanced or metastatic. Gastric cancer begins with a mutation in

the structure of DNA in cells, which can affect how they grow. Gastric cancer is the fourth leading cause of cancer-related deaths and accounts for approximately 750000 deaths each year worldwide^{6,7}

Trifluridine and Tipiracil HCl combination therapy (TAS-102; Lon surf) comprises an antineoplastic thymidine-based nucleoside analogue, trifluridine, and thymidine phosphorylase (TPase) inhibitor, Tipiracil HCl, at a molar ratio 1:0.5. following uptake into cancer cells, trifluridine is phosphorylated by thymidine kinase, further metabolized in cells to a DNA substrate, and incorporated directly into DNA, thereby interfering with DNA function to prevent cell proliferation. Trifluridine is rapidly degraded by TPase and readily metabolized by a first-pass effect, hence the inclusion of the TPase inhibitor, Tipiracil HCl. TFD/TP HCl combination therapy is in development for the treatment of metastatic gastric cancer^{7,8}

1.1 Objectives

Design and Development of sustained release Trifluridine/Tipiracil floating microsphere. Development of UV analytical method for estimation of Trifluridine/Tipiracil. Screening of various polymers/ excipients required for formulation. Compatibility study of polymers/ excipients with Trifluridine/Tipiracil. Preliminary Evaluation of microspheres for various evaluation parameters in consideration of Gastro-retentive properties. Optimization of the drug: Polymer ratio for required sustained release profile by performing *in vitro* drug release studies. Accelerated stability studies of optimized formulation.

2. MATERIAL AND METHODS

2.1 Chemicals and Reagents

Trifluridine and Tipiracil HCl were kindly supplied as Emcure pharmaceuticals, Ahmedabad, Gujarat, and excipients were procured as gift samples from Colorcon pvt ltd.

2.3 Preparation of microspheres

Floating microspheres were prepared using water in oil in oil emulsion (w/o/o) with different polymer ratios. The drug was dissolved in an aqueous solvent (distilled water) and the polymer mixture was dissolved in the organic solvent mixture. Then the aqueous solution was mixed with the organic phase containing the polymer to obtain the primary emulsion (w/o). This primary emulsion was slowly to light liquid paraffin-containing surfactant with constant stirring for 2h. the microspheres were separated by filtration, which made them free from liquid paraffin and by washing with pet ether and air-dried throughout 12 hrs.¹⁰

2.4 Evaluation of floating microspheres¹¹

Particle size:

The particle size of the microspheres was measured using an optical microscopic method and the mean microsphere size was calculated by measuring 100 particles with the help of a calibrated ocular micrometer.

Micromeritic properties:

Floating microspheres are characterized by their Micromeritic properties such as flow properties (Angle of Repose, Hausner's Ratio), and density. The angle of repose is determined by the fixed funnel method and the compressibility index is determined by measuring the change in volume using a bulk density apparatus.

(a) Bulk density:

Bulk density is defined as the mass of powder divided by bulk volume. Accurately weighed sample of microsphere was placed into 25 ml measuring cylinder. The volume occupied by the granules was noted without disturbing the cylinder and the bulk density was calculated using the equation (values expressed in gm/cm³)

Bulk density = weight of the sample/Volume of sample

(b) Tapped density:

The tapping method is used for the determination of tapped density. In this method, hollow microsphere sample is placed in a 25 ml measuring cylinder and dropped at a height of one

inch onto a hard wooden surface 100 times at an interval of 2 seconds. The final volume was recorded and the tapped density is calculated by the following equation (expressed in gm/cm³).

Tapped density = Weight of microspheres/Tapped volume

(c) Carr's index:

The Carr's index indicates the flowability and compressibility of a powder. This is calculated from the values of bulk density and tapped density by using the formula:

Carr's Index (%) = Tapped Density-Bulk density/Tapped density

(d) Hausner's ratio:

The Hausner's ratio indicates the compressibility and flow property of powder. This is calculated from the values of bulk density and tapped density by using the formula:

Hausner's ratio = [Tapped density / Bulk density]

Angle of repose:

The angle of repose is indicative of the flowability of the substance. This can be determined by the funnel method. The height of the funnel is adjusted in such a way that stem is 2.5 cm above the horizontal surface. The sample powder was allowed to flow from the funnel adjusted at a height of 2.5 cm from the stem. The diameter of the pile was determined by drawing a boundary along the circumference of the pile and taking the average of three diameters. It is calculated by the formula.

Angle of repose (θ) = $\tan (h/r)$

Where θ is the angle of repose, h, is the height of the pile; r is the radius of the pile.

Percentage yield:

The percentage yield of floating microspheres was calculated by dividing the actual weight of the product by the total amount of all non-volatile components that are used in the preparation of floating microspheres and is represented by the formula.

% yield = (actual weight of product/total weight of drug and Excipients) \times 100

Drug-Excipients (DE) interactions:

This is done using Fourier-transform infrared spectroscopy (FTIR). The appearance of a new peak and/or disappearance of the original drug or excipients peak indicate the DE interaction.

Scanning electron microscopy (SEM):

Morphological examination of the surface and internal structure of the floating multiarticulate is performed by using a scanning electron microscope (SEM).

Floating Behavior:

Appropriate quantity (100mg) of the floating microspheres is placed in 100 ml of the simulated gastric fluid (SGF, pH 1.2), and the mixture is stirred with a magnetic stirrer. After 12 hours, the layer of buoyant microspheres is a pipette and separated by filtration. Separate the particles in the sinking particulate layer by filtration. Particles of both types are dried in a desiccator until constant weight is achieved. Both the fractions of microspheres are weighed and buoyancy is determined by the weight ratio of floating particles to the sum of floating and sinking particles.

Buoyancy (%) = $(W_f / W_f + W_s) \times 100$

Where W_f and W_s are the weights of the floating and settled microspheres

Percentage drug entrapment:

Appropriate quantity (100mg) of the floating microspheres is thoroughly triturated and suspended in a minimal amount of solvent. The suspension was filtered to separate shell fragments. Drug contents were analyzed and the percentage of drug entrapment is calculated by using the following equation.

% Drug Entrapment = (Actual drug content /Theoretical drug content) \times 100

In- Vitro Dissolution Tests:

Drug release studies of the prepared floating microsphere were performed, in triplicate, in a USP Dissolution Tester Apparatus, type- II (Paddle method) at $37 \pm 0.5^\circ\text{C}$. The paddles were rotated at a speed of 100 rpm. The microsphere (weight equivalent to one dose) was placed in empty tea bag and dissolution study was performed in simulated Gastric pH using 900 ml of 0.1N HCl solution (pH 1.2). Aliquots of 10 ml were withdrawn from the dissolution apparatus at different time intervals and replaced by 10ml of fresh dissolution medium. The drug content

was determined spectrophotometrically at a wavelength of 276 nm and 262nm. The release profile of all prepared gastroretentive microsphere batches were compared with the theoretical release of the drug by calculating similarity and dissimilarity factors.

Drug Release Kinetics Study

To analyze the mechanism for the release and release rate kinetics of the dosage form, the data obtained were fitted in to, zero order, First order, Higuchi matrix, Peppas and Hixson Crowell model. In this by comparing the R-values obtained, the best-fit model was selected.

Stability studies:

According to ICH guidelines, 3 months of accelerated stability study at $40\pm 2^\circ\text{C}$, and $75\pm 5\%$ was carried out for optimized formulations. Optimized drug formulation is evaluated for appearance, size, and buoyant properties before and after 3 months of storage at $40\pm 2^\circ\text{C}$ & $75\pm 5\%$ RH.

3. RESULTS AND DISCUSSION

3.1 OPTIMIZATION OF VARIABLES USING BOX BEHNKEN DESIGN

DOE is an approach for effectively and efficiently exploring the cause-and-effect relationship between numerous process variables and the output. A sequence of experiments was performed that would yield the most information about the factors and their interactions in as few experiments as possible (15 runs). A 3-factor 3-level factorial Box Behnken experimental design technique was employed to investigate the variables. Independent variables with their levels and the dependent variables selected are listed in (Table 4.7.1). An interactive second-order polynomial model was utilized to evaluate both the response variables. The polynomial equation generated by this experimental design using Microsoft Excel and Statistica is described as equation 1:

$$Y_i = b_0 + b_1X_1 + b_2X_2 + b_3X_3 + b_{12}X_1X_2 + b_{13}X_1X_3 + b_{23}X_2X_3 + b_{11}X_1^2 + b_{22}X_2^2 + b_{33}X_3^2 \quad (1)$$

Where Y_i is the dependent variable while b_0 is the intercept; b_1 to b_{33} are the regression coefficients which were determined from the results of the experiment to identify the statistically significant terms, X_1 , X_2 , and X_3 are the independent variables and levels of independent variables were selected from the preliminary experiments. Coefficients with more than one-factor term (b_{12} , b_{13} , and b_{23}) and those with higher-order terms (b_{11} , b_{22} , and b_{33}) represent interaction terms and quadratic relationships, respectively.^{12,13,14}

Table 3.1: OPTIMIZED BATCHES FOR BOX BAHNKEN DESIGN

Batch	Coded value			% Ratio		Polymer weight (X1)	DCM: Acetone	RPM
	X1	X2	X3	X1 (HPMC15:EC45)	HPMC15(mg)	EC (mg)	X2	X3
1	-1	-1	0	25:75	34	101	20	1500
2	1	-1	0	75:25	101	34	20	1500
3	-1	1	0	25:75	34	101	40	1500
4	1	1	0	75:25	101	34	40	1500
5	-1	0	-1	25:75	34	101	30	1300
6	1	0	-1	75:25	101	34	30	1300
7	-1	0	1	25:75	34	101	30	1800
8	1	0	1	75:25	101	34	30	1800

9	0	-1	-1	50:50	68	67	20	1300
10	0	1	-1	50:50	68	67	40	1300
11	0	-1	1	50:50	68	67	20	1800
12	0	1	1	50:50	68	67	40	1800
13	0	0	0	50:50	68	67	30	1500
14	0	0	0	50:50	68	67	30	1500
15	0	0	0	50:50	68	67	30	1500

Table 3.2 : Results analysis of design expert formula

Batch No.	HPMC 15: EC15 X1	DCM: Acetone X2	RPM X3	Y1 EE (%)	Y2 Drug release after 6 hrs		Y3 Drug release after 12 hrs		Y4 t ₉₀		Y5 Particle size	
					TP	TFD	TP	TFD	TP	TFD	TP	TFD
1	-1	-1	0	78.5	78.9	34.1	35.08	59.05	59.83	18.50	18.63	320.6
2	1	-1	0	78.0	77.5	68.10	67.56	99.20	100.26	8.73	9.24	323.2
3	-1	1	0	76.3	76.2	38.3	37.56	63.1	64.36	17.92	17.67	280.1
4	1	1	0	76.2	76.2	68	68.98	100	101.29	8.56	8.47	287.4
5	-1	0	-1	78.6	78.9	28.56	29.45	57.12	58	19.62	19.28	344.9
6	1	0	-1	79.2	78.1	66.21	65.23	98.2	99	9.15	9.11	349.23
7	-1	0	1	73.3	73.1	32.23	33.17	59	59.98	18.74	18.66	250.0
8	1	0	1	73.2	73.1	69.02	69.81	99.21	101.01	7.91	7.90	256.5
9	0	-1	-1	80.1	80.2	53.14	53.68	96.56	97.18	10.95	10.83	370.0
10	0	1	-1	79.0	78.9	55.6	56.38	97.4	98.23	10.74	10.64	330.6
11	0	-1	1	74.1	74.0	57.4	58.02	99.02	99.85	9.58	9.56	270.4
12	0	1	1	71.6	72.0	58.82	59.75	100.02	102.73	9.45	9.29	220.0
13	0	0	0	76.8	76.3	58.89	59	100.32	99.3	10.48	10.35	300.0
14	0	0	0	76.7	77.2	57.12	58.02	99	99.96	10.48	10.36	300.0
15	0	0	0	76.5	77.0	57.01	57.87	100	101.12	10.43	10.38	300.0

TABLE 3.3 Summary of ANOVA table for response parameters for Box-Behnken design for floating microsphere

Source	Sum of Squares	Degree of freedom	Mean Square	F Value	P-value
% Entrapment Efficiency (TP HCl)					
Regression	84.30	10	8.430185367	41	0.0013
Residual	1.15	5	0.228459777		
Total	85.4	15			
% Entrapment Efficiency (TFD)					
Regression	88.21980167	10	8.821980167	60.77062287	0.000630292
Residual	0.806491667	5	0.161298333		
Total	89.02629333	15			
Drug release after 6 hrs (TP HCl)					
Regression	2587.761393	10	258.7761393	93.26657719	0.000270453
Residual	15.41436667	5	3.082873333		
Total	2603.17576	15			
Drug release after 6 hrs (TFD)					
Regression	2566.337192	10	256.6337192	160.1968797	0.00009
Residual	8.899941667	5	1.779988333		
Total	2575.237133	15			

Drug release after 12 hrs (TP HCl)					
Regression	4538.956148	10	453.8956148	435.8260489	0.00001
Residual	5.785891667	5	1.157178333		
Total	4544.74204	15			
Drug release after 12 hrs (TFD)					
Regression	4581.547152	10	458.1547152	319.33	0.00002
Residual	7.970541667	5	1.594108333		
Total	4589.517693	15			
t90 (TP HCl)					
Regression	249.4498346	10	24.94498346	213.8508907	0.00005
Residual	0.648036775	5	0.129607355		
Total	250.0978713	15			
t90 (TFD)					
Regression	242.2757835	10	24.22757835	140.2843938	0.000120
Residual	0.959462802	5	0.19189256		
Total	243.2352463	15			
Particle size					
Regression	23367.96178	10	2336.796178	149.9328485	0.000105444
Residual	86.58676944	5	17.31735389		
Total	23454.54855	15			

3.2 Multiple regression analysis for dependent variables

Y1- % Entrapment Efficiency

$$(%EE-TP) = 76.85 + 0.29X_1 - 0.90X_2 - 3.00X_3 + 0.32X_1X_2 + 0.23X_1X_3 - 0.18X_2X_3 - 0.07X_1^2 + 0.40X_2^2 - 0.96X_3^2$$

$$(%EE-TFD) = 76.69 + 0.01X_1 - 0.96X_2 - 3.10X_3 + 0.09X_1X_2 - 0.17X_1X_3 - 0.37X_2X_3 + 0.20X_1^2 + 0.34X_2^2 - 0.83X_3^2$$

The coefficient of X_1 that is b_1 bear positive sign whereas coefficient of X_2 and X_3 that is b_2 and b_3 respectively bear negative sign indicating that the % entrapment efficiency is increased with increase in level of X_1 whereas as there is increase in the level of X_2 and X_3 there is decrease in % entrapment efficiency. Furthermore, the coefficient value of X_3 is higher than other two independent variable (X_1 & X_2) reveals that the X_3 (RPM) has greater influence on % entrapment efficiency (Tipiracil HCl). The significance level of coefficient b_2 , b_3 and b_{33} was found to be less than $p=0.05$, thus they were significance effect on % Entrapment Efficiency (Tipiracil HCl). The results of statistical analysis are shown in table 5.7.7. **The Figure 5.7.4** shows surface response plot and contour plot for the interaction between independent variables and % entrapment efficiency. It reveals that the % EE is affected by all three independent variables. The effect of X_2 and X_3 is stronger on % EE than the effect of X_1 . There is sharp decrease in % EE with increase in level of X_2 and X_3 from -1 to 1 which It shows that as the results clearly indicate that the dependent variables (% **Entrapment Efficiency**) are dependent on the independent variables.

Figure 3.1: Surface Response Plot for effect of independent variable on % EE

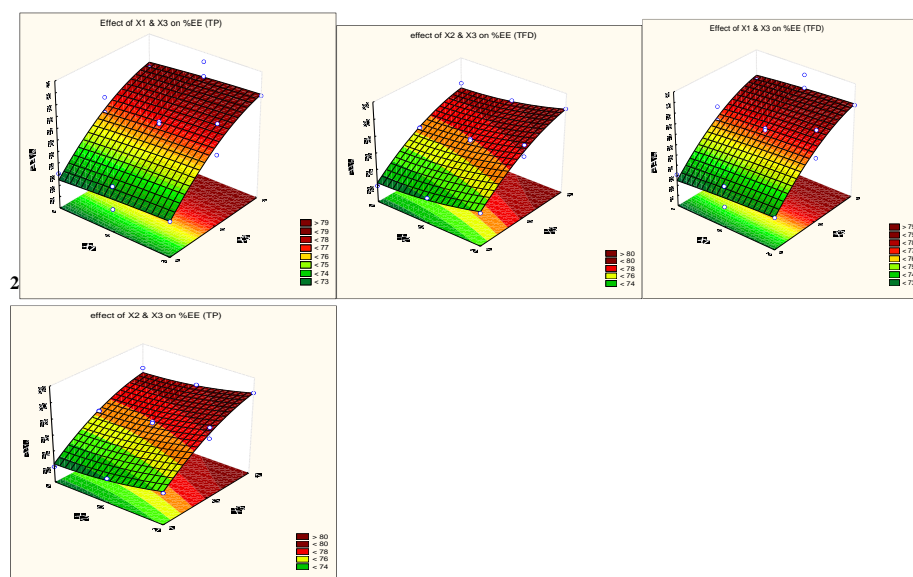
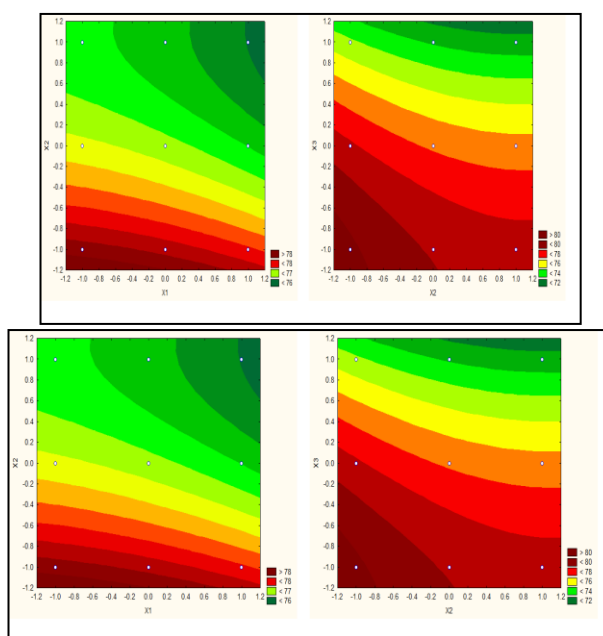


Figure 3.2 : Contour Plot for effect of independent variable on % EE



Response surface plot and contour plot shows that X1 increase from level -1 to 1 to increase in % Entrapment Efficiency (Tipiracil HCl) and X2 and X3 increase from level -1 to 1 decrease in % Entrapment Efficiency (Tipiracil HCl).

Y2- Drug Release after 6 hours

$$(Q_6 - TP) = 57.44 + 17.26X_1 + 0.99X_2 + 1.74X_3 - 1.07X_1X_2 - 0.21X_1X_3 - 0.26X_2X_3 - 6.27X_1^2 + 0.95X_2^2 - 2.16X_3^2$$

$$(Q_6 - TFD) = 58.30 + 17.11X_1 + 0.97X_2 + 2.00X_3 - 0.40X_1X_2 + 0.21X_1X_3 - 0.24X_2X_3 - 6.70X_1^2 + 0.84X_2^2 - 2.18X_3^2$$

Fig 3.3 : Surface Response Plot for effect of independent variable on drug release after 6 hrs.

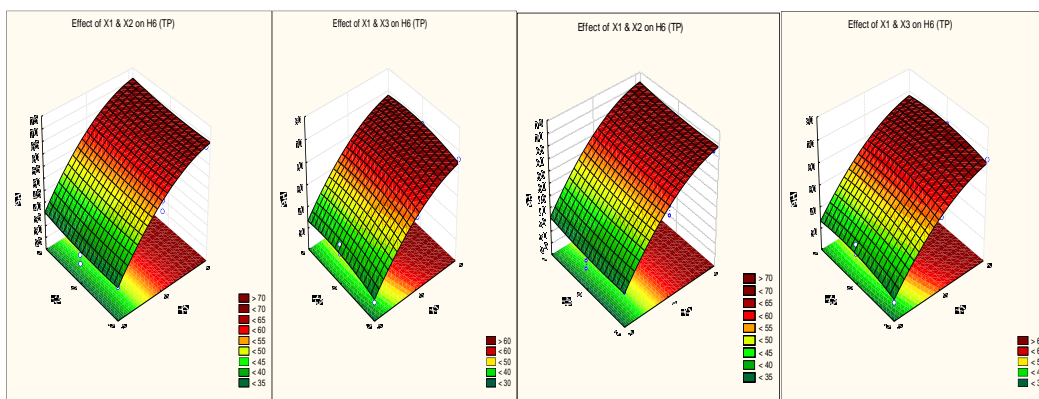
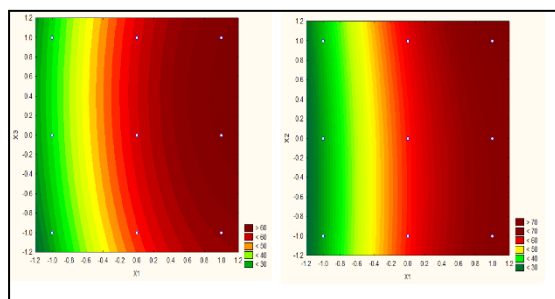


Fig: Table 3.4 : Coutor Plot for effect of independent variable on drug release after 6 hrs.



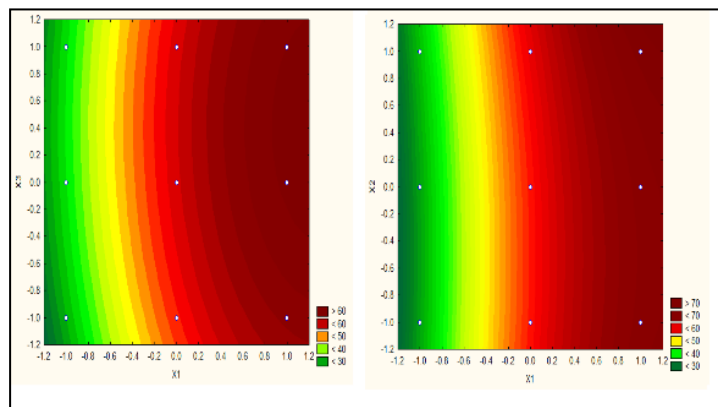
The coefficient values for all the variables carries positive sign and the p value for coefficient of X1 and X3 is less than 0.05. The positive sign indicates the increased drug release with higher level of all three selected independent variables however the higher value of b_1 stands for significant stronger effect of X1 on drug released at 6th hours. The results of statistical analysis are shown in table. The surface response plot and coutor plot shows that shifting of X1 from lower level (-1) TO Higher level (1) shows greater feet on total amount of drug released at sixth hours. The rotational speed (RPM) has lesser effect on drug released at sixth hours than the X1.

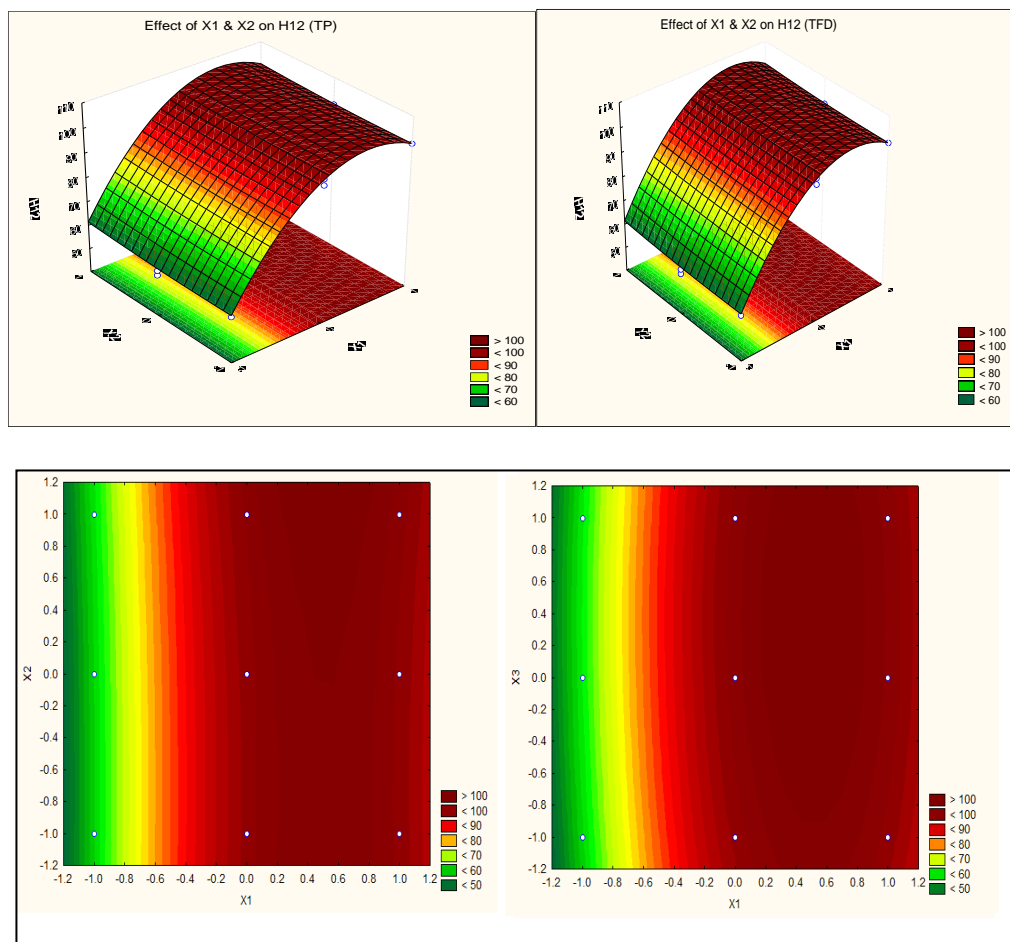
Y3- Drug Release after 12 hours

$$(Q_{12}-TP) = 99.03 + 19.79X1 + 0.83X2 + 0.99X3 - 0.81X1X2 - 0.21X1X3 + 0.04X2X3 - 19.28X1^2 + 0.58X2^2 - 1.36X3^2$$

$$(Q_{12}-TFD) = 100.13 + 19.79X1 + 1.32X2 + 1.40X3 - 0.61X1X2 + 0.01X1X3 - 0.46X2X3 - 19.48X1^2 + 0.52X2^2 - 1.15X3^2$$

Fig 3.5 : Surface Response Plot for effect of independent variable on drug release after 12 hrs.





Y4- t_{90} (Trifluridine)

$$(t_{90}\text{-TFD}) = 10.36 - 4.94X_1 - 0.27X_2 - 0.56X_3 + 0.05X_1X_2 - 0.14X_1X_3 - 0.02X_2X_3 + 3.40X_1^2 - 0.26X_2^2 - 0.02X_3^2$$

$$(t_{90}\text{-TFD}) = 10.47 - 5.05X_1 - 0.13X_2 - 0.60X_3 + 0.10X_1X_2 - 0.09X_1X_3 + 0.02X_2X_3 + 3.32X_1^2 - 0.36X_2^2 + 0.07X_3^2$$

The coefficient of X_1 that is b_1 bear positive sign and coefficient of X_2 and X_3 that is b_2 and b_3 bear negative sign and thus X_1 increases the Particle size whereas X_2 and X_3 decrease the Particle size. The significance level of coefficient b_2 and b_3 was found to be less than $p=0.05$, thus they were significance effect on particle size. The results of statistical analysis are shown in table. The plot shows that the particle size of microspheres was greatly dependent and influenced by changes in level of X_3 and X_2 from -1 to 1. There is a significant decrease in particle size was revealed with increase in level of X_2 and X_3 . The effect of X_1 is not as prominent as the effect of X_2 and X_3 .

Fig 3.6: Surface Response Plot for the effect of the independent variable on drug release on t90

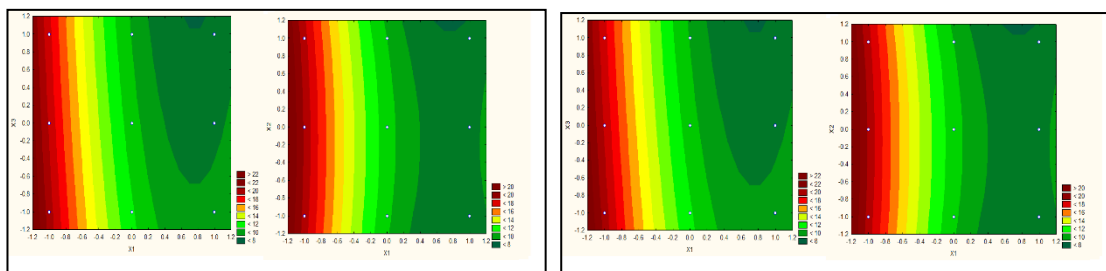


Fig 3.7: Contour Plot for the effect of the independent variable on drug release on t90

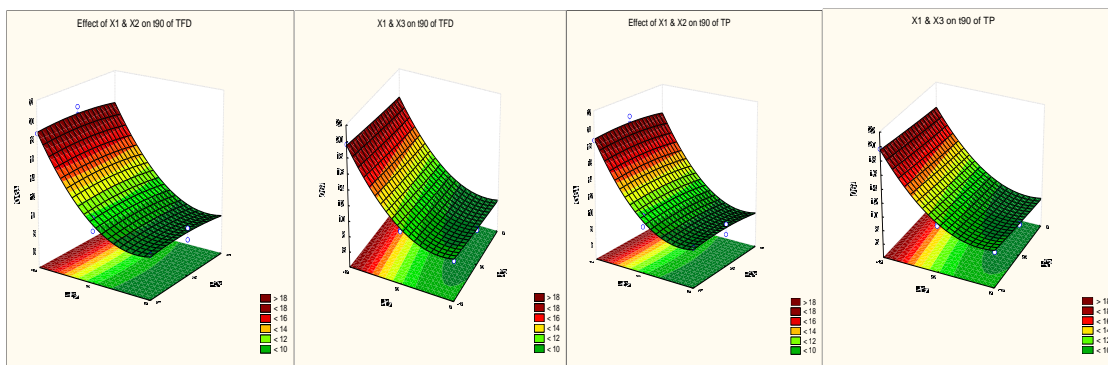
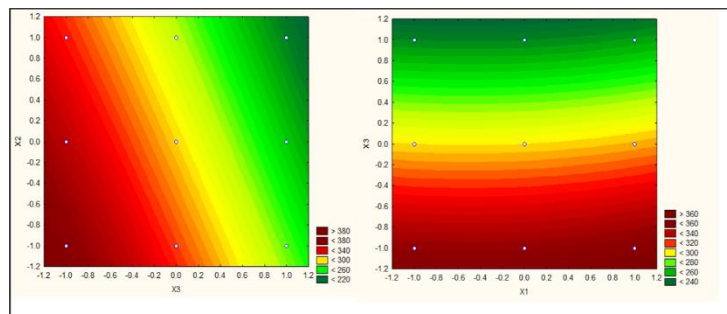


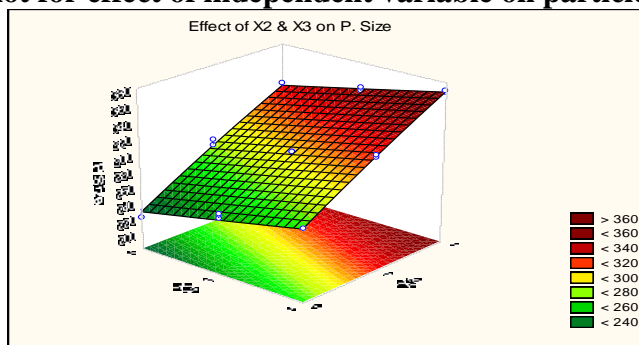
Fig 3.8: Surface Response Plot for effect of independent variable on particle size



Y5- Particle size

$$Y_i (P. size) = 300 + 2.59X_1 - 20.77X_2 - 49.72X_3 + 1.19X_1X_2 + 0.53X_1X_3 - 2.75X_2X_3 + 2.62X_1^2 + 0.22X_2^2 - 2.47X_3^2$$

Fig 3.9: Contour Plot for effect of independent variable on particle size



Validation of Model by Checkpoint batch

The three components of **Box-Behnken design** were run with one check point composition of which is shown in Table. Batch CP1 was prepared to validate the derived equation for *selected responses*. The data for the predicted and observed values are shown in table.

Table 3.4: Evaluation parameters for check point batch

Check point batch (CP1)	Drug	Evolution Parameter	Predicted value	Observed value	% Error
X1=0.5; X2=1.0 ; X3=0.5	<i>Tipiracil HCl</i>	t90	10.46	10.1	3.44
		H6	66.79	64.5	3.43
		H12	105.68	101.5	3.96
		%EE	74.44	71.5	3.95
	<i>Trifluridine</i>	t90	10.21	9.85	3.53
		H6	63.14	61.45	2.68
		H12	101.28	97.31	3.92
		%EE	72.34	70.35	2.72
	P size		255.91	249.5	2.50

Table3.11: t-Test: Paired Two Sample for Means

t-Test: Paired Two Sample for Means		
	Variable 1	Variable 2
Mean	84.47222	81.78444
Variance	5266.429	5002.529
Observations	9	9
Pearson Correlation	0.999962	
Hypothesized Mean Difference	0	
df	8	
t Stat	4.14547	
P(T<=t) one-tail	0.001615	
t Critical one-tail	1.859548	
P(T<=t) two-tail	0.003229	
t Critical two-tail	2.306004	

Figure 3.5: Profile for predicted value and desirability of CP1 batch

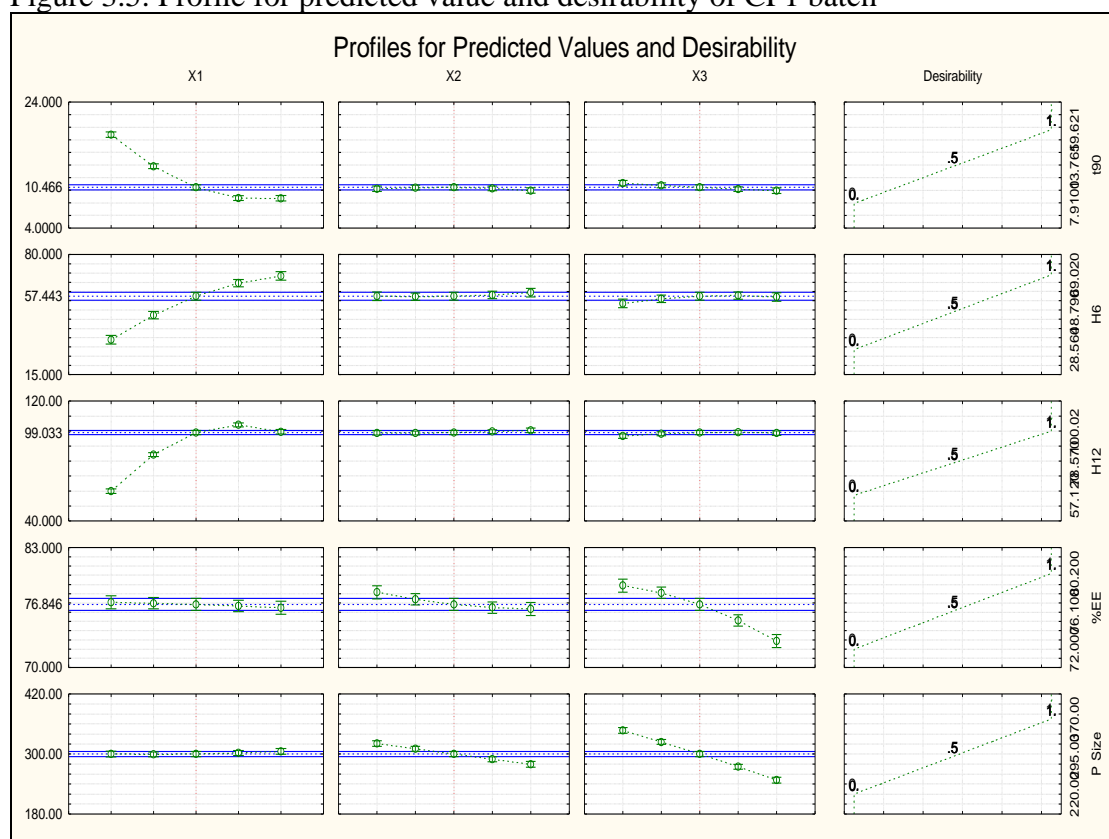


Fig 3.10: Identification of Tipiracil HCl by FTIR

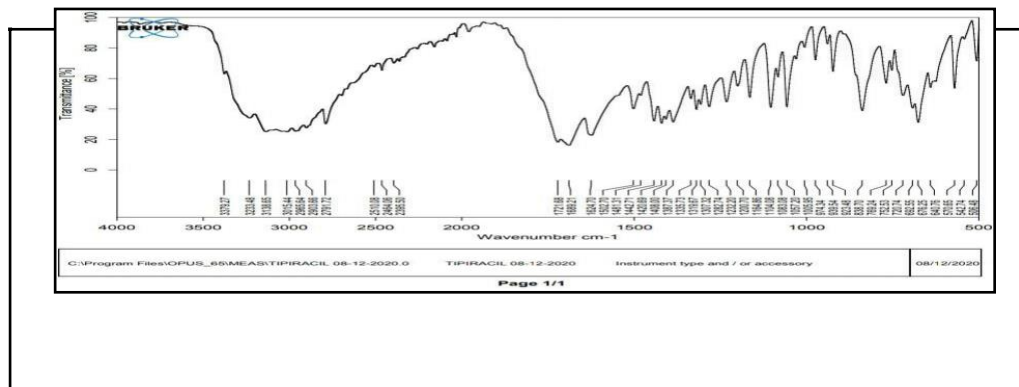


Fig 3.11: Identification of Trifluridine by FTIR

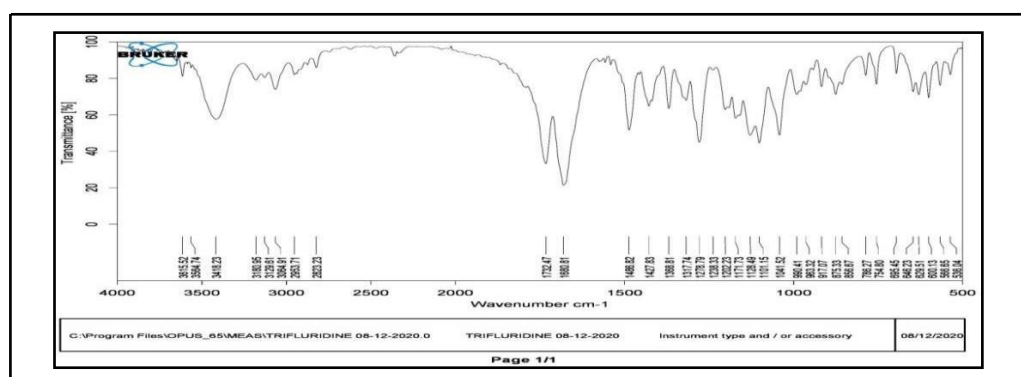


Fig 3.12: FTIR for optimized formulation

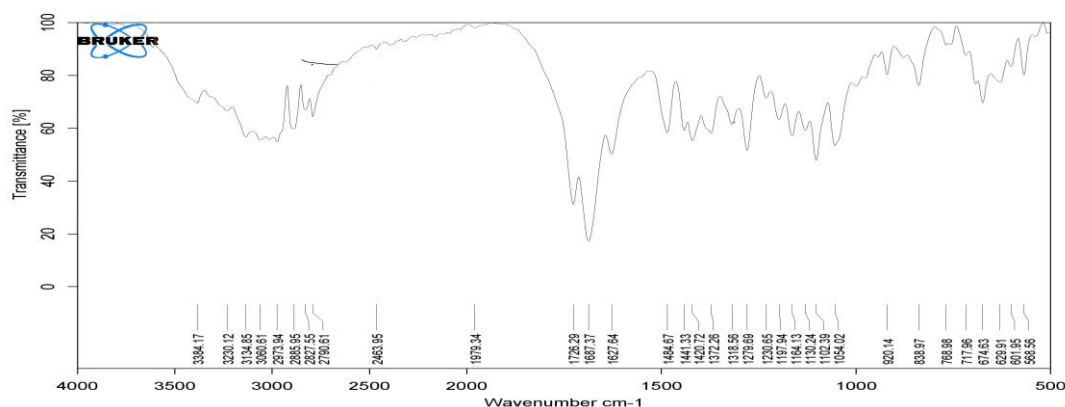


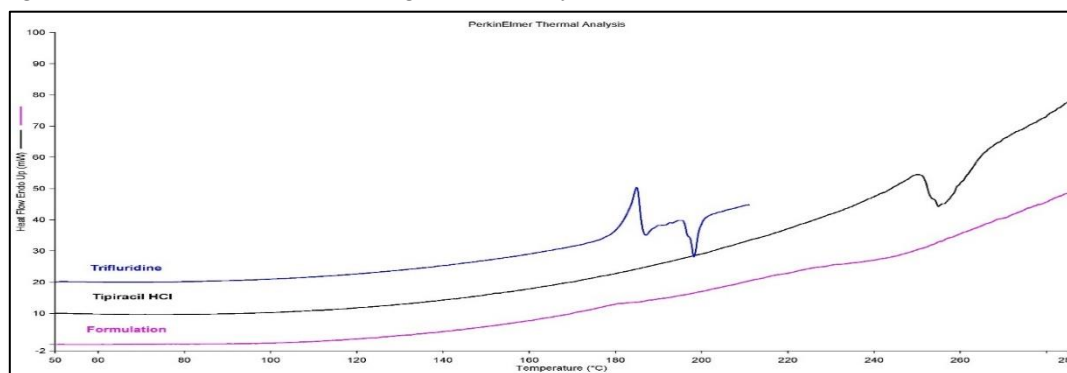
Table 3.6: Interpretation of FTIR graph of B13 Batch

Functional group	(TFD) Pure Drug (cm ⁻¹)	Functional Group	(TP)pure Drug (cm ⁻¹)	Microsphere
O-H	3615.52	N-H	3379.27	3384.17
N-H	3564	C=O	1721.68	1726.29
C=O	1732.47	C=N	1689	1687.37
C-F	1278	C-H Aromatic	3233	3230
C-O	1128.49	C-O	1104.08	1054.02

DSC thermograms of pure Trifluridine, Tipiracil HCl, and Trifluridine/Tipiracil HCl loaded floating microsphere. They exhibited a sharp endothermic peak of trifluridine at about 186.28°C corresponding to its melting point (186-189°C), and Tipiracil HCl exhibited a sharp endothermic peak at 253.45°C corresponding to its melting point (251-253°C) representing its crystalline nature. The thermogram of the physical mixture of polymer and drug and formulation gave the peaks at 185.09°C, respectively, there was a slight decrease in the melting point of the drug when prepared in the form of microspheres. It was also observed that there was a noticeable reduction in the enthalpy of the crystals in comparison with pure drugs. The evaluation of the thermograms obtained from DSC revealed no interaction between the polymer and the drug in the microspheres.

Differential Scanning Calorimetry (DSC)

Figure 3.12: Differential Scanning Calorimetry (DSC)



Transmission electron microscope (TEM)

The high-resolution transmission electron microscope was used to investigate the microstructures. Transmission electron microscopy (TEM) images were taken with a FEG - TRANSMISSION ELECTRON MICROSCOPE (HR-TEM), Thermo Fisher Scientific, Talos F200i S/TEM using an accelerating voltage of 200 kV was further investigated by TEM. Fig. a and b shows TEM images of the as-prepared floating microspheres with different magnifications. Low-magnification TEM image as indicated in Fig. a shows that the as-prepared product is composed of microspheres with a uniform diameter of about 300 μm , which is consistent with the observed result in SEM images. Fig. 3b is a high-magnification it can be seen that the sample is a hollow structure with a spherical shell thickness of about 303 nm. The hollow structure was formed in the sphere, and the structure was broken in the microspheres. From the high-magnification TEM image shown in fig , the microspheres were porous structure was observed.

Figure 3.13. TEM images of the sample. (a): TEM images of the microsphere with low magnification; (b): TEM images of the high magnification.

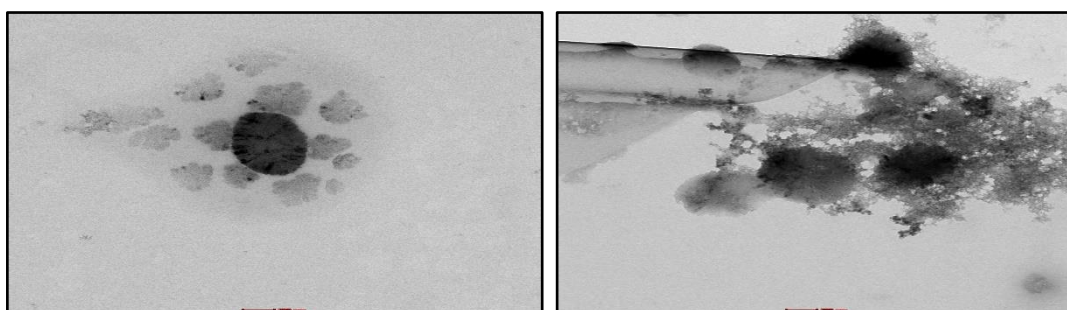


Figure 3.14: GC Scan of B13 formulation, solution prepared in DMSO

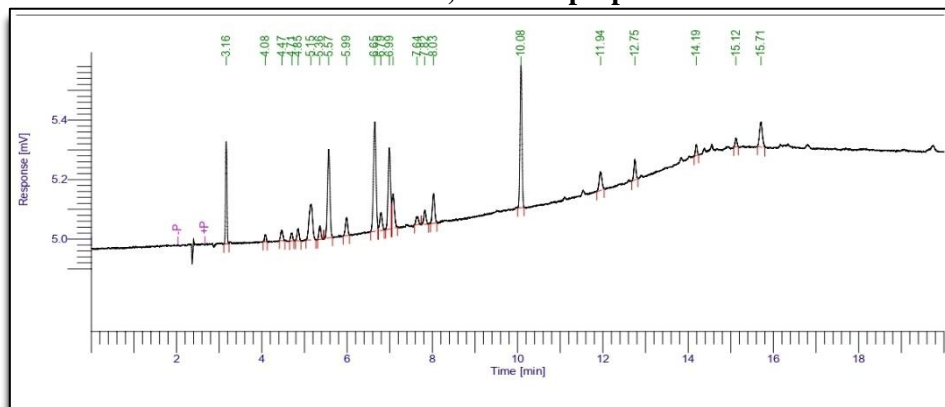


Table 3.7: Residual Solvent Analysis for microsphere

Sr. No	Sample Name	Acetone (ppm)	Dichloromethane (ppm)
1	Microsphere	0.30	0.62

CONCLUSION

Floating microspheres of Trifluridine/Tipiracil HCl were prepared to absorption in stomach necessities development of sustained drug delivery system forms which retained in stomach with improved drug efficiency and decreased dose requirements for prolonged period of time. The systems provide an easy way of maintaining constant blood level with an ease of administration and better patient compliance in case of gastric cancer.

REFERENCES

1. Susan Hua (2020). Advances in Oral Drug Delivery for Regional Targeting in the Gastrointestinal Tract - Influence of Physiological, Pathophysiological and Pharmaceutical Factors. *frontiers in pharmacology*, 11(524).
2. Debjit Bhowmik, Harish Gopinath, B. Pragati Kumar, S. Duraivel, K. P. Sampath Kumar. (2-12) Controlled Release Drug Delivery Systems, *The pharma innovation*, 1(10).
3. Satinderkakar, Ramandeep Singh and Shallusandhan (2015). Gastro retentive drug delivery systems: A review, *African Journal of Pharmacy and Pharmacology*, 9(12),
4. Julu Tripathi, Prakash Thapa, Ravi Maharjan and Seong Hoon Jeong (2019). Current State and Future Perspectives on Gastro retentive Drug Delivery Systems, *pharmaceutics*.
5. Saurabh Sharma, Arun Nanda and Lalit Singh (2014). Gastro retentive Drug Delivery System: An Overview, *International Journal of Research in Pharmaceutical and Biomedical Sciences*.
6. CHMP extension of indication variation assessment report, *European medicines Agency science medicines health*, 2019.
7. <https://go.drugbank.com/drugs/DB00432>
8. <https://go.drugbank.com/salts/DBSALT001349#:~:text=Tipiracil%20hydrochlorideProduct%20ingredient%20for%20Tipiracil&text=Tipiracil%20is%20a%20thymidine%20phosphorylase,bioavailability%20by%20inhibiting%20its%20catabolism>.
9. <https://pubchem.ncbi.nlm.nih.gov/compound/Tipiracil-hydrochloride>
10. Krishna Sailaja and Anusha K (2017), Review on microspheres as a drug delivery carrier, *International Journal of Advances in Pharmaceutics*, 6(5).
11. Gayathri devi M, J. Adlin Jino Nesalin and T. Tamizh Mani, 2016. Floating microsphere: a review, *IJRPC*, 6(03).
12. Yu Huang, Yumeng Wei, Hongru Yang, Hao Pi, Hao Liu, Yun Ye, Ling Zhao, (2016). A 5-fluorouracil-loaded floating gastro retentive hollow microsphere: development, pharmacokinetic in rabbits, and biodistribution in tumor-bearing mice, *Drug Design, Development and Therapy*.
13. Dharmendra Rai, Durga Pandey, Nishi Prakash Jain, Surendra Kumar Jain, (2019). Formulation Development and Evaluation of Floating Microsphere of Famotidine for the Treatment of Peptic Ulcer, *Journal of Drug Delivery & Therapeutics*, 9(4),
14. D. Ridhima, P. Sweta, KJ. Upendra (2012) "Formulation and Evaluation of floating microspheres of curcumin", *International Journal of Pharmacy and Pharmaceutical Sciences*, 4(3).
15. Bathini Sree Tejaswi, Durgaramani Sivadasan and Shalini Devi. P, (2011) "Formulation and in vitro evaluation of clarithromycin floating microspheres for eradication of Helicobacter Pylori" *Scholars Research Library*, 3(6).
16. Rajeev Garg and GD Gupta (2010) "Gastroretentive Floating Microspheres of Silymarin: Preparation and In Vitro Evaluation" *Tropical Journal of Pharmaceutical Research*, 9(1).
17. S.K. Singh, C. H. Borkhataria. N.R. Seth, Dr. R. P. Patel, S. Singh and G. R. Parma (2009), Formulation and in vitro evaluation of lansoprazole micro pellets, *International Journal of PharmTech Research*, 1(4),
18. Kumaresh S. Soppimath, Anandrao R. Kulkarni, Tejrj M. Aminabhavi (2001) "Development of Hollow Microspheres as Floating Controlled-Release Systems for Cardiovascular Drugs: Preparation and Release Characteristics" *Drug Development and Industrial Pharmacy*, 27(6),

PCP377

PHARMACEUTICAL 3-D PRINTING TECHNOLOGY AT A GLANCE

AP0366
Dr. Chetan H. Borkhataria
Assistant Professor (GES
Class-2)
B.K.Mody Govt. Pharmacy
College Rajkot
chetanborkhataria@gmail.com

AP0352
Mr. Jaydeep Mehta
M. Pharm
(Pharmaceutics)
B.K.Mody Govt.
Pharmacy College Rajkot
Jaydip30mehta@gmail.com

AP0354
Mr. Dhruv C. Sakhiya
PhD Scholar
Gujarat technological
university Gandhinagar
199999901526@gtu.edu.in

Abstract: -

The process of digital fabrication, commonly known as 3D printing or additive manufacturing, involves gradually adding materials to a geometric representation to make physical objects. Dr. Kodama receives the first 3D printing efforts in exchange for his creation of a quick prototyping method. He was the first to explain a layer-by-layer manufacturing process and develop the photosensitive resin that served as the prototype of SLA. 3D printing is now widely used throughout the world. 3D printing technology is progressively being applied for mass modification and manufacture of open-source designs in agricultural, healthcare, automobile, locomotive, and aviation industries. A significant amount of 3D printing technology is currently being employed in the pharmaceutical production chain to change what pharmacies do when producing particular drugs. The advantages include extremely reproducible results, a variety of pharmaceutical release patterns, and individualized pharmacological therapy. Patients may benefit from a variety of advantages provided by 3DP's customized medications. It may be better to provide a patient a printable dosage form on paper rather than one printed with powder. Used in the creation of complicated release profile formulation and customized delivery, as well as drug printing in picoliters and minimizing API side effects or adverse effects.

Keywords: Three-dimensional printing, Solid oral dosage forms, medical devices, pharmaceutical development, Personalized medication, Controlled release

THREE-DIMENSIONAL PRINTING: -

The purpose of 3D printing is to deliver customized and complex product in much easy way than the conventional manufacturing techniques [1]. Digitized production technologies are anticipated to bring striking benefits for companies and businesses, but in practice, such gains are rarely realized. Product Innovators are advised to be extraordinary and agile to turn to three-dimensional (3D) printing [2]. 3D printing is a relatively fresh technology that was first illustrated in the early 1990s[3]. Medicinal and pharmaceutical 3D printing applications are growing quickly and are expected to develop the health care industry [4]. Examples of personalized drugs, including dose, dose combination, or even actively tailored to the patient's genetics, are not yet fully understood [5, 6]. 3D printing is all about digital drawing and fabrication of article layer-by-layer [7]. In realistic terms, this means that users can create practically anything that can be designed in a digital platform using computer-aided design (CAD) software [8, 9]. Virtual must be created as stereolithography (.stl) or object (.obj) files for use as templates in commercially available object printers [10]. Democratization of design and production, enhanced collaboration, reduced time, customized geometrically complex objects in small quantities have helped reduce material use [3,11]. The term 3D printing refers to a series of additive mechanized processes, which construct products straight from digital design by creating layers of plastics, metals or other materials [12]. Due to the all-embracing

research being done in this vicinity and all the investigational drug delivery systems intended and described in numerous papers over the past few years, pharmaceutical company like *Apresia*® launched its first approved 3DP manufactured product [13].

3D printing is built-up technique in which objects fabricate by depositing material like, plastic, metal, resin, powder, liquid, etc. to construct 3D object [14].

3D printers are similar to the traditional inkjet printers though, the ending creation differs within that a 3D printed object is produced.

BRIEF HISTORY: -

Hull, in 1980s, was working at the Ultra Violet Products Company in California to manufacture plastic making objects from Photopoly Limers invented 3D printing [4]. In 1988, 1st commercial 3D printer, SLA-250, was launched. Later, Austin filed a patent designed for selective laser sintering; a process scan over a powder bed is by laser beam to produce a solid object after repetitions [15].

MIT Professors are accredited first for using the expression “3D printer” with their invention of a layering technique using standard inkjet print head to deposit “ink” or a binder solution into the powder bed to bind powder, again repeating this process layer-by-layer to produce the desired geometry [16].

Thomas J. Bradbury and his colleagues created design of anatomically correct implants for a patient. Radiological data representing anatomical structure of anatomical body, which is to be altered, repaired or augmented and created multidimensional model, can be used [17]. David Russell and colleagues invented apparatus and method to produce 3D object [18].

TYPES OF 3D PRINTING TECHNOLOGIES: -

Over the past 20 years, wide varieties of 3D printing technologies were introduced. 3D printing is also known as the additive manufacturing (AM) process. Although other highly competitive processes, such as laser-based writing systems or nozzle-based deposition systems, have been extensively developed, printing-based inkjet systems is a frequently used procedure in three-dimensional method [19].

It can furthermore be classified, figure 1, into 3-D printing systems. 3- D printing processes may also be related to (1) melt and solidify method, (2) fusing method and (3) cut and join methods. Fused deposition production method uses melting followed by liquid-based printing [20].

In stereolithographic printing, a laser is used to photo polymerize a resin. StereoLithography translate liquid polymers into solid layers by means of photo-curing UV blue light and used to manufacture complex nanocomposites [21, 22, 23]. Polyjet printing is a quite novel form of rapid printing manufacture [24]. The process was patented in 1994 by Sachs et al. under US patent [25].

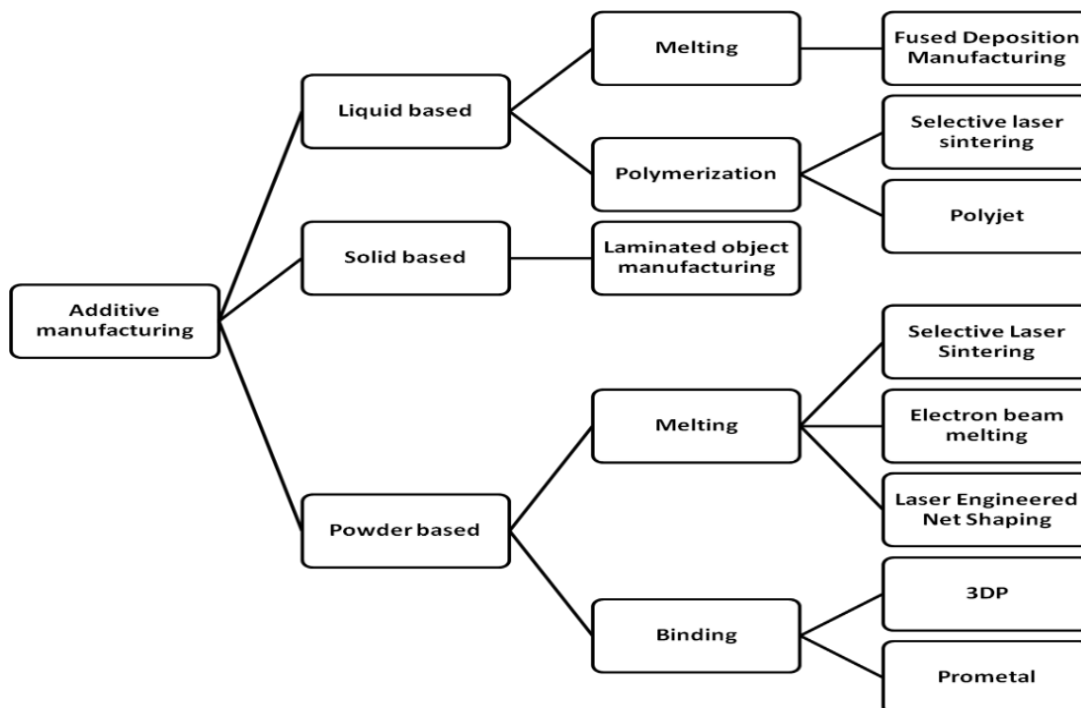
It uses inkjet technologies to produce physical model groups [26, 27] Laminated Object Manufacturing is ideal for large parts production [28].

The layers are bound together by pressure and temperature application and by means of a thermal adhesive coating. In selective laser sintering process, the powder is sintered or fused using carbon dioxide laser beams [20].

Electron beam melting used mostly for fabricating complex polymer prototypes that have now become well established [29,30]. Laser engineered net shaping (LENS) uses virgin metal powder as the user's choice, as processes build material [31- 33].

In MIT-licensed procedures, 3DP and prometal, a liquid binder is installed on a powder medium using inkjets for printing using computer-aided design (CAD) data [20,28].

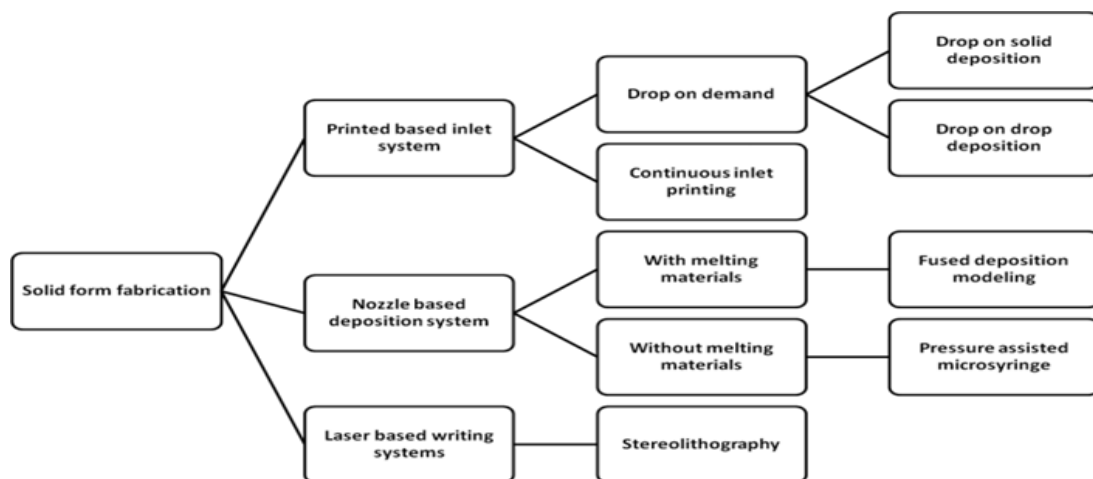
Figure 1: Categorization of 3D printing general additive manufacturing techniques based on type of base



TECHNIQUES WIDELY USED BY THE PHARMACEUTICAL COMPANIES:

Pharmaceutical industry uses 3D printing techniques bases on solid form fabrication that are further classified in printed based inlet system, nozzle-based deposition system and laser-based writing systems (figure 2).

Figure 2: 3D printing technologies that supports medicine manufactures for solid form fabrication



1. Printing-based inkjet systems: -

Inkjet printing is the overall term for describing systems that are capable of digitally controlled configuration and residency of small liquid droplets on a substrate with a pattern-generating mechanism. There are two categories of printing-based inkjet systems: 1) continuous inkjet printing (CIJ) and 2) drop-on demand (DoD) inkjet printing [19, 35]. Inkjet printing is based on Lord Rayleigh's instability theory, developed in 1878, which explains the breaking of a liquid stream or jet into droplets [34, 36].

1. Drop-on-demand (DoD) inkjet printing: -

DoD inkjet printers fabricate individual drops when considered necessary and are therefore more economical with ink delivery than CIJ systems [37]. DoD classifies into two types: drop-on solid deposition and drop-on-drop deposition. The most regular types of work with DOD printing are thermal (sometimes referred to as bubbles) and piezoelectric [19, 34]. In thermal type, its heads utilize a resistor that the electrical pulses in the reservoir heat up swiftly and make a vapor bubble, these bubbles then drive the ink out of the print head; then the bubble breaks down, producing negative pressure that pulls the ink out of the reservoir to refill the chamber. In piezoelectric type, a piezoelectric component such as a crystal or ceramic is used to manufacture mechanical movement when voltage is applied. The element deformation creates a pressure signal that drains the fluid out of the nozzle. breaks down, producing negative pressure that pulls the ink out of the reservoir to refill the chamber. In piezoelectric type, a piezoelectric component such as a crystal or ceramic is used to manufacture mechanical movement when voltage is applied. The element deformation creates a pressure signal that drains the fluid out of the nozzle.

2. Drop-on- solid deposition

Drop-on-solid deposition uses a mixture of powder-bed and binder-ink to generate a solid structure in a level-by-level way. The stability of the final product is often achieved by thermal sintering, which permits the elimination of residual volatile solvents. The binder may reason the particles of the ink to stick or the powder bed may play a role after its own solidification. These techniques are prejudiced by two powder characteristics: powder topology and the response of materials with binder.

1.1.1. Drop-on-drop deposition

The drop-on-drop deposition is a direct-writing inkjet printing method capable of creating microscopic drug formulations with diverse geometries and comparatively high drug loadings. Multi-droplets allow the creation of overlapping, high-resolution three-dimensional compositions. Piezoelectric print heads are frequently used because they do not restrict the selection of solvent. The droplets produced are characterized by the volume of some picoliters, which corresponds to the normal range of 18-50 μm . The major negative aspect of the process is that the three-dimensional structures are very fragile and irregular, deficient hardness, unconvinced resolution finish, and low drug loadings. The unbound powder serves as a supporting material during the process and is removed after the forgery [19,34,36].

3. Continuous inkjet printing (CIJ):-

CIJ printing uses a pressure stream to generate a continuous flow of drops. The droplets are taken after exiting the nozzle and are directed to the substrate or the waste again by electrostatic plates [37,38].

2.Nozzle-based deposition systems: -

Technologies are ever evolving and new technologies are continuously developed to overcome limitations of previous ones [39]. The nozzle-based deposition method consists of a combination of drugs and polymers and other solid materials prior to 3D printing. Nozzle-based deposition systems permit direct writing, which is based on computer-controlled production methods that ink through the nozzle to create a 3D pattern layer-bilayer with controlled structure and architecture. Such systems can be divided into processes based on content melting and non- melting processes. There are two types of printing, depending on the kind of material use: fused deposition modeling, which uses dissolved components, and pressure-assisted micro syringes, which do not use dissolved materials.

1. Fused deposition modeling:

In Fused deposition modeling process, the copy or part is usually produced by extruding slim 200-400 μm threads of polymer-based matter that alleviate immediately to structure a solid layer [20]. Process has limitation of various shapes that can be fabricated. Yet, using a detachable hold up structure, any form can be constructed. These thin supports are added without human intervention to the model throughout processing and can be broken down during the finishing procedure.

2. Pressure-assisted micro-syringes (PAM):

This technique uses a syringe extruder for oily and semi-liquid material deposition according to the geometry design. Viscosity, apparent elastic limit and viscoelasticity, are the root parameters that establish the fertility of this technology. It has the potential to work continuously with an oven and at room temperature. Solvents used can be sometimes toxic to health and may cause stability problem in certain APIs. Tissue printing substitutes or soft tissue scaffolds, as well as multifaceted medicine delivery systems are its key applications [19, 34].

3. Stereolithography:

In stereolithographic printing, a laser is used to photo polymerize a resin. Stereo Lithography converts liquid polymer resins and composites into solid layers using photo-curing UV blue light [17]. This technology produces high-quality components for biomedical applications or gears with integrated moving components and complex nanocomposites.

BIOLOGICAL APPLICATIONS/ MEDICAL APPLICATION FOR 3D PRINTING:-

Additive manufacturing was used to design and manufacture lightweight machines for various purposes like parts of rocket, plane, formula one car [40, 41]. In the early 2000s, the expertise was first used to create dental implants and custom prosthetics [4, 34]. After that, medical applications of 3D printing have advanced extensively. Recently published reviews tell the use of 3D printing intended for skeleton, ears, exoskeleton, windpipes, stem cells, jawbones, spectacles, vascular network, cell culture, blood vessels, organs and tissues, novel dosage forms, and drug delivery devices [42]. Additive manufacturing have been extensively used as a tool for bioengineered tissue, varying in composition from bone and tooth to vascular and organ sca olding. However, in some cases the required scaffolds area is so large that autogenous tissue sampling is not possible for the patient [36]. 3D printing has become an attractive booth for the development of biological material that is reproducible. Table 1 shows the various biological applications of 3D printing.

Table 1: Biological applications of 3D printing

Tissue Engineering	The current treatment for organ failure is largely based on organ transplantation of live or else deceased donors. On the other hand, present is a stretched scarcity of human organs obtainable for transplantation [43]. Researchers are working on methods to grow complete human organs, which can be used, for selection purposes at some stage in drug discovery [4, 32]. 3D bioprinting have been doing well in produce knee meniscus, heart valves, artificial ears as well as the manufacture of custom-made barrier absorbable trachea, which has already been implanted in neonates with tracheobronchomalacia [34, 44].
Customized Implants and Prostheses	Planting and prosthesis can be made in almost any conceivable geometry by translating X-ray, MRI or CT scan digital.stl 3D print documents. 3D printing is productively used in the health care, both standard and complex, used for surgical implant and prostheses, sometimes within 24 hours [4]. Used for fabricating dental, spinal, and hip implants.
Surgical Anatomical Models	3D Printed neuro anatomical providing can be especially helpful for neurosurgeons by introducing some of the most complex structures in the human body. A real model, modeling the relationship between lesions with regular brain structure, can help determine the safest surgical corridors and may be useful for rehearsing challenging cases for neurosurgeons. Multipart spinal deformity can be better studied using the 3D model. Models for colonoscopy and liver transplant studies have been designed in USA and Japan, respectively. Polypeptide chain models with secondary folds structures were designed by inclusion of bond rotating barriers.
Aesthetic Surgery	In the future, using a three-dimensional printed model will be able to print personalized breast implants to suit any patient's anatomy and personal needs. Not only the shape but also the implant's design can be adjusted, giving the breast a more natural appearance and a natural experience.
Hand Surgery	Recently, customized three-dimensionally printed prostheses have emerged, and various commercial companies offer personalized three-dimensionally printed finger, hand, and arm prosthetics. It is now doable to order a 3D printed finger or arm prosthetic for only \$20 to \$50. Print biomimetic prosthetics combined with diverse neurons layers may probably make prosthetic limbs a entirely functional piece of the body.
Treatment of Burn Wounds	Researchers at the Wake Forrest Institute of Regenerative Medicine used this method to bioprint amniotic fluid-derived stem cells and skin cells directly onto wounds and burn defects. The escalating speed and resolution of three-dimensional bioprinters, this approach may develop into viable for the in vivo regeneration of tissues straight away after injury or during surgery.

PHARMACEUTICAL APPLICATIONS: -

1. Commercially existing 3D Printed Drugs:

The FDA granted approval to the antiepileptic API, the first 3D printed drug-containing levetiracetam, Spritam® (Aprecia Pharmaceuticals, East Windsor, NJ, USA). Pharmacological effectiveness was found to be analogous conventional tablets, but porous and soluble matrix composition led to improved dissolution [34]. Also used for tablets with immediate-release, monolithic sustained-release, pulsatile drug release, biphasic release, fast-disintegrating, enteric release, and zero-order release, orodispersible films, floating drug delivery system (FDDS), multi-active solid dosage forms, and nanocapsule formulation [39].

2. Personalized Topical Treatment Device

Nose-shaped masks for acne treatment filled with salicylic acid have been developed efficiently. Here, facial scan of patient was exported to the program, after which the section was selected. The most promising technique was for mask manufacturing, allowing high drug loading for the significant conductivity of salicylic acid during 3D printing [34].

3. 3D printing of transdermal delivery systems

To avoid first-pass metabolism and/or pH mediated degeneration or ease of administration for patients with chronic illnesses such as diabetes, transdermal delivery systems may be beneficial. Layer-by-layer 3D printing technology can with no trouble used for the foundation of multifaceted transdermal patches of films. 3D technology offers the unique advantage of printing drug-filled microneedles for transdermal delivery. Microneedles are usually less than 500 µm in height and are meant to penetrate the stratum corneum (10-15 µm) to deliver active agents [12]. SL was used to produce microneedles of biodegradable polymer (methyl vinyl ether-alt-maleic anhydride). To coat a quantum dotted needle as a model active agent inkjet printing can be used.

SUMMARY OF RESEARCH CARRIED OUT USING 3D PRINTING FOR DOSAGE FORM DEVELOPMENT

Variety of research has been carried out on dosage form development ranging from controlled release profile of drug to immediate release solid dispersions. Table 2 summarizes various research reported and their outcome to guide further course of research in future.

Table 2: Studies of 3D printing for use in drug formulation development:

The 3D technique (equipment)	API and/or Dosage form	Application/Remark	Reference
Selective laser sintering and fused deposition modeling or UV curing of resin as in stereolithography	Captopril, Nifedipine Glipizide	3D extrusion-based printing was used as a drug product technology. It was used to produce a multi-active tablet with well-defined and separate controlled release profile, for three different drugs.	[45]
FDM (fused deposition *Modeling)	Metronidazole	Printed 3D printed tablet, which has a hole of 2.0 mm, air volume of 132 mm ³ , is released zero-order drug. In this research, indicate That has promised in the	[47]

		development of the existing 3D printing tablet housing platform Floating drug delivery systems.	
The desktop extrusion-based 3D printer (Fab@Home)	Guaifenesin	This research was a noteworthy step towards the revelation and validation of easy, low-cost 3D printing for the adapted manufacture of medicines, with the impending possibility to play a decisive role in future developments, both in personalized care and treatment.	[48]
RegenHU 3D printer(3D based extrusion)	Ramipril, pravastatin sodium, Atenolol, aspirin, and hydrochlorothiazide	Demonstrate 5 drugs in one tablet (polypill) in one tablet, immediate and sustained release, shun incompatibility of drug, no detection of interaction.	[49]
Fused deposition Modeling (FDM) 3D printing and Hot Melt Extrusion (HME)	Theophylline	FDM-based 3D printing proved compatible with the drug load filament produced by HME.	[50]
3DP	Chlorpheniramine maleate, Diclofenac sodium	3DP technology different release mechanism (erosion, diffusion), Pulsatory devices fabrication one pulse generate in stomach and second pulse generate in the intestine. 3DP techniques used for fabricating pulsatile release fabrication.	[51]
Thermal Ink-Jet (TIJ) Printing	Salbutamol Sulphate	Salbutamol Sulphate used as a model drug and treatment of Asthma in pediatric patient. TIJ printing makes it possible to personalized dose as per patient age, body surface area and sex.	[52]
Inkjet printing	Riboflavin sodium phosphate, propranolol hydrochloride	Inkjet-printed solid dose forms showed excellent content Consistency for both APIs. Also used for water-insoluble and oxygen labile drug and increase the stability of the drug.	[53]

FDM 3DP	Paracetamol	Five diverse shaped tablets were printed - pyramid, cube, sphere, cylinder, and torus. Here, it was concluded that drug release was dependant on surface area to volume ratio rather than simply on surface area and there comes the role of geometric shape.	[54]
Inkjet printing	Rifampicin	Antibiotic and calcium eluting micropatterns were revealed as fresh means of prevention. Microfluidic motile cultures were used. Rifampicin absolutely kills the ability of the micropattern to have as an effective means of preventing biofilm colony. <i>S. Epidermidis</i> composition is an effective means of preventing biofilm colony development.	[55]
Inkjet printing	Levofloxacin(LVFX)	A 3D printing process that yields a dual-model profile i.e., pulsatile and sustains release from an implant was developed.	[56]
Hot-melt 3D inkjet printing	Fenofibrate	Higher spatial resolution is achieved by the formulation testifies to and benefits from very small volumes of ink (picoliters). Accurate dose is be very desirable when managing Chronic illnesses like hypertension and anti-depression for maximum therapeutic reasons.	[57]
Piezoelectric inkjet printing	Paclitaxel (PTX)	PTX loaded PLGA microparticles with different geometries display different drugs release rate mainly due to different surface areas to volume ratio. The release rate was a downward rate categorized as honeycomb > grid, ring > circle.	[58]

Extrusion printing	dexamethasone-21-phosphate disodium salt (Dex21P)	The printed 3-dimensional compositions are represented by the spatial distribution of the drug. Two types of drug encapsulation designs (rolled and sealed as well as layer-by-layer) were successfully fabricated using printing technology.	[59]
ZMorph® 3D printer(co-extrusion based 3D printing)	Aripiprazole	The underlying principle of this research was to estimate the value of dual co-extrusion fluid- loaded soluble free filament and insoluble drug-free with 3D printed tablet with aripiprazole (ARP) assigned to BCS class II. The synchronized co-extrusion of drug-free filament was chosen because feedstock material demonstrates a promising approach to be a viable preparation method for prints with modified release.	[60]
Fused Deposition Modeling (a.k.a. FDM-3D printing)	Metformin and glimepiride	Formulated bilayer tablet dosage form encloses two anti-diabetic drugs having different daily dosage regimens. It is desirable to include added more than one API into the formulation, as it increase patient fulfillment and reduce the cost of treatment, especially when different doses of API are tailored to the explicit requirements of each patient, provided by printing.	[61]
Dual extrusion fused deposition modeling	Pantoprazole sodium	The model drug used different printing plans for tablets with the acid- and thermo-labile drug pantoprazole sodium were evaluated for various characteristics. The acetate phthalate bottom and the almost insoluble polycaprolactone at the top are printed only at 58 °C. Coated tablets with a thermo-labile API were successfully implemented	[62]

		showing no visible signs of thermal degradation.	
Hot melt ram extruder 3D printers	Paracetamol	Paracetamol used as the model drug in Orodispersible film (ODF). This work describes a novel approach to print ODF intended for adapted therapy. This should be the uniformity of the drug amount per unit of medicinal products Goals for the benefit of patients can be certain.	[63]
3DP	Paracetamol	3DP technology development of new oral fast- disintegrating dosage form devices. The porosity of the pellets is inversely related to the compressive pressure. However, high compression pressure is needed to ensure sufficient strength of the tablet. 3DP has some advantages over traditional compression techniques for the manufacture of solid dosage forms and can grant inventive strategies for the design, development, production, and commercialization of many types of solid dosage forms.	[64]
3DP	Acetaminophen	Desired drug release in conventional manufacture techniques requires multistep process different materials used in the different processes and unfriendly effect on accuracy repeatability. Desired release profile tablet formulated in single easy step. Also powerful way to compete with controlled-release tablets formulating.	[65]

3-DPT TM Technology	Pseudoephedrine hydrochloride (PEH)	Primary difficulties in maintaining a constant release rate include initial dose explosion, loss of driving force to maintain target release rate over the desired period, and premature changes in its properties due to the length of the drug release path. Prepare the near zero-order release of water-soluble drug by this technology. These techniques produce products insensitive to both changes in pH and hydrodynamic stress of the dissolution medium.	[66]
Inkjet printing	Felodipine	Felodipine is poorly water-soluble anti-hypertensive drug and bioavailability and dissolution is poor, inkjet printing able to produce droplet size in picoliters so adverse/side effect is reduced. This technology used to prepare the solid dispersion to boost the dissolution profile.	[67]
3DP technology	Fenofibrate (FEN) and Cinnarizine (CINN)	Fenofibrate (FEN) and cinnarizine (CINN) are used as the model drug for the preparation of solid self-emulsifying drug delivery systems (SSMEDDS) with defined surface area to volume (SA/V) ratios. Drugs selection was based on their poor water solubility and their broad use as lipophilic compounds in a variety of studies with lipid-based drug formulations. These formulations controlled three-dimensional geometry without a solid-phase carrier. The dispersal kinetics of the drug-filled S-SMEDDS formulation showed a clear dependence on the SA / V ratio values, showing the effect of geometric shaping on the dispersion time.	[68]

HME FDM	Haloperidol	In 3D printed tablet drug in amorphous state and drug, release is faster and immediate. Potential delivery of medicine avoidance of side effects by personalized delivery, 3D printed tablets prepared by fused deposition modeling with the aim of would afford comparatively rapid drug release.	[69]
---------	-------------	--	------

FUTURE TRENDS: -

3D printing is anticipated to execute a significant role in the attitude towards individual medicine, the use of customize dietary foodstuffs, drugs and organs. Pharmaceutical API/dosage forms could be made-up on demand. Drug manufacturing and distribution will be more cost effective. 3D printing in fabricating the complex organ and prosthetics for the individual patient will surely help healthcare system. Pharmaceutical industry, like aerospace, could use the complex designed equipment for manufacturing processes. The advances in the programmed bioprinters and robot-assisted surgical treatment may also be fundamental in the direction of the development of this technology. There are challenges but a promising progress is continuing.

CONCLUSION: -

Our well-thought-out review summarizes the accessible literature on current techniques designed for pharmaceutical manufacturing and dosage form development. Useful individual/personalized drug delivery for the narrow therapeutic window drug in 3D printing technology printing in the picoliters and reduce the adverse effect or side effect of the API for pediatrics and geriatrics. 3D printed fabrication of the products with complex release profile and personalized delivery. Effect of formulation geometry on release rate was studied which gives a way and idea to study other factors using printing technology produced dosage forms.

REFERENCE:

1. Perrot A. 3D Printing in Concrete: General Considerations and Technologies. In: Perrot A, Amziane S, editors. 3D Printing in Concrete, London and New Jersey: ISTE Ltd and John Wiley & Sons, Inc; 2019, p. 1–40. <https://doi.org/10.1002/9781119610755.ch1>
2. Candi M, Beltagui A. Effective use of 3D printing in the innovation process. *Technovation* 2019; 80–81: 63–73. <https://doi.org/10.1016/j.technovation.2018.05.002>
3. Rengier F, Mehndiratta A, Tengg-Kobligk H, Zechmann C M, Unterhinninghofen R, Kauczor HU, Giesel F L. 3D printing based on imaging data: review of medical applications. *Int J CARS* 2010;5: 335–341. <https://doi.org/10.1007/s11548-010-0476-x>
4. Ventola CL. Medical applications for 3D printing: current and projected uses. *Pharmacy and Therapeutics* 2014;39(10):704..
5. Kalaskar DM. 3D printed pharmaceutical products. In: Gaisford S, editor. 3D Printing in Medicine. Duxford: Woodhead publishing, 2017; p. 155–166. <https://doi.org/10.1016/B978-0-08-100717-4.00007-7>
6. Kamali P, Dean D, Skoracki R, Koolen PGL, Paul MA, Ibrahim AMS, Lin SJ. The Current Role of Three-Dimensional Printing in Plastic Surgery. *Plast Reconstr Surg* 2016;137(3): 1045–1055. <https://doi.org/10.1097/01.prs.0000479977.37428.8e>
7. Norman J, Madurawe RD, Moore CMV, Khan MA, Khairuzzaman A. A new chapter in pharmaceutical manufacturing : 3D-printed drug products. *Adv Drug Deliv Rev* 2017;108: 39– 50. <https://doi.org/10.1016/j.addr.2016.03.001>

8. Souto EB, Campos JC, Filho SC, Teixeira MC, Martins-Gomes C, Zielinska A, Carbone C, Silva AM. 3D printing in the design of pharmaceutical dosage forms. *Pharm Dev Technol* 2019;24(8):1044–1053. <https://doi.org/10.1080/10837450.2019.1630426>
9. Izdebska J, Thoma S. 3-D Printing. In: Thomas DJ, Claypole TC, editors. *Printing on Polymers: Fundamentals and applications*, Oxford: William Andrew; 2016, p.293–306. <https://doi.org/10.1016/B978-0-323-37468-2.00018-X>
10. Panesar SS, Belo JTA, D'Souza RN. Feasibility of Clinician-Facilitated Three-Dimensional Printing of Synthetic Cranioplasty Flaps. *World Neurosurg* 2018;113: e628–e637. <https://doi.org/10.1016/j.wneu.2018.02.111>
11. Ursan I, Chiu L, Pierce A. Three-dimensional drug printing : A structured review. *JAPhA* 2013; 53(2):136-144. <https://doi.org/10.1331/JAPhA.2013.12217>
12. Prasad LK, Smyth H. 3D Printing technologies for drug delivery : a review. *Drug Dev Ind Pharm* 2016; 42(7): 1019–1031. <https://doi.org/10.3109/03639045.2015.1120743>
13. Fink JK. *3D Industrial Printing with Polymers*, 1st ed. : John Wiley & Sons Inc: 2019. <https://doi.org/10.1002/9781119555308.ch6>
14. Ngo TD, Kashani A, Imbalzano G, Nguyen KTQ, Hui D. Additive manufacturing (3D printing A review of materials, methods, applications and challenges. *Compos Part B-Eng* 2018; 143: 172–196. <https://doi.org/10.1016/j.compositesb.2018.02.012>
15. Deckard CR. Method and apparatus for producing parts by selective sintering. US4863538, 1989.
16. Sachs EM, Haggerty JS, Cima MJ, Williams PA. Three-dimensional printing techniques. US5204055, 1993.
17. Bradbury TJ, Gaylo CM, Fairweather JA, Chesmel KD, Materna PA, Youssef A. System and method for rapidly customizing design, manufacturing and/or selection of biomedical devices. US6772026B2, 2004.
18. Russell ID, Hernandez A, Kinslly J, Berlin A. Apparatus and methods for 3D printing, US7291002B2, 2007.
19. Goole J, Amighi K. 3D printing in pharmaceuticals: A new tool for designing customized drug delivery systems. *Int J Pharm* 2016; 499(1–2): 376–394. <https://doi.org/10.1016/j.ijpharm.2015.12.071>.
20. Kaufui VW, Aldo H. A Review of Additive Manufacturing. *Int Sch Res Notices* 2012;2012:1- 10. doi:10.5402/2012/208760.
21. Melchels FPW, Feijen J, Grijpma DW. A review on stereolithography and its applications in biomedical engineering. *Biomater* 2010;31(24): 6121–6130. <https://doi.org/10.1016/j.biomaterials.2010.04.050>
22. Manapat JZ, Chen Q, Ye P, Advincula, RC. 3D Printing of Polymer Nanocomposites via Stereolithography. *Macromol Mater Eng* 2017;302(9): 1600553. <https://doi.org/10.1002/mame.201600553>
23. Gibson I, Rosen D, Stucker B. *Additive manufacturing technologies: 3D printing, rapid prototyping, and direct digital manufacturing*, 2nd ed. London: Springer New York Heidelberg Dordrecht; 2015. <https://doi.org/10.1007/978-1-4939-2113-3>
24. Singh R. Process capability study of polyjet printing for plastic components. *J Mech Sci Technol* 2011;25 (4): 1011-1015. <https://doi.org/10.1007/s12206-011-0203-8>
25. Sachs EM. *Three-Dimensional Printing Techniques*, US5340656, 1994. Vehse M, Petersen S, Sternberg K, Schmitz K, Seitz H. Drug Delivery From Poly (ethylene glycol) Diacrylate Scaffolds Produced by DLC Based Micro-Stereolithography. *Macromol Symp* 2014; 346(1):43-47. <https://doi.org/10.1002/masy.201400060>
26. Taylor P, Petrovic V, Vicente J, Gonzalez H, Jordá O, Gordillo JD, Blasco JR, Griñan LP. Additive layered manufacturing : sectors of industrial application shown through case studies. *Int J Prod Res* 2011;49(4):1061-1079. <https://doi.org/10.1080/00207540903479786>
27. Cooper KG. *Rapid Prototyping Technology: Selection and Application*. 1st ed. New York: Marcel Dekker, Inc; 2001.
28. Murr LE, Gaytan SM, Ramirez DA, Martinez E, Hernandez J, Amato KN, Shindo PW, Medina FR, Wicker RB. Invited review metal fabrication by additive manufacturing using laser and electron beam melting technologies. *J Mater Sci Technol* 2012;28(1):1–14. [https://doi.org/10.1016/S1005-0302\(12\)60016-4](https://doi.org/10.1016/S1005-0302(12)60016-4)
29. Murr LE, Gaytan SM, Ceylan A, Martinez E, Martinez JL. Characterization of titanium aluminide alloy components fabricated by additive manufacturing using electron beam melting. *Acta Mater* 2010;58:1887–1894. <https://doi.org/10.1016/j.actamat.2009.11.032>

30. Clint A, Griffith M, Harwell L, Schlienger E, Mark E, John S, Tony R, Don G, Daryl R. Laser engineered net shaping (LENS®): A tool for direct fabrication of metal parts, in: Proceedings of ICALEO '98, vol 85, Orlando, FL, USA, 1998, p E-1.
31. Perrot A. 3D Printing in Concrete: General Considerations and Technologies. In: Perrot A, Amziane S, editors. 3D Printing in Concrete, London and New Jersey: ISTE Ltd and John Wiley & Sons, Inc; 2019, p. 1–40. <https://doi.org/10.1002/9781119610755.ch1>
32. Acosta-vélez GF, Wu BM. 3D pharming: Direct printing of personalized pharmaceutical tablets. *Polymer Sciences* 2016;2(1):1-10. <https://doi.org/10.4172/2471-9935.100011>
33. Hofmeister W, Wert M, Smugeresky J, Philliber JA, Griffith M, Ensz M. Investigating solidification with the laser- engineered net shaping (LENSTM) Process. *JOM* 1999;51(7):1-6.
34. Konta AA, Garc M, Serrano DR. Personalised 3D Printed Medicines : Which Techniques and Polymers Are More Successful?. *Bioeng* 2017;4(79):1-16. <https://doi.org/10.3390/bioengineering4040079>
35. Yamada K, Henares TG, Suzuki K, Citterio D. Paper-based inkjet-printed microfluidic analytical devices. *Angew Chem Int Ed* 2015;54(18):5294-310. <https://doi.org/10.1002/anie.201411508>
36. Gross BC, Erkal JL, Lockwood SY, Che C, Spence DM. Evaluation of 3D printing and its potential impact on biotechnology and the chemical sciences. *Anal Chem* 2014;86(7):3240–3253. <https://doi.org/10.1021/ac403397r>
37. Derby B. Inkjet printing of functional and structural materials: Fluid property requirements, feature stability, and resolution. *Annu Rev Mater Res* 2010;40(1):395–414. <https://doi.org/10.1146/annurev-matsci-070909-104502>
38. Cooley P, Wallace D, Antohe B. Applications of Ink-Jet Printing Technology to BioMEMS and Microfluidic Systems. *JALA* 2002;7(5):33-39. doi:10.1016/S1535-5535(04)00214-X
39. Khatri P, Shah MK, Vora N. Formulation strategies for solid oral dosage form using 3D printing technology : A mini-review. *J Drug Deliv Sci Technol* 2018;46:148–155. <https://doi.org/10.1016/j.jddst.2018.05.009>
40. Bletzinger KU, Ramm E. Structural optimization and form finding of light weight structures. *Comput Struct* 2001;79(22-25):2053–2062. [https://doi.org/10.1016/S0045-7949\(01\)00052-9](https://doi.org/10.1016/S0045-7949(01)00052-9)
41. Milewski JO. Additive manufacturing of metals. From Fundamental Technology to Rocket Nozzles, Medical Implants, and Custom Jewelry,. 2017:134-57. <https://doi.org/10.1007/978-3-319-58205-4>
42. Schubert C, Van Langeveld MC, Donoso LA. Innovations in 3D printing: A 3D overview from optics to organs. *Br J Ophthalmol* 2014;98(2):159–161. <https://doi.org/10.1136/bjophthalmol-2013-304446>
43. Cui X, Boland T, D’Lima D, Lotz M. Thermal inkjet printing in tissue engineering and regenerative medicine. *Recent Pat Drug Deliv Formul* 2012;6(2):149–155. <https://doi.org/10.2174/187221112800672949>
44. Ji S, Guvendiren M. Recent advances in bioink design for 3d bioprinting of tissues and organs. *Front Bioeng Biotechnol* 2017;23(5):1–8. <https://doi.org/10.3389/fbioe.2017.00023>
45. Khaled SA, Burley JC, Alexander MR, Yang J, Roberts CJ. 3D printing of tablets containing multiple drugs with defined release profiles. *Int J Pharm* 2015; 494(2): 643–650. <https://doi.org/10.1016/j.ijpharm.2015.07.067>
46. Katstra WE, Palazzolo RD, Rowe CW, Giritlioglu B, Teung P, Cima MJ. Oral dosage forms fabricated by Three Dimensional Printing™. *J Controlled Release* 2000;66(1):1–9. [https://doi.org/10.1016/S0168-3659\(99\)00225-4](https://doi.org/10.1016/S0168-3659(99)00225-4)
47. Huanbutta K, Sangnim T. Design and development of zero-order drug release gastroretentive floating tablets fabricated by 3D printing technology. *J Drug Deliv Sci Technol* 2019; 52:831-7. <https://doi.org/10.1016/j.jddst.2019.06.004>
48. Khaled SA, Burley JC, Alexander MR, Roberts CJ. Desktop 3D printing of controlled release pharmaceutical bilayer tablets. *Int J Pharm* 2014;461(1-2):105-11. <https://doi.org/10.1016/j.ijpharm.2013.11.021>
49. Khaled SA, Burley JC, Alexander MR, Yang J, Roberts CJ. 3D printing of five-in-one dose combination polypill with defined immediate and sustained release profiles. *J Controlled Release*, 2015;217:308–314. <https://doi.org/10.1016/j.jconrel.2015.09.028>
50. Pietrzak K, Isreb A, Alhnan MA. A flexible-dose dispenser for immediate and extended release 3D printed tablets. *Eur J Pharm Biopharm* 2015;96:380–387. <https://doi.org/10.1016/j.ejpb.2015.07.027>
51. Rowe CW, Katstra WE, Palazzolo RD, Giritlioglu B, Teung P, Cima MJ. Multimechanism oral dosage forms fabricated by three dimensional printing™. *J Controlled Release* 2000;66(1):11-17.

52. Buanz ABM, Saunders MH, Basit AW, Gaisford S. Preparation of personalized-dose salbutamol sulphate oral films with thermal ink-jet printing. *Pharm Res* 2011;28(10):2386–2392. <https://doi.org/10.1007/s11095-011-0450-5>
53. Genina N, Fors D, Vakili H, Ihalainen P, Pohjala L, Ehlers H, Kassamakov I, Haeggström E, Vuorela P, Peltonen J, Sandler N. Tailoring controlled-release oral dosage forms by combining inkjet and flexographic printing techniques. *Eur J Pharm Sci* 2012;47(3):615–623. <https://doi.org/10.1016/j.ejps.2012.07.020>
54. Goyanes A, Robles Martinez P, Buanz A, Basit AW, Gaisford S. Effect of geometry on drug release from 3D printed tablets. *Int J Pharm* 2015; 494(2):657–663. <https://doi.org/10.1016/j.ijpharm.2015.04.069>
55. Gu Y, Chen X, Lee JH, Monteiro DA, Wang H, Lee WY. Inkjet printed antibiotic- and calcium- eluting bioresorbable nanocomposite micropatterns for orthopedic implants. *Acta Biomater*, 2012;8(1):424–431. <https://doi.org/10.1016/j.actbio.2011.08.006>
56. Huang W, Zheng Q, Sun W, Xu H, Yang X. Levofloxacin implants with predefined microstructure fabricated by three-dimensional printing technique. *Int J Pharm* 2007;339(1- 2):33–38. <https://doi.org/10.1016/j.ijpharm.2007.02.021>
57. Kyobula M, Adedeji A, Alexander MR, Saleh E, Wildman R, Ashcroft I, Gellert PR, Roberts CJ. 3D inkjet printing of tablets exploiting bespoke complex geometries for controlled and tuneable drug release. *J. Control. Release* 2017;261:207–215. <https://doi.org/10.1016/j.jconrel.2017.06.025>
58. Lee BK, Yun YH, Choi JS, Choi YC, Kim JD, Cho YW. Fabrication of drug-loaded polymer microparticles with arbitrary geometries using a piezoelectric inkjet printing system. *Int J Pharm* 2012;427:305–310. <https://doi.org/10.1016/j.ijpharm.2012.02.011>
59. Rattanakit P, Moulton SE, Santiago KS, Liawruangrath S, Wallace GG. Extrusion printed polymer structures: A facile and versatile approach to tailored drug delivery platforms. *Int J Pharm* 2012;422:254–263. <https://doi.org/10.1016/j.ijpharm.2011.11.007>
60. Jamróz W, Kurek M, Czech A, Szafraniec J, Gawlak K, Jachowicz R. 3D printing of tablets containing amorphous aripiprazole by filaments co-extrusion. *Eur J Pharm Biopharm* 2018;131:44–47. <https://doi.org/10.1016/j.ejpb.2018.07.017>
61. Gioumouxouzis CI, Baklavaridis A, Katsamenis OL, Markopoulou CK, Bouropoulos N, Tzetzis D, Fatouros DG. A 3D printed bilayer oral solid dosage form combining metformin for prolonged and glimepiride for immediate drug delivery. *Eur J Pharm Sci* 2018;120:40–52. <https://doi.org/10.1016/j.ejps.2018.04.020>
62. Kempin W, Domsta V, Brecht I, Semmling B, Tillmann S, Weitschies W, Seidlitz A. Development of a dual extrusion printing technique for an acid- and thermo-labile drug. *Eur J Pharm Sci* 2018;123:191–198. <https://doi.org/10.1016/j.ejps.2018.07.041>
63. Musazzi UM, Selmin F, Ortenzi MA, Mohammed GK, Franzé S, Minghetti P, Cilirzo F. Personalized orodispersible films by hot melt ram extrusion 3D printing. *Int J Pharm* 2018;551(1-2):52–59. <https://doi.org/10.1016/j.ijpharm.2018.09.013>
64. Yu DG, Shen XX, Branford-White C, Zhu LM, White K, Yang XL. Novel oral fast- disintegrating drug delivery devices with predefined inner structure fabricated by Three- Dimensional Printing. *J Pharm Pharmacol* 2009;61(3):323–329. <https://doi.org/10.1211/jpp/61.03.0006>
65. Yu DG, Branford-White C, Yang YC, Zhu LM, Welbeck EW, Yang XL. A novel fast disintegrating tablet fabricated by three-dimensional printing. *Drug Dev Ind Pharm* 2009. 35(12), 1530–1536. <https://doi.org/10.3109/03639040903059359>
66. Wang CC, Tejwani MR, Roach WJ, Kay JL, Yoo J, Surprenant HL, Monkhouse DC, Pryor TJ. Development of near zero-order release dosage forms using three-dimensional printing (3-DP™) technology. *Drug Dev Ind Pharm* 2006;32(3):367–376. <https://doi.org/10.1080/03639040500519300>
67. Scoutaris N, Alexander MR, Gellert PR, Roberts CJ. Inkjet printing as a novel medicine formulation technique. *J Controlled Release* 2011;156(2):179–185. <https://doi.org/10.1016/j.jconrel.2011.07.033>
68. Vithani K, Goyanes A, Jannin V, Basit AW, Gaisford S, Boyd BJ. A proof of concept for 3D printing of solid lipid-based formulations of poorly water-soluble drugs to control formulation dispersion kinetics. *Pharm Res* 2019;36(7):102. <https://doi.org/10.1007/s11095-019-2639-y>
69. Solanki NG, Tahsin M, Shah AV, Serajuddin ATM. Formulation of 3D Printed Tablet for Rapid Drug Release by Fused Deposition Modeling: Screening Polymers for Drug Release, Drug- Polymer Miscibility and Printability. *J. Pharm. Sci.* 2018; 107(1):390–401. <https://doi.org/10.1016/j.xphs.2017.10.021>

PCP394

AUGUMENTED REALITY AND VIRTUAL REALITY IN PHARMACEUTICAL INDUSTRY

AP0385	AP0384	AP0	AP0188
Ravin Malam	Dishita Parmar	Dr. D. M. Patel	Dr. Sanjay Chauhan
M. Pharm	M. Pharm	Associate	Director
Graduate School of	Graduate School of	Professor	Graduate School of
Pharmacy	Pharmacy	Graduate School	Pharmacy
Ravinmalam786@g	Dishitaparmar54@g	of Pharmacy	Prof_sanjay_chauhan
mai.com	mail.com	asso_dmpatel@gt	@gtu.ed.in
		u.edu.in	

Abstract

Immersive technologies that combine virtual and real-world components are virtual reality and augmented reality. These technologies have helped and enhanced human skills in a variety of areas. There are several medical applications for virtual and augmented reality systems. They work well in the majority of patient therapy and medical procedure phases. Therefore, the goal of this study is to evaluate and rate the many uses of virtual and augmented reality in the field of pharmaceutical. A new technique called augmented reality (AR) involves superimposing computer visuals on the actual environment. A large pharmaceutical firm used augmented reality to boost production and decrease mistakes. Virtual reality (VR) is a simulation of reality in which users are immersed in a synthetic or virtual environment that doesn't actually exist but gives the impression that it does. VR technology was first applied to video games, but it is now utilised in a variety of industries, including pharmaceutical industry. The main objective of this review is to shed light on the applications of VR in pharmaceutical industry to discuss some applications showing how the pharmaceutical field has already started reaping the benefits of VR.

Keywords: Augmented Reality, Virtual Reality, Medicine, Pharmaceutical industry.

PCP401

FORMULATION AND EVALUATION OF FLOATING MICROBALLOONS OF ALLOPURINOL

AP0398

Prachi Gohil

M. Pharm Student

Pioneer Pharmacy Degree College, Vadodara

prachigohil2@gmail.com

Abstract:

To formulate physically and chemically sustained release formulation of allopurinol by using a gastro retentive drug delivery system with the floating approach. Sustained release floating microballoons containing allopurinol was formulated by solvent evaporation method with sustained release polymer, DCM and ethanol as organic solvents and tween 80 as a processing medium by using 3² factorial designs. The independent factors were concentration of Eudragit RS 100 and tween 80 whereas dependent factors were % entrapment efficiency and % drug release. The prepared batches were evaluated for particle size, % entrapment efficiency, drug loading, floating time, total floating time and in-vitro drug release. During experiment the concentration of polymer increases shows decrease in entrapment, drug release and also affect the floating property. Thus, in moderate concentration of polymer shows excellent result of % entrapment efficiency, % drug release, floating property and sustained drug delivery. Evaluations were performed for optimized batch (B3) shows 1.04 seconds floating time, 97.45% drug entrapment efficiency, 98.19% drug release at 12 hours and total floating time up to 12hours. The sustained release floating microballoons system is a promising novel drug delivery system for the treatment of gout using allopurinol as a drug. This system is used because it enhances the floating behavior at upper part of GIT as microballoons have low density and hollow space, also the drug has solubility on upperpart of GIT.

Keywords: Floating, microparticulate, hollow sphere, allopurinol

1. INTRODUCTION

Floating drug delivery systems are low density systems that have abundant buoyancy to float over gastric content and remain in the stomach for a prolonged period. The systems float over to the gastric contents, and the drug is released slowly at the desired rate, which results in increased gastro retention time and reduces the fluctuation. Microballoons (hollow microspheres) is the multiunit floating system which are spherical empty particles without a core. These microballoons are characteristically free flowing powder. It consists of proteins or a synthetic materials and ideally having size less than 200 micrometer. Microballoons are considered as one of the most promising buoyancy systems, as they possess the unique merits of multiple unit system as well as better floating properties because of the central hollow space inside the microsphere.

Allopurinol was first reported in 1965 synthesized by Roland k. Robins. It is used in the treatment of gout. Gout is the purine metabolism disorder resulting from an excess uric acid present in the blood stream. Allopurinol reduces the production of uric acid in our body. It is potent xanthine oxidase inhibitor. It is BCS class I drug has high aqueous solubility and permeability.

2. METHOD OF PREPARATION

Microballoons were prepared by using solvent evaporation method. Allopurinol and Eudragit RS100 in different ratio were dissolved in mixture of dichloromethane and ethanol (1:1) in a beaker. The above mixture was poured in the water containing surfactant (Tween 80) solution at a room temperature while stirred on magnetic stirrer at 300rpm agitation speed and volatile

solvent was allowed to be evaporated. The obtained microballoons was filtered and washed with distilled water and dried at 40° C.

Table 1: Composition of floating microballoons of allopurinol

Batch	Allopurinol (mg)	Eudragit RS 100 (mg) X1	Tween 80 (%) X2	DCM : Ethanol	Distilled water (ml)
B1	100	75	0.05	1:1	200
B2	100	75	0.1	1:1	200
B3	100	75	0.15	1:1	200
B4	100	100	0.05	1:1	200
B5	100	100	0.1	1:1	200
B6	100	100	0.15	1:1	200
B7	100	125	0.05	1:1	200
B8	100	125	0.1	1:1	200
B9	100	125	0.15	1:1	200

3. EVALUATION OF FLOATING MICROBALLOONS

3.1 Production yield

The production yield of the microparticles was determined by accurately calculating the initial weight of the raw materials and the last weight of the microballoons obtained.

3.2 Loading efficiency

The loading efficiency (%) of the microballoons was calculated according to the following equation:

$$\text{Loading Efficiency} = \frac{\text{Amount of drug in microballoons}}{\text{Weight of Microballoons}} \times 100$$

3.3 Drug entrapment efficiency (DEE)

The amount of drug was estimated by crushing the microballoons equivalent to 100mg of allopurinol and extracting with aliquots of 0.1 N HCl repeatedly. The extract was further transferred in to a 100 ml volumetric flask and the volume was made up using 0.1 N HCl. The solution was filtered and absorbance was measured by the spectrophotometer against the appropriate blank. The amount of drug entrapped in microballoons was calculated by;

$$\text{DEE} = \left(\frac{\text{Amount of drug actually present}}{\text{Theoretical drug load expected}} \right) \times 100$$

3.4 Floating lag time:

The 100 mg of floating microballoons were placed in the 100 ml of 0.1N HCl and is raised to upper of the beaker. The duration of time was noted.

3.5 Buoyancy time (total floating time):

100 mg microballoons were dispersed in 0.1 N HCl solution containing Tween 80 (0.1 w/v %) to stimulate gastric fluid and the mixture was stirred with a paddle at 75 rpm. After 12 hours, the layer of the buoyant particles was pipette out and the floating particles were separated by filtration and particles in sinking particulate layer were separated by filtration. Both particles were dried overnight and each weight was measured and buoyancy was determined by the weight ratio of the floating particles to the sum of floating and sinking particles.

$$\text{Buoyancy (\%)} = \frac{Q_f}{Q_f + Q_s} \times 100$$

Where Q_f and Q_s are the masses of floating and settled microballoons.

3.6 In-vitro drug release study

In vitro release study was carried out by taking microballoons equivalent to 100 mg of allopurinol in capsules in basket type dissolution apparatus. Dissolution study was carried out in pH 1.2 dissolution media for 12 hrs at 37 °C. Allopurinol amount in withdrawn samples was determined by spectrophotometrically at λ_{\max} 250nm.

3.7 SEM analysis

The surface structure of microballoons was examined using scanning electron microscopy (SEM- JSM 5610 LV) technique. The prepared microballoons were coated with gold palladium under an argon atmosphere at room temperature, and then SEM images were recorded at the required magnification.

3.8 Kinetic data analysis

The mathematical models were used to evaluate the kinetics and mechanism of drug release from the tablets. The model that best fits the release data was selected based on the correlation coefficient (r) value in various models the model that gives high r² value was considered as the best fit of the release data.

4. RESULT AND DISCUSSION

Table 2: Evaluation of floating microballoons of allopurinol

Batch	Mean Size ($\mu\text{m} \pm \text{S.D.}$, n=3)	Production Yield (%)	Entrapment Efficiency (% \pm S.D., n=3)	Drug Loading (% \pm S.D., n=3)	Floating time (sec) (\pm S.D., n=3)	Total floating time (hrs) (\pm S.D., n=3)
B1	193.66 \pm 0.06	84.08 \pm 0.01	95.14 \pm 0.01	83.14 \pm 0.05	1.33 \pm 0.04	>12
B2	195.94 \pm 0.02	93.17 \pm 0.05	91.78 \pm 0.04	79.91 \pm 0.08	2.00 \pm 0.12	>12
B3	191.47 \pm 0.07	98.23 \pm 0.07	97.45 \pm 0.03	92.57 \pm 0.07	1.04 \pm 0.05	>12
B4	192.07 \pm 0.01	85.31 \pm 0.15	96.32 \pm 0.08	90.43 \pm 0.06	2.56 \pm 0.09	>12
B5	194.84 \pm 0.01	94.23 \pm 0.09	91.45 \pm 0.07	77.09 \pm 0.09	1.81 \pm 0.01	>12
B6	195.85 \pm 0.08	95.45 \pm 0.11	89.14 \pm 0.04	68.37 \pm 0.03	2.00 \pm 0.03	>12
B7	194.98 \pm 0.07	90.45 \pm 0.06	92.08 \pm 0.05	85.57 \pm 0.01	2.55 \pm 0.01	>12
B8	197.85 \pm 0.05	95.98 \pm 0.03	81.45 \pm 0.02	73.38 \pm 0.02	2.00 \pm 0.41	>12
B9	198.62 \pm 0.04	97.15 \pm 0.10	73.65 \pm 0.09	60.07 \pm 0.04	3.30 \pm 0.22	>12

Figure no 1: In vitro drug release of B1-B3

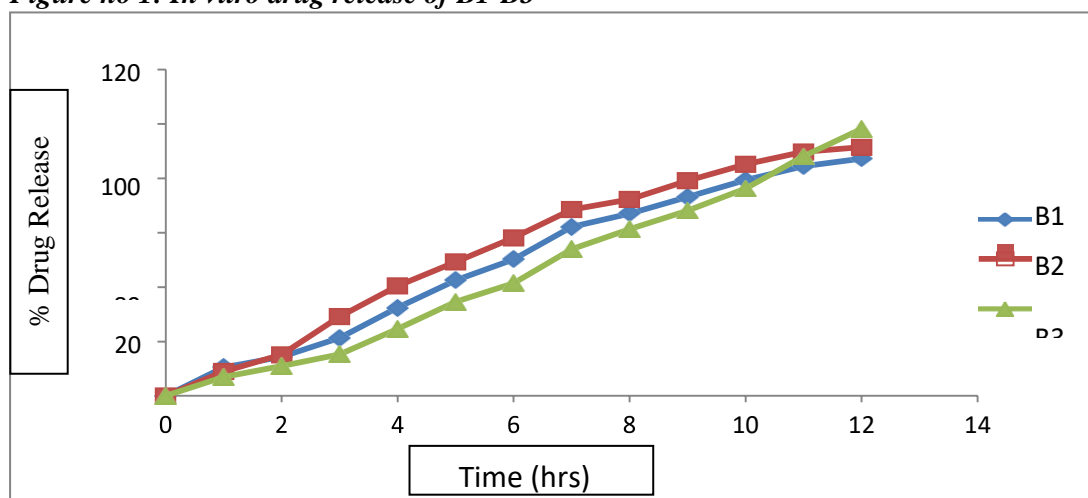


Figure no 2: In vitro drug release of B4-B6

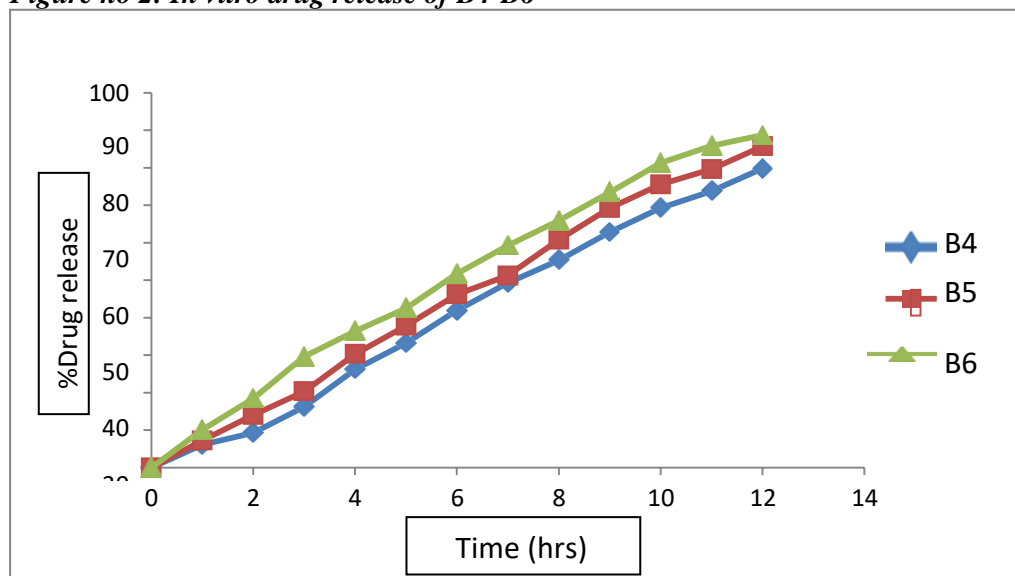


Figure no 3: In vitro drug release of B7-B9

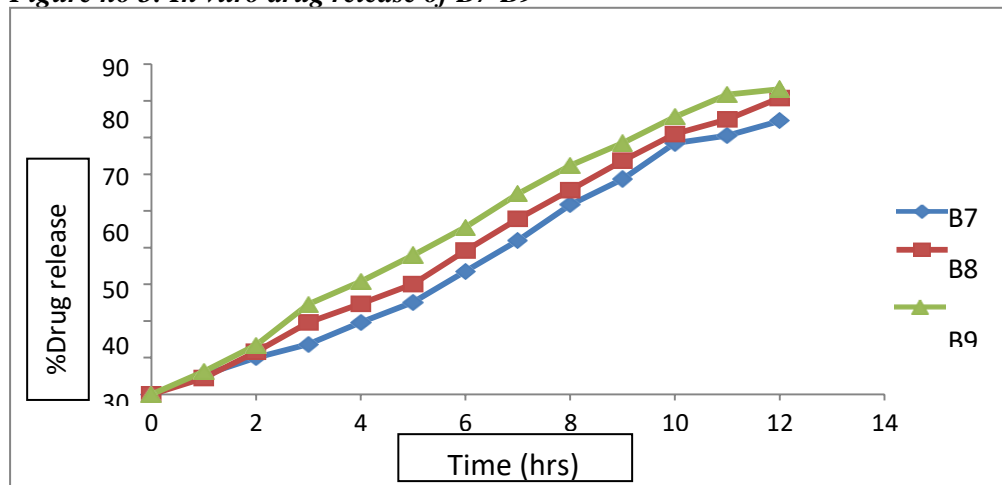
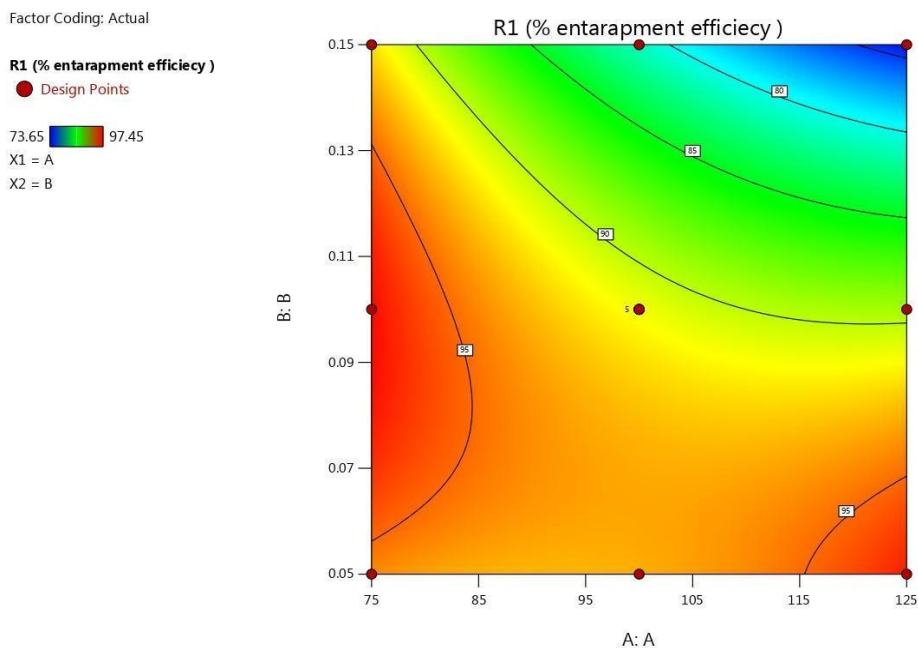


Figure no 4: Contour plot showing the effect of Eudragit RS 100 (X1) and Tween 80 (X2) on response Y1 (% Entrapment efficiency)



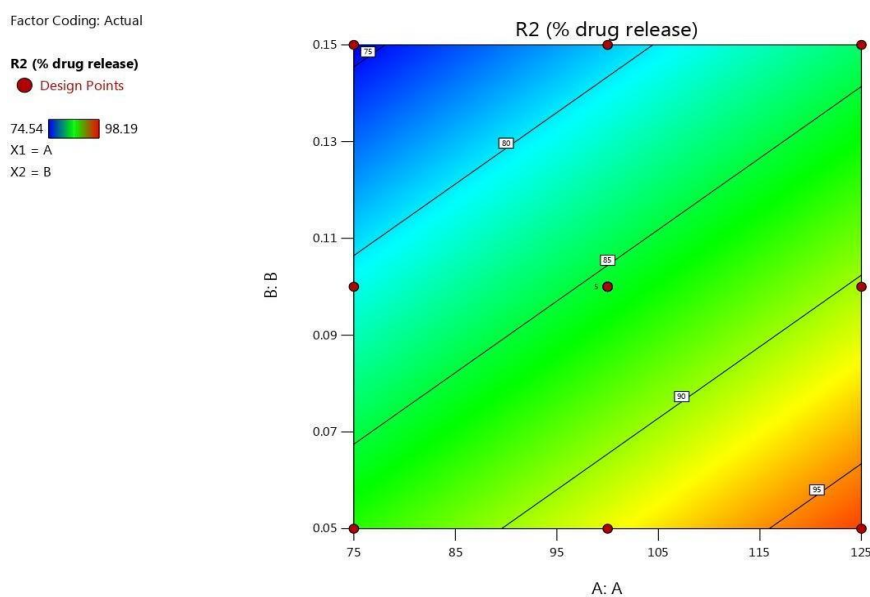
Final equation in term of coded factors

$$\text{Entrapment efficiency} = +91.22 - 6.20 * A - 3.88 * B - 5.18 * AB - 4.20 * A^2 + 2.90 * B^2$$

Final equation in term of actual factors

$$\text{Entrapment efficiency} = +91.21759 - 6.19833 * A - 3.88333 * B - 5.18500 \text{ concentration of Eudragit RS 100 and tween 80} - 4.02155 * A^2 + 2.0945 * B^2$$

Figure no 5: Contour plot showing the effect of Eudragit RS 100 (X1) and Tween 80(X2) on response Y2 (% Drug release) at 12 hours



Final equation in term of coded factors

$$\% \text{ Drug release} = +85.59 - 6.41 * A + 4.74 * B$$

Final equation in term of actual factors

$$\% \text{ Drug release} = +85.59000 - 6.41333 \text{ concentration of Eudragit RS 100} + 4.74167 \text{ concentration of tween 80}$$

Figure no 6: Response surface plot showing the effect of Eudragit RS 100 (X1) and Tween 80 (X2) on response Y1 (% Entrapment Efficiency)

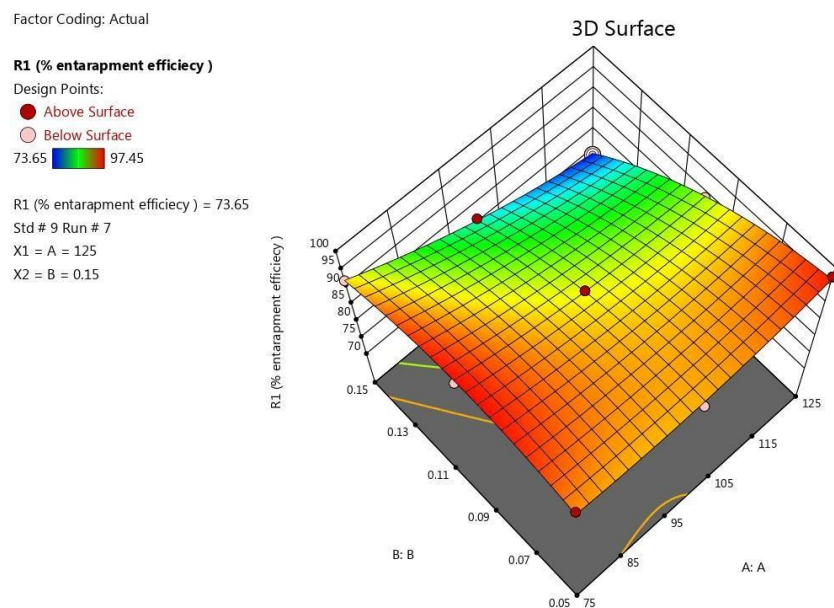


Figure no 7: Response surface plot showing the effect of Eudragit RS 100 (X1) and Tween 80 (X2) on response Y2 (%drug release)

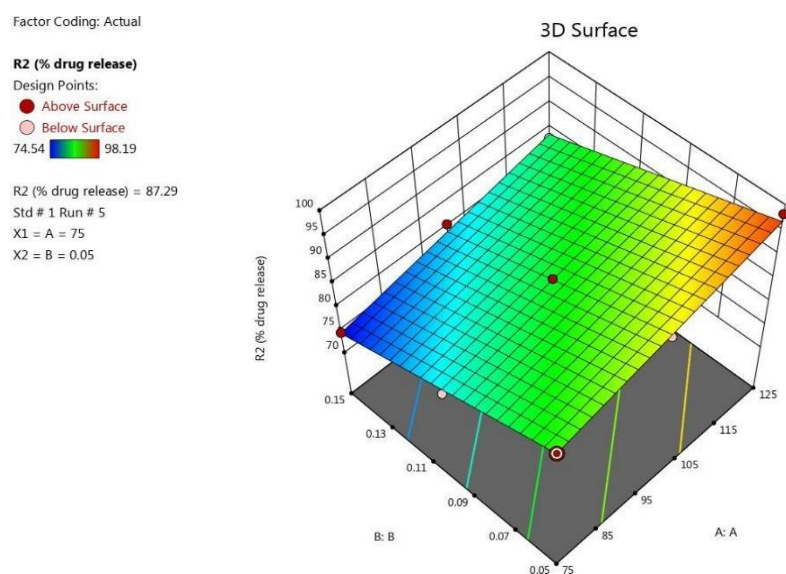


Figure no 8: SEM image of floating microballoons of allopurinol



Figure no 9: SEM image of floating microballoons of allopurinol



The morphology of Allopurinol loaded microballoon prepared by solvent evaporation method was investigated by SEM studies. The images showed that prepared microballoon were nearly spherical. Closer view of a microballoon revealed characteristics hollow on surface.

Table no 3: Release kinetics model of Floating Microballoons of allopurinol

Batch	Zero order	Higuchi model	First order	Hixon- Crowell Model	Peppas model
B3	0.9929	0.9496	0.9303	0.9745	0.9835

Figure no 10: Zero order graph

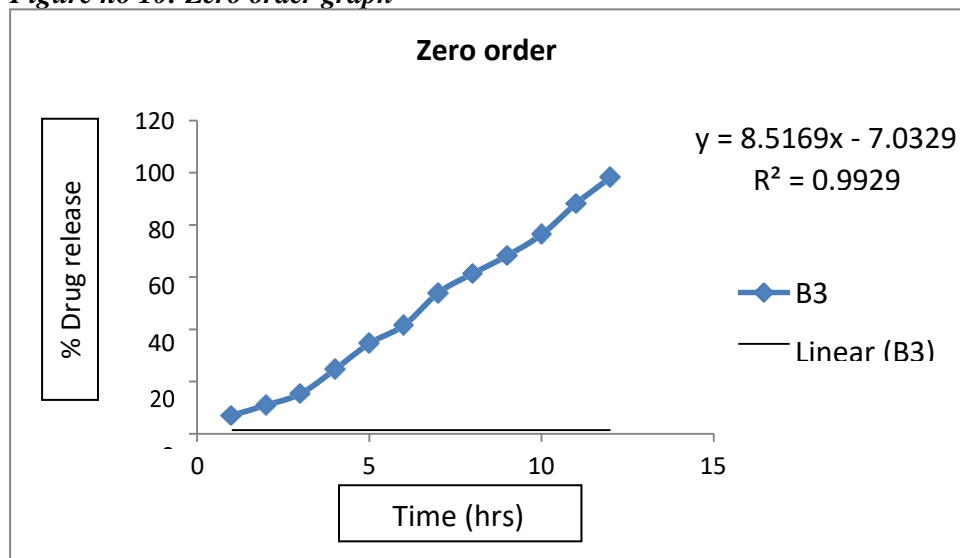
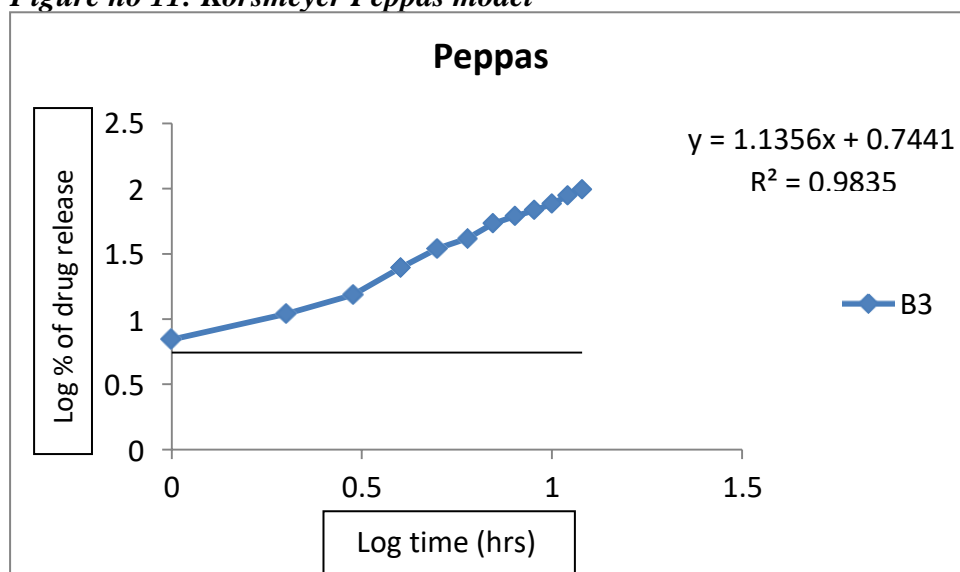


Figure no 11: Korsmeyer Peppas model



5 CONCLUSIONS

Floating microballoons of allopurinol was successfully prepared by taking polymer Eudragit RS 100 by solvent evaporation method. 3^2 factorial designs were employed to optimize the floating microballoons of allopurinol by selecting the concentration of Eudragit RS 100. From the factorial design it can be concluded that as the concentration of polymer decreases shows increase in yield and drug release. As the concentration of polymer increases shows decrease in entrapment, drug release and also affect the floating property. Thus, in moderate concentration of polymer shows excellent result of % entrapment efficiency, % drug release, floating property. From 3^2 factorial design it can be concluded that 75 mg of Eudragit RS 100 and 0.15 % of tween 80 (B3) formulation imparts good result for formulation. Evaluations were performed for optimized batch shows 1.04 seconds floating time, 97.45% drug entrapment efficiency, 98.19% drug release at 12 hours and total floating time up to 12 hours.

6. REFERENCES

1. Ghule PN, Deshmukh AS and Mahajan VR, (2014) , Floating drug delivery system (FDDS): An overview. *Research Journal of Pharmaceutical Dosage Forms and Technology*, 6(3), 174-182.
2. Dubey J and Verma N, (2013), Floating drug delivery systems: A review. *International Journal of Pharmaceutical Sciences and research*, 4(8), 2893-2899.
3. Kumar R, et al., (2016), Microballoons: An advance avenue for gastroretentive drug delivery system- A review." *UK Journal of Pharmaceutical and Bioscience*, 4(4), 29-40.
4. Patel S, et al., (2016), Microballoons: A novel approach in in gastro-retention floating drug delivery system (FDDS). *An International Journal of Pharmaceutical Science*, 7(2), 332-345.
5. Senthil PR, Senthil C and Sathali AH, (2016), Microballoons - from formulation to pharmaceutical design and applications." *World Journal of Pharmacy and Pharmaceutical Sciences*, 5(5), 341-352.
6. Patel D, et al, (2016), Formulation and evaluation of floating microsponges of allopurinol. *An International Journal of Pharmaceutical Sciences*, 7(3), 135-154.
7. Ragab G, Elshahaly M and Bardin T, (2017), Gout: An old disease in new perspective: A review. *Journal of Advanced Research*, 8(5), 495-511.
8. Pancheddula M and Shayeda, (2018), Development and in vitro characterization of acetohydroxamic acid floating microballoons. *International Journal of Pharmacy and Biological Sciences*, 8(3), 698-709.

9. Gupta P, Kumar M and Kaushik D, (2017), Pantoprazole sodium loaded microballoons for the systemic approach: *in vitro* and *in vivo* evaluation. *Advanced Pharmaceutical Bulletin*, 7(3), 461-467.
10. Gurnany E, Jain A and Jain R, (2014), Preparation and characterization of gastro-retentive floating microballoons of Acrycoat S-100 bearing carvedilol. *Asian Journal of Pharmaceutics*, 9(2), 120.
11. Ahmed SM, Ahmed Ali A, Ali AM and Hassan OA, (2016), Design and *in vitro/in vivo* evaluation of sustained-release floating tablets of itopride hydrochloride. *Drug Design, Development and Therapy*, 10, 4061-4071.
12. Jelvehgari M, Maghsoodi M and Nemati H, (2010), Development of theophylline floating microballoons using cellulose acetate butyrate and/or Eudragit RL 100 polymers with different permeability characteristics. *Research in Pharmaceutical Science*, 5(1), 29-39.
13. Jain A, et al., (2014), Formulation and characterization of floating microballoons of nizatidine for effective treatment of gastric ulcers in murine model. *Journal of Drug Delivery*, 22(3), 306-311.
14. Yogesh JM, Rohan BK and Nisharani SR, (2012), Floating microsphere: a review. *Brazilian journal of Pharmaceutical Science*, 48(1), 17-30.
15. Porwal A, Swami G and Saraf SA, (2011), Preparation and evaluation of sustained release microballoons of propranolol. *DARU Journal of Pharmaceutical Sciences*, 19(3), 193-201.
16. Rishikesh G, Sunil KP, Snigdha P and Peeyush B, (2014), Formulation and evaluation of novel stomach specific floating microspheres bearing famotidine for treatment of gastric ulcer and their radiographic study. *Asian Pacific Journal of Tropical Biomedicine*, 4(9), 729-735.
17. Shaikh HK, Kshirsagar RV and Patil SG, (2015), Mathematical models for drug release characterization: A review. *World Journal of Pharmacy and Pharmaceutical Sciences*, 4(04), 324-338.

PCP409

**INSIGHTS OF MEDICAL DEVICE RULES 2017 AND IT'S
AMENDMENTS**

AP0415

Hardi Patel

M. Pharm Student,
Graduate School of Pharmacy
Gujarat Technological University
hardi.patel2011@gmail.com

AP0420

Bhumika Maheriya

Assistant Professor,
Graduate School of Pharmacy
Gujarat Technological University
ra_pharmacy@gtu.edu.in

Abstract

Indian market for Medical Device is the 4th largest in Asia and is in one of the top 20 Medical Device market across the World. It was valued as Rs. 75,611 crore (US\$10.36 billion) in 2020 and is presumed to reach US\$ 50 billion in 2025 at a rate of 37% CAGR (Compound Annual Growth Rate). Medical Devices are used for various functions in the field of healthcare, as but not limited to, screening and diagnosis, treatment/care, restoration, and monitoring. Since 1940, medical devices were regulated as per Drug and Cosmetic Act 1940 and Rules 1945, CDSCO (Central Drug Standards Control Organization) regulated only a handful of medical devices through gazette notifications, these devices being called as notified devices. This system was not in consonance with the international standards and was rudimentary in character of CDSCO. After recognizing the requirement to establish more stringent and specific regulations for separating medical device from drug, refurbish the regulatory framework for medical device by passing the Medical Device rules 2017. This rule came into effect from 1st January 2018 which majorly focuses on the manufacture, sale, import, distribution and clinical investigation of Medical Device in India. Till date there are 37 Medical Devices registered to CDSCO under the Medical Device Rules 2017. In the subsequent amendments of the guidelines CDSCO is coming with the concept to cover all the medical device under one umbrella, making the similar rules and norms for all the medical devices. These regulations will provide a great number of opportunities for the manufacture of medical devices to invest in India and ease of doing a medical device business in India.

Keywords: CDSCO, Medical Device Rules 2017, Notified Devices

PCP413
**A MINI REVIEW ON PHAGE THERAPEUTICS AND
FORMULATION STRATEGIES-SUPPLEMENTING THE
MODERN MEDICINE SYSTEM**

AP0429
Charmi Soni
Student,
L.M.college of pharmacy
bpsonicharmi@lmcp.ac.in

AP0430
Aajvi Jansari
Student,
L.M.college of pharmacy
bpjansariaajvi@lmcp.ac.in

Guide:
Dr. Radhika Pandya
Assistant professor,
LMcollege of Pharmacy

Abstract

Recent advancements in phage encapsulation techniques reveal possible areas for innovation in the field of study that might have a big influence on the industry's future prospects. Therapeutic investigations, phage host identification, phage treatment effectiveness, and official procedures are required to assess the efficacy of phage therapy in combination with antibiotics, as well as their clinical applications. It has also enlightened the importance of human microbiota. Phage cocktails, rather than a single phage preparation, may be the most effective way to treat infections, according to research on animals. As designation of modern anti-biotics and many possible forms of therapy are needed to point out the universal problem of anti-biotics resistance. The phage therapy is the best concept which basically solves the problem related to multi-drug resist organisms. This paper reviews and summarises the use of phage therapy for various infections and focuses on the therapeutic demands and issues related to treat acute and chronic infections.

Keywords: Anti-biotics resistance, Human microbiota, Phage encapsulation, Clinical studies.

1. INTRODUCTION

Bacteriophages are biological creatures that aren't alive but yet have genetic material such as DNA and RNA that is essentially coated by a protein shell called a capsid that allows them to infect and multiply inside the cells of bacteria. We know that the exposure of anti-biotic resistance entities leads to fundamental threat to public health all over the world. That's why, phage therapy represents promising alternative approach to fight emerging pathogens. Phage therapy is defined as the administration of virulent phages directly to a patient for causing lysis of the bacterial pathogen which may leads to cause any infections.

1.1.1 History

History of phage therapy, has been full of with conflicting observations, poor understanding and misinterpretation. But understanding the extra scientific aspects of its history can help to explain the course of phage therapy.

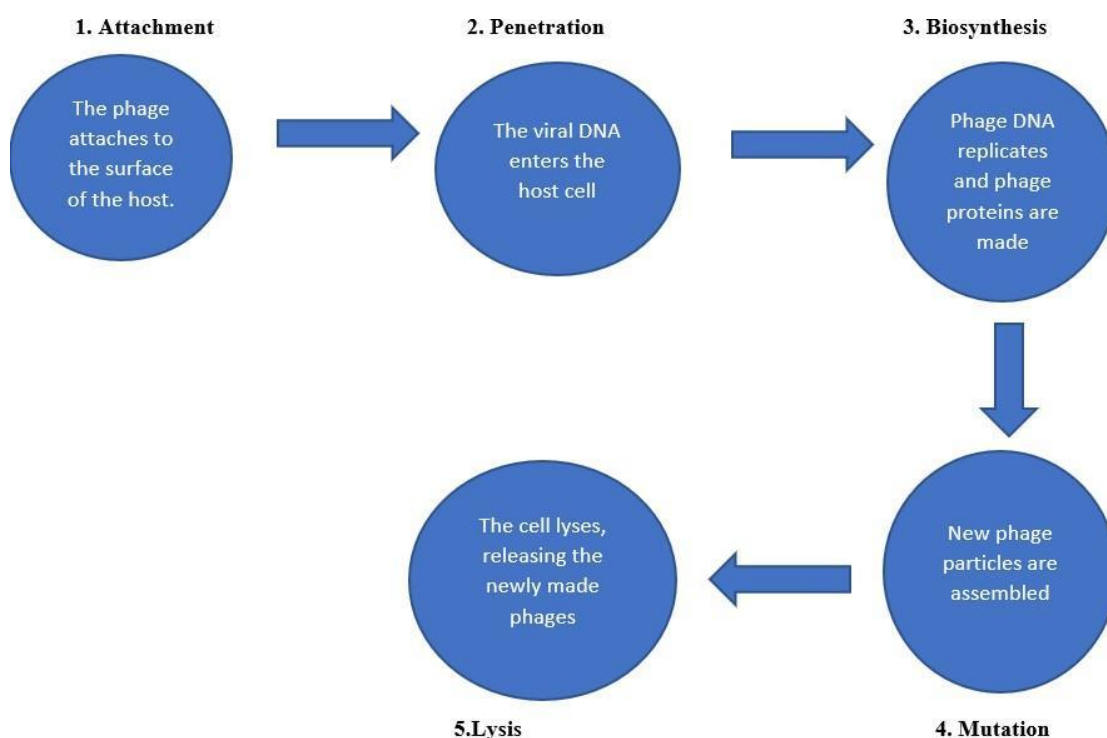
1. Stages of phage therapy development

- 1915 - First report of phage by Fredenck Tworth
- 1917 - Felix D'Herelle characterizes phage
- 1919 - Beginning of phage therapy
- 1920 - Use of phage therapy in western world
- 1928 - Discovery of penicillin by Alexander Fleming
- 1930 - Decline of phage therapy, rise of antibiotic use
- 1940 - Golden age of anti-biotics
- 1948 - Emergence of penicillin resistant S. aureus
- 1959 - Rise of MRSA

1983 - Phages used to treat drug - resistant bacterial infections
 2001 - First use of purified endolysin in vivo
 2009 - First regulated clinical trial of phage therapy
 2013 - Phase 1 clinical trial of lysin SAL-1
 2017 - Pharmacokinetic analysis of endolysin based drug SAL-200
 2020 - Phase 1/2 a clinical trial of lysin XZ.700 from microcos

1.1.2 Mechanism of action of bacteriophage therapy

Figure: 1 Lytic lifecycle of bacteriophage:



2. ADVANTAGES OF BACTERIOPHAGES OVER ANTI-BIOTICS

Table:1 Comparison of bacteriophages with antibiotics

Bacteriophages	Anti-biotics
Ables to kill anti-biotic resistant bacteria	Cannot kill anti-biotic resistant bacteria
It is very specific so the chances of developing secondary infections are avoided	This may affect the microbial balance in the patient, which may lead to serious secondary infection
No serious side effects have been described	Multiple side effects have been observed and secondary infections have been reported
Available where they are most needed	Do not necessarily concentrate at the site of infection
Do not harm microbiome that is found inside of our bodies	Anti-biotics tend to kill good bacteria
Bacteria do not regain their viability, means once it is killed it remains dead.	They only stop the growth of bacteria
They are non-toxic.	They may toxic.

3.APPLICATION OF BACTERIOPHAGE:

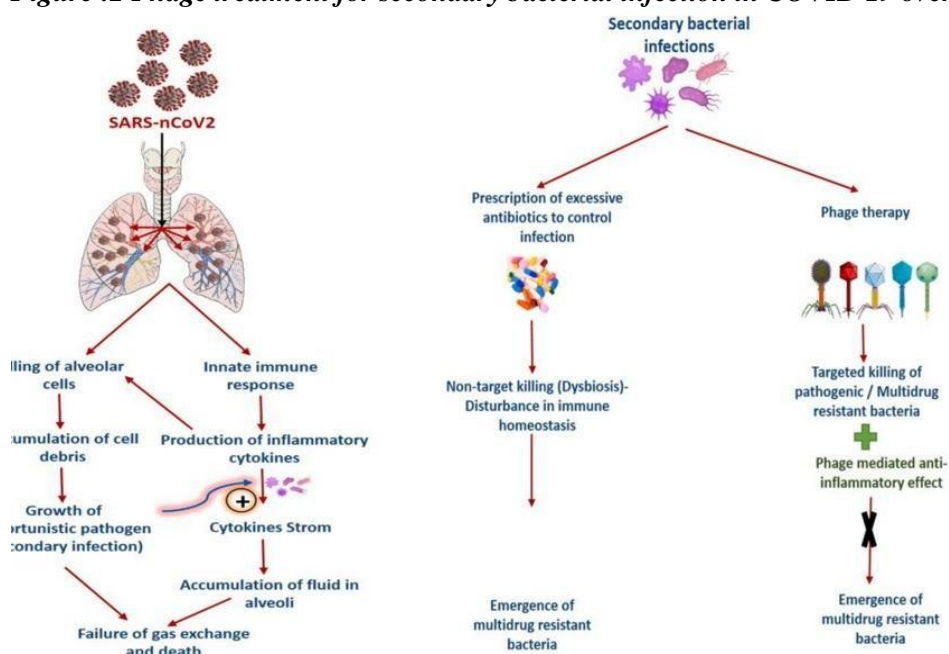
- Antiviral activities SARS-nCOV 2
- Treatment of Multi drug resistant bacteria
- Phage therapy: Treating human infectious disease
Prevention of human infectious disease
- Veterinary medicine: Treating animal infectious disease
Prevention of animal infectious disease
- Phage encapsulation
- Phage associated protein synthesis

1.3.1 Phage therapy: A novel approach to secondary bacterial infection treatment in COVID 19

One of the most well-known pandemics of the 20th century was COVID-19 (World Health Organization 2020). Numerous questions remain about the prevalence, manifestation, and symptoms of bacterial infections in SARSCoV-2 (COVID-19) patients. According to reports, only 8.4% of COVID-19 patients acquire a secondary bacterial infection. In comparison, 74.6% are given antibiotics as a preventative measure. Antibiotics are still prescribed to patients with secondary bacterial infections and/or co-infections, even though they are worthless for the treatment of COVID-19. This presumption, though, increases the risk of antibiotic overuse and, eventually, widespread bacterial resistance. A great option would be phage treatment, which has a long history of effectiveness. The moment has arrived to revive it as an antibiotic substitute. High specificity (targeted killing) and anti-inflammatory bacteriophages will be very helpful in the treatment of diseases like Covid-19. There are two potential pathways for Phage's anti-inflammatory action:

- 1.indirect impact by lowering bacterial burden by killing the targeted pathogen directly or facilitating their evacuation from the body.
- 2.direct effect by engaging with the host immune system. Bacteriophages aid in the removal of their respective hosts from the body in addition to killing (lysing) them directly.

Figure :2 Phage treatment for secondary bacterial infection in COVID 19 over antibiotics



Source:

<https://doi.org/10.1016/j.crmicr.2022.100115>

4. DEVELOPING A BACTERIOPHAGE DELIVERY METHOD USING ENCAPSULATION AND POSSIBLE IMMOBILISATION APPLICATIONS

It is essential to deliver medicinal substances to the area of action. Although many chemical compounds, such as beta-lactam antibiotics, can reach therapeutic levels in the majority of the human body after administration, chemicals with a greater molecular weight, such as therapeutic proteins, may not be able to reach the site of action (such as an infection), and are thus useless. However, the use of therapeutic proteins has been shown to be successful. Phage therapy is a highly promising technique, particularly for infections caused by multidrug-resistant bacteria. Encapsulation, or their immobilization is one of the most frequently employed methods. Encapsulated phages, such as those found inside liposomes, provide a variety of therapeutic advantages over the administration of free phages. The goal of any encapsulation method is to generate monodisperse particles that are identical in size and other physicochemical features and do not agglomerate during manufacture or application.

Table: 2 Summary of the advantages and disadvantages of mass manufacturing of encapsulated therapeutic phage compositions.

Encapsulation method	Advantages	Disadvantages
Emulsification	Material produced ideal for cream type treatments Promote absorption when applied topically	Difficult to transport Prone to bacterial contamination
Freeze drying	Final product: easy to store Variety of applications	Time consuming and costly
Spray drying	Final product: easy to store Variety of applications	Energy consuming process

Table :3 A summary of advantages and disadvantages of several bacteriophage immobilization procedures for the development of therapeutic phage formulations

Immobilization Approach	Advantages	Disadvantages
Physical	Adsorption Simple process Inexpensive	Undirected, inconsistent phage not strongly bound to substrate
Protein-Ligand	Strongly bound phage High binding efficiency Tail-up orientation	Complicated process Expensive
Electrostatic	High binding efficiency Applicable to most tailed phages Tail-up Orientation	Electrostatically charged surface may not be desirable
Covalent Linkage	Strongly bound phage Potentially longer shelf life	Can be a costly and complex process (in the case of linker-based immobilization)

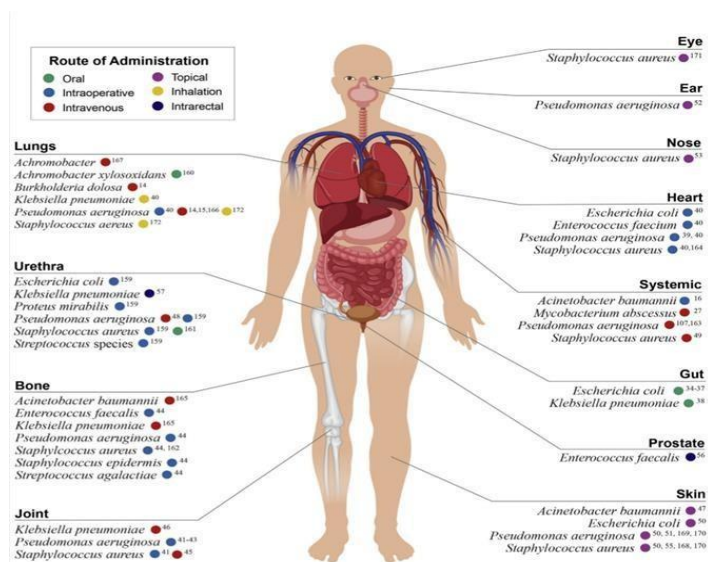
5. Bacteriophage therapy a successful clinical trial :

The combining of both, i.e., bacteriophage and antibiotics, or phage alone, may produce potentially successful treatment options for bacterial infections as opposed to totally replacing antibiotics, as proven by past clinical case studies. In order to increase the use of bacteriophage treatment against multi-drug resistant infections, significant challenges must be overcome in the design of improved clinical studies. When antibiotics fail to work, antibacterial medications

can be administered alone or in combination with bacteriophages, known as bacteriophage-antibiotic combination therapy.

1. Bone and joint infections
2. Urinary tract infections
3. Biofilm infections
4. Heart/pulmonary infections
5. Gastrointestinal infections
6. Septicemia/bloodstream infections
7. Skin and soft tissue infections

Figure :3 Summary of the phage therapy clinical trials and compassionate use case reports from 2005 to 2020. Case reports are categorized by the site of infection and target pathogen. The color coding represents the primary route of phage administration in each case report



<https://doi.org/10.1016/j.clinthera.2020.07.014>.

Table: 4 A summary of clinical trials using bacteriophages to treat infections of the bones and joints

Case study	Description	Administration	Result	Reference
Using bacteriophage therapy to treat of PKI	A 79-year-old female with a resistant <i>Staphylococcus epidermidis</i> PKI was given phage treatment following debridement and implant retention surgery	Phage#- Local instillation Antibiotics (colistin, meropenem and ceftazidime) — Intravenous	Bacteria eradicated successfully following combination therapy	Doub et al. 2021
Bacteriophage treatment for chronic PJI infection of the knee and persistent pain femoral osteomyelitis.	Following a gunshot wound, an 80-year-old patient suffering from T2DM2 and CKD were identified with	Phage cocktail (SA- BHU1, SA-BHU2, SA-BHU8, SA- BHU15, SA-BHU21, SA-BHU37, SA-BHU47)— Intralesionally	Bacteria were successfully eliminated as a result of combination treatment.	Tkhilaishvili et al. 2020

	PJI and chronic kidney disease. Osteomyelitis caused by Pseudomonas aeruginosa MDR infection			
--	--	--	--	--

PJI prosthetic joint infection, **PKI** prosthetic knee infection, **T2DM2** type 2 diabetes mellitus, **CKD** chronic kidney disease **MDR** multi-drug resistant, **Phage#:** Collection (No identification Case study given) received from George Eliava Institute of Bacteriophages, Microbiology and Virology (Tbilisi, Georgia).

Table: 5 A summary of clinical trials using bacteriophages for the treatment urinary tract infections

CASE STUDY	DESCRIPTION	ADMINISTRATI ON	RESULT	Reference
Identifying intravesical Using phage therapy to treat UTI	Men over the age of 18 with acute UTI but no signs of systemic disease were included in a placebo-controlled, double-blind clinical research. Uropathogens (Enterococcus spp., Escherichia coli, Proteus mirabilis, Pseudomonas aeruginosa, Staphylococcus spp., and Streptococcus spp.)	Phage cocktail (Pyobacteriophage)-Intravesical suprapubic	Intravesical phage therapy was non-inferior to antibiotic treatment. In terms of efficacy and safety, bladder irrigation (placebo) was not superior. safety	Leitner et al. 2021
Case report of effective therapy for chronic relapsing UTI treated with phage	A 58-year-old renal transplant patient experienced epididymitis after developing a post-transplant UTI caused by ESBL Klebsiella pneumoniae (MDR).	Phage#-Oral, Intravesical and bladder irrigation Antibiotic (meropenem)- Intravenous	After receiving combination treatment, sterile urine culture was obtained.	Kuipers et al. 2020

UTI urinary tract infection, **ESBL** extended-spectrum β -lactamase; **Phage#:** Solution (No identification given) received from Eliava Institute in Tbilisi, Georgia

Table: 6 A summary of clinical trials using bacteriophages for the treatment of biofilm infections

CASE STUDIES	DESCRIPTION	ADMINISTRATION	RESULT	Reference
Using bacteriophage therapy to treat of animal-based paranasal biofilm model	Pseudomonas aeruginosa infection was simulated in sheep frontal sinuses to create an infection and produce a biofilm.	Phage cocktail (CT- PA containing Pa193, Pa204, Pa222 and Pa223)- Intranasal	A statistically significant decrease in the bacterial population of the biofilm was observed.	Fong et al. 2019
Phages and antibiotics work together to destroy biological films.	In microtiter plates, Pseudomonas aeruginosa biofilm has been grown in vitro to mimic the in-vivo environment	Phage (NP1 & NP3) and antibiotic (ceftazidime, ciprofloxacin, colistin, gentamycin & tobramycin)-Direct inoculation	As compared to other drugs, the synergistic effect of phages and drugs was highest with tobramycin	Chaudhry et al. 2017

Table: 7 A summary of clinical trials using bacteriophages for the treatment of heart and pulmonary diseases

CASE STUDY	DESCRIPTION	ADMINISTRATION	RESULT	Reference
Phage therapy for critical Infections associated with Cardiothoracic surgery	Eight patients with immunosuppression after organ transplantation were infected via MDR Staphylococcus aureus, Enterococcus faecium, Pseudomonas aeruginosa, Klebsiella pneumoniae, and Escherichia coli	Phage (CH1, Enf1, PA5, PA10, KPV811, KPV15, Sa30, SCH1, SCH111, ECD7, V18)-local, intraoperatively, inhalation and intranasal Antibiotics (cefepime, daptomycin, linezolid, tobramycin, ceftazidime, colistin, meropenem, cotrimoxazole, rifampicin, fucloxacillin, sultamicillin and clindamycin)—oral and intravenous	No major adverse effects, seven out of eight people got their target bacteria eradicate	Rubalskii et al. 2020 9056 A
Bacteriophage therapy for an aortic graft infection	A 76-year-old patient underwent surgery for an aortic aneurysm with Dacron graft, which resulted in MDR Pseudomonas aeruginosa infection	Phage (OMKO1) and antibiotics (ceftazidime)-direct injection into the site (mediastinal fistula)	Infection eradicated with no signs of recurrence in 18 months	Chan et al. 2018

MDR: Multi drug resistant

Table: 8 A summary of clinical trials using bacteriophages for the treatment of skin and soft tissue infections

Case studies	Description	Administration	Result	Reference
A clinical trial for the treatment of wounds via a bacteriophage cocktail	Patients aged between 12 to 60 years with chronic non-healing wounds caused by Escherichia coli, Staphylococcus aureus and Pseudomonas aeruginosa	Phage#- Topical	Seven patient infections eradicated, while the remaining 13 wound sizes decreased significantly	Gupta et al. 2019
Transfersomal phage cocktail treatment against SSTIs in a rat model	The posterior portion of both thighs of 4–6-week-old female rats was intramuscularly injected with Staphylococcus aureus	Phage (MR-5 & MR-10)- Intramuscular	100% survival rate was observed for both 30 min and 12 h post-infection	Chhibber et al. 2017

SSTIs: Skin and soft tissue infections; Phage#: Cocktail of phages (No identification given)

Table: 9 A summary of clinical trials using bacteriophages for the treatment of septicemia/bloodstream infections

Case studies	Description	Administration	Result	Reference
A case report of bacteriophage therapy for the treatment of septicaemia in a patient	A 61-year-old man with peritonitis infection and other complications developed large necrotic pressure sores by MDR Pseudomonas aeruginosa leading to septicaemia	Phage (BFC1)- Intavenous and Topical	Fever disappeared, CRP level dropped, and blood culture turned negative for P. aeruginosa	Jennes et al. 2017
Experimental phage therapy for the treatment of liver abscesses and bacteremia	The mice intragastrical inoculation of Klebsiella	Phage (NK5)- Oral or Intraperitoneal	The bacterial count was eliminated virtually from	Hung et al. 2011
pneumoniae led to the development of liver abscesses, necrosis of liver tissues and bacteremia			both blood and liver tissues	

MDR: Multidrug-resistant; CRP: C-reactive prote.

Table: 10 A summary of clinical trials using bacteriophages for the treatment of gastrointestinal infections

Case studies	Description	Administration	Result	Reference
Bacteriophage therapy for intestinal MDR bacteria eradication	Due to increased antimicrobial resistance in gut bacteria, the effect of single-dose of bacteriophage on MDR <i>Klebsiella pneumoniae</i> isolated from albino mice use faeces	Phage#-Oral	The colony-forming unit of <i>Klebsiella pneumoniae</i> gradually decreased as the days progressed, leading to full eradication in 6 days	Chaturvedi and Nath 2018
Combined bacteriophage treatment for septic	Female mice inoculated with a lethal dose of VRE disseminated intraperitoneally to intra and extra-peritoneal organs	peritonitis Phage (EFDGI and EFLK1) and antibiotics (ampicillin)- Intraperitoneal	100% successful treatment via bacteriophage cocktail alone for critically ill mice and 60% the success rate for combination therapy	Gelman et al. 2018

MDR multi-drug resistant, VRE vancomycin-resistant *Enterococcus faecalis*; Phage#: Customized Phage cocktail (No identification given)

6. CURRENT ISSUES AND NEW STRATEGIES IN PHAGE TREATMENT.

Currently, phage therapy encounters obstacles including:

1. sustaining existing standards of quality and safety
2. ensuring the longevity of phage preparations
3. developing a high-throughput test for phage screening
4. overcoming phages' restricted activity in biofilms
5. preventing and combating the development of bacterial phage resistance
6. developing a regulatory system more suited to phage products.
7. the use of combined strategies, such as the combination of phages and antibiotics.
8. the use of synthetic biology technologies to create phages with enhanced characteristics

7. CONCLUSION

Since bacteriophages are particular to their host, their effectiveness against resistant bacteria offers them a possible treatment for resistant bacterial infections, which is especially important given the rise in AR bacterial illnesses. According to previous clinical case studies, bacteriophage and antibiotics combined or phage alone might produce potentially effective treatment alternatives against bacterial pathogens rather than completely replacing antibiotics. The possible benefits of bacteriophage treatment include improved bacterial clearance, more effective adsorption into biofilms, and a reduced risk of bacteriophage resistance development. They also hold great promise for the treatment of bacterial co-illnesses or secondary infections during viral pandemics like the ongoing COVID-19 pandemic. Despite tremendous advances in medicine, we are unable to halt the spread of diseases caused by AMR infections. More study on the nature of host-phage interactions is needed in the future to help clarify and expedite the notion of bacteriophage treatment, as well as advocate for its regulatory adoption in modern medicine.

8. REFERENCES:

1. Bhargava, Kanika, et al. "Phage Therapeutics: From Promises to Practices and Prospectives." *Applied Microbiology and Biotechnology*, vol. 105, no. 24, 2021, pp. 9047–9067., <https://doi.org/10.1007/s00253-021-11695-z>.
2. Doub JB, Ng VY, Wilson E, Corsini L, Chan BK (2021) Successful Treatment of a Recalcitrant Staphylococcus epidermidis Prosthetic Knee Infection with Intraoperative Bacteriophage Therapy. *Pharmaceuticals* 14(3):231. <https://doi.org/10.3390/2Fph14030231>
3. Tkhlilaishvili T, Winkler T, Muller M, Perka C, Trampuz A (2020) Bacteriophages as adjuvant to antibiotics for the treatment of periprosthetic joint infection caused by multidrug-resistant *Pseudomonas aeruginosa*. *Antimicrob Agents Chemother* 64(1):e00924-e1019. <https://doi.org/10.1128/AAC.00924-19>
4. Leitner L, Ujmajuridze A, Chanishvili N, Goderdzishvili M, Chkonia I, Rigvava S, Chkhotua A, Changashvili G, McCallin S, Schneider MP, Liechti MD, Mehnert U, Bachmann LM, Sybesma W, Kessler TM (2021) Intravesical bacteriophages for treating urinary tract infections in patients undergoing transurethral resection of the prostate: A randomised, placebo-controlled, double-blind clinical trial. *Lancet Infect Dis* 21(3):427–436. [https://doi.org/10.1016/s1473-3099\(20\)30330-3](https://doi.org/10.1016/s1473-3099(20)30330-3)
5. Kuipers S, Ruth MM, Mientjes M, de Sevaux RG, van Ingen J (2020) A Dutch case report of successful treatment of chronic relapsing urinary tract infection with bacteriophages in a renal transplant patient. *Antimicrob Agents Chemother* 64(1):e01281-e1319. <https://doi.org/10.1128/aac.01281-19>
6. Chaudhry WN, Concepcion-Acevedo J, Park T, Andleeb S, Bull JJ, Levin BR (2017) Synergy and order effects of antibiotics and phages in killing *Pseudomonas aeruginosa* biofilms. *PLoS One* 12(1):e0168615. <https://doi.org/10.1371/journal.pone.0168615>
7. Fong SA, Drilling AJ, Ooi ML, Paramasivan S, Finnie JW, Morales S, Psaltis AJ, Vreugde S, Wormald PJ (2019) Safety and efficacy of a bacteriophage cocktail in an in vivo model of *Pseudomonas aeruginosa* sinusitis. *Transl Res* 206:41–56. <https://doi.org/10.1016/j.trsl.2018.12.002>
8. Rubalskii E, Ruemke S, Salmoukas C, Boyle EC, Warnecke G, Tudorache I, Shrestha M, Schmitto JD, Martens A, Rojas SV, Ziesing S, Bochkareva S, Kuehn C, Haverich A (2020) Bacteriophage therapy for critical infections related to cardiothoracic surgery. *Antibiotics* 9(5):232. <https://doi.org/10.3390/2Fantibiotics9050232>
9. Chan BK, Turner PE, Kim S, Mojibian HR, Eleftheriades JA (2018) Narayan D (2018) Phage treatment of an aortic graft infected with *Pseudomonas aeruginosa*. *Evol Med Public Health* 1:60–66. <https://doi.org/10.1093/emph/eoy005>
10. Chhibber S, Shukla A, Kaur S (2017) Transfersomal phage cocktail is an effective treatment against methicillin-resistant *Staphylococcus aureus*-mediated skin and soft tissue infections. *Antimicrob Agents Chemother* 61(10). <https://doi.org/10.1128/aac.02146-16>
11. Gupta P, Singh HS, Shukla VK, Nath G, Bhartiya SK (2019) Bacteriophage therapy of chronic non-healing wound: clinical study. *Int J Low Extrem Wounds* 18(2):171–175. <https://doi.org/10.1177/1534734619835115>
12. Jennes S, Merabishvili M, Soentjens P, Pang KW, Rose T, Keersebilck E, Soete O, Francois PM, Teodorescu S, Verween G, Verbeken G, De Vos D, Pirnay JP (2017) Use of bacteriophages in the treatment of colistin-only-sensitive *Pseudomonas aeruginosa* septicemia in a patient with acute kidney injury—a case report. *Crit Care* 21(1):129.
13. Gelman D, Beyth S, Lerer V, Adler K, Poradosu-Cohen R, Copenhagen-Glazer S, Hazan R (2018) Combined bacteriophages and antibiotics as a therapy against VRE *Enterococcus faecalis* in a mouse model. *Res Microbiol* 169(9):531–539. <https://doi.org/10.1016/j.resmic.2018.04.008>

14. Chaturvedi A, Nath G (2018) Oral administration of Klebsiella pneumoniae bacteriophage eradicates the bacteria in albino mice. *Indian J Med Microbiol* 36(2):293–294. https://doi.org/10.4103/ijmm.IJMM_18_154
15. Bacteriophage Therapy: An Alternative Solution for Antibiotics.” *DHR Proceedings*, 2022, <https://doi.org/10.47488/dhrp.v2is2.58>.
16. AL-Ishaq, Raghad Khalid, et al. “Bacteriophage Treatment: Critical Evaluation of Its Application on World Health Organization Priority Pathogens.” *Viruses*, vol. 13, no. 1, 2020, p. 51., <https://doi.org/10.3390/v13010051>.
17. Gordillo Altamirano, Fernando L., and Jeremy J. Barr. “Phage Therapy in the Postantibiotic Era.” *Clinical Microbiology Reviews*, vol. 32, no. 2, 2019, <https://doi.org/10.1128/cmr.00066-18>.
18. Drulis-Kawa, Zuzanna, et al. “Learning from Bacteriophages - Advantages and Limitations of Phage and Phage-Encoded Protein Applications.” *Current Protein and Peptide Science*, vol. 13, no. 8, 2012, pp. 699–722., <https://doi.org/10.2174/138920312804871193>.
19. Gordillo Altamirano, Fernando L., and Jeremy J. Barr. “Phage Therapy in the Postantibiotic Era.” *Clinical Microbiology Reviews*, vol. 32, no. 2, 2019, <https://doi.org/10.1128/cmr.00066-18>.

PCP415

FORMULATION AND EVALUATION OF ORALLY DISINTEGRATING TABLETS OF BRIVARACETAM

AP0435 Jay Patel GTU Student, M.pharm Sem-3 Shree Swaminarayan Sanskar Pharmacy College jaypatidar361@gmail.com	AP0436 Sejal M Solanki Associate professor Pharmaceutics Department Shree Swaminarayan Sanskar Pharmacy College sejalkharadi@gmail.com	AP0439 Nehang Raval Trainee Q.C Citrus research center Rx.jaypatidar@gmail.com
---	--	--

ABSTRACT:

Oro-dispersible tablets of Brivaracetam were successfully formulated by the direct compression method. Pre-formulation studies of the drug were performed; the infrared spectral analysis studies revealed that there is no chemical interaction with excipients used in the formulation of the drug. Risk Assessment of formulation variables using Quality by Design (QbD) showed that diluent selection and type and level of disintegrants were most likely to affect the Critical Quality Attributes (CQA) of the Orally Disintegrating Tablets (ODT). Hence were ranked high. Based on weight variation, hardness, friability, disintegration time, and dissolution, it was found that all the formulations were satisfactory as per pharmacopeial standards. Disintegration time was 90% of drug release at 10 minutes with the least disintegrant level. Further optimization of the formulation was done using 2^2 factorial designs (2 factors 2 levels) using Minitab 16 and established control strategy and design space of the formulation. Validation of design was done and the final optimized batch P7 was chosen from the design space. The final formulation P7 was tested for accelerated stability studies for 3 months and found stable.

Keywords: Brivaracetam, Orally Disintegrating Tablets (ODT), Critical Quality Attributes (CQA)

1 INTRODUCTION

1.1 Introduction of Drug Delivery System

Formulation of drugs into a presentable form is the basic requirement and need of today. The dosage form is a means of drug delivery system, used for the application of drugs to a living body. Various type of dosage forms is available such as tablets, syrups, suspensions, suppositories, injections, transdermal, and patches having different type of drug delivery mechanisms.¹

These classical/modern dosage forms have some advantages and disadvantages therefore the development of an ideal drug delivery system is a big challenge to the pharmacist in the present scenario. To get the desired effect the drug should be delivered to its site of action at such rate and concentration to achieve the maximum therapeutic effect and minimum adverse effect. For the development of a suitable dosage form a thorough study of the physicochemical principles that govern a specific formulation of a drug should be subjected.¹

1.1.1 ORAL DISPERSIBLE TABLETS:-¹

Drinking water is mostly required for the oral administration of drugs, like tablets and capsules, in which some patients experience nuisance in swallowing bulky conventional dosage forms. To prevent the dysphagia and improve patient compliance, orodispersible tablets are introduced as a substitute in oral DDS, designed to disintegrate in the mouth without the aid of water. So they are useful in such conditions in which water is not available, or prohibited as before operation, in kinetosis, cough episodes due to neurological stimulation, or chest infections.

Different methods are adopted to manufacture the orodispersible tablets to give fast disintegration to the dosage form as it gets in contact with saliva with a good agreeable mouth feeling.

These orodispersible tablets (ODT) can be administered to any patient having difficulty swallowing. They are also recognized as mouth dissolvable, melt-in-mouth, fast dissolving, rapid-melts, or porous tablets.

1.1.2 PREREQUISITE OF FAST DISINTEGRATING TABLETS:-²

There are some prerequisites for fast disintegrating tablets which are mentioned as,

- ✓ Tablet must disintegrate and disperse in the oral cavity without water intake.
- ✓ It can hold high drug quantities.
- ✓ It should be compatible with taste-masking agents and excipients and have an optimum sensation effect.
- ✓ Leave minimum to no residue after administration.
- ✓ It should have the optimum capacity to remain intact in formulation processes.
- ✓ It should be stable in the range of temperature and humidity.
- ✓ It should be adaptable and amenable to existing processing and packaging machinery.
- ✓ It should be manufactured at a low cost.

1.1.3 SUITABILITY OF DRUGS FOR FAST DISINTEGRATING TABLETS:-³

For developing FDT of a specific drug several factors should be kept forth while selecting the drug, excipients, and formulation method. These are as follows:

- ✓ Drugs to be used for sustained action are not suitable candidates for FDT.
- ✓ Drugs having very disagreeable taste are not suitable like clopidogrel.
- ✓ Patients suffering from Sjogren's syndrome and those with less saliva secretion and not suitable for FDT dosage form.
- ✓ Drugs of very short half-life and requiring frequent dosing are not an appropriate candidates.
- ✓ Patients on Anticholinergic therapy are not suitable for FDT.
- ✓ Drugs showing altered pharmacokinetic behavior if formulated in such dosage form concerning their conventional dosage form are not suitable, like selegiline, apomorphine, and Buspirone.
- ✓ Drugs producing considerable amounts of toxic metabolites on first-pass metabolism and in GIT and having substantial absorption in oral and pregastric areas are good candidates.
- ✓ Drugs permeable to upper GIT and oral mucosal epithelial cell lining are considered good candidates for FDT.

1.1.4 TECHNIQUES FOR PREPARING ORODISPERSIBLE TABLETS:-³

Various techniques are currently used in preparing fast disintegrating/dissolving tablets;

- Direct compression
- Freeze drying or Lyophilization
- Molding method
- Sublimation
- Spray-drying
- Mass-extrusion
- Cotton candy process
- Nanonization
- Compaction
- Phase-transition method

1.1.5 ADVANTAGES OF ODT'S:-⁴

- ✓ Administration to the patients who cannot swallow, such as the elderly, stroke victims, bedridden patients, patients affected by renal failure, and patients who refuse to swallow such as pediatric, geriatric, and psychiatric patients.

- ✓ Rapid drug therapy intervention.
- ✓ Achieve increased bioavailability/rapid absorption through pre-gastric absorption of drugs from the mouth, pharynx, and oesophagus as saliva passes down.
- ✓ Convenient for administration and patient compliance for disabled, bedridden patients and for travelers and busy people, who do not always have access to water.
- ✓ Good mouth feel property helps to change the perception of medication as bitter pill particularly in pediatric patients.

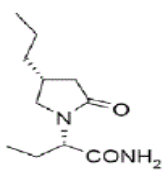
1.1.6 DISADVANTAGES OF FAST DISSOLVING TABLETS:-⁴

- ✓ Low amount of drug can be incorporated in each dose.
- ✓ Sometimes it possesses mouth feeling
- ✓ ODT requires special packaging for proper stabilization & safety of stable products.
- ✓ Eating and drinking may become restricted

1.2 Introduction of Drug

- **Brivaracetam:**⁷⁻¹⁰

Table 01 Drug Information

General Properties:-	
Name	Brivaracetam
Description	Brivaracetam is a racetam derivative of levetiracetam used in the treatment of partial-onset seizures. Brivaracetam binds SV2A with 20 times higher affinity than levetiracetam.
Appearance	Brivaracetam is a white to off-white crystalline powder.
Structure	
CAS number	357336-20-0
Category	Antiepileptic
Molecular Weight	212.28 g/mol
Chemical Formula	C ₁₁ H ₂₀ N ₂ O ₂
IUPAC Name	(2S)-2-[(4R)-2-oxo-4-propylpyrrolidin-1-yl]butanamide
Solubility	It is very soluble in water, buffer (pH 1.2, 4.5, and 7.4), ethanol, methanol, and glacial acetic acid. It is freely soluble in acetonitrile and acetone and soluble in toluene. It is very slightly soluble in n-hexane.
Water Solubility	46.8 mg/mL
Log P	0.86
pKa	16.29
Melting point (°C)	72 to 77 °C
Hygroscopic	Non-Hygroscopic
Identification	FTIR, UV

BCS Class	I	
Dose	10/25/50/75/100 mg	
Pharmacokinetic Properties:-		
Absorption of drug	Brivaracetam is highly permeable and is rapidly and almost completely absorbed after oral administration.	
Protein binding of drug	Brivaracetam is weakly bound to plasma proteins ($\leq 20\%$)	
Metabolism of drug	Brivaracetam is primarily metabolized by hydrolysis of the amide moiety to form the corresponding carboxylic acid metabolite, and secondarily by hydroxylation on the propyl side chain to form the hydroxy metabolite	
Half life	9 hours	
Excretion	Brivaracetam is eliminated primarily by metabolism and by excretion in the urine.	
Pharmacological Properties:-		
Drug Indication	Used as adjunctive therapy for partial-onset seizures in patients 16 years of age or older.	
Mechanism / Modes of action	Brivaracetam displays a high and selective affinity for synaptic vesicle protein 2A (SV2A) in the brain, which may contribute to the anticonvulsant effect.	
Marketed Preparations:-		
Brand/Generic Name	Availability	Company Name
BRIVIACT	Tablet: 10/25/50/75/100 mg	UCB Pharma

Figure 1 Marketed Preparations



2 AIM & OBJECTIVES

2.1 Aim of Work

Present research work aims to formulate and evaluate the Orally Disintegrating tablets of Brivaracetam.

2.2 Rationale

- ✓ Patient inconvenience due to swallowing difficulty (dysphagia) may minimize the drug treatment efficacy. Dysphagia is common in elderly patients and those with dementia, whereas patient rejection is frequently perceived.
- ✓ Formulation of drugs as orally disintegrating Tablets (ODTs) is one of the approaches to achieve enhanced patient acceptance toward orally solid dosage forms.

- ✓ Orally disintegrating Tablets are solid dosage forms that disintegrate rapidly when placed upon the tongue, usually within a matter of seconds.
- ✓ Brivaracetam is a racetam derivative used in the treatment of partial-onset seizures. Its oral recommended dose is 10/25/50/75/100 mg two to three times in a day.
- ✓ It is only available as simple conventional tablets under the brand name of Briviact.
- ✓ Its molecular weight is 212.28 g/mol. The half-life is about 9 hours. Also, the drug has good water solubility.
- ✓ Brivaracetam is belongs to the Antiepileptic category which is used in the emergency condition of seizures. This condition required quick onset of the action to the patient for instant recovery.
- ✓ Hence, by making Brivaracetam as orally disintegrating tablets (ODT's) can provide several patient advantages as they disintegrate rapidly (<1 min) in the mouth with or without water. Fast disintegration provides immediate drug release and fast drug absorption which ultimately gives quick onset of action.
- ✓ In addition, Brivaracetam ODT's provide ease of administration & swallowing, in addition to an acceptable mouth feel. Also the tablet swallowing difficulty can be minimizing for elderly patients.

2.3 Objectives of Work

- ✓ To formulate and evaluate orally disintegrating tablets of Brivaracetam using QbD approach.
- ✓ To investigate the impact of critical quality attributes (CQAs) and critical process parameters (CPPs) on quality target product profile (QTPP) attributes of orally disintegrating tablets of Brivaracetam.
- ✓ To check drug excipient compatibility study.
- ✓ To prepare orally disintegrating tablets of Brivaracetam using direct compression method.
- ✓ To screen various super disintegrating agents for satisfactory Disintegration time and In-Vitro Drug release.
- ✓ To evaluate pre and post compression parameters.
- ✓ To carry out stability study on final formulation.

3 RESEARCH METHODOLOGY

Quality Target Product Profile

The quality target product profile (QTPP) is “a prospective summary of the quality characteristics of a drug product that ideally will be achieved to ensure the desired quality, taking into account safety and efficacy of the drug product.”

Table 3 QTPP of the product

QTPP Elements	Target	Justification
Dosage Form	ODT	Patient Compliance
Dosage Design	Immediate Release tablet without scoring	For suitable replacement of marketed product
Route of Administration	Oral	Same route of administration
Dosage Strength	Similar to marketed product	Pharmaceutical Equivalence
Pharmacokinetics	Similar to marketed product	
Stability	Similar to marketed product	
	Physical Attribute	Pharmaceutically Equivalent to Marketed Product

Drug Product Quality Attributes	Identification		
	Assay		
	Disintegration Time		
	Content Uniformity		
	Dissolution		
Administration/Concurrence with labeling		Similar food effect	To achieve similar Pharmacokinetics
Alternative methods of administration		None	None

4 LITERATURE REVIEW

4.1 Review of Literature on Drug Delivery System

Maria M et al¹² formulated and evaluated fast-disintegrating tablets (FDTs) having Flurbiprofen (FP) and Metoclopramide HCl (MHCl) in combination. Direct compression was used to formulate FDTs of FP and MHCl as a combination regimen in six formulations. FDTs are defined as solid oral dosage form that disintegrates rapidly within seconds when placed in the oral cavity. FDT-1, FDT-2, FDT-3, FDT-4, FDT-5, and FDT-6 were formulated using crospovidone, croscarmellose sodium, and sodium starch glycolate as super disintegrants each in two formulations. Several pre-compression tests (angle of repose, bulk density, tapped density, Hausner's ratio, and compressibility index), post-compression evaluation (weight variation, friability, hardness, disintegration time, wetting time, assay, in vitro dissolution study, release kinetics study, statistical analysis, and stability study), and drug compatibility study were done for all six formulations.

Gozde G et al¹⁴ prepared different oral disintegrating tablet formulations and tested by changing the usage of co-formulated disintegrating excipient and other disintegrant combined with sodium starch glycolate and mannitol. Powder flow characteristics were examined. Suitable formulations compressed via direct compression method at two different pressure levels. Compressed tablets were tested physically and chemically. The results thus obtained were evaluated in the Artificial Neural Network and Gene Expression Programming modules.

Buket A et al¹⁵ investigated the impact of critical quality attributes (CQAs) and critical process parameters (CPPs) on quality target product profile (QTPP) attributes of orally disintegrating tablet (ODT) containing Ondansetron (OND) using two artificial neural network (ANN) programs.

Ashwini R et al¹⁷ focused on application of QbD approach to see the effect of formulation variables on oral disintegrating tablets containing antiemetic drug, Granisetron HCl. Risk assessment of critical material and process parameters are linked to critical quality attributes (CQAs) of the product with respect to obtain target quality product profile (TQPP). Preliminary screening was done to characterize the effects of microcrystalline cellulose, crospovidone, croscarmellose sodium and magnesium stearate on drug release. The effects of critical parameters (concentration of two super disintegrants crospovidone and croscarmellose sodium) were investigated by executing design of experimentation (DoE) using 3 level full factorial designs

Biswajit B et al¹⁸ worked on aims to propose control strategy for commercial manufacturing of Loratadine as an ODT. The control strategies include proposal of different parameters including strategies for raw materials, mixing time, speed of impeller and chopper, inlet temperature, screen size and mill speed, blending and lubrication time, and tablet compression.

Swapnil S et al¹⁹ reviewed all the aspects of ODTs which are necessary to develop the drug products as Super generics. The future perspective of ODTs about QbD is also provided to bank the researchers & manufacturers towards ODTs.

Priyanka N et al²⁰ focused on ideal characteristics, advantages and disadvantages, formulation aspects, formulation technologies, evaluation of products and future potential. Various marketed preparations along with numerous scientific advancements made so far in this avenue have also been discussed.

Niranjan B et al²¹ prepared ODT by direct compression method by using crospovidone as a superdisintegrating agent and optimized by 3² factorial design. Independent variables were concentration of crospovidone (X1) and hydroxypropyl cellulose (X2) while dependent variables were disintegration time and percent drug released. Optimized formulation, F4, showed drug content (97.90±0.37%), disintegration time (20.33±0.317 sec), percent drug released (101.5±0.59%), water absorption ratio (113.5±1.26%).

5 PREPARATIONS OF FORMULATION:

5.1 Direct Compression Method:

Direct Compression Method was adopted as it is the simplest of approach for ODT tablet fabrication. It involves least number of unit operations and is cost effective when it comes to commercialization of the product. Detailed formulae mentioned in table below.

Table 02 Formulation Table

Sr. No.	Ingredients	Screening of Diluent			Screening of Super Disintegrants			Optimization of Super Disintegrant		
		F1	F2	F3	F4	F5	F6	F7	F8	F9
1	Brivaracetam	10.0	10.0	10.0	10.0	10.0	10.0	10.0	10.0	10.0
2	Pharmaburst 500	50.0	-	-	50.0	50.0	50.0	50.0	50.0	50.0
3	Ludiflash	-	50.0	-	-	-	-	-	-	-
4	Pearlitol	-	-	50.0	-	-	-	-	-	-
5	Crospovidone	-	-	-	7.5	-	-	5.0	7.5	10.0
6	Croscarmellose Sodium	-	-	-	-	7.5	-	-	-	-
7	Sodium Starch Glycolate	-	-	-	-	-	7.5	-	-	-
8	Avicel pH 102	76.0	76.0	76.0	68.5	68.5	68.5	66.5	68.5	76.5
9	Sucralose	4.0	4.0	4.0	4.0	4.0	4.0	4.0	4.0	4.0
10	Colloidal Silicon Dioxide	4.0	4.0	4.0	4.0	4.0	4.0	4.0	4.0	4.0
11	Talc	2.0	2.00	2.0	2.0	2.0	2.0	2.0	2.0	2.0
12	Magnesium Stearate	4.0	4.0	4.0	4.0	4.0	4.0	4.0	4.0	4.0
	Total	150.0	150.0	150.0	150.0	150.0	150.0	150.0	150.0	150.0

5.2 Procedure:

5.2.1 Dispensing and Sifting

- a) Dispensed quantity of Drug, Pharmaburst 500 / Ludiflash / Pearlitol, Crospovidone / Croscarmellose Sodium / Sodium Starch Glycolate, Avicel pH 102, Sucralose and Colloidal Silicon dioxide were sifted through #40 mesh.
- b) Talc and Magnesium Stearate were sifted through #60 mesh.

5.2.2 Blending and Lubrication:

- a) Material of Step 1.a was transferred to a Double Cone blender and the material was blended for 15 minutes at 20 RPM.
- b) To the above blended material, sifted Magnesium Stearate was added and the blend was lubricated for 5 minutes at 20 RPM.

The blend was then evaluated for pre-compaction parameters.

5.2.3 Compression:

The blend from step 2.b was compressed using Multi punch Tablet compression machine from Cadmach machinery using a 5.5 mm round tip punch sets.

The tablets were then evaluated for post compression parameters of ODT.

5.3 Application of factorial design

Based on the trial batches results, statistical design was applied for optimization of final formulation. It was observed that the amount of super disintegrant and the directly compressible excipient is critical and the physicochemical parameters was depends on the both factors. Hence, factorial design was applied by taking crospovidone and Pharmaburst 500 as an independent variable. 2^2 factor 2 level factorial design was applied as per below;

Table 03 Factorial Design table

Independent Variable	Low	Center Point	High
Crospovidone	5.0	7.5	10
Pharmaburst 500	40	50	60
Dependant Variable			
Y1=Disintegration Time			
Y2=Drug Release at 2 min			

Table 04 Formulation table for Factorial batches

Sr. No.	Ingredients (mg)	P1	P2	P3	P4
1	Brivaracetam	10.0	10.0	10.0	10.0
2	Pharmaburst 500 [®]	40.00	40.00	60.00	60.00
3	Crospovidone	5.0	10.0	5.0	10.0
4	Avicel pH 102	81	76	61	56
5	Sucralose	4.0	4.00	4.00	4.00
6	Colloidal Silicon Dioxide	4.0	4.00	4.00	4.00
7	Talc	2.0	2.00	2.00	2.00
8	Magnesium Stearate	4.0	4.00	4.00	4.00
	Total	150.0	150.0	150.0	150.0

Evaluation of factorial batches was done as per trial batches and the results were recorded in results and discussion chapter.

5.4 PRE-COMPRESSION PARAMETERS

Precompression parameters of all the blends (F1 to F9) and it was observed that there was no significant difference amongst all the blends in terms of flowability and compressibility. It could be possible because of the fact that most of the property of the blend is governed by the excipients which include diluents in major. All pre compression parameters are tabulated below:

Table 05 Results of Pre-Compression Parameters of blend

Batch	Angle of Repose (θ) (n=3)	Bulk Density (g/ml) (n=3)	Tapped Density (g/ml) (n=3)	Hausner's Ratio (n=3)	Carr's Consolidation Index (%) (n=3)
F1	22.8 \pm 0.3	0.311 \pm 0.004	0.482 \pm 0.003	1.550 \pm 0.021	35.477 \pm 0.035
F2	23.9 \pm 0.5	0.350 \pm 0.001	0.468 \pm 0.004	1.337 \pm 0.011	25.214 \pm 0.024
F3	25.0 \pm 0.7	0.341 \pm 0.002	0.480 \pm 0.001	1.408 \pm 0.023	28.958 \pm 0.032
F4	27.4 \pm 0.4	0.372 \pm 0.002	0.489 \pm 0.003	1.315 \pm 0.020	23.926 \pm 0.014
F5	26.3 \pm 0.6	0.339 \pm 0.004	0.479 \pm 0.001	1.413 \pm 0.011	29.228 \pm 0.031
F6	24.5 \pm 0.5	0.352 \pm 0.003	0.457 \pm 0.002	1.298 \pm 0.013	22.976 \pm 0.025
F7	25.7 \pm 0.5	0.361 \pm 0.002	0.469 \pm 0.001	1.299 \pm 0.031	23.028 \pm 0.017
F8	22.0 \pm 0.3	0.340 \pm 0.005	0.472 \pm 0.002	1.388 \pm 0.022	27.966 \pm 0.031
F9	23.4 \pm 0.4	0.345 \pm 0.003	0.461 \pm 0.003	1.336 \pm 0.010	25.163 \pm 0.031

5.5 Post Compression Parameters:

5.5.1 Weight Variation:

Weight variation was performed to ensure dosage uniformity. The test was carried out by weighing the 20 tablets individually using analytical balance, then calculating the average weight, and comparing the individual tablet weights to the average. The percentage of weight variation was calculated by using the following formula.

Table 06 Weight Variation

Sr. No.	Average Weight of tablets (mg)	Maximum % difference allowed
1	<130	+ 10%
2	130-324	+ 7.5%
3	>324	+ 5%

5.5.2 Thickness:

Thickness will affect the physical appearance of the tablet and will be governed by the compressibility of the blend and the target hardness. It is measured in mm.

5.5.3 Hardness:

Hardness is also so called crushing strength. It is the load required to crush the tablet when placed on its edge. Tablets must be able to withstand the rigors of handling and transportation experienced in the manufacturing plant, in the drug distribution system, and in the field at the hands of the end users (patients/consumers). For these reasons, the mechanical strength of tablets is of considerable importance and is routinely measured. It is measured in Newton or kg/cm² or kilo Newton.

Hardness is a Critical Quality Attribute as it governs a balance between Disintegration Time and Friability.

5.5.4 Friability:

Friability is defined as the % weight loss by tablets due to mechanical action during the test. It refers to the ability of the compressed tablet to avoid fracture and breaking during transport.

Friability of a tablet is calculated by below mentioned formula:

$$\% \text{friability} = (1 - \text{Final weight} / \text{Initial weight}) * 100$$

5.5.5 Disintegration Time:

Disintegration Time is the most important Critical Quality Attribute for an Orodispersible. The in vitro disintegration studies were carried out using a digital tablet disintegration test apparatus (Electrolab, India). One tablet was placed in each of the 6 tubes of the basket assembly and then disk was added to each tube. This assembly was then suspended in a 1-liter beaker containing water with its temperature being maintained at $37 \pm 2^\circ\text{C}$. The basket was then moved up and down through a distance of 5 to 6 cm, at the frequency of 28 to 32 cycles per minute. The time required for complete disintegration of the tablet was recorded.

5.5.6 Wetting Time and Water Absorption Ratio:

The Wetting Time of the tablets was evaluated (n = 6). This experiment mimics the action of saliva in contact with tablet. A Whatman filter paper disk folded once diametrically was placed in a petri dish. A small volume (10 ml) of water containing the water soluble dye, Rhodamine B (0.1 g) was added to the filter paper on the petri dish. The tablet was carefully placed on the filter paper at t = 0 and the time for complete wetting were measured. Complete coloring the tablet was taken as a sign for complete wetting. The wetted tablet was then weighed and water AR was determined according to the Equation mentioned below

$$\text{Absorption Ratio} = 100 \times (W_a - W_b) / W_b$$

Where W_a and W_b are the tablet weights after and before wetting

5.5.7 Dissolution:

The release rate of Brivaracetam from ODTs was determined using United State Pharmacopoeia (USP) dissolution testing apparatus Type II (paddle method). The dissolution test was performed using 900 ml of 0.1N HCl pH 1.2 as dissolution medium, at $37 \pm 0.5^\circ\text{C}$ and 50 rpm. A sample (5 ml) of the solution was withdrawn from the dissolution apparatus at 5, 10, 15, 20 and 30 minutes. The samples were filtered through a 0.45 membrane filter. The absorbance of these solutions was measured at 225 nm using a Shimadzu spectrophotometer. The cumulative percentage of drug release was calculated using an equation obtained from a standard curve.

6 RESULTS & DISCUSSION

6.1 Preformulation Study

The results and conclusion of the Preformulation studies carried out on Active Ingredients are documented below.

6.1.1 Melting Point Determination:

The melting point of the Active Ingredient was found to be 76°C , which is found to be consistent with that of the reported melting point of pure Brivaracetam. This confirms the purity of the material.

6.1.3 Physical Characterization of the drug:

Observations from the test results of physical characterization of the drug are tabulated below:

Table 0.7 Results of Physical Characterization of Brivaracetam

Sr. No.	Test	Results	Inference
1	Angle of Repose	47.8	Poor flow
2	Bulk Density (g/ml)	0.15	-
3	Tapped Density (g/ml)	0.21	-
4	Hausner's Ratio	1.40	Poor flow
5	Carr's Consolidation Index	28.6	Poor flow

6.1.4 Solubility Studies:

The solubility of pure Brivaracetam was evaluated in different media and the results were recorded in the table below. Results are tabulated below:

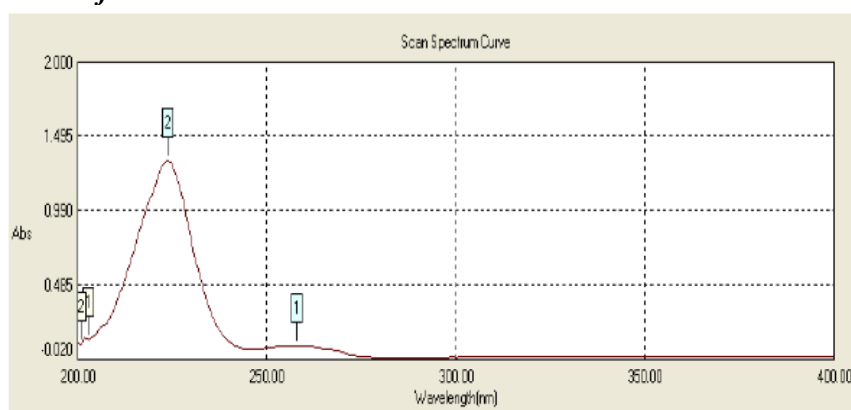
Table 0.8 Solubility Studies Data

Sr. No.	Media	Solubility (mg/ml)
1	Purified Water	8.2
2	pH 1.2 HCl buffer	9.5
3	pH 4.5 acetate buffer	7.5
4	pH 6.8 phosphate buffer	8.4

6.1.5 ANALYTICAL METHOD FOR ESTIMATION

6.1.5.1 UV ABSORPTION

Figure 0.2 λ_{max} of Pure Brivaracetam



Scanning the Brivaracetam stock solution showed that the λ_{max} of drug was 225 nm and all further analysis will be done at this particular wavelength.

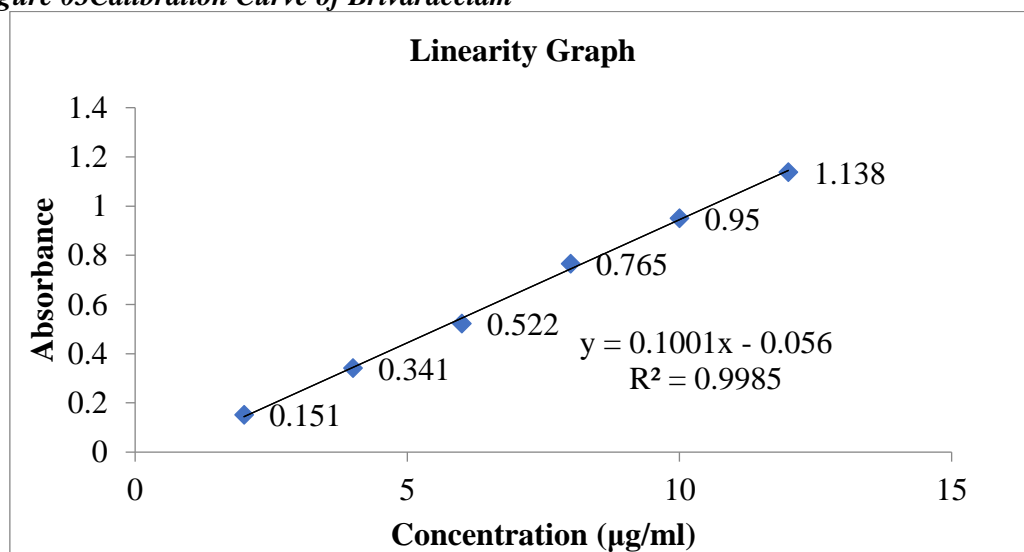
6.1.5.2 STANDARD CALIBRATION CURVE

The calibration curve was found to be linear in the concentration range of 2-12 $\mu\text{g/ml}$ In 0.1 N HCl at its λ_{max} , 225 nm. The coefficient of correlation (R^2) was found to be $R^2 = 0.998$.

Table 9 Calibration curve

Concentration (µg/ml)	I	II	III	Absorbance ± SD
2	0.150	0.151	0.152	0.151 ± 0.04
4	0.343	0.341	0.339	0.341 ± 0.03
6	0.520	0.522	0.524	0.522 ± 0.02
8	0.760	0.770	0.765	0.765 ± 0.02
10	0.950	0.945	0.955	0.950 ± 0.03
12	1.135	1.138	1.141	1.138 ± 0.05

Figure 03 Calibration Curve of Brivaracetam



6.1.6 DRUG-EXCIPIENT COMPATIBILITY

Figure 04 FT-IR Spectrum of Brivaracetam

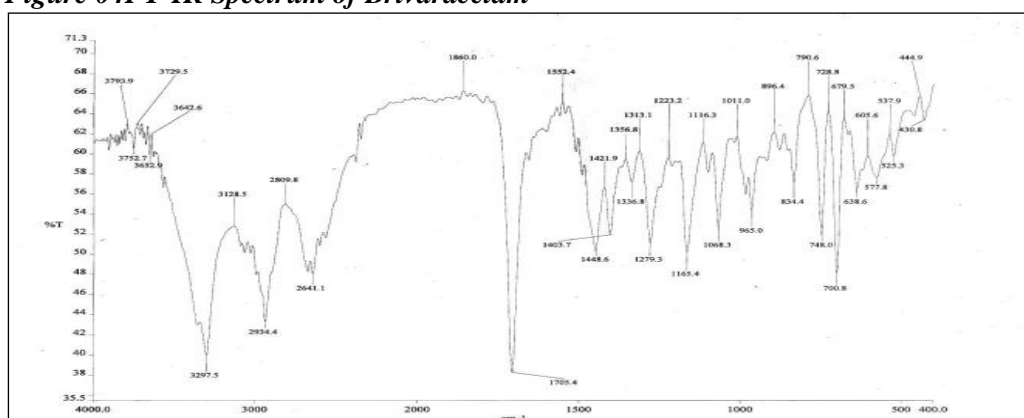
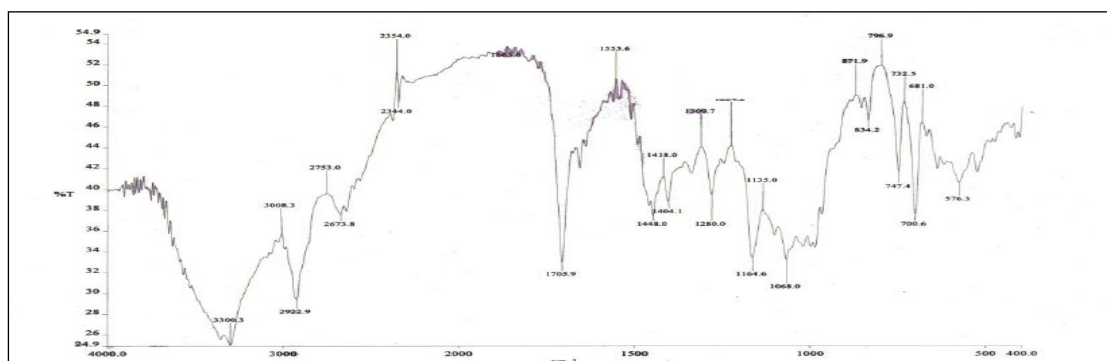


Figure 05 FT-IR Spectrum of Brivaracetam + excipients of optimized formulation



The graph is evident of the fact that all the functional groups of Brivaracetam are maintained in the spectrum of drug + excipients. Hence it can be concluded that all the excipients used in the formulation of ODT are compatible with the drug.

Table 010 FTIR Interpretation

Functional group	FTIR Region	Observed frequency in Pure Drug (cm ⁻¹)	Observed frequency in Formulation (cm ⁻¹)	Conclusion
C-H	2960-2850	2809.8	2922.9	<i>No Interaction</i>
C=O	1700-1725	1705.4	1705.9	
O-H	1200-1500	1279.3	1280.0	
N-H	1500-1700	1448.6	1448.0	

6.2.2 PRE-COMPRESSION PARAMETERS

Precompression parameters of all the blends (F1 to F9) and it was observed that there was no significant difference amongst all the blends in terms of flowability and compressibility. It could be possible because most of the property of the blend is governed by the excipients which include diluents in major. All pre-compression parameters are tabulated below:

Table 011 Results of Pre-Compression Parameters of blend

Batch	Angle of Repose (θ) (n=3)	Bulk Density (g/ml) (n=3)	Tapped Density (g/ml) (n=3)	Hausner's Ratio (n=3)	Carr's Consolidation Index (%) (n=3)
F1	22.8 ± 0.3	0.311 ± 0.004	0.482 ± 0.003	1.550 ± 0.021	35.477 ± 0.035
F2	23.9 ± 0.5	0.350 ± 0.001	0.468 ± 0.004	1.337 ± 0.011	25.214 ± 0.024
F3	25.0 ± 0.7	0.341 ± 0.002	0.480 ± 0.001	1.408 ± 0.023	28.958 ± 0.032
F4	27.4 ± 0.4	0.372 ± 0.002	0.489 ± 0.003	1.315 ± 0.020	23.926 ± 0.014
F5	26.3 ± 0.6	0.339 ± 0.004	0.479 ± 0.001	1.413 ± 0.011	29.228 ± 0.031
F6	24.5 ± 0.5	0.352 ± 0.003	0.457 ± 0.002	1.298 ± 0.013	22.976 ± 0.025
F7	25.7 ± 0.5	0.361 ± 0.002	0.469 ± 0.001	1.299 ± 0.031	23.028 ± 0.017
F8	22.0 ± 0.3	0.340 ± 0.005	0.472 ± 0.002	1.388 ± 0.022	27.966 ± 0.031
F9	23.4 ± 0.4	0.345 ± 0.003	0.461 ± 0.003	1.336 ± 0.010	25.163 ± 0.031

6.2.2 POST COMPRESSION PARAMETERS:

6.2.2.1 Weight Variation:

Weight Variation of all the Formulations was found well within the prescribed Pharmacopoeial limits of NMT 7.5 %. A good flow could be attributed to diluent selection which has a substantial effect on powder flow.

6.2.2.2 Thickness:

All the formulations were compacted to achieve a target hardness of 4.5 kg/cm². All the formulations showed a similar thickness profile.

6.2.2.3 Hardness:

Target Hardness was optimized to 4.5 kg/cm² keeping in mind the tablet weight and dimensions. All the formulations showed very good compressibility which could be due to choice of ODT platform used in the formulation.

6.2.2.4 Friability:

Friability for all the formulation was well below the Pharmacopoeial limit of NMT 1.0%. Proper selection of hardness and a good compactability of the blend resulted in a satisfactory friability result.

6.2.2.5 Disintegration Time:

The most important attribute of an ODT is Disintegration Time. For an Orodispersible tablet, the Pharmacopoeial limit is NMT 3 minutes. All the formulations passed this limit. However, for a tablet to be claimed as an Orally Disintegrating Tablet, as per USP, the limit is not more than 30 sec. Formulations F8 and F9 matched these criteria. Hence the level of super disintegrant was finalized as per trial F8.

6.2.2.6 Wetting Time and Water Absorption Ratio:

Wetting Time results were comparable to the Disintegration Time showing a good correlation to the grade and level of super disintegrants. Formulation F9 with the highest level of Crospovidone XL 10 showed the least amount of Wetting Time. Since Crospovidone XL 10 absorbs a great amount of water by a wicking mechanism, its Water Absorption Ratio is also the highest.

6.2.2.7 Dissolution:

Dissolution was rapid for all the formulations as all the formulations had a disintegration time below 2 minutes. All formulations showed comparable dissolution with F8 showing >90% of drug release at 10 minutes with least disintegrant level.

Table 012 Results of Post-Compression Parameters

Formulations	Weight Variation (mg) (n=20)	Thickness (mm) (n=3)	Hardness (kg/cm ²) (n=3)	Friability (%)
F1	148 ± 2.6	3.80 ± 0.23	5.3 ± 0.9	0.39
F2	151 ± 3.1	3.78 ± 0.31	4.1 ± 1.2	0.31
F3	150 ± 3.7	3.76 ± 0.11	7.4 ± 0.8	0.41
F4	149 ± 2.1	4.08 ± 0.20	6.9 ± 1.1	0.30
F5	152 ± 3.3	4.05 ± 0.17	5.5 ± 0.4	0.32
F6	151 ± 2.0	4.03 ± 0.11	4.9 ± 0.3	0.34
F7	153 ± 3.0	4.05 ± 0.22	4.7 ± 0.4	0.31
F8	149 ± 2.4	4.09 ± 0.15	5.5 ± 0.3	0.29
F9	152 ± 2.9	4.00 ± 0.11	4.9 ± 0.1	0.28

Table 013 Results of Post-Compression Parameters

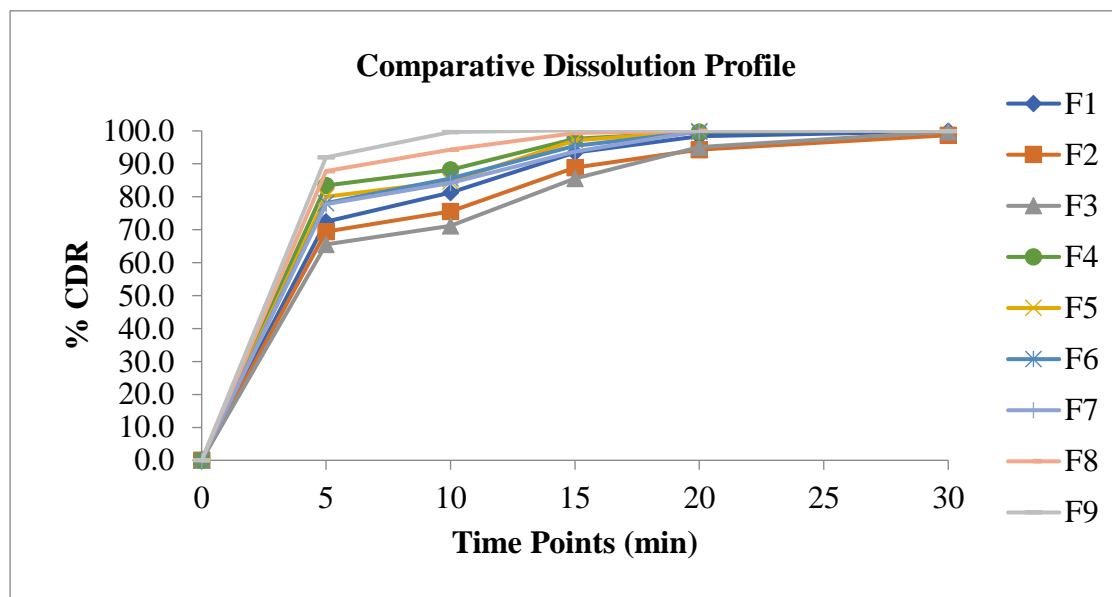
Formulations	Disintegration Time (sec) (n=6)	Water Absorption Ratio (%) (n=3)	Wetting Time (sec) (n=3)	Assay (%) (n=3)
F1	37 ± 3.5	61.7 ± 4.5	75 ± 5.9	98.9 ± 1.3
F2	49 ± 1.9	48.6 ± 2.9	84 ± 4.8	99.2 ± 1.2
F3	62 ± 2.8	35.3 ± 1.9	92 ± 6.5	100.3 ± 0.3
F4	31 ± 4.6	68.4 ± 2.7	65 ± 5.4	99.6 ± 0.4
F5	35 ± 3.4	65.9 ± 3.9	72 ± 3.6	99.4 ± 1.0
F6	38 ± 3.7	57.3 ± 1.8	75 ± 4.8	99.9 ± 0.6
F7	34 ± 4.6	67.9 ± 1.8	70 ± 4.9	100.1 ± 0.2
F8	27 ± 1.9	75.1 ± 3.8	54 ± 6.1	101.3 ± 0.1
F9	24 ± 3.7	85.3 ± 4.1	51 ± 2.3	100.4 ± 0.3

Table 014 Results of Dissolution Studies

Formulations	% Cumulative Drug Release in 900 ml, 0.1N HCl, at 50 RPM Paddle					
	Time	5 min	10 min	15 min	20 min	30 min
F1	%CDR	72.4	81.3	93.4	98.4	99.9
	SD	3.4	3.2	3.0	2.2	1.7
F2	%CDR	69.4	75.6	88.9	94.3	98.7
	SD	3.1	3.6	3.1	2.2	2.1
F3	%CDR	65.5	71.2	85.6	95.1	99.8
	SD	2.3	2.4	1.6	1.4	1.2
F4	%CDR	83.4	88.2	97.6	99.7	100.2
	SD	4.9	3.2	2.1	1.7	1.6
F5	%CDR	80.0	84.7	97.1	99.9	101.3
	SD	4.5	3.2	1.4	1.5	1.5
F6	%CDR	78.1	85.6	95.5	99.8	100.1
	SD	4.1	4.2	3.1	2.7	1.9
F7	%CDR	77.8	84.2	93.7	99.9	100.4
	%SD	3.2	2.1	3.0	2.7	2.2
F8	%CDR	87.8	94.3	99.4	100.0	100.3
	%SD	2.1	3.9	3.1	1.7	1.6
F9	%CDR	92.0	99.7	100.2	100.1	99.9
	%SD	3.3	1.6	1.5	1.5	1.4

Figure 6.4 Comparative Dissolution Profile

6.4 Analysis of Factorial Design



Factorial batches were taken and their evaluation parameters were compiled to check the effect of independent factors. 2 factors 2 levels of full factorial design was selected and the data was fitted in Minitab software for analysis. Following are the details collected from DoE software.

Table 09 Factorial Design table

Run Order	Center Pt	Blocs	Crospovidone	Pharmaburst 500	Disintegration Time (sec)	Dissolution at 2 min
1	1	1	5	60	19	33.4
2	1	1	5	40	42	25.8
3	1	1	10	60	8	49.1
4	1	1	10	40	29	40.9

ANOVA for Drug release at 2 min

Table 010 Analysis of Variance for Drug release at 2 min

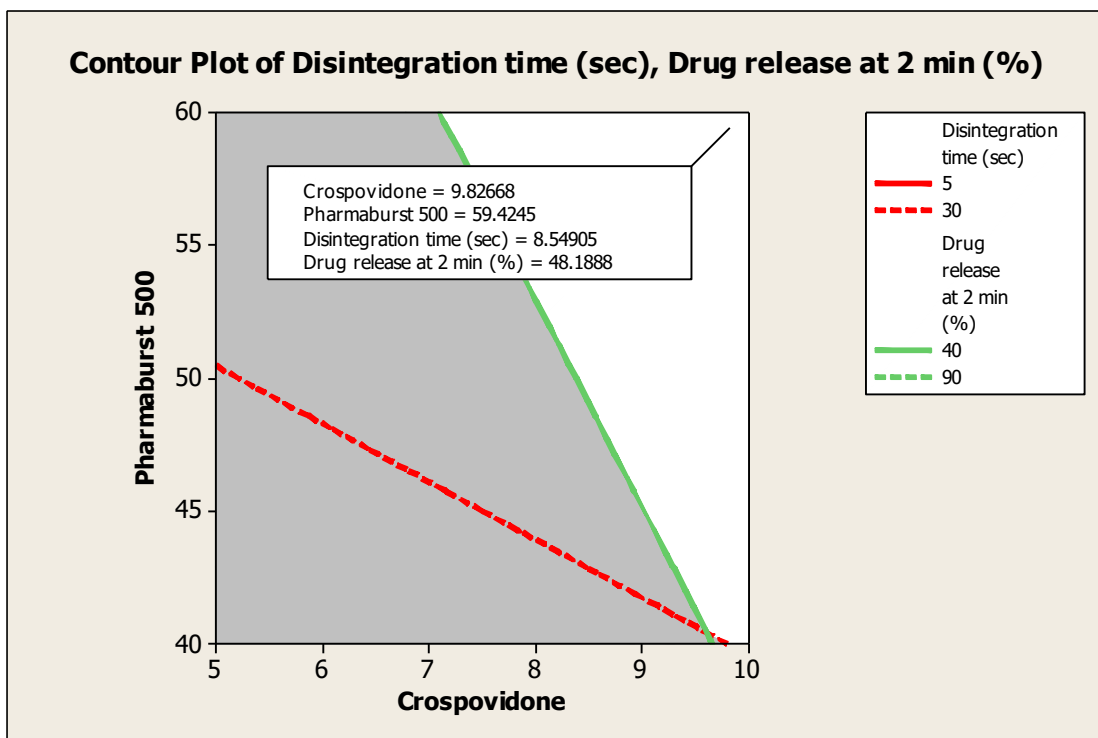
Source	DF	Seq SS	Adj SS	F value	P value	Remarks
Main Effects	2	299.570	299.570	1664.28	0.017	<i>Significant</i>
Crospovidone	1	237.160	237.160	2635.11	0.012	<i>Significant</i>
Pharmaburst 500	1	62.410	62.410	693.44	0.024	<i>Significant</i>
Residual Error	1	0.090	0.090	-	-	-
Total	3	299.660	-	-	-	-

ANOVA table for Drug release at 2 min shows that the Crospovidone and Pharmaburst 500 both have a significant impact.

6.5 Optimized Batch

Based on Factorial Design data, final optimized batch selected from the Contour plot to achieve desired drug release and disintegration. Complete analysis of this batch done and recorded below.

Figure 05 Overlay contour plot for optimized batch



Sr. No.	Ingredients (mg)	P7
1	Brivaracetam	10
2	Pharmaburst 500 [®]	59.4
3	Crospovidone	9.8
4	Avicel pH 102	56.8
5	Sucralose	4.00
6	Colloidal Silicon Dioxide	4.00
7	Talc	2.00
8	Magnesium Stearate	4.00
	Total	150.0

Results of optimized batch

Table 011 Results of Optimized batch

Evaluation Parameters		P7				
Weight Variation (mg) (n=20)		150 ± 2.1				
Thickness (mm) (n=3)		4.10 ± 0.03				
Hardness (kg/cm ²) (n=3)		5.5 ± 0.3				
Friability (%)		0.25				
Disintegration Time (sec) (n=6)		9 ± 2				
Wetting Time (sec) (n=3)		19 ± 1.1				
Water Absorption Ratio (%) (n=3)		70.8 ± 1.7				
Assay (%) (n=3)		99.4 ± 0.8				
Batch	0 min	2 min	4 min	6 min	8 min	10 min
P7	0	47.2 ± 1.6	96.8 ± 1.5	98.2 ± 2.6	99.8 ± 1.1	99.9 ± 0.5

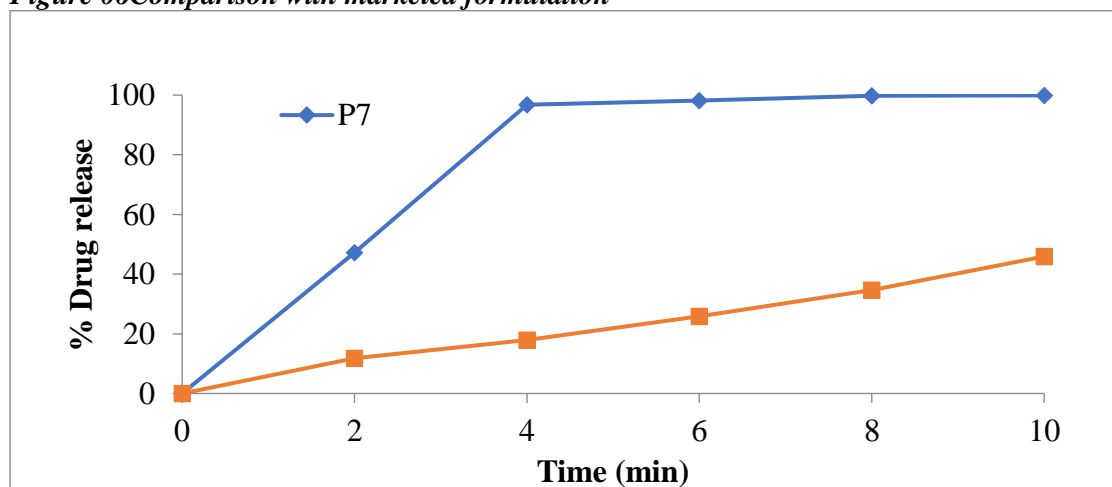
6.6 Comparison with Marketed Product

Final batch P7 was optimized with the marketed product. The dissolution profile was shown below. As the marketed formulation was only conventional tablet hence it gives release more than 85% after 30 min.

Table 012 Comparison with marketed formulation

Batch	2 min	4 min	6 min	8 min	10 min
P7	47.2 ± 1.6	96.8 ± 1.5	98.2 ± 2.6	99.8 ± 1.1	99.9 ± 0.5
Marketed Product	11.8 ± 2.6	17.9 ± 3.4	25.8 ± 1.9	34.6 ± 2.8	45.9 ± 1.7

Figure 06 Comparison with marketed formulation



6.7 Stability Study

Stability study of final optimized batch P7 performed for 1 month at 40°C and 75% RH. Initial results and after 1 month results compared and found satisfactory. The batch was found stable during stability. The results were recorded in below table.

Table 013 Stability study of P7 batch

Evaluation Parameters	Initial	After 1 month
Appearance	Complies	Complies
Disintegration Time (sec)	9 ± 2	10 ± 2.2
Assay (%)	99.4 ± 0.8	99.1 ± 1.1
% Drug release after 10 min	99.9 ± 0.5	99.9 ± 0.2

7 CONCLUSION

Orodispersible tablets of Brivaracetam were successfully formulated by Direct Compression method. Preformulation studies of drug were performed; the infrared spectral analysis studies revealed that there is no chemical interaction with excipients used was compatible with drugs. Risk Assessment of Formulation Variables showed that Diluent selection and Type and level of Disintegrants were most likely to affect the CQAs of the ODT. Hence were ranked high. Based on Weight variation, Hardness, friability, Disintegration Time and Dissolution it was found that all the formulation were satisfactory as per Pharmacopoeial Standards. Disintegration Time was <30 sec for formulation F8 and F9. Dissolution was rapid for all the formulations as all the formulations had disintegration time below 2 minutes. All formulations showed comparable dissolution with F9 showing >90% of drug release at 10 minutes with least disintegrant level. Further Optimization of formulation was done using Factorial design (2 factor 2 levels) and established control strategy and design space of the formulation. Validation of design was done and final optimized batch P7 was chosen from the design space. The final formulation P7 was tested for Accelerated Stability Studies for 1 month and found stable.

8 REFERENCES

1. Chinwala M, "Recent Formulation Advances and Therapeutic Usefulness of Orally Disintegrating Tablets (ODTs)." *Pharmacy*, **2020**,8, 186.
2. Hannan P, Khan A and Safiullah S, "Oral dispersible system: A new approach in drug delivery system", *Indian Journal of Pharmaceutical Science*, **2016**, 78 (1), 2-7.
3. Vrushali Mogal, Jaydeep D, Pankaj B, Priya T, Sanjay K, "A review on quality by design", *Pharmaceutical And Biological Evaluations*, **2016**,3(3), 313-319.
4. Lawrence X, Gregory A, Mansoor A, Stephen W, James P, Raju G and Janet W, "Understanding Pharmaceutical Quality by Design", *The AAPS Journal*, **2014**, 16(4), 771-783.
5. Pooja A and Vandana A, "Orodispersible Tablets: A Comprehensive Review," *International Journal of Research and Development in Pharmacy and Life Sciences*, **2013**, 2(2), 270-284.
6. Harsh V, Darshan M, Vikram P, Praful B, Maulik P, "Oral Dispersible Tablet: A Popular Growing Technology", *Asian Journal of Pharmaceutical Research and Development*, **2013**, 1(6), 138-155.
7. Drug Information, December 2021, <https://go.drugbank.com/drugs/DB05541>.
8. Drug Information, December 2021, <https://pubchem.ncbi.nlm.nih.gov/compound/Brivaracetam>.
9. Drug Information, December 2021, <https://www.rxlist.com/briviact-drug.htm>.
10. Drug Information, December 2021, <https://www.drugs.com/briviact.html>.
11. Drug Information, December 2021, https://www.accessdata.fda.gov/drugsatfda_docs/label/2018/205836s005,205837s004,205838s003lbl.pdf.
12. Mushtaq M, Fazal N, "Formulation and Evaluation of Fast-disintegrating Tablets of Flurbiprofen and Metoclopramide." *J Pharm Innov*, **2020**, 1-20.
13. Mane S, Bathe R, Awatade S, "Formulation and Evaluation of Fast Disintegrating Tablets of Atenolol Using Natural and Synthetic Superdisintegrants." *JDDT*, **2019**, 9(2-s), 150-158.

14. Gozde G, Gizem Y, Burcu M, Buket A, Yıldız O, "Formulation Design of the Oral Disintegrating Tablets Including Alfuzosin Hydrochloride with Risk Evaluation via Quality by Design," *Acta Pharmaceutica Scientia*, **2017**, 55 (2), 57-76.
15. Buket A, Gizem Y, Sevim P, Erdal C and Yıldız O, "Optimization of Ondansetron Orally Disintegrating Tablets Using Artificial Neural Networks", *Tropical Journal of Pharmaceutical Research*, **2014**, 13(9), 1374-1383.
16. Tejas B, Tushar R and Suhagia B, "Formulation Development of Donepezil Hydrochloride Oral Disintegrating Tablets Using Quality By Design Approach", *International Journal of Pharmaceutical Sciences and Research*, **2016**, 7(5), 2097-2108.
17. Ashwini R and Bhogale V, "Process Development, Evaluation and Controlling of Parameters during Formulation Development of Granisetron HCl as an ODT by QBD Concept" *International Journal for Pharmaceutical Research Scholars*, **2016**, 5(2), 189-201.
18. Biswajit B, Sajari B, Swati Rawat, "Control strategy of generic loratadine orally disintegrating tablets 10 mg during scalable manufacturing", *Innovations in Pharmaceuticals and Pharmacotherapy*, **2016**, 4(2), 189-195.
19. Swapnil S, Deeliprao V, Ashish B, Sharmin J, Nikita D, "A Review on: Orodispersible Tablet (ODT) Technology - A Novel Approach to Develop the Supergenerics", *International Journal of Pharmaceutical Sciences Review and Research*, **2014**, 26(2), 231-236.
20. Priyanka N, Kusum S, Iti C, Madhu V, Mohd Y, Azad K, Rajat S and Nandini G, "Orally disintegrating tablets : formulation, preparation techniques and evaluation", *Journal of Applied Pharmaceutical Science*, **2011**, 01(04), 35-45.
21. Niranjana B, Swati R, Upendra G, "Formulation and Evaluation of Oral Disintegrating Tablets of Lornoxicam by 3² Factorial Design", *Journal of Applied Pharmaceutical Science*, **2013**, 3(8), S42-S52.
22. Shahabaz S, Soujanya C and Kishore M, "Formulation and Evaluation of Oral Disintegrating Tablets of Nimodipine", *World Journal of Pharmacy And Pharmaceutical Sciences*, **2018**, 7(1), 926-946.
23. Phulzalkar S, Kate B, Bagade M, Shete R, "Formulation Development and Evaluation of Orodispersible Tablets of Quetiapine Fumarate by Sublimation Method", *Asian Journal of Biomedical and Pharmaceutical Sciences*, **2015**, 6 (57), 22-31.
24. Joel M, "Brivaracetam: a newly approved medication for epilepsy", *Future Neurol.* **2019**, 14(3), 1-22.
25. Christian O, Shikiko W, Suzanne M, Armel S, "Relative Bioavailability and Bioequivalence of Brivaracetam 10 mg/mL Oral Solution and 50-mg Film-Coated Tablet", *Clinical Pharmacology in Drug Development*, **2017**, 6(3), 313-317.
26. Stefano B, Gian L, Mariarosaria V, "Brivaracetam for the treatment of focal-onset seizures: pharmacokinetic and pharmacodynamic evaluations." *Expert Opinion on Drug Metabolism & Toxicology*, **2020**, 16(10), 853-863.

PCP425
SCREENING STUDY OF TRANSFEROSOMAL FORMULATION
OF RASAGILINE MESYLATE BY PLACKETT - BURMAN
DESIGN

AP0454
Shivani M. Patel
PhD, Research Scholar
Parul university
rxpatelshivani@gmail.com

AP0412
Dr. Lalit Lata Jha

Parul university

Abstract

The aim of the given study is to perform screening of various process and formulation parameters to check its significant effect on formulation of Transfersomes by using Plackett-Burman design. Screening of lipid, edge activators and other process parameters are crucial as they significantly affect the formulation of Transfersomes. These factors can affect the vesicle size and entrapment efficiency of formulation. Transfersomes are vesicular carriers used in transdermal drug delivery systems and therefore effect of variables on vesicle size must be taken into consideration. In the present study 8 factors including amount of lipid, amount of edge activators and other process variables were taken for the preparation of Transfersomes of Rasagiline Mesylate. By using Plackett and Burman domain of matrix total 12 batches were obtained and responses taken were vesicle size and entrapment efficiency of Transfersomes. For particle size value of sb^2 is 5.747 and among 11 factors 3 factors shows b value higher than 5.74, for entrapment efficiency value of sb^2 is 3.44 and among 11 factors 3 factors shows b value higher than 3.44. Based on results co-efficient of 12 batches for each variable, amount of lipid, amount of edge activator and sonication time are selected as significant variables. Further optimization study of Transfersomes of Rasagiline Mesylate can be done by using these three variables.

Key words: Screening, Variables, Plackett and Burman design, Transfersomes.

INTRODUCTION:

The Plackett Burman screening design was used for identification of various process variables and formulation variable to check significant effect. The Plackett Burman design is also known as Hadamard design of screening. Total 12 experimental batches were obtained for the screening The Plackett Burman design estimate eight coefficient or effects and additionally a constant term. This design is shortest screening design which gives design matrix in multiplication of 4 experiments the design is also very well known as Hadamard design.[1-7] 8 quantitative variables are selected for the screening at 2 levels +1 and -1. Here, X1 to X8 are real variables and X 10 to 12 are dummy or false variables and do not correspond to any actual factor and therefor omitted. So, experimental domain shows 12 variables with 12 experimental runs. Variable to be studied are amount of lipid, amount of edge activator, amount of hydration media, amount of alcohol, hydration time, temperature, sonication time and rotation speed.[8,9] Calculation of the effect

b_0 = average of responses

$$b_1 = (y_1 - y_2 + y_3 - y_4 - y_5 - y_6 + y_7 + y_8 + y_9 - y_{10} + y_{11} - y_{12}) / 12$$

$$b_2 = (y_1 + y_2 - y_3 + y_4 - y_5 - y_6 - y_7 + y_8 + y_9 + y_{10} - y_{11} - y_{12}) / 12$$

$$b_3 = (-y_1 + y_2 + y_3 - y_4 + y_5 - y_6 - y_7 - y_8 + y_9 + y_{10} + y_{11} - y_{12}) / 12$$

$$b_4 = (y_1 - y_2 + y_3 + y_4 - y_5 + y_6 - y_7 - y_8 - y_9 + y_{10} + y_{11} - y_{12}) / 12$$

$$b_5 = (y_1 + y_2 - y_3 + y_4 + y_5 - y_6 + y_7 - y_8 - y_9 - y_{10} + y_{11} - y_{12}) / 12$$

$$b_6 = (y_1 + y_2 + y_3 - y_4 + y_5 + y_6 - y_7 + y_8 - y_9 - y_{10} - y_{11} - y_{12}) / 12$$

$$b_7 = (-y_1 + y_2 + y_3 + y_4 - y_5 + y_6 + y_7 - y_8 + y_9 - y_{10} - y_{11} - y_{12}) / 12$$

$$b_8 = (-y_1 - y_2 + y_3 + y_4 + y_5 + y_6 + y_7 + y_8 - y_9 + y_{10} - y_{11} - y_{12}) / 12$$

$$b_9 = (-y_1 - y_2 - y_3 + y_4 + y_5 + y_6 - y_7 + y_8 + y_9 - y_{10} + y_{11} - y_{12})/12$$

$$b_{10} = (y_1 - y_2 - y_3 - y_4 + y_5 + y_6 + y_7 - y_8 + y_9 + y_{10} - y_{11} - y_{12})/12$$

$$b_{11} = (-y_1 + y_2 - y_3 - y_4 - y_5 + y_6 + y_7 + y_8 - y_9 + y_{10} + y_{11} - y_{12})/12$$

sb² = average value of responses form dummy variable (X9+X10+X11/3)²

MATERIALS AND METHOD

Rasagiline mesylate was procured from Benzchem Enterprise Vadodara, Phospholipon 90 G was gifted by lipoid Germany, Sodium Deoxycholate, dihydrogen potassium phosphate, dihydrogen sodium phosphate and sodium chloride were procured Chemdyes Corporation, Rajkot.

METHOD FOR PREPARATION OF TRANSFEROSOMES

The film hydration method was used to prepare Transferosomes. Given quantity of lipid and edge activator were dissolved in chloroform in round bottom flask. Round bottom flask was attached to rotary evaporator to form thin and uniform film. Hydrated formed film with 7.4 pH phosphate buffer saline in which Rasagiline mesylate was dissolved. Allow vesicles to hydrate for about 2 hours at room temperature. The hydrated Transferosomal solution was then subjected to sonication for further size reduction.[10-12]

METHOD FOR DETERMINATION OF ENTRAPMENT EFFICIENCY

Transferosomal solution equivalent to 1 mg API was placed in centrifuge tube and centrifugation was done. Supernatant was collected and absorbance was checked to find concentration. Following equation was used to determine %EE[13,14].

$$\text{Entrapment efficiency} = (\text{amount entrapped} / \text{total amount added}) * 100$$

METHOD FOR DETERMINATION OF VESICLE SIZE

Vesicle size of Transferosomes was determined by using zeta sizer. Transferosomal solution was kept in cuvette and allowed to scan [13,14].

Table:1 Experimental domain for a screening of significant factors

Factors	Associated variables	Levels	
		-1	+1
Amount of lipid(gm)	X1	0.5	2
Amount of edge activator(mg)	X2	25	100
Amount of hydration media(ml)	X3	10	30
Amount of alcohol(ml)	X4	5	10
Hydration time(hrs)	X5	0.5	2
Temperature(°C)	X6	40	60
Sonication time(min)	X7	05	15
Rotation speed (RPM)	X8	50	100

Table:2 Placket-Burman design matrix for 11 factors and 12 runs

No of runs	X1	X2	X3	X4	X5	X6	X7	X8	X9	X10	X11
1	+	+	-	+	+	+	-	-	-	+	-
2	-	+	+	-	+	+	+	-	-	-	+
3	+	-	+	+	-	+	+	+	-	-	-
4	-	+	-	+	+	-	+	+	+	-	-
5	-	-	+	-	+	+	-	+	+	+	-
6	-	-	-	+	-	+	+	-	+	+	+
7	+	-	-	-	+	-	+	+	-	+	+
8	+	+	-	-	-	+	-	+	+	-	+
9	+	+	+	-	-	-	+	-	+	+	-

10	-	+	+	+	-	-	-	+	-	+	+
11	+	-	+	+	+	-	-	-	+	-	+
12	-	-	-	-	-	-	-	-	-	-	-

RESULTS

For formulation of Transfersomes of Rotigotine HCL and Rasagiline mesylate various factors were taken for screening purpose, two responses were taken to identify significant and non-significant factors and are particle size and entrapment efficiency. Trial batches were taken with the reference of experimental domain and results were recorded. Effects, b_0 and Sb^2 values were calculated with given formula. The effects give values from b^1 to b^u were compared and significance of factors were checked by using Sb^2 values for each response. Value of b greater than Sb^2 is consider as significant factors and others are nonsignificant. For particle size value of Sb^2 is 5.74 so among 11 factors 3 factors shows b value higher than 5.74, For entrapment efficiency value of Sb^2 is 3.44 so among 11 factors 3 factors shows b value higher than 3.44. These three factors are considered as significant factors and are amount of lipid, amount of edge activator, sonication time (table no.4). The responses result obtained were plotted in pareto chart.

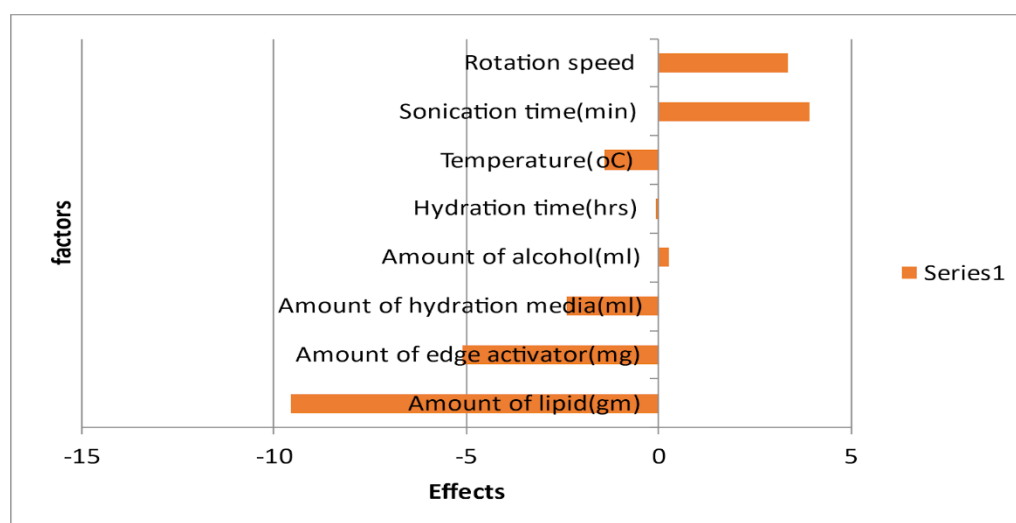
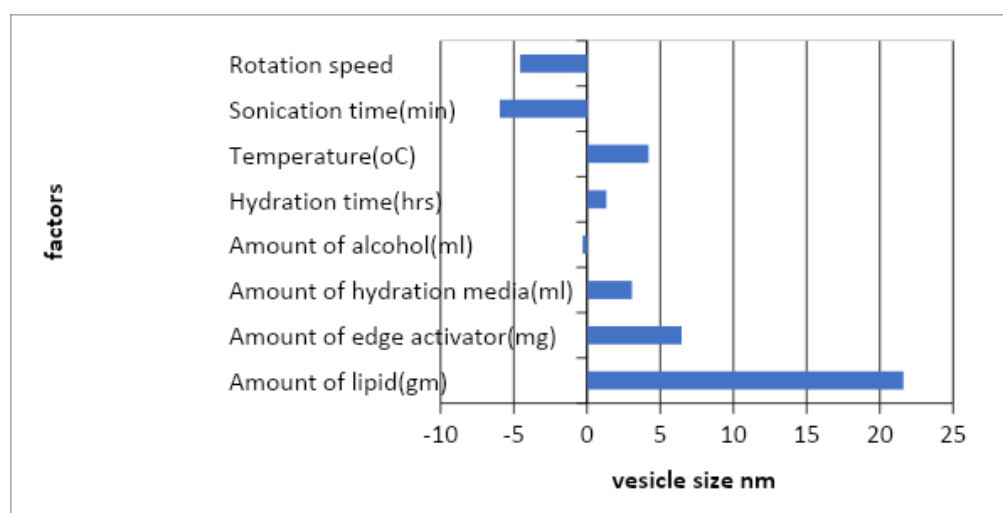
Table:3 Placket-Burman design matrix with results

Runs	X1 (gm)	X2 (mg)	X3 (ml)	X4 (ml)	X5 (hr)	X6 (°C)	X7 (min)	X8 (RPM)	Y1 (nm)	Y2 (%)
1	2	100	10	10	2	60	10	50	112	32
2	0.5	100	30	5	2	60	30	50	88.58	42
3	2	25	30	10	0.5	60	30	100	98.8	45
4	0.5	100	10	10	2	40	30	100	62.8	70
5	0.5	25	30	5	2	60	10	100	59.69	71
6	0.5	25	10	10	0.5	60	30	50	55.17	73
7	2	25	10	5	2	40	30	100	77.89	54
8	2	100	10	5	0.5	60	10	100	132	35
9	2	100	30	5	0.5	40	30	50	102	46
10	0.5	100	30	10	0.5	40	10	100	62.4	51
11	2	25	30	10	2	40	10	50	128	37
12	0.5	25	10	5	0.5	40	10	50	62.68	57

Table:4 Results of Packet-Burman (Hadamard) design

Parameters	Parameters	vesicle size (Sb^2)	%EE(Sb^2)
Average	B0	86.8	51.01
Amount of lipid	B1	21.61	-9.58

Amount of E. E	B2	6.46	-5.08
Amount of hydration media	B3	3.08	-2.42
Amount of alcohol	B4	-0.31	0.25
Hydration time	B5	1.33	-0.083
Temperature	B6	4.21	-1.412
Sonication time	B7	-5.96	3.92
Rotation speed	B8	-4.57	3.25
Sb ²	Sb ²	5.75	3.44



DISCUSSION

The aim of this presented study was screening of significant and non-significant factors which affects the formulation. With 8 independent and 2 dependent variable, 12 batches were obtained by using design expert software (version 7.0.0). Total 8 factors were selected for the study and were checked that which of them are most effective. Particle size and entrapment efficiency of resultant batches were checked. For further analysis pareto chart was obtained and from which standardized effects gave significant and non-significant factors. Particle size of different batches was obtained in the range of 55.17nm to 122nm, entrapment efficiency was obtained in the range of 32-73%. Significant factors were used for optimization of formulation. Amount of lipid, amount of surfactant and sonication time.

CONCLUSION

The study was carried out for screening of significant and non-significant variable which can affects the vesicle size and entrapment efficiency of transferosomes. The study has been performed by formulating batches obtained from design expert software (version 7.0.0). vesicle size and entrapment efficiency of all 12 batches were checked. Amount of lipid, amount of surfactant and sonication time were found to be most effective variables for the formulation of transferosomes based on sb^2 value. The result of ANOVA shows p value $> F$ for both responses. These significant variables will be optimized by using box-Behnken design for the formulation of transferosomes for the treatment of Parkinson's disease.

REFERENCES

1. Karlapudi AP, Krupanidhi S, Reddy R, et al.(2018). Plackett-Burman design for screening of process components and their effects on production of lactase by newly isolated *Bacillus* sp. VUVD101 strain from Dairy effluent. Beni-Suef University journal of basic and applied sciences 7(4),pp. 543-546.
2. Smith ZD, Keller JR, Bello M, et al.(2016). Plackett–Burman experimental design to facilitate syntactic foam development. Journal of Applied Polymer Science 133(1).
3. Sahu PK, Ramiseti NR, Cecchi T, et al.(2018). An overview of experimental designs in HPLC method development and validation. Journal of pharmaceutical and biomedical analysis 147,pp. 590-611.
4. Sahu AK, Jain V.(2017). Screening of process variables using Plackett–Burman design in the fabrication of gedunin-loaded liposomes. Artificial cells, nanomedicine, and biotechnology 45(5), pp. 1011-1022.
5. Mueanmas C, Indum P.(2019). Application of plackett-burman design on screening the factors affecting torrefaction of palm kernel shell. IOP Conference Series: Earth and Environmental Science;IOP Publishing.
6. Kuchekar AB, Pawar AP.(2014). Screening of factors using Plackett Burman design in the preparation of Capecitabine-loaded nano polymeric micelles. Int J Pharm Pharm Sci 6(4),pp. 489-496.
7. Ekpenyong MG, Antai SP, Asitok AD, et al.(2017). Plackett-Burman design and response surface optimization of medium trace nutrients for glycolipopeptide biosurfactant production. Iranian Biomedical Journal 21(4),pp. 249.
8. Rutu BP, Parikh R.(2012). Preparation and formulation of transferosomes containing an antifungal agent for transdermal delivery: Application of Plackett-Burman design to identify significant factors influencing vesicle size. Journal of Pharmacy & Bioallied Sciences.
9. Lewis GA, Mathieu D, Phan-Tan-Luu R.(1998). Pharmaceutical experimental design. CRC press.
10. Dudhipala N, Phasha Mohammed R, Adel Ali Youssef A, et al.(2020). Effect of lipid and edge activator concentration on development of aceclofenac-loaded transferosomes gel for transdermal application: In vitro and ex vivo skin permeation. Drug development and industrial pharmacy 46(8),pp. 1334-1344.
11. Wu P-S, Li Y-S, Kuo Y-C, et al.(2019). Preparation and evaluation of novel transferosomes combined with the natural antioxidant resveratrol. Molecules 24(3),pp. 600.
12. Ahmed TA.(2015). Preparation of transferosomes encapsulating sildenafil aimed for transdermal drug delivery: Plackett–Burman design and characterization. Journal of liposome research 25(1),pp. 1-10.
13. Tawfeek HM, Abdellatif AA, Abdel-Aleem JA, et al.(2020). Transferosomal gel nanocarriers for enhancement the permeation of lornoxicam. Journal of Drug Delivery Science and Technology 56:101540.
14. Yeo S, Yoon I, Lee WK.(2022). Design and Characterisation of pH-Responsive Photosensitizer-Loaded Nano-Transferosomes for Enhanced Photodynamic Therapy. Pharmaceutics 14(1),pp. 210.

PCP437

**COLOSTRUM ENRICHED READY-TO-SPRINKLE
IMMUNOMODULATORY HEMATINIC NUTRACEUTICAL
SUPPLEMENT FOR PAEDIATRIC SUBPOPULATION**

AP0037

Jayvin Raval

Trainee Executive
Amneal Pharmaceuticals,
jayvinraval@gmail.com

AP0464

Vivek Joshi

PG Student
Graduate School of Pharmacy,
Gujarat Technological
University
rx.jvd.198@gmail.com

AP0187

Dr. Manju Misra

Associate Professor
Graduate School of Pharmacy,
Gujarat Technological
University
asso-manju_misra@gtu.edu.in

Abstract

Currently, very few food options or nutritional supplements are available for paediatric group that offers the combined benefit of fulfilling nutritional requirement and immunoprotection. A nutritional supplement providing both these advantages is highly desirable and forms the basis of our present investigation. The first sustenance of life, Colostrum, created by a natural process called colostrogenesis, referred to as liquid gold or immune milk was used. It possesses immunomodulatory action along with anti-inflammatory activity. A unique ready-to-sprinkle nutraceutical containing Colostrum and *Opuntia elatior* Mill. (*O. elatior*; Prickly pear) fruit was formulated that may serve as an immunomodulator and a hematinic. Fruits of *O. elatior* are known to contain Betanin that exhibit medicinal benefits as antioxidant and haematinic; in treatment of such as rheumatoid arthritis, hypertension, diabetes, asthma, gastric mucosal issues, coronary disease, etc. Fresh juice of *O. elatior* fruits was blended with fresh bovine liquid colostrum followed by lyophilization to produce the intended formulation. Formulation was characterized by estimating total Betanin content using RP-HPLC method, while IgG content was assayed using ELISA kit, proving immunomodulatory potential. Accelerated stability studies were carried out at $40\text{ }^{\circ}\text{C} \pm 5\text{ }^{\circ}\text{C}$ and $75\% \pm 5\%$ RH for 30 days, which resulted into loss of around 4% total Betanin content. Final formulation batch was also scaled up for marketing the product as a Nutraceutical or Food supplement for pediatrics.

Keywords: Paediatric, Hematinic, Colostrum, Prickly pear fruit, Immunomodulatory.

PCP450

INTRODUCING DIGITAL PILL: A STEP AHEAD TO CONVENTIONAL DRUG FORMULATIONS.

AP0495

Flora Pujara

Mpharm student,

L.M. College of Pharmacy

Gujarat Technological University

florapoojara@gmail.com

AP0496

Hetvi Prajapati

Mpharm student,

L.M. College of Pharmacy

Gujarat Technological University

hetusahi@gmail.com

Abstract

Drugs alone seem to be insufficient in the face of holistic and complex medical approaches in an era of constant technological quantum leaps and increasing patient demands. This is resulting in the emergence of 'beyond the drug' services, which provide the opportunity for improved health outcomes, gaining competitive advantage, and new business models. The concept of digital pill emerged in Nov, 2017 when the FDA approved world's first "digital pill". Also popularly known as the "Smart Pill" is indeed an ingestible drug that incorporates technology that can track and regulate drug release, as well as record data about drug release such as when, where, drug amount, body temperature, and heart rate. It is ingestible miniaturized electromechanical device embedded with sensors that serve as a point of convergence for biomedical technology, medicine, and the pharmaceutical industry. This is used to measure the dosage level of a tablet in real-time. When medical professionals are provided with the information, they can prescribe a treatment regimen which is more likely to lead to medication adherence, increasing the drug's therapeutic effects. The whole adherence assistance comes with serious implications for the patient's privacy. This review article addresses that despite having regulatory challenges, this pill remains a remarkable advancement in the field of medical science when it comes to medication adherence in patients especially those suffering from psychological disorders.

Keywords: digital pill, smart pill, medication adherence, psychological disorders.

1. INTRODUCTION

Despite sounding like something out of a science-fiction narrative, advanced pill technology that really can transmit relevant information of real-time adherence data to clinicians is by now being used and approved - "The Digital Pill" (Istory & Ackground, 2018). In an era where there are huge technological leaps occurring every day, the main focus of pharmaceutical industry lies in advancement of technology which can be inbuilt in dosage forms itself for betterment of patient compliance having ultimate goal of improvement in treatment. There arise innovative business models which provides services 'beyond the pill' in combination with advance technology(Liebmann-Smith, 1993).

Pharma companies must proceed beyond innovative features to compete effectively at this crossroads of technology, facilities, patient requirement, and market opportunity, and they have a number of factors to consider along the case, such as,

1. economic evaluation and future prospects for digital health tools
2. which services are meaningful and add value for both patient populations and pharmaceutical industry
3. a broader assessment of the patient satisfaction(Liebmann-Smith, 1993)

Even in modern medication system, the main issue faced by physicians for failing of treatment is medication non-adherence. Digitalizing medication adherence can have advantages in medical field. (Chai, Goodman, et al., 2021; Wong & Chan, 2016). Patients with serious mental illness (SMI), which account for roughly 4% of US adults, possess elevated risk of chronic physical comorbidities than the normal community (Merikangas et al., 2010). Patients who suffer from depression seem to develop cardiovascular disease 1.5 times more. Patients suffering from bipolar disorder or schizophrenia seem to be 2-3 times more likely to suffer from cardiovascular disease (Carney et al., 2006; Carney & Jones, 2006; Dixon et al., 1999; Kilbourne et al., 2004, 2007; MacEwan et al., 2018b; Merikangas et al., 2010). Diabetes mellitus seems to be 2-3 times more common in patients with bipolar disorder. All of these are caused by medication non-adherence (de Hert et al., 2011; MacEwan et al., 2018a).

TABLE 1: Differences between conventional and digital pill formulation.

Conventional Formulation	Digital Pill Formulation
It has high level of non-Adherence	It has low level of non-Adherence
Partial or complete loss of response	Increase in overall response
High Cost of payers	Low cost of payers
Health cost is higher	Reducing health cost
Revenue is low	Revenue is high

(Ilan, 2021)

A digital pill is boon in this area. Digital pills are an answer to the issue of nonadherence. There is plethora of proof promoting the usage of digital pills system in clinical trials, and technological breakthroughs in system trustworthiness as well as improve end user compliance enhance the effectiveness observed in monitoring adherence in a manner trying to ease process of implementing pill. Digital pill system rules over conventional drug formulations as it is enriched with dozens of advantages over conventional formulations (TABLE 1). In long-term, the reliability as well as quality of appropriate data of adherence, along with the decline of variances, will reap rewards (Klein, 2021). Digital pill or smart pill or smart tablet contains special electronic sensors and monitoring devices that can be consumed and used to collect and transmit data while still within your body. They can be used to catch and transmit images, detect chemical and hormone level changes, start releasing medications, or plainly alert ones doctor that users did take the medication. The AbilifyMycite digital tablet from Proteus Digital Health and Otsuka Pharmaceutical was the very first to be approved, and it consisted of a swallowable sensor to record patient's commitment to the medication regimen. This was applied for treating mentally ill patients, who profited immensely from it (Martani et al., 2020a; Rawat et al., 2015; Sharma, 2022).

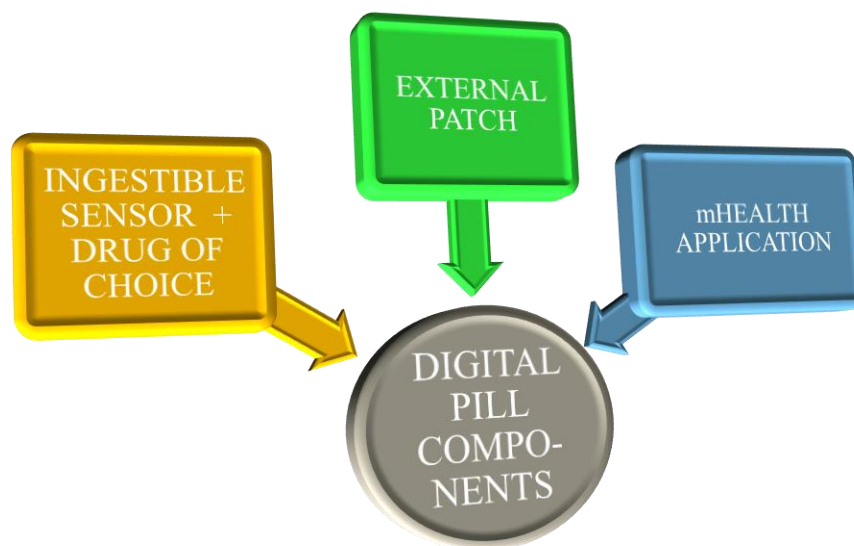
2. WHAT DO WE UNDERSTAND BY "DIGITAL PILL"

Digital pills are orally administered event markers which allow for adherence assessment via an integrated swallowable sensor combined with exterior receiver. The orally administered medications are enclosed in a suitable capsule shell having appropriate pharmaceutical-grade that holds a biocompatible sensor that is enabled by gastrointestinal fluid exposure. A digital signal emits real-time drug therapy ingestion information. A wearable technological device detects the output and forwards it to the physician and researcher. The method for using digital pill is equivalent to that of over-encapsulating an active study drug, however the capsule also includes an ingestible sensor (Browne et al., 2018; Chai, Goodman, et al., 2021). Patients can learn very quickly how to use and understand such systems. In a latest usability study, users have been capable of using the system as originally meant, safely and effectively; in performance evaluations, they ascertained that this device was having simple usage and possessed potential to become a beneficial tool in order to assist them organise their medicines (Baumgartner et al., 2021b; Shtrichman et al., 2018).

2.1. Components of digital pill.

There are various advancements in components of this pill. The main components of the first digital pill approved by FDA, developed by Proteus are shown in FIGURE 1.

FIGURE1: Components of Digital Pill developed by Proteus.



(Istory & Ackground, 2018)

The ingestible sensor, which is only one mm long and one-third of a mm thick, is inaccessible to patients and is encapsulated in medications such as Abilify. The sensor along with the main drug is encapsulated in a smart pill or capsule. Whenever the patient consumes the pill, the sensor made of copper, silicon, and magnesium establish a circuit with human's gastric acid. The extraneous patch is applied to the patient's skin mainly at torso part. The patch tracks and system log the dates and times the pill is consumed, in addition to other vital signs like the patient's pulse rate, temperature, function, and respiratory rate(Istory & Ackground, 2018; Martani et al., 2020a; Plowman et al., 2018)

2.2. How does a Digital Pill work?

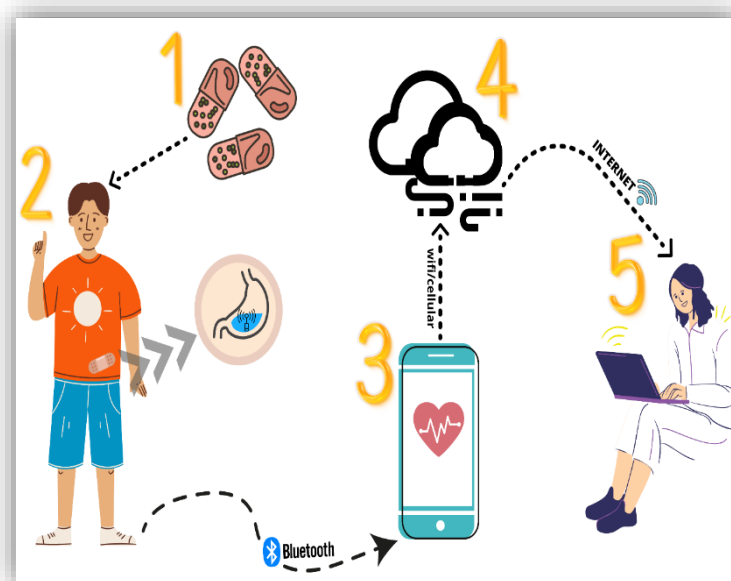
As complicated as it sounds, the working of this pill quite simple and does wonders when it comes to safety and patient compliance. FIGURE 2 clearly demonstrates the process of working of digital pill.

This FDA-approved form of treatment encompasses an ingestible sensor having length and width of a sand's grain into a capsule or pill. So, when sensor reaches the stomach, the electrolytes on its surface (copper and magnesium) interact with the electrolytes in stomach acid to form a bio galvanic-like battery. The sensor is able to use these voltages to produce an electric field, that is spotted by the Proteus Personal Monitor, an extrinsically worn adhesive monitor(Diedericks, 2019; Voelker, 2018). The orally administered sensor can interact with the monitor for 5 to 10 minutes until becoming unresponsive, crossing through the end of the gastrointestinal tract, and then being excreted with faecal matter(Diedericks, 2019).

The patients should be provided with some training before implementing it. They should be aware about the overview of the System, setup of charger and tracker for the first time, routine usage of the system without use of the patient application, routine use of the system with use

of the patient application, application navigation and functionality(Baumgartner et al., 2021a; Chai, Bustamante, et al., 2021).

FIGURE2: Demonstration of working of digital pill system (DPS).



1. The ingestible sensor infused with drug pill is taken by patient who has to wear an adhesive tracker on his body mainly on the torso part. 2. This sensor emits a reduced power RF (radio frequency) signal when stimulated by person's gastrointestinal fluid. 3. The tracker analyses the output signal emitted from the consumed sensor and transmits it to the patient's mobile App via Bluetooth. 4. The mobile application shows the information and then sends it to the central secure server. 5. The server transmits data about drug ingestion to the physician dashboard.

The detector can record numerous different parameters including heart rate and activity level in addition to tracing whenever the ingestible sensor signal is received, making it a useful platform for both clinicians and scientists. Records from the tracker is encrypted and distributed to the person's smartphone via Bluetooth technology prior to getting shared online to a centralized server, enabling evidence gathered by the tracker to be assimilated into electronic medical records(di Carlo et al., 2012a; Kane et al., 2013; Park et al., 2015). When health practitioners are provided with the data, they can recommend a medication regimen which is more likely to lead in medication adherence, enhancing the medication's therapeutic benefits. Digital pill establishes an assistance system that links both patients and caregivers, thereby minimizing the healthcare workers required to guarantee patient's medication compliance. Furthermore, by enhancing patient adherence, cumulative cost of treatment for both patient populations and insurance providers are scaled back by avoiding unwanted expenditures(Insinga et al., 2011; *The True Cost of Skipping Prescription Medications*, n.d.). This structure has proven good detection accuracy of the ingestible sensor, low ill consequences in patients (currently restricted to skin rash and one case of nausea), and an increased rates of patient compliance. This even requires little coaching, making it a good fit for medication adherence tracking(Belknap et al., 2013a).

2.3. Which are the available types of Digital Pill?

The Food and Drug Administration (FDA) has given green signal in sales promotion of two digital pill systems as ingestible event identifiers. Otsuka Pharmaceutical Co., Ltd. (Tokyo, Japan) partnered with Proteus Digital Health to establish and market Abilify MyCite®, the very

first adherence-enabled drug-device combination product (Otsuka eventually acquired the Proteus technology)(Abilify MyCite (Otsuka America Pharmaceutical, Inc.): FDA Package Insert, n.d.; Otsuka America Pharmaceutical, Inc., Purchases the Assets of Proteus Digital Health, Inc. / Discover Otsuka, n.d.).

In December of 2019, the FDA granted 510(k) clearance to etectRx (Gainesville, FL, USA) for the ID-Cap™ System. This scheme is an engaging technology capable of incorporating a huge spectrum of oral medications.

3. WHAT REGULATORY BODIES HAVE TO SAY ABOUT DIGITAL PILL?

The very first medication in the country with a digital ingestion tracking system was given approval by the US Food and Drug Administration in Nov, 2017. The ingestible sensor in the aripiprazole tablets identified as Abilify MyCite (with sensor) keeps track of the timing of medication consumed. This medication is approved for acute treatment of manic and mixed episodes linked to bipolar I disorder as well as for usage in adjunctive therapy in adult depression. According to FDA officials, the recently approved aripiprazole framework hasn't yet to be proven to upgrade' adherence to his/her treatment. Proteus Digital Health Inc of Redwood City, California, and Otsuka Pharmaceutical Co Ltd of Tokyo, Japan, the platform's manufacturers, stated that the program's ramp - up will comprise a narrow number of health insurance framework, doctors, and patients in order to enhance user feedback response. Adults taking Abilify in clinical studies most frequently reported experiencing the following adverse effects: nausea, vomiting, constipation, headache, dizziness, uncontrollable limb and body movements (akathisia), anxiety, sleeplessness, and restlessness. Some individuals may have skin irritation where they applied the MyCite patch(FDA Approves Pill with Sensor That Digitally Tracks If Patients Have Ingested Their Medication / FDA, n.d.).

In both clinical and research settings, Digital pill are combination of drug-device that record and communicate patient-specific measurement information to track certain health-related lifestyle behaviours, particularly medication-taking behaviour(Martani et al., 2020b).

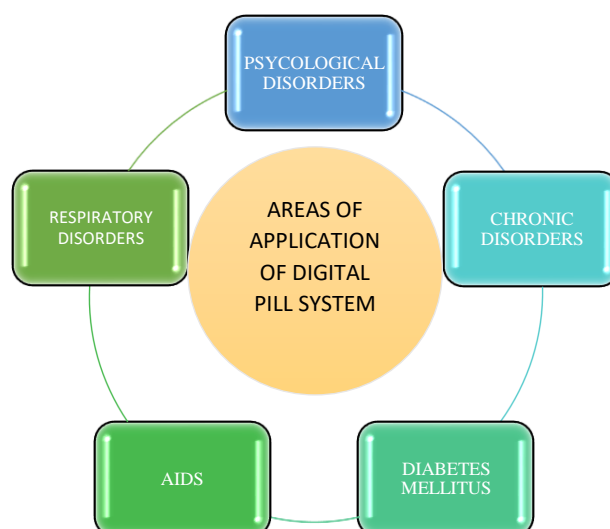
The ingestible sensor have ability to be co-encapsulated with conventional medications in DP, which allows higher reliability in monitoring of medication-taking behaviour as well as gathering information about other lifestyle activities related to health(Chai et al., 2015).

In 2016, the European Medicines Agency (EMA) issued an opinion recognising DP as "a qualified tool for evaluating adherence in clinical studies."(European Medicines Agency /, n.d.)

4. AREAS OF APPLICATION OF DIGITAL PILL:

This system has its role in numerous areas where medication non-adherence stands as a major issue. Brief areas and diseases where these pills can be used is mentioned in figure 3.

FIGURE3. List of areas where DPS can be applied.



(Baroletti & Dell'Orfano, 2010; Briesacher et al., 2008; Browne et al., 2015)

The very first drug of its type, marketed to public as Abilify MyCite, is an aripiprazole dosage formulation manufactured with a sensor administered in the pill. Aripiprazole is indeed an antipsychotic medication that is administered to treat schizophrenia, bipolar disorder, and depressive symptoms. In a comment, Mitchell Mathis, MD, director of the FDA's Division of Psychiatry Products, told reporters, "Being able to track ingestion of medications prescribed for mental illness may be useful for some patients." Mathis added that perhaps the organisation is keen to investigate how truly innovative prescription medication technology can assist both patients and professionals (Voelker, 2018). Multiple previous studies utilized a DPS i.e., Digital Pill System to assess adherence, which would include diabetes treating drugs, antiretroviral therapy (ART), tuberculosis treatment, and antipsychotic medication for schizophrenia (Browne et al., 2015, 2017; Kamal et al., 2020; Peters-Strickland et al., 2016). 90% terms of confidence shown with a digital pill system was documented in a study designed to examine opioid use patterns (Chai et al., 2017; Hoppe et al., 2015).

Although it hasn't been authorised for clinical use, Belknap et al have used early design of the system designed by Proteus Digital Health, Inc to illustrate considerably better medication compliance for tuberculosis disease management (Belknap et al., 2013b). Modernizing medication compliance may also have a substantial effect in the area of cardiovascular diseases, under which medication nonadherence is observed in 60% patients, along with a wide range of some of the other chronic diseases such as rheumatoid arthritis, chronic myeloid leukaemia, diabetes mellitus, and sickle cell anaemia (Baroletti & Dell'Orfano, 2010; Briesacher et al., 2008; Creary et al., 2014).

In addition to the above-mentioned fields, this technology can be used in various other fields like oncology, neurology, Parkinson's disease, infectious diseases etc. where medication non-adherence is a major drawback in treatment therapy (Burks et al., 2017; Chai et al., 2020; Klein, 2021; Marin et al., 2010)

5. CHALLENGES

Amidst its ability to transform universal health care, digitalizing medication adherence does have a few important shortcomings and issues to be concerned of. One or more of the mentioned hurdles may impact a user's interest in long-term use: (1) problems with the application, tracker, and/or charger's technology; (2) design issues with the tracker and/or charger; (3) a perceived lack of personal adherence challenges. (4) observed side effects on user's body. (5) patient's privacy issues. (Chai et al., 2022).

5.1. Important issues to consider:

The majority of the problems with the application, tracker, and charger revolve around user-friendliness. At this point in time, the layout of this specific ingestible sensor confines its use to prescription medications taken orally. Furthermore, there are issues that integrating an ingestible sensor into treatments and medications will substantially increase healthcare costs. As medication accessibility is a hinderance to medication adherence, especially for individuals without drug insurance coverage, this medication adherence strategic approach may be pricey for the patients who require it the most. One more concern with implementing digital medical adherence is patient privacy, due to the problems associated of capturing and maintaining private health data on some kind of central server not controlled by the patient (di Carlo et al., 2012b; Wong & Chan, 2016).

There has been some debate about privacy rules and laws apply to data created and communicated by digital sensors, as well as whether existing practices to privacy data protection implement to this technological innovation. Patient records, in specific, is highly individualized and private to patients and might be advantageous to businesses, including insurers, when evaluating insurance premiums (*Fears of Hackers Targeting US Hospitals, Medical Devices for Cyber Attacks - ABC News*, n.d.). This is true especially for

such evidence gathered and transferred by the digital pill. Patients must have faith that his\her personal medical data will be considered confidential, notably since the medication itself tales to those who receive it. Also, because Supreme Court has ruled that people with mental illnesses have all the liberty not to be coerced into therapies(Canter, 2010), which would also include taking medication, the digital pill may emerge controversial as a remedy to medication adherence in mentally ill people. Abilify MyCite can raise the mortality risk in elderly patients with dementia-related psychosis. It may lead to increasing the probability of suicidal thoughts and hormonal change development in children, adolescents, and young adults who consume pills(Voelker, 2018).

5.2. Solution:

A mere equilibrium must be seen among the confidentiality threats posed to users by the digital pill as well as the issues of excessive regulation, which might prevent whatever perks from being discovered. Having provided a printed privacy policy to an advanced digital pill user wouldn't be an efficient method of providing the patient with the greatest security protection available. Similar to how a client might scroll through a privacy policy on an installed app on one's device prior to actually clicking "accept," an end user of the digital pill might do the same. Agreement derived from a health care professional offers the patient with a stronger possibility for consideration, understand regarding the user privacy posed by the technology, as well as seek clarification with his\her doctor prior to actually using or spending for the digital pill. No individual should be mandated to take the digital pill unless they have given their full explicit consent. Adherence technology has the capability to be employed against clients as a requirement for health insurance, occupation, or admission to a school. To protect the same, federally mandated usage of such advanced technology are considered necessary. Ultimately, even though this innovation proficiently detects medication adherence, it ought to be aided by suitable and efficient patient counselling to be sincerely efficient in enhancing patient treatment adherence(Istory & Ackground, 2018; Iuga & McGuire, 2014).

6. FUTURE ASPECTS:

In the future, the principle could be broadened to produce low-cost, high-efficiency easily curable smart pills that also provide diagnosis. As a result, all patients can be supervised and treated within the same time(Chen et al., 2021). Wearable devices like fitbits and smartwatches should be incorporated into this concept. It enables patients to monitor his/her health and keep record of a wide range of indicators in his\her bodies. This collects details including heartbeat, blood pressure, and calories burned. Such systems can monitor and alert on health problems such as seizures. In addition to the individual's tracking, wearable data could be used to convey health outcomes to physician during consultations. Furthermore, wearables may occur in the form of rings, garments, and possibly other items as technology evolves (Swarna et al., 2021). Some users further suggested for optimizing the software of the smartphone application in order to enhance overall user experience(Chai et al., 2022).

7. CONCLUSION:

Overall, there have been mixed feeling about this innovation in the opinion of users, physicians and caretakers. As the traditional mode of operation has become redundant, smart pills are becoming more trustable and serve as one of the least harmful and endurable diagnostic techniques in the present society. To function properly, the system necessitates sophisticated design knowledge. Only aripiprazole currently has ingestible sensor approval, but it shouldn't be astounding if the edible sensor will be embedded into certain other medications in the upcoming years. Despite its advantages, concerns about healthcare costs, confidentiality of the patient, and patient autonomy might have to be clarified prior to it being widely used. By enacting appropriate legislation, upgrading existing safeguards, and establishing protections, the digital pill can indeed be smoothly launched onto the market, allowing us to reap the entirety of its benefits. The "digital pill," however, provides a novel workable alternative to a long-

standing challenge in health care services and could soon become an excellent component in the forthcoming physician's toolbox for achieving optimum health outcome.

REFERENCES:

1. *Abilify MyCite (Otsuka America Pharmaceutical, Inc.): FDA Package Insert*. (n.d.). Retrieved September 3, 2022, from <https://medlibrary.org/lib/rx/meds/abilify-mycite/>
2. Baroletti, S., & Dell'Orfano, H. (2010). Medication adherence in cardiovascular disease. *Circulation*, *121*(12), 1455–1458. <https://doi.org/10.1161/CIRCULATIONAHA.109.904003>
3. Baumgartner, S. L., Buffkin, D. E., Rukavina, E., Jones, J., Weiler, E., & Carnes, T. C. (2021a). A novel digital pill system for medication adherence measurement and reporting: Usability validation study. *JMIR Human Factors*, *8*(4), 3–4. <https://doi.org/10.2196/30786>
4. Baumgartner, S. L., Buffkin, D. E., Rukavina, E., Jones, J., Weiler, E., & Carnes, T. C. (2021b). A Novel Digital Pill System for Medication Adherence Measurement and Reporting: Usability Validation Study. *JMIR Human Factors*, *8*(4). <https://doi.org/10.2196/30786>
5. Belknap, R., Weis, S., Brookens, A., Au-Yeung, K. Y., Moon, G., DiCarlo, L., & Reves, R. (2013a). Feasibility of an ingestible sensor-based system for monitoring adherence to tuberculosis therapy. *PloS One*, *8*(1). <https://doi.org/10.1371/JOURNAL.PONE.0053373>
6. Belknap, R., Weis, S., Brookens, A., Au-Yeung, K. Y., Moon, G., DiCarlo, L., & Reves, R. (2013b). Feasibility of an ingestible sensor-based system for monitoring adherence to tuberculosis therapy. *PloS One*, *8*(1). <https://doi.org/10.1371/JOURNAL.PONE.0053373>
7. Briesacher, B. A., Andrade, S. E., Fouayzi, H., & Chan, K. A. (2008). Comparison of drug adherence rates among patients with seven different medical conditions. *Pharmacotherapy*, *28*(4), 437–443. <https://doi.org/10.1592/PHCO.28.4.437>
8. Browne, S. H., Behzadi, Y., & Littlewort, G. (2015). Let Visuals Tell the Story: Medication Adherence in Patients with Type II Diabetes Captured by a Novel Ingestion Sensor Platform. *JMIR MHealth and UHealth*, *3*(4). <https://doi.org/10.2196/MHEALTH.4292>
9. Browne, S. H., Peloquin, C., Santillo, F., Haubrich, R., Muttera, L., Moser, K., Savage, G. M., Benson, C. A., & Blaschke, T. F. (2017). Digitizing Medicines for Remote Capture of Oral Medication Adherence Using Co-encapsulation. *Clinical Pharmacology and Therapeutics*, *103*(3), 502–510. <https://doi.org/10.1002/CPT.760>
10. Browne, S. H., Peloquin, C., Santillo, F., Haubrich, R., Muttera, L., Moser, K., Savage, G. M., Benson, C. A., & Blaschke, T. F. (2018). Digitizing Medicines for Remote Capture of Oral Medication Adherence Using Co-encapsulation. *Undefined*, *103*(3), 502–510. <https://doi.org/10.1002/CPT.760>
11. Burks, J., Marshall, T. S., & Ye, X. (2017). Adherence to disease-modifying therapies and its impact on relapse, health resource utilization, and costs among patients with multiple sclerosis. *ClinicoEconomics and Outcomes Research: CEOR*, *9*, 251–260. <https://doi.org/10.2147/CEOR.S130334>
12. Canter, D. (2010). *Forensic Psychology*. <https://doi.org/10.1093/ACTRADE/9780199550203.001.0001>
13. Carney, C. P., & Jones, L. E. (2006). Medical comorbidity in women and men with bipolar disorders: a population-based controlled study. *Psychosomatic Medicine*, *68*(5), 684–691. <https://doi.org/10.1097/01.PSY.0000237316.09601.88>
14. Carney, C. P., Jones, L., & Woolson, R. F. (2006). Medical comorbidity in women and men with schizophrenia: A population-based controlled study. *Journal of General Internal Medicine*, *21*(11), 1133–1137. <https://doi.org/10.1111/j.1525-1497.2006.00563.x>
15. Chai, P. R., Bustamante, M. J., Goodman, G., Mohamed, Y., Najarro, J., Sullivan, M. C., Castillo-Mancilla, J., Coyle, R. P., Mayer, K. H., Rosen, R. K., Baumgartner, S. L., Alpert, P. E., Boyer, E. W., & O'Cleirigh, C. (2021). A brief training program to support the use of a digital pill system for medication adherence: Pilot descriptive study. *JMIR Formative Research*, *5*(4). <https://doi.org/10.2196/26213>
16. Chai, P. R., Carreiro, S., Innes, B. J., Rosen, R. K., O'Cleirigh, C., Mayer, K. H., & Boyer, E. W. (2017). Digital Pills to Measure Opioid Ingestion Patterns in Emergency Department Patients With Acute Fracture Pain: A Pilot Study. *Journal of Medical Internet Research*, *19*(1). <https://doi.org/10.2196/JMIR.7050>
17. Chai, P. R., Castillo-Mancilla, J., Buffkin, E., Darling, C., Rosen, R. K., Horvath, K. J., Boudreaux, E. D., Robbins, G. K., Hibberd, P. L., & Boyer, E. W. (2015). Utilizing an Ingestible Biosensor to

- Assess Real-Time Medication Adherence. *Journal of Medical Toxicology* 2015 11:4, 11(4), 439–444. <https://doi.org/10.1007/S13181-015-0494-8>
18. Chai, P. R., Goodman, G., Bustamante, M. J., Mohamed, Y., Castillo-Mancilla, J., Boyer, E. W., Mayer, K. H., Rosen, R. K., Baumgartner, S. L., Buffkin, E., & O’Cleirigh, C. (2021). Long-Term Stability of the Electronic Sensor Component of a Digital Pill System in Real-World Storage Settings. *Journal of Pharmacy Technology*, 37(3), 135–139. <https://doi.org/10.1177/8755122520985219>
 19. Chai, P. R., Goodman, G., Bustamante, M., Mendez, L., Mohamed, Y., Mayer, K. H., Boyer, E. W., Rosen, R. K., & O’Cleirigh, C. (2020). Design and Delivery of Real-Time Adherence Data to Men Who Have Sex with Men Using Antiretroviral Pre-exposure Prophylaxis via an Ingestible Electronic Sensor. *Undefined*, 25(6), 1661–1674. <https://doi.org/10.1007/S10461-020-03082-Y>
 20. Chai, P. R., Goodman, G. R., Bronzi, O., Gonzales, G., Baez, A., Bustamante, M. J., Najarro, J., Mohamed, Y., Sullivan, M. C., Mayer, K. H., Boyer, E. W., O’Cleirigh, C., & Rosen, R. K. (2022). Real-World User Experiences with a Digital Pill System to Measure PrEP Adherence: Perspectives from MSM with Substance Use. *AIDS and Behavior*, 26(7), 2459–2468. <https://doi.org/10.1007/s10461-022-03594-9>
 21. Chen, Y., Xiang, W., Opitz, M., Toxins, B. P., Valincius, G., & Budvytyte, R. (2021). *Swallowable Glass Pill for Digestive Motility & Toxin Detection Using Cell-Based Biosensor Retraction Retraction : Swallowable Glass Pill for Digestive Motility & Toxin Detection Using Cell-Based Biosensor (J . Phys . : Conf .*
 22. Creary, S. E., Gladwin, M. T., Byrne, M., Hildesheim, M., & Krishnamurti, L. (2014). A pilot study of electronic directly observed therapy to improve hydroxyurea adherence in pediatric patients with sickle-cell disease. *Pediatric Blood & Cancer*, 61(6), 1068–1073. <https://doi.org/10.1002/PBC.24931>
 23. de Hert, M., Correll, C. U., Bobes, J., Cetkovich-Bakmas, M., Cohen, D. A. N., Asai, I., Detraux, J., Gautam, S., Möller, H. J., Ndeti, D. M., Newcomer, J. W., Uwakwe, R., & Leucht, S. (2011). Physical illness in patients with severe mental disorders. I. Prevalence, impact of medications and disparities in health care. *World Psychiatry : Official Journal of the World Psychiatric Association (WPA)*, 10(1), 52–77. <https://doi.org/10.1002/J.2051-5545.2011.TB00014.X>
 24. di Carlo, L., Moon, G., Intondi, A., Duck, R., Frank, J., Hafazi, H., Behzadi, Y., Robertson, T., Costello, B., Savage, G., & Zdeblick, M. (2012a). A digital health solution for using and managing medications: wirelessly observed therapy. *IEEE Pulse*, 3(5), 23–26. <https://doi.org/10.1109/MPUL.2012.2205777>
 25. di Carlo, L., Moon, G., Intondi, A., Duck, R., Frank, J., Hafazi, H., Behzadi, Y., Robertson, T., Costello, B., Savage, G., & Zdeblick, M. (2012b). A digital health solution for using and managing medications: wirelessly observed therapy. *IEEE Pulse*, 3(5), 23–26. <https://doi.org/10.1109/MPUL.2012.2205777>
 26. Diedericks, H. (2019). *Digital Pills and Promises*. 63–67. <https://doi.org/10.1145/3357729.3357746>
 27. Dixon, L., Postrado, L., Delahanty, J., Fischer, P. J., & Lehman, A. (1999). The association of medical comorbidity in schizophrenia with poor physical and mental health. *The Journal of Nervous and Mental Disease*, 187(8), 496–502. <https://doi.org/10.1097/00005053-199908000-00006>
 28. *European Medicines Agency* /. (n.d.). Retrieved September 4, 2022, from <https://www.ema.europa.eu/en>
 29. *FDA approves pill with sensor that digitally tracks if patients have ingested their medication* | FDA. (n.d.). Retrieved September 4, 2022, from <https://www.fda.gov/news-events/press-announcements/fda-approves-pill-sensor-digitally-tracks-if-patients-have-ingested-their-medication>
 30. *Fears of hackers targeting US hospitals, medical devices for cyber attacks - ABC News*. (n.d.). Retrieved September 3, 2022, from <https://abcnews.go.com/Health/fears-hackers-targeting-us-hospitals-medical-devices-cyber/story?id=48348384>
 31. Hoppe, J. A., Nelson, L. S., Perrone, J., Weiner, S. G., Rathlev, N. K., Sanchez, L. D., Babineau, M., Griggs, C. A., Mitchell, P. M., Ma, J., Hoch, W. B., Totten, V., Salzman, M. S., Karmakar, R., Iwanicki, J. L., Morgan, B. W., Pomerleau, A. C., Delgado, J., Medoro, A., ... Koploy, A. (2015). Opioid Prescribing in a Cross Section of US Emergency Departments. *Annals of Emergency Medicine*, 66(3), 253-259.E1. <https://doi.org/10.1016/j.annemergmed.2015.03.026>
 32. Ilan, Y. (2021). Improving Global Healthcare and Reducing Costs Using Second-Generation Artificial Intelligence-Based Digital Pills: A Market Disruptor. *International Journal of Environmental Research and Public Health*, 18(2), 1–12. <https://doi.org/10.3390/IJERPH18020811>

33. Insinga, R. P., Ng-Mak, D. S., & Hanson, M. E. (2011). Costs associated with outpatient, emergency room and inpatient care for migraine in the USA. *Cephalalgia: An International Journal of Headache*, 31(15), 1570–1575. <https://doi.org/10.1177/0333102411425960>
34. Istory, I. I. H., & Ackground, B. (2018). *A TOUGH [DIGITAL] PILL TO SWALLOW* Alexa Nagy * I. I. 228–242.
35. Iuga, A. O., & McGuire, M. J. (2014). Adherence and health care costs. In *Risk Management and Healthcare Policy* (Vol. 7, pp. 35–44). <https://doi.org/10.2147/RMHP.S19801>
36. Kamal, S., Rosen, M. I., Lazar, C., Siqueiros, L., Wang, Y., Daar, E. S., & Liu, H. (2020). Perceptions of People Living with HIV and HIV Healthcare Providers on Real-Time Measuring and Monitoring of Antiretroviral Adherence Using Ingestible Sensors: A Qualitative Study. *AIDS Research and Treatment*, 2020, 1098109. <https://doi.org/10.1155/2020/1098109>
37. Kane, J. M., Perlis, R. H., DiCarlo, L. A., Au-Yeung, K., Duong, J., & Petrides, G. (2013). First experience with a wireless system incorporating physiologic assessments and direct confirmation of digital tablet ingestions in ambulatory patients with schizophrenia or bipolar disorder. *The Journal of Clinical Psychiatry*, 74(6), e533-40. <https://doi.org/10.4088/JCP.12m08222>
38. Kilbourne, A. M., Brar, J. S., Drayer, R. A., Xu, X., & Post, E. P. (2007). Cardiovascular disease and metabolic risk factors in male patients with schizophrenia, schizoaffective disorder, and bipolar disorder. *Psychosomatics*, 48(5), 412–417. <https://doi.org/10.1176/APPI.PSY.48.5.412>
39. Kilbourne, A. M., Cornelius, J. R., Han, X., Pincus, H. A., Shad, M., Salloum, I., Conigliaro, J., & Haas, G. L. (2004). Burden of general medical conditions among individuals with bipolar disorder. *Bipolar Disorders*, 6(5), 368–373. <https://doi.org/10.1111/J.1399-5618.2004.00138.X>
40. Klein, G. L. (2021). The Case for Digital Pill Use in Clinical Trials. *Clinical Trials and Practice – Open Journal*, 4(1), 16–21. <https://doi.org/10.17140/ctpoj-4-120>
41. Liebmann-Smith, J. (1993). Beyond the pill. *American Druggist*, 207(4), 38–41. <https://doi.org/10.1093/wentk/9780190069674.003.0005>
42. MacEwan, J. P., Silverstein, A. R., Shafrin, J., Lakdawalla, D. N., Hatch, A., & Forma, F. M. (2018a). Medication Adherence Patterns Among Patients with Multiple Serious Mental and Physical Illnesses. *Advances in Therapy*, 35(5), 671–685. <https://doi.org/10.1007/s12325-018-0700-6>
43. MacEwan, J. P., Silverstein, A. R., Shafrin, J., Lakdawalla, D. N., Hatch, A., & Forma, F. M. (2018b). Medication Adherence Patterns Among Patients with Multiple Serious Mental and Physical Illnesses. *Advances in Therapy*, 35(5), 671–685. <https://doi.org/10.1007/s12325-018-0700-6>
44. Marin, D., Bazeos, A., Mahon, F. X., Eliasson, L., Milojkovic, D., Bua, M., Apperley, J. F., Szydlo, R., Desai, R., Kozlowski, K., Paliompeis, C., Latham, V., Foroni, L., Molimard, M., Reid, A., Rezvani, K., de Lavallade, H., Guallar, C., Goldman, J., & Khorashad, J. S. (2010). Adherence is the critical factor for achieving molecular responses in patients with chronic myeloid leukemia who achieve complete cytogenetic responses on imatinib. *Journal of Clinical Oncology: Official Journal of the American Society of Clinical Oncology*, 28(14), 2381–2388. <https://doi.org/10.1200/JCO.2009.26.3087>
45. Martani, A., Geneviève, L. D., Poppe, C., Casonato, C., & Wangmo, T. (2020a). Digital pills: A scoping review of the empirical literature and analysis of the ethical aspects. *BMC Medical Ethics*, 21(1). <https://doi.org/10.1186/s12910-019-0443-1>
46. Martani, A., Geneviève, L. D., Poppe, C., Casonato, C., & Wangmo, T. (2020b). Digital pills: A scoping review of the empirical literature and analysis of the ethical aspects. *BMC Medical Ethics*, 21(1), 1–13. <https://doi.org/10.1186/S12910-019-0443-1/FIGURES/2>
47. Merikangas, K. R., He, J. P., Burstein, M., Swanson, S. A., Avenevoli, S., Cui, L., Benjet, C., Georgiades, K., & Swendsen, J. (2010). Lifetime prevalence of mental disorders in U.S. adolescents: Results from the national comorbidity survey replication-adolescent supplement (NCS-A). *Journal of the American Academy of Child and Adolescent Psychiatry*, 49(10), 980–989. <https://doi.org/10.1016/j.jaac.2010.05.017>
48. *Otsuka America Pharmaceutical, Inc., Purchases the Assets of Proteus Digital Health, Inc. | Discover Otsuka*. (n.d.). Retrieved September 3, 2022, from <https://www.otsuka-us.com/discover/proteus-assets-purchase>
49. Park, L. G., Howie-Esquivel, J., & Dracup, K. (2015). Electronic Measurement of Medication Adherence. *Western Journal of Nursing Research*, 37(1), 28–49. <https://doi.org/10.1177/0193945914524492>
50. Peters-Strickland, T., Pestreich, L., Hatch, A., Rohatagi, S., Baker, R. A., Docherty, J. P., Markovtsova, L., Raja, P., Weiden, P. J., & Walling, D. P. (2016). Usability of a novel digital medicine system in adults with schizophrenia treated with sensor-embedded tablets of aripiprazole. *Neuropsychiatric Disease and Treatment*, 12, 2587–2594. <https://doi.org/10.2147/NDT.S116029>

51. Plowman, R. S., Peters-Strickland, T., & Savage, G. M. (2018). Digital medicines: clinical review on the safety of tablets with sensors. *Expert Opinion on Drug Safety*, 17(9), 849–852. <https://doi.org/10.1080/14740338.2018.1508447>
52. Rawat, J., Singh, A., Bhadauria, H. S., & Virmani, J. (2015). Computer Aided Diagnostic System for Detection of Leukemia Using Microscopic Images. *Procedia Computer Science*, 70, 748–756. <https://doi.org/10.1016/J.PROCS.2015.10.113>
53. Sharma, S. (2022). *Smart Pill Technology in Machine Learning*. May. <https://doi.org/10.15680/IJIRCCE.2022.1005083>
54. Shtrichman, R., Conrad, S., Schimo, K., Shachar, R., Machluf, E., Mindal, E., Epstein, H., Epstein, S., & Paz, A. (2018). Use of a Digital Medication Management System for Effective Assessment and Enhancement of Patient Adherence to Therapy (ReX): Feasibility Study. *JMIR Human Factors*, 5(4), e10128. <https://doi.org/10.2196/10128>
55. Swarna, S. R., Kumar, A., Dixit, P., & Sairam, T. V. M. (2021). Parkinson's disease prediction using adaptive quantum computing. *Proceedings of the 3rd International Conference on Intelligent Communication Technologies and Virtual Mobile Networks, ICICV 2021*, 1396–1401. <https://doi.org/10.1109/ICICV50876.2021.9388628>
56. *The True Cost of Skipping Prescription Medications*. (n.d.). Retrieved September 3, 2022, from <https://www.innovu.com/post/the-true-cost-of-skipping-prescription-medications>
57. Voelker, R. (2018). News from the food and drug administration. *JAMA - Journal of the American Medical Association*, 320(1), 23. <https://doi.org/10.1001/jama.2018.8554>
58. Wong, S., & Chan, V. (2016). *The digital pill Tracking medication adherence through electronic modalities*. 38–40.

ABSTRACT

SESSION 2 - QUALITY ASSURANCE
BY ADVANCE ANALYTICAL
TECHNIQUES

PCP372

COMPARATIVE STUDY OF UV SPECTROSCOPIC AND RP-HPLC METHOD FOR THE ESTIMATION OF EFONIDIPINE HCL ETHANOLATE AND METOPROLOL SUCCINATE IN THEIR COMBINED DOSAGE FORM

AP0342

Hitanshi Darji
Research Scholar
Pioneer Pharmacy Degree
College
hpdarji9@gmail.com

AP0350

Dr. Prasanna Pradhan
Associate Professor
Pioneer Pharmacy Degree College
pkpwithu@gmail.com

Abstract

Ratio derivative UV spectroscopic method and RP-HPLC method were developed, validated and compared for the quantitative determination of Efonidipine HCl Ethanolate (EFD) and Metoprolol Succinate (METO) in their combined dosage form. Both the methods were validated as per ICH Q2R1 guideline. The UV spectroscopic method utilizes 285 nm and 274 nm for EFD and METO, respectively, whereas 230 nm was used in case of RP-HPLC method. Methanol is used as solvent in both methods. Both the methods were found to be linear in the range 10-60 μ g/ml for RP-HPLC and 10-50 μ g/ml and 25-125 μ g/ml for EFD and METO respectively in UV-spectroscopic methods with a good correlation i.e. $r^2 > 0.999$. ANOVA analysis of Assay result indicates both methods can be applied for estimation of EFD and METO in their combined dosage formulations in quality control laboratories.

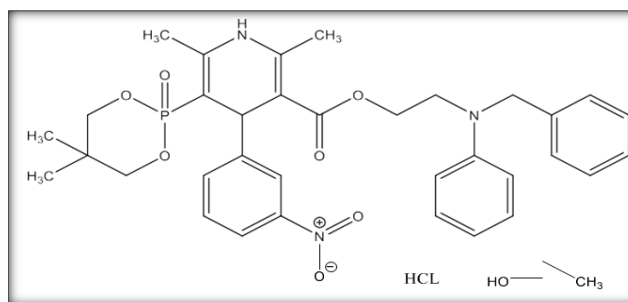
KEY WORDS: Efonidipine Hydrochloride Ethanolate, Metoprolol Succinate, Ratio derivative Method, RP-HPLC, Validation, ANOVA

INTRODUCTION

Efonidipine Hydrochloride Ethanolate (EFD) is a 2-(N-benzyl anilino) ethyl 5-(5,5-dimethyl-2-oxo-1,3,2 λ 5 - dioxaphosphinan-2-yl)-2,6-dimethyl-4-(3-nitrophenyl)- 1,4-dihydropyridine-3 carboxylate; ethanol; hydrochloride (Figure 1). It belongs to 1,4-dihydropyridine calcium channel blocker and used to cure hypertension and angina pectoris. It leads to vasodilation and lower the automaticity of heart by blocking the L and T type of calcium channels. It employs negative chronotropic effect by hindering T-type calcium channel action of sinoatrial node, it delays the late phase-4 depolarization of sinoatrial action potential and reducing the heart rate. (1, 2)

Metoprolol succinate (METO) is chemically known as (RS)-1-isopropylamino-3-*p*-(2-methoxyethyl) phenoxypropan-2-ol (2*R*,3*R*)-succinate (Figure 2). It is a cardio-selective β -blocker, used in the treatment of various disease of the cardiovascular system, commonly hypertension. (3, 4)

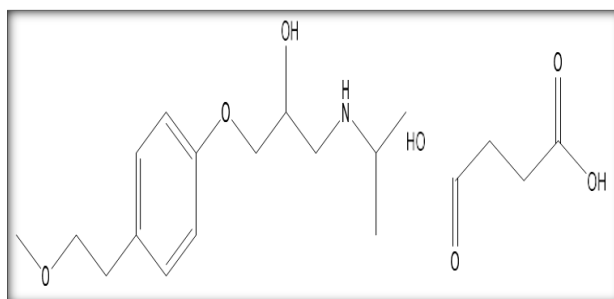
Figure 1: Efonidipine HCl Ethanolate ⁽¹⁾



Source: “Efonidipine Hydrochloride Ethanolate”

<https://pubchem.ncbi.nlm.nih.gov/compound/Efonidipine-hydrochloride-ethanolate#section=3D-Conformer>

Figure 2: Metoprolol succinate ⁽³⁾



Source: “Metoprolol succinate” <https://pubchem.ncbi.nlm.nih.gov/compound/Metoprolol-succinate#section=3D-Conformer>

OBJECTIVE

During literature survey ⁽⁵⁻¹⁶⁾, till date there is no analytical UV spectrophotometric method and RP-HPLC are available for simultaneous determination of Efonidipine HCl Ethanolate and Metoprolol succinate. Therefore, the objectives of this study were to develop a simple, rapid, and validated method for simultaneous estimation of Efonidipine HCl Ethanolate and Metoprolol succinate and to validate the method in accordance with International Conference on Harmonization (ICH) guidelines and evaluate the data using Statistical analysis.

RESEARCH METHODOLOGY

Materials and Methods

Reagents and Chemicals

Pure drug sample of EFD was procured from Purechem Pvt Ltd, Ankleshwar and METO was procured from CTX lifescience Pvt Ltd, Surat. LR and AR grade Methanol was used as solvent. Calibrated glass wares were used throughout the work.

Instrumentation

Instrument used was an UV-Visible double beam spectrophotometer, SHIMADZU (Model-UV-1800) with a pair of 1cm matched quartz cells. The software was used UV Probe 2.33.

The HPLC used Shimadzu LC 20AD binary pump system, equipped with a UV-detector with manual injector, Enables C₁₈. The software was used LC win 5.

Preparation of standard stock solution

An accurately weighed quantity of EFD and METO (25 mg) was transferred to a separate 25 ml volumetric flask and dissolved and diluted to the mark with methanol to obtain standard solution having concentration of EFD and METO (1000 µg/ml). For **Method I** (Ratio derivative method), Accurately measured of both the solutions were transferred into a 25 ml of volumetric flask and diluted to the mark with Methanol to obtain solution having concentration of 200 µg/ml of EFD and 500 µg/ml of METO and for **Method II** (RP-HPLC), solution having concentration of 500 µg/ml of EFD and METO.

Selection of detection wavelength

Method I: EFD 30µg/ml spectrum was divided with the divisor spectra of METO (25µg/ml). New spectrum was obtained which is then derivatized in to first and higher orders. Mixture spectra was similarly divided with the same divisor and derivatized. EFD and mixture shows same absorbance at 285nm in 2nd derivative spectra with Delta lambda 20 and scaling factor 10. Same as METO 75µg/ml spectrum was divided with the divisor spectra of EFD (10µg/ml). New spectrum was obtained which is then derivatized in to first and higher orders. Mixture spectra was similarly divided with the same divisor and derivatized. METO and mixture shows same absorbance at 274nm in 1st derivative spectra with Delta lambda 5 and scaling factor 10.

Method II: In the present study individual drug solutions were prepared in HPLC grade Methanol. These drug solutions were scanned in the UV-region of 200-400 nm and the spectrum were recorded to get maximum of analytes in mobile phase.

EFD and METO were scanned in UV in which both EFD and METO show reasonably good response at 230 nm.

VALIDATION OF PROPOSED METHOD

The proposed methods were validated according to the International Conference on Harmonization (ICH) guidelines. ⁽¹⁷⁾

Method I: Ratio Derivative Method

Linearity

The calibration curves were plotted over a concentration range of EFD and METO. Absorbance of the solutions was measured at respective wavelength against Methanol as blank. The calibration curves were constructed by plotting absorbance *versus* concentrations and the regression equations were calculated.

Method precision

The precision of the instrument was checked by repeated scanning and measurement of absorbance of solutions ($n = 6$) for EFD and METO.

Intermediate precision

The intra-day and inter-day precision of the proposed method was determined by analyzing the corresponding responses three times on the same day and on three different days three different concentrations of standard solutions of EFD and METO.

Accuracy

Accuracy was determined by performing recovery studies by spiking different concentration of drug in pre-analysed sample solution. To pre-analysed sample solution, a known amount of working standard solution of EFD and METO were added in 10ml volumetric flask and made

up to mark with different level i.e. 80%, 100% and 120%. The experiment was performed in triplicate.

Limit of Detection and limit of Quantification

The limit of detection (LOD) and the limit of quantification (LOQ) of the drug were derived by calculating the signal-to-noise ratio (S/N) using the following equations designated by International Conference on Harmonization (ICH) guidelines.

$$\text{LOD} = 3.3 \times \sigma/S$$

$$\text{LOQ} = 10 \times \sigma/S$$

Where σ is the standard deviation of the response and S is the slope of the calibration curve.

Analysis of EFD and METO in a combined tablet dosage form

The obtained spectra of test concentration scanned in range of 200 – 400 nm and the absorbance were measured at respective wavelengths as per developed method. From recorded absorbancies concentrations were found out and % purity was calculated for both EFD and METO.

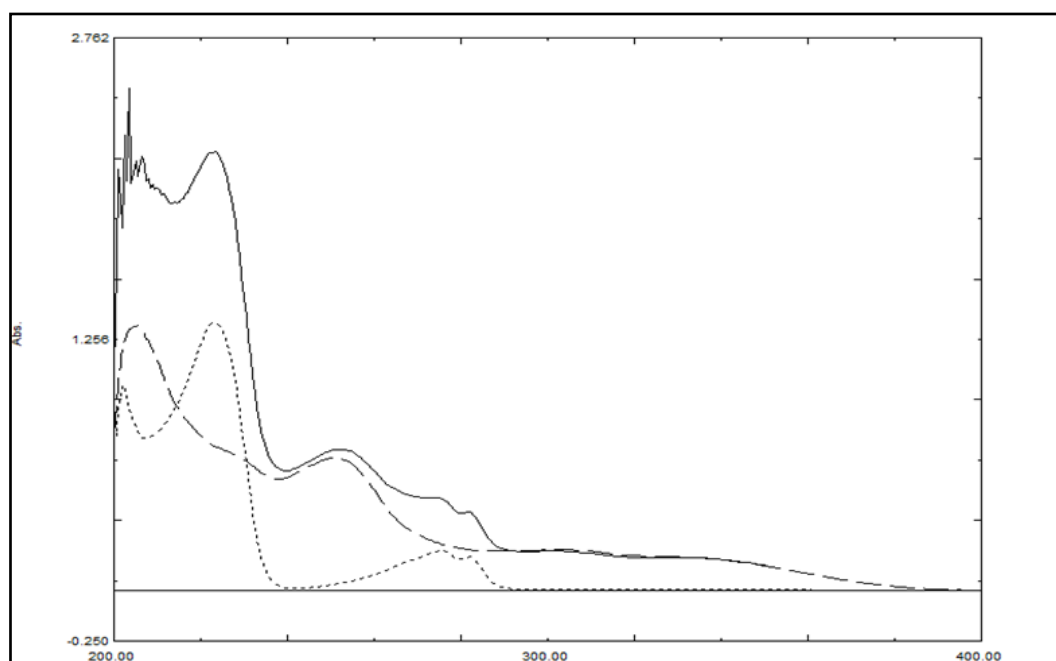
Robustness

Robustness of proposed method was evaluated by deliberately substituting the parameters and found out the % RSD.

RESULTS AND DISCUSSION

Ratio spectra derivative spectroscopic method based on dividing the spectrum for a mixture into the standard spectra for each of the analyses and driving the proportion to obtain a spectrum that is independent of the analyte concentration used as a divisor. The use of standardized spectra as divisors minimizes experimental errors and background noise. ⁽¹⁸⁾

Figure 3: Overlain zero order spectrum of EFD (---- , 20 µg/ml), METO (.... , 50 µg/ml) and Mixture (____, 20+50 µg/ml)



Linearity

Figure 4: Overlain spectra of EFD (10- 50 µg/ml)

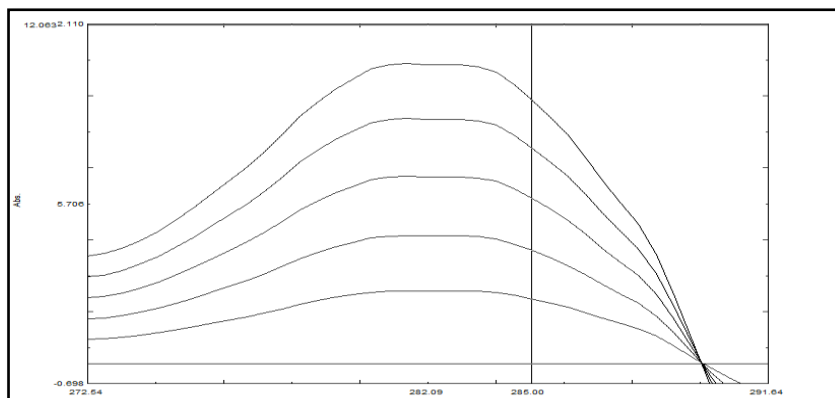


Figure 5: Overlain spectra of METO (25-125µg/ml)

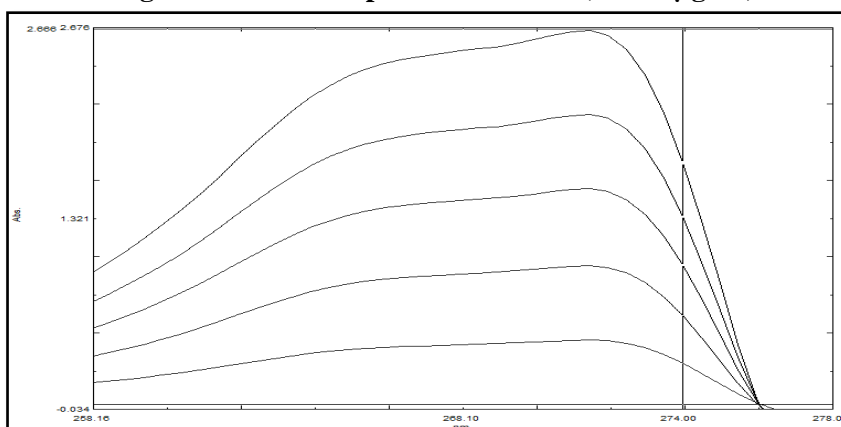


Table 1: Calibration curve

Conc. (µg/ml) (EFD)	Mean Absorbance (n=3)	% RSD	Conc. (µg/ml) (METO)	Mean Absorbance (n=3)	% RSD
10	2.312	0.04	25	0.294	0.34
20	4.042	0.03	50	0.631	0.24
30	5.897	0.01	75	0.991	0.15
40	7.703	0.01	100	1.332	0.07
50	9.411	0.01	125	1.716	0.05

Precision

Table 2: Repeatability

Concentration (µg/ml)		Mean Absorbance (n=6)		% RSD	
EFD	METO	EFD	METO	EFD	METO
30	75	5.896	0.992	0.02	0.07

Intermediate Precision

Table 3: Intra day and Inter day precision

Conc. (µg/ml)	Intraday precision		Interday precision	
	Mean absorbance	% RSD	Mean Absorbance	% RSD
EFD				
10	2.310	0.08	2.320	0.28
30	5.892	0.04	5.894	0.05
50	9.610	0.02	9.616	0.07
METO				
25	0.287	0.43	0.288	0.75
75	0.993	0.23	0.993	0.14
125	1.717	0.11	1.715	0.14

Accuracy

Table 5: % Recovery study

Level (%)	Mean Abs. (n = 3) EFD	% Recovery	% RSD	Mean Abs. (n = 3) METO	% Recovery	% RSD
80	6.854	98.29	1.54	1.208	100.83	1.32
100	7.681	101.79		1.334	98.43	
120	8.362	100.72		1.497	101.18	

LOD and LOQ

Table 6: LOD and LOQ of EFD and METO

Parameters	EFD	METO
LOD (µg/ml)	0.669	1.334
LOQ (µg/ml)	2.027	4.044

Assay

Table 7: Analysis of EFD and METO in formulation (n=6)

Drug	Tablet content (mg)	Mean of Abs (n=6)	% Assay	% RSD	Tablet content found (mg)
EFD	20	5.896	100.43	0.02	20.08
METO	50	0.992	99.97	0.99	49.98

Robustness

Table 8: Robustness of EFD and METO

	Solvent Source		Instrument Model		Different Analyst	
	EFD	METO	EFD	METO	EFD	METO
% RSD	0.03	0.09	0.04	0.19	0.02	0.12

Method II: RP-HPLC

Selection of mobile phase

Mobile phase was selected on the basis of best separation, peak symmetry and theoretical plate. So, numbers of trials were taken for the selection of mobile phase.

Preparation of mobile phase

Mobile phase was prepared 85 ml of Methanol and 15 ml of Water. The mobile phase was filtered through 0.45 μ m membrane filter paper.

Table 9: Chromatographic Conditions

Chromatographic Conditions		Results
Elution		Isocratic
Column		Phenomenex Kinetex $\text{\textcircled{R}}$ 5 μ C18 Size: 150 * 4.6mm
Mobile phase composition (% v/v)		Methanol: Water (85: 15 % V/V)
Flow rate (ml/min)		1 ml/min
Detection wavelength (nm)		230 nm
Injection volume		20 μ l
Run time		10 min
Retention time (min)	EFD	2.3 min
	METO	3.9 min

Table 10: System Suitability Parameters

Parameters	Data obtained	
	EFD (30 μ g/ml)	METO (75 μ g/ml)
Retention time (Rt) \pm SD	2.32 \pm 0.03	3.91 \pm 0.06
Area \pm SD	2707110 \pm 50.84	1297445 \pm 478.93
Theoretical plates per column (N) \pm SD	7254 \pm 42.50	3672 \pm 20.95
Symmetry factor/Tailing factor (As) \pm SD	1.24 \pm 0.04	1.44 \pm 0.04
Resolution (Rs) \pm SD	2.45 \pm 0.02	

Linearity

Figure 6: Linearity of EFD and METO

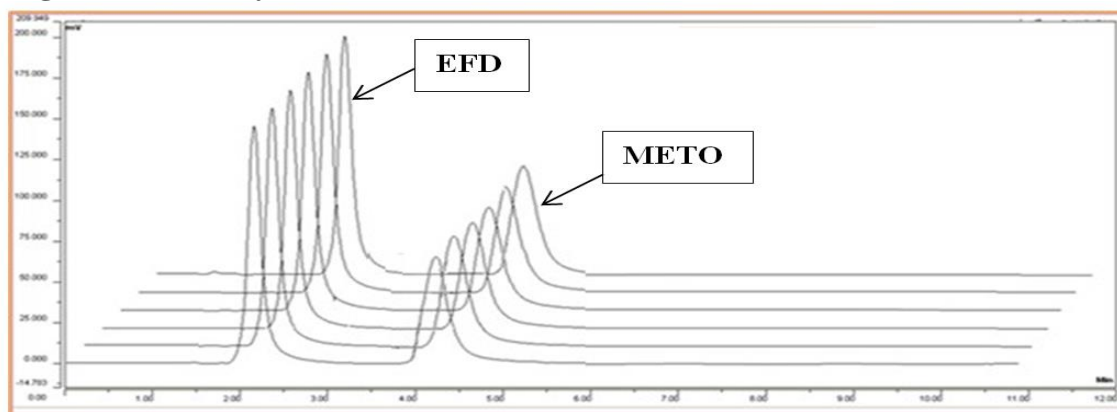


Table 11: Linearity data

Conc. (μ g/ml) EFD	Average area	% RSD	Conc. (μ g/ml) METO	Average area	% RSD
10	800223	0.01	25	421463	0.26
20	1734261	0.005	50	865462	0.04

30	2707110	0.001	75	1297445	0.03
40	3595092	0.004	100	1788400	0.05
50	4492412	0.004	125	2219640	0.01
60	5526749	0.07	150	2714620	0.04

Precision

Table 12: Repeatability of EFD and METO

Concentration (µg/ml)		Mean area (n = 3)		% RSD	
EFD	METO	EFD	METO	EFD	METO
30	75	2707223	1295502	0.005	0.228

Intermediate Precision

Table 13: Intraday and Interday Precision

Conc. (µg/ml)	Intraday Precision		Interday Precision	
	Mean area	% RSD	Mean area	% RSD
EFD				
10	800465	0.02	800652	0.02
30	2707460	0.01	2705670	0.04
60	5522794	0.03	5523516	0.03
METO				
25	422769	0.31	422516	0.17
75	1297539	0.02	1296497	0.13
150	2714848	0.05	2716063	0.13

Accuracy

Table 14: % Recovery

Level (%)	% Recovery EFD	Mean % Recovery	% RSD	% Recovery METO	Mean % Recovery	% RSD
80	100.52	100.63	0.98	99.10	99.94	0.97
100	99.61			100.38		
120	101.76			100.34		

LOD and LOQ

Table 15: LOD and LOQ of EFD and METO

Parameters	EFD	METO
LOD (µg/ml)	0.04	0.18
LOQ (µg/ml)	0.13	0.55

Analysis of EFD and METO in formulation

Table 16: % Assay of EFD and METO

Drug	Drug Content (mg)	Mean % Purity	%RSD	Content found (mg)
EFD	20	101.18	0.05	20.23
METO	50	100.30	0.16	50.18

Robustness

Table 17: Robustness of EFD and METO

	Peak area		Theoretical plates		Tailing factor	
	EFD	METO	EFD	METO	EFD	METO
Flow rate (ml/min) % RSD	0.07	0.06	0.46	0.52	1.86	1.73
Mobile phase composition (%V/V) % RSD	0.07	0.19	0.29	1.18	1.32	1.36

STATISTICAL COMPARISON

The statistical evaluation of % Assay of Ratio derivative method and RP-HPLC method done by ANOVA: Single Factor and found out the F value.

Discussion: F value was found to be smaller compared to F_{crit} value ($F < F_{crit}$), therefore there were no significant differences between the groups.

CONCLUSION

Statistically compared, the LC method is more precise and accurate than the UV method. Statistical tests revealed that there was no significant difference between the groups during the analysis with both methods. It is clear from the report that both of the recommended UV and RP-HPLC methods are applicable to the determination of EFD and METO in drug formulation appropriately. Excipients in pharmaceutical preparations have not interfered and the mobile phase can be prepared very easily. Both suggested analytical methods are reproducible, precise and linear and can be used for routine analysis of EFD and METO in pharmaceutical dosage forms.

REFERENCES

1. "Efonidipine Hydrochloride Ethanolate" accessed on July 2019
<https://pubchem.ncbi.nlm.nih.gov/compound/Efonidipine-hydrochloride-ethanolate#section=3D-Conformer>
2. Solanki MD, Patel DV, Meshram DB. (2022). Development and validation of UV Spectrophotometric method for simultaneous estimation of Efonidipine hydrochloride ethanolate and Chlorthalidone in their synthetic mixture. *Drug Anal. Res.* (6), pp. 27-34.
3. "Metoprolol succinate" accessed on July 2019
<https://pubchem.ncbi.nlm.nih.gov/compound/Metoprolol-succinate#section=3D-Conformer>
4. Madhukar, A et al. (2016). Analytical method development and validation for the determination of Metoprolol succinate in tablet dosage form by RP-HPLC techniques. *Sci. Res. Phar.* 5(6), pp. 74-77.
5. Kumar, A. (2017). Development and Validation of Liquid Chromatography (RPHPLC) Methodology for Estimation of Efonidipine HCl Ethanolate (EFD). *Pharm Anal Acta* (8), pp. 547.
6. Liu, M et al. (2016). A chiral LC-MS/MS method for the stereospecific determination of Efonidipine in human plasma. *J Pharm Biomed Anal* 122, pp. 35-41.
7. Liu, H. (2014). Determination of efonidipine in human plasma by LC-MS/MS for pharmacokinetic applications. *Journal of Pharmaceutical and Biomedical Analysis*, pp. 1-23.
8. Otsukaa, M et al. (2015). Developmental considerations for ethanolate with regard to stability and physicochemical characterization of efonidipine hydrochloride Ethanolate. *CrystEngComm*, pp. 1-5.
9. Wang, N. (2008). Spectroscopic studies on the interaction of efonidipine with bovine serum albumin. *Brazilian Journal of Medical and Biological Research* (41), pp. 589-595.
10. Jadhav, RS. and Bharad, VJ. (2017). Analytical Method Development and Validation of Spectroscopic Method for Estimation of Metoprolol Succinate. *Der Pharmacia Lettre*, 9 (6), pp. 285-297.

11. Gopika VC and Remi, SL. (2018). Validated UV spectrophotometric method for simultaneous estimation of metoprolol succinate and benidipine hydrochloride in their combined tablet dosage form. *Asian J. Pharm. Hea. Sci.* (8), pp. 1968-1975.
12. Shanmugasundaram, P and Kamarapu, SK. (2018). Method Development And Validation For The Simultaneous Determination Of Metoprolol And Atorvastatin By Reversed-Phase High-Performance Liquid Chromatography In Its Bulk And Pharmaceutical Tablet Dosage Form Using Biorelevant Dissolution Media (Fasted State Small Intestinal Fluid). *Asian J Pharm Clin Res.* 11(4), pp. 1-8.
13. Agrawal S, Gurjar P and katheriya B. (2019). Analytical Method Development and Validation for Simultaneous Estimation of Trimetazidine Hydrochloride and Metoprolol Succinate Using HPTLC. 15(3), pp. 243-250.
14. Rao DS, Venkateswarlu T and Rama Krishna G. (2015). Development and Validation of HPLC Method Of Dissolution Test For Metoprolol Succinate And Cilnidipine. *IJPCBS* 5(4), pp. 971-981.
15. Corina MS, Hancianu M, Agoroaei L and Butnaru E. (2015). Preparation of Biological Samples Containing Metoprolol and Bisoprolol for Applying Methods for Quantitative Analysis. *Acta Medica Marisiensis* 61(4), pp. 356-360.
16. Saravanan G, Naga PN, and Visagaperumal D. (2015). Development and validation of stability indicating RP-HPLC method for the simultaneous estimation of Metoprolol succinate and Cilnidipine in bulk and pharmaceutical dosage form. *Int J Pharm Pharm Sci.* (7), pp. 150-154.
17. Geneva, Switzerland: International Conference on Harmonization; 2005. ICH, Q2 (R1) Validation of Analytical Procedure: Text and Methodology.
18. Nikam AD, Pawar SS and Gandhi SV. (2008). Estimation of paracetamol and aceclofenac in tablet formulation by ratio spectra derivative spectroscopy. *Indian J Pharm Sci.* 70(5), pp. 635-637.

PCP385

RISK ASSESSMENT OF NITROSAMINES IN PHARMACEUTICALS: A LOOK AHEAD OF DRUG DEVELOPMENT

AP0363 Mr. Ravi Patel	AP0367 Mr. Ravisinh Solanki	AP0380 Dr. Rajesh Patel	AP0335 Mr. Shalin Parikh	AP0374 Dr. Dignesh khunt
Assistant Professor GSP-GTU ap_ravi_patel@ gtu.edu.in	Assistant Professor GSP-GTU ravisinh@gt u.edu.in	Associate Professor GSP-GTU rajeshpatel@g tu.edu.in	Senior Manager Senores Pharmaceuticals PVT LTD Shalin.parikh2011 @gmail.com	Assistant Professor GSP-GTU digneshkhunt@ gtu.edu.in

Abstract

Since June of 2018, thousands of pharmaceuticals from all over the world have been recalled due to the unexpected presence of nitrosamines (NAs). Beginning with the class of pharmaceuticals known as sartans, subsequent lines of inquiry included antidiabetic medicines, antihistamines, and antibiotics. The problem can be mainly ascribed to naively adopted approval revisions and the lack of sufficient current analytical technologies that can detect those contaminants in time. The impact on the global pharmaceutical market has been enormous, and the problem can be traced to both of these factors. Because of the presence of NAs, it has become clear that pharmaceutical corporations and regulatory bodies in the past did not place sufficient emphasis on these chemicals while they were developing new drugs. Because NAs are known to cause cancer, it is imperative that these cancer-causing substances be eradicated or, at the at least, severely restricted in order to protect patients who are dependent on these medications. This work contributes a procedure that may be utilized in the preapproval development of drugs as well as the post approval risk assessment in order to prevent unexpected finding in the future.

Keywords: Nitrosamines, Drug Development, Impurity

PCP392

NITROSAMINE IMPURITIES AND LONG-TERM MEDICATION: THE NEED FOR INVESTIGATION IN GUJARAT REGION

AP0367 Mr. Ravisinh Solanki Assistant Professor GSP-GTU ravisinh@gtu.edu.in	AP0363 Mr. Ravi Patel Assistant Professor GSP-GTU ap_ravi_patel@gtu.edu.in	AP0380 Dr. Rajesh Patel Associate Professor GSP-GTU rajeshpatel@gtu.edu.in	AP0335 Mr. Shalin Parikh Senior Manager Senores Pharmaceuticals PVT LTD Shalin.parikh2011@gmail.com	AP0387 Mr. Bhavinkumar Gayakvad Assistant Professor GSP-GTU ap_gsp_bhavin@gtu.edu.in
---	--	--	--	--

Abstract

The prevalence of diabetes in India's 15 states was 73% (95 % CI 70–7.5), according to the study. In urban Gujarat alone, 9.8 percent of diabetes were documented, whereas in rural Gujarat, 5.1 percent of diabetics were reported. Increased usage of Metformin and its combinations has been found in both urban and rural populations, coupled with this rise in the incidence of diabetes. Metformin and its combinations with other medicines are widely used as a therapy for type 2 diabetes. Combinations of these other medications include Glipizide, Rosiglitazone, Pioglitazone, Nateglinide, Vidagliptine, Fenofibrate, Sitagliptin, Glimepiride and Fenofibrate. In recent months, the U.S. Food and Drug Administration (and European Medical Agency (EMA), Therapeutic Goods Administration (TGA), and Health Canada (HC)) have placed a greater emphasis on the probable presence of human carcinogenic and genotoxic nitrosamine contaminants in Metformin formulations. According to ICH M7, the USFDA advisory paper specifies seven potentially carcinogenic nitrosamine impurities with maximum daily allowable intake. In the interest of public health, a systematic market survey of Metformin with other drug combinations in Gujarat is necessary, followed by a short risk evaluation of the failed samples. Due to the nanograms per milliliter limitations of certain contaminants, analytical procedures such as LC-MS/MS, LC-HRMS, or GC-MS/MS are necessary. Present article shows the need and the methodology on accordance with regulatory guidance to carry out systematic survey on marketed metformin combinations in Gujarat Region.

Keywords: Nitrosamine, long term medication, impurity.

PCP410

ISOLATION AND CHARACTERIZATION OF SELECTIVE HERBAL MARKERS FROM *GARCINIA INDICA* EXTRACT

AP0419 Kankshi Pathak Student Graduate school of pharmacy-GTU knp462000@gmail.com	AP0425 Monika Sorathiya Student Graduate school of pharmacy- GTU monikasorathiya421999@gmail.com	AP0427 Dr. Sanjay Chauhan Director Graduate school of pharmacy- GTU Prof_Sanjay_chauhan@gtu.edu.in
--	---	---

Abstract

As the market for herbal goods grows, it will be necessary to build trustworthy, cutting-edge technical interventions to find fake, mislabeled, and contaminated products. In this case, we have established cutting-edge technical ways to test the *Garcinia indica* (*G. indica*) which is known as Kokum-member of *Guttiferae* family. It prevents obesity and functions as an antioxidant and digestive tonic, and treats liver conditions, sunstroke, cancer, and heart conditions. Garcinol, citric acid (CA), hydroxycitric acid (HCA), hydroxycitric acid lactone (HCAL), tannins, carbs, fiber, lipids, proteins, and anthocyanin pigments are some of the phytoconstituents discovered in it. Garcinol isolation by vacuum column chromatography and size exclusion chromatography was performed after dichloromethane: methanol (1:1) extraction of dried fruit rinds. Toluene, ethyl acetate and acetic acid (7:3:0.2 v/v/v), used as the mobile phase, were used to develop the high-performance thin layer chromatography (HPTLC) method. The high-performance liquid chromatography (HPLC) method was established using C18 (250mm x 4.6mm, 5 m) as the stationary phase, 0.01M potassium dihydrogen phosphate (KH₂PO₄) as the mobile phase A, and acetonitrile: 0.01M KH₂PO₄ (90:10 v/v) as the mobile phase B. The samples were then detected at 215nm and 276nm. Garcinol had a 0.69 retention factor (R_f) according to the HPTLC technique. HCAL, HCA, CA, and Garcinol all had HPLC retention times that were, respectively, 2.941, 4.25, 8.666 and 18.467 minutes. This study may aid in the prevention of adulteration as well as quality assurance, standardization and phytoconstituent identification in *G. indica* formulations.

Keywords: *Garcinia indica*, phytoconstituents, HPLC, HPTLC, standardization.

PCP417

**STABILITY INDICATING HPLC METHOD DEVELOPMENT
AND VALIDATION FOR SIMULTANEOUS ESTIMATION OF
CELECOXIB AND TRAMADOL HYDROCHLORIDE IN
COMBINATION**

AP0440 HARMISH ASODARIYA^{1*} M. Pharm Student SSSPC, Zundal *asodariyaharmish009@gmail.com	AP0442 DR. HIRAL PANCHAL² Professor SSSPC, Zundal hir_panchal@ymail.com	AP0443 YAYATI PATEL³ M. Pharm Student SSSPC, Zundal ynp1911@gmail.com	AP0441 NITYA PATEL⁴ M. Pharm Student SSSPC, Zundal nityapatel2016@gmail.com
---	--	--	---

ABSTRACT

A simple, accurate Stability-Indicating High-Performance Liquid Chromatographic (HPLC) method was developed and validated for Simultaneous estimation of Celecoxib and Tramadol hydrochloride in combination. Chromatography was carried out on Phenomenex luna C18 (4.6 mm LD x 250 mm, 5µm) column using a mixture of Water: Methanol (15:85, v/v) as the mobile phase at a flow rate of 0.8ml/min, the detection was carried out at 275nm respectively for Celecoxib and Tramadol hydrochloride. The retention time of the Celecoxib and Tramadol hydrochloride was 5.79 and 3.89 min respectively. The method procedure linear response of Celecoxib and Tramadol hydrochloride was found to be 1 and 0.997 respectively. The method precision for the determination of assay was below 2.0% RSD. The method was statistically validated for linearity, accuracy, precision and selectivity. Due to its simplicity and accuracy this method will be useful for routine quality control analysis.

Key words: Celecoxib, Tramadol hydrochloride, HPLC, Method Validation, Stability study

PCP418

CURRENT TRENDS IN GREEN CHEMISTRY BASED ON PHARMACEUTICAL APPROACH

AP0431

Kartiksinh Solanki

GTU Student,

Graduate School of Pharmacy-GTU

kartiksolanki081@gmail.com

Abstract

Green chemistry is the utilisation of a set of principles that reduces or eliminates the use or generation of hazardous substances in the design, manufacture and application of chemical products. Chemicals are a part of modern life. Products are the main emissions of the chemical and pharmaceutical industries. Very often they do not become degraded or fully broken down to water, carbon dioxide and inorganic salts. Often, unknown transformation products are formed in the environment. Therefore, according to the principles of green chemistry, the functionality of a chemical should not only include the properties of a chemical necessary for its application, but also easy and fast degradability after its use. Green Chemistry is simply a new environmental priority when accomplishing the science already being performed regardless of the scientific discipline or the techniques applied. Pharmaceutical Green Chemistry will translate to higher synthetic efficiency and better chemical processes, which will in turn reduce impact upon the environment. The main objective of this review is to shed light upon key aspects with regard to the philosophy of pharmaceutical green chemistry and to reduce environmental risks, hazards and pollution caused by chemicals in pharmaceutical industry.

Keywords: Green Chemistry, Green Pharmacy, Sustainable products, Green analytical techniques.

PCP429

A REVIEW ON IMPURITY PROFILING IN PHARMACEUTICALS

AP0460

Shraddha Patil

Student

GSP-GTU

patilshraddha@gmail.com

AP0380

Dr. Rajesh Patel

Associate Professor

GSP-GTU

rajeshpatel@gtu.edu.in

Abstract

Any component of the new drug substance that is not a chemical entity is considered an impurity. The identified and unidentified impurities present in a new drug substance are referred to as the impurity profile. Impurity profiling is the common name for a set of analytical activities aimed at detecting, identifying, elucidating, and determining organic and inorganic impurities in pharmaceuticals. The impurity may be developed during Formulation or upon aging of API'S. Toxic impurities are dangerous to health and increase the safety of drug therapy; therefore, impurities should be identified and determined using any selective methods. Regulatory bodies include the international council for harmonization (ICH), United States Food and drug administration (USFDA) and Canadian Drug and Health Agency (CDHA). Catalysts, reagents, heavy metals, and degraded end products obtained during the manufacturing of bulk drugs via hydrolysis, oxidation, and de-carboxylation are some of the various sources in pharmaceutical products. To identify impurities in pharmaceuticals, various methods such as ultraviolet spectroscopy, infrared spectroscopy, liquid chromatography-mass spectroscopy (LC-MS), gas chromatography-mass spectroscopy (GC-MS), nuclear magnetic resonance (NMR) spectroscopy, and others are used.

Keywords: Impurity Profile, Chromatography, Impurities, Elucidation.

PCP434

METABOLIC FINGERPRINTING WITH FTIR SPECTROSCOPY FOR ANTIBIOTIC SCREENING ASSAY

AP0458

Shikha Sharma

PG Student

GSP-GTU

sharmashikhak@gmail.com

AP0380

Dr. Rajeshkumar Patel

Associate professor

GSP-GTU

rajeshpatel@gtu.edu.in

Abstract:

Despite a slowdown in antibiotic development, identifying the mechanism of action (MOA) remains a significant barrier. To identify the metabolic fingerprint of 15 antibiotics induced on *Escherichia coli* metabolism, a high-throughput whole-cell FTIR spectroscopy-based bioassay was developed. Since each biochemical fingerprint was unique, it was possible to distinguish between several antibiotics in various separate cultures using FTIR spectroscopy. These fingerprints matched the known MOA of each tested antibiotic. High throughput screening for antibiotic development and a better knowledge of the MOA of existing antibiotics both offer considerable promise for FTIR spectroscopy.

Keywords: Antibiotic discovery; Fourier-Transform infrared (FTIR) spectroscopy; high-throughput screening; metabolic fingerprinting; multivariate analysis.

PCP446

A NOVEL AND ROBUST STABILITY INDICATING RP-HPLC-DAD METHOD FOR SIMULTANEOUS ESTIMATION OF MONTELUKAST AND ACEBROPHYLLINE CONTAINING THEOPHYLLINE-7-ACETIC ACID AND AMBROXOL BASE IN ITS MARKETED TABLET DOSAGE FORM

AP0489

Janki Goswami

Research Scholar
Graduate School of
Pharmacy

jankigoswami5@gmail.com

AP0367

Ravisinh Solanki

Assistant Professor
Graduate School of
Pharmacy

ravisinh@gtu.edu.in

AP0363

Ravi Patel

Assistant Professor
Graduate School of
Pharmacy

ap_ravi_patel@gtu.edu.in

Abstract:

A precise, robust, simple and accurate stability indicating RP-HPLC method was developed and validated for simultaneous estimation of Acebrophylline and Montelukast in marketed formulations. Presented analytical method had challenges due to extreme sensitive nature of montelukast i.e., heat and light sensitive and hygroscopic. According to the literature review, Acebrophylline is composed of two different components, each with different properties and pKa values. Therefore, the chromatogram would have shown two distinct peaks. (One for theophylline -7- acetic acid and other for ambroxol base). Unfortunately, none of the reported more than four HPLC methods shown two individual peaks. Theophylline-7-acetic acid and ambroxol base are components of Acebrophylline which requires more reliable data using forced degradation studies and stability studies. In this work, marketed sample was subjected to various degradation conditions. The developed method was analyzed by Eclipse Plus C18 (150mm x 4.6mm, 5 μ m) as stationary phase using mobile phase in ratio of Phase A 90:10 % v/v and Phase B 10:90% v/v at flow rate of 1.0ml/min. Quantification was achieved at 296 nm with PDA detector. The retention time was Montelukast 21.73min and Acebrophylline Peak 1=4.75min and Peak 2= 7.95min. The linearity of method was found in the range of 10-30 and 200-600 μ g/ml with mean accuracies of 100.69%-99.83% and 99.921%-100.369% respectively. The developed method meets all the acceptance criteria as per ICH Q2 R1 guideline.

Keywords: RP-HPLC, Acebrophylline, Montelukast, Method Validation, Stress Testing, IR spectrum

INTRODUCTION:

Introduction To the Drug Combination

Acebrophylline is a mucolytic. It is used for the treatment of Respiratory Tract Infection. Acebrophylline cyclohexanol is the salt obtained by reaction of equimolar amounts of theophylline-7-acetic acid, which is a xanthine derivative with specific bronchodilator activity, and ambroxol, which is a mucolytic and expectorant. Montelukast is a leukotriene antagonist. It works by blocking the action of leukotriene, a chemical messenger. Monosodium salt is a selective and orally active leukotriene receptor antagonist that inhibits the cysteinyl leukotriene CysLT1 receptor. The combination of these two drugs are available in the market for the treatment of COPD and bronchial asthma and also clinical trials have been reported for this combination in India^[1].

Acebrophylline: CAS no. is 96989-76-3, IUPAC name is 4-[(2-amino-3,5-dibromophenyl) methylamino] cyclohexan-1-ol;2-(1,3-dimethyl-2,6-dioxopurin-7-yl) acetic acid (Fig. 1a) and mechanism of action is that Acebrophylline is obtained by reaction of the Ambroxol base and theophylline-7-acetic acid^[2,3]. The Carboxyl group of theophylline-7-acetic acid was satisfied with Ambroxol's amine group in a stoichiometric ratio 38.7% acid and 61.3% base that ensures,

after absorption, high plasma levels of Ambroxol with low levels of the xanthine derivative which are nevertheless high enough to ensure a carrier effect for ambroxol [4,5].

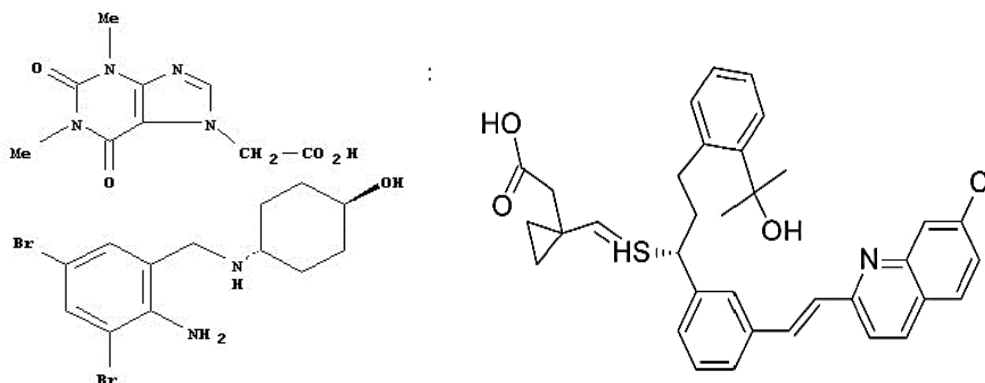


Figure 1: a) Structure of Acebrophylline, b) Structure of Montelukast

Montelukast: CAS no. is 151767-02-01, IUPAC name is [R-(E)]-1-[[[1-[3-[2-(7-chloro-2quinolinyl) ethenyl] phenyl]-3-[2-(1-hydroxy-1ethylrhtyl) phenyl] propyl] thio] methyl] cyclopropane acetic acid, monosodium salt (Fig. 1b) and mechanism of action is that Montelukast selectively antagonizes LTD₄ at the cysteinyl leukotriene receptor, CysL0054₁, in a human airway, Montelukast inhibits the actions of LTD₄ at the CysLT₁ receptor, preventing airway edema, smooth muscle contraction, and enhanced secretion of viscous and thick mucus [6,7].

In the proposed method, both the drugs are applied for forced degradation in acid, alkaline, oxidative, photolytic, and thermal environments and these solutions were analyzed by the RP-HPLC method. A stress study or degradation study was performed according to ICH guidelines for stability testing. The method was developed and validated according to ICH Q2R1 guidelines. After a detailed and systematic study, the following procedures are recommended for the determination of Montelukast sodium and Acebrophylline in pharmaceutical formulations.

Literature Review

Several reports are available describing various methods for the estimation of the Montelukast and Acebrophylline individually and in a combination in a variety of matrices like bulk drug and dosage forms. Literature review for the combination presented in table 1.

Table 1. Literature review

Sr. no.	Sample matrix	Analytical method	Method description	Ref. No.
1	Combination drug	RP-HPLC method	(Combination with levocetirizine) Column C- 18 BEH 2.1 x 50 mm (1.7 μm) Flow rate: 0.6 ml/min Wavelength: 230 nm Mobile phase; methanol: acetonitrile: Buffer (30:40:30) potassium dihydrogen phosphate buffer was used with pH 6.0. Run time 4.5 min.	9
2	Marketed formulation (MONT+ ACB+ LEVO)	HPLC method	Column: C18 4.6 mm * 250 mm (5 μm) Mobile phase: Ammonium acetate buffer of pH 3.5 (pH adjusted with glacial acetic acid) and methanol in the ratio 15:85 v/v	10

3	Tablet	RP-HPLC method	Column: BDS Hypersil, C18, (250 x 4.6mm, 5 μ m) Mobile phase: 10 mm phosphate buffer (pH 4): Acetonitrile (15:85)	11
4	Marketed formulation (MONT+ ACB+ Desloratadine)	RP-HPLC-PDA method	Column: BDS C8 Column (150 x 4.6mm, 5 μ m) Mobile phase: Potassium hydrogen ortho-phosphate buffer: acetonitrile (40:60) Flow rate: 1ml/min	12
5	Combined dosage form	HPLC method	Column: C18 Hibar Lichrospher® (250 mm x 4.6 mm, 5 μ m) Mobile phase: Acetonitrile: Methanol (60:40 %v/v) Flow rate: 0.8 ml/min	13

Justification

The literature review and studies concluded that Acebrophylline made up of two different components i.e., **theophylline -7- acetic acid**, a xanthine derivative, and **ambroxol base**, a mucolytic and expectorant. So, the chromatogram would show two separate peaks for both components. None of the reported HPLC methods did show two individual peaks for Acebrophylline. (One for **theophylline -7- acetic acid** and the other for **ambroxol base**). So, the requirement of generation of more reliable data with forced degradation study was required. That would result in a robust, accurate, precise and reliable analytical method on HPLC for simultaneous estimation and assay calculation of Acebrophylline and Montelukast formulations.

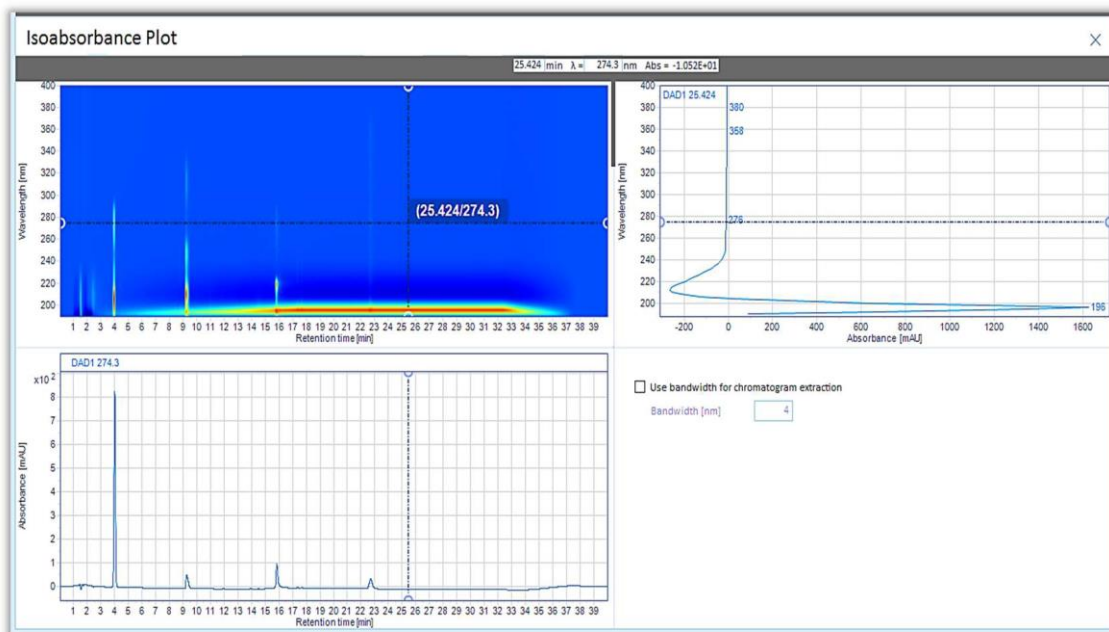
MATERIALS AND METHODS

Chemicals and Reagents

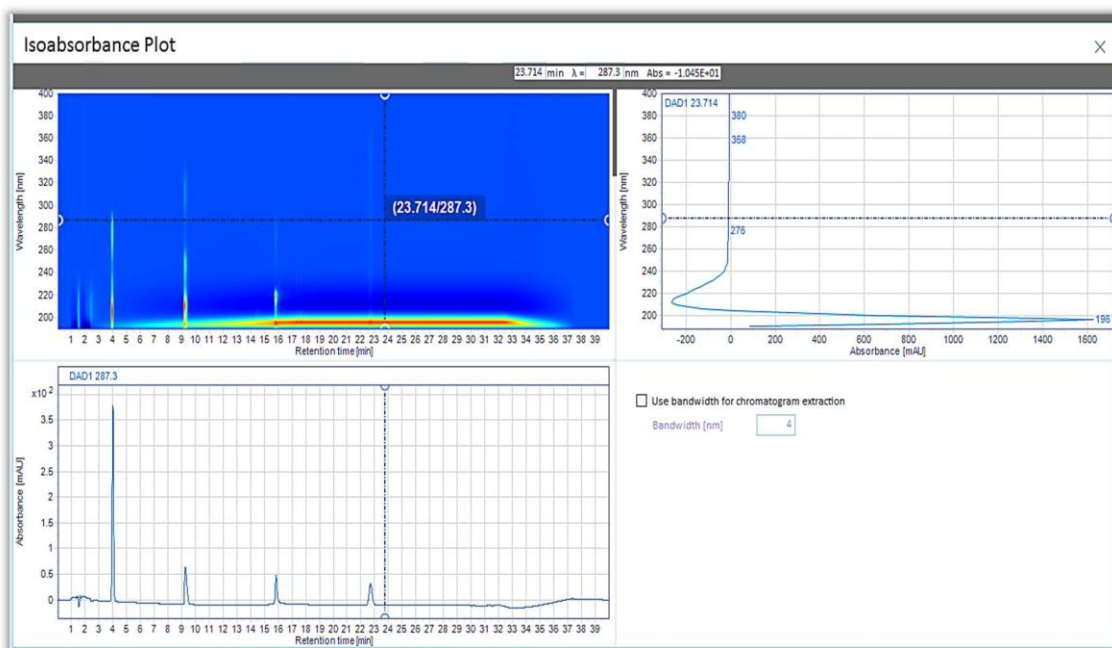
Acebrophylline and Montelukast both standards were obtained from Synochem Pharmaceuticals. HPLC grade solvents methanol purchased from Rankem lab, Milli Q water, and AR grade reagents ammonium formate buffer, O- phosphoric acid are of research-grade used without further purification.

Instrumentation and Chromatographic Conditions

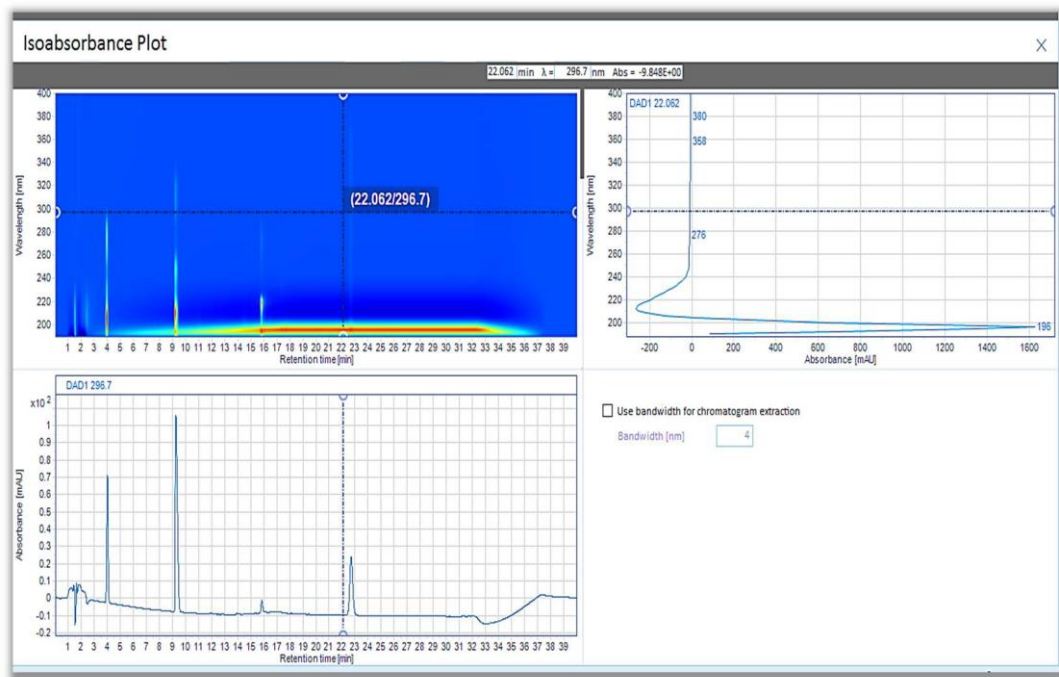
The chromatographic analysis was performed using Agilent HPLC (1260 Infinity II) system equipped with a prominence PDA detector (G7115A) and quaternary pump (G7111B) system operational with an auto-sampler (G7129A). The data interpretation and analysis were done using software Open Lab CDS. Chromatographic separation was carried out using Eclipse Plus C₁₈ analytical column (150mm x 4.6mm internal diameter, 5 μ m particle size) at a column temperature of 10 °C. The optimized Mobile phase A= Ammonium formate buffer was adjusted to pH 2.8 with OPA: Methanol (90:10 V/V) and Mobile phase B= Ammonium formate buffer were adjusted to pH 2.8 with OPA: Methanol (10:90 V/V) and pumped through column at a flow rate of 1.0 mL/ min. Prior to use, the mobile phase was filtered through the 0.45 μ m Millipore filter and ultrasonically degassed. The volume of injection was kept at 10 μ L for the sample analysis. The optimum wavelength i.e., 296nm was used for simultaneous estimation (Fig. 2).



Isoabsorbance plot at 274 nm (λ_{max} of Acebrophylline)



Isoabsorbance plot at 287.3nm (λ_{max} of Montelukast)



Isoabsorbance plot at 296nm (Selected λ_{max})
Figure 2: Isoabsorbance plots

NOTE:

Montelukast is heat and light-sensitive drug.

Carried out all the experimental work in minimum light to avoid the light exposure

Carried out all the experimental work at room temperature (25 °C)

Preparation Of Mobile Phase And Diluent

0.7 mg of Ammonium formate buffer was weighed and make the volume up to 1000 mL then sonicated it for 15 min (Observed pH was 6.54), Adjusted the pH 2.8 with 1 mL of O-phosphoric acid. Filtered the solution.

Mobile phase A= Ammonium formate buffer: Methanol= 90:10 V/V

Mobile phase B= Ammonium formate buffer: Methanol= 10:90 V/V

Diluent: Methanol: Ammonium formate buffer: 70:30 V/V

Preparation of Standard solutions

Standard stock solution of ACBR (4000 μ g/ mL) and MTKT (200 μ g/ mL) were prepared in diluent (Methanol: Ammonium formate buffer – 70:30 V/V). 100 mg of Acebrophylline and 5 mg of Montelukast were weighed into a 50 ml volumetric flask. Add about 35 ml of diluent and sonicated to dissolve. Diluted up to mark with diluents (Acebrophylline 4000 μ g/mL and Montelukast 200 μ g/ml). 5 mL of stock solution and diluted up to 25 mL with diluent (400 μ g/mL of Acebrophylline and 20 μ g/mL of Montelukast). Primary standards were stored in well manners to protect from light and heat until analysis.

Preparation of Sample solutions

Twenty tablets were weighed accurately and a quantity of tablet powder equivalent to 100 mg Acebrophylline and 5 mg Montelukast was transferred to 50 ml volumetric flask, 35 ml of diluent was added, sonicated for 5 min and made upto mark with diluent (4000 μ g/ml and 200 μ g/ml of ACBR and MTKT respectively). The sample solution was scanned in the wavelength range of 400–200 nm. 296 nm wavelength was selected for further analysis on HPLC owing to measurable response of all three components.

METHODS

The development of a method for simultaneous analysis of Acebrophylline and Montelukast was performed by using different mobile phase gradient and mobile phase pH. According to ICH guidelines, the validation of the developed method was done for linearity, the limit of quantification (LOQ), the limit of detection (LOD), accuracy, precision, robustness, specificity.

System Suitability Test (SST)

The SST ensures that validating the power of the analytical method as well as confirms the resolution between different peaks of interest. All critical parameters tested met the acceptance criteria on all days. The system suitability assessment for the analytical HPLC method established instrument performance parameters such as resolution, %RSD, Theoretical Plates (*N*), and Tailing factor (*Tf*) for both the analytes.

Precision

Repeatability was determined by analysing a solution containing a mixture of Acebrophylline and Montelukast having a concentration of 400 µg/ml and 20 µg/ml respectively. The Peak area of the same concentration was measured six times and % RSD was calculated.

Intraday Precision: Solution containing a mixture of Acebrophylline and Montelukast as 200 µg/ml and 10 µg/ml, 400 and 20 µg/ml and 600 and 30 µg/ml were analysed on 3 different days, peak areas were determined and % RSD was calculated.

Interday Precision: Solution containing a mixture of Acebrophylline and Montelukast as 200 µg/ml and 10 µg/ml, 400 and 20 µg/ml and 600 and 30 µg/ml were analysed on 3 times on same days, peak areas were determined and % RSD was calculated.

Linearity

The linearity of the method was evaluated by injecting different concentrations of the standard solution of Acebrophylline and Montelukast. A stock solution was prepared of Acebrophylline 400 µg/ml and Montelukast 20 µg/ml. Further dilutions are 0.5, 0.8, 1.0, 1.2 and 1.5 mL of stock solution and diluted up to 10mL which gives concentrations 200, 320, 400, 480 and 600 µg/ml of Acebrophylline while 10, 16, 20, 24 and 30µg/ml of Montelukast.

Accuracy (%Recovery)

The assay method was evaluated with the recovery of the standards from excipients. Three different quantities (50%, 100% and 150%) of the standards were added to the pre analyzed formulation and were analyzed using the developed HPLC method.

Specificity

The specificity of the method was ascertained by analyzing diluent, placebo, standard and tablet formulation to examine the % interference of excipients and their impurities with analytes peak. The specificity of the proposed method was determined by analyzing spiking of placebo to sample and calculated the % interference.

Robustness

As defined by the ICH, the robustness of an analytical procedure refers to its Capability to remain unaffected by small and deliberate variations in method Parameters here changes in different conditions were considered:

- 1) Change in wavelength (296 nm ± 2)
- 2) Change in Flow rate (1 ml/min ± 0.2)
- 3) Column Temperature (25°C ± 5°C)
- 4) Mobile phase pH (2.8 ± 0.2)

LOD and LOQ

From the linearity curve equation, the standard deviation (SD) of the intercepts (response) was calculated. The limit of detection (LOD) of the drug was calculated by using the following equation designated by International Conference on Harmonization (ICH) guideline:

$$\text{LOD} = 3.3 \times \text{Standard deviation} / \text{Slope}$$

The limit of quantitation (LOQ) of the drug was calculated by using the following equation designated by International Conference on Harmonization (ICH) guideline:

$$\text{LOQ} = 10 \times \text{Standard deviation} / \text{Slope}$$

Stability Studies (Forced Degradation):

Stability Studies were carried out on the drug in order to check the stability of the drug by providing various stress conditions like acid, base, oxidation, thermal, photo, and UV Control degradation compared with normal conditions as recommended by ICH. The purpose of the force degradation method is to provide evidence that the analytical method is efficient in the determination of drug substances in the commercial drug product in the presence of its degradation products.

NOTE: Stability studies (forced degradation) were performed on the marketed formulation (Telekast A by Lupin Ltd.; Label claim= Acebrophylline 100 mg, Montelukast 10 mg)

Acid Hydrolysis

Tablet powder equivalent to 773.5mg of Acebrophylline and Montelukast (1 tablet) was transferred in a 50 mL volumetric flask. Add 1mL of 1N HCl was added and kept for 15min at 60°C in the water bath. Neutralization was done by using 1mL of 1N NaOH. Add about 35mL with diluent and sonicate it for 10min, make up the volume up to the mark (400 µg/mL and 20 µg/mL of Acebrophylline and Montelukast respectively) centrifuge it for 10min at 5000 rpm maintaining 10°C filter the solution with 0.45 µm syringe filter.

Base Hydrolysis

Tablet powder equivalent to 773.5mg of Acebrophylline and Montelukast (1 tablet) was transferred in a 50 mL volumetric flask. Add 1mL of 1N NaOH was added and kept for 15min at 60°C in the water bath. Neutralization was done by using 1mL of 1N HCl. Add about 35mL with diluent and sonicate it for 10min, make up the volume up to the mark (400 µg/mL and 20 µg/mL of Acebrophylline and Montelukast respectively) centrifuge it for 10min at 5000 rpm maintaining 10°C filter the solution with 0.45 µm syringe filter.

Oxidative Hydrolysis

Tablet powder equivalent to 773.5mg of Acebrophylline and Montelukast (1 tablet) was transferred in a 50 mL volumetric flask. 0.5mL of 6 % H₂O₂ was added and kept for 15min at 60°C in the water bath. Add about 35mL with diluent and sonicate it for 10min, make up the volume up to the mark (400 µg/mL and 20 µg/mL of Acebrophylline and Montelukast respectively) centrifuge it for 10min at 5000 rpm maintaining 10°C filter the solution with 0.45 µm syringe filter.

Thermal Degradation

Tablet powder equivalent to 773.5mg of Acebrophylline and Montelukast (1 tablet) was transferred in 50 mL volumetric flask and kept in the water bath for 20min at 60°C. To it, 70 % of diluent was added and sonicated for 20 min. Add about 35mL with diluent and sonicate it for 10min, make up the volume up to the mark (400 µg/mL and 20 µg/mL of Acebrophylline and Montelukast respectively) centrifuge it for 10min at 5000 rpm maintaining 10°C filter the solution with 0.45 µm syringe filter.

Photo Degradation:

Tablet powder equivalent to 773.5mg of Acebrophylline and Montelukast (1 tablet) was transferred in 50 mL volumetric flask and kept in UV chamber for 2Hrs. Add about 35mL with diluent and sonicate it for 10min, make up the volume up to the mark (400 µg/mL and 20 µg/mL of Acebrophylline and Montelukast respectively) centrifuge it for 10min at 5000 rpm maintaining 10°C filter the solution with 0.45 µm syringe filter.

UV Control Degradation:

Tablet powder equivalent to 773.5mg of Acebrophylline and Montelukast (1 tablet) was transferred in 50 mL volumetric flask and kept in UV chamber (wrapped with aluminum foil) for 2Hrs. Add about 35mL with diluent and sonicate it for 10min, make up the volume up to the mark (400 µg/mL and 20 µg/mL of Acebrophylline and Montelukast respectively) centrifuge it for 10min at 5000 rpm maintaining 10°C filter the solution with 0.45 µm syringe filter.

RESULTS AND DISCUSSION

Development and optimization of a method

A robust and new RP-HPLC method was established for the simultaneous determination of Acebrophylline and Montelukast. The different parameters such as mobile phase composition, their pH and flow rate, wavelength and column oven temperature were optimized for the development of an effective chromatographic method. The mobile phase was selected based on pKa and pH values of both the drugs, solubility, peak symmetry, best separation etc. A number of trials were taken for the selection of mobile phase as mentioned here. Initially according to the pKa value and solubility of Acebrophylline and Montelukast, methanol and ammonium formate buffer were tried in different ratio and it gives satisfactory results. Finally mobile phase consisting of Mobile phase A= ammonium formate buffer: methanol [pH 2.8 optimized by 1mL OPA] in the ratio of **90:10 v/v** and mobile phase B= ammonium formate buffer: methanol in ratio of **10:90 v/v** gave good separation and resolution. The effect of various flow rates on formulation and separation of peaks of the analytes was studied and a flow rate, 1.0 mL/min was optimum with reasonable time of analysis. Montelukast having a retention time of 21.73 min and Acebrophylline having retention time Peak 1=4.75 min and Peak 2= 7.95min. (Fig. 3).

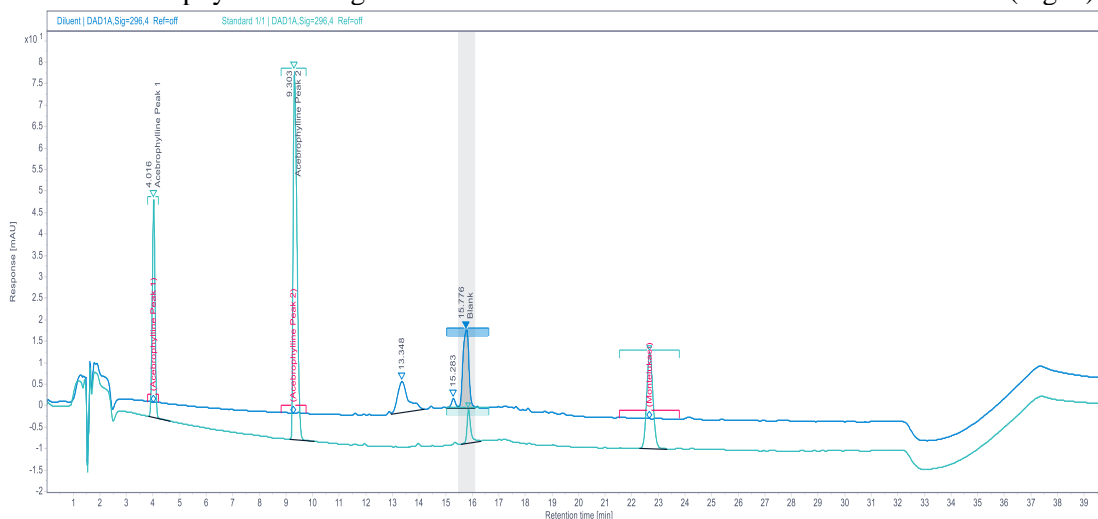


Figure 3: Chromatogram of both standards

Method validation

Validation of analytical method deals with the aim to ensure that the developed method is acceptable and reliable for its deliberate purpose. As per ICH guidelines (Q2R1), the developed HPLC method was validated for different validation characteristics such as system suitability, linearity, accuracy, precision, LOD, LOQ, robustness, and specificity (Table 2).

Table 2. Summary of validation parameters

Parameters	Result	
	Acebrophylline	Montelukast
Linearity	0.9998	0.9994
Accuracy at 50%, 100% & 150%	99.92- 101.07 %	99.83- 100.69 %
Precision Interday Precision Intraday Precision	0.504	0.795
Robustness		
Change in wavelength (296 nm ± 2)	0.125 (294nm) and 0.392 (298nm)	0.402 (294nm) and 0.955 (298nm)
Change in Flow rate (1 ml/min ± 0.1)	0.738 (0.9 ml/min) and 0.87 (1.1 ml/min)	0.131 (0.9 ml/min) and 0.187 (1.1 ml/min)
Temperature (25 °C ± 5 °C)	0.742 (20 °C) and 0.824 (30 °C)	0.345 (20 °C) and 0.688 (30 °C)
Change in pH (2.8 ± 0.2)	0.606 (2.6) and 0.849 (3)	0.426 (2.6) and 0.315 (3)
LOD	0.335 µg/ml	2.767 µg/ml
LOQ	1.015 µg/ml	8.387 µg/ml

System suitability

The system suitability ensures that the validity and specificity of the developed method. This test represents an essential component of the method development and is utilized to confirm the resolution and reproducibility of the developed technique, for performing chromatographic analysis. The percent RSD of different parameters such as peak area, retention time, theoretical plates and tailing factor were determined (Table 3). The peaks obtained for Acebrophylline and Montelukast were found to be sharp, well separated and with high resolution.

Table 3. System suitability parameters

Parameters	Observation				Specification
	Acebrophylline			Montelukast	
	Peak 1	Peak 2	Sum		
Resolution (RS)	000	22.64	22.64	21.10	RS > 18
Tailing Factor (T)	0.97	1.63	-	1.10	T ≤ 2
Theoretical Plates (N)	6962	18249	-	45412	> 3000
% RSD	-	-	0.274	0.618	< 2%

RSD: Relative standard deviation

Precision

Precision is a measure of degree of scattered readings of the developed method between the numbers of reading resulted from various samplings of a similar sample under the specified analytical procedures. In the present study, intra-day and inter-day assays were used to test the precision. Analysis of precision was done on the same day at different time intervals by determining repeatability (intra-day precision), and on three consecutive days, by determining intermediate precision (inter-day precision).

Linearity

Linearity is the ability of the analytically developed procedure to check the result of the sample analytes whether it is to its concentration. The linearity of the method was tested by analysing

different concentration ranges 200-600 $\mu\text{g/mL}$ of Acebrophylline and 10-30 $\mu\text{g/mL}$ Montelukast, at 296nm. The regression analysis data for the calibration curve shows linear relation over this concentration range. The correlation coefficient values for both drugs were found to be $R^2 > 0.999$ (Fig. 4).

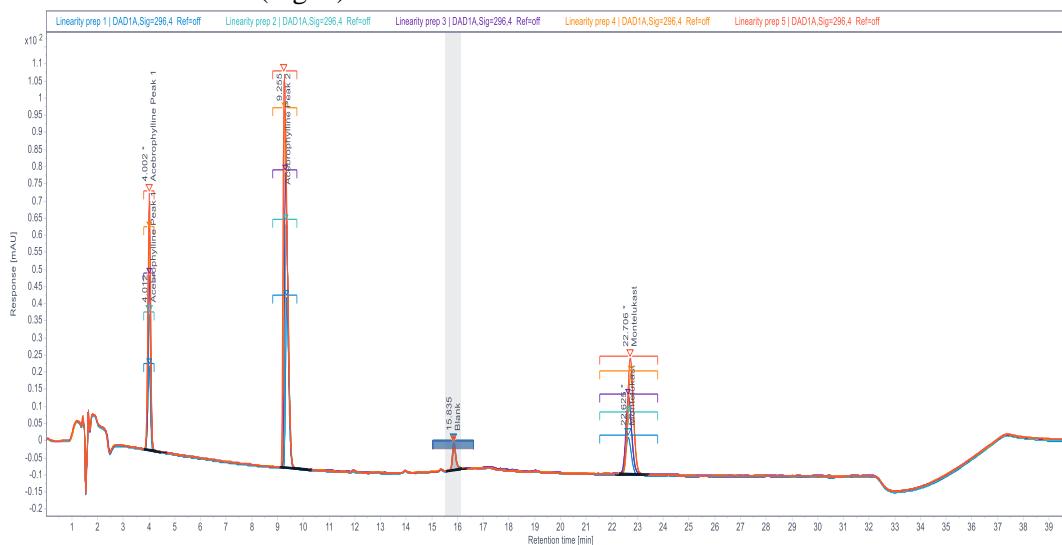


Figure 4: Linearity overlay of Acebrophylline and Montelukast

Accuracy (% Recovery)

The closeness of experimental and true value or an accepted reference value signifies the accuracy of analytical procedure. The data for accuracy for Acebrophylline and Montelukast is presented in table 10 and 11 respectively. The recovery range for Acebrophylline and Montelukast was found to be 99.921- 100.369% and 100.69- 99.83% respectively.

Specificity

Specificity is the ability to assess unequivocally the analyte in the presence of components that may be expected to be present. Typically, these might include impurities, degradants, etc. It is proven by comparing chromatogram of blank, standard solution and sample preparation solution, there was no interference of excipients with peak of Acebrophylline and Montelukast.

Robustness

Deliberate changes in different parameters like i) Flow rate, ii) Wavelength, iii) pH and iv) Column oven.

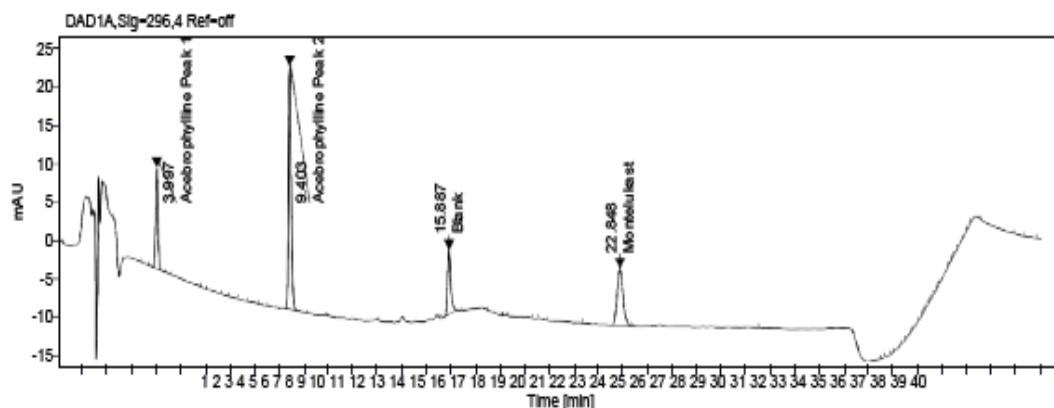
LOD and LOQ

From the LOD and LOQ values, it was inferred that the optimized method was sensitive to determine the entrapment efficiency. LOD found from the equation was 0.055 and 0.114 while LOQ was 0.167 and 0.346 for Acebrophylline and Montelukast respectively.

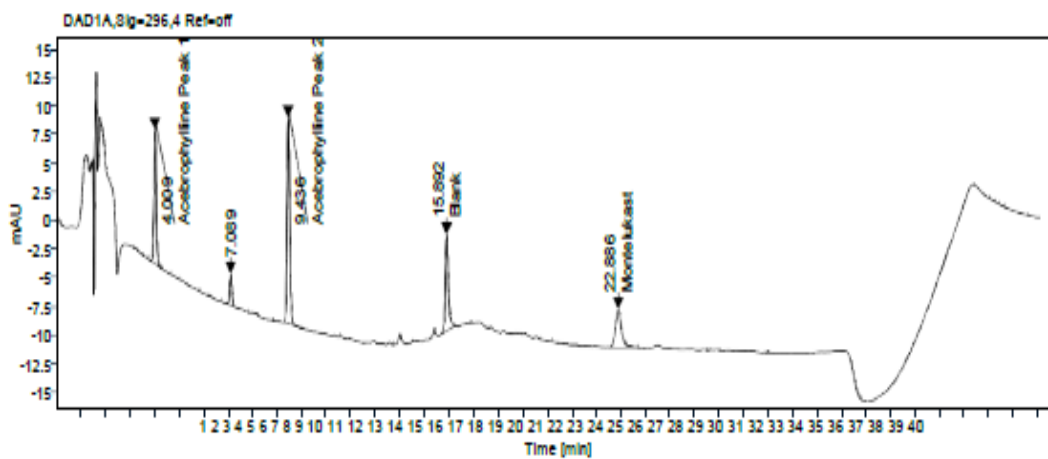
Forced degradation study

ACBR and MTKT were subjected to various forced degradation conditions to effect partial degradation of the drug preferably in 10-30% range. Data of degradations presented in table 4 for Acebrophylline and Montelukast as well as in Fig. 5.

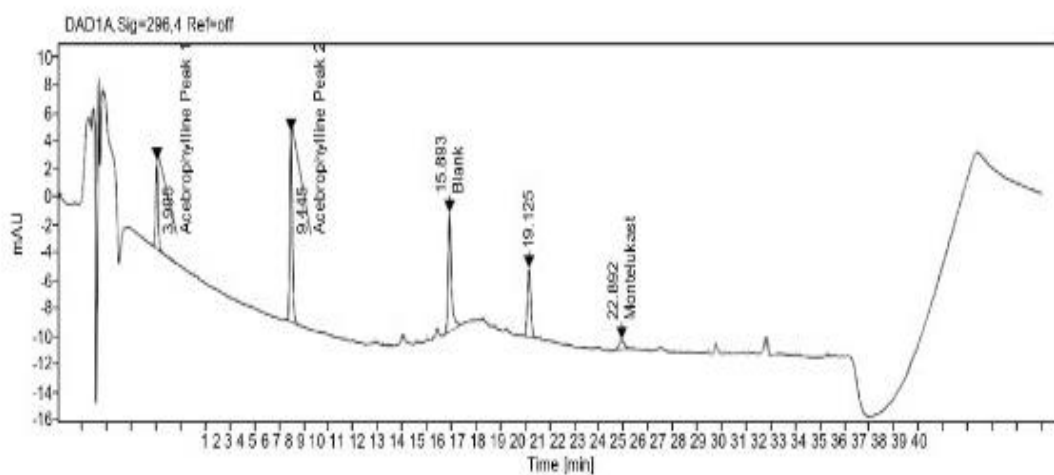
Figure 5: A) Acid Degradation, B) Alkali Degradation, C) Peroxide Degradation, D) Thermal Degradation, E) UV Degradation and D) UV Control Degradation



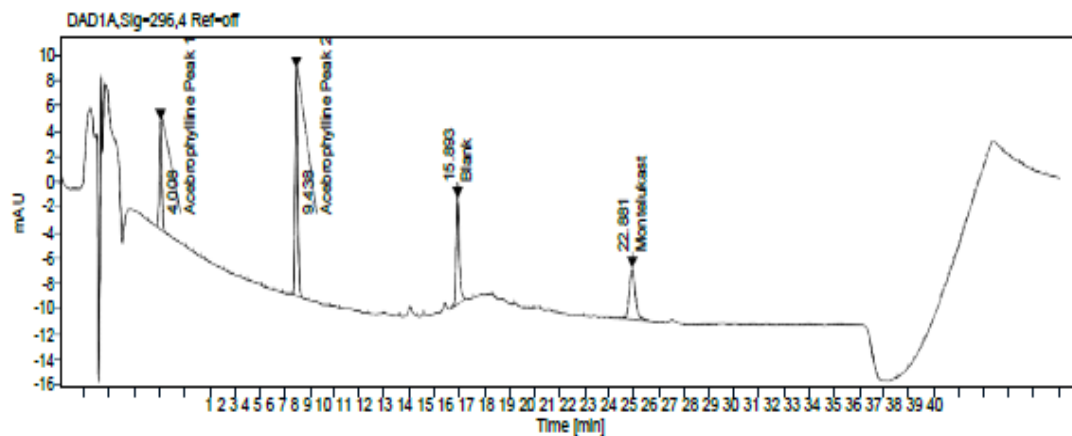
A



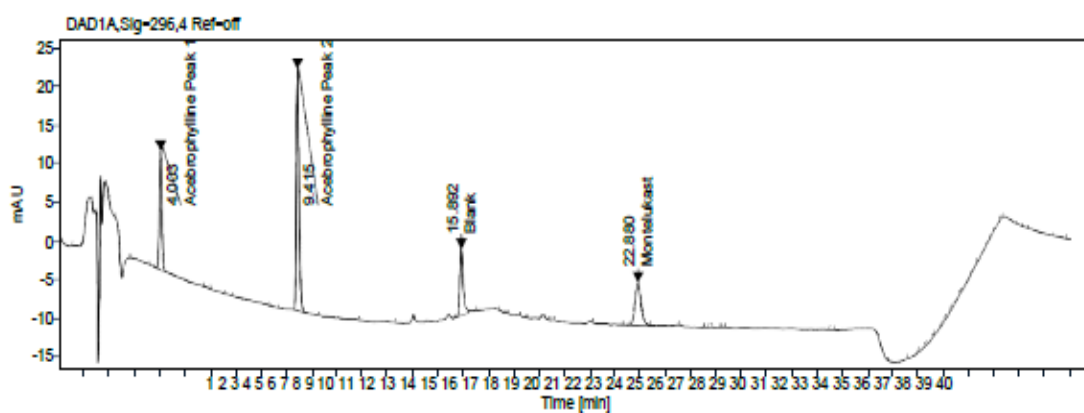
B



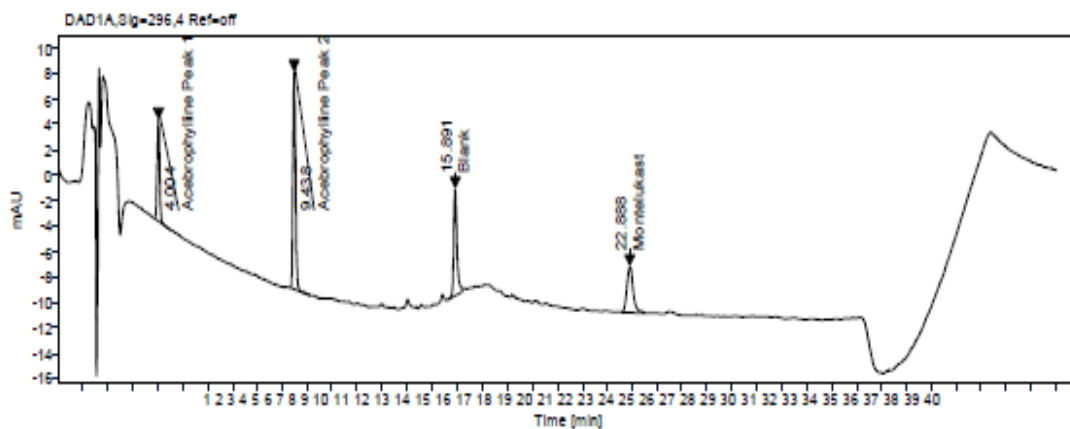
C



D



E



F

Table 4. Forced Degradation

Acebrophylline % Degradation				
Parameter	Area			% Degradation
	Peak 1	Peak 2	Sum	
Acid	311.46	631.15	942.61	22.71
Alkali	304.53	752.83	1057.36	13.50
Oxidation	295.44	832.45	1127.90	7.16
Thermal	326.03	638.25	964.28	20.98
Photolytic	310.11	832.24	1142.36	6.48
UV Control	428.75	782.96	1211.72	0.98
Montelukast % Degradation				
Parameter	Area		% Degradation	
Acid	251.65		30.37	
Alkali	368.15		25.96	
Oxidation	251.46		30.46	
Thermal	285.78		20.62	
Photolytic	219.32		39.41	
UV Control	244.83		32.48	

Dosage form analysis

Formulations was procured commercially from the market. The tablet formulations Telekast A (Lupin Ltd), Montek AB (Sun Pharmaceutical Industries Ltd), Glemont-A (Glenmark Pharmaceuticals Ltd) and Montair AB (Cipla Pharmaceuticals) containing 200 mg Acebrophylline and 10 mg Montelukast when analyzed using the developed method, showed separated peak at Retention time and assay as observed in standard with slight change in the chromatogram of tablet formulations indicating no interference of the excipients. Data presented in table 5.

Table 5. Dosage form analysis

Telekast A		
	Retention time	
Acebrophylline peak 1	3.598	Mean: 102.94
Acebrophylline peak 2	9.346	SD: 0.812
Montelukast	22.625	%RSD: 0.794
Montek AB		
Acebrophylline peak 1	4.003	Mean: 102.75
Acebrophylline peak 2	9.300	SD: 0.517
Montelukast	22.662	%RSD: 0.503
Glemont-A		
Acebrophylline peak 1	4.013	Mean: 102.29
Acebrophylline peak 2	9.290	SD: 0.461
Montelukast	22.636	%RSD: 0.451
Montair AB		
Acebrophylline peak 1	4.009	Mean: 102.34
Acebrophylline peak 2	9.306	SD: 0.397
Montelukast	22.670	%RSD: 0.388

CONCLUSION

A simple, sensitive, accurate, precise and specific RP-HPLC method has been developed for the simultaneous quantification of Montelukast and Acebrophylline in bulk and marketed tablet dosage form. The developed method was validated by linearity, precision, accuracy, specificity, robustness, LOD and LOQ. The proposed method is satisfactorily applied for the separation of analyte peaks in presence of degradation products. The chromatograms showed that there were no interference peaks due to degradants, hence the method is stability indicating and can be applied for quality control of Acebrophylline and Montelukast combination tablets.

REFERENCES

1. Asthma. Accessed February 16, 2022. <https://www.who.int/news-room/fact-sheets/detail/asthma>
2. Tapadar SR, Das M, Chaudhuri AD, Basak S, Mahapatra ABS. The Effect of Acebrophylline vs Sustained Release Theophylline in Patients of COPD- A Comparative Study. *J Clin Diagn Res.* 2014;8(9):MC11. doi:10.7860/JCDR/2014/8176.4869
3. Pozzi E. Acebrophylline: an airway mucoregulator and anti-inflammatory agent. *Monaldi Arch chest Dis = Arch Monaldi per le Mal del torace.* 2007;67(2):106-115. doi:10.4081/MONALDI.2007.498
4. Acebrophylline | C22H28Br2N6O5 - PubChem. Accessed March 25, 2021. <https://pubchem.ncbi.nlm.nih.gov/compound/176595>
5. Ambroxol acefyllinate | DrugBank Online. Accessed March 25, 2021. <https://go.drugbank.com/drugs/DB13141>
6. Montelukast | DrugBank Online. Accessed March 25, 2021. <https://go.drugbank.com/drugs/DB00471>
7. Montelukast sodium | DrugBank Online. Accessed March 25, 2021. <https://go.drugbank.com/salts/DBSALT001043>
8. ICH Official web site : ICH. Accessed February 16, 2022. <https://www.ich.org/page/quality-guidelines>
9. Sangeetha S, Alexandar S, Jaykar B. *Simultaneous Estimation of Acebrophylline, Montelukast Sodium and Levocetirizine by RP-UPLC Method in Combined Dosage Forms.* Vol 4.; 2020.
10. Simultaneous estimation of acebrophylline, montelukast, and levocetirizine dihydrochloride in marketed formulation by high-performance liquid chromatography method. Accessed February 16, 2022.
11. Kumar Naraharisetti S. Reverse Phase-Hplc/Uv Spectrophotometric Method for Estimation of Acebrophylline and Montelukast Sodium in Dosage forms. Published online 2014.
12. Mamatha J, Devanna N. RP-HPLC-PDA method for simultaneous quantification of montelukast, acebrophylline and desloratadine tablets. *Asian J Chem.* 2018;30(6):1383-1386. doi:10.14233/ajchem.2018.21269
13. Article | Stability Indicating Hplc Method Development For Estimation Of Montelukast Sodium And Acebrophylline In Combined Dosage Form | Inventi Journals Pvt.Ltd. Accessed March 27, 2021.

PCP452

A REVIEW OF AZIDO IMPURITY IN DRUG SUBSTANCES AND ITS PRODUCTS

AP0459

Kinnari Patel

Student

GSP-GTU

kinnari3264patel@gmail.com

AP0380

Dr. Rajesh Patel

Associate Professor

GSP-GTU

rajeshpatel@gtu.edu.in

Abstract

An Azido impurity is an Azidomethyl-biphenyl-tetrazole (AZBT). It is present in sartan medicine which is used to treat high blood pressure(hypertension). Sartan drugs (Losartan, Irbesartan, Telmisartan, Olmesartan, Valsartan) are Angiotensin II Receptor Blockers (ARBs). An Azido impurity is mutagenic impurity that is produced during the API manufacturing process. In April 2021, AZBT-contaminated sartans were first identified as result, EDQM immediately ordered a market recall. After numerous recalls were issued as a result of this azido impurity by regulatory authorities such as Health Canada, TGA, MHRA etc. This review talks about mechanism of formation of azido, health risk, currently available analytical methods like LC-MS/MS, HPLC-UV-MS etc.

Keywords: Azido Impurity, AZBT, Mutagenic, Sartan drugs, Analytical Methods

PCP454

RISK ASSESSMENT, ANALYSIS AND CONTROL OF GENOTOXIC IMPURITIES IN DRUG SUBSTANCES AND PRODUCTS

AP0501
JAITRI NAYANBHAI
MEHTA
GTU STUDENT,
L.M. COLLEGE OF
PHARMACY
jaitrimehta12@gmail.co
m

AP0498
DR. JAYANT B. DAVE
FACULTY/RESEARCH
SCHOLAR/ACADEMICIA
N
L.M. COLLEGE OF
PHARMACY
jayant.dave@lmcp.ac.in

AP0502
AMI SURESHBHAI
GADHIYA
GTU STUDENT,
L.M. COLLEGE OF
PHARMACY
ami.gadhiya64@gmail.co
m

Abstract:

The substances reacting with DNA have a potential to cause gene mutations at low concentration and are called Genotoxic Impurities (GTI) which may cause cancer. Their assessment at ppm/ppb levels demands highly sensitive analytical methods. Hazard assessment helps in Impurities classification with respect to mutagenic and carcinogenic potential (Class 1-5). The EMEA guideline focusing on Threshold of Toxicological Concern (TTC) gives a value of 1.5 $\mu\text{g}/\text{day}$ corresponding to a theoretical 10^{-5} excess lifetime risk of cancer. Identification of these GTIs can be done using in-silico structure-based approaches, (Q)SAR methodologies. Since Genotoxic Impurities should be controlled at ppm level, the analytical method used for their assessment should be highly sensitive, specific and reliable. Recent analytical approaches for assessment of GTI like two dimensional (2D)-GC, Hydrophilic-interaction chromatography (HILIC), Ultra-performance Liquid Chromatography (UPLC-MS/MS), Extractive ESI-MS/MS, Molecular Imprinted Polymers (MIP), matrix deactivation are described in the paper to reduce matrix interference and enhance sensitivity. The risk assessment is based on the physicochemical properties and factors that influence the fate and purge studies of the impurity. This paper describes updated information about GTIs and reviews the regulatory aspects centered on ICH M7 for GTIs in drug substance/products as well as its control strategies.

Keywords: Genotoxic Impurities, ICH M7, Gene mutation, Carcinogenic impurities, HILIC, GC-MS, UPLC-MS/MS.

1. INTRODUCTION:

The manufacturing of active pharmaceutical ingredients (API) may lead to inevitable entry of some starting material, intermediates or by-products in the final end products in the form of impurities (Majid et al., 2018). A small number of these possible impurities, referred to as Genotoxic Impurities (GTIs), are of particular concern because of their propensity to interact with DNA and resulting in genetic abnormalities. Additionally, GTIs may interfere with DNA replication resulting in the growth of tumors or other serious health issues (Helmy et al., n.d.). Genotoxicity has been defined as "any deleterious change in the genetic material, regardless of the mechanism by which the change is induced" in the ICH S2 (R1) Guideline1 ("Genotoxic Impurities in Pharmaceutical Products," n.d.). International Council on Harmonisation of Technical Requirements for Registration of Pharmaceuticals for Human Use (ICH) guidelines Q3A and Q3B addresses the control of impurities in APIs as well as drug products. Based on the estimated clinical dose, route of administration, and various mitigating factors, these standards specify the reporting, identification, and qualification levels of impurities in APIs and

final medicinal products. These recommendations acknowledge that "unusually toxic" impurities like GTIs do not fall within the purview of the ICH-defined impurity levels (Helmy et al., n.d.). It is difficult to determine the acceptable limits of Genotoxic Impurities as the data available for GTIs is quite variable. In case of absence of appropriate data, a general approach as explained by Threshold of Toxicological Concern (TTC) is implemented. The intake of genotoxic impurities with a TTC value of 1.5 µg/day is considered to have tolerable risk (excess cancer risk of 1 in 100,000 over a lifetime) for the majority of pharmaceuticals. (Giordani et al., 2011). The TTC value is not applicable when the GTI belongs to the class of aflatoxin-like compounds or N-nitroso or azoxy compounds. For these highly genotoxic compounds the lower limit (0.15 µg/person/day) must be applied, alternatively the risk assessment requires compound-specific toxicity data (Giordani et al., 2011).

A staged TTC is one that has been adjusted to account for both the dose and the length of the clinical trials; as a result, it is lower for higher doses and higher for shorter durations. The reason for this is that overall exposure in clinical research is kept to a minimum and dosage durations are kept to a minimum. For most potent carcinogens, this technique yields considerable safety margins due to the original TTC's conservative risk assessment. If there are multiple genotoxic impurities present, the staged TTC values should be applied to each chemical at every stage of development. Exceptions to this rule include extremely potent carcinogens (PhRMA, n.d.).

The Europeans Medicines Agency (EMA) is the first regulatory agency to implement comprehensive rules for handling genotoxic impurities. The recommendation established the idea of limiting impurity levels to "as low as reasonably possible" (ALARP) for potential genotoxic contaminants lacking sufficient evidence of a threshold-related mechanism. The recommendation in the guideline calls for the implementation of a risk assessment, such as an estimation of daily exposure at and below levels where there is a negligible risk to human health, if the formation of genotoxic impurities cannot be prevented and if the impurities cannot be totally removed (EMA, Committee for Medicinal Products (CHMP), 2006)

Table 1: Acceptable qualification thresholds for GTIs for Pharmaceuticals in Clinical studies

Duration of Exposure	Limit (µg/day)		
	PhRMA	USFDA	EMA
Single dose	120	120	120
Less than 14 days	120	60	120
14 days to 1 month	120	60	60
1 to 3 months	40	20	20
3 to 6 months	20	10	10
6 to 12 months	10	5	5
More than 12 months	1.5	1.5	1.5

Source: (FDA Draft guidance, 2008)(European Medicines Agency, 2018) (PhRMA, n.d.)

Genotoxic tests are in vitro and in vivo procedures used to identify substances that cause genetic damage either directly or indirectly through a various mechanisms. With regard to DNA damage and its fixing, these tests should be able to identify potential hazards (Guidance for Industry S2B Genotoxicity ICH, 1997). A single test is not able to detect all the genotoxic impurities that are possibly present. Thus, complementary tests or battery tests are performed in genotoxicity studies.

Examples are provided for some of the often identified potentially genotoxic structural motifs. Alkylating agents, which include alkyl halides, alkyl sulfonates, and related structures, are a subtype of these. These compounds could be produced during chemical synthesis or employed as reagents. For instance, an alkyl halide is created when an alcohol combines with the salt counter ion of a basic molecule like HX (X = halogens).

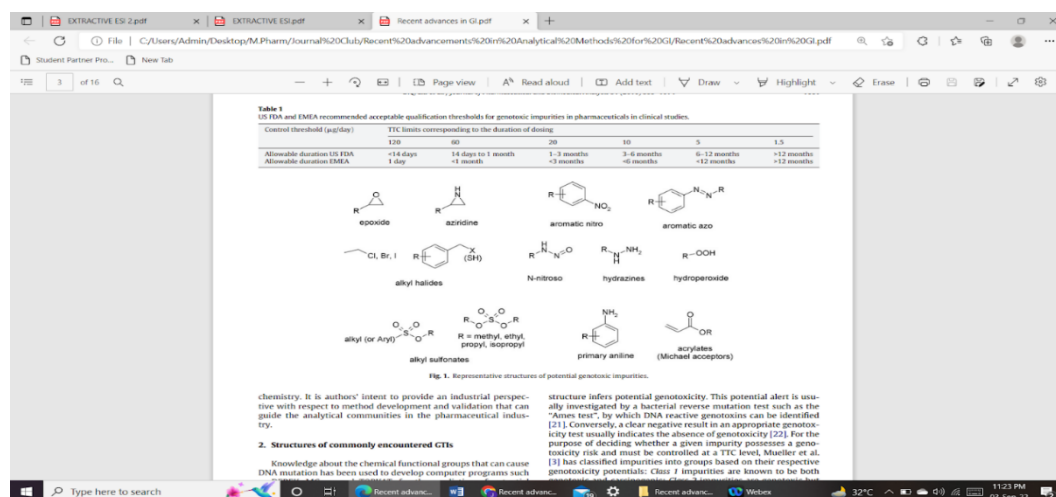
Table 2: In Vitro and In Vivo Tests for the Detection of Genotoxicity:

Tests to be performed	Species used	Observed End Point
In-vivo test methods: <ul style="list-style-type: none"> Comet assay test Immunoassays and mass spectrometry Somatic and germ cell gene mutation assay for transgenic rodents Micronucleus test Chromosome aberration test 	<ul style="list-style-type: none"> Mammalian tissues Mammalian liver cells, Mammalian tissue and peripheral blood cells Transgenic rats or mice Mammal blood cells Mammalian bone marrow and spermatogonial cells 	<ul style="list-style-type: none"> Breaking of DNA strand Induction of DNA repair Mutagenicity Chromosomal damage Chromosomal damage
In-vitro test methods: <ul style="list-style-type: none"> Ames test Hrpt test Thymidine kinase/ Mouse lymphoma assay Chromosome aberration test Micronucleus test Comet assay test Immunoassays and mass spectrometry 	<ul style="list-style-type: none"> Salmonella thyphimurium, Escherchia coli Mammalian cell lines TK6 human lymphoblastoid cell line Mammalian cell lines Human and mammalian primary lymphocytes and cell lines Cell and cell lines Cell and cell lines 	<ul style="list-style-type: none"> Reverse mutation Forward mutation Forward mutation or chromosomal damage Chromosomal damage Chromosomal damage Breaking of DNA strand Induction of DNA repair and adduct

Source: (Cartus & Schrenk, 2016)

Alkylation agents are frequently employed in chemical synthesis, and examples include alkyl esters of sulphate, methanesulfonic acid (mesylate), benzenesulfonic acid (besylate), and p-toluenesulfonic acid (tosylate). After being bioactivated in vivo, aromatic amines and nitro compounds may cause genotoxicity (Liu et al., 2010). Some common GTI atructures are depicted below.

Figure 1: Representative Structures of common GTIs



Source: (Sun, Liu, et al., 2010)

A case study on control of NDMA impurities in Metformin:

Metformin is one of the most widely used drugs in the treatment of type 2 diabetes mellitus (T2DM). It is used as a chronic therapeutic agent (administered for more than 10 years), a TTC-based acceptable intake of a mutagenic impurity of 1.5 µg/person/day, is considered to be associated with a negligible risk. Metformin, being an important medicine for diabetic care, is consumed by a large number of patient populations with high dose. The presence of nitrosamine impurities like NDMA (Nitrosodimethylamine) in Metformin may be a resultant of cross-contamination, nitrosating reagent, or degradation of starting and intermediate products. Since NDMA is classified as probable human carcinogen by WHO/IARC, the allowable daily intake for NDMA is 0.096 µg/day as per USFDA and EMA. Still several marketed products of Metformin like Glycomet IR (max. dose 3000mg) and Glycomet SR (max. dose 2000mg) have controlled levels of NDMA up to 0.03 µg/day to avoid its carcinogenic effects (Doshi et al., 2021). Since the synthesis of Metformin includes a reaction between Dicyandiamide (DCDA) and Dimethylamine HCl (DMA), there are chances of them occurring as impurities in the final product. As per Indian Pharmacopoeia, test for Related Substances should be performed to check the presence of such impurities. The limit of dicyandiamide should be not more than 0.02% and impurity should not be more than 0.1%. (Government of India, Ministry of Health, (1955), Pharmacopoeia of India (the Indian Pharmacopoeia), 2018)

Figure 2: Schematic diagram of metformin synthesis

The screenshot displays a PDF document with the following content:

- Text:** "during the synthesis and/or subsequent degradation of drug substances or by-products. Genotoxic impurities are uncommon in most of the drug substances, and synthesis of few chemical entities results in genotoxic impurity."
- Chemical Structure (Figure 3):** Structure of nitrosodimethylamine, CN(C)N=O.
- Text:** "The USV's risk assessment consists of the following quality elements, as follows:"
- List:**
 - Route of synthesis of metformin
 - Route of synthesis of starting materials and reagents
 - Use of highly sensitive analytical methods
 - Impurities in the starting materials
 - Solvents (including water, recovered or recycled)
 - Processing conditions
 - Processing steps
 - Facilities and equipment used
 - Disinfectants used
 - Process monitoring and data analytics
- Chemical Reaction (Figure 4):** Schematic diagram of metformin synthesis. It shows the reaction of Dicyandiamide (DCDA), NC(=N)N, and Dimethylamine HCl (DMA), CN(C)Cl, to form Metformin HCl, CN(C)NC(=N)N.

Source: (Doshi et al., 2021)

2. IDENTIFICATION AND CLASSIFICATION OF GENOTOXIC IMPURITIES:

As per ICH M7, genotoxic impurities can be classified based on hazard assessment by analyzing impurities through database of carcinogenicity and bacterial mutagenicity test or by Structural Activity Relationship methodologies. Using (Q)SAR techniques that forecast the results of a bacterial mutagenicity assay, a novel computational toxicology assessment should be carried out. The fundamental validation guidelines outlined by the Organization for Economic Cooperation and Development (OECD) should be adhered to by (Q)SAR models using these prediction approaches (ICH M7(R1), 2017). The absence of structural alerts is sufficient to conclude that the impurity is non-mutagenic and thus, no further testing is needed (e.g. Class

V). In case of a relevant structural alert, adequate control measures in addition with bacterial mutagenicity assay can be applied (e.g. Class III). If the bacterial mutagenic assay gives negative test results no further assessment is required. Additionally, if an impurity has same structural alert, position and chemical environment as the drug substance it can only be considered as non-mutagenic if the bacterial mutagenicity assay gives a negative result (e.g. Class IV).

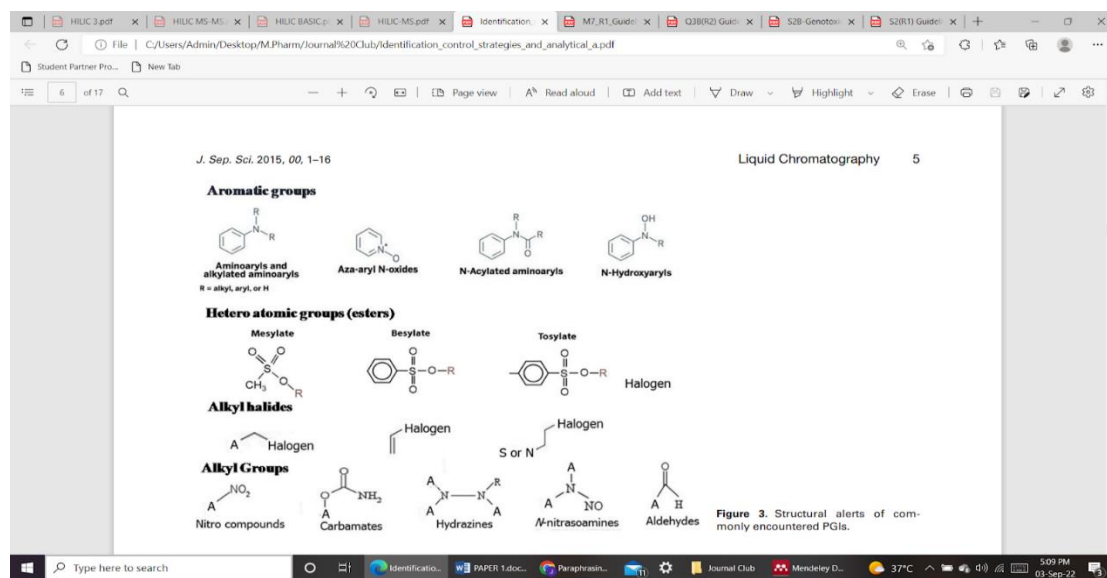
Table 3: Classification based on Carcinogenic/Mutagenic potential and required Control actions:

Class	Description	Control Action
I	Impurities with known mutagenic carcinogen	Should be controlled at or below the compound specific acceptable limit
II	Impurities with known mutagens but unknown carcinogenic potential	Should be controlled at or below acceptable TTC limits
III	Impurities with alerting structure, not related to drug substance and no mutagenicity data available	Should be controlled at or below appropriate TTC/ bacterial mutagenicity assay should be conducted. If positive= Class V If negative= Class II
IV	Impurities with same alerting structure with the drug substance which are tested as non-mutagenic	Should be treated as non-mutagenic impurity
V	Impurities with no structural alerts, or data to prove mutagenicity or carcinogenicity	Should be treated as non-mutagenic impurity

Source: (ICH M7(R1), 2017)

A comprehensive review by Bhaskar Reddy, Jaafar and colleagues shows some of the structural alerts in some common Genotoxic impurities including alkylating agents, like alkyl halides, alkyl sulfonates, and other closely. These compounds are frequently employed as reagents or may even be produced during chemical synthesis. They have the impact of cytotoxicity, which inhibits cell development or starts apoptosis or programmed cell death. Additionally, nitro compounds and aromatic amines do not directly establish covalent bonds with DNA bases, but rather, gets metabolically active before reacting with DNA bases and becoming genotoxic (Majid et al., 2018)

Figure 3: Structural alerts of commonly encountered GTIs:



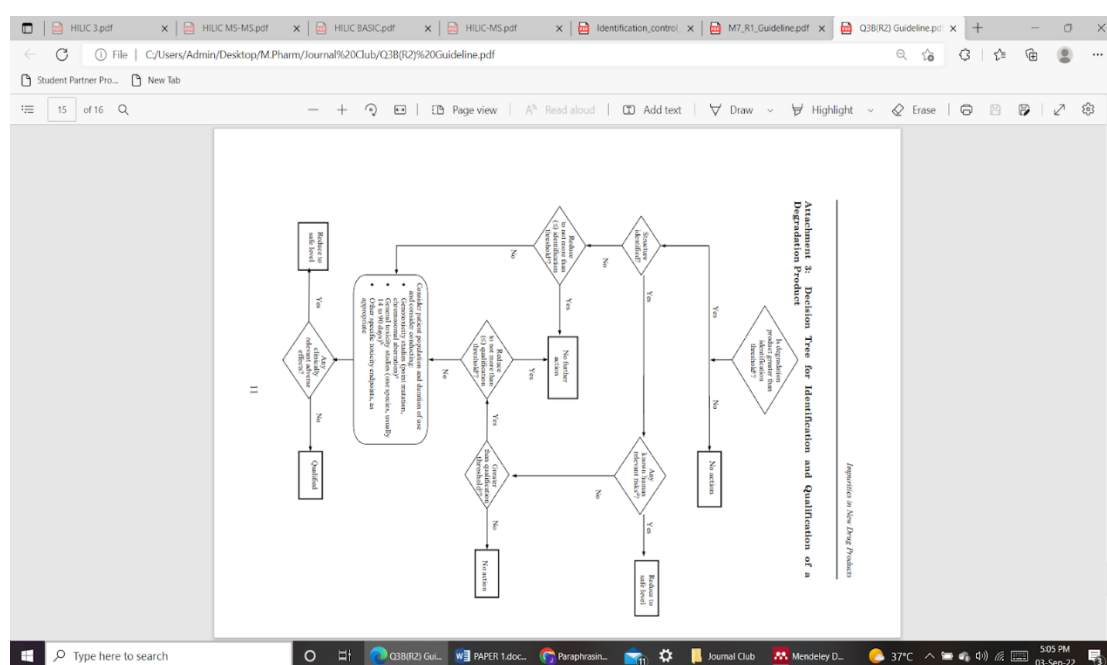
Source: (Majid et al., 2018)

Before qualifying a Genotoxic impurity, one must consider the following points (Q3B(R2) IMPURITIES IN NEW DRUG PRODUCTS, 2006):

- In order to distinguish between qualified and unqualified material, more than one studies should be designed for general genotoxic studies.
- The duration of studies should be based on appropriate data and should be performed amongst the species that are most likely to show maximum potential to detect the toxicity of an impurity.
- Single dose drug studies are recommended for case-by-case studies only.
- Generally the studies should be conducted for at least 14 days and at the most 90 days.
- If the genotoxic impurity is unusually toxic, lower thresholds can be considered.

Attachment 3 of ICH Q3(B) gives a decision tree for identification as well as qualification of degradation products based on threshold levels and identified structures.

Figure 4: Decision Tree for Identification and Qualification of Degradation Product:



Source: (Q3B(R2) IMPURITIES IN NEW DRUG PRODUCTS, 2006)

3. RISK ASSESSMENT METHODS FOR GENOTOXIC IMPURITIES:

In current toxicological studies, a thorough understanding of the compound's mode of action (MoA) is a vital prerequisite for a substantial risk assessment. The presence of a threshold and an absolutely safe level, for compounds having a genotoxic mechanism of action, particularly if they were carcinogenic in people or experimental animals, thus cannot be assumed. It is rare for legal residues to necessitate a risk assessment of genotoxic substances because genotoxicity is typically a requirement for excluding a chemical from legal authorisation (and subsequent use) (Cartus & Schrenk, 2016).

Some of the common approaches for risk assessment have been developed, they are:

- For the evaluation of non-genotoxic compounds, the No Observed Adverse Effect Level (NOAEL), or the maximum dose level that does not significantly induce an

adverse effect, can be employed. However, it is not found suitable for the evaluation of substances that are both genotoxic and carcinogenic.

- b. The dose-response data are fitted using several mathematical functions to determine the modelled Point of detection (PODs). These modelled functions have confidence intervals that are statistically specified.
- c. If the benchmark or critical level of effect is predefined, the estimation of dose levels which would induce the degree of effect is allowed by the modelled functions. Lower Confidence Level of a Benchmark Dose (BMD) with 10% Effect can be derived from the lower level of the associated confidence interval (for example, 95% confidence)(Davis et al., 2011). A free in-silico software like BMDS or PROAST is available.
- d. A staged TTC approach by PhRMA task force also suggests use of computer-based structure-activity relationship tools such as DEREK (Deductive Estimation of Risk from Existing Knowledge, <http://www.chem.leeds.ac.uk/luk/derek/>) or MCASE (Multi Computer Automated Structure Evaluation, <http://www.multicase.com/products/prod01.htm>) along with the in vitro assay for point mutations such as Ames test. (Humfrey, 2007)

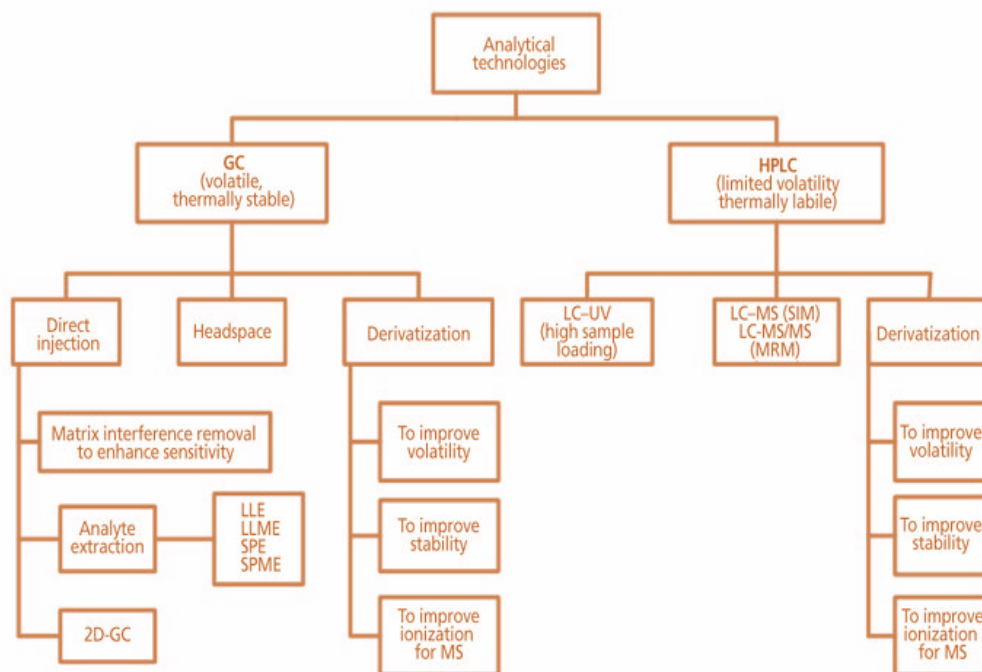
4. CURRENT APPROACHES IN ANALYSIS OF GENOTOXIC IMPURITIES:

At the commercial stage, GTIs were controlled at a TTC of 1.5 g/day. According to the ICH Q3 guidance for traditional pharmaceutical impurities analysis, a GTI would need to be controlled at a level of 1.5 ppm for a 1-g daily dose of the marketed product ($[1.5 \text{ g/day}]/[1 \text{ g/day}] = 1.5 \text{ ppm}$), which is hundreds of times lower than the 0.05% (500 ppm) control standard. Additionally, for clinical development and commercial products, the total amount of mutagenic impurities shall not exceed 5µg/day in cases when three or more mutagenic impurities are present in the drug substance specification. Robust and sensitive analytical techniques are essential for the monitoring and analysis of GTIs given their low level (Wigman et al., 2015). Prior to creating a strategy, it is crucial to comprehend the following:

- a. The purpose of testing; if the technique will be utilised for API release testing or during development (spiking and purging studies)
- b. The requirements for method validation differ depending on whether a limit test or quantitative method is performed
- c. The analyte's physicochemical characteristics
- d. The method's ultimate user, which could be a manufacturing laboratory, a commercial user, or a development laboratory.

Two of the most used analytical techniques, gas chromatography (GC) or high performance liquid chromatography (HPLC), may be used depending on the physicochemical characteristics of the analyte. The following figure shows the common strategy used to select an appropriate analytical method for the assessment of genotoxic impurities.

Figure 5: Analytical Method Selection Strategy.



Source: (Wigman et al., 2015)

Analytical challenges in identification, quantification as well as assessment of genotoxic impurities: (Raman et al., 2011):

- Diverse structural forms of GTIs which necessitate the use of numerous analytical methods,
- GTIs lacking structural characteristics friendly to conventional analytical detectors,
- Chemically reactive or Low recovery and poor sensitivity are caused by unstable GTIs, which call for unique handling methods,
- Sample matrix interference resulted from increased API test concentration to obtain lower limits on detection

Some innovative analytical methods used for genotoxic impurities are described below:

1. 2D Gas Chromatography Technique:

Volatile compounds are generally separated by gas chromatography. In this analysis, the headspace injection adds another dimension of separation along with chromatographic separation, where nonvolatile API is not introduced into the GC system. Thus, for thermally stable volatile compound headspace sample injection is preferable. Since use of direct injection leads to introduction of a large amount of API into the chromatography system, there is a high risk of column, detector or injection port contamination. Currently, GTI analysis has benefited from the application of two-dimensional (2-D) GC techniques such back flush and heart cut analysis, which only inject a small portion of the volume containing the target analyte into the MS detector or second column, limiting the instrument contamination (Sun, Liu, et al., 2010). The most common detector used along with GC is flame ionization detector (FID). When GTIs contain halogens, electron capture detection (ECD) can be a good alternative to FID in GC as they add an extra level of selectivity to the detection process. Recent study makes it clear that sensitive and selective mass spectrometry detection is a key component of GTI analysis. The most popular detection modes are selective ion monitoring (SIM) or multiple reaction monitoring (MRM), while quadrupole mass analyzers are the industry standard for quantification. While MRM demands more advanced triple quadrupole MS instruments, SIM is commonly achieved with single quadrupole MS instruments. Impurities analysed by GC are enlisted below (R POUNIKAR et al., 2020):

- i. Five genotoxic impurities were assessed and quantified in the drug substance Divalproex sodium (DPS) using GC-EI-MS with SIM mode at very low levels: methyl bromide, ethyl bromide, isopropyl bromide, n-propyl bromide, and n-butyl bromide.
- ii. Methyl-p-toluene sulfonate ethyl p-toluene sulfonate and isopropyl p-toluene sulfonate are analysed in Dobutamine drug substance.
- iii. 1, 3-dichloropropane, 3-chloropropylacetate, and chloropropyl hydroxypropyl ether are detected as residual GTIs by GC-MS in SIM mode with helium as the carrier gas.

2. HILIC-MS/MS Approach:

Depending on the volatility of the analytes, HPLC or GC are selected most commonly. GTIs can be classified into two classes based on their volatility. Reversed phase (RP)-HPLC is the most widely used chromatography method for nonvolatile analytes. For the separation of different pharmaceutical compounds, numerous varieties of RP-HPLC column stationary phases are well known. In addition to RP-HPLC, hydrophilic interaction liquid chromatography (HILIC) is beneficial for separating extremely polar analytes (An et al., 2008). Hydrophilic interaction LC (HILIC) was developed as a substitute for NPLC. A hydrophilic SP and an aqueous-polar organic solvent MP are characteristics of HILIC. Similar to NPLC, retention rises with higher polarity of the analysed compounds, higher polarity of the SP, lower polarity of the MP, and so on (Dejaegher & Vander Heyden, 2010). Due to HILIC's MP characteristics, the drawback of insolubility of hydrophilic chemicals in NPLC is essentially resolved. Since the SP develops a water-enriched liquid layer, a portion of the MP becomes a fundamental component of the SP. Generally the stationary phase used for HILIC is silica based and polymer based. The mechanism of retention is surface adsorption, electrostatic interaction with the charges present on the stationary phase, or hydrophilic portioning between mobile phase and hydrophilic stationary phase (Dejaegher & Vander Heyden, 2010). For the detection of trace amounts of genotoxic contaminants, the hydrophilic interaction liquid chromatography-tandem mass spectrometry (HILIC-MS/MS) method was developed and validated (Mullangi et al., 2021). The pharmaceutical sector has a significant analytical challenge with the trace-level analysis of PGIs in drug substances. For ppm or lower level detection of PGIs in pharmacological compounds, complex and expensive procedures like LCMS, GC-MS, and ICP-MS are typically used. In order to examine contaminants at such a low level, a straightforward, sensitive, and affordable method through HPLC utilizing an HILIC technique is not thoroughly explored. To evaluate genotoxic impurities at lower levels, an HPLC method as sensitive as LCMS was established and validated (Jain et al., 2017). The advantages and disadvantages of HILIC over conventional RP-HPLC are enlisted in the below table.

Table 4: Advantages and Disadvantages of HILIC:

Sr. no.	Advantage of HILIC	Disadvantage of HILIC
1.	Ability to retain highly polar compounds using mobile phase containing major portion of organic solvents	In case of analysis of hydrophobic compounds is HILIC leads to precipitation.
2.	Less matrix interference, high signaling and high sensitivity	
3.	It can be applied in analysis of polar and less polar compounds as it is strictly selective towards polar compounds.	

Source: (Jain et al., 2017)

Some of the common impurities analyzed using HILIC are as follows:

- i. The intermediates, 2, 3-dichloro aniline, bis (2-chloroethyl) amine, and 2-chloro ethylamine used in synthesis of Aripiprazole can be present as GTI in the final product (Mullangi et al., 2021)

- ii. (Pyridine-4-carboxamide), (3-Aminopyridine), (1, 2-bis (4-pyridyl) hydrazine), (1, 3-Di (pyridin-4-yl) urea), and (4-Aminopyridine-N-oxide) are often produced as GTIs during the manufacture of Dalfampridine (Jain et al., 2017)
- iii. 2-chloro-N-(2-chloroethyl)ethanamine hydrochloride (BCEA), a well-known genotoxic contaminant, is used in the crucial stage of this synthesis process for Vortioxetine (VOR), the amount of BCEA in the final product must be strictly controlled (Douša et al., 2016)

4.3 UPLC-MS/MS Technique:

Several HPLC methods are developed and reported for quantification of various GTIs, but only a few LC-MS methods are reported for detection as well as qualification of known and unknown GTIs in drugs like Zolmitriptan. The major disadvantage of HPLC method of analysis is low separation efficiency and longer analysis time (sometimes more than 20 minutes). For trace analysis of GTIs there is a need to develop better analytical methods as the existing methods have reported some drawbacks (e.g. variation in retention time for HPLC). Novel approaches like Ultra Performance Liquid Chromatography coupled with Mass Spectrometry (UPLC-MS/MS) has major advantages over conventional analytical methods as it can simultaneously separate and quantify multiple GTIs without modifications in the chromatographic or mass spectrometric parameters (Vijaya Bhaskar Reddy et al., 2013). When compared to high-performance liquid chromatography, ultra performance liquid chromatography (UPLC) is effective for particles with a diameter of less than 2 μ m and can achieve excellent resolution, speed, and sensitivity (HPLC). Pharmaceutical industries are focused on innovative strategies to increase efficiency and speed up medication development in the twenty-first century. Analytical laboratories are not an exception to this trend as UPLC analysis now results in better-quality products. In UPLC, the separation and quantification are carried out at extreme pressure (up to 100M Pa). In comparison to HPLC, it has been found that high pressure has no adverse effects on the analytical column, and that time and solvent consumption are lower in UPLC (M* et al., 2015). UPLC chromatograms show superior resolution and separation. They also perform more sensitive analyses, use less solvent, and analyse data rapidly (Wu et al., 2004). UPLC can be used in assessment of epoxide impurity in sarpogrelate hydrochloride intermediate, 4-nitrobenzenesulfonic acid, methyl 4-nitrobenzenesulfonate, ethyl 4-nitrobenzenesulfonate, and isopropyl 4-nitrobenzenesulfonate, APP, NPA, NPP 11 and MNA as common intermediates in synthesis of Zolmitriptan that acts as GTIs (Vijaya Bhaskar Reddy et al., 2013)

4.4 Matrix Deactivation Method:

A challenging problem in pharmaceutical analysis is the trace identification of reactive and unstable pharmaceutical genotoxic impurities (GTIs). The instability of analytes is frequently a direct cause of numerous experimental problems, including insufficient sensitivity, poor accuracy, and anomalous (too high/low) spiking recovery. The matrix deactivation approach chemically deactivates the synthetic reactive species in the sample matrix, in contrast to the traditional chemical derivatization strategy where the analytes are changed into stable observable species. It chemically stabilizes the analyte for analytical method development. The matrix deactivation method was created under the idea that interactions between specific analytes and low level reactive species in the sample matrix leads to the instability of certain analytes at trace levels. The unstable and reactive analytes could therefore be stabilised by quenching the reactivity of the reactive species. Matrix deactivation is used to chemically reduce the reactivity of the reactive species. Based on the analytes' reactivity and any potential degradation pathways, the matrix deactivation reagents should be chosen. There is no need for any additional steps; the matrix deactivation reagents can simply be injected into the diluents. As a result, matrix deactivation is a straightforward sample preparation technique that can be utilised to increase the stability of analyte solutions. Scavenging or protonation by acids can be used to achieve this (Sun, Bai, et al., 2010).

4.5 Extractive ESI-LC/MS:

Basic analytes can be analysed by atmospheric pressure ionisation MS with high sensitivity since they have a strong affinity for protons. The compounds that contains multiple nitrogen molecules are ideal for electrospray ionization (ESI) LC/MS (Liu et al., 2010). Sensitivity and selectivity can be assessed for both atmosphere pressure electrospray ionisation (AP-ESI) and atmospheric pressure chemical ionisation (APCI), whether they are functioning in the positive ion (PI) or negative ion (NI) detection mode. For instance, despite the fact that one mode may produce a larger absolute response when combined with lesser selectivity and/or higher background, the overall performance of another ionisation mode may be superior for the particular application. Here, the employment of a multimode ESI/APCI source, flow injection of GTI/PGI solution, MS acquisition in alternate + or - scan mode, and can be helpful (Jacq et al., n.d.). For the purpose of detecting the genotoxic impurity (GTI), methyl p-toluenesulfonate (MTS), atmosphere pressure thermal desorption-extractive electrospray-mass spectrometry (AP/TD-EESI-MS) is being used. A new method aims to enhance both retention and sensitivity derivatization with dansyl chloride followed by LC/ESI-MS detection. For the study of (p-chlorophenyl)-aniline, electrochemical oxidation and ESI-MS/MS are combined. Additionally, HILIC interfaced with ESI-MS may be used to investigate this class of chemicals. In this method, polar analytes are retained on a column whereas non-polar APIs elute close to the void (Hsieh, 2008).

4.6 Molecular Imprinted Polymers (MIP) Approach:

Removal of GTIs from the API is of utmost importance for pharmaceutical safety assessment as well as regulatory compliance. Molecular imprinted polymers is a novel technique used to address this concern. MIP are used as GTI scavenger resins in selectively removing the impurities (Székely, Bandarra, et al., 2012). For impurities like Acetamide and Aryl sulfonate impurities that act as carcinogenic as if contains p-toluene sulfonic acid like compounds during manufacturing needs to be controlled below TTC limits. It is generally known that the purification process plays a significant part in GMP quality production and enhances product risk assessment. Typically, multiple-step procedures including recrystallization, fractional distillation, and other chromatographic methods are used to remove these contaminants. These time-consuming purifying procedures result in a significant proportion of API loss, which increases the cost of the final API. This demands the development of new purification methods that will efficiently separate genotoxins and other contaminants from APIs. Recently, selective API purification techniques have been developed using molecularly imprinted solid phase adsorbents, molecularly imprinted membranes, and nanofiltration (Székely, Fritz, et al., 2012)

4.7 Some other Approaches for Assessment of GTIs include:

For the purpose of identifying residual alkylating impurities in the API, several researchers, including Steen and Zeinab, evaluated a number of electrically driven modes of separation techniques, including capillary zone electrophoresis (CZE), micellar electrokinetic chromatography (MEKC), and microemulsion micellar electrokinetic chromatography (MEEKC).

The novel analytical method of micellar electrokinetic chromatography (MEKC) can distinguish between neutral and charged analytes. High separation efficiency, extremely low chemical usage, and user-friendly operation are further benefits of MEKC. Other intrinsic characteristics of the MEKC process include increased separation effectiveness and less solvent consumption. It is used in determination of 4-hydrazine benzene sulphonamide impurity in Celecoxib (Elder et al., 2011).

A microemulsion is employed as the carrier electrolyte in the interesting capillary electrophoretic method known as micro-emulsion electrokinetic chromatography (MEEKC). Analytes may partition between the microemulsion's aqueous phase and its oil droplets, which function as a pseudostationary phase. Although it can also be used for charged analytes, this mode works well for the separation of neutral analytes (Al Azzam & Aboul-Enein, 2016)

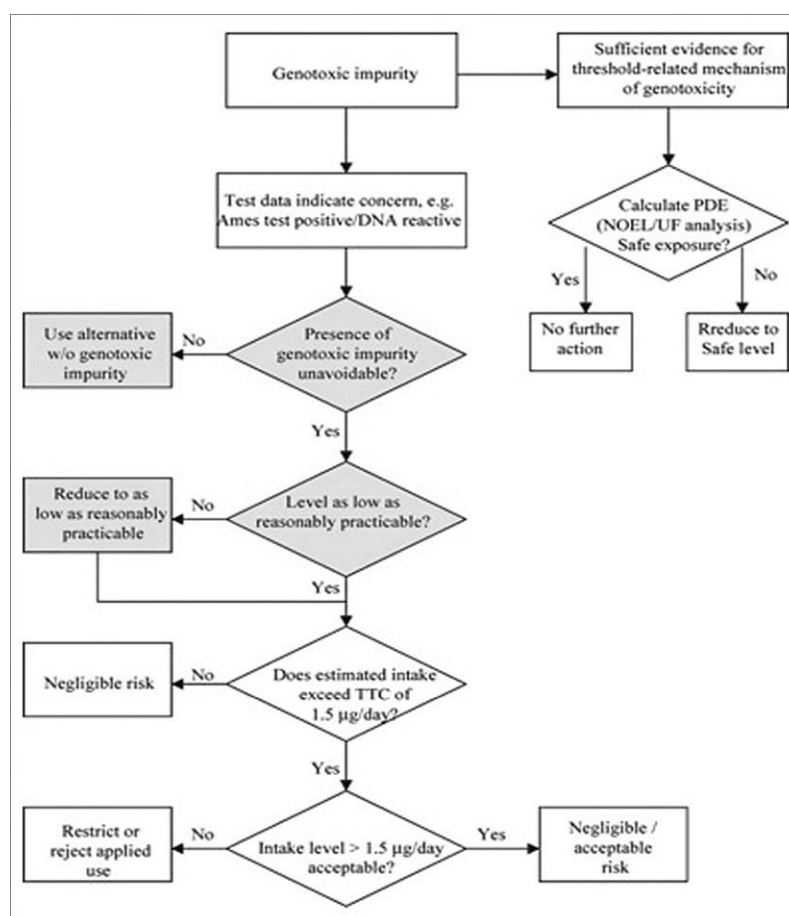
5. CONTROL STRATEGY FOR GENOTOXIC IMPURITIES:

Monitoring impurities that develop, particularly in the penultimate and final stages of synthesis of a drug substances, is the key objective of the risk assessment. By modifying the synthetic

pathway and reagents employed, the genotoxic impurity may be eliminated if it develops during the synthesis of the API. However, this is not a feasible option since, the synthesis of API is a complex procedure and is limited to chemicals and availability of reagents. Additional purification steps can be implemented to the synthetic route in order to get rid of the impurities. But, this may not be a good choice in case of impurities formation after the synthesis of the API, like degradation products or by interaction with the container-closure system. Testing for an impurity that developed during the synthesis of an API might only be necessary for the intermediate that follows the introduction of the impurity (rather than the final product). If the amount of impurity in the first intermediate test exceeds a specific threshold further testing will be necessary on subsequent intermediates. Spiking studies can be implemented in order to assess the pre-determined levels, while the test points and impurity level specifications varies for different compounds. It is easier to conduct risk assessment on the synthetic route to identify all the theoretical GTIs present in the end product. It is possible to exclude an impurity from the final API specification if it is added before the last step of the synthesis. On the other hand, if the impurity is added during the last stage of synthesis, it should be considered in the final API (Majid et al., 2018). The following steps can be followed to control the presence of GTIs once it is identified (Raillard, 2012).

- (1) Change the route of synthesis to completely eliminate the PGI
- (2) Change relevant process parameters to lower the PGI to a level that is not concerning.
- (3) Use chemical and mechanistic reasoning, ideally supported by experimental evidence, to show that the PGI will not be present at a substantial level.
- (4) Carry out tests to show that the PGI at its average API level is not actually hazardous.

Figure 6: Strategies to control Genotoxic Impurities:



Source: (Doshi et al., 2021)

6. CONCLUSION:

Identification, control and assessment of Genotoxic impurities should be strictly monitored due to the hazardous effect of the GTIs present in the API. Literature data, structural alerts, and specialised software along with correct toxicological assays and genotoxicity tests (e.g. Ames test) can all be used to identify GTI. It takes scientific judgement to measure the risk that can result from the GTI's presence in the drug substance against the potential for impurity production and carryover. Subsequently, limits for the impurities will be set using either the TTC or the available toxicological data. These limits allow for the development of appropriate analytical methodologies to determine the presence of the GTI in the drug substance and during the production process. It is a challenging task to develop analytical methods that are highly sensitive, robust, and reliable that can accurately monitor GTIs at very low levels (ppm level). Although simple separation and detection techniques are preferred in manufacturing quality control laboratories, MS detection in tandem with GC or HPLC is essential for tracing GTI at various pre-clinical and clinical drug development stages. The key to developing reliable methods for GTI assessment is to have a solid understanding of the molecular characteristics and structure of GTIs. Low recovery and inadequate sensitivity constitute a real difficulty in trace analysis because many GTIs have reactive properties and are unstable for direct analysis. Development of novel approaches like Extractive ESI, 2D Gas Chromatography, UPLC, HILIC-MS/MS is a breakthrough in assessment and quantification of Genotoxic impurities at ppm level. These novel techniques not only save time but are cost efficient and gives better sensitivity and reliability as compared to the conventional chromatography techniques. In addition, a sample treatment method called "matrix deactivation" has been devised to efficiently quench interfering elements in the sample matrices, which can be brought on by either the API itself or low level contaminants and solvents. This enables direct examination of some GTIs that are reactive or unstable. Although initial guidance on controlling and assessment of impurities with genotoxic potential has been provided by regulatory guidelines such as ICH M7, ICH Q3(B), ICH S2(R1), EMA, and USFDA, additional challenges are still being identified as all stakeholders acquire further experience in this area and these challenges be acknowledged. As technology and risk assessment approaches advance, it is expected that the assessment and regulation of genotoxic impurities will evolve.

7. REFERENCES:

1. Al Azzam, K. M., & Aboul-Enein, H. Y. (2016). Recent advances in analysis of hazardous genotoxic impurities in pharmaceuticals by HPLC, GC, and CE. *Journal of Liquid Chromatography and Related Technologies*, 39(1), 1–7. <https://doi.org/10.1080/10826076.2015.1111794>
2. An, J., Sun, M., Bai, L., Chen, T., Liu, D. Q., & Kord, A. (2008). A practical derivatization LC/MS approach for determination of trace level alkyl sulfonates and dialkyl sulfates genotoxic impurities in drug substances. *Journal of Pharmaceutical and Biomedical Analysis*, 48(3), 1006–1010. <https://doi.org/10.1016/j.jpba.2008.06.019>
3. Cartus, A., & Schrenk, D. (2016). Current methods in risk assessment of genotoxic chemicals. *Food and Chemical Toxicology*. <https://doi.org/10.1016/j.fct.2016.09.012>
4. Davis, J. A., Gift, J. S., & Zhao, Q. J. (2011). Introduction to benchmark dose methods and U . S . EPA ' s benchmark dose software (BMDs) version 2 . 1 . 1. *Toxicology and Applied Pharmacology*, 254(2), 181–191. <https://doi.org/10.1016/j.taap.2010.10.016>
5. Dejaegher, B., & Vander Heyden, Y. (2010). HILIC methods in pharmaceutical analysis. *Journal of Separation Science*, 33(6–7), 698–715. <https://doi.org/10.1002/jssc.200900742>
6. Doshi, C., Malayandi, R., Namjoshi, G., Kadam, P., & Mule, D. (2021). Nitrosodimethylamine impurities in metformin drug products: Physician insight. *Journal of Diabetology*, 12(2), 120. https://doi.org/10.4103/jod.jod_60_20
7. Douša, M., Klvaňa, R., Doubský, J., Srbek, J., Richter, J., Exner, M., & Gibala, P. (2016). HILIC-MS Determination of Genotoxic Impurity of 2-Chloro-N-(2-Chloroethyl)Ethanamine in the Vortioxetine Manufacturing Process. *Journal of Chromatographic Science*, 54(2), 119–124. <https://doi.org/10.1093/chromsci/bmv107>

8. Elder, D. P., Snodin, D., & Teasdale, A. (2011). Control and analysis of hydrazine, hydrazides and hydrazones-Genotoxic impurities in active pharmaceutical ingredients (APIs) and drug products. *Journal of Pharmaceutical and Biomedical Analysis*, 54(5), 900–910. <https://doi.org/10.1016/j.jpba.2010.11.007>
9. EMEA, Committee for Medicinal Products (CHMP). (2006). *Guideline on the Limits of Genotoxic Impurities 2006*.
10. European Medicines Agency, E. of M. for H. U. (2018). GUIDELINE ON THE LIMITS OF GENOTOXIC IMPURITIES. In *Ema* (Issue January 2007).
11. FDA Draft guidance. (2008). *Genotoxic and Carcinogenic Impurities in Drug Substances and Products: Recommended approaches*.
12. Genotoxic impurities in pharmaceutical products. (n.d.). *Agilent Technologies*.
13. Giordani, A., Kobel, W., & Ulrich, H. (2011). European Journal of Pharmaceutical Sciences Overall impact of the regulatory requirements for genotoxic impurities on the drug development process. *European Journal of Pharmaceutical Sciences*, 43(1–2), 1–15. <https://doi.org/10.1016/j.ejps.2011.03.004>
14. Government of India, Ministry of Health. (1955), Pharmacopoeia of India (the Indian Pharmacopoeia). (2018). N. 2, 2548.
15. Guidance for Industry S2B Genotoxicity ICH. (1997). *Guidance for Industry S2B Genotoxicity : A Standard Guidance for Industry S2B Genotoxicity : A Standard* (Issue July).
16. Helmy, R., Strickfuss, S., Hamilton, S., & Bu, X. (n.d.). *Quantification of Genotoxic Impurities in*.
17. Hsieh, Y. (2008). Potential of HILIC-MS in quantitative bioanalysis of drugs and drug metabolites. *Journal of Separation Science*, 31(9), 1481–1491. <https://doi.org/10.1002/jssc.200700451>
18. Humfrey, C. D. N. (2007). Recent developments in the risk assessment of potentially genotoxic impurities in pharmaceutical drug substances. *Toxicological Sciences*, 100(1), 24–28. <https://doi.org/10.1093/toxsci/kfm173>
19. ICH M7(R1). (2017). *ASSESSMENT AND CONTROL OF DNA REACTIVE (MUTAGENIC) IMPURITIES IN PHARMACEUTICALS TO LIMIT POTENTIAL CARCINOGENIC RISK M7(R1)* (Vol. 7, Issue March).
20. Jacq, K., Baker, A., David, F., Vanhoenacker, G., & Sandra, P. (n.d.). Method Selection for Trace Analysis of Genotoxic Impurities in Pharmaceuticals. *LCGC Europe, Volume 22*(Issue 11), Pages: 552–561.
21. Jain, M., Srivastava, V., Kumar, R., Dangi, V., Hiriyanna, S. G., Kumar, A., & Kumar, P. (2017). Determination of five potential genotoxic impurities in dalfampridine using liquid chromatography. *Journal of Pharmaceutical and Biomedical Analysis*, 133, 27–31. <https://doi.org/10.1016/j.jpba.2016.10.013>
22. Liu, D. Q., Sun, M., & Kord, A. S. (2010). Recent advances in trace analysis of pharmaceutical genotoxic impurities. *Journal of Pharmaceutical and Biomedical Analysis*, 51(5), 999–1014. <https://doi.org/10.1016/j.jpba.2009.11.009>
23. M*, T., S, A., SJ, G., SS, I., & A, H. (2015). Ultra Performance Liquid Chromatography (UPLC) - A Review. *Austin J Anal Pharm Chemistry*, 1–10. www.austinpublishinggroup.com
24. Majid, Z. A., Aris, A. Bin, & Talib, J. (2018). *Identification , control strategies , and analytical approaches for the determination of potential genotoxic impurities in pharmaceuticals : A analytical approaches for the determination of potential genotoxic impurities in pharmaceuticals : A comprehensi. October*. <https://doi.org/10.1002/jssc.201401143>
25. Mullangi, S., Ravindhranath, K., & Panchakarla, R. K. (2021). An efficient HILIC-MS/MS method for the trace level determination of three potential genotoxic impurities in aripiprazole active drug substance. *Journal of Analytical Science and Technology*, 12(1), 1–35. <https://doi.org/10.1186/s40543-021-00273-7>
26. PhRMA. (n.d.). *A Rationale for Determining, Testing and Controlling Specific Impurities in Pharmaceuticals that Possess Potential for Genotoxicity*.
27. Q3B(R2) IMPURITIES IN NEW DRUG PRODUCTS, I. (2006). ICH Q3B (R2) Impurities in New Drug Products (ICH/v02062006). In *ICH Quality Guidelines* (Issue June).
28. R POUNIKAR, A., J UMEKAR, M., & R GUPTA, K. (2020). Genotoxic Impurities: an Important Regulatory Aspect. *Asian Journal of Pharmaceutical and Clinical Research*, June, 10–25. <https://doi.org/10.22159/ajpcr.2020.v13i6.37370>

29. Raillard, S. P. (2012). Control of genotoxic impurities: In active pharmaceutical ingredients. *Chimica Oggi*, 30(1), 28–30.
30. Raman, N. V. V. S. S., Prasad, A. V. S. S., & Ratnakar Reddy, K. (2011). Strategies for the identification, control and determination of genotoxic impurities in drug substances: A pharmaceutical industry perspective. *Journal of Pharmaceutical and Biomedical Analysis*, 55(4), 662–667. <https://doi.org/10.1016/j.jpba.2010.11.039>
31. Sun, M., Bai, L., Terfloth, G. J., Liu, D. Q., & Kord, A. S. (2010). Matrix deactivation: A general approach to improve stability of unstable and reactive pharmaceutical genotoxic impurities for trace analysis. *Journal of Pharmaceutical and Biomedical Analysis*, 52(1), 30–36. <https://doi.org/10.1016/j.jpba.2009.11.027>
32. Sun, M., Liu, D. Q., & Kord, A. S. (2010). A systematic method development strategy for determination of pharmaceutical genotoxic impurities. *Organic Process Research and Development*, 14(4), 977–985. <https://doi.org/10.1021/op100089p>
33. Székely, G., Bandarra, J., Heggie, W., Ferreira, F. C., & Sellergren, B. (2012). Design, preparation and characterization of novel molecularly imprinted polymers for removal of potentially genotoxic 1,3-diisopropylurea from API solutions. *Separation and Purification Technology*, 86, 190–198. <https://doi.org/10.1016/j.seppur.2011.11.004>
34. Székely, G., Fritz, E., Bandarra, J., Heggie, W., & Sellergren, B. (2012). Removal of potentially genotoxic acetamide and arylsulfonate impurities from crude drugs by molecular imprinting. *Journal of Chromatography A*, 1240, 52–58. <https://doi.org/10.1016/j.chroma.2012.03.092>
35. Vijaya Bhaskar Reddy, A., Venugopal, N., Madhavi, G., Gangadhara Reddy, K., & Madhavi, V. (2013). A selective and sensitive UPLC-MS/MS approach for trace level quantification of four potential genotoxic impurities in zolmitriptan drug substance. *Journal of Pharmaceutical and Biomedical Analysis*, 84, 84–89. <https://doi.org/10.1016/j.jpba.2013.05.047>
36. Wigman, L., Zhang, K., & Kumar, A. (2015). Analytical Technologies for Genotoxic Impurities in Pharmaceutical Compounds. *LCGC North America*, Volume 33(Issue 5), Pages: 344–359.
37. Wu, N., Dempsey, J., Yehl, P. M., Dovletoglou, A., Ellison, D., & Wyvratt, J. (2004). Practical aspects of fast HPLC separations for pharmaceutical process development using monolithic columns. *Analytica Chimica Acta*, 523(2), 149–156. <https://doi.org/10.1016/j.aca.2004.07.069>

ABSTRACT

SESSION 3 – DESIGN & INNOVATION
IN MEDICINAL & PHYTOMEDICAL
CHEMISTRY

PCP376

PREPARATION AND EVALUATION OF HERBAL LOZENGES FOR THE TREATMENT OF SORE THROAT

AP0355	AP0362	AP0356	AP0343
Ms. Kanchiben Pandya	Ms. Pooja Patel	Mr. Kaish Pathan	Ms. Pooja Goswami
Student (M. Pharm), Krishna School of Pharmacy & Research	Student (M. Pharm), Krishna School of Pharmacy & Research	Student (M. Pharm), Krishna School of Pharmacy & Research	Assistant Professor, Babaria Institute of Pharmacy
pandyakanchi@gmail.com	pooja1200patel@gmail.com	kaishfpathan98@gmail.com	poojagoswami241@gmail.com

ABSTRACT

Herbal medicines are widely improved for primary health care because of better acceptability, better compatibility with the human body, and lesser side effects. Lozenges are palatable solid unit dosage forms to be administered in the oral cavity. The benefits of the medicated lozenges are: they increase the retention time which increases bioavailability, reduces gastric irritation, and bypasses first-pass metabolism. These are the flavoured medicated dosage forms proposed to be held in the oral cavity usually prepared in a sweetened base. Lozenges show local effects in the oral cavity and systemic effects by absorption into the systemic circulation. The emerging pandemic of coronavirus disease 2019 presents a new challenge for healthcare systems globally. The clinical presentation of severe acute respiratory syndrome coronavirus 2 (SARS-CoV-2) mainly targets the respiratory tract, for the treatment of which large numbers of drugs are prescribed. These flavoured lozenges reduce the number of medications and improve patient compliance in the treatment of sore throat associated with respiratory infections. In the present study different herbal medicinal plants were selected and the extract was prepared. These lozenges are formulated with hard lozenges candy base using different ingredients like binders, lubricants, flavouring, colouring, whipping agent, humectants, and herbal extract. Lozenges are evaluated for hardness, friability, diameter and thickness, weight variation, moisture content, drug content/ assay, etc. Lozenges provide easy administration, convenience to the patient, patient compliance, efficient treatment of low drug dosing, immediate onset of action, reduced dosage regimen, and cost-effectiveness.

Keywords: Lozenges, Herbal medicament, Cough drops, COVID, Sore throat.

1. INTRODUCTION

Cough is the most common infection which has been increasing and is considered to be an evidence defense mechanism for eradication of foreign material from the respiratory tract. Acute sore throat is a symptom often caused by an inflammatory process in the pharynx, tonsils, or nasopharynx. A sore throat is pain, scratchiness or irritation of the throat that often worsens when you swallow. The most common cause of a sore throat (pharyngitis) is a viral infection, such as a cold or the flu. A sore throat caused by a virus resolves on its own. Strep throat (streptococcal infection), a less common type of sore throat caused by bacteria, requires treatment with antibiotics to prevent complications. Sore throats may be caused by viral infections, Bacterial infections, Irritants and injuries. The microscopic organism that most

normally causes sore throat is streptococci. A sore throat can also occur by aggravation, smoking, air contamination, unnecessary shouting, and postnasal trickle brought about by hypersensitivities and breathing through the mouth. To conquer these issues such as difficulty in swallowing and conditions such as sore throat, formulators have significantly devoted their push to build up a novel kind of tablet dosage form for the oral route, that is, one, which deteriorates and breaks up quickly in salivation without the requirement swallowing the dosage form as a whole. These tablets are lozenges that break down from 15 s to 2 min. The quicker the medication breaks, the faster the assimilation and beginning of clinical impact. (Polyherbal Extract Based Linkus Lozenges for Symptomatic Relief: Design, Development and Evaluation)

Introduction of Lozenge (Suchitra Pundir, 2014) (Alton, 2016)

Lozenges are solid unit dosage forms containing a drug, flavoring, and sweetening agents. Lozenges are candies manufactured in a simple way, that are intended to be dissolved or disintegrated slowly in the mouth. (Edwards, 2017) They are commonly used for localized effects in the oral cavity as well as for systemic effects through absorption via the *oral* mucosa. Lozenges are a solid preparation consisting of sugar and gum, the latter giving strength and cohesiveness to the lozenge and facilitating the slow release of the medicament. Lozenges may contain an anesthetic, a demulcent, or an antiseptic. (Sevinc Kurbanoglu, 2017)

Classification of lozenges: (Majekodunmi, A Review on Lozenges, 2015)

Lozenges can be classified into various classes based on various methods. According to Site of Action 1. Local effect. Ex. Antiseptic, Decongestants 2. Systemic effect. Ex. Vitamins, Nicotine According to texture and Composition 1. Chewy or caramel-based medicated lozenges 2. Compressed tablet lozenges 3. Soft lozenges 4. Hard candy lozenges

Hard Candy Lozenges Hard candy lozenges are mixtures of sugar and other carbohydrates in an amorphous (non-crystalline) or glassy state. They can also be regarded as solid syrups of sugars. To slow the rate of dissolution, polymers such as peps and HPMC may be added. Another type of hard lozenge may be made of compressed powders. An example of this is clotrimazole troches (lozenges) made as a large compressed tablet that is slowly dissolved in the mouth. The tablet base material is made of dextrose, MCC, and povidone. The moisture content and weight of hard candy lozenge should be between, 0.5 to 1.5% and 1.5-4.5g respectively. These should undergo a slow and uniform dissolution or erosion over 5- 10min., and should not disintegrate. The temperature requirements for their preparation are usually high hence heat labile materials cannot be incorporated into them. Excipients such as sorbitol and sugar have demulcent effects, which relieve the discomfort of abraded tissue resulting from irritation due to cough and sore throat. A portion of the active drug product actually may be absorbed through the buccal mucosa, thereby escaping the first-pass metabolism which occurs when a drug is swallowed and absorbed through the gut. Acidulants, such as citric, tartaric, fumaric and malic acid may be added to the candy base to strengthen the flavor characteristics of the finished product and to control pH to preserve the stability of the incorporated medication. Regular hard candy has a pH of about 5.0 to 6.0 but with the addition of acidulants, it may be as low as 2.5 to 3.0. (Pothu, 2014)

Soft lozenges are often made using PEGs of sufficient molecular weight to provide slow dissolution in the saliva. Additionally, hydrocolloids such as acacia may also be added as an adhesive agent. Soft clotrimazole troches can be made this way by adding drug and acacia to melted PEG 1450 base and pouring into troche molded cavities.

Chewable lozenges are typically based on glycerinated gelatin; a base of glycerin, gelatin, and water. This base can be mixed with drug, acacia, and suitable flavoring and sweetening agents. (D. Mastropietro, 2017)

Drug candidates which can be incorporated into lozenges, belong to one of the following categories: Antiseptics, Local anaesthetics, Antibiotics, Antihistaminic, Antitussives, Analgesics, Decongestant, and Antifungal. (Majekodunmi, 2015)

Storage, packing and dispensing (Chandrawanshi Mayuri, (2018)) (Majekodunmi, 2015)

Storage: Lozenges should be stored away from heat and out of the reach of children. They should be protected from extremes of humidity.

Packaging: Hard candies are hygroscopic and frequently prone to absorption of atmospheric moisture. Considerations must include the hygroscopic nature of the candy base, storage conditions of the lozenges, the length of time they are stored, and the potential for drug interactions. These products should be stored in tight containers to avoid drying. This is especially true for chewable lozenges which can be overly dry and difficult to chew. If a disposable mold with a cardboard sleeve is used, it is best to slip this unit into a properly labelled, sealable plastic bag. Packaging should be proper and attractive

Introduction of herbal plant: (D. M. Kannur *, 2018)

The word “**herb**” has been obtained from the Latin word, “*herba*” and also an old French word “*herbe*”. Radditional medicine and herbal formulations have been used by making for the cure and treatment of various diseases and disorders. According to the Indian System of medicine, Ayurveda, Siddha, Unani plants are prepared in various types of dosage forms. Various formulations are commonly used with Ayurvedic reference or as home remedies or folk medicine. Considering the importance of patient compliance and market competition with modern dosage forms, the present study included phytochemical analysis of the extracts used and their formulation into lozenges, jellies and dispersibles.

Introduction of drug extract: (CK Kokate, 2008)

Table 15: Introduction of Drug Extract

Sr. no	Drug Name	Biological Name	Biological Source	Family	Geographical Source	Used To
1	TULSI	Sacred Basil, Holy Basil	fresh and dried leaves of <i>Ocimum sanctum</i> Linn	Labiatae	Cultivated in garden	respiratory problems, used to cure fever, common cold and sore throat
2	TURMERIC	Indian saffron, Curcuma	Dried, also fresh rhizome of the <i>curcuma longa</i> Linn.	Zingieraeae	southern Asia, India, China	sore throat, sneezing, stuffy nose, cough and even asthma
3	BLACK PEEPER	Peeper	The dried unripe fruit of perennial climbing vine <i>piper nigrum</i> Linn.	Piperaceae	south India, Indonesia, Brazil	arthritis, asthma, stuffy nose
4	CASTOR OIL	Ricinus oil	Obtained by the cold expression of the seeds of <i>Ricinus communis</i> .	Euphorbiacea	India, South America, Africa	antiviral and antimicrobial

2. OBJECTIVE

The aim of this study was to extract the herbal medicinal plant having a beneficial role in respiratory tract infections related sore throat treatment and to formulate the lozenge tablets in order to investigate a profitable dosage form.

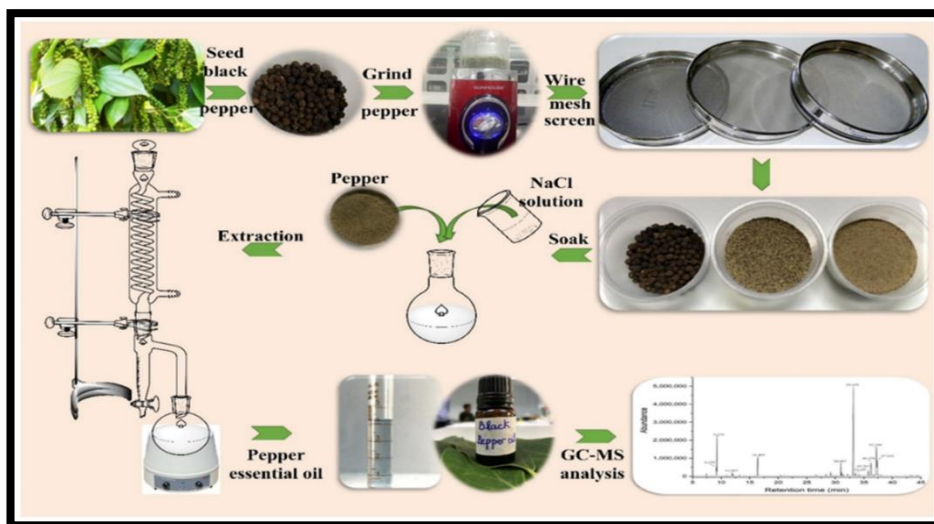
3. RESEARCH METHODOLOGY:

3.1 Methodology

3.1.1 Preparation of Black Pepper Extract: -

Extraction with ethanol (Tiwari, 2020): 10 gm of black pepper powder extracted with 150 ml 95% ethanol in Soxhlet extractor for 2 hours. The solution was filtered and concentrated in the water bath at 60°C. 10 ml 10% of alcoholic potassium hydroxide was added to the filtrate with continuous stirring. The insoluble residue was filtered and the alcoholic solution was left overnight and filtered by a membrane filter.

Figure 1: Chart of Black Pepper Extract



3.1.2 Preparation of Tulsi Extract: -

1. **Preparation of raw material** (Jagdish, 2021): The leaves were dried in order to reduce the initial moisture content (90 % of humidity), in an oven with air renewal and circulation. The drying temperature was 50 °C and was held constant for 5 hours. After drying, the sheets were grinded in order to increase the contact surface reducing the resistance to oil extraction. The dried leaves were placed in sealed plastic bags, protected from light and moisture, and stored in a refrigerator with low humidity.

Extraction with ethanol (Pradeep Mutttagadur Chandrappa, 2015): Tulsi extract for the study was obtained by finely powdering the dried leaves. The powder was macerated with 100% ethanol followed by filtration. 18 grams of tulsi extract (residue 6% w/w) was obtained by dissolving 300 g of tulsi powder in 1 liter of ethanol.

Figure 2: Tulsi Extract



3.2 METHOD OF PREPARATION OF HERBAL LOZENGES: - (Luber, 2013)

Hard lozenges. The hard lozenges were prepared by heating and congealing technique. The quantity of each ingredient needed for compounding was calculated for 20 lozenges and the enough material for two extra lozenges were calculated and weighed. Candy base was prepared by dissolving desired quantity of sugar, dextrose, SMC, and gelatin in one-third amount of water (into 10ml to) at a temperature of about 100°C -105°C (in beaker 1). In the second beaker add sucrose in 5ml water just to dissolve and form a clear viscous solution using a water bath, the temperature should be kept in between 156C- 160°C. After 5 minutes, mix the solution of Beaker 2 with the solution in beaker 1 and again put it in a water bath until the syrup color became golden. After 35 min, 2-4% black pepper, turmeric powder, tulsi extract, and ginger powder are incorporated in formulation at 160°C. Color is added to it in the form of solution or paste and mixed uniformly. Poured into a mold of desired shape and size to form candy. The weight of the candy mass is checked. (S. Vidyadhara1)

3.3 INGREDIENTS FOR PREPARATION OF HERBAL LOZENGES: (Luber, 2013)

Table 16: Ingredients and quantity of drugs utilized for preparation

Sr. No.	INGREDIENT	QUANTITY	USED As
1	Black Peeper Extract	10mg	Antimicrobial
2	Turmeric Powder	500mg	Anti-bacterial, Antioxidant
3	Tulsi Extract	10ml	Anti-Septic, Cold and Cough
4	Ginger Powder	4g	Anti-inflammatory
5	SMC	2g	Binder
6	Gelatin	1g	Pouring the Mould
7	Sugar	4g	Candy base
8	Water	15ml	Candy Base
9	Dextrose	5gm	Candy Base
10	Sucrose	2.5gm	Candy Base

4. LITERATURE REVIEW

Table 17: Literature review

Sr. No.	Ingredient	Scientific Name	Used As	References
1	Black Peeper Extract	Piper Nigrum	Antimicrobial, Bone healing activity, Anti-obesity activity, Anti-ulcerative activity, Antioxidant and free radical scavenging-activity, Analgesic, anti-inflammatory and stimulatory activity	(Sundaran J, 2020)
2	Turmeric Powder	Curcuma Longa	Anti-bacterial, Antioxidant, anti-inflammatory, antioxidant, anticancer, antimutagenic, antimicrobial, antiobesity, hypolipidemic, cardioprotective, and neuroprotective effects	(Ahmad, 2020)
3	Tulsi Extract	Ocimum Tenuiflorum	Anti-Septic, in curing a Cold and Cough, Anxiolytic and anti-depressant	(MM, 2014)
4	Ginger Powder	Zingiber Officinale	anti-inflammatory, antioxidant, anticancer, antimutagenic, antimicrobial, antiobesity,	(Rahmani AH, 2014)

			hypolipidemic, cardioprotective, and neuroprotective effects	
--	--	--	--	--

5. ANALYSIS

Evaluation Parameters of Herbal lozenges (Peters, 2005) (Chandrawanshi Mayuri J., 2019) (S. Vidyadhara1)

5.1.1 Physical Appearance: The physical appearance was visually checked for the appearance, color, size, shape, and the feel on application of prepared herbal lozenges formulations.

5.1.2 Hardness: Hardness of the lozenges is determined by Monsanto hardness tester by taking six lozenges from the formulation. The values were expressed in Kg / cm² and mean \pm SD values were calculated. Resistance to shipping or breakage under conditions of storage, transportation and handling prior usage of lozenges depends on its hardness.

5.1.3 Diameter and Thickness: A vernier caliper is an instrument used for the determination of the diameter and thickness of the lozenges.

5.1.4 Friability: Roche friabilator is used for the determination of the friability of lozenges. Twenty pre weighed lozenges were rotated at 25 rpm for 4 min. After the revolution the lozenges were de-dusted and weighed again accurately. The observed value should not be more than 1 %. Friability is calculated by following formula,

$$\% \text{ friability} = (1 - W_t / W) \times 100$$

Where, W= initial weight of lozenges, W_t= weight of lozenges after revolution

5.1.5 Weight Variation: Twenty lozenges were randomly selected and individually weighed using an electronic balance. The average weight and standard deviation of 20 tablets was calculated or initial weight is compared with the calculated average weight. The weight of not more than two lozenges should deviate from the average weight by more than 5 %.

5.1.6 pH: For the determination we take small quantity of lozenges solution in another party plate and dip the pH strip in it and with the help of color change is pH noted.

5.1.7 Moisture Analysis: Moisture analysis can be done by using three methods like, Karl fisher titration, Gravimetric analysis, Azeotropic distillation method. Here we followed Gravimetric analysis Method

5.1.7.1 Gravimetric Analysis: Weigh accurately about 1g of sample and note the initial weight. It is then placed in a vacuum oven at 60-70 °C for 12- 16 hours. After a specific period of time, once again weigh the sample and moisture content can be calculated by subtraction of final weight from the initial weight.

5.1.7.2 Stability Studies: The products should show satisfactory stability of organoleptic characteristics at elevated temperatures and elevated humidity. Because lozenges are flavoured, flavour stability is important. There is, however, no objective method for measuring flavour stability in a finished dosage form, although gas chromatography may be used for the chemical analysis of flavour compounds. The stability studies were performed for all the prepared formulations at room temperature. The stability study was conducted for a period of 3 weeks. The parameters like physical appearance, pH, and colour were tested every week. The results are tabulated. All the formulations were equally good with respect to appearance, homogeneity, and pH.

6. FINDING

6.1 Physical Appearance or Various Quality Control Parameters

Table 4 : The physical appearance of lozenges

Sr. No.	Parameter	Result
1	Color	Greenish
2	State	Solid
3	Smell	Characteristic
4	Shape	Round
5	Hardness	12.68 kg/cm ²
6	Thickness	10.57 mm
7	Average diameter	6.29 mm
9	Net weight	3gm

Figure 3: Image of Prepared Lozenges



6.2 pH:

With the help of pH Strip, We determine pH=7

6.3 Stability Studies:

Table 5: Stability studies of Herbal lozenges formulations

Sr. No.	Parameter	Observation			
		Initial	1 week	2 week	3 week
1	Appearance	Solid and Greenish	Solid and Greenish	Solid and Greenish	Solid and Greenish
2	PH	7	7	6.5	6.5

6.4 Moisture Analysis

The moisture content of herbal lozenges was found in between 1.0 – 1.5%.

7 CONCLUSION

Lozenges are organoleptically accepted formulations which provide easy administration, convenience to patient, large patient compliance and efficient treatment of low drug dosing, immediate onset of action, reduced dosage regimen and cost-effectiveness. New drug development in this field is always beneficial for the patient, the physician and the pharmaceutical industry. In the present study different herbal medicinal plants were selected and the extract was prepared and incorporated into hard candy-based lozenges. The clinical presentation of severe acute respiratory syndrome coronavirus 2 (SARS-CoV-2) mainly targets the respiratory tract, for the treatment of which large numbers of drugs are prescribed. These flavored lozenges reduce the number of medications and improve patient compliance in the treatment of sore throat associated with respiratory infections. This discovery will be useful for further improvement and development of this plant or other herbal plants for better compliance.

8 REFERENCES

1. Ahmad, R. S. (2020). Biochemistry, Safety, Pharmacological Activities, and Clinical Applications of Turmeric: A Mechanistic Review. *Evidence-Based Complement Alternat Medicine*.
2. Alton, M. E. (2016). *Pharmaceutics the Science of Dosage Form Design*. Churchill Livingstone.
3. Chandrawanshi Mayuri J., S. R. (2019). a review on medicated lozenges . *World Journal Of Pharmaceutical Research volume*, 396-412.
4. Chandrawanshi Mayuri, J. S. ((2018)). A REVIEW ON MEDICATED LOZENGES. *world journal of pharmacy and pharmaceutical sciences*, 396-412.
5. CK Kokate, A. P. (2008). Text book of Pharmacognosy. *Nirali prakashan*, 81-94.
6. D. M. Kannur *, S. S. (2018). FORMULATION AND EVALUATION OF TRADITIONAL MEDICINE BASED HERBAL LOZENGES, JELLIES AND DISPERSIBLE TABLETS. *INTERNATIONAL JOURNAL OF PHARMACEUTICAL SCIENCES AND RESEARCH*, 3501-3505.
7. D. Mastropietro, .. H. (2017). Biocompatibility, Surface Engineering, and Delivery of Drugs, Genes and Other Molecules.
8. Edwards, W. (2017). Development of a potential probiotic lozenge containing *Enterococcus faecium* CRL 183. 193-199.
9. Irene Thomas, B. P. (n.d.). Formulation and Evaluation of Herbal Lozenges Containing Eucalyptus Oil and Coleus Aromaticus Oil Binu Anand*, .
10. Jagdish. (2021). tulsi-oil-extraction-process-benefits-uses. *agri farming*.
11. Jing-RuHea, J.-J. S.-W.-Q. (2021). Bioaccessibility and intracellular antioxidant activity of phloretin embodied by gliadin/sodium carboxymethyl cellulose nanoparticles. *Food Hydrocolloids*.
12. Luber, T. S. (2013). "Antacid Products," Handbook of Nonprescription. *United States Patent*.
13. Majekodunmi, S. O. (2015). A Review on Lozenges. *American Journal of Medicine and Medical Sciences*, 99-104.
14. Majekodunmi, S. O. (2015). A Review on Lozenges. *American Journal of Medicine and Medical Sciences*, 99-104.
15. MM, C. (2014). Tulsi - *Ocimum sanctum*: A herb for all reasons. *J Ayurveda Integr Med*, 251.
16. Peters, D. L. (2005). Medicated Lozenges Pharmaceutical Dosage Forms: Tablets. *New York: Marcel Dekker*, 419-577.
17. Polyherbal Extract Based Linkus Lozenges for Symptomatic Relief: Design, Development and Evaluation. (n.d.).
18. Pothu, R. &. (2014). LOZENGES FORMULATION AND EVALUATION: A REVIEW. *IJAPR*, 290-294.
19. Pradeep Muttagadur Chandrappa, A. D. (2015). Antimicrobial activity of herbal medicines (tulsi extract, neem extract) and chlorhexidine against *Enterococcus faecalis* in Endodontics: An in vitro study. *Journal of International Society of Preventive and Community Dentistry*, 89-92.
20. Rahmani AH, S. F. (2014). Active ingredients of ginger as potential candidates in the prevention and treatment of diseases via modulation of biological activities. *Int J Physiol Pathophysiol Pharmacol*, 125-36.
21. S. Vidyadhara1, R. S. (n.d.). Formulation and Evaluation of Amoxicillin Trihydrate Lozenges.
22. Sevign Kurbanoglu, .. S. (2017). Carbon-based nanostructures for electrochemical analysis of oral medicines.
23. Shingate PN, D. P. (2013). New method development for extraction and isolation of Piperine from Black Pepper. *Int J Pharm Sci* , 3165-3170.
24. Suchitra Pundir, A. M. (2014). A review on lozenges. *Journal der Pharmazie Forschung*, 1- 10.

25. Sundaran J, B. R. (2020). A short review on pharmacological activity of *Cissus quadrangularis*. *Bioinformation*, 579-585.
26. Tiwari, A. M. (2020). Piperine: A comprehensive review of methods of isolation, purification, and biological properties. *Medicine in Drug Discovery*, 100027.

PCP430

DESIGN, SYNTHESIS AND EVALUATION OF SOME PIPERAZINE-ARYLAMIDE ANALOGUES AS ANTITUBERCULAR AGENTS

AP0402

Divya Teli

Assistant Professor,
Department of
Pharmaceutical
Chemistry,
L. M. College of
Pharmacy
divya.teli@lmcp.ac.in

AP0452

Palak Vadodariya

Assistant Professor,
Department of Pharmacy,
Marwadi University
Palakvadodariya812@gmail.com

AP0453

Mahesh Chhabria,

Professor,
Department of
Pharmaceutical Chemistry,
L. M. College of Pharmacy
mahesh.chhabria@lmcp.ac.in

Abstract

Tuberculosis (TB) has been historically a deadly infectious disease. Compared to the 1.8 million deaths brought on by COVID-19, TB alone caused 1.5 million fatalities in the world in 2021. According to the World Health Organization, in order to stop the pandemic, and in line with the END-TB strategy, new TB medications must be investigated. Piperazine has been recognized as one of the important heterocyclic scaffolds among the nitrogen-containing heterocycles acting against *Mycobacterium tuberculosis*. The current work summarizes the recent development of piperazine-arylamide analogues as anti-TB agents, including their design, synthesis and anti-mycobacterial evaluation of suitable drug candidates. In order to find *InhA* inhibitors, virtual screening of 2,00,000 ligands from the Enamine Hit locator library, ADMET analysis, application of Lipinski filters, and MD simulations have been carried out. The best promising four piperazine aryl-amides (LMPV-1 to LMPV-4) have been synthesized and characterized. Three of them (LMPV-1, 3, and 4) showed comparable inhibitory concentrations to that of Isoniazid when screened by the MABA antimycobacterial assay. Thus, such piperazine-arylamides can be potential hits in antitubercular drug discovery.

Keywords: Tuberculosis, InhA, Piperazine-arylamide, Docking, MABA

1 Introduction

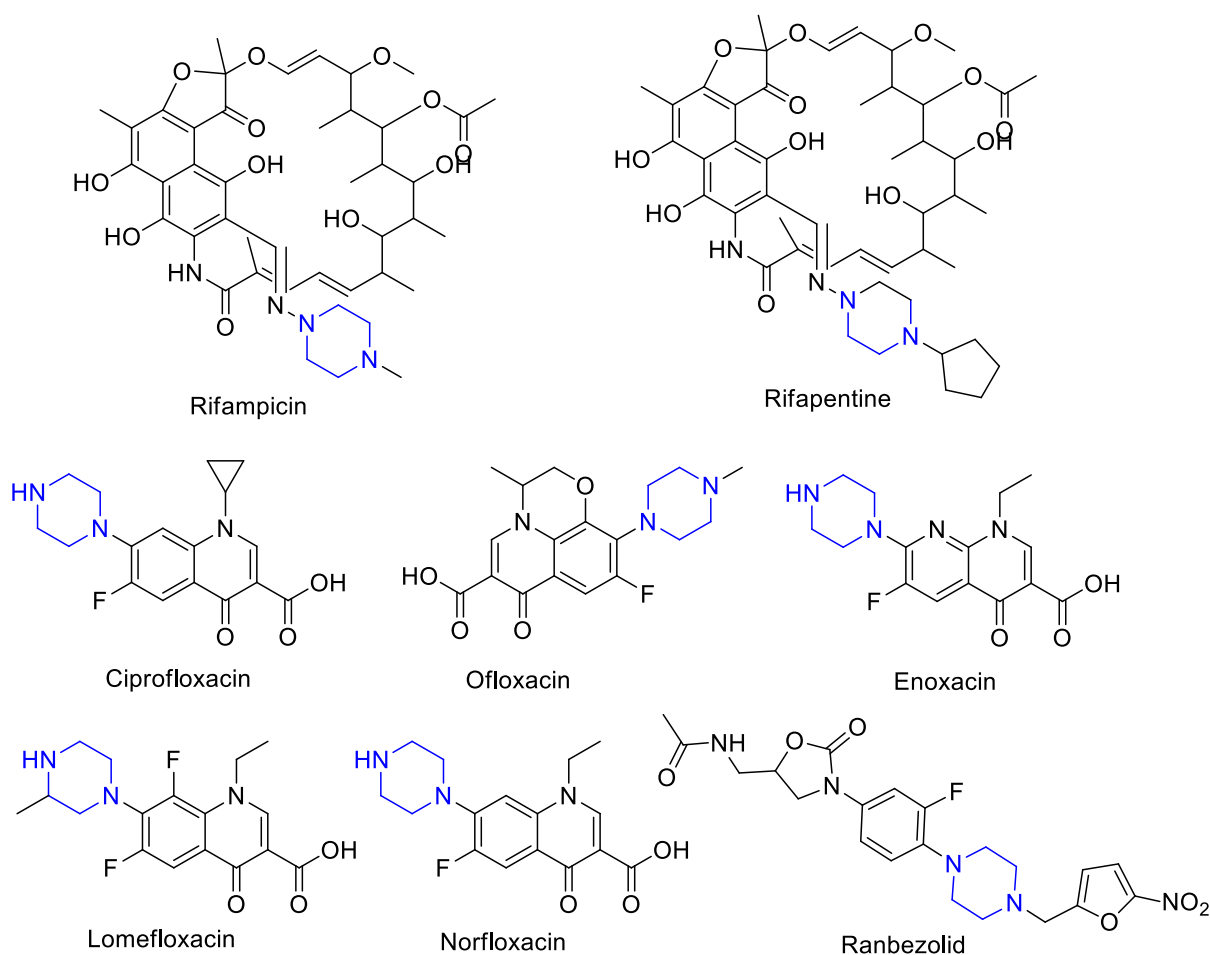
Tuberculosis (TB) is a severe infectious illness caused by several strains of *Mycobacterium tuberculosis*. It is highly contagious and fatal. Furthermore, it is the leading cause of death worldwide, followed by COVID-19, with significant economic and health problems, especially in developing countries. After COVID-19, TB is anticipated to rank second as a cause of death from a single infectious agent in 2020. As per WHO global tuberculosis report 2021, the number of deaths officially categorised as caused by tuberculosis (1.3 million) was about 2 times that of HIV/AIDS (0.68 million) in 2020, and the COVID-19 pandemic had a greater impact on TB mortality (*World Health Organisation Global tuberculosis report, 2020*).

In addition, taking high doses of anti-TB medications over an extended length of time induces lung tissue inflammation in tuberculosis patients. It is due to the oxidative stress brought on by the generation of free radicals by activated macrophages and anti-TB drugs. Hence, owing to side effect as well as complexity of recently used anti-TB drugs, the search of new chemical entities as anti-TB agents has been strongly urged which further sensitized through the recent approvals of bedaquiline and delamanid from the United States food and drug administration (USFDA) and European medical agency (EMA) (Gualano et al., 2016), respectively for the treatment of drug resistant TB. Many of the newly discovered chemical entities and other several drug candidates have been under the clinical trial phase for the treatment of the pulmonary tuberculosis (Oh et al., 2021).

The mycobacterial enoyl acyl carrier protein reductase (InhA) is a key enzyme involved in the biosynthesis of mycolic acid of *M. tuberculosis*. Isoniazid (INH), a first-line anti-TB drug targets InhA, from the mycobacterial type II fatty acid production pathway. Importantly, KatG, the enzyme that converts isoniazid into its active form, is mutated in the majority of INH-resistant clinical isolate (Jain et al., 2020). Therefore, drugs that block InhA without first activating KatG will be effective against the majority of INH-resistant Mycobacterium tuberculosis strains. Thus, the InhA direct inhibitors which do not need prior activation by KatG embarks the potential strategy to combat resistance. Some of the categories of molecules like aryl amide, piperazine, benzamide, quinazoline, thiaziazole, etc. have been recognized as direct InhA inhibitors (Prasad et al., 2021).

Piperazine, a six membered nitrogen containing heterocycle is a privileged scaffold. In recent years several potent molecules containing piperazine as an essential subunit of the structural frame have been reported, especially against *Mycobacterium tuberculosis*. Moreover, many of these reported molecules also displayed potential activity against multidrug-resistant (MDR), and extremely drug-resistant (XDR) strains of the mycobacteria. (Girase et al., 2021). These piperazine derivatives have been investigated as antitubercular agents through different mechanism of actions like InhA inhibition, MmpL3 inhibitors, DprE1 inhibitors, etc. Various antitubercular agents also possess the piperazine heterocycles, which is depicted in figure 1.

Figure 1 Structures of Antitubercular agents containing piperazine heterocycle



2 Objectives

Recently, development of drug resistance, toxicity and side effects of currently available antitubercular agents and re-occurrence of TB as multidrug resistant (MDR) and extensively drug resistant (XDR) tuberculosis highlight the need for the identification and characterization of new chemical entities.

Recently anti-tubercular drug discovery programs like 'End-TB' focuses on the discovery and development of novel agents which can inhibits the enzymes involved in the life cycle of the mycobacteria. InhA is involved in Fatty acid synthesis (FAS II). So, it is the viable target for drug development, because eukaryotic cells only use a FAS-I enzymes to synthesize fatty acids. As per the literature search, direct InhA inhibitors are developed (to avoid the activation of KatG and avoiding drug resistance) which gave considerable enzyme inhibitory effect.

Therefore, in this research article, the novel piperazine-arylamide scaffold has been identified through virtual screening against InhA. The better analogues of piperazine-amide were designed in terms of better binding affinity with the receptor and optimized pharmacokinetic parameters. These analogues have been synthesized, characterized and evaluated for their anti-tubercular potential.

3 Research Methodology/ Experimental

3.1 Computational study

3.3.1 Structure-based virtual screening

Structure-based virtual screening was employed to search the novel InhA inhibitors from Enamine Hit Locator (HLL-200) library having 2,00,000 ligands (<https://enamine.net/compound-libraries/diversity-libraries/hit-locator-library-200>). Initially, all the compounds were prepared for computational study at physiological pH condition using OPLS3e forcefield by LigPrep module of Schrödinger (Schrödinger, LLC, New York, NY, 2020).

The 3D crystal structure of InhA (PDB ID: 4TZK) has been retrieved from RCSB Protein Data Bank. It was prepared to ensure structural correctness for hydrogen consistency, bond orders, steric clashes and charges using Protein Preparation Wizard in Schrodinger Suite supported by OPLS3e force field. Thus, the prepared structure was used for receptor grid generation required for the docking protocol. The receptor grid was generated considering centroid of co-crystallized ligand. The docking protocol was validated by calculating all-atom RMSD between re-docked ligand and co-crystallized ligand which came 0.12 Å.

At the first, high-throughput virtual screening (HTVS) method was used for molecular docking of 2,00,000 compounds using Glide module of Schrödinger. From the result, the best scored 20,000 compounds were picked up and subjected for next standard precision (SP) docking. From the SP docking result, 2000 molecules were carried forward for extra-precision (XP) docking. By evaluating the docking results of XP method, piperazine containing compounds showed good binding with the receptor. So, it was selected as a hit and the substitutions were modified to obtain the good fit into the receptor active site pocket. The 4 best fitting compounds have been identified based on their docking scores, binding energy study and the key interactions with the enzyme.

3.3.2 Pharmacokinetic properties prediction

The pharmacokinetic parameters of designed compounds have been investigated using QikProp tool of Schrödinger. The best promising compound's molecular dynamic study has been carried out to understand the ligand-receptor stability.

3.3.3 Molecular dynamics (MD)

To establish the time-dependent stability of the complexes between the most promising compounds LMPV-1 and InhA enzyme, MD study was carried out. The study was performed over a period of 10 ns using Gromacs2020.1 package. The docked pose of the ligands in complex with enzyme was considered as the reference frame for MD study. Some statistical parameters such as RMSD-L, RMSD-P, RMSF-P, and H-bond were determined.

3.2 Synthesis of designed piperazine-arylamides

All the reagents and solvents required for the synthesis of the compounds were procured from Sigma-Aldrich, Spectrochem, and S. d. fine chemicals. Reaction monitoring was carried out by thin-layer chromatography (TLC), using silica gel precoated plates (60F254, Merck, 0.25 mm thickness) and visualized under ultraviolet (UV) light ($\lambda = 254$ nm) or in an iodine chamber. Melting points were determined in glass capillary tubes using a silicon oil-bath type melting point apparatus (Veego) and the reported melting points are uncorrected. The IR spectra were recorded on in FT-IR 8400S Shimadzu spectrophotometer using KBr. Mass spectra were obtained using 2010EV LCMS Shimadzu instrument at 70 eV. ¹H NMR spectra were recorded in DMSO-*d*₆ on BRUKER Avance-II at 400 MHz and chemical shift were measured as parts per million downfield from tetramethylsilane (TMS) as internal standard.

3.2.1 General method for the synthesis of ethyl substituted-benzoates

To a previously stirred solution of benzoic acid/ substituted benzoic acid (5.0 g) in ethanol (50 mL) was added conc. sulfuric acid (5 mL) at room temperature. The reaction mixture was then refluxed for 6 h.

After cooling down to room temperature, the solution was basified with sodium bicarbonate to remove the traces of benzoic acid. The basified aqueous mixture was extracted with ethyl acetate (3 x 100 mL). The organic extracts were combined, dried over sodium sulfate and concentrated under reduced pressure, which was used in the next step as such.

3.2.1.1 Ethyl benzoate

The title compound was synthesized using benzoic acid (5.0 g, 41 mmol). Yield: 5.9 g, 96.7% as colorless oil, b.p. 212-214 °C (lit b.p. 210-212 °C) (Fathi et al., 2019).

3.2.1.2 ethyl 2-methylbenzoate

The title compound was synthesized using *o*-toluic acid (5.0 g, 36.7 mmol). Yield: 5.7 g, 95% as colorless oil, b.p. 221-223 °C (lit b.p. 226-227 °C) (Gavara et al., 2020).

3.2.1.2 ethyl 4-methylbenzoate

The title compound was synthesized using *p*-toluic acid (5.0 g, 36.7 mmol). Yield: 5.4 g, 90% as colorless oil, b.p. 230-232 °C (lit b.p. 232-233 °C) (Qiu et al., 2017).

3.2.2 General method for the synthesis of mono-substituted benzoyl piperazines

In to a round bottom flask provided with a stirrer, thermopocket and condenser set up were taken piperazine (5.0 equiv.) and ethyl benzoate (1.0 equiv.). The reaction mixture was heated for 10 h to reach a temperature of about 110° C while stirring. After completion of reaction, the reaction mixture was allowed to cool to room temperature, dissolved in chloroform and washed with saturated sodium bicarbonate solution followed by water. The organic layer was acidified to pH 2 with 10% aqueous hydrochloric acid. The organic layer was then separated, and an aqueous layer was washed with chloroform. This aqueous portion was basified with solid sodium bicarbonate to pH 8 and was extracted with chloroform. The chloroform layer was evaporated to obtain the desired substituted benzoyl piperazines.

3.2.2.1 Benzoyl piperazine

The title compound was synthesized using ethyl benzoate (5.9 g, 39.2 mmol) and piperazine (16.9 g, 196.4 mmol). Yield: 4.3 g, 70.5% as white solid, m.p. 132-133 °C (Joseph et al., 2019).

3.2.2.2 Piperazin-1-yl(*o*-tolyl)methanone

The title compound was synthesized using ethyl 2-methylbenzoate (5.7 g, 34.7 mmol) and piperazine (11.8 g, 173.6 mmol). Yield: 5.2 g, 75% as brown solid, m.p. 140-141 °C (Shan, Y. et al, 2015).

3.2.2.3 Piperazin-1-yl(*p*-tolyl)methanone

The title compound was synthesized using ethyl 4-methylbenzoate (5.4 g, 32.9 mmol) and piperazine (14.1 g, 164.6 mmol). Yield: 4.8 g, 67.7% as brown solid, m.p. 137-138 °C (Lai et al., 2001).

3.2.3 General method for the synthesis of piperazine-arylamides

To a previously stirred solution of 4-sulfamoyl benzoic acid (1.07 equiv.) in DMF (5 mL) was added HATU (1.5 equiv.) and DIPEA (2.0 equiv.) at room temperature and reaction mixture was allowed to stir for 15 minutes. To the resulting reaction mixture was then added mono-substituted benzoyl piperazine (1.0 equiv.) and stirred for 2 h at room temperature. After completion of reaction, it was poured in ice-cold water to obtain the white colored precipitates which was filtered and dried under reduced pressure. The obtained product was recrystallized using isopropyl alcohol to yield the titled compound.

3.2.3.1 4-(4-benzoylpiperazine-1-carbonyl)benzenesulfonamide

The title compound was synthesized using benzoyl piperazine (0.5 g, 2.6 mmol) and 4-sulfamoyl benzoic acid (0.58 g, 2.8 mmol). Yield: 0.3 g, 33% as white solid, m.p. 239-241 °C. IR (KBr, cm⁻¹): 3346, 2922, 1621, 1329, 1169. ¹H NMR (DMSO-*d*₆): δ 7.33 - 7.31 (d, 2H, ArH), 7.24 - 7.21 (m, 4H, ArH), 7.02 (d, 2H, NH₂), 6.53 - 6.51 (d, 2H, ArH), 6.16 - 6.14 (d, 1H, ArH), 3.67 - 3.48 (m, 4H, CH₂), 3.42 - 3.34 (m, 4H, CH₂); MS (m/z): 374.2 [M+H]⁺.

3.2.3.2 4-(4-(2-methylbenzoyl)piperazine-1-carbonyl) benzene sulfonamide

The title compound was synthesized using piperazin-1-yl(*o*-tolyl)methanone (0.5 g, 2.4 mmol) and 4-sulfamoyl benzoic acid (0.54 g, 2.6 mmol). Yield: 0.41 g, 43.6% as off-white solid, m.p. 217-218 °C. IR (KBr, cm⁻¹): 3350, 2923, 1628, 1331, 1255. ¹H NMR (DMSO-*d*₆): δ 7.89 - 7.87 (d, 2H, ArH), 7.63 - 7.61 (d, 2H, ArH), 7.49 - 7.47 (m, 2H, ArH), 7.46 (s, 2H, NH₂), 7.45 - 7.43 (m, 2H, ArH), 3.67 - 3.34 (m, 8H, CH₂), 2.34 (t, 3H, CH₃); MS (m/z): 388.2 [M+H]⁺.

3.2.3.3 4-(4-(4-methylbenzoyl)piperazine-1-carbonyl)benzene sulfonamide

The title compound was synthesized using piperazin-1-yl(*p*-tolyl)methanone (0.5 g, 2.4 mmol) and 4-sulfamoyl benzoic acid (0.54 g, 2.6 mmol). Yield: 0.32 g, 34% as off-white solid, m.p. 197-199 °C. IR (KBr, cm⁻¹): 3355, 2905, 1624, 1331, 1168. ¹H NMR (DMSO-*d*₆): δ 7.89 - 7.85 (d, 2H, ArH), 7.62 - 7.53 (m, 2H, ArH), 7.49 (s, 2H, NH₂), 7.36 - 7.21 (s, 4H, ArH), 3.77 - 3.39 (m, 8H, CH₂), 2.22 (s, 3H, CH₃); MS (m/z): 388.3 [M+H]⁺.

3.2.3.4 4-(4-(methylamino)benzoyl)piperazin-1-yl(*p*-tolyl) methanone

The title compound was synthesized using piperazin-1-yl(*p*-tolyl)methanone (0.5 g, 2.4 mmol) and 4-(methylamino)benzoic acid (0.37 g, 2.4 mmol). Yield: 0.25 g, 30.5% as white solid, m.p. 174-176 °C. IR (KBr, cm^{-1}): 3346, 2923, 1621, 1329, 1169. $^1\text{H NMR}$ ($\text{DMSO-}d_6$): δ 7.33 - 7.31 (d, 2H, ArH), 7.26 - 7.21 (m, 4H, ArH), 6.53 - 6.51 (d, 2H, ArH), 6.16 - 6.14 (d, 1H, NH), 3.54 - 3.34 (m, 8H, CH_2), 2.68 (s, 3H, CH_3), 2.34 (s, 3H, CH_3); MS (m/z): 338.4 $[\text{M}+\text{H}]^+$.

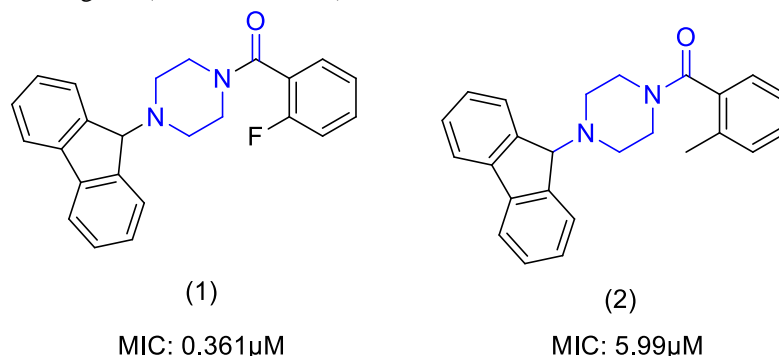
3.3 Pharmacological screening- Anti-mycobacterial assay

The antimycobacterial activity of all the synthesized compounds were assessed *in vitro* against *Mycobacterium tuberculosis H37Rv* strain. The values of the minimum inhibitory concentration (MIC) were measured using the serial dilution procedure with microplate alamar blue assay (MABA) method. To prevent medium evaporation during incubation in the test wells, 200 μL of sterile deionized water was applied to all sterile 96 wells plate outside perimeter wells. The 96 well plate was made entirely of Middle brook 7H9 broth, and successive dilutions of substances were taken primarily on the plate. The reference standard antitubercular drugs' and synthesized compounds' final concentrations ranged from 100 to 0.2 $\mu\text{g/mL}$. Plates were coated with parafilm and sealed before being incubated at 37°C for five days. Between 80 and 24 hours of incubation, 25 μL of freshly made 1:1 mixture of alamar blue reagent and 10% of alamar blue reagent were added. A blue colour meant there was no bacterial growth in the well, whereas a pink colour meant there was. The MIC is defined as the lowest medication concentration that prevents the colour change from pink to blue.

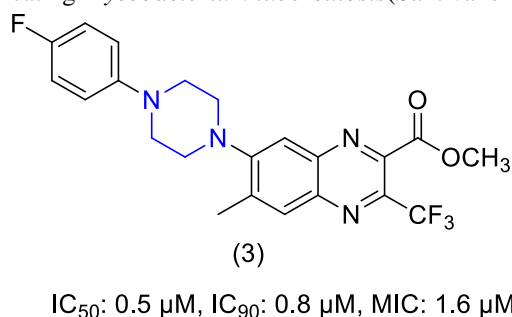
4. Literature Review

Many nitrogen containing heterocycles have been found important in drug design. Amongst them, piperazine has attracted interest in medicinal chemistry because of its extensive pharmacological action. Piperazine skeleton has been very well acknowledged as a useful pharmacophore against mycobacterial infections (Singh et al., 2019). Many researchers have designed and tested numerous piperazine-containing analogues for their anti-TB activity the pursuit of discovering novel anti-TB hybrids. Some of them have been described below.

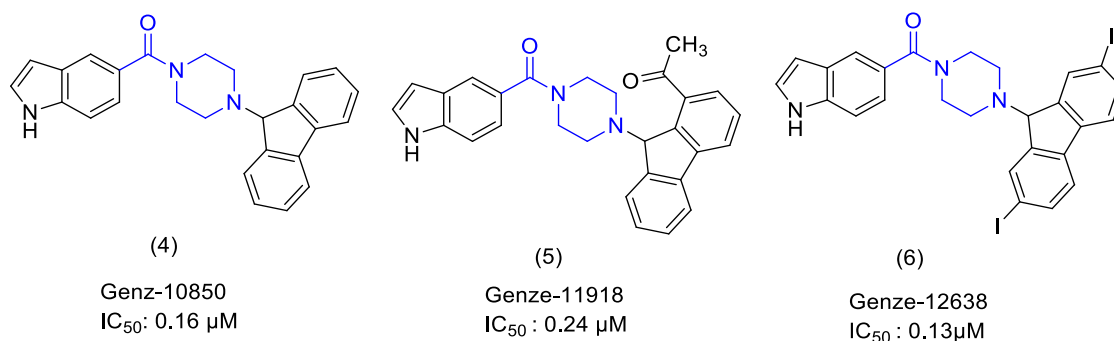
Mariane Rotta *et al.*, synthesized and perform the SAR studies for the 9*H*-fluoren-9-yl-piperazine containing compounds interact with *M. tuberculosis* InhA at the enoyl thioester (2-*trans*-dodecenoyl-CoA) substrate binding site (Rotta et al., 2015).



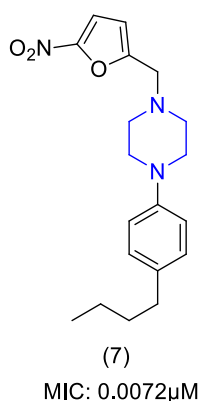
Mery Santivanez *et al.*, design and synthesized novel quinoxaline derivatives among which 5 compound shows MIC value < 3.1 μM and IC_{50} values < 1.5 μM in primarily screening. In addition, compound 3 was potent against non-replicating *Mycobacterium tuberculosis* (Santivañez-Veliz et al., 2016).



Mack R. Kuo *et al.*, synthesized Genz-10850, Genze-11918, Genze-12638 shows potent anti-tubercular activity against mycobacterium species (Kuo et al., 2003).



Yempalla K Reddy *et al.*, performed the in-vitro studies on nitrofuranyl methyl piperazine as new anti-TB agents. Based on overall in vitro profiles, compound 7 was found to have comparatively better solubility than other tested and acceptable pharmacokinetic properties with MIC value 0.0072 μM (Yempalla *et al.*, 2015).



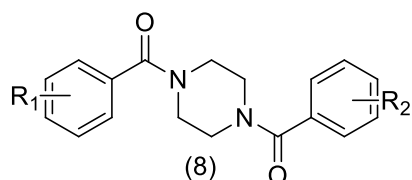
5. Analysis and Findings or Results and Discussion

5.1 Computational study

5.1.1 Structure-based virtual screening

Molecular docking is a part of the structure-based drug design approach conveying knowledge of receptor-ligand complex with respect to binding affinity and binding mode. The 2,00,000 ligands from Enamine Hit Locator library were subjected for molecular docking based virtual screening using Glide module of Schrodinger. After virtual screening, piperazine-arylamide scaffold was found interacting with the active site residues of InhA. As per the literature search also, it has been found that piperazine-arylamide related molecules have been reported as direct InhA inhibitors. So, this scaffold has been selected as a hit and the different substitutions of aryl ring have been explored to achieve the better fitting in the binding pocket of enzyme. The best scored molecules have been discussed in the table 1. The receptor-ligand interaction of compound 1 and co-crystal ligand with the active site of InhA has been shown in figure 2.

Compound 1 to 4 exhibited better docking score and ligand efficiency when it was compared with co-crystal ligand. Compound 1 showed -12.087 kcal/mol docking score. One of the keto groups of piperazine-arylamide showed hydrogen bonding with active site amino acid Tyr158. The similar kind of hydrogen bond was observed between keto of pyrrolidinone of cocrystal ligand and Tyr158. Sulphonamide group of Compound 1 exhibited hydrogen bonding with Gly96 residue. Apart from this, the compound 1 also showed the hydrophobic interactions with Phe97, Met98, Thr196, Ala198, and Met199. It has been noticed that the compound was not showing any interaction with NAD.



Common structure of piperazine-arylamides

Table: 1 Docking score of top 4 compounds

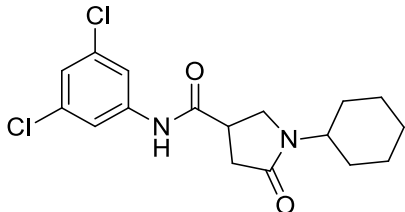
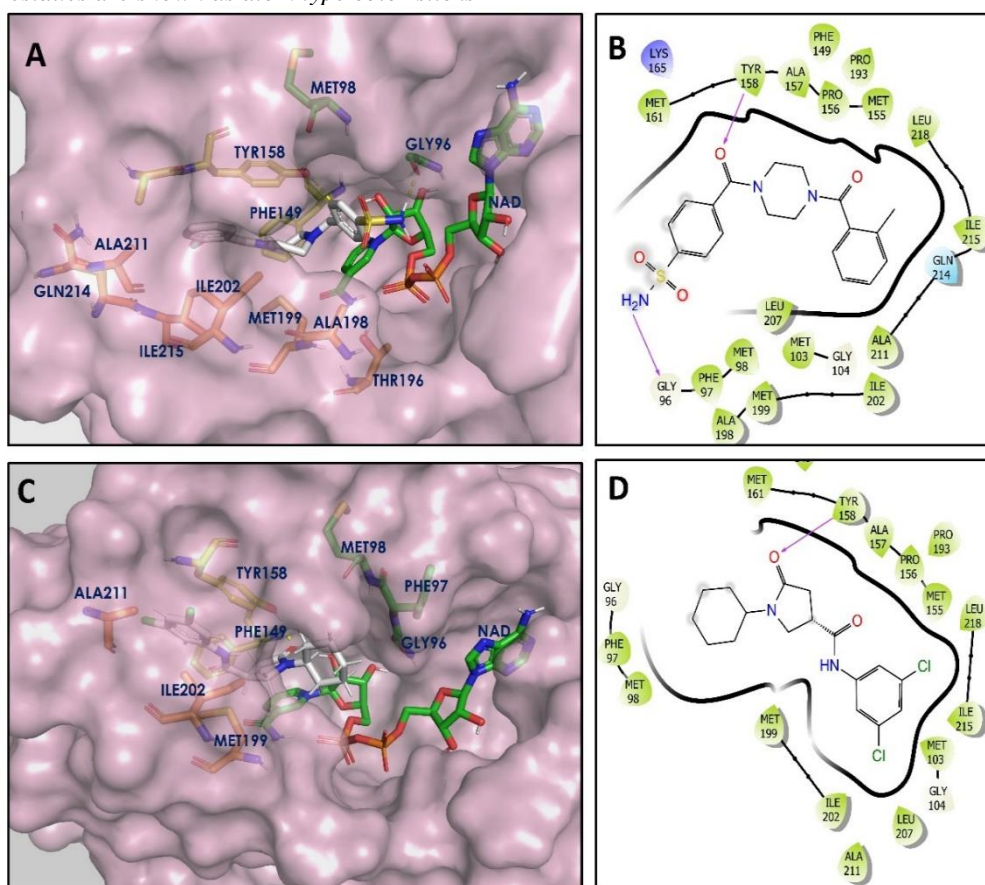
Comp. No.	R ₁	R ₂	Docking score (kcal/mol)	Ligand efficiency	Interacting amino acid residues
8a	-2-Me	-SO ₂ NH ₂	-12.087	-0.455	Tyr158, Gly96
8b	-H	-SO ₂ NH ₂	-11.841	-0.446	Tyr158, Gly96
8c	-4-Me	-SO ₂ NH ₂	-11.171	-0.414	Tyr158, Gly96
8d	-4-Me	-NHMe	-10.654	-0.426	Tyr158, Gly96
Co-crystal ligand			-10.021	-0.402	Tyr158

Figure 2 Docking interactions of compound 1 and co-crystal ligand of PDB: 4TZK with InhA. A and C: 3D-Binding mode of compound 8a and co-crystal ligand respectively. B and D: 2D-Binding mode of compound 8a and co-crystal ligand respectively. Ligands are shown as gray sticks, InhA residues are shown as atom type color sticks



5.1.2 Physicochemical and pharmacokinetic parameter prediction

Modern drug research places a strong emphasis on physicochemical property optimization in order to balance activity and efficacy while minimizing the side effects. The most “druglike” molecules should have $\text{LogP} \leq 5$, molecular weight ≤ 500 , number of hydrogen bond acceptors ≤ 10 , and number of hydrogen bond donors ≤ 5 according to Lipinski (Lipinski et al., 1997). Topological polar surface area (TPSA) and a number of rotatable bonds are the other two parameters introduced by Veber and co-

workers (Veber et al., 2002). All the designed compounds obey the rules of Lipinski and Veber, as shown in Table 2.

Table: 2 Physicochemical parameters of compound 8a to 8d^a

Comp. No.	MW	LogP	HBD	HBA	TPSA	NRB
8a	387.46	1.24	2	10	121.26	4
8b	373.43	0.93	2	10	123.87	4
8c	387.46	1.22	2	10	121.26	4
8d	337.42	3.13	1	7	72.01	3

^aMW, molecular weight; HBA, hydrogen-bond acceptor atoms; HBD, hydrogen-bond donor atoms; LogP, predicted oil/water partition coefficient; TPSA, polar surface area; NRB, number of rotatable bonds

The prediction of pharmacokinetic indicators for compounds 1 to 4 has been shown in Table 3. QPlogHERG gives the predicted value for blockage of HERG K⁺ channels, an indicator for cardiotoxicity. It should be above -5. QPlogBB is the predicted brain/blood barrier coefficient. QPPCaco is the indicator for oral absorption of molecules. It estimates the alleged gut-blood barrier permeability. A value less than 25 predicts poor oral absorption. All the compounds exhibited better oral absorption which can also be explained by percentage human oral absorption values of the compounds. QPlogKhsa shows the predicted binding affinity of compounds with human serum albumin. All the designed compounds displayed the values of the abovementioned pharmacokinetic parameters in the desired range.

Table: 3 Pharmacokinetic parameters of compound 8a to 8d^b

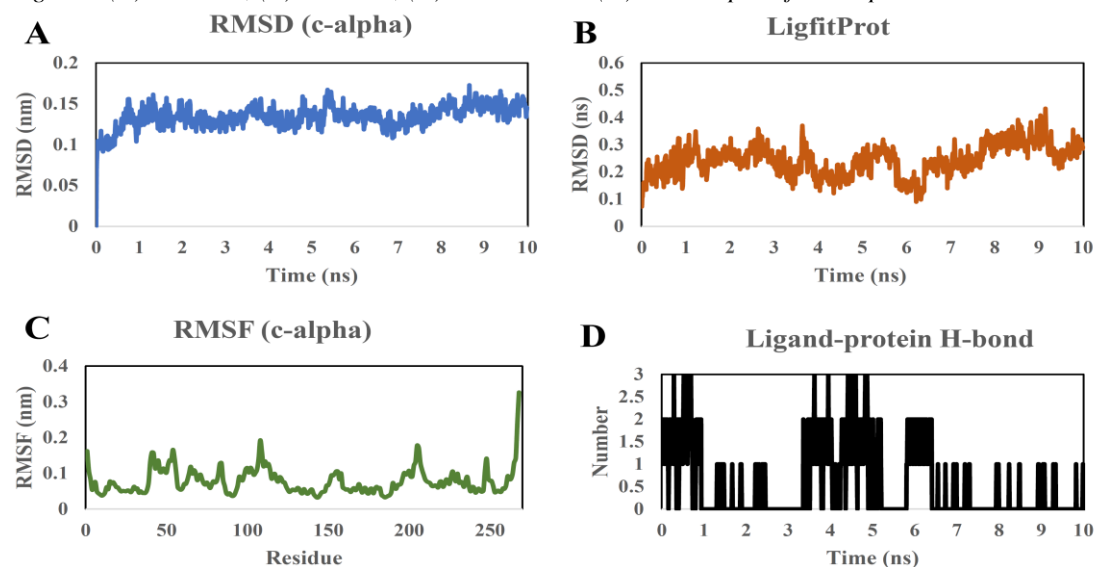
Comp. No.	QPlogHERG	QPPCaco	QPlogBB	CYP3A4 inhibitor	QPlogKhsa	%Human oral absorption
8a	-5.80	946.79	-1.8	No	-0.12	88.7
8b	-6.03	803.18	-1.9	No	-0.17	85.2
8c	-5.95	804.40	-1.9	No	-0.11	87.6
8d	-5.92	1070.89	-0.6	No	0.224	100

^bQPlogHERG, Predicted IC₅₀ value for blockage of HERG K⁺ channels; QPPCaco, caco-2 cell permeability; QPlogBB, brain/blood partition coefficient; QPlogKhsa, prediction of binding to human serum albumin

5.1.3 Molecular dynamic study

The molecular dynamic study of best scored compound 8a was performed and statistical parameters have been derived to assess its stability with InhA protein over a period of time.

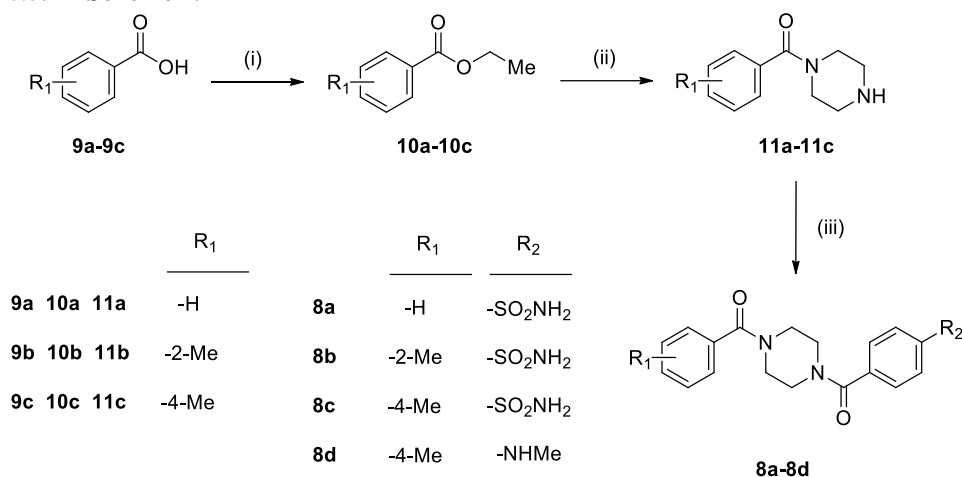
Figure 3 (A) RMSD-P, (B) RMSD-L, (C) RMSF-P and (D) H-bond plots for compound 8a with InhA



The protein RMSD-P was analysed to understand the extent of movement of protein or atoms while putting the ligand in the active site and offering the structural stability, deviation, and conformations of the protein over the simulation time. The RMSD-P for InhA in complexation with compound 8a was in the range of 0.17 - 0.09 with an average of 0.13 nm (Figure 3A). This signifies the stability of the protein while having compound 8a in the active site of InhA over this simulation time. RMSD-L value was in the range of 0.43 - 0.07 with an average of 0.24 nm implies the protein-ligand stability without a major change in orientation of the ligand in the active site over a period of simulation time. (Figure 3B). RMSF value describes the residual mobility and integrity of the structure. The observed RMSF-P for the residues up to 260 was below 0.34 nm, whereas the protein tail beyond residue number 260 displayed a greater fluctuation (Figure 3C). Hydrogen bonds between the ligand and protein over the period of the simulation were determined with Gromacs g_hbond utility. A maximum of three hydrogen bonds were observed between ligand and protein during MD simulation, whereas one hydrogen bond was observed consistently throughout the simulation time (Figure 3D). The average value of observed short-range electrostatic energy (Coul-SR) is -22.5188 ± 3.9 kJ/mol, and van der Waals/hydrophobic energy (LJ-SR) is -156.534 ± 2.1 kJ/mol. These values propose that the hydrophobic interactions have more contribution in stabilizing the complex than the electrostatic interactions.

5.2 Chemistry

The designed piperazine arylamide derivatives (**8a-d**) were synthesized from substituted benzoic acids as depicted in **Scheme 1**.



Scheme 1. General synthetic route for the synthesis of designed compounds (**8a-8d**); Reagents and conditions: (i) H₂SO₄, ethanol, reflux; (ii) anhydrous piperazine, 110 °C; (iii) ArNH₂, HATU, DIPEA, DMF.

The whole procedure is comprised of three synthetic steps. In the first step, the substituted benzoic acids were first converted to respective ethyl esters by Fischer esterification method. The obtained ethyl esters of benzoic acids were pure enough and were used in the next step without further purification. These ethyl esters of substituted benzoic acid, in presence of 5 equivalent of anhydrous piperazine were heated to 110 °C for 10-12 h to obtain the desired mono-substituted piperazines. During the last step, the reaction of mono-substituted piperazines with substituted benzoic acid was carried out by HATU as coupling agent, DIPEA as a base and DMF as a solvent. All the synthesized compounds were purified and confirmed by IR, Mass and ¹H-NMR spectroscopy.

5.3 Pharmacological screening

All the synthesized compounds were investigated for anti-mycobacterial activity using the Microplate Alamar Blue Assay (MABA). This technology is a non-toxic, high-performance assay and low-cost method that uses a thermally stable reagent and is very compatible with the radiometric proportion test and BACTEC. This method utilizes a resazurin dye (a dark blue dye and non-fluorescent). The Tubercule bacilli are used to convert resazurin to resorufin which is of blue colour. The minimum inhibitory concentrations (MICs) of the compounds found by *in vitro* antitubercular assay have been shown in Table 1 and the results have also been compared with the standard drugs- Isoniazid, Ethambutol, Pyrazinamide, Rifampicin and streptomycin.

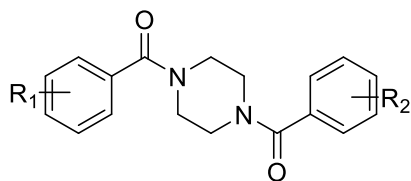


Table: 1 *In vitro* Antimycobacterial activity of compounds

Comp. No.	R ₁	R ₂	MIC (µg/mL)
8a	-H	-SO ₂ NH ₂	1.6
8b	-2-Me	-SO ₂ NH ₂	3.12
8c	-4-Me	-SO ₂ NH ₂	1.6
8d	-4-Me	-NHMe	1.6
Isoniazid	-	-	1.6
Ethambutol	-	-	1.6
Pyrazinamide	-	-	3.12
Rifampicin	-	-	0.8
Streptomycin	-	-	0.8

Compound 8a, 8c, and 8d were found to be most potent molecule amongst the synthesized compounds, with MIC value 1.6 µg/ml, which is same as Isoniazid and Ethambutol. Compound 8b was found to be less potent with MIC value 3.12 µg/ml, which is comparable with Pyrazinamide.

6. Conclusion

The modern drug discovery paradigm has been more bent towards rational drug design rather than traditional drug design in pursuit of viable drug candidates with potent activity, desirable pharmacokinetic and pharmacodynamic characteristics. One of such approaches, structure-based virtual screening was used to identify novel piperazine-arylamide scaffold as anti-TB agent. The drug-likeness features of discovered hits were confirmed using the Lipinski's Ro5 and ADMET parameter calculations. Molecular dynamic simulation studies using appropriate statistical descriptors indicated the stability of the best hit with their docked complex. The best 4 compounds (8a-8d) were synthesized and evaluated using *in vitro* MABA assay. The compounds 8a, 8c and 8c showed MIC 1.6µg/mL which is similar to isoniazid. Thus, such piperazine-arylamide analogues can be potential hits in antitubercular drug discovery.

7. References

- Fathi, M. A. A., Abd El-Hafeez, A. A., Abdelhamid, D., Abbas, S. H., Montano, M. M., & Abdel-Aziz, M. (2019). 1,3,4-oxadiazole/chalcone hybrids: Design, synthesis, and inhibition of leukemia cell growth and EGFR, Src, IL-6 and STAT3 activities. *Bioorganic Chemistry*, 84, 150–163. <https://doi.org/10.1016/j.bioorg.2018.11.032>
- Gavara, L., Sevaille, L., De Luca, F., Mercuri, P., Bebrone, C., Feller, G., Legru, A., Cerboni, G., Tanfoni, S., Baud, D., Cutolo, G., Bestgen, B., Chelini, G., Verdirosa, F., Sannio, F., Pozzi, C., Benvenuti, M., Kwapien, K., Fischer, M., ... Hernandez, J. F. (2020). 4-Amino-1,2,4-triazole-3-thione-derived Schiff bases as metallo-β-lactamase inhibitors. *European Journal of Medicinal Chemistry*, 208. <https://doi.org/10.1016/j.ejmech.2020.112720>
- Girase, P. S., Dhawan, S., Kumar, V., Shinde, S. R., Palkar, M. B., & Karpoornath, R. (2021). An appraisal of anti-mycobacterial activity with structure-activity relationship of piperazine and its analogues: A review. *European Journal of Medicinal Chemistry*, 210. <https://doi.org/10.1016/j.ejmech.2020.112967>
- Gualano, G., Capone, S., Matteelli, A., & Palmieri, F. (2016). New antituberculosis drugs: From clinical trial to programmatic use. *Infectious Disease Reports*, 8(2), 43–49. <https://doi.org/10.4081/idr.2016.6569>
- Jain, S., Sharma, S., Sen, D. J., & Pandya, S. S. (2020). Enoyl-Acyl Carrier Protein Reductase (INHA): A Remarkable Target to Exterminate Tuberculosis. *Anti-Infective Agents*, 19(3), 252–266. <https://doi.org/10.2174/2211352518999201201114426>
- Joseph, J., Dixit, S. R., & Pujar, G. V. (2019). Design , Synthesis and In Vitro Evaluation of Aryl Amides as Potent Inhibitors against Mycobacterium Tuberculosis. *J. Pharm. Sci. & Res.*, 11(9),

- 3166–3173.
7. Kuo, M. R., Morbidoni, H. R., Alland, D., Sneddon, S. F., Gourlie, B. B., Staveski, M. M., Leonard, M., Gregory, J. S., Janjigian, A. D., Yee, C., Musser, J. M., Kreiswirth, B., Iwamoto, H., Perozzo, R., Jacobs, W. R., Sacchettini, J. C., & Fidock, D. A. (2003). Targeting Tuberculosis and Malaria through Inhibition of Enoyl Reductase. *Journal of Biological Chemistry*, 278(23), 20851–20859. <https://doi.org/10.1074/jbc.m211968200>
 8. Lai, L. L., Wang, E., & Luh, B. J. (2001). Reaction of piperazine with trimethylacetic arylcarboxylic anhydride; a convenient method for preparing monoacylated piperazine derivatives. *Synthesis*, 3, 361–363. <https://doi.org/10.1055/s-2001-11425>
 9. Lipinski, C. A., Lombardo, F., Dominy, B. W., & Feeney, P. J. (1997). Experimental and computational approaches to estimate solubility and permeability in drug discovery and development settings. *Advanced Drug Delivery Reviews*, 64(SUPPL.), 4–17. <https://doi.org/10.1016/j.addr.2012.09.019>
 10. Oh, S., Trifonov, L., Yadav, V. D., Barry, C. E., & Boshoff, H. I. (2021). Tuberculosis Drug Discovery: A Decade of Hit Assessment for Defined Targets. *Frontiers in Cellular and Infection Microbiology*, 11. <https://doi.org/10.3389/fcimb.2021.611304>
 11. Prasad, M. S., Bhole, R. P., Khedekar, P. B., & Chikhale, R. V. (2021). Mycobacterium enoyl acyl carrier protein reductase (InhA): A key target for antitubercular drug discovery. *Bioorganic Chemistry*, 115. <https://doi.org/10.1016/j.bioorg.2021.105242>
 12. Qiu, H. Y., Zhu, X., Luo, Y. L., Lin, H. Y., Tang, C. Y., Qi, J. L., Pang, Y. J., Yang, R. W., Lu, G. H., Wang, X. M., & Yang, Y. H. (2017). Identification of new shikonin derivatives as antitumor agents targeting STAT3 SH2 domain. *Scientific Reports*, 7(1). <https://doi.org/10.1038/s41598-017-02671-7>
 13. Rotta, M., Pissinate, K., Villela, A. D., Back, D. F., Timmers, L. F. S. M., Bachega, J. F. R., De Souza, O. N., Santos, D. S., Basso, L. A., & Machado, P. (2015). Piperazine derivatives: Synthesis, inhibition of the Mycobacterium tuberculosis enoyl-acyl carrier protein reductase and SAR studies. *European Journal of Medicinal Chemistry*, 90, 436–447. <https://doi.org/10.1016/j.ejmech.2014.11.034>
 14. Santivañez-Veliz, M., Pérez-Silanes, S., Torres, E., & Moreno-Viguri, E. (2016). Design and synthesis of novel quinoxaline derivatives as potential candidates for treatment of multidrug-resistant and latent tuberculosis. *Bioorganic and Medicinal Chemistry Letters*, 26(9), 2188–2193. <https://doi.org/10.1016/j.bmcl.2016.03.066>
 15. Shan, Y., Dong, J., Pan, X., Zhang, L., Zhang, J., Dong, Y., & Wang, M. (2015). Expanding the structural diversity of Bcr-Abl inhibitors: Dibenzoylpiperazine incorporated with 1H-indazol-3-amine. *European Journal of Medicinal Chemistry*, 104, 139–147.
 16. Singh, V., Pacitto, A., Donini, S., Ferraris, D. M., Boros, S., Illyés, E., Szokol, B., Rizzi, M., Blundell, T. L., Ascher, D. B., Pato, J., & Mizrahi, V. (2019). Synthesis and Structure–Activity relationship of 1-(5-isoquinolinesulfonyl)piperazine analogues as inhibitors of Mycobacterium tuberculosis IMPDH. *European Journal of Medicinal Chemistry*, 174, 309–329. <https://doi.org/10.1016/j.ejmech.2019.04.027>
 17. Veber, D. F., Johnson, S. R., Cheng, H. Y., Smith, B. R., Ward, K. W., & Kopple, K. D. (2002). Molecular properties that influence the oral bioavailability of drug candidates. *Journal of Medicinal Chemistry*, 45(12), 2615–2623. <https://doi.org/10.1021/jm020017n>
 18. *World Health Organisation Global tuberculosis report*. (2020).
 19. Yempalla, K. R., Munagala, G., Singh, S., Magotra, A., Kumar, S., Rajput, V. S., Bharate, S. S., Tikoo, M., Singh, G. D., Khan, I. A., Vishwakarma, R. A., & Singh, P. P. (2015). Nitrofuranyl Methyl Piperazines as New Anti-TB Agents: Identification, Validation, Medicinal Chemistry, and PK Studies. *ACS Medicinal Chemistry Letters*, 6(10), 1041–1046. <https://doi.org/10.1021/acsmchemlett.5b00141>

This page Intentionally left Blank

ABSTRACT

SESSION 4 – NOVEL APPROACHES IN
BIOLOGICAL EVALUATION OF
PHARMACEUTICALS & NATURAL
PRODUCTS

PCP389

CURRENT UPDATES IN ANTISENSE THERAPY

AP0384 Dishita Parmar M. Pharm Graduate School of Pharmacy Dishitaparmar54@g mail.com	AP0385 Ravin Malam M. Pharm Graduate School of Pharmacy Ravinmalam786@g mai.com	AP0 Dr. D. M. Patel Associate Professor Graduate School of Pharmacy asso_dmpatel@g u.edu.in	AP0188 Dr. Sanjay Chauhan Director Graduate School of Pharmacy Prof_sanjay_chauhan @gtu.ed.in
---	---	--	---

Abstract:

The antisense concept derives from an understanding of nucleic acid structure and function and depends on Watson–Crick hybridization. A novel and effective method for managing a cell's gene expression is antisense technology. It targets genes at the level of mRNA rather than DNA and stops them from making proteins by using synthetic antisense oligonucleotides. More people are accepting antisense oligonucleotides (ASO) as promising therapies for several ailments. Nine single-stranded antisense oligonucleotide (ASO) medicines with two modes of action, four methods of administration, and four chemical classes have been developed. Antisense medications work more specifically and have the ability to be less harmful and more effective than traditional medications. A fascinating and promising method for treating a variety of disorders is antisense therapy. The present review will provide a current updates and research of the antisense therapy in various neurodegenerative, cancer and neuromuscular disorder.

Keyword: Antisense, oligonucleotide, Influenza, molecular targets, phosphorothioate

PCP391

CHROMATOGRAPHIC FINGERPRINTING AND ASSESSMENT OF ANTIINFLAMMATORY ACTIVITY OF *CUMINUM CYMINUM* AND *ZINGIBER OFFICINALE* EXTRACTS

AP0369

Hirvita Bhatt

Research Scholar

Gujarat Technological University

hirvitabhatter19@gmail.com

AP0386

Dr. Deepti K. Jani

Associate Professor

Gujarat Technological University

deeptikjani@gmail.com

ABSTRACT

Several factors like environmental, procurement, packing, storage etc. are responsible for variations in the amount of phytoconstituents in different plant samples. Hence, pharmacognostic evaluation is also required with pharmacological investigation for proper evaluation of therapeutic effects of herbal extracts. In the present study, aqueous extracts from the fruit of *Cuminum cyminum* and rhizomes of *Zingiber officinale* was evaluated for *in-vitro* anti-oxidant and anti-inflammatory activity. *In-vitro* anti-inflammatory action was evaluated by HRBC membrane stabilization and protein denaturation method. The antioxidant activity of plant extracts was assessed by DPPH radical scavenging and FRAP method. Total phenolic content was determined by using Folin-Ciocalteu method. Pharmacognostic evaluation and Chromatographic fingerprint of selected bioactive constituents cuminaldehyde and 6-gingerol of selected plant was also done. Our results indicated significant anti-inflammatory and anti-oxidant action of selected extracts. Therefore, selected extracts possess potential as anti-inflammatory and anti-oxidant agents.

Keywords: 6-Gingerol, Cuminaldehyde, Chromatographic fingerprints, Anti-inflammatory

1. INTRODUCTION

Inflammation is defense response to tissue injury caused by physical trauma, destructive chemicals, microorganisms and some environmental agents. The objective of inflammation is to destroy or remove the injurious stimuli and initiate the healing process. Various components can contribute and associated with inflammatory reaction, symptoms and injury. At one set of inflammation, mast cells undergo activation and release variety of inflammatory mediators including cytokines, chemokines, histamine, protease, prostaglandins, leukotrienes, serotonin, oxygen and nitrogen derived free radicals. Inflammation regularly progress to Acute and chronically, Acute inflammation's main features are the release of fluid and various plasma proteins and occurs very rapidly. When acute inflammation occurs rapidly and continuously chronic inflammation will take place, this process lasting for several weeks to months and even years which is also known as adaptive immunity^[1,2,3].

Ginger (*Zingiber officinale* Roxb.) belongs to family Zingiberaceae. It is originated in South-East Asia and then used in many countries as a condiment to add flavor to food as a spice. The rhizome part of ginger is used traditionally for the health promoting perspective because of rich source of phytoconstituents. Ginger has a potential activity to treat number of ailments including degenerative disorders like arthritis, rheumatism, digestive problems like constipation, indigestion, ulcers etc., cardiovascular disorders, vomiting, diabetes mellitus and cancer. Cumin (*Cuminum cyminum* Linn.) is an aromatic plant included in Apiaceae/ Umbelliferae family which is used as flavoring agents, added to fragrances and having medicinal properties like astringent, carminative, emmenagogue for the treatment of corneal opacities, ulcers, boils, relieve cough, inflammation and anti-oxidant activity^[4,5,6].

2. OBJECTIVE:

The present research work focus on the In-vitro Anti-inflammatory activity and Anti-oxidant activity of the selected plant aqueous extracts. HRBC membrane stabilization and protein denaturation activity were included for the significance study of Anti-inflammatory by In-vitro method. Further that research work included for the quantitative estimation of various phytochemical analysis and the HPTLC and HPLC chromatographic technique.

3. MATERIAL AND METHODS

The rhizomes of *Zingiber officinale* Roxb. and fruit of *cuminum cyminum* Linn. both were collected from the Local market of Baroda, Gujarat, India. Identification of the ginger and cumin were authenticated at the Department of Botany, The Maharaja Sayajirao University of Baroda, and a voucher specimen has been submitted in the departmental herbarium. The phytochemical screening of both the plant was performed with use of chemical reagents and other solvents were purchased as a laboratory grade. For chromatographic techniques all the solvents used were of chromatographic grade and other chemicals were of analytical reagent grade.

3.1 Extraction Method and Preparation of Plant Extracts

Ginger rhizome and Cumin fruits were dried in the shade and then pulverized to attain the powder. The 100 gm of dried powder of ginger rhizome and cumin fruit were extracted with distilled water through Soxhlet apparatus technique. Dried extract of both plant collect individually and packed in separate bottle and placed extract bottles were store in desiccator for further investigation of the phytochemical screening and analytical research work.

3.2 Estimation of Secondary Metabolites

3.2.1 Determination of total phenolics content ^[7]

The concentration of phenolics in plant extracts was determined using Spectrophotometric method. Folin-Ciocalteu assay method was used for the determination of the total phenol content ^[7]. 10 mg/ml stock solutions of plant extracts were prepared. The reaction mixture consists of 1 ml or 0.5 ml of extract and 9 ml of distilled water was taken in a volumetric flask (25 ml). One milliliter of Folin-Ciocalteu phenol reagent was treated to the mixture and shaken well. After 5 minutes, 10 ml of 7 % Sodium carbonate (Na_2CO_3) solution was treated to the mixture. The volume was made up to 25 ml. A set of standard solutions of Gallic acid (20, 40, 40, 60, 80 and 100 $\mu\text{g}/\text{ml}$) were prepared in the same manner as described earlier. Incubated for 90 min at room temperature and the absorbance for test and standard solutions were determined against the reagent blank at 550 nm with an Ultraviolet (UV) /Visible spectrophotometer. Percentages of total phenolics of all plant extracts were calculated.

3.2.2 Determination of total tannins content ^[8]

The concentration of total tannins in plant extracts was determined by titrimetric method. Preparation of plant extracts infusion: accurately weighed 0.5 g of plant extracts and add 25ml of water to make infusion. Preparation of Indigo carmine: 6 g of Indigo carmine was dissolved in 500 ml of distilled deionized water by heating, after cooling 50 ml of 95-97% H_2SO_4 was added and the solution was diluted to 1000 ml and then filtered. Take 25ml of plant extracts infusion into 1 liter of conical flask, and then 25 ml of indigo carmine solution and 750 ml of distilled deionized water were added. These solutions titrated against 0.1 N aqueous solution of KMnO_4 until blue colored solution changes to green colour. Few drops added until solution becomes golden yellow. The blank determination was carried out. Calculated percentage of total tannins by using following formula:

$$T(\%) = (V - V_0) * 0.004157 * 250 * 100 \\ \text{g} * 25$$

Where,

V - Volume of 0.1 N aqueous solution of KMnO₄ for titration of sample (ml)

V₀ - Volume of 0.1 N aqueous solution of KMnO₄ for the titration of blank sample

0.004157 – tannins equivalent in 1 ml of 0.1 N aqueous solution of KMnO₄

g- Mass of the sample taken for the analysis

250- Volume of the volumetric flask (ml)

100 – Percentage (%)

25 – Volume of plant extracts infusion

3.2.3 Determination of total flavonoid content ^[7]

Total flavonoid content was measured by the aluminium chloride colorimetric assay. Aluminum chloride forms stable complexes with C-4 keto group and either the C-3 or C-5 hydroxyl group of flavones and flavonols that estimate in aqueous extracts by uv-spectroscopy method. 10 mg/ml stock solutions of plant extracts were prepared. The reaction mixture consists of 0.5 ml or 0.3 ml of extract and 4 ml of distilled water was taken in a 10 ml volumetric flask. To the flask, 0.30 ml of 5 % sodium nitrite was treated and after 5 minutes, 0.3 ml of 10 % aluminium chloride was mixed. After 5 minutes, 2 ml of 1M Sodium hydroxide was treated and diluted to 10 ml with distilled water. A set of reference standard solutions of Quercetin (20, 40, 60, 80 and 100 µg/ml) were prepared in the same manner as described earlier. The absorbance for test and standard solutions were determined against the reagent blank at 510 nm with an UV/Visible spectrophotometer. Percentages of total flavonoid content of all plant extracts were calculated.

3.3 Chromatography Techniques

3.3.1 High Performance Thin Layer Chromatography ^[9]

3.3.1.1 Sample preparation

Aqueous extract of *Zingiber officinale* and *cuminum cyminum* were prepared individually, from that a concentration of 10mg/ml of both the sample extracts were prepared in methanol respectively and the solutions were filtered through Whatman filter paper No. 1 and filtrates were used for analysis. Diethyl ether, Toluene, Ethyl acetate, Methanol chemical solvents used were of Analytical grade (Renkem).

3.3.1.2 Chromatographic conditions:

Samples were spotted in the form of bands of width 6mm on Pre-coated Silica gel 60 F254 aluminum plates for HPTLC technique were procured from Merck using Camag linomat V. For determination of aqueous extract of ginger the mobile phase was Toluene: Ethyl acetate: Diethyl ether (3.0: 6.0: 1.0) and for cumin aqueous extract mobile phase Toluene: Ethyl acetate: Methanol (7.5: 2: 0.5) was used. Automated TLC sampler applicator Linomat V with nitrogen as inert gas is used as sample applicator. Hamilton 100 µl HPTLC syringe was used for sample application. Linear ascending development was carried out in twin trough (20 × 20 cm) saturated glass chamber. The optimized chamber saturation time was 45 minutes at room temperature. Length of chromatogram run was 80 mm. Densitometry scanning was performed using Camag TLC scanner 3 in absorbance mode at 254nm UV light.

3.3.2 High Performance Liquid Chromatography ^[10]

3.3.2.1 Sample preparation

Aqueous extract of *Zingiber officinale* and *Cuminum cyminum* were prepared individually, from that a concentration of 10mg/ml of both the sample extracts were prepared in methanol respectively and the solutions were filtered through Whatman filter paper No. 1 and filtrates were used for analysis. Acetonitrile, Methanol solvents used were of HPLC grade (Renkem). Mono potassium dihydrogen phosphate and Ortho-Phosphoric acid of Analytical reagent grade were used. Double distilled water was used throughout the study. All the reagents were filtered through 0.2 µm Ultipor® Nylon 66 membrane filter.

3.3.2 Chromatographic conditions:

HPLC system consisting of Shimadzu LC 20-A Prominence Controller with Pump LC-20AD, System controller SBM20Alite and UV/VIS Detector SPD-20A was used. C18G column (Dimensions: 5µm, 250× 4.6 mm) was used as stationary phase at ambient temperature. Rheodyne fixed loop injector of 20 µl is used for sample injection. For determination of aqueous extract of ginger the mobile phase was Acetonitrile: water (55:45) and Acetonitrile: Methanol: Phosphate buffer pH 2.88 in ratio of (55:01:44) and for cumin aqueous extract mobile phase Acetonitrile: Methanol: Phosphate buffer pH 2.88 in ratio of (25:45:30) was used. Sonication time of mobile phase was 10 min. Column saturation time should be 40 minutes. Flow rate of mobile phase was 1ml/min and pressure should be maintaining 126 kgf at ambient temperature. Detection wavelength of ginger extract was 282 nm and for cumin 205 nm with UV 254 nm and 365 nm.

3.4 Anti-Oxidant Activity

3.4.1 DPPH Free Radical Scavenging Activity ^[11]

The antioxidant activities were determined as the measure of radical scavenging using DPPH assay. Free radical scavenging potential of the extracts were tested against a methanol solution of a α, α Diphenyl- β Picryl Hydrazyl (DPPH). Antioxidants react with DPPH and convert it to α, α Diphenyl- β Picryl Hydrazine. The degree of discoloration indicates scavenging potentials of the antioxidant.

3.4.1.1 Preparation of Standard and Sample solution

Required quantity of ascorbic acid was dissolved in methanol to give the concentration of 100,200,400,600,800 and 1000 µg/ml. The individual test samples aqueous extract of ginger and cumin were dissolved in methanol to give stock solution of 1000µg/ml. Test samples were prepared by proper dilution of the stock solution with methanol to give a series of 100, 200, 300, 400, 500, 600, 800 and 1000 µg/ml.

3.4.1.2 Estimation of DPPH free radical scavenging activity

DPPH was prepared in methanol having concentration of 1.3 mg/ml. It was protected from light by covering the test tube with aluminum foil. 75 µl DPPH solution was added to 3 ml methanol and the absorbance was taken immediately at 516 nm for control reading. Different concentrations of standard and test samples were diluted with methanol up to and 75 µl of DPPH was added. The absorbance was taken immediately after addition of DPPH solution at 516 nm using methanol as a blank at zero minute. Decrease in absorbance in presence of test samples at different concentration was noted after 10, 20 and 30 min.

The % reduction was calculated as follows

$$\text{Percentage (\%)} \text{ Antioxidant activity} = \frac{\text{Control absorbance} - \text{Sample absorbance}}{\text{Control absorbance}} \times 100$$

3.5 FRAP (ferric reducing antioxidant power) assay ^[11]

3.5.1 Chemicals and reagents

Phosphate buffer was prepared according to I.P.1996. 10% Trichloro acetic acid, 1% Potassium ferricyanide solution and 0.1% ferric chloride solution prepared using laboratory grade solvents.

3.5.2 Preparation of standard solution

Ascorbic acid (10 mg) was dissolved in 10 ml distilled water. Proper dilutions were made with distilled water to get 10, 20, 40, 60, 80 and 100 µg/ml solutions. Aqueous extract of ginger and cumin were dissolved in sufficient quantity of methanol to give stock solution of 10mg/ml.

Stock solution was further diluted with phosphate buffer to give concentration of 20, 40, 60, 80, 100, 200 and 400 µg/ml.

3.5.3 Estimation for reducing power by FeCl₃

2 ml of each sample and standard solutions were spiked with 2.5 ml of 1 % potassium ferricyanide solution. This mixture was kept at 50 °C in water bath for 20 min. After cooling, added with 2.5 ml of 10 % trichloro acetic acid, centrifuged at 3000 rpm for 10 min. 2.5 ml of supernatant was mixed with 2.5 ml of distilled water and 1 ml of 0.1 % ferric chloride and kept for 10 min. Control was prepared in similar manner excluding samples. The absorbance of resulting solution was measured at 700 nm and those of samples were compared with standard solution.

3.6 In-vitro Anti-Inflammatory Activity

3.6.1 HRBC Membrane Stabilization Method ^[4,12]

The HRBC membrane stabilization method was performed. In the HRBC suspension, the content of hemoglobin was adjudged by using ultraviolet-visible (UV) spectrophotometer at 570 nm.

3.6.1.1 HRBC Suspension Preparation

The fresh blood was collected from human's volunteers for the experiment which mixed with the sterilized Alsever solution. Alsever solution was prepared by adding 2% dextrose, 0.85% sodium citrate, 0.06% citric acid, and 0.44% sodium chloride in water. The centrifugation of blood was done at 3000 rpm for 10 minutes, and sediment cells obtained after centrifugation were washed three times with isosaline solution having pH 7.2. The blood volume was measured and having been formed again as a 10% v/v suspension with isosaline solution.

3.6.1.2 Herbal Sample Preparation

Ginger and Cumin aqueous extract 25 µg was taken and dissolved in 10 mL of methanol, and after that, this is boiled for 10 minutes and cooled. After that, it was centrifuged for 10 minutes at 2,500 rpm, and after the centrifugation, the supernatant was collected and used for further study.

The assay mixture contained the secondary metabolite from the plant extract, 1 mL phosphate buffer (0.15 M, pH 7.4), 2 mL hyposaline (0.36%), and 0.5 mL HRBC suspension. Diclofenac was used as a reference drug. Instead of the hyposaline, 2 mL distilled water was used as the control. The assay mixtures were incubated at 37 °C for 30 min and centrifuged at 3000 rpm for 25 minutes. In the supernatant solution, the hemoglobin content in the supernatant was estimated using a UV-Visible spectrophotometer at 560 nm. Diclofenac sodium (25 µg/10 mL) was used as a reference standard, and control was prepared by excluding the drug samples. The percentage inhibition of hemolysis or membrane stabilization was calculated according to the modified method

The formula used for the calculation of % hemolysis of HRBC membrane is given below:

$$\text{Percentage of hemolysis} = (\text{Test sample's optical density} / \text{Control sample's optical density}) \times 100$$

The formula used for the calculation of % protection of HRBC membrane is given below:

$$\text{Percentage of protection} = 100 - (\text{Test sample's optical density} / \text{Control sample's optical density}) \times 100$$

3.7 Protein Denaturation Method ^[4,12]

The protein denaturation method was performed using mixture 0.2 mL egg albumin + 2.8 mL phosphate buffer saline pH 6.4 + 2 mL of aqueous extract (Ginger and cumin individually) was incubated at 37 ± 2 °C for 10 minutes and heated at 60 °C for 10 minutes. At 640 nm in the UV spectrophotometer by using a vehicle as blank absorbance is assessed. Distilled water is used

as a control. Diclofenac sodium with a 1 mg/mL concentration was used as a reference standard and prepared the same as a test solution for the measurement of absorbance.

The formula for the calculation of protein denaturation is given below:

Percentage of inhibition = (Absorbance of control - absorbance of sample)/Absorbance of control × 100

3.8 Statistical method:

Data represented as mean ± S. The comparison between standard and test group was done by t test. The P value less the 0.05 considered as significant. Microsoft excel was used for calculations and statistical analysis.

4. LITERATURE REVIEW:

The mechanisms of inflammation involve a series of events in which the metabolism of arachidonic acid plays an important role. It is metabolized by the Cyclooxygenase (COX) pathway to prostaglandins and thromboxane A₂, whereas the 5-lipoxygenase (5-LOX) pathway to eicosanoids and leukotrienes (LT's), which are known to act as chemical mediators in a variety of inflammatory events^[1,2,3]. Ginger possess non volatile pungent compounds are gingerols, shogaols, paradols and zingerone. It has also anti-inflammatory and anti-oxidant properties for controlling aging. Aqueous extract of ginger plant have rich fraction of 6-Gingerol, 8-Gingerol, 10-Gingerol and 6-Shogaol phytoconstituents that fraction have targets various inflammatory and pro-inflammatory mediators like prostaglandins, leukotrienes, histamine, bradykinin, TNF- α etc.; suppression of both cyclooxygenase and lipoxygenase metabolites of arachidonic acid and also inhibited LPS-induced TNF- α , IL- β , IL-6 and PGE₂ production^[4]. The Cumin (*Cuminum cyminum* Linn.) fruit traditionally used in the treatment of toothache, dyspepsia, diarrhoea, epilepsy and jaundice. Cumin contains various monoterpenes compounds such as linalool, γ -terpinene, α -pinene and β -pinene, cuminaldehyde (32.4%), protein, flavonoid glycosides including apigenin-7-glucoside, luteolin-7-glucoside. Aqueous extract of cumin fruit have inhibiting action to release of histamine, serotonin and kinins. Lipoxygenase (LOX) inhibitors leads for developing dual COX-LOX inhibitors as well as LPS-induced inflammatory response via NF- κ B, JNK and ERK pathways^[5,6].

5. RESULTS & ANALYSIS

Table 1: phytochemical screening analysis

Plant Name	% Total Phenolics content	% of Total Tannis	% Total Flavonoids
Aqueous extract of <i>Zingiber officinale</i>	1.892 % w/w	6.6512 % w/w	0.54 % w/w
Aqueous extract of <i>Cuminum cyminum</i>	1.0495 % w/w	9.9768 % w/w	1.565 % w/w

Table 2: HPTLC Chromatographic parameters

Aqueous extract of <i>Zingiber officinale</i>		Aqueous extract of <i>Cuminum cyminum</i>	
Rf Value	Peak area	Rf Value	Peak area
0.38	1324	0.46	520.6
0.72	2009	0.57	374.9
0.82	2712.7	0.73	615.8
0.87	2900.4	0.75	210.2

Figure 1: HPTLC Chromatogram of (a) Aqueous extract of *Zingiber officinale* (b) Aqueous extract of *Cuminum cyminum*

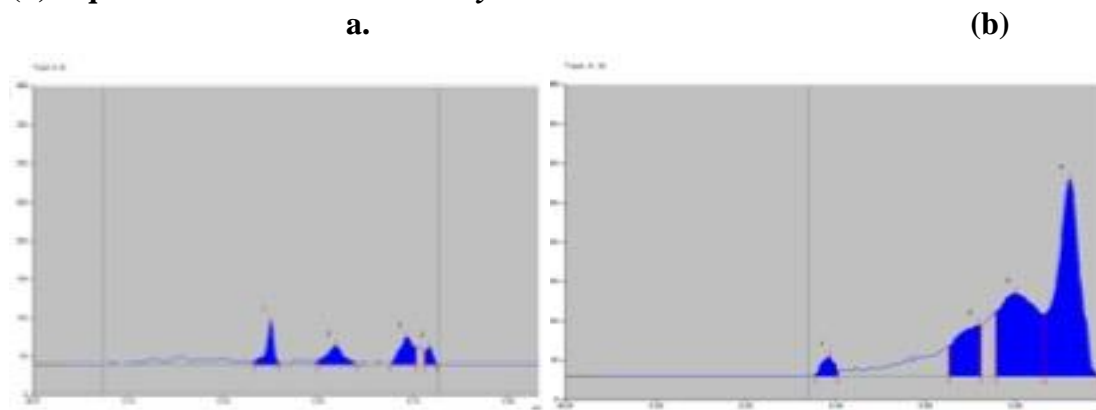


Figure 2: HPTLC Chromatogram of 6-gingerol form *Zingiber officinale* plant

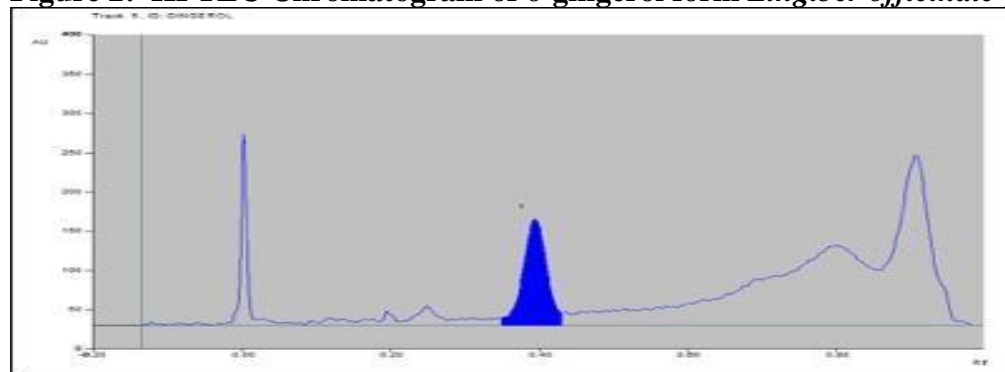


Figure 3: HPTLC Chromatogram of Cuminaldehyde form *Cuminum cyminum* fruit

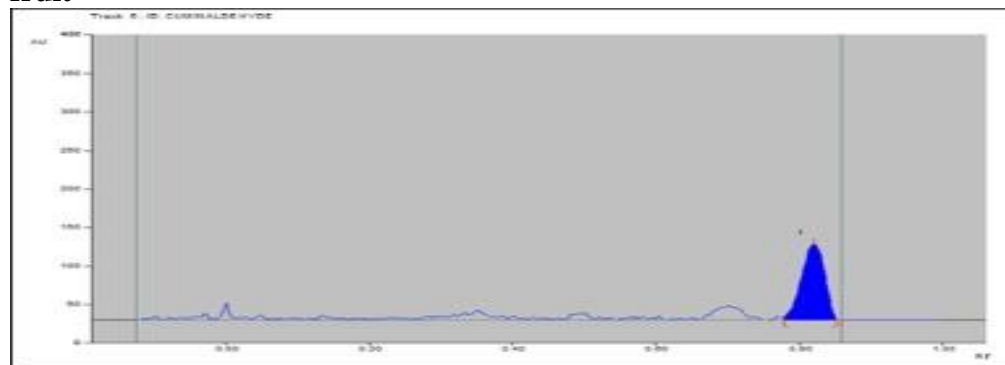


Table 3: HPLC Chromatographic system suitability parameters

System Suitability Parameters	Aqueous extract of <i>Zingiber officinale</i>			Aqueous extract of <i>Cuminum cyminum</i>		
	Rt1	Rt2	Rt3	Rt1	Rt2	Rt3
Retention time	2.8	7.2	9.4	2.82	8.522	11.83
Peak area	368592	299464	208557	388592	575899	375528
Theoretical plates	9875.5	8739.184	11154.554	9875.5	7501.313	6202.948
HETP	15.32	17.164	13.447	15.32	19.997	24.182
Tailing factor	1.025	1.134	0.948	0.987	1.456	1.730

Resolution	5.023	-	6.502	0.03	0.0	6.351
Capacity factor (k')	0.19	0.00	0.299	0.19	0.0	0.367

Figure 4: HPLC Chromatogram of Aqueous extract of *Zingiber officinale*

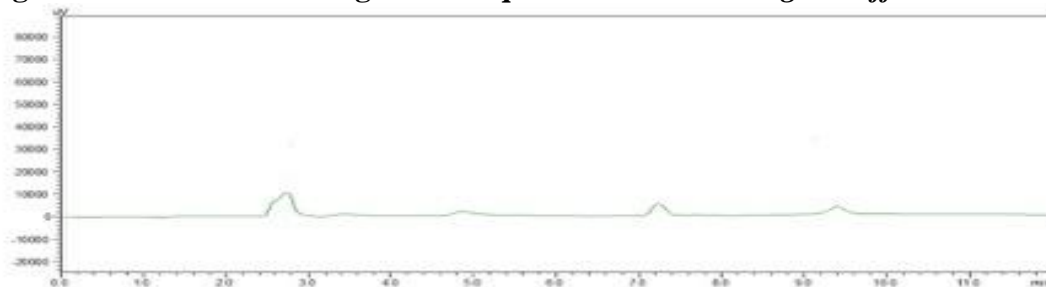


Figure 5: HPLC Chromatogram of Aqueous extract of *Cuminum cyminum*

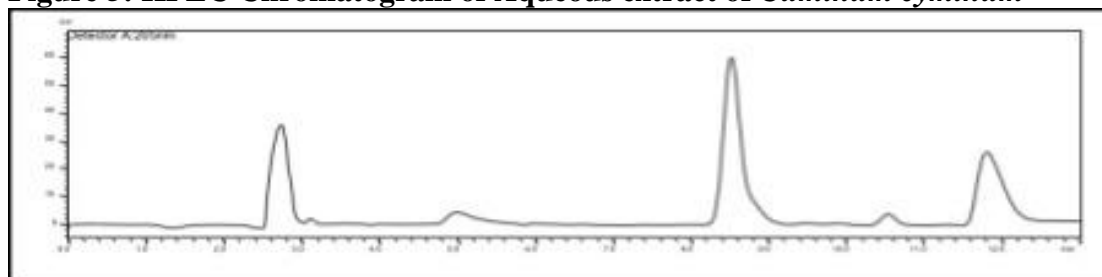


Table 4: Anti-oxidant: DPPH free radical scavenging activity

Ascorbic Acid		Aqueous extract of <i>Zingiber officinale</i>		Aqueous extract of <i>Cuminum cyminum</i>	
Concentration (µg/ml)	% reduction	Concentration (µg/ml)	% reduction	Concentration (µg/ml)	% reduction
10	30.4	50	46.3 ± 5.409	50	23.69 ± 9.411
20	49.35	100	54.9 ± 5.409	100	35.46 ± 9.411
40	54.76	200	60.0 ± 0.001	200	44.35 ± 0.001
60	69.64	300	65.2 ± 0.001	300	55.99 ± 0.001
80	88.78	400	71.6 ± 0.001	400	65.99 ± 0.001
100	91.8	500	80.3 ± 0.001	500	81.55 ± 0.001
EC50 µg	27.84 µg	EC50 µg	209.5 µg	EC50 µg	196.1 µg

Figure 6: Percentage reduction of (a) Ascorbic Acid and (b) Aqueous extracts of *Zingiber officinale* and *Cuminum cyminum*

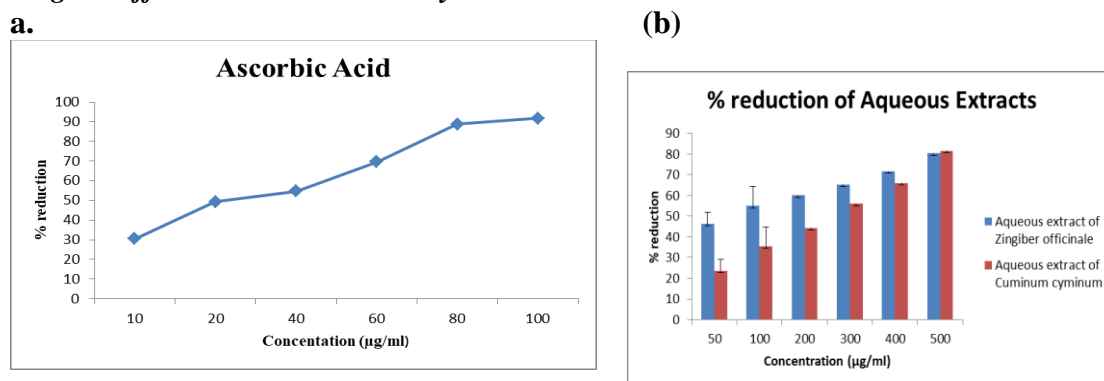


Figure 7: Comparative free radical scavenging activity

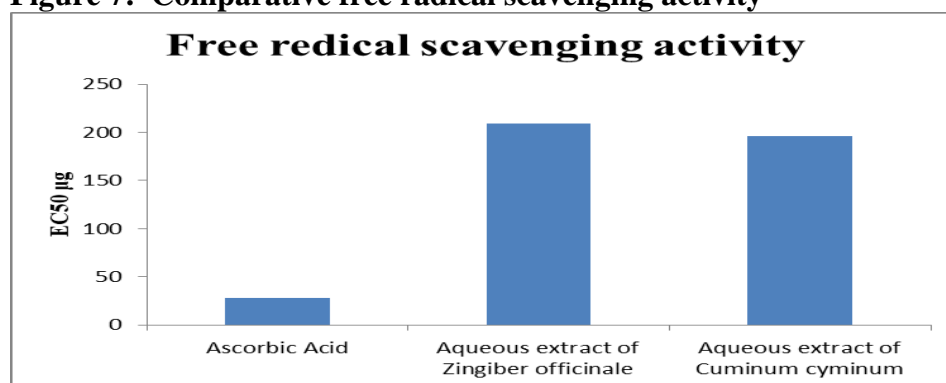


Table 5: Reducing power by FeCl₃

Ascorbic Acid		Aqueous extract of <i>Zingiber officinale</i>		Aqueous extract of <i>Cuminum cyminum</i>	
Concentration (µg/ml)	Absorbance	Concentration (µg/ml)	Absorbance	Concentration (µg/ml)	Absorbance
10	0.361	50	0.268	50	0.246
20	0.483	100	0.358	100	0.381
40	0.731	200	0.509	200	0.603
60	0.916	300	0.706	300	0.731
80	1.156	400	1.196	400	1.034
100	1.43	500	1.218	500	1.323

Figure 8: Anti-oxidant activity through reducing power by FeCl₃, (a) Ascorbic acid (b) Aqueous extract of *Zingiber officinale* and *Cuminum cyminum*

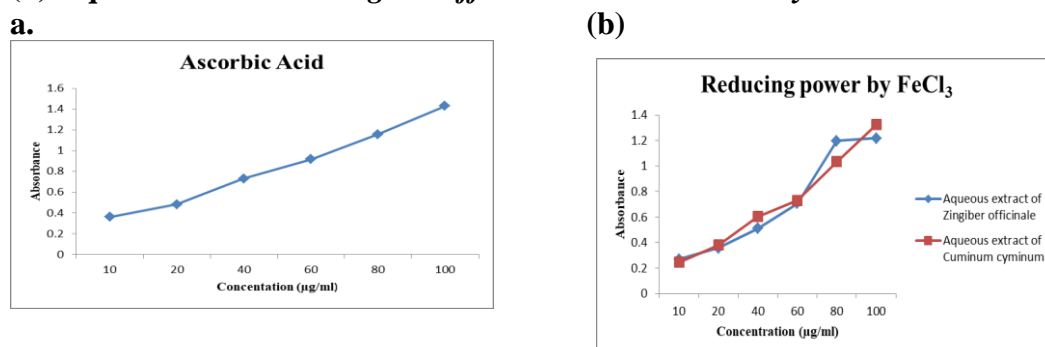


Table: 6 In-vitro Anti-inflammatory activity of Aqueous extracts of *Zingiber officinale* and *Cuminum cyminum* by HRBC membrane hemolysis and membrane protection

Concentration (µg/ml)	% hemolysis of Diclofenac sodium	% protection of Diclofenac sodium	% hemolysis of Aqueous extracts of <i>Zingiber officinale</i>	% protection of Aqueous extracts of <i>Zingiber officinale</i>	% hemolysis of Aqueous extracts of <i>Cuminum cyminum</i>	% protection of Aqueous extracts of <i>Cuminum cyminum</i>
50	71.89 ± 9.30	30.35 ± 9.38	27.98 ± 7.99	72.09 ± 7.81	32.89 ± 8.357	84.36 ± 12.61
100	56.98 ± 9.30	41.92 ± 9.38	38.23 ± 7.99	61.98 ± 7.81	43.29 ± 8.357	75.32 ± 12.61
200	42.94 ± 9.30	57.18 ± 9.38	53.58 ± 7.99	45.98 ± 7.81	59.36 ± 8.357	45.87 ± 12.61
250	35.84 ± 0.01	66.67 ± 0.01	65.36 ± 0.01	35.85 ± 0.01	69.89 ± 0.01	29.54 ± 0.01
500	17.15 ± 0.01	84.12 ± 0.01	70.32 ± 0.01	29.89 ± 0.01	78.36 ± 0.01	19.54 ± 0.01

Figure 9: Percentage Hemolysis by HRBC membrane activity

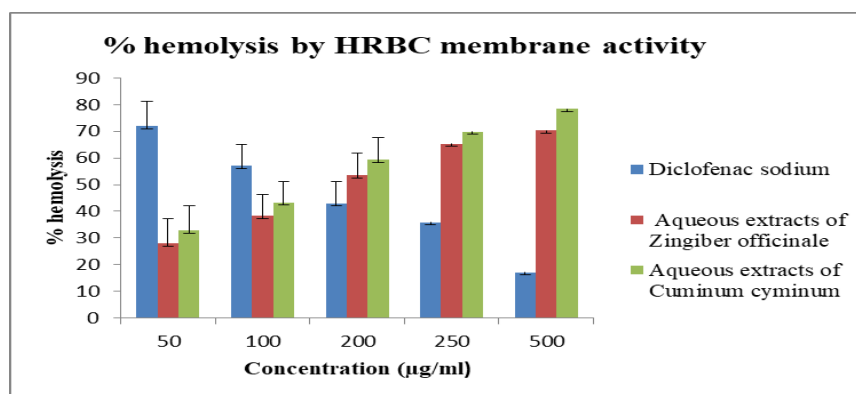


Figure 10: Percentage protection by HRBC membrane activity

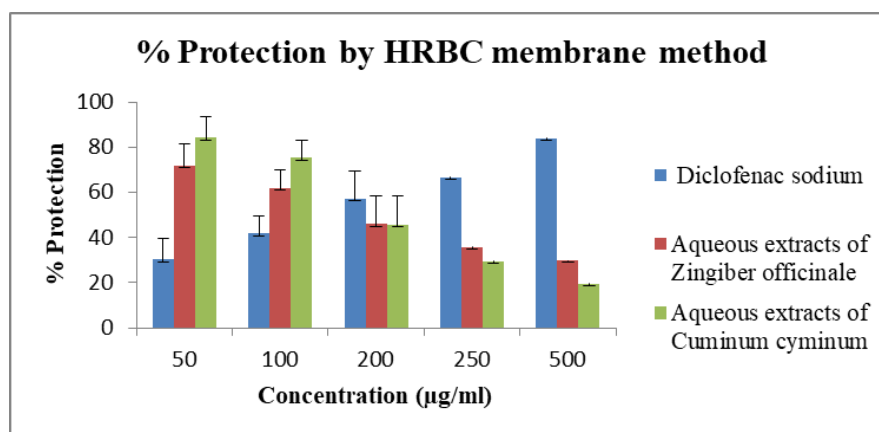
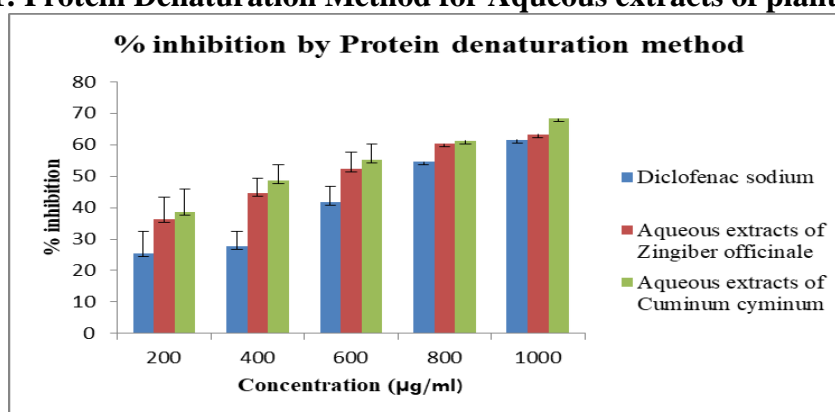


Table 7: In-vitro Anti-inflammatory activity of Aqueous extracts of *Zingiber officinale* and *Cuminum cyminum* by Protein Denaturation Method

Concentration (µg/ml)	% inhibition of Diclofenac sodium	% inhibition of Aqueous extracts of <i>Zingiber officinale</i>	% inhibition of Aqueous extracts of <i>Cuminum cyminum</i>
200	25.28 ± 7.16	36.23 ± 4.99	38.69 ± 5.10
400	27.58 ± 7.16	44.48 ± 4.99	48.56 ± 5.10
600	41.65 ± 7.16	52.41 ± 4.99	55.25 ± 5.10
800	54.56 ± 0.01	60.33 ± 0.01	61.25 ± 0.01
1000	61.56 ± 0.01	63.25 ± 0.01	68.25 ± 0.01

Figure 11: Protein Denaturation Method for Aqueous extracts of plant



6. STATISTICAL ANALYSIS

Estimation of the absorbance data were calculated as linearity. Equation $y = mx + c$ is used and EC50 values are also calculated for the same. All the Statistical analysis data of bar graphs were expressed as means ± standard deviation calculated by standard error mean of measurement. All graphical presentations show the error bars.

7. FINDINGS

For quantitative estimation of various secondary metabolites from aqueous extract of *Zingiber officinale* and *Cuminum cyminum* plants were observed as 1.892 and 1.0495 %w/w as total phenolics contents; 6.6512 and 9.9768 %w/w of total tannins and 0.54 and 1.565 %w/w of total flavonoids contents respectively. Aqueous extract of *Zingiber officinale* shows 0.38, 0.72, 0.82, 0.87 Rf value by performing HPTLC analysis and specific phytoconstituent 6-gingerol Rf value 0.44 was found thorough using densitometry analysis. By HPTLC analysis *Cuminum cyminum* aqueous extracts observed 0.46, 0.57, 0.73, 0.75 Rf value and Cuminaldehyde chief volatile oil have 0.87 Rf value by densitometry analysis. By performing HPLC chromatographic analysis Aqueous extract of ginger and cumin plant were observed 2.8, 7.2, 9.4 and 2.82, 8.522, 11.83 retention time respectively. Both the plant aqueous extract shows 209.5 µg and 196.1µg EC50 value were observed by estimating DPPH free radical scavenging activity. % reduction of Aqueous extracts graph shows the significant Ant-oxidant activity in selected plant. FRAP method were perform and reducing power by FeCl₃ complex determine the anti-oxidant activity in both the extracts. In-vitro Anti-inflammatory activity by HRBC membrane method, % of hemolysis in higher concentration of the aqueous extract of ginger and cumin plant were found to be 70.32 and 78.36 and % protection were observed 29.89 and 19.54 respectively. Percentage inhibition by Protein Denaturation method 63.25 and 68.25 % were found in higher concentration of aqueous extract of ginger and cumin respectively.

8. CONCLUSION

Our results indicated that aqueous extracts of rhizomes of *Zingiber officinale* Roxb. and fruit of *cuminum cyminum* possess both antioxidant and anti-inflammatory action in dose dependent

manner. These anti-inflammatory activities may be due to the occurrence of bioactive compounds, such as polyphenols, flavonoids, tannins etc in the extract. Aqueous extracts of both plant target various inflammatory mediators specifically for the suppression action of cyclooxygenase and lipoxygenase metabolism both the extracts may stabilize lysosomal membranes. Both plants commonly used therefore have potential use as a candidate component in polyherbal formulations for various inflammatory diseases like arthritis, rheumatoid diseases and inflammation associated respiratory disorders.

9. REFERENCES

1. Singh, B. M., Negi, G., Bhole, P., & Jaiprakash, M. (2012). Pain and inflammation: a review. *International Journal of Pharmaceutical Sciences and Research*, 3(12), 4697.
2. Schug, S. A., Daly, H. C., & Stannard, K. J. (2018). Pathophysiology of pain. *Mechanism of vascular disease – NCBI Bookshelf*. A service of the National Library of Medicine, National Institutes of Health
3. Abdulkhaleq, L. A., Assi, M. A., Abdullah, R., Zamri-Saad, M., Taufiq-Yap, Y. H., & Hezmee, M. N. M. (2018). The crucial roles of inflammatory mediators in inflammation: A review. *Veterinary world*, 11(5), 627.
4. Thakur M.D., Sheth N.R., Raval M.K. (2020) Assessment of In-vitro Anti-inflammatory Activity of Ginger and Diclofenac sodium combination. *International Journal of Pharmaceutical Sciences and Drug Research*, 12(5), 442-447.
5. Amin, B., & Hosseinzadeh, H. (2016). Black cumin (*Nigella sativa*) and its active constituent, thymoquinone: an overview on the analgesic and anti-inflammatory effects. *Planta medica*, 82(01/02), 8-16.
6. Bhat, S. P., Rizvi, W., & Kumar, A. (2014). Effect of *Cuminum cyminum* L. seed extracts on pain and inflammation. *Journal of natural remedies*, 14(2), 186-192.
7. Tambe, V. D., & Bhambhar, R. S. (2014). Estimation of total phenol, tannin, alkaloid and flavonoid in *Hibiscus tiliaceus* Linn. wood extracts. *Journal of pharmacognosy and phytochemistry*, 2(4), 41-47.
8. Atanassova, M., & Christova-Bagdassarian, V. (2009). Determination of tannins content by titrimetric method for comparison of different plant species. *Journal of the University of Chemical Technology and Metallurgy*, 44(4), 413-415.
9. Kumar, K. S., Manasa, B., Rahman, K., & Sudhakar, B. (2012). Development and validation of HPTLC method for estimation of 6-gingerol in herbal formulations and extracts. *International Journal of Pharmaceutical Sciences and Research*, 3(10), 3762.
10. Pratap, S. R., Gangadharappa, H. V., Ramakant, N. M., & Pooja, J. V. Development and Validation of Stability-Indicating RP-HPLC Method for the Estimation of Cuminaldehyde.
11. Qamar, M., Akhtar, S., Ismail, T., Yuan, Y., Ahmad, N., Tawab, A., ... & Ziora, Z. M. (2021). *Syzygium cumini* (L.), Skeels fruit extracts: In vitro and in vivo anti-inflammatory properties. *Journal of Ethnopharmacology*, 271, 113805.
12. Parameswari, P., Devika, R., & Vijayaraghavan, P. In vitro anti-inflammatory and antimicrobial potential of leaf extract from *Artemisia nilagirica* (Clarke) Pamp. *Saudi J Biol Sci*, 2019; 26 (3): 460-463.

PCP393

PRODUCING, PURIFYING, AND REGULATING BIOSIMILARS: A STEP-BY-STEP GUIDE

AP0335

Mr. Shalin Parikh

Senior Manager Senores
Pharmaceuticals PVT LTD
Shalin.parikh2011@gmail.com

AP0367

Mr. Ravisinh Solanki

Assistant Professor
GSP-GTU
ravisinh@gtu.edu.in

AP0363

Mr. Ravi Patel

Assistant Professor
GSP-GTU
ap_ravi_patel@gtu.edu.in

Abstract:

There are no clinically relevant differences between a biosimilar and a reference/originator or innovator product. By 2026, the global market value for biosimilars is expected to rise by about 25 percent compared to 2020. Any cell type, from viruses to whole animals, may be used in bioprocessing, which is broadly defined as the manufacture of a value-added product from a living source. Cells that produce the desired protein are grown in the upstream process, and the medicinal material is purified in the downstream phase. An authorized regulatory agency must approve applications from biosimilar manufacturers. They need to show that their product is structurally and functionally similar to the innovator product and that the remaining variations identified are not clinically significant. Producing biopharmaceuticals requires a totally different strategy. Living cells, such as blood and plasma products, vaccines, and recombinant proteins, are employed to make them. In the recent decade, a number of biologic medications have been developed and approved for use in the treatment of a variety of disorders. There is a high price tag for biological treatments, and several of their patents have already expired. As a result, biosimilars are becoming more widely available in Europe, the United States, and other regions of the world as a result of the expiration of patents on biologics.

Keywords: Biosimilar, biopharmaceuticals, regulation of biologics

PCP 411

ASSESSMENT OF APHRODISIAC ACTIVITY USING A POLY HERBAL FORMULATION IN RATS

AP0426

Modhiya Raini

M. Pham. Scholar,
Department of Pharmacology,
L. M. College of Pharmacy,
Gujarat Technological University
modhiaraini@gmail.com

AP0428

Goswami Sunita

HOD and Associate professor,
Department of Pharmacology,
L. M. College of Pharmacy,
Gujarat Technological University
Sunita.goswami@lmcp.ac.in

ABSTRACT

Background: Our study has reported as Aphrodisiac, Rejuvenating, Revitalizing and Nutritive tonic potential of Poly herbal Formulation (PHF) based on traditional knowledge. The combination of the plants can help enhancing sexual behavior. Therefore, we aim to study scientific basis of the PHF which is comprising of extract of different herbs to assess aphrodisiac activity. **Methods:** Aphrodisiac potential is determined following the oral administration of different doses (100 and 200 mg/kg) of PHF in rats. The study was performed using sexual behavior, biochemical parameters, and histopathology. The sexual behavior was examined by mating behavior on day 0 and 14th and sexual organ weight on 14th day. Biochemical parameters were evaluated by using different methods such as serum and testicular cholesterol, serum testosterone level, serum nitric oxide, protein estimation. Antioxidant activity was tested using testicular homogenate which included reduced glutathione (GSH), Lipid peroxidase (MDA), catalase (CAT), and sodium dismutase (SOD) along with sperm analysis. All the serum parameters were performed on day 0 and 14th while testicular parameters were performed on day 14th. In addition, histopathology of testis was performed on day 14th. **Results:** Rats treated with PHF 100, and 200 mg/kg exhibited significant increase in serum testosterone level [(14.71±1.03; 19.28±0.86), nitric oxide levels (20.2± 0.39; 20.64± 0.77) and total protein (7.31±0.68 ;7.09±0.78). Further, we observed increase in sperm viability (p< 0.01), motility (p < 0.01) in a dose- dependent manner and sperm count (p < 0.01) at 200 mg/kg. Sexual behavior in terms of number of mountings was increased while other sexual parameters remained unaltered. Further, serum and testicular cholesterol levels have also not changed statistically significant. Chronic treatment with high dose of PHF showed significant increase in SOD (p<0.01) and CAT (p<0.01). Contrary to this, GSH and MDA remained unaltered. **Conclusion:** The aphrodisiac potential of PHF can be attributed to increased testosterone levels and increased antioxidant activity. Also, the Presence of spermatozoa might be the reason for the sperm motility.

Key words: Aphrodisiac potential, Poly herbal formulation, Sexual behavior.

1 INTRODUCTION

A person's physical, psychological, and social health are critically related to their sexual relationships, and sexual health is a vital part of an individual's exceptional well-being (Ojatula et al., 2020). The sexual act is the most cherished, integral, and fundamental part of individual personality, and is likely the source of the greatest pleasure and satisfaction (Erhabor & Idu, 2017)

Mating is defined as sexual behavior. Sexual dysfunction (SD) can be defined as when the male cannot perform a satisfactory sexual act repeatedly or when he is suffering from any disorder that interferes with him being able to perform his sexual reaction cycle as a whole. Undoubtedly male sexual dysfunction contributes strongly to male infertility, with approximately 30%–50% of infertility cases being attributable only to difficulties faced by men (Ojatula et al., 2020).

It has been previously demonstrated that sexual dysfunction is the most common disorder in both sexes; men and women, particularly those over 40 years of age. In particular, erectile dysfunction and untimely ejaculation are enormously universal issues that have a negative impact on millions of fellows across the globe (Aydogan et al., 2020a). Erectile dysfunction (ED) refers to a man's inability to maintain or acquire a penile erection for sexual pleasure (Preedapirom et al., 2018).

However, aphrodisiacs have been shown to be effective in treating/managing those aforementioned disorders. Many aphrodisiacs may be described as stimulating parts of the senses, such as light, touch, smell, taste, and hearing. Sensual attention is stepping forward, which results in a desire to engage in sexual activity. Many regionally widespread parts had been regarded to boom libido in a few continents of the world (Erhabor & Idu, 2017). The definition of an aphrodisiac, then, is any substance or agent (food, drug, scent, or device) that stimulates the erotic instinct, induces venereal preference, increases sexual satisfaction and performance, and also modifies impaired sexual functions (Ojatula et al., 2020). In Greek mythology, the word 'aphrodisiac' refers to Aphrodite, the goddess of love and sexuality. Since ancient times, mankind has been infatuated with aphrodisiac substances. Both sexes can use aphrodisiacs for some time, whether or not there is any theoretical basis for their use to improve sexual satisfaction or even without any connection to their structure (Agrahari et al., 2021).

An aphrodisiac material can be tested for its potential by two methods: the observatory method, which involves the assessment of mating behavior, and the biochemical method. It is advantageous to use both *in vivo* and *in vitro* animal models in order to analyze aphrodisiac interest within laboratory animals such as rats, mice, and guinea pigs (Ojatula et al., 2020).

Sexual inadequacy in humans has led to an improvement in some of the available remedies, resulting in a continuous search for powerful herbal agents that can be used to develop new, safe, and effective treatment formulas addressing male sexual inadequacy. Therefore, medicinal plants with marked pharmacological activities are readily available all year round, reasonably priced, and easily accessible, and can be used regularly with minimal side effects, and are being explored worldwide as sources of alternative medicine. The Ayurvedic literature provides an explanation of aphrodisiacs, their benefits, extent, and limitations. The promise of these Ayurvedic medical literature findings is that the poly herbal ayurvedic formulations do provide the desired outcomes. Nevertheless, it is vital to analyze and judge their effectiveness in numerous conditions by means of the study of different correlating variables, which is the aim of this research (Ojatula et al., 2020).

2 OBJECTIVES

Our primary objective was to evaluate aphrodisiac activity and the secondary objectives were to evaluate mating behavior, sperm analysis along with testicular and serum cholesterol and testosterone level, serum nitric oxide and antioxidant activity.

3 MATERIALS AND METHODS

3.1 Animals

Sexually active Wistar albino rats (36 male and 36 female), weighing about 180-220g (8-10 weeks old), were used for the study. The male animals were trained through pairing with mature female rats, 2 times, for 5 days before the beginning of the test. Males and females, who did not reveal sexual interest during the experimental duration were taken into consideration as gradual animals. The female rats were artificially brought in estrous phase by administering estradiol valerate (10µg/kg body weight, PO) 24 hr. prior to experimentation. The receptivity of the female animals was confirmed by taking vaginal smear (Aydoğan et al., 2020a; Gill et al., 2018). The experimental protocol was approved by Institutional Animal Ethical Committee as per the guidance of Committee for the Purpose of Control and Supervision of Experiments on Animals (CPCSEA), animal welfare division, Ministry of environment, forest & climate change, and Government of India with protocol number **LMCP/IAEC/22/0022**. Prior permission of experiment on animal was taken from the Institutional Animal Ethics Committee (IAEC). The rats of either sex was isolated and housed in separate cages at room temperature ($24 \pm 2^\circ\text{C}$) on a 12hr dark and light cycle with relative humidity of 50%–55% while the experimental period. The animals were fed with a standard pellet diet and provided water (Gill et al., 2018).

3.2 Drugs, Assay Kits, and Other Reagents

The PHF used under the study includes different sources of herbs such as whole plant, seed, fruit, and essential oil. PHF comprises of extracts of *Glycyrrhiza glabra*, *Withaniasomnifera*, *Asparagus racemosus*, *Mucuna pruriens*, *Curculigoorchioides*, *Asteracantha longifolia*, *Tribulus terrestris*, *Grewia populifolia*, *Balasisida cordifolia*, *Anacyclus pyrethrum*, *Zingiber officinale* Rhizome, *Piper cubeba*, *Piper longum*, *Caryophyllusaromaticus*, *Santalum album*, *Nutmeg* and *Cardamom*. All of these were processed with *sesamum indicum* and *Ghrit*. All chemicals used in this study were of analytical grade. Testosterone and antioxidant kits were acquired from Krishgen, Cholesterol kit was acquired from erba, and total protein kit was acquired from truechemie. Estradiol valerate used under the brand name Intas.

3.3 Grouping and Dosing of Animals

All the animals were randomly divided into three groups. Group one received 0.5% sodium CMC b.i.d., group two and three received 100mg/kg and 200mg/kg body weight PO, twice a day respectively. The test was performed at 17:00 h in a peaceful room below faint red light in transparent cages. 30 min after administering test substance, female rats were brought into the male cages with one female to one male ratio, and the male sexual behavior were right away examined (Aydoğan et al., 2020a). The observation for mating behavior started after 10 min of introducing the paired animals withinside the cage and were recorded with the useful resource of a video digital digicam (Erhabor & Idu, 2017).

3.4 Sexual Behaviors (Singh et al., 2013)

3.4.1 Mount frequency (MF):

Mounting is described as the climbing of one animal to another generally from the posterior cease with the aim of introducing one organ into another. Mount can also be operationally defined as the male assuming the copulatory characteristic but failing to acquire intromission.

Therefore, mount frequency defined as the number of mounts without intromission from the time of introduction of the female till ejaculation.

3.4.2 Intromission frequency (IF):

Intromission is the introduction of one organ or element into another. e.g., the penis into the vagina. Intromission Frequency is described as the number of intromissions from the time of the introduction of the female till ejaculation.

3.4.3 Mount latency (ML):

Mount latency is defined as the time interval between the appearance of the female and the primary mount through the male.

3.4.4 Intromission latency (IL):

Intromission latency is described as the time interval from the time of the advent of the female to the first intromission with the aid of using the male. This is commonly characterized with the aid of using pelvic thrusting, and springing dismounts.

3.4.5 Ejaculatory latency (EL):

Ejaculation is the act of ejecting semen introduced with the aid of using a reflex movement that takes place as the end result of sexual stimulation. Ejaculatory latency is described as the time interval among the first intromission and ejaculation. This is normally characterized with the aid of using longer, deeper pelvic thrusting and sluggish dismount observed with the aid of using a duration of inaction or reduced activity.

3.4.6 post-ejaculatory interval (PEI):

Post-ejaculatory interval is the time interval between ejaculation and the first intromission of the following series.

3.4.7 Copulatory rate:

Copulatory rate is calculated by determining the number of mounts plus number of intromissions divided by the time from the first mount until ejaculation.

$$\text{Copulatory rate} = \frac{\text{Number of mounts} + \text{Number of intromissions}}{\text{Time from first mount till ejaculation}}$$

3.4.8 Index of libido:

Index of Libido is describing as the ratio of number mated to number paired expressed in percentage. This can be expressed mathematically as:

$$\% \text{ Index of libido} = \frac{\text{Number mated}}{\text{Number paired}} \times 100$$

3.4.9 Computed male sexual behavior parameters Using the above parameters of sexual behavior, the following can thus be computed:

The parameters can be counted as:

$$3.4.9.1 \% \text{ Mounted} = \frac{\text{Number mounted}}{\text{Number paired}} \times 100$$

$$3.4.9.2 \% \text{ Intromitted} = \frac{\text{Number of intromissions}}{\text{Number paired}} \times 100$$

$$3.4.9.3 \text{ Intromission ratio} = \frac{\text{Number of Intromission}}{\text{Number of mounts} + \text{Number of intromissions}} \times 100$$

$$3.4.9.4 \% \text{ Ejaculated} = \frac{\text{Number of ejaculations}}{\text{Number paired}} \times 100$$

3.4.9.5 *Copulatory efficiency* = Amount of intromissions/ Number of mounts \times 100

3.4.9.6 *Intercopulatory efficiency* = Average time between intromissions

3.5 Evaluation Parameter for Biochemical Studies

3.5.1 Testicular and serum cholesterol concentrations

Testicular and serum cholesterol concentrations were performed through the Chod-PAP method. Serum cholesterol was performed at day 0 and 14 while testicular cholesterol was performed at day 14 only.

3.5.2 Serum testosterone determination

Blood samples were collected and centrifuge at 2, 200 rpm for 15 min at 4°C. The serum was saved at -35°C for analysis. Serum testosterone levels were measured with the aid of using an ELISA Kit. Serum testosterone was performed at day 0 and 14.

3.5.3 Measurement of nitric oxide (NO) concentration

The test was performed at day 0 and 14 using the method described by (Gul et al., 2013; Pinto et al., 2020) with a few modifications, 500 μ l of supernatant were incubated with an equal volume of freshly prepared Griess reagent [1.5% Phosphoric acid, 0.1% N-1-naphthylethylenediamine in deionized water] for 30 minutes at room temperature. The product is protected from light. Against a reagent blank, the violet color absorbance was determined at 540nm. By substituting deionized water for the sample, a reagent blank was prepared.

3.5.4 Protein estimation

As described in the manufacturer's test procedure, we used a total protein kit to estimate the protein content. Total protein level was checked on day 0 and day 14.

3.5.5 Antioxidant stress measurement

The test was performed by using ELISA kit as described in the manufacturer's test procedure. All the antioxidant parameters were performed at the end of the study using tissue homogenates.

3.5.6 Sperm analysis (Khalil et al., 2019; Sharma et al., 2013)

The motility, viability, and count of spermatozoa withinside the cauda epididymis was assessed in the present investigation. The animals were sacrificed, and the cauda epididymis were transacted on the point of beginning of the vas deferens at the distal end and positioned in a watch glass containing 0.5 mL of phosphate buffer maintained at 37 °C. The tissues were minced cautiously with the assist of fine forceps and scissors to make sure the extrusion of spermatozoa. The tissue fractions were eliminated by the usage of the fine forceps and a needle, and the suspension was used for sperm analysis. Sperm analysis was performed at the end of the study.

3.5.6.1 Sperm motility

A drop of sperm suspension was placed on a clean glass slide after which covered with a coverslip slip. The slide was then tested below the microscope at 40 \times and the motility were scored in distinct fields of view. Spermatozoa displaying any degree of motion may be taken into consideration to be motile. All spermatozoa (motile in addition to immotile) may be counted with the assist of a blood cell counter. Sperm motility may be calculated by the usage of the subsequent formula:

Motility (%) = quantity of motile spermatozoa/overall quantity of spermatozoa (motile +immotile) \times 100

3.5.6.2 Sperm viability

Sperm viability could be assessed the use of a supravital staining approach primarily based totally on the precept that cells with damaged plasma membrane absorb the stain, while viable ones do not. All glassware, in addition to the eosin– nigrosin stain were maintained at 37 C. A drop of sperm suspension and a drop of eosin–nigrosine stain (1% eosin + 5% nigrosine, 1:1) were placed on a clean glass slide and blended very well with the assist of a fine glass rod. A part of the mixture was transferred to a 2nd slide, and a skinny film was prepared. The slide was then tested below the microscope (40×). Spermatozoa appearing pinkish (stained) could be taken into consideration to be dead, while the ones appearing colorless (unstained) could be counted as possible. Sperm viability could be calculated in percentage through the use of the subsequent formula:

$$\text{Viability (\%)} = \frac{\text{quantity of viable spermatozoa}}{\text{Overall quantity of spermatozoa (viable + dead)}} \times 100$$

3.5.6.3 Sperm count

A hemocytometer with Neubauer ruling were used for counting the spermatozoa. A 20-fold dilution were made via mixing the sperm suspension with Phosphate buffer. The preparation was then very well mixed, and one drop was added to both sides of the hemocytometer. The number of spermatozoa was counted from the 4 corner squares of the hemocytometer below a microscope at 40×. If the spermatozoa crossed the lines of the grid, simplest the ones on the top and right-hand sides of the squares were counted. Spermatozoa on both sides of the hemocytometer were counted, and the average quantity was recorded. The number of spermatozoa per cauda epididymis was expressed as follows:

$$\text{Sperm number} = \text{average no. of spermatozoa counted (N)} \times \text{multiplication factor (10'000)} \times \text{dilution factor (20)} = N \times 10'000 \times 20 \times 106 \text{ spermatozoa}$$

3.5.7 Effect on sexual organ weight

After 14 days of treatment, the body weights of animals were taken, and then all animals were sacrificed. Testis, seminal vesicles, epididymis, and prostate glands were cautiously eliminated and weighed (Gill et al., 2018; Ojatula et al., 2020).

3.6 Histological studies

The animals were sacrificed at the end of the study and the testis of animals were cut into small pieces, fixed with Bovine's fixative and after that dehydrated with varying possibilities of ethanol for histological studies. Sections were cut, stained with hematoxylin and eosin and then analyzed microscopically (Khalil et al., 2019).

3.7 Statistical Analysis

All the values were expressed as Mean \pm SEM, where $p < 0.05$ was considered statistically significant. The data obtained was statistically analyzed using Graph Pad Prism version 8 software. Statistical comparison was performed using one- way ANOVA followed by Dunnett's multiple comparison test, t- test and non-parametric test Kruskal–Wallis.

4 LITERATURE REVIEW

The aphrodisiac activity can be observed in terms of increased libido and enhanced sensory experience during sexual activity (Ojatula et al., 2020). Aphrodisiac activity often compromised in persons who are having pre-existing diseases like diabetes, chronic alcoholic, vascular disease, muscle sclerosis, atherosclerosis, kidney diseases, and Neurologic disorders (Singh et al., 2013). In order to correct sexual disorders Viagra, Stendra and Cialis like drugs are available

globally. However, those drugs are having untoward effects like flushing, visual disturbance, dizziness etc (Agrahari et al., 2021).

In the Indian traditional system of medicine, many herbs are said to affect males and females differ in terms of their sexual behavior. There has been little scientific documentation of these herbs. Despite the availability of effective conventional medical treatment, plant-derived and herbal remedies continue to serve as a popular alternative for people seeking to improve their sexual health. This is due to the fact that plant-derived and herbal products are associated with relatively fewer side effects. Furthermore, there are relatively few empirically supported, pharmacologically based approved treatments available for sexual problems, which may partially explain the use and efficacy of herbal remedies; however, these remedies are far fewer in number for women than they are for men. Many plants such as Berberine, Crocus sativus, Epimedium extract (horny goat weed), yohimbine and Morinda officinalis are believed to have the potential to improve sexual behavior according to the Ayurvedic system of medicine in India. Unfortunately, most of these claims have not been scientifically proven (Agrahari et al., 2021; Rowland & Tai, 2003).

5 RESULTS

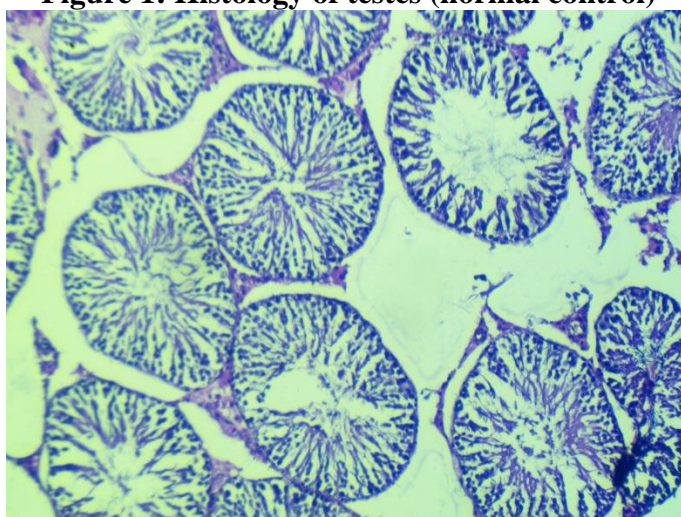
Baseline biochemical parameters are listed in table 1.

Table 1: Baseline biochemical parameters on day 0

Parameters	Control	100mg/kg	200mg/kg
Serum cholesterol analysis (mg/dl)	50.17± 4.84	49.06± 16.03	51.52± 8.2
Serum testosterone (pg/ml)	13.20±0.14	13.86±0.22	13.62±0.31
nitric oxide (NO) concentration(μmol/ml)	19.51± 0.83	28.168± 2.24	36.37± 2.9
Protein estimation (g/dl)	3.25±0.21	3.87±0.41	3.15±0.45

All data expressed in mean ± SEM. n=6; control- Normal control group

Figure 1: Histology of testes (normal control)



The administration of the PHF to male rats on day 0 did not manifest any noticeable effect on sexual behavioral parameters. While on 14th day, attempt of mounts were observed. However, sexual behavioral parameters were not significantly changed on 14th day also. Further, there were no significant differences observed in the organs such as testes, prostate glands, and seminal vesicles on day 0 & 14, but epididymis weight increased significantly in animals receiving 200 mg/kg dose on 14th day (table 2).

Table 2: Effect of PHF on sperm analysis, physical and biochemical parameters on day 14

Parameters	Control	100mg/kg	200mg/kg
Biochemical parameters			
Serum cholesterol (mg/dl)	56.46± 3.07	58.5± 2.51	55.78± 3.23
testicular cholesterol(mg/dl)	51.33± 3.07	64.88± 11.65	75.78± 3.12
Serum testosterone (pg/ml)	13.72±0.34	14.712±1.03	19.28±0.85**
nitric oxide (NO) concentration (µmol/ml)	19.39± 1.36	20.2± 0.39*	20.644± 0.76**
Protein estimation (g/dl)	4.54±0.26	7.31±0.68*	7.09±0.78**
Reduced glutathione (µ/ml)	12.38±1.03	14.05±0.76	14.02±0.39
Superoxide dismutase (ng/ml)	17.01±2.1	21.61±1.10	28.22±1.86**
Lipid peroxidase (nmol/ml)	5.80±0.39	4.82±0.29	4.94±0.14
Catalase (u/min/mg protien)	20.35±0.83	23.07±1.28	27.32±1.15**
Sexual organ weight (g)			
Epididymis (g)	0.6825 ± 0.03	0.722 ± 0.03	0.88 ± 0.02**
Testes (g)	1.57 ± 0.12	1.66 ± 0.13	1.794 ± 0.08
prostate glands (g)	0.4 ± 0.05	0.46 ± 0.04	0.56 ± 0.05
seminal vesicles (g)	0.52 ± 0.05	0.628 ± 0.09	0.75 ± 0.18
Sperm Analysis			
Sperm count (n)	83.4±1.75	74±1.65	71.75±2.13**
Sperm motility (%)	72.6 %	80.68%*	83.72%**
Sperm viability (%)	75.5 %	81.32%**	85.78%**

All data expressed in mean ± SEM. n=6; control- Normal control group * p<0.05, ** p<0.01 statistically significant.

Figure 3: Histology of testes using PHF (200mg/kg)

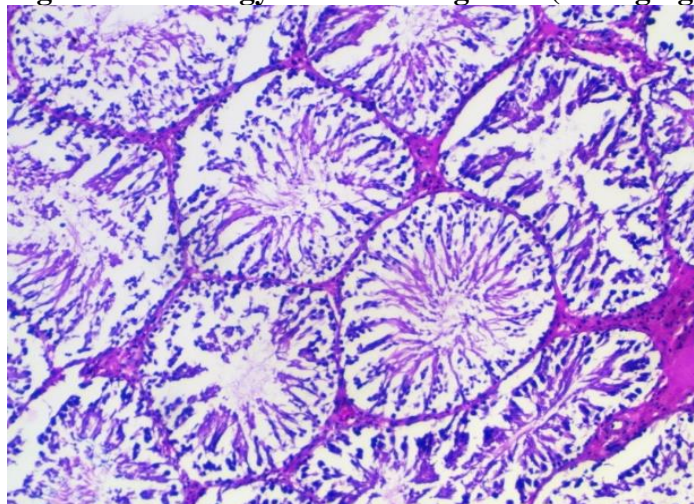
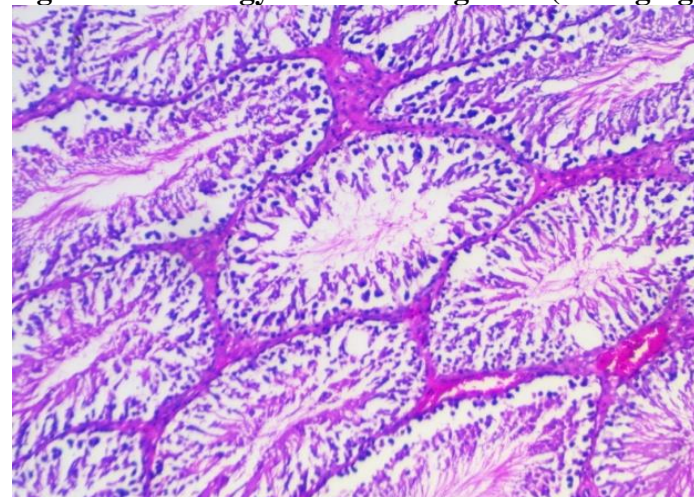


Figure 2: Histology of testes using PHF (100mg/kg)



Serum cholesterol levels (mg/dl) were measured on day 0, and 14 whereas testicular cholesterol was performed on day 14. As can be seen in table 1&2, there was no significant change in serum total cholesterol on day 0 and day 14 as well as testicular cholesterol. Total protein content increased significantly in those animals treated with 100 (7.31 ± 0.68) and 200 (7.09 ± 0.78) mg/kg dose on day 14 (table 2). Similarly, significant changes were observed in serum nitric oxide on day 14th with the mean value of 20.2 ± 0.39 for 100 mg/kg and 20.644 ± 0.76 for 200 mg/kg. table 2 depicted significant changes in serum testosterone at 200 mg/kg dose (19.28 ± 0.85) on 14th day.

After the treatment with PHF for 14 days, there was no significant difference observed at low dose (100 mg/kg) in GSH, MDA, CAT and SOD activity as compared to control group. Whereas in high dose (200 mg/kg), significant improvement in SOD and catalase activity observed. Contrary to this, GSH and MDA levels were not affected significantly at higher dose treatment (table 2).

In vivo sperm count was performed after 14 days of treatment of all the animal groups. The epididymal sperm counts significantly increased ($p < 0.01$) at dose of 200 mg/kg (71.75 ± 2.136)

as compared to normal control (83.4 ± 1.754045). The motility of caudal epididymal spermatozoa was increased significantly ($p < 0.01$) in a dose-dependent manner as compared to the control rats that exhibited normal sperm motility. Sperm motility in the 100, and 200 mg/kg group was 80.68%, and 83.72%, respectively, as compared to 72.6 % in the control group (table 2). The viability of spermatozoa was increased significantly ($p < 0.01$) in a dose-dependent manner as compared to control rats that exhibited normal sperm viability. Sperm viability in the 100, and 200 mg/kg group was 81.32%, and 85.78%, respectively, compared to 75.5 % in the control group (table 2).

Testes section of control group animals showed that seminiferous tubules having maximum diameter were not abundant. Germinal epithelium showed normal shape and size. Spermatozoa were embedded in Sertoli cells, showed normal cytoplasmic granulation. Leydig cells had normal appearance. Luminal part of the tubule was not excessively filled with spermatozoa (Fig 1). The testes section of low dose (100 mg/kg) treated group animal showed increased spermatogenesis evident from high numbers of spermatozoa in seminiferous tubules. Almost all seminiferous tubules showed greater diameter. Lumen of every tubule was overcrowded with enormous numbers of spermatozoa. Germinal epithelial cells were hyperactive. Large numbers of different cells at different stages of spermatogenesis were seen. Cytoplasm of sertoli cells was found highly granulated. Nucleus of the Leydig cells was enlarged and cytoplasm appeared to be stained darkly (Fig 2). Histo architecture of high dose (200 mg/kg) treated group also exhibited similar profile to that of low dose treated group (Fig 3).

6 DISCUSSION

Sexual dysfunction is a health problem that can occur at any age in both the genders. Sexual dysfunction is characterized by a lack of interest for sexual activity or reduced libido. Infertility is a major health problem nowadays (Du et al., 2020). Therefore, Aphrodisiac agents are introduced globally. The aphrodisiac agents can be obtained from plant or animal origin (Ojatula et al., 2020).

The worldwide available synthetic compounds like Avanafil, sildenafil, tadalafil and vardenafil can be used for increasing sexual activity. They are known as PDE5 inhibitors. Though they are used to increase sexual activity, they have major side effects such as retinal defects, headaches, flushing, dizziness, visual disturbances, nasal congestion, and other disorders caused by inhibition of PDE6. Therefore, medicinal plants with marked pharmacological activities are readily available all year round, cheap, and accessible and often with minimal side effect. Historically, medicinal plants have been one of the most valuable resources in therapeutic practices associated with human diseases and some have been used as aphrodisiac tonics for centuries (Agrahari et al., 2021).

Herbal medicine and products derived from plants are still being used in medical practice, though the mechanisms of action of many herbal drugs are unknown, and the active principles in these drugs are seldom understood.

Sexual behaviour parameters supposed to be increased in libido but in our finding, we were unable to observe such behaviour.

Significant increases in the weight of the epididymis may be a result of an increased androgen synthesis, as evidenced by significant increases in serum testosterone levels in the experimental rats. It has been demonstrated that androgen levels correlate positively with the weight of the testis, epididymis, seminal vesicle, and prostate glands, and that androgens are necessary for the development, growth, and normal functioning of the testes and male accessory reproductive glands (Sharma et al., 2013). In our finding there were no significant increase in testes, seminal vesicles and prostate gland however, there was significant increase in the weight of epididymis.

There is evidence that cholesterol is a precursor in androgen biosynthesis and its level are closely related to fertility and sperm production. With the ability for aphrodisiac lead significant increase in testicular and or serum cholesterol concentrations. Along with the ability to act as an aphrodisiac, the PHF results in significant increases in testicular cholesterol and/or serum cholesterol levels. It is possible that such increase might stimulate testosterone synthesis, which could result in an elevated testosterone concentration. Generally, an increase in testosterone concentration is associated with a rise in libido (Singh et al., 2013). However, there were no significant changes observed in both the cases of serum and testicular cholesterol.

The increased stimulation of GnRH- LH signalling may be responsible for the increase in testosterone concentration in serum. Luteinizing hormone stimulates the synthesis and secretion of testosterone by Leydig cells in the testes by binding to their receptors. Rats treated with PHF (100 and 200 mg/kg) may experience sexual arousal as a result of the release of testosterone in the serum, which stimulates dopamine receptor synthesis. In addition to regulating tumescence and rigidity, testosterone also contributes to ejaculation and penetration. An increase in the concentration of serum testosterone with PHF (100 and 200 mg/kg) can thus be considered one of the factors responsible for aphrodisiac activities in rats (Khalil et al., 2019).

eNOS and nNOS have been discovered to contain an important activating compound (AC). In CC nNOS and eNOS are activated by the PHF. This increases the production of NO, which activates the enzyme guanylate cyclase to convert GTP into cyclic GMP. Cyclic GMP (cGMP) regulates smooth muscle tone in the CC as well as penile erection. There is a decrease in intracellular calcium levels that leads to relaxation. These pathways are mediated by cGMP and cAMP. Consequently, AC may induce aphrodisiac effects through the cGMP-mediated pathway by activating eNOS and nNOS. AC stimulates erectile function in CC. AC could simultaneously affect CC and CNS signalling. Sexual arousal is one of the many functions of the neuronal NOS in men and women. By increasing the formation of cGMP from GTP, the PHF could increase the levels of cGMP, while Viagra (sildenafil citrate) inhibits phosphodiesterase 5, which specifically degrades cGMP. In addition, it is interesting to note that both the poly herbal drug and Viagra can increase cGMP levels. The poly herbal drug increases cGMP formation from GTP, whereas Viagra inhibits cGMP degradation. It appears that the poly herbal drug has the potential to serve as an alternative to Viagra (Subramoniam et al., 2013).

It is possible that the increased protein level in the group treated with PHF may be because of steroids and other antioxidants, that favors protein metabolism by reducing oxidative damage. Among the drug-treated group, weight gain is mainly due to a rise in protein mass (Balamurugan et al., 2010).

The reactive oxygen metabolites, including hydrogen peroxide, superoxide radicals, nitric oxide radicals, and so on, seem to play a variety of roles in maintaining and disrupting cellular functions. On one hand, they are found to play a role in cell signalling in different cell types, including spermatozoa; on the other hand, they have also been implicated in aging, disease, and apoptosis. Several studies have shown that oxidative stress has an important role in male infertility. High levels of these reactive oxygen species (ROS) are associated with sperm motility decline and decreased ability to fuse with the oocyte, making the health of the sperm dependent on antioxidants. Based on the results, superoxide dismutase activity as well as catalase activity, were significantly higher in the testicular homogenate of the animals treated with PHF when compared to the control. By neutralizing the deleterious effects of the ROS, these enzymes can help maintain the motility and viability of the sperm and thereby enhance the success rate of treating male infertility (Padashetty & Mishra, 2007). In our study GSH and MDA did not produce significant change.

As a result of high testosterone levels, rats administered PHF were observed to have favorable and increased spermatogenic activities. In the development of sperm cells, testosterone plays a

critical role, and its disruption may result in testicular steroidogenic disorder and Leydig cell dysfunction. The epididymis plays a significant role in the maturation of sperm, which is essential for their viability and ability to become fertile. As a result, an increase in the activity of the epididymis in experimental rats could have contributed to the progression of sperm motility. The increased sperm count, and motility are, therefore, evidence that treatment with PHF enhances and improves the fertilization capability of the sperm (Padashetty & Mishra, 2007).

Histological studies along with in vitro and biochemical studies, suggested probable role of fraction in synthesizing or stimulating testosterone release from Leydig cells (Vyas & Raval, 2016).

7 CONCLUSIONS

Our data suggest aphrodisiac potential of the PHF used under the study. The mechanism of action of its aphrodisiac activity can be attributed to increased testosterone level, nitric oxide level, spermatogenic activity, along with rise in SOD and CAT level.

8. ACKNOWLEDGEMENT

We are gratefully acknowledging Vandana Mody Madam, Vice President, Cadila Pharmaceutical Limited for providing poly herbal formulation.

8 REFERENCES

1. Agrahari, N., Lakshameesha, C., & Roy, S. (2021). Regulatory Insight for Aphrodisiac Drugs. *J Drug Des Res*, 8(1), 1–7. <https://www.jsccimedcentral.com/DrugDesign/drugdesign-8-1077.pdf>
2. Aydogan, F., Baykan, S., Soliman, G. A., Yusufoglu, H., & Bedir, E. (2020a). Evaluation of the potential aphrodisiac activity of sesquiterpenoids from roots of *Ferula huber-morathii* Peşmen in male rats. *Journal of Ethnopharmacology*, 257, 112868.
3. Balamurugan, G., Muralidharan, P., & Polapala, S. (2010). Aphrodisiac activity and curative effects of *Pedaliium murex* (L.) against ethanol-induced infertility in male rats. *Turkish Journal of Biology*, 34(2), 153–163.
4. Du, Q., Huang, Y. H., Bajpai, A., Frosig- Jorgensen, M., Zhao, G., & Craik, D. J. (2020). Evaluation of the in Vivo Aphrodisiac Activity of a Cyclotide Extract from *Hybanthus enneaspermus*. *Journal of Natural Products*, 83(12), 3736–3743.
5. Erhabor, J. O., & Idu, M. D. (2017). Aphrodisiac potentials of the ethanol extract of *Aloe barbadensis* Mill. root in male Wistar rats. *BMC Complementary and Alternative Medicine*, 17(1), 1–10.
6. Gill, M., Rai, A., Kinra, M., Sumalatha, S., Rao, C. M., Cheruku, S. P., Devkar, R., & Kumar, N. (2018). Chemically characterised extract of *Saraca asoca* improves the sexual function in male Wistar rats. *Andrologia*, 50(7), 1–10.
7. Gul, M. Z., Ahmad, F., Kondapi, A. K., Qureshi, I. A., & Ghazi, I. A. (2013). Antioxidant and antiproliferative activities of *Abrus precatorius* leaf extracts - an in vitro study. *BMC Complementary and Alternative Medicine*, 13, 1–12.
8. Khalil, I., Khan, M. R., Ghani, M., & Akbar, F. (2019). *Abutilon pannosum* stem bark enhances the aphrodisiac activities and spermatogenesis in rat. *Andrologia*, 51(10), 1–11.
9. Ojatula, A., Idu, M., & Timothy, O. (2020). Aphrodisiac Potentials of *Pausinystalia yohimbe* (K. Schum.) Pierre ex Beille Methanol Root Extract in Male Wistar Rats. *Journal of Integrative Nephrology and Andrology*, 7(2), 47.
10. Padashetty, S. A., & Mishra, S. H. (2007). Aphrodisiac studies of *Tricholepis glaberrima* with supportive action from antioxidant enzymes. *Pharmaceutical Biology*, 45(7), 580–586.
11. Pinto, R. V., Antunes, F., Pires, J., Silva-Herdade, A., & Pinto, M. L. (2020). A comparison of different approaches to quantify nitric oxide release from NO-releasing materials in relevant biological media. *Molecules*, 25(11).
12. Preedapirom, W., Changwichit, K., Srisawang, P., Ingkaninan, K., & Taepavarapruk, P. (2018). Aphrodisiac Activity of *Eulophia macrobulbon* Extract on Erectile Dysfunction in Male Aged Rats. *BioMed Research International*, 2018.
13. Rowland, D. L., & Tai, W. (2003). A review of plant-derived and herbal approaches to the treatment of sexual dysfunctions. *Journal of Sex and Marital Therapy*, 29(3), 185–205.
14. Sharma, V., Boonen, J., De Spiegeleer, B., & Dixit, V. K. (2013). Androgenic and spermatogenic activity of alkylamide-rich ethanol solution extract of *anacyclus pyrethrum* dc. *Phytotherapy Research*, 27(1), 99–106.

15. Singh, R., Ali, A., Jeyabalan, G., Semwal, A., & Jaikishan. (2013). An overview of the current methodologies used for evaluation of aphrodisiac agents. *Journal of Acute Disease*, 2(2), 85–91.
16. Subramoniam, A., Gangaprasad, A., Sureshkumar, P. K., Radhika, J., & Arun, B. K. (2013). A novel aphrodisiac compound from an orchid that activates nitric oxide synthases. *International Journal of Impotence Research*, 25(6), 212–216.
17. Vyas, N. Y., & Raval, M. A. (2016). Aphrodisiac and spermatogenic potential of alkaloidal fraction of *Hygrophila spinosa* T. Ander in rats. *Journal of Ethnopharmacology*, 194, 947–953.

PCP416

DESIGN OF EXPERIMENT (DoE) BASED APPROACH FOR FORMULATION AND OPTIMIZATION OF CURCUMIN TRANSFEROSOMES FOR WOUND HEALING

AP0405

Manisha Jadav
Research Scholar
Parul University

manisha.jadav121112@parul
university.ac.in

AP0409

Dr. Vandana B. Patel
Founder & Director
Teacher Talks
Academy, Vadodara

vbpatel04@yahoo.com

AP0412

Dr. Lalit Lata Jha
Principal
School of Pharmacy,
Parul University

lalit.jha@paruluniversity
.ac.in

Abstract

The aim of the present study was to investigate the potential of a transferosome formulation for transdermal delivery of Curcumin. Curcumin is widely used as a potent anti-inflammatory herbal drug ingredient in various topical preparations. The only challenge of Curcumin in topical application is its poor permeability, therefore it was decided to formulate transferosomal based gel of Curcumin. The preformulation study of curcumin was carried out initially in terms of identification (physical appearance, melting point and IR spectra), solubility study, λ -max determination and the results obtained were directed for the further course of formulation. The transferosomes were formulated by lipid thin film hydration method. Screening of lipids were done in which Phospholipon 90G gave good results in terms of Entrapping Efficiency (EE) and Vesicle Size (VS). Various process variables such as temperature, pressure, rotation, time for film making, time for hydration and consistency of film were also screened for best values. Further optimization of the formulation was carried out using 3^2 full factorial design in which Span 80 and Sonication time were taken as independent variables (factors) and Entrapment Efficiency (EE) and Vesicle Size (VS) were taken as dependent variables (response). The data was analyzed using Stat-ease Design-Expert v7.0.0 software. The batch F8 gave highest entrapment efficiency of 91.18 ± 2.7 and average vesicle size 87.75nm. The formulation F8 can be taken further for its incorporation into suitable gel and In-Vitro drug diffusion studies will be carried out to check the permeation enhancement of the drug.

Keywords: Curcumin, factorial design, span 80, thin film hydration

1. INTRODUCTION

Transferosomes are the optimized ultra-deformable lipid supramolecular aggregates able to penetrate mammalian skin. The edge activator is incorporated into the layers such as span 80, tween 80. They consist of at least inner aqueous phase surrounded by lipid bilayer. A Transferosome carrier is an artificial vesicle designed to exhibit the characteristics of a cell vesicle or a cell engaged in exocytosis, and thus suitable for controlled and, potentially, targeted drug delivery. A Transferosome carrier is an artificial vesicle designed to exhibit the characteristics of a cell vesicle or a cell engaged in exocytosis, and thus suitable for controlled and potentially targeted drug delivery.

Curcumin is chemically (1E, 6E)-1, 7-bis (4-hydroxy-3-methoxyphenyl) hepta-1, 6-diene-3, 5-Dione. Curcumin is used for the treatment of anti-cancer, anti-oxidant, anti-inflammatory, hyperlipidemic, antibacterial, wound healing and hepatoprotective activities. Apart from its pharmacological actions, it has also been investigated as photostabilizing agent to protect photo-labile drugs in solution, topical preparations and soft gelatin capsules. Despite the presence of large number of pharmacological actions, the therapeutic efficacy of curcumin is limited due to its poor oral bioavailability. The poor oral bioavailability of curcumin has been

attributed to its poor aqueous solubility as its partition coefficient 3.2 and extensive first pass metabolism.⁴

2. OBJECTIVES

The objective of the study to investigate the potential of a transferosome formulation for enhanced bioavailability and transdermal delivery of Curcumin for wound healing.

3. RESEARCH METHODOLOGY

3.1 Material

Curcumin was obtained from HIMEDIA, Mumbai. PHOSPHOLIPON 90G procured from LIPOID, Germany. Span 80 was procured from Chemdyes, Vadodara. Chloroform, Di sodium hydrogen phosphate and Potassium dihydrogen phosphate was purchased from S D Fine Chemical Limited, Vadodara.

3.2 Method

Transferosomes were prepared by thin film hydration method using Chloroform as Solvent. Take phospholipid and edge activator and curcumin in round bottom flask. Add chloroform and dissolve it. Put the round bottom flask on Rota evaporator until thin film form. Hydrate it with phosphate buffer 7.4 and gently shake for 15 min. Yellowish colored transferosomal suspension is formed.

Characterization of curcumin loaded-Transferosomes:

Vesicle size distribution and zeta potential

Vesicle size, size distribution and zeta potential were determined by Dynamic Light Scattering system by Malvern Zetasizer.

Entrapment efficiency:

Percentage of drug which are entrapped into a delivery system is known as entrapment efficiency. By the use of Mini column centrifugation method the first separation of the untrapped drug can be determined. After centrifugation, the vesicles were disrupted using 0.1% Triton X-100 or 50% n-propanol. The entrapment efficiency is expressed as:

$$\text{Entrapment efficiency} = \left(\frac{\text{Amount entrapped}}{\text{Total amount added}} \right) \times 100$$

Surface charge and charge density

Surface charge and charge density can be determined by zeta sizer analysis.

4. LITERATURE REVIEW

Many literatures reveal the various methods for the preparation of transferosomes of curcumin by using different lipids. In this research study an attempt is made to curcumin by using two lipids and applying 3² Full factorial design.

5. ANALYSIS PART

5.1. Process Parameter optimization:

In this research various process parameters were optimized as their effect is directly on film formation. These are listed in table 1.

Table 1: Optimization of Process Parameters

X1: Temperature (°C)	X2: Pressure (mm Hg)	3: Rotation (rpm)	X4: Time of making film	X5: Time for Hydration	Y: Consistency of film
45	300	50	2 hr	1.8 hr	Thick
50	400	60	1.5 hr	1 hr	Slightly thin
55	500	80	50-60 min	1 hr	Thin

5.2. Formulation Parameter Optimization

Screening of Phospholipids were done on the basis of % Entrapment Efficiency and Vesicle size as per given in the Table 2.

Table 2: Screening of Phospholipid

	PHOSPHOLIPON 90G	PHOSPHOLIPON 90H
Lipid	850 mg	850 mg
Drug	30 mg	30 mg
Chloroform	10 ml	10ml
Edge activator (span 80)	150 mg	150 mg
% Encapsulation Efficiency	89.27±2.48	72.56±5.87
Vesicle size (nm)	79.24±3.71	120.23±4.56

Formulation Optimization by 3² Full Factorial Design

Table 3: Variable selected for Formulation prepared by using Phospholipon 90G

Dependent variables	Independent variables
X1: Amount of Edge activator (mg)	Particle Size (nm) and Entrapment Efficiency (%)
X2: Sonication time (minutes)	

6. FINDINGS

After the Trial and error which was hereby listed optimized process parameter

Table 4: Optimized Process Parameters

Temperature	55 °C
Pressure	500 mm Hg
Rotation	80 rpm
Time for making film	50-60 min
Time for hydration	1 hr

After the Screening of Phospholipid formulation containing PHOSPHOLIPON 90G have good entrapment efficiency and vesicle size compare to PHOSPHOLIPON 90H.

Table 5: Formulation Optimization By 3² Full Factorial Design

Batch	Variables in coded form		Variables in actual form		Response Variables	
	X1: Amount of Edge activator	X2: Sonication time	X1: Amount of Edge activator (mg)	X2: Sonication time (min)	Particle Size (nm)	Entrapment Efficiency (%)
F1	-1	-1	100	10	79.02±2.84	45.01±1.85
F2	0	-1	150	10	107.01±3.12	74.09±5.25
F3	+1	-1	200	10	156.19±2.15	65.91±3.49
F4	-1	0	100	15	67.9±3.47	52.18±1.87
F5	0	0	150	15	96.02±4.89	81.91±2.46
F6	+1	0	200	15	129.93±1.28	69.01±3.18
F7	-1	+1	100	20	59.12±2.78	60.05±3.42
F8	0	+1	150	20	87.75±3.74	91.18±2.71
F9	+1	+1	200	20	113.09±2.89	71.09±3.61
F10	0	0	150	15	93.12±5.67	78.91±4.58
F11	0	0	150	15	94.02±2.87	82.12±2.96

From above Optimization study Batch F8 contain minimum particle size and more entrapment efficiency.

Figure 1 Zeta potential of optimized formulation



Effect of factors on Particle Size:

Table 6: ANOVA for Response surface quadratic model of Particle size

Source	Sum of squares	df	Mean Square	F value	P value Prob > F	
Model	7605.87	5	1521.17	146.71	<0.0001	Significant
A-amount of edge activator	6219.11	1	6219.11	599.82	<0.0001	Significant
B-Sonication time	1151.49	1	1151.49	111.06	0.0001	Significant
AB	134.56	1	134.56	12.98	0.0155	
A2	56.60	1	56.60	5.46	0.0667	
B2	19.32	1	19.32	1.86	0.2305	
Residual	51.84	5	10.37			
Lack of Fit	47.43	3	15.81	7.18	0.1248	Not Significant
Pure Error	4.41	2	2.20			
Cor Total	7657.71	10				

Figure 2 Counter Plot of Particle Size

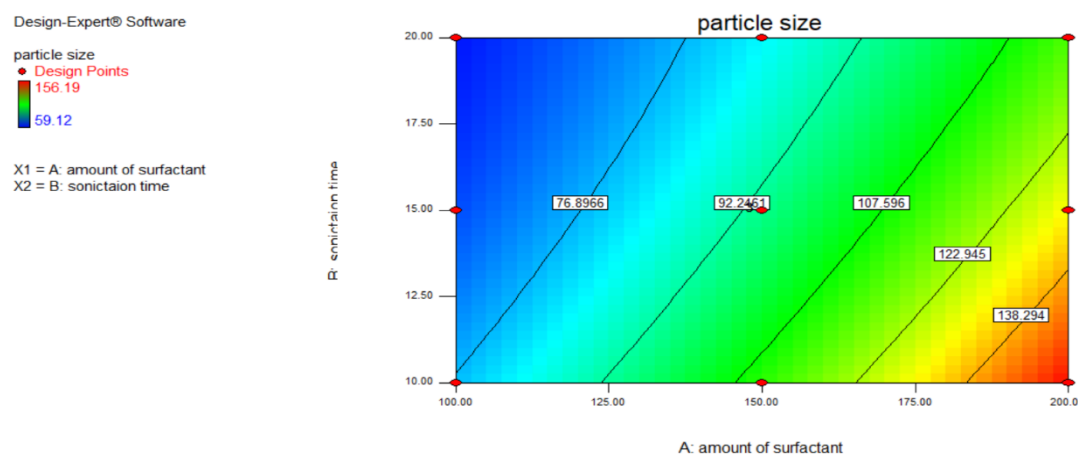
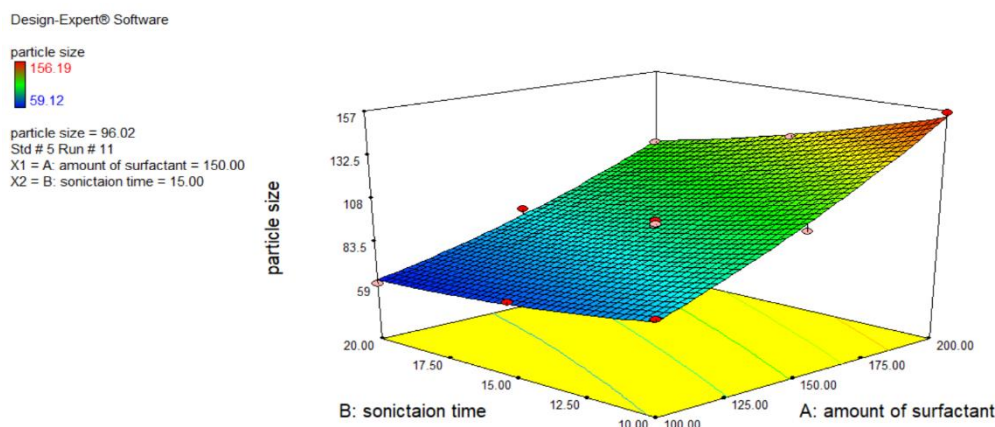


Figure 3 Response surface Plot of Particle Size



The plot showed the optimal region of the formulation by considering the particle size. In both the plots for blue region was the optimized region which shows the particle size minimum for the formulation.

Polynomial equation of Particle size

$$\text{Particle size} = +94.31 + 32.20 * A - 13.85 * B - 5.80 * A * B + 4.73 A^2 + 2.76 * B^2$$

Reduce polynomial equation

$$\text{Particle size} = +94.31 + 32.20 * A - 13.85 * B + 4.73 A^2 + 2.76 * B^2$$

$$R^2 = 0.9521$$

Discussion: The equation represents the effect of independent variables on the response i.e. particle size, which indicates that amount of surfactant has positive effect on particle size, so as the amount of surfactant increases particle size also increases. whereas sonication time has negative effect on particle size, so as the sonication time increases gradually particle size decreases.

Effect of factors on Entrapment efficiency

Table 7: ANOVA for Response surface quadratic model of Entrapment efficiency

Source	Sum of squares	df	Mean Square	F value	P value Prob > F	
Model	1868.37	5	373.67	75.22	0.0001	Significant
A-amount of edge activator	396.42	1	396.42	79.80	0.0003	Significant
B-Sonication time	232.01	1	232.01	46.71	0.0010	Significant
AB	24.30	1	24.30	4.89	0.0779	
A ²	1149.15	1	1149.15	231.34	<0.0001	
B ²	1.39	1	1.39	0.28	0.6189	
Residual	24.84	5	4.97			

Lack of Fit	18.39	3	6.13	1.90	0.3630	Not significant
Pure Error	6.45	2	3.22			
Cor Total	1893.21	10				

Figure 4 Counter Plot of Entrapment efficiency

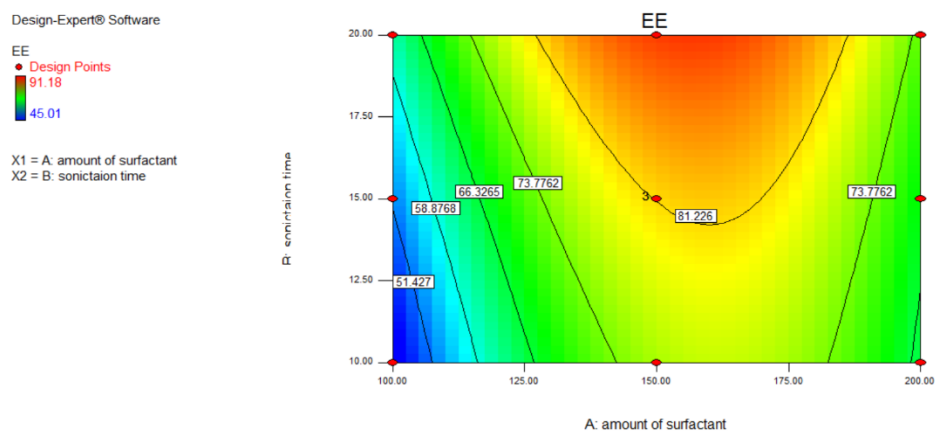
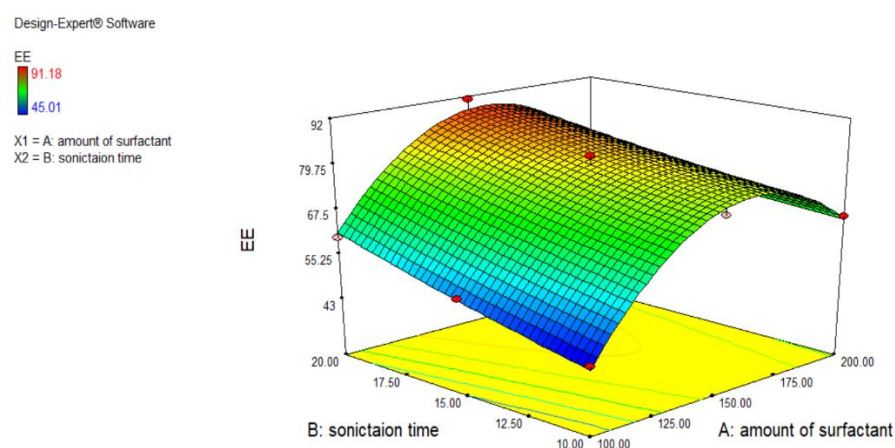


Figure 5 Response surface Plot of Entrapment efficiency



To get the effective formulation, maximum Entrapment efficiency should be done on formulation. In above response surface plot, orange area showed the maximum Entrapment efficiency.

Polynomial equation of Entrapment efficiency

$$\text{Entrapment efficiency} = +81.35 + 8.13 * A + 6.22 * B - 2.47 * A * B - 21.30 A^2 + 0.74 * B^2$$

Reduce polynomial equation

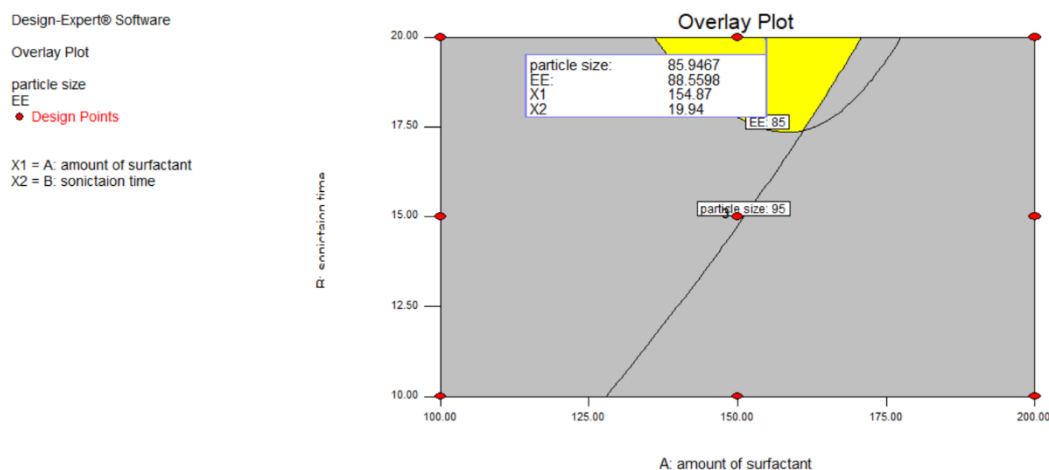
$$\text{Entrapment efficiency} = +81.35 + 8.13 * A + 6.22 * B - 21.30 A^2 + 0.74 * B^2$$

$$R^2 = 0.9371$$

Discussion: The equation represents the effect of independent variables on the response i.e. entrapment efficiency, which indicates that amount of surfactant and sonication time have

positive effect on entrapment efficiency, so as the amount of surfactant and sonication time increase entrapment efficiency also increases.

Figure 6 Overlay plot of Particle size and Entrapment efficiency



Check Point method

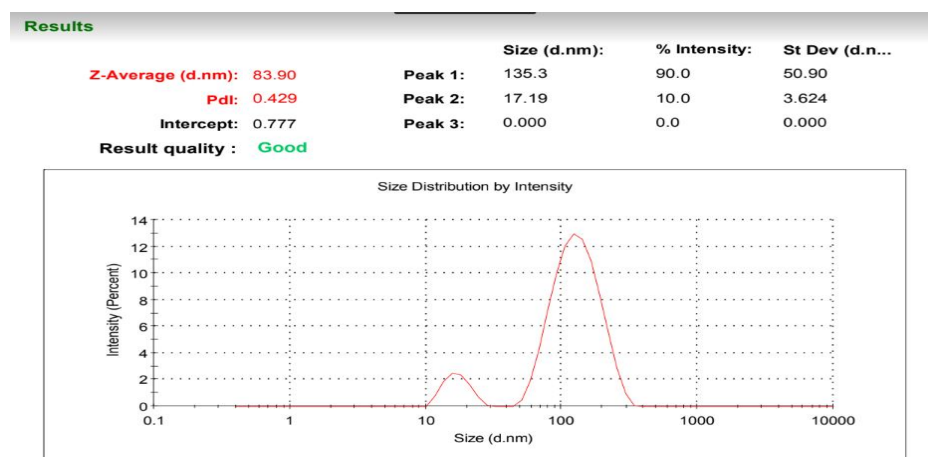
Check point batch was prepared by taken amount of edge activator 150 mg and sonication time 20 minutes (C1 batch). Actual check point batch was based on overlay plot in that amount of edge activator 154.87 mg and Sonication time was 19.94 minutes.

Table 8: Comparison of result of performed Check point batch (C1 batch) with Actual check point batch (C2 batch) and Optimized batch (F3 batch)

	Y1: Particle size (nm)	Y2: Entrapment Efficiency (%)
Performed Check point batch (C1 batch)	83.9+1.26	90.55+1.05
Actual check point batch (C2 batch)	85.94	88.55
Optimized batch (F8 batch)	87.75+3.74	91.18+2.71

From the analysis it was shown that there were no significant difference between actual and performed value on responses Y1 and Y2. So the close resemblance between the experimental and predicted response value assessed the robustness of prediction. Thus F8 batch was selected as optimized batch as transferosome formulation.

Figure 7 Particle Size graph of Performed Check Point Batch



7. CONCLUSION

It can be concluded that the application of experimental design is helpful tool for the development of Curcumin Transferosomes. During the preliminary studies, it was found that there are various factors that affect the preparation of Transferosomes. 3² Full Factorial design was employed as the optimization technique to determine the most significant factors that affected the formulation of Transferosomes using Design-Expert v7.0.0 software. In this study amount of edge activator and sonication time plays an important role for the preparation of Transferosomes. From the screening study formulation containing PHOSPHOLIPON 90G have good entrapment efficiency and vesicle size compare to PHOSPHOLIPON 90H.

The dependent responses including entrapment efficiency and vesicle size were evaluated and results were statistically analyzed by Design expert software. The batch F8 gave highest entrapment efficiency and good vesicle size.

REFERENCES

1. Sharma, M. (2019). Transdermal and intravenous nano drug delivery systems: present and future. In *Applications of targeted nano drugs and delivery systems* (pp. 499-550). Elsevier.
2. Ogihara-Umeda, I., Sasaki, T., Toyama, H., Oda, K., Senda, M., & Nishigori, H. (1997). Rapid diagnostic imaging of cancer using radiolabeled liposomes. *Cancer detection and prevention*, 21(6), 490-496.
3. Prajapati, S. T., Patel, C. G., & Patel, C. N. (2011). Transferosomes: a vesicular carrier system for transdermal drug delivery. *Asian Journal of Biochemical and Pharmaceutical Research*, 2(1), 507-524.
4. Patel, R., Singh, S. K., Singh, S., Sheth, N. R., & Gendle, R. (2009). Development and characterization of curcumin loaded transferosome for transdermal delivery. *Journal of pharmaceutical sciences and research*, 1(4), 71.
5. Sheraz, M. A., Ahmed, S., Ahmad, I., Shaikh, R. H., Vaid, F. H. M., & Iqbal, K. (2011). Formulation and Stability of Ascorbic Acid in Topical Preparations. *Surgical Neurology International*, 2(2).
6. Gupta, T., Singh, J., Kaur, S., Sandhu, S., Singh, G., & Kaur, I. P. (2020). Enhancing bioavailability and stability of curcumin using solid lipid nanoparticles (CLEN): A covenant for its effectiveness. *Frontiers in bioengineering and biotechnology*, 8, 879.
7. Patel, R., Singh, S. K., Singh, S., Sheth, N. R., & Gendle, R. (2009). Development and characterization of curcumin loaded transferosome for transdermal delivery. *Journal of pharmaceutical sciences and research*, 1(4), 71.
8. Boateng, J. S., Matthews, K. H., Stevens, H. N., & Eccleston, G. M. (2008). Wound healing dressings and drug delivery systems: a review. *Journal of pharmaceutical sciences*, 97(8), 2892-2923.
9. Strodbeck, F. (2001). Physiology of wound healing. *Newborn and infant nursing reviews*, 1(1), 43-52.
10. Tatsioni, A., Balk, E., O'Donnell, T., & Lau, J. (2007). Usual care in the management of chronic wounds: a review of the recent literature. *Journal of the American College of Surgeons*, 205(4), 617-624e57.
11. Shetty, T., Dubey, A., Ravi, G. S., Hebbar, S., Shastri, C. S., & Charyulu, N. (2017). Antifungal and antioxidant therapy for the treatment of fungal infection with microemulsion gel containing curcumin and vitamin C. *Asian J Pharm*, 11(Suppl), S717-S725.
12. Vasanth, S., Dubey, A., GS, R., Lewis, S. A., Ghate, V. M., El-Zahaby, S. A., & Hebbar, S. (2020). Development and investigation of vitamin C-enriched adapalene-loaded

- transfersome gel: a collegial approach for the treatment of acne vulgaris. *AAPS PharmSciTech*, 21(2), 1-17.
13. Arora, R. I. Y. A., Aggarwal, G. E. E. T. A., Dhingra, G. A., & Nagpal, M. A. N. J. U. (2019). Herbal active ingredients used in skin cosmetics. *Asian J. Pharm. Clin. Res*, 12(9), 7-15.
 14. Patel, N. A., Patel, N. J., & Patel, R. P. (2009). Formulation and evaluation of curcumin gel for topical application. *Pharmaceutical Development and Technology*, 14(1), 83-92.
 15. Sahu, J. P., Khan, A. I., Maurya, R., & Shukla, A. K. (2019). Formulation development and evaluation of Transferosomal drug delivery for effective treatment of acne. *Advance Pharmaceutical Journal*, 4(1), 26-34.
 16. Thakur, N., Jain, P., & Jain, V. (2018). Formulation development and evaluation of transferosomal gel. *Journal of Drug Delivery and Therapeutics*, 8(5), 168-177.
 17. Gayathri, H., & Sangeetha, S. (2022). PHARMACEUTICAL DEVELOPMENT OF TAMOXIFEN CITRATE LOADED TRANSFEROSOMAL GEL FOR SKIN CANCER BY DOE APPROACH. *Journal of Positive School Psychology*, 1879-1890.

PCP435

**TO STUDY THE DEVELOPMENT OF
PHYTOPHARMACEUTICAL MEDICATED JELLY
FORMULATION OF CURCUMIN AND TULSI AND ITS
REGULATORY ASPECTS IN INDIA**

AP0451

Rutvi Tandel

M.PHARM Student,
Department of Drug Regulatory Affairs,
Graduate School of Pharmacy-GTU
rutvirtandel@gmail.com

AP0413

Asmatbanu Pathan

Assistant Professor,
Department of Drug Regulatory Affairs,
Graduate School of Pharmacy-GTU
asmatbanu236@gmail.com

Abstract

Phytopharmaceuticals are a novel class of medication developed using advanced techniques of solvent extraction, fractionation, potentiating steps, modern formulation development, etc. The most preferred route for better patient compliance and easy administration is oral route. Difficulties in swallowing oral formulations are common among all age groups, especially in elderly and paediatrics. Medicated oral jellies are the most attractive dosage forms for all age groups and can be ingested without water. Present study was aimed to formulate oral medicated jelly formulation of Curcumin and Tulsi using polymer like pectin with various pharmacological activities including the antioxidant, and anti-inflammatory effects, immunomodulatory agent, anti-cancer agent and describe regulatory requirements of Phytopharmaceutical drugs in India. Thus, the study confirmed that the oral medicated jelly formulation of Curcumin and Tulsi can be used as a possible alternative to recently available oral formulations.

Keywords: Phytopharmaceutical drug, Curcumin, Tulsi, Medicated jelly.

PCP439

ESTIMATION OF HEAVY METALS AND EVALUATION OF MICROBIAL CONTAMINATION IN SHATAVARI TABLETS

AP0442

Ms. Vanessa James

Shree Swaminarayan Sanskar Pharmacy College,
Gujarat Technological University
Gujarat Technological University
vanessajames807@yahoo.com

AP0466

Dr. Hiral Panchal

PhD Research Scholar
Professor & HOD (Quality Assurance),
Shree Swaminarayan Sanskar Pharmacy
College,
hir_panchal@ymail.com

Abstract

Herbal formulations are widely consumed across the World and even in India due to their therapeutic benefits. Shatavari tablets of different brands were collected from herbal stores. Shatavari tablets are consumed due to their various benefits. The aim of the study is the estimation of heavy metals and the evaluation of microbial contamination of different brands of Shatavari tablets. Heavy metals estimation was carried out by Inductively Coupled Plasma Mass spectroscopy with microwave assisted sample digestion. Microbial evaluation was carried out as per procedure mentioned in Ayurvedic Pharmacopoeia. Mercury content in one sample of Shatavari tablets was not within acceptable level mentioned in Ayurvedic Pharmacopoeia. The microbial determination complies with the standards of Ayurvedic Pharmacopoeia. Regular quality control of Shatavari tablets should be performed to ensure heavy metals are within the acceptable level.

Key Words: Tablets, Microbial determination, Heavy metals

1. INTRODUCTION

Herbal formulations are widely consumed throughout the world for the treatment and prevention of chronic diseases and several ailments ¹. In India, people tend to depend on traditional medicine on regular basis for improving immunity, improving stomach problems, cosmetic purposes etc. Herbal products contain parts of plants or herbs or a combination of other plants as active ingredients. However, the safety of herbal medicines is compromised by a lack of quality controls, and inappropriate manufacturing, packaging and storage conditions ².

Trace elements such as Iron, Manganese, Zinc and Copper are required for certain physiological functions in the human body ³. Heavy metals like Cadmium, Arsenic, Lead, and Mercury are very toxic to humans causing hepatotoxicity, cardiovascular diseases, diabetes mellitus, cancer, etc.⁴. Heavy metals contamination could be due to various reasons such as the usage of fertilizers and pesticides, waste disposal, industrial processes like mining and smelting, etc. ^{5,6}. Heavy metals are not easily metabolized by human body and gets accumulated in tissues causing health troubles⁷.

It is also essential to evaluate herbal medicines for their microbial contamination as this could be the cause of gastroenteritis, diarrhoea and food poisoning ⁸. The lack of routine checks for contaminants may pose risks to human health. Quality and safety assessment requirements of herbal formulations should be in place for microbial contamination and heavy metals ⁹. The

World Health Organization (WHO) has set guidelines for contaminants and residues and their acceptable limits for herbal medicines.¹⁰

The extract obtained from the roots of the Shatavari plant is used to prepare Shatavari tablets. Shatavari's (Wild asparagus) scientific name is *Asparagus racemosus* Willd. and Family is Liliaceae¹¹. Shatavari plant is extensively cultivated in tropical and subtropical parts of India¹². Shatavari has shown galactogogue activity by increasing prolactin levels.¹³ *Asparagus racemosus* is beneficial in nervous disorders, dyspepsia, diarrhoea, hyperacidity, ulcers, cough, bronchitis and various diseases^{14, 15}. Shatavari has been reported to have Antibacterial activity¹⁶, Antiprotozoal activity¹⁷, Hepatoprotective activity¹⁸, Antioxidant activity¹⁹, Anti-inflammatory activity²⁰, Antidepressant activity²¹. Shatavari has significant role in Immunomodulatory and immunoadjuvant potential activity^{22, 23}.

The aim of the study is the estimation of heavy metals and the evaluation of microbial contamination in three brands of Shatavari Tablets. Estimation of heavy metals was carried out by Inductively Coupled Plasma Mass Spectroscopy and evaluation of microbial contamination was carried out as per Ayurvedic Pharmacopoeia.

2. MATERIALS and METHODS

2.1 Sample collection

Three different brand formulations of Shatavari tablets were selected for the present study. Three samples of Shatavari Tablets were considered for heavy metal and microbial analysis. Samples of Shatavari Tablets (ST1, ST2, ST3) were collected from herbal stores in Ahmedabad city.

2.2 Chemicals and reagents

Nitric acid Ultrapure grade, Hydrogen peroxide 30 %, Milli – Q Ultrapure Water, and Heavy metal Certified Reference Material were used for the analysis of the heavy metals.

Sterile buffered Sodium chloride peptone solution pH 7, Nutrient agar medium, Soyabean casein digest agar medium, Cetrimide Agar medium, Baird Parker Agar medium, MacConkey agar medium, Xylose-lysine-deoxy-cholate agar medium, Brilliant Green Agar and Bismuth Sulphate Agar medium were used for the evaluation of microbial contamination.

2.3 Heavy metal analysis

Microwave-assisted sample digestion was carried out in Microwave digester for Shatavari Tablets. 0.50 g sample is powdered and taken in a digestion container. Nitric acid and Hydrogen peroxide reagents were used for the digestion of the sample. Nitric acid and hydrogen peroxide blanks were considered in every digestion series. 4 ml of HNO₃: 1 ml H₂O₂ to each container. The samples were diluted with Milli Q water and used in the quantitative determination of heavy metals by ICP-MS.

2.4 Quantitative elemental analysis

The stock solution of individual samples was prepared and a 0.5 mg/l concentration of working standards were prepared in 4% nitric acid.

Calibration standards of 0.001, 0.002, 0.004, 0.008, 0.016, and 0.032 mg/ml were prepared by diluting the working standard solution. Standard curves of Arsenic, Cadmium, Mercury, and Lead are shown in Figure 1. The concentration of samples was calculated as parts per million and is shown in Table 1.

Figure 1 Standard curves for Arsenic, Cadmium, Mercury and Lead

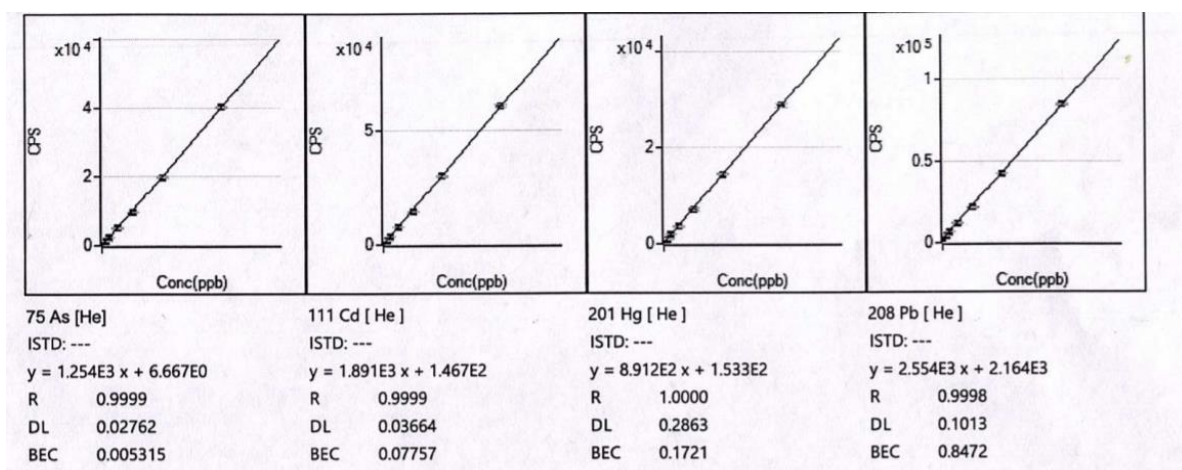


Table 1: Results of Heavy metals in Shatavari Tablets

Heavy metals	Limit of Heavy metals as per Ayurvedic Pharmacopoeia (ppm)	ST1	ST2	ST3
Lead	10	1.36	0.08	2.68
Arsenic	3	0.65	0.09	BLQ
Cadmium	0.3	BLQ	BLQ	BLQ
Mercury	1	1.98	0.30	0.065

2.5 Evaluation of Microbial contamination

Microbiological testing was performed as per the procedure in the Ayurvedic Pharmacopoeia. Tests included for analysis were Total plate count, Yeast and Mould count, Escherichia coli, Staphylococcus aureus, Salmonella, and Pseudomonas aeruginosa for the presence of pathogens in samples.

2.6 Media preparation and Inoculation

The media mentioned were procured and prepared as per Ayurvedic Pharmacopoeia. Media were sterilized in Autoclave. Media were transferred to the aseptic area with laminar air flow after inoculation with samples.

The samples ST1, ST2 and ST3 were separately transferred to 50 ml sterile media under a laminar flow cabinet. For Total plate count and yeast and mould count, the serial dilutions of samples were carried out. The media which were inoculated with samples were mixed homogeneously and kept in incubators to cultivate and preserve microbial plates for 1-5 days as per Ayurvedic Pharmacopoeia.

3. RESULTS and DISCUSSION

3.1 Heavy metal analysis

The samples ST2 and ST3 were found to be safe for human consumption. The sample ST1 was above the permissible limit of Ayurvedic Pharmacopoeia.

Mercury concentration was obtained in **1.98 ppm** which is above permissible limit (1 ppm) of Ayurvedic Pharmacopoeia.

Lead was found to be below Ayurvedic Pharmacopoeia permissible limit in all samples. Arsenic was below permissible limits of Ayurvedic Pharmacopoeia in all samples.

Cadmium was found to be below quantitation limit in all samples of Shatavari Tablets.

Heavy metals in herbal medicines could be due to industrial emissions, use of fertilizers, composition of soil, waste water for irrigation and various reasons²⁴. The heavy metals in medicines could be due to improper manufacturing process, raw material contamination or adulteration and storage conditions²⁵. Measures to follow safety standards and possible sources of contamination should be evaluated. Authorities should create awareness for benefits and side effects of herbal medicines to consumers and storage practices for manufacturers and retailers. Manufacturers should also ensure proper manufacturing practices and quality testing for finished herbal medicines.

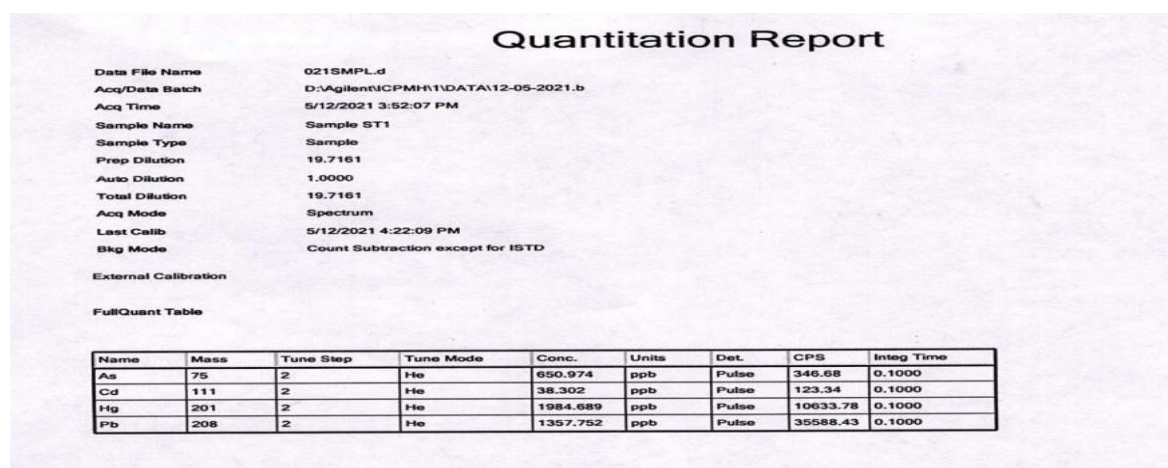


Figure 2: Quantitation report of ST1 sample

3.2 Microbiological contamination

Table 2: Results of Microbial Contamination in Shatavari Tablets

Microbial Tests	Limit of Microbial contamination as per Ayurvedic Pharmacopoeia (ppm)	ST1	ST2	ST3
Total Plate Count cfu/g	10 ⁵ /g	18000 cfu	50 cfu	480 cfu
Yeast and mould count cfu/g	10 ³ /g	<10	<10	30
Staphylococcus aureus	Absent	Absent	Absent	Absent
Salmonella	Absent	Absent	Absent	Absent
Pseudomonas aeruginosa	Absent	Absent	Absent	Absent
E. coli	Absent	Absent	Absent	Absent

Total aerobic plate count and Total Yeast and Mould count was within the allowable limit mentioned in Ayurvedic Pharmacopoeia for all samples of Shatavari tablets.

Staphylococcus aureus, Salmonella, Pseudomonas aeruginosa and E.coli tests were found to be absent in all Shatavari Tablets samples. Quality checks need to be regularly performed and proper storage conditions should be maintained at all outlets.

4. CONCLUSION

Shatavari tablets samples ST2 and ST3 were found to be safe for human consumption. Mercury in ST1 sample poses serious threat to human health. Heavy metals variation in Churna could be due to contamination in raw materials and process due to improper handling and storage practices. Herbal manufacturers should ensure routine quality tests and proper packaging of finished products along with their storage. Awareness amongst consumers about health risks should be carried out for herbal medicines.

REFERENCES

1. Ekor, M., The growing use of herbal medicines: issues relating to adverse reactions and challenges in monitoring safety. *Front Pharmacol* **2014**, *4*, 177.
2. Raynor, D. K.; Dickinson, R.; Knapp, P.; Long, A. F.; Nicolson, D. J., Buyer beware? Does the information provided with herbal products available over the counter enable safe use? *BMC Med* **2011**, *9*, 94.
3. Pajarillo, E. A. B.; Lee, E.; Kang, D. K., Trace metals and animal health: Interplay of the gut microbiota with iron, manganese, zinc, and copper. *Anim Nutr* **2021**, *7* (3), 750-761.
4. Jaishankar, M.; Tseten, T.; Anbalagan, N.; Mathew, B. B.; Beeregowda, K. N., Toxicity, mechanism and health effects of some heavy metals. *Interdiscip Toxicol* **2014**, *7* (2), 60-72. doi:10.2478/intox-2014-0009.
5. McConnell, J. R.; Edwards, R., Coal burning leaves toxic heavy metal legacy in the Arctic. *Proc Natl Acad Sci U S A* **2008**, *105* (34), 12140-4.
6. Yang, Y.; Wei, S.; Zhang, B.; Li, W., Recent Progress in Environmental Toxins-Induced Cardiotoxicity and Protective Potential of Natural Products. *Front Pharmacol* **2021**, *12*, 699193.
7. Alengebawy, A.; Abdelkhalek, S. T.; Qureshi, S. R.; Wang, M. Q., Heavy Metals and Pesticides Toxicity in Agricultural Soil and Plants: Ecological Risks and Human Health Implications. *Toxics* **2021**, *9* (3).
8. Kalumbi, M. H.; Likongwe, M. C.; Mponda, J.; Zimba, B. L.; Phiri, O.; Lipenga, T.; Mguntha, T.; Kumphanda, J., Bacterial and heavy metal contamination in selected commonly sold herbal medicine in Blantyre, Malawi. *Malawi Med J* **2020**, *32* (3), 153-159.
9. Organization, W. H., *WHO global report on traditional and complementary medicine 2019*. World Health Organization: **2019**.
10. Organization, W. H., *WHO guidelines for assessing quality of herbal medicines with reference to contaminants and residues*. World Health Organization: **2007**.
11. Alok, S.; Jain, S. K.; Verma, A.; Kumar, M.; Mahor, A.; Sabharwal, M., *Plant profile, phytochemistry and pharmacology of Asparagus racemosus (Shatavari): A review*. *Asian Pac J Trop Dis*. **2013** Jun;3(3):242-51.
12. Bopana, N.; Saxena, S., Asparagus racemosus - Ethnopharmacological evaluation and conservation needs. *Journal of ethnopharmacology* **2007**, *110*, 1-15. doi:10.1016/j.jep.2007.01.001.
13. Gupta, M.; Shaw, B., A Double-Blind Randomized Clinical Trial for Evaluation of Galactogogue Activity of Asparagus racemosus Willd. *Iran J Pharm Res* **2011**, *10* (1), 167-72.
14. Sairam, K.; Priyambada, S.; Aryya, N. C.; Goel, R. K., Gastroduodenal ulcer protective

- activity of *Asparagus racemosus*: an experimental, biochemical and histological study. *J Ethnopharmacol* **2003**, *86* (1), 1-10.
15. Goyal, R. K.; Singh, J.; Lal, H., *Asparagus racemosus*--an update. *Indian J Med Sci* **2003**, *57* (9), 408-14.
 16. Mandal, S. C.; Nandy, A.; Pal, M.; Saha, B. P., Evaluation of antibacterial activity of *Asparagus racemosus* willd. root. *Phytother Res* **2000**, *14* (2), 118-9.
 17. Roy, R.; Bhagwager, S.; Chavan, S.; Dutta, N. J. J. R. I. M., Preliminary pharmacological studies on extracts of root of *Asparagus racemosus* (Satavari), Willd, Lilliaceae. *J Res Indian Med* **1971**, *6*, 132-138.
 18. Zhu, X.; Zhang, W.; Zhao, J.; Wang, J.; Qu, W., Hypolipidaemic and hepatoprotective effects of ethanolic and aqueous extracts from *Asparagus officinalis* L. by-products in mice fed a high-fat diet. *J Sci Food Agric* **2010**, *90* (7), 1129-35.
 19. Kamat, J. P.; Bloor, K. K.; Devasagayam, T. P.; Venkatachalam, S. R., Antioxidant properties of *Asparagus racemosus* against damage induced by gamma-radiation in rat liver mitochondria. *J Ethnopharmacol* **2000**, *71* (3), 425-35.
 20. Plangsombat, N.; Rungsardthong, K.; Kongkanermit, L.; Waranuch, N.; Sarisuta, N., Anti-inflammatory activity of liposomes of *Asparagus racemosus* root extracts prepared by various methods. *Exp Ther Med* **2016**, *12* (4), 2790-2796.
 21. Singh, G. K.; Garabadu, D.; Muruganandam, A. V.; Joshi, V. K.; Krishnamurthy, S., Antidepressant activity of *Asparagus racemosus* in rodent models. *Pharmacol Biochem Behav* **2009**, *91* (3), 283-90.
 22. Gautam, M.; Saha, S.; Bani, S.; Kaul, A.; Mishra, S.; Patil, D.; Satti, N. K.; Suri, K. A.; Gairola, S.; Suresh, K.; Jadhav, S.; Qazi, G. N.; Patwardhan, B., Immunomodulatory activity of *Asparagus racemosus* on systemic Th1/Th2 immunity: implications for immunoadjuvant potential. *J Ethnopharmacol* **2009**, *121* (2), 241-7.
 23. Sharma, P.; Chauhan, P. S.; Dutt, P.; Amina, M.; Suri, K. A.; Gupta, B. D.; Suri, O. P.; Dhar, K. L.; Sharma, D.; Gupta, V.; Satti, N. K., A unique immuno-stimulant steroidal sapogenin acid from the roots of *Asparagus racemosus*. *Steroids* **2011**, *76* (4), 358-64.
 24. Briffa, J.; Sinagra, E.; Blundell, R., Heavy metal pollution in the environment and their toxicological effects on humans. *Heliyon* **2020**, *6* (9), e04691.
 25. Mukhopadhyay, S.; Abraham, S. E.; Holla, B.; Ramakrishna, K. K.; Gopalakrishna, K. L.; Soman, A.; Chikkanna, U. C.; Bharath, M. M. S.; Bhargav, H.; Varambally, S.; Gangadhar, B. N., Heavy Metals in Indian Traditional Systems of Medicine: A Systematic Scoping Review and Recommendations for Integrative Medicine Practice. *J Altern. Complement. Med. (New York, N.Y.)* **2021**, *27* (11), 915-929.

PCP441

Cerebroprotective Effect of *Pistia Stratiotes L.* against Cerebral Ischemic Reperfusion Injury

AP0469 Rumana Patel Research Scholar Parul Institute of Pharmacy, Faculty of Pharmacy, Parul University, Vadodara, Gujarat. rumin55540@gmail.com	AP0470 Naisargi Pathak Research Scholar Parul Institute of Pharmacy, Faculty of Pharmacy, Parul University, Vadodara, Gujarat. pathaknaisargi05@gmail.com	AP0472 Dr. Jitendra Vaghasiya Professor Parul Institute of Pharmacy, Faculty of Pharmacy, Parul University, Vadodara, Gujarat. j_vaghasiya@yahoo.com
--	--	--

Abstract

Pistia Stratiotes L. (PS) is well reported to modify inflammatory response, oxidative stress which are key pathophysiological finding of cerebral reperfusion injury, alongside it is reported to reduce cholesterol and blood glucose levels, and therefore present work was designed to investigate the effect of PS on cerebral reperfusion injury in normal and diabetic rats. Each protocol comprised cerebral ischemia (CI) for 30 min followed by reperfusion (R) for 1 h. Animals were treated with PS (50 mg/kg p.o.) for seven days. At the end of the experiment, brain tissue was utilized for the measurement of oxidative stress markers, inflammatory response, infarct size and histopathological findings. PS treated rats demonstrated a significant reduction in infarct sizes ($p < 0.05$) when compared with CI/R and Diabetic CI/R (DCI/R) group of rats. PS treatment demonstrated a significant decreased in malondialdehyde ($p < 0.05$), nitric oxide ($p < 0.05$) and blood glucose levels ($p < 0.001$) and a significant increase in the level of reduced glutathione, superoxide ($p < 0.01$) dismutase catalase ($p < 0.01$) and insulin levels ($p < 0.001$), indicated modification in oxidative stress. PS treatment confirmed a significant decrease in myeloperoxidase ($p < 0.01$), C - reactive protein ($p < 0.05$) and TNF- α ($p < 0.01$) levels indicated a change in the inflammatory response. Histopathological findings revealed a reversal of damage in PS treated rats. PS treatment reduced DNA fragmentation of brain tissue of PS was found to normal and diabetic rats. The result of present study demonstrated that PS showed cerebro-protective against CI/R along with DCI/R group of rats by anti-inflammatory and antioxidant activities.

Keywords: Diabetes Mellitus Type 2; *Pistia Stratiotes*; Cerebral Ischemia Reperfusion Injury; Inflammatory Response; Oxidative Stress

Introduction

Type 2 Diabetes Mellitus (T2DM) is associated with an increased risk of cerebral complications. Diabetic patients are at a higher risk for ischemic conditions caused by decreased blood flow.^[1] Cerebral injury caused by ischemia-reperfusion (I/R) during surgery may induce cell death, which is considered essential in developing dysfunction and traumatic events in ischemic neuropathy. I/R is worsening cellular dysfunction and death following the restoration of blood flow to previously ischaemic tissues.^[2] The reestablishment of blood flow is essential to salvage ischaemic tissues. However, reperfusion itself paradoxically causes further damage, threatening the function and viability of the organ. I/R occurs in many organs, including the heart, lung, kidney, gut, skeletal muscle and brain. It may involve not only the ischaemic organ itself but may also induce systemic damage to organs, potentially leading to multi-system organ failure.

Cerebral ischemia/reperfusion injury (CI/RI) is a common feature of ischemic stroke, involving a period of impaired blood supply to the brain, followed by the restoration of cerebral perfusion through medical intervention. Although ischemia and reperfusion brain damage is a complex pathological process with an unclear physiological mechanism, more attention is currently focused on the neuro inflammatory response of an ischemia/reperfusion origin, and anti-inflammatory appears to be a potential therapeutic strategy following ischemic stroke. There is no doubt that CI/RI has become an increasingly critical challenge for a stroke patient. Up to date, a series of researches indicated that the main underlying mechanisms of CI/RI included inflammatory response, oxidative/nitrative stress, mitochondrial dysfunction, calcium overload, activation of apoptotic and autophagic pathways, platelet activation and aggregation, leukocyte infiltration, and complement activation.^[3-7]

Pistia stratiotes L. (PS) commonly known as water lettuce belongs to Araceae. It has been used in various medicines for the treatment of eczema, leprosy, ulcers, piles, stomach disorder, throat and mouth inflammation, a few to mention. Information regarding the uses and effects of different extract (ethanolic and methanolic) of this plant is also documented. *Pistia stratiotes* possess different useful activities like, diuretic, antidiabetic, antidermatophytic, antifungal, and antimicrobial properties against harmful diseases.^[8]⁴⁰ It has great potential for absorption of heavy metals (Fe, Zn, Cu, Cr, and Cd) without developing any toxicity or reduction in growth due to metal accumulation and has shown a wide range of tolerance to all the selected metals and therefore can be used for water purification and to combat water pollution in waste water bodies such as drainage ditches and channels carrying industrial effluents. Plant also well documented for its antioxidant and anti-inflammatory activities, hence in the present study it has been hypothesized that these plants may be effective against I/R injury.

Materials & Methodology

Animals

The Wistar Rats were housed in polypropylene cages, maintained under standardized condition (12-h light/dark cycle, 24°C, 35 to 60% humidity) and provided free access to palleted CHAKKAN diet (Nav Maharashtra Oil Mills Pvt. Ltd., Pune) and purified drinking water ad libitum. The protocol described here was approved by the Institutional Animal Ethical Committee (No PIPH16/18 921/PO/ReBi/S/05/CPCSEA) and conducted according to the guidelines of CPCSEA. Permission was obtained from the committee for the purpose of control and supervision of experiments on Animals (CPCSEA), Ministry of Social Justice and Empowerment, Government of India.

Plant materials and preparation of the extract

PS was collected from the School of Science Botany Department, Gujarat University and Authenticated by the taxonomist. The plant materials (leaves, root, shoot) were washed with distilled water and dried under shadow then plant material was chopped into small pieces. Plant materials (leaves, root, shoot) extracts were prepared using soxhlet extraction unit, a quantity

of 10gm plant materials (leaves, root, shoot) were weighed and suspended with 200 ml of solvent. The extraction for each plant material is carried out by using ethanol solvent. The extracts were dried by using rotor evaporator, which were store in a refrigerator at 4 °C until needed for analysis.^[8]

Induction of Diabetes Mellitus Type-II

T2DM was induced in rats by the administration of nicotinamide (NAD) (230 mg/kg, *i.p.*), 15 min prior to the single dose of streptozotocin (STZ) (65 mg/kg, *i.v.*).^[9] Control animals received an equal volume of saline. The STZ solution contained STZ in saline and a sodium citrate buffer, pH 4.0. Food, water consumption, weight gain, blood glucose levels and serum insulin level were recorded to monitor the degree of diabetes. Four weeks were allowed to elapse in between the induction of diabetes and ischemic injury.

Measurement of Blood Glucose Concentration and Serum Insulin

In vitro quantitative determination of blood glucose concentrations (BCG) was done using enzymatic kit (Beacon Diagnostics Pvt. Limited). Serum insulin was estimated by using commercially available radioimmunoassay kit.

Cerebral Ischemia Injury in Normal and Diabetic Rats

Rats were anesthetized by ketamine (60 mg/kg *i.p.*) and diazepam (5 mg/kg *i.p.*). Bilateral carotid arteries were exposed and occluded with thread for 30 min to induce ischemia. It was followed by reperfusion for 2 hr.⁴³ Experimental procedure and design are as follows.

Group	Group Name	Experimental Procedure
Group: 1	NSO	Normal rats underwent all surgical procedures without I/R
Group: 2	CI/R	Normal rats; Cerebral ischemia was produced for 30 min followed by reperfusion for 2hr
Group: 3	DSO	Diabetic rats underwent all surgical procedures without I/R
Group: 4	DCIR	Diabetic rats; Cerebral ischemia was produced for 30 min followed by reperfusion for 2hr
Group: 5	NPS	In Normal rats; treatment of PS (50mg/kg) ^[8] p.o was given once a day for two weeks and on the 15 th day CI/R was produced.
Group: 6	DPS	In Diabetic rats; treatment of PS (50mg/kg) ^[8] p.o was given once a day for two weeks and on the 15 th day CI/R was induced.

Determination of infarct size and area of infarction

Evaluation of infarct size carried out by 2, 3, 5-triphenyl tetrazolium chloride (TTC) staining method.^[10] Following CI/R, animals were decapitated; the brains were removed and placed in cold saline. Coronal brain slices (2 mm thick) were made. Then the slices were incubated in phosphate buffer saline (pH 7.4) containing 2% TTC at 37°C for 10 min and then kept overnight in neutral-buffered formalin. A high-resolution scanner acquired the images of the TTC-stained section. The infarct size was measured by using Primostar Trinocular Microscope and compared between treatment groups and CI/R control group of rats.^[11]

Histopathological Analysis

For histopathological analysis brain was fixed in 10% formalin and embedded in paraffin. The paraffin-embedded tissues were sectioned and stained with hematoxylin-eosin and analyzed by light microscopy. The histological sections were examined by an observer blinded to the treatment regimen, for the extent of brain tissue injury. The following morphological criteria were used to determine the histopathological damage: score 0, no damage; score 1 (mild), interstitial edema and focal necrosis; score 2 (moderate), diffuse brain cell swelling and necrosis; score 3 (severe), necrosis with the presence of contraction bands, neutrophil infiltration, and the capillaries were compressed; and score 4 (highly severe), widespread

necrosis with the presence of contraction bands, neutrophil infiltration, capillaries compressing and hemorrhage.^[12]

Estimation of oxidative stress and inflammatory response

The cerebral tissue was assayed for levels of lipid peroxidation (MDA content) and endogenous antioxidant enzymes like reduced glutathione (GSH), superoxide dismutase (SOD), catalase (CAT), glutathione peroxidase (GSHPx), xanthine oxidase (XO) activity, and nitric oxide (NO). C-reactive protein (by using diagnostic kits, Nicholas India Pvt. Ltd., India) and TNF- α (Endogen, mouse TNF- α kit, Pierce Biotech Int., Rockford, Illinois, USA) were determined at serum level. cerebral tissue analyzed for MPO activity as neutrophils infiltration.^[13-14]

DNA Fragmentation

Genomic DNA was extracted from brain tissue using a DNA extraction kit (DNeasy kit, Axygen). Ten micrograms of DNA were loaded into 1.5% agarose gel containing 0.5 mg/mL ethidium bromide. DNA electrophoresis was carried out at 80 V for 1–2 h. DNA ladders, an indicator of tissue apoptotic nucleosomal DNA fragmentation, were visualized under ultraviolet light and photographed for permanent records.^[15]

Statistical Analysis

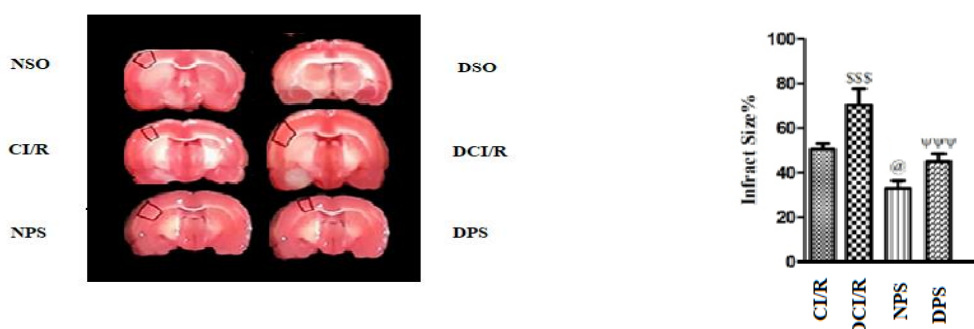
All the values are expressed as mean \pm SEM. Statistical significance was tested between more than two groups using one-way ANOVA followed by the Bonferroni multiple comparisons test by using a computer-based fitting program (Prism, Graphpad 5). Differences were considered to be statistically significant when $P < 0.05$.

Result

Effect of PS on Infarct Size and Are of Infraction

A large infarction area observed mainly in the caudal and rostral side of the hippocampus in the damaged brain of CI/R and DCI/R, whereas the infarction was markedly reduced in the rat brains treated with PS compared to CI/R and DCI/R group of rats.

Figure 1: Effect of PS on Infarct Size. Values are mean \pm SEM (n = 6), analyzed by one-way ANOVA followed by Bonferroni's multiple comparison tests, \$\$\$ denote ($P < 0.001$) for chance differences vs CI/R, @ denotes ($p < 0.05$) for chance differences vs CI/R and ^^^ denotes ($p < 0.001$) for chance differences vs DCI/R.



Effect of PS on Serum Glucose and Serum Insulin

Serum insulin and serum glucose levels were found to significantly ($p < 0.001$) far above the ground in DSO rats compared to NSO groups of rats indicated insulin resistant diabetes in rats. PS treated in the diabetic rats demonstrated significant lower serum insulin ($p < 0.001$) and glucose ($p < 0.001$) when compared CI/R and DCI/R respectively.

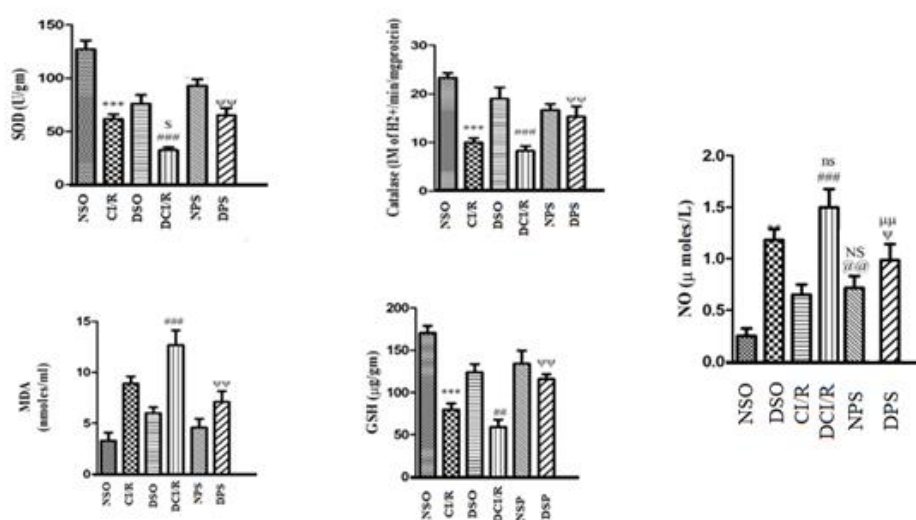
Figure 2: Effect of PS on serum glucose and insulin level during experiments. Values are mean \pm SEM (n = 6), analyzed by one-way ANOVA followed by Bonferroni's multiple comparison, \$\$\$ denote (p < 0.001) for chance differences vs CI/R, $\Psi\Psi\Psi$ denote (p < 0.001) for chance differences vs DCI/R.



Effect of PS on Oxidative Stress Markers

The MDA activity, NO level was significantly (p < 0.05) increased in CI/R, DCI/R group in comparison with the NSO, DSO group. On the other hand, the MDA activity was also found to be significantly (p < 0.05 or p < 0.001) minimized when compared in between CI/R, DCI/R in PS treated NPS and DPS groups of rats. The tissue level of SOD, CAT, GSH were decreased significantly (p < 0.001) in CI/R group in comparison with the NSO group. The SOD activity, CAT activity, GSH activity was found to be significantly (p < 0.05 or p < 0.01 or p < 0.001) increased in normal and diabetic PS treated NPS and DPS groups of rats.

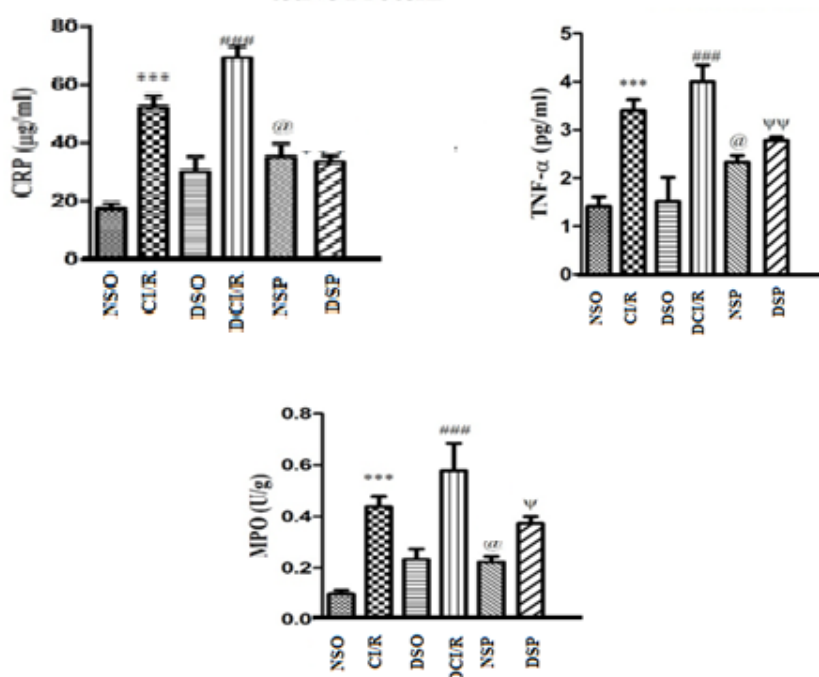
Figure 3: Effect of PS on oxidative stress markers. Values are mean \pm SEM (n = 6), analyzed by one-way ANOVA followed by Bonferroni's multiple comparison tests ***denotes (p < 0.001) significance for chance differences vs NSO, ####denotes (p < 0.001) significance for chance differences vs DSO, \$denote (p < 0.05) for chance differences vs CI/R, ## denotes (p < 0.01) for chance differences vs DSO, @@@ denotes (p < 0.001) for chance differences vs CI/R and, $\Psi\Psi$ denotes (p < 0.001) for chance difference vs DCI/R group.



Effect of PS on Inflammatory response

CRP activity, TNF- α activity, MPO activity was significantly ($p < 0.001$) raised in CI/R, DCI/R group in comparison with the NSO, DSO group. Treatment with PS to normal and diabetic rats demonstrated significant lower TNF- α ($p < 0.001$), CRP ($p < 0.05$), and MPO ($p < 0.001$) activities when compared with CI/R and DCI/R group of rats.

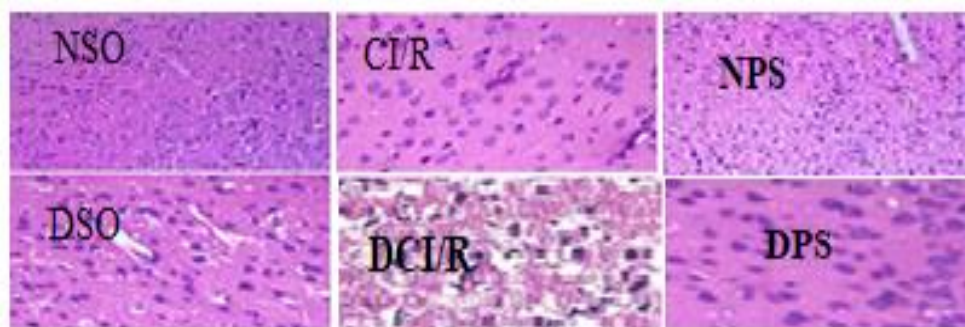
Figure 4: Effect of PS on inflammatory response. Values are mean \pm SEM ($n = 6$), analyzed by one-way ANOVA followed by Bonferroni's multiple comparison tests *** denotes ($p < 0.001$) significance for chance differences vs NSO, ### denotes ($p < 0.001$) significance for chance differences vs DSO, @ denotes ($p < 0.05$) for chance differences vs CI/R, $\Psi\Psi$ denotes ($p < 0.01$), Ψ denotes ($p < 0.05$) for chance differences vs DCI/R group of rats.



Effect of PS on Histopathological Evaluation

The photomicrographs of Brains sections stained with hematoxylin and eosin, 10X from I/R groups demonstrated lymphocytic proliferation and neuronal necrosis in CI/R, and DCI/R, as compared with NSO and DSO. There is a significant reversal of damage observed in PS treated group of rats. (Figure 5)

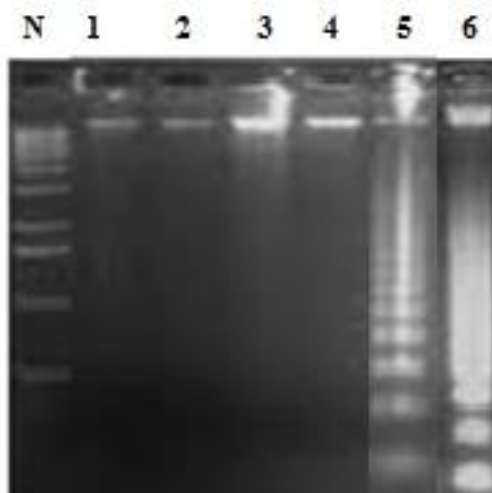
Figure 5: Effect of PS on hematoxylin and eosin-stained brain sections.



Effect of PS on DNA Fragmentation

Apoptosis was evaluated by DNA fragmentation analysis. The typical DNA laddering activity was observed in the CI/R and DCI/R groups, which indicates cell apoptosis. PS treated CI/R and DCI/R group demonstrated decreased DNA fragmentation and necrosis in comparison to the CI/R and DCI/R group respectively. (Figure 6)

Figure: 6 Effect of PS on DNA Fragmentation. 1) Normal sham- operated (NSO); 2) Cerebral ischemia/reperfusion in normal rats (CI/R), 3) Diabetic sham-operated (DSO), 4) Cerebral ischemia/reperfusion in diabetic rats (DCI/R), 5) PS treated normal rats (NPS), 6) PS treated diabetic rats (DPS)



Discussion

Several existing drugs with potential neuroprotective activity have been used or are being tested in treating stroke. However, most of them do not exhibit satisfactory clinical outcomes due to a variety of patients and drug-associated factors. For example, a series of novel drugs that interfere with distinct processes of stroke pathogenesis, such as neuron apoptosis, excitotoxicity, inflammation, and angiogenesis, are under development.^[16] These results imply that I/R causes organ injury (cerebral) and DM can exacerbate that injury, and PS treatment has a protective effect against that injury. We found significantly higher lipid peroxidation in the brain tissue of both non-diabetic and diabetic rats after induction of cerebral I/R injury, which is a major index of oxidative stress and it might be due to ROS production via inflammatory response. Inflammatory reactions are activated during the process of I/R injury, resulting in the formation of inflammatory cytokines, like TNF- α , interleukin-1 (IL-1) and arachidonic acid metabolites.^[17] Cytokines are thought to be important in the pathophysiology of cerebral injury. TNF- α mediated apoptosis is one of the proposed mechanisms for its association with organ dysfunction.^[18] In this study, we found increase in TNF- α . These increases were accompanied by increased cerebral after I/R tissue MPO activity, consistent with leukocyte infiltration and activation in the cerebral tissue.^[19] These increased in MPO activity was attenuated by selected drug treatment in present investigation demonstrated PS prevented cerebral I/R. Modifications in inflammatory response by PS treatment could also result in lower lipid peroxidation that we observed in our study, because activation of neutrophils causes the generation of ROS.

Nitrite/ nitrate levels, as the end products of nitric oxide conversion, were increased in brain tissue in diabetic animals compared to non-diabetic animals,^[20] which was confirmed by elevated NO levels in our study. PS treatment in diabetic I/R animals normalized the high tissue NO level, which might be attributed to the inhibition of inducible nitric oxide synthase (iNOS) enzyme since STZ-induced diabetes caused an increase in activity and expression of cerebral iNOS.^[21] Selected drug reported for the anti-diabetic effect may decrease activity and

expression of iNOS in cerebral tissue. The present results have verified the involvement of iNOS in the inflammatory process, and it might have a role in cerebral injury induced via activated iNOS-producing cells.

The results of the present work confirmed that the PS treatment causes a decrease in lipid peroxidation in cerebral tissue after cerebral I/R. Antioxidant enzymes like GSH, GSHPx, CAT and SOD were increased following PS treatment in cerebral tissue followed cerebral I/R in diabetic rats. Also, PS lowered elevated MPO activity in cerebral organs. Thus, PS protected against cerebral damage by preventing neutrophil activation and ROS production and decreasing XO activity. Several mechanisms might be responsible for the protective effects of PS as PS might reduce oxidative stress, as shown in our study. In addition, the PS treatment was found to be decreased cell apoptosis that signifying it might reduce nuclear oxidative stress. In addition, modification in oxidative stress and inflammatory response by PS treatment could explain the cerebral protective effect of PS. This study further strengthens our previous report's modification of oxidative stress and inflammatory response by selected drugs.

Conclusion

In conclusion, in rats, diabetes overstated I/R via oxidative stress, the inflammatory process in STZ-NAD-induced diabetes. Also, PS treatment attenuated cerebral injury induced by I/R in diabetic rats. This is the first study in which PS is used to prevent cerebral damage induced by cerebral I/R in diabetes. The prevention was shown to achieve via NO generation and neutrophil sequestration.

References

1. Amos, A. F.; McCarty, D. J.; Zimmet, P. The Rising Global Burden of Diabetes and Its Complications: Estimates and Projections to the Year 2010. *Diabetic Medicine* **1997**, *14* (S5), S7–S85. <https://doi.org/3.0.co;2-r>>10.1002/(sici)1096-9136(199712)14:5+3.0.co;2-r.
2. Hyperglycemia, Diabetes and Vascular Disease. *General Pharmacology: The Vascular System* **1993**, *24* (4), 1035. [https://doi.org/10.1016/0306-3623\(93\)90189-5](https://doi.org/10.1016/0306-3623(93)90189-5).
3. Shvedova, M.; Anfinogenova, Y.; Atochina-Vasserman, E. N.; Schepetkin, I. A.; Atochin, D. N. C-Jun N-Terminal Kinases (JNKs) in Myocardial and Cerebral Ischemia/Reperfusion Injury. *Frontiers in Pharmacology* **2018**, *9*. <https://doi.org/10.3389/fphar.2018.00715>.
4. Krenz, M.; Baines, C.; Kalogeris, T.; Korthuis, R. Cell Survival Programs and Ischemia/Reperfusion: Hormesis, Preconditioning, and Cardioprotection. *Colloquium Series on Integrated Systems Physiology: From Molecule to Function* **2013**, *5* (3), 1–122. <https://doi.org/10.4199/c00090ed1v01y201309isp044>.
5. Pan, J.; Konostas, A.-A.; Bateman, B.; Ortolano, G. A.; Pile-Spellman, J. Reperfusion Injury Following Cerebral Ischemia: Pathophysiology, MR Imaging, and Potential Therapies. *Neuroradiology* **2006**, *49* (2), 93–102. <https://doi.org/10.1007/s00234-006-0183-z>.
6. Gorsuch, W. B.; Chrysanthou, E.; Schwaeble, W. J.; Stahl, G. L. The Complement System in Ischemia–Reperfusion Injuries. *Immunobiology* **2012**, *217* (11), 1026–1033. <https://doi.org/10.1016/j.imbio.2012.07.024>.
7. Mishra, J.; Dent, C.; Tarabishi, R.; Mitsnefes, M. M.; Ma, Q.; Kelly, C.; Ruff, S. M.; Zahedi, K.; Shao, M.; Bean, J.; Mori, K.; Barasch, J.; Devarajan, P. Neutrophil Gelatinase-Associated Lipocalin (NGAL) as a Biomarker for Acute Renal Injury after Cardiac Surgery. *Lancet (London, England)* **2005**, *365* (9466), 1231–1238. [https://doi.org/10.1016/S0140-6736\(05\)74811-X](https://doi.org/10.1016/S0140-6736(05)74811-X).
8. Tulika, T.; Puneet, P.; Mala, A. Qualitative Phytochemical Analysis and Antioxidant Activity of Methonolic Extract of Eichhornia Crassipes (Mart.) Solms and

- Pistia. *International Journal of Pharmacognosy and Phytochemical Research* **2017**, 9 (5). <https://doi.org/10.25258/phyto.v9i5.8139>.
9. Masiello, P.; Broca, C.; Gross, R.; Roye, M.; Manteghetti, M.; Hillaire-Buys, D.; Novelli, M.; Ribes, G. Experimental NIDDM: Development of a New Model in Adult Rats Administered Streptozotocin and Nicotinamide. *Diabetes* **1998**, 47 (2), 224–229. <https://doi.org/10.2337/diabetes.47.2.224>.
 10. Isayama, K.; Pitts, L. H.; Nishimura, M. C. Evaluation of 2,3,5-Triphenyltetrazolium Chloride Staining to Delineate Rat Brain Infarcts. *Stroke* **1991**, 22 (11), 1394–1398. <https://doi.org/10.1161/01.str.22.11.1394>.
 11. Mehta, S. L.; Manhas, N.; Raghubir, R. Molecular Targets in Cerebral Ischemia for Developing Novel Therapeutics. *Brain Research Reviews* **2007**, 54 (1), 34–66. <https://doi.org/10.1016/j.brainresrev.2006.11.003>.
 12. Sundararajan, S.; Landreth, G. E. Antiinflammatory Properties of PPARgamma Agonists Following Ischemia. *Drug News & Perspectives* **2004**, 17 (4), 229. <https://doi.org/10.1358/dnp.2004.17.4.829049>.
 13. Slater, T. F.; Sawyer, B. C. The Stimulatory Effects of Carbon Tetrachloride and Other Halogenoalkanes on Peroxidative Reactions in Rat Liver Fractions in Vitro. General Features of the Systems Used. *The Biochemical Journal* **1971**, 123 (5), 805–814. <https://doi.org/10.1042/bj1230805>.
 14. Bryant, D.; Becker, L.; Richardson, J.; Shelton, J.; Franco, F.; Peshock, R.; Thompson, M.; Giroir, B. Cardiac Failure in Transgenic Mice with Myocardial Expression of Tumor Necrosis Factor- α . *Circulation* **1998**, 97 (14), 1375–1381. <https://doi.org/10.1161/01.cir.97.14.1375>.
 15. Abbate, A.; Morales, C.; De Falco, M.; Fedele, V.; Biondi Zoccai, G. G. L.; Santini, D.; Palleiro, J.; Vasaturo, F.; Scarpa, S.; Liuzzo, G.; Severino, A.; Baldi, F.; Crea, F.; Biasucci, L. M.; Vetovec, G. W.; Gelpi, R. J.; Baldi, A. Ischemia and Apoptosis in an Animal Model of Permanent Infarct-Related Artery Occlusion. *International Journal of Cardiology* **2007**, 121 (1), 109–111. <https://doi.org/10.1016/j.ijcard.2006.08.077>.
 16. Hagar, H. H. Folic Acid and Vitamin B12 Supplementation Attenuates Isoprenaline-Induced Myocardial Infarction In Experimental Hyperhomocysteinemic Rats. *Pharmacological Research* **2002**, 46 (3), 213–219. [https://doi.org/10.1016/s1043-6618\(02\)00095-6](https://doi.org/10.1016/s1043-6618(02)00095-6).
 17. Gesquière, L.; Loreau, N.; Minnich, A.; Davignon, J.; Blache, D. Oxidative Stress Leads to Cholesterol Accumulation in Vascular Smooth Muscle Cells. *Free Radical Biology and Medicine* **1999**, 27 (1-2), 134–145. [https://doi.org/10.1016/s0891-5849\(99\)00055-6](https://doi.org/10.1016/s0891-5849(99)00055-6).
 18. Bryant, D.; Becker, L.; Richardson, J.; Shelton, J.; Franco, F.; Peshock, R.; Thompson, M.; Giroir, B. Cardiac Failure in Transgenic Mice with Myocardial Expression of Tumor Necrosis Factor- α . *Circulation* **1998**, 97 (14), 1375–1381. <https://doi.org/10.1161/01.cir.97.14.1375>.
 19. Salas, A.; Panés, J.; Elizalde, J. I.; Granger, D. N.; Piqué, J. M. Reperfusion-Induced Oxidative Stress in Diabetes: Cellular and Enzymatic Sources. *Journal of Leukocyte Biology* **1999**, 66 (1), 59–66. <https://doi.org/10.1002/jlb.66.1.59>.
 20. Entman, M. L.; Smith, C. W. Postreperfusion Inflammation: A Model for Reaction to Injury in Cardiovascular Disease. *Cardiovascular Research* **1994**, 28 (9), 1301–1311. <https://doi.org/10.1093/cvr/28.9.1301>.
 21. Timmers, L.; Henriques, J. P. S.; de Kleijn, D. P. V.; Devries, J. H.; Kemperman, H.; Steendijk, P.; Verlaan, C. W. J.; Kerver, M.; Piek, J. J.; Doevendans, P. A.; Pasterkamp, G.; Hofer, I. E. Exenatide Reduces Infarct Size and Improves Cardiac Function in a Porcine Model of Ischemia and Reperfusion Injury. *Journal of the American College of Cardiology* **2009**, 53 (6), 501–510. <https://doi.org/10.1016/j.jacc.2008.10.033>.

PCP443

PREPARATION AND EVALUATION OF ANTIACNE HERBAL CREAM OF *TAGETES ERECTA* FLOWER PETALS

AP0478
Dr. D. B.
Meshram
Principal,
PPC, Vadodara
GTU
dbmeshram@y
ahoo.com

AP0480
Ms. Prachi K.
Rathod
Student,
Pioneer
Pharmacy
College,
Vadodara
GTU
prachi.k.rathod@
gmail.com

AP0479
Mrs. Rashmi
Rajeghorpade
Assistant Professor,
PPC, Vadodara
GTU
rashmmerajeghorpade
y@gmail.com

AP0481
Mr. Hiren Prajapati
Student,
PPC, Vadodara
GTU
prajapatihiren1201
@gmail.com

Abstract

Acne is a chronic inflammatory state, which occurs in skin due to acne vulgaris. The number of antibiotics resistant to acne including acterial strains are increasing day by day. To avoid this herbal anti-acne cream is best and safe alternative. In the present study, we formulated and evaluated anti-acne herbal cream using methanolic extract of *Tagetes erecta* (Marigold) flower petals. *Tagetes erecta* contains abundant amount of flavanoids that is responsible for showing anti-microbial activity. The antimicrobial activity of methanolic extract in different concentrations (12.5%, 50%, 100% w/v) was investigated against *Streptococcus aureus* and *Escherichia coli* by using agar well diffusion method. The results showed that 12.5%, 50% and 100% w/v extracts of *T. erecta* exhibited good antimicrobial activity by inhibiting bacterial growth which was confirmed by their zone of inhibition 22mm, 25mm and 100mm respectively. The research lays emphasis on flavanoids exhibiting anti-acne effect of *T. erecta* extracts, significantly affecting the gram positive and gram-negative bacteria. The present work confirmed the successful antimicrobial activity of *Tagetes erecta* flower petals. Three batches (F1, F2 and F3) were formulated using o/w type emulsion method. Evaluation of cream was carried out based on physical appearance, pH, viscosity, homogeneity, irritancy testing, dye test, spreadability and wetness. Among all the formulations (F1-F3), F3 had shown satisfactory results.

Keywords: *Tagetes erecta*, Antimicrobial activity, Anti-acne herbal cream, Acne vulgaris.

1 INTRODUCTION

Antibiotic resistance among bacterial strains is a serious situation. It may be so rapid that the effectiveness of common antibiotics may be lost within a span of 5 years due to genetic changes.¹ One of the surveys conducted by the World Health Organization (WHO) reports that more than 80% of the world's population still depends upon the traditional medicines for various diseases. Forced with the growing resistance of MDR microbe strains to antibiotics and other drugs, the search for alternatives is serious.¹⁻² In the past few years, the interest in Traditional Medicines from varied cultures has increased tremendously in modern countries, owing to the fact that many prescription drugs worldwide have originated from the tropical flora. Traditional plants have long been used in many parts of the world as a safe, inexpensive, and dependable alternative to chemical drugs. The lower incidence of adverse reactions in plant preparations compared to modern conventional pharmaceuticals, combined with lower cost, encourages researchers to consider plant medicines as an alternative to synthetic drugs.³

Nature has provided us with numerous medicinal plants, which have become a storehouse of remedies to cure all of mankind's ailments. Herbal plants are a rich source of health care for the prevention and treatment of various pathological states. In this article we have shed light on microbiological activity of *Tagetes Erecta* (Marigold).⁴

Figure1. TAGETES ERECTA FLOWERS



Source: <https://en.m.wikipedia.org/wiki/Tagetes>

Chemical cosmetics and skin care products are gaining attention due to their negative effects on skin and health. Chemical additives in skin care products can cause skin irritation and allergic reactions, such as the harmful effect of some skin bleaching preparations containing steroids. Herbal or medicinal plants have recently been used as a source for skin care products. Herb extracts have higher antioxidant activity and keep the skin looking not only healthy but also younger. The most significant advantage of herbal extracts in skin care is due to the presence of natural agents such as omega-3, vitamins, and flavonoids compounds such as apigenin and quercetin. Plant part extracts contain natural nutrients such as vitamin E, which keeps skin healthy.

Tagetes Erecta is an aromatic, erect, annual herb belongs to the family asteraceae, it contained a wide range of chemical constituents including saponins, triterpenes, triterpenoid esters, flavonoids, steroids, tannin, quinines, coumarins, carotenoids, amino acids, polysaccharides, essential and volatile oils and many other chemical groups. Marigold has shown prominent benefits to skin especially in terms of treating acne due to the constituent flavonoid. *Tagetes Erecta* exerted many therapeutic effects including antibacterial, antifungal, anthelmintic, antiviral, cytotoxic, antioxidant, anti-inflammatory, analgesic, hepatoprotective, cardioprotective, gastroprotective, wound healing and many other effects. The present study will highlight the chemical constituents and the antimicrobial effect of *Tagetes Erecta* especially in curing acne.⁵

2 OBJECTIVES

- To do preliminary phytochemical screening of *Tagetes erecta* flower petals extract.
- To evaluate antimicrobial activity of *Tagetes erecta* flower petals extract.
- To prepare and evaluate anti-acne herbal cream of *Tagetes erecta* flower petals extract.

3 MATERIALS AND METHODS

3.1 Collection and Authentication of Flowers

Fresh flowers of *T. erecta* were purchased from the local market and authenticated by botanist from the Department of Botany, Shardabai Pawar Mahila Mahavidyalaya, Baramati, Maharashtra.

3.2 Preparation of Extract

The shade dried *Tagetes erecta* flowers were finely powdered and extracted in soxhlet apparatus by using methanol as a solvent. The solvent used in the extraction was allowed to evaporate. The extract was kept in the dessicator until further use. Percentage yield of the extracts in methanol was found as 47.3%.⁶

Figure 2. Flowers Kept for Drying



Figure 3. Dry Powder of Marigold



Figure 4. Soxhlet Apparatus



3.3 Preliminary Phytochemical Screening

Preliminary phytochemical analysis was done to find out the active chemical principle of particular plant.

3.3.1 Test for carbohydrates:

1 ml of Molisch's reagent and a few drops of concentrated sulphuric acid were added to 2 ml of plant extract. The presence of carbohydrates was indicated by the presence of purple or reddish color.⁷

3.3.2 Test for reducing sugars:

3.3.2.1 Fehling's test- 1ml Fehling's A and 1ml Fehling's B solution was combined and boiled for 1 minute. Added the same amount of test solution. For 5-10 minutes, heat in a boiling water bath. A yellow and then a brick red precipitation were observed.

3.3.2.2 Benedict's test- In a test tube, combined an equal volume of Benedict's reagent and test solution. Kept for 5 minutes in a bath of boiling water. Depending on the amount of reducing sugar in the test solution, the solution appears green, yellow, or red.⁷

3.3.3 Test for terpenoids:

2ml of chloroform and 0.5ml of concentrated sulphuric acid were carefully added to 0.5ml of extract. The presence of terpenoids was indicated by the formation of a red brown color at the interface.⁸

3.3.4 Test for saponins(Foam Test):

When the extract was vigorously shaken with water, it produced persistent stable foam.⁸

3.3.5 Test for alkaloids:

The alcoholic extract was removed and evaporated. The residue was treated with diluted HCl. The following tests were performed after thoroughly shaking and filtering.

1. **Dragendroff's test:** A few drops of Dragendroff's reagent were added to 2-3 ml of filtrate. Orange brown precipitation was formed.
2. **Mayer's test:** 2-3 ml filtrate with a few drops Mayer's reagent yields ppt.
3. **Hager's test:** 2-3 ml filtrate with a few drops of Hager's reagent yields yellow ppt.
4. **Wagner's test:** 2-3 ml filtrate with a few drops of Wagner's reagent yields reddish brown ppt.⁷

3.3.6 Test for tannins and phenolic compounds:

A few drops of 5% FeCl₃ solution were added to 2-3 ml of aqueous or alcoholic extract, deep blue-black color, alternatively, bromine water discoloration seen.⁸

3.3.7 Test for flavonoids (Sulphuric acid test):

1. When sulphuric acid (66%) is added, flavones and flavonoid dissolve and produce a deep yellow solution. Flavones are responsible for the orange and red hues.
2. Ethanolic KOH (2ml) was added to ml of ethanolic extract of marigold flowers; the presence of flavanoids is indicated by the yellow color.

3.3.8 Test for quinones:

1 ml of concentrated sulphuric acid was added to 1 ml of extract. The presence of quinines was indicated by the formation of a red color.⁸

3.3.9 Test for coumarins:

1ml of 10% NaOH was added to 1ml of extract. The presence of coumarins was indicated by the formation of yellow color.⁸

3.3.10 Test for glycosides:

2ml of plant extract was mixed with 3ml of chloroform and 10% ammonia solution. The presence of glycosides was indicated by the formation of pink color.⁹

3.3.11 Borntrager's test:

1 ml dilute H_2SO_4 was added to 2ml extract for anthraquinone glycosides. Boiled and strained. An equal volume of chloroform was added to the cold filtrate. Shaken vigorously. The organic solvent removed. Ammonia should be added. The ammoniacal layer turns pink or red.⁶

3.4 Antimicrobial Activity

3.4.1 Preparation of inoculum

Methanolic extracts of *Tagetes erecta* flowers were tested for antimicrobial properties against Gram-positive bacteria [*Bacillus Staphylococcus aureus* (SA)] and Gram-negative bacteria [*Escherichia coli* (EC)]. For preparation of inoculum gram positive and gram negative bacteria's were provided by Microbiology laboratory section in Pioneer Pharmacy Degree College, Vadodara.¹⁰

3.4.2 Antimicrobial screening

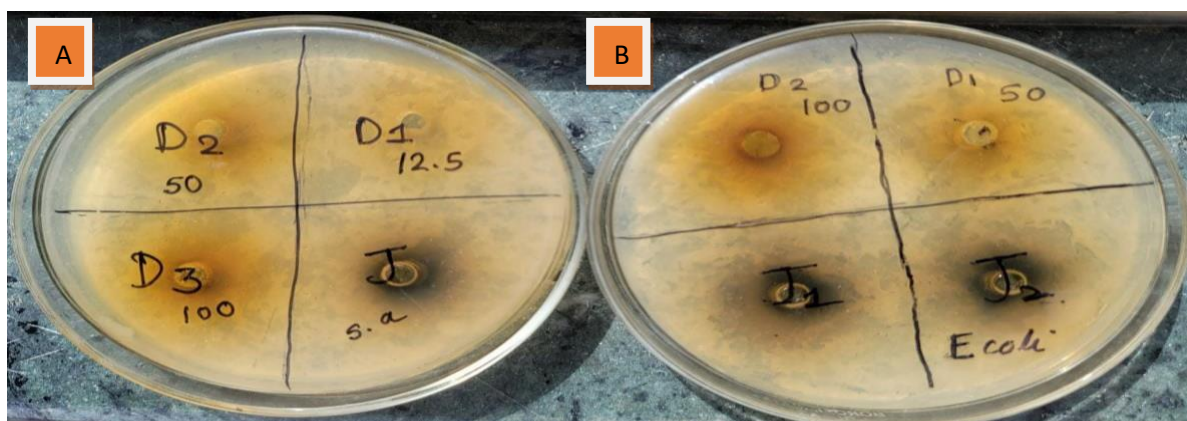
The antimicrobial activity of extracts were tested using the agar well diffusion method. For the inoculum preparation, 2 ml of fresh bacterial culture were used. The sterile Petri dish was then filled with nutrient Agar and bacteria thoroughly mixed. Upon solidification, wells were drilled into agar plates containing inoculums with a sterile cork borer (6 mm in diameter). After that, 1 ml of each extract (12.5, 50, 100% w/v) was added to the appropriate wells. The concentration of extracts (12.5, 50, and 100% w/v) was chosen based on preliminary experiments and previous literature. The plates were then incubated at 37 °C for 18 hours. Antimicrobial activity was determined by measuring the zone of inhibition (including the diameter of the wells) that appeared after incubation. DMSO at a concentration of 10% was employed as a negative control.¹¹

3.4.3 Determination of minimum inhibitory concentrations

Tagetes erecta flower extracts exhibited antimicrobial activity in all the concentrations; especially (100% w/v) concentration had exhibited maximum inhibitory action. Therefore, this concentration was taken to determine their minimum inhibitory concentrations (MIC) using agar well diffusion method. The MIC was considered as the lowest concentration which inhibited the growth of the respective microorganisms. DMSO was used as a control for methanol extracts.¹⁰

Figure 5 The Inhibition Zone (mm) of Ethanolic Extract (A, B) of *Tagetes erecta* against *Escherichia coli* (EC) (B) and *Staphylococcus aureus* (SA).

A- at concentration of 12.5, 50, 100% (w/v) (D1, D2, D3) for (SA) and B- 50,100% for (EC).



3.5 Formulation of Anti-acne Herbal Cream

Melted stearic acid in a china dish over a 70°C water bath. Potassium hydroxide and methyl paraben (methyl parahydroxybenzoate) was dissolved in water in a beaker, and then glycerin was added to it. On a water bath, this aqueous solution was heated up to 70°C. When both the aqueous and oily phases have reached the same temperature (70°C), the aqueous phase was added to the melted stearic acid while stirring continuously. Continued to stir after removing the pan from the heat. When the temperature reached 40°C, the perfume added and mixed uniformly until it cooled and became homogeneous (smooth) cream. The necessary percentage of extracts (12.5, 50, 100% w/v) was measured. Three batches of same cream base formula with different extract concentration were prepared.¹²

Figure 6 Cream Prepared using 12.5, 50, 100%w/v *Tagetes erecta* flowers extract



Table 1 Formulation of Marigold Cream

Compositions	F1	F2	F3
<i>Tagetes erecta</i> Flower extract	2ml (12.5%)	2ml (50%)	2ml (100%)
Stearic acid	5.5g	5.5g	5.5g
Potassium hydroxide	0.176g	0.176g	0.176g
Glycerine	2.2ml	2.2ml	2.2ml
Methyl paraben	0.044g	0.044g	0.044g
Perfume	q.s	q.s	q.s
Water	14.10ml	14.10ml	14.10ml

3.6 Evaluation of Cream

3.6.1 pH:

The pH of the prepared cream was measured with a pH meter and calibrated with a standard buffer solution. The pH of the cream was measured after 0.5g of cream was weighed and dissolved in 50.0 ml of distilled water.¹³⁻¹⁴

3.6.2 Physical appearance:

The physical appearance of cream was visually inspected against a dark background.¹³⁻¹⁴

3.6.3 Viscosity:

Viscosity of cream was determined using a Brookfield viscometer at 20 rpm with spindle no.64.¹⁶

3.6.4 Homogeneity:

The formulated cream was tested for homogeneity through visual appearance and touch.¹³⁻¹⁴

3.6.5 Washability:

The cream applied to the skin was easily removed by washing with tap water.¹⁴

3.6.6 Irritation test:

1cm square mark was made on the left dorsal surface of skin. The cream was applied to the designated area, and the time was recorded. Irritation, erythema, and edema were assessed and reported at regular intervals up to 24 hours.¹³

3.6.7 Dye test:

Sudan red dye was mixed with cream. A drop of the cream was placed on a microscopic slide, which was then covered with a cover slip and examined under a microscope. If the dispersed globules are red and the background is white. The cream is of the o/w variety. The opposite condition occurs in w/o type cream, in which the dispersed globules appear colorless.¹⁵

3.6.8 Spreadability:

The cream sample was applied between the two glass slides and was compressed to uniform thickness by placing 100 gm of weight for 5 minutes before adding weight to the weighing pan. The time it took the upper glass slide to move over the lower glass slide was used to calculate spreadability.¹⁴

3.6.9 Emollience:

Observation revealed that the cream did not leave any residue on the skin's surface after application.

3.6.10 Wetness:

Wetness was measured by applying cream to a human skin.

3.6.11 Determination of Moisture Content-

In a crucible, 5 g of powdered *Tagetes erecta* flowers were precisely weighed. It was dried in a hot air oven at 105 degrees Celsius. The percentage of moisture content was then calculated using the air-dried sample as a reference.¹⁷

3.6.12 Determination of Total Ash Value:

In a dried silica crucible, 5 g of powdered *Tagetes erecta* flowers were precisely weighed. It was incinerated at 450 degrees Celsius until free of carbon, and then cooled. The ash was weighed and the percentage was calculated using the air-dried sample as a reference.

3.6.13 Determination of Acid Insoluble Ash Value:

Followed procedure given in point 3.6.12 and the obtained total ash was boiled for 5 minutes in 25 ml of 2 N HCl, filtered, and the insoluble matter were collected on ashless filter paper. The residue was then washed with hot water, ignited in a silica crucible for 15 minutes at a temperature no higher than 450 C, cooled, and weighed. With reference to the air-dried sample, the percentage of acid insoluble ash was calculated.

3.6.14 Determination of Water Soluble Ash Value:

Followed procedure given in point 3.6.12. The obtained total ash was boiled for a few minutes with 25 ml of water, filtered, and the insoluble matter was collected on ashless filter paper. The residue was then washed with hot water, ignited in a silica crucible for 15 minutes at a temperature not exceeding 450 C, cooled, and weighed. The weight difference represents the water soluble ash. Finally, the percentage of water soluble ash was calculated using the air-dried sample as a reference.¹⁷

3.6.15 Determination of Alcohol and Water Soluble Extractive Value:

20 g of *Tagetes erecta* flower petals, which had been air dried and ground into a coarse powder, were macerated in 100 ml of methanol for 24 hours, stirring frequently for the first 6 hours, and then left to stand for 18 hours. Then it was quickly filtered, and measures were taken to prevent methanol loss. In a Petri dish, 25 ml of the filtrate was dried, weighted, and evaporated to dryness. With reference to the sample that had been air dried, the percentages of methanol soluble extracts were computed. For a water soluble extract, the same process as above was followed but with water instead of methanol.¹⁷

4 LITERATURE REVIEW

- 4.1 **Gupta P et al. (2012):** They discussed the genus of marigold that is *Tagetes erecta* which is a rich source of compounds with possible pharmacological values such as carotenoids that are used as food colorants, and possess anticancer and anti-ageing effects, essential oil known insecticidal properties, and summarized the biological activities and phytoconstituents of this genus.⁵
- 4.2 **Mehta D et al. (2012):** This paper discussed the genus of marigold that is *Canidia officinalis* herbal plant, having prospects of wide areas of therapeutic activity, in a way as an important medicinal source.³
- 4.3 **Shinde P et al. (2020):** The purpose of this research article is to formulate and evaluate the vanishing herbal cream.¹⁸
- 4.4 **Niyomkam P et al. (2010):** In this paper they focused on antibacterial activity of various herbal extracts on acne involved microorganism.¹⁹
- 4.5 **Vora J et al. (2019):** In this they have reviewed about *R. officinalis*, *M. chamomilla* and *A. nilotica* plant extracts could be possible to use as the natural anti-acne formulations.²⁰

5 FINDINGS

Table 2 Physical Characteristics of Extracts *Tagetes erecta* Flower Petals

Sr. No.	Solvent used	Physical Characteristics		
		Colour	Consistency	Odor
1	Methanol	Dark brown	Solid sticky	Organic

Table 3 Percentage Yield of Methanolic Extract of *Tagetes erecta* Flower Petals

Sr. No.	Solvent used	Physical Characteristics	Amount (g)

1	Methanol	Weight of dry powder (g)	30
		Weight of extract (g)	14.2
		% Yield	47.3%

Table 4 Proximate analysis

Moisture content	Ash value			Extractive value	
	Total ash	Acid Insoluble Ash	Water Soluble Ash	Methanol	Water
10%	8.6%	5.5%	3.1%	8%	9.6%

Table 5 Phytochemical Analysis of *Tagetes erecta*

Sr. No.	Phytochemical Tests	Methanolic Extract
1	Carbohydrates	+
2	Reducing Sugar : Fehling's test	+
	Benedict's test	+
3	Terpenoids	+
4	Saponins : Foam test	+
5	Alkaloids : Dragendroff's test	+
	Mayer's test	+
	Hager's test	+
	Wagner's test	+
6	Tannins and Phenolic compounds	+
7	Flavonoids : Sulphuric acid test	+
8	Quinines	+
9	Coumarins	+
10	Glycosides	+
11	Borntrager's test	-

Figure 7 Flavonoids Test



Figure 8 Terpenoids Test



Figure 9 Dragendroff's Test



Figure 10 Benedict's test

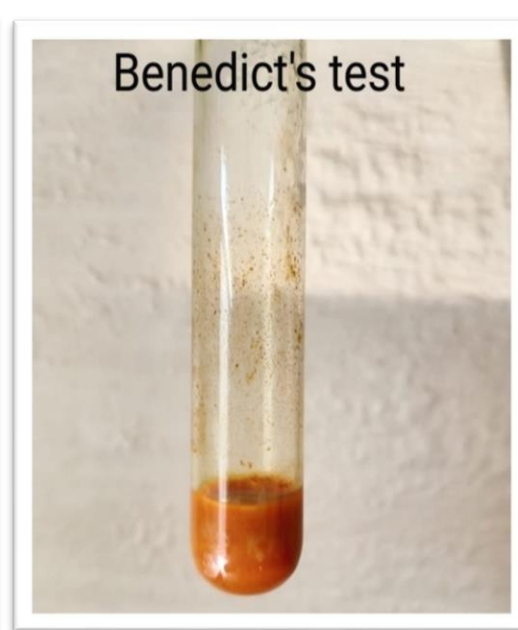


Table 6 Antimicrobial activity of methanolic extract of *Tagetes erecta* flower petals against different strains

Group of Bacterial Strains	The Bacterial Strain	<i>T. erecta</i> Extract Concentrations (w/v)	Antimicrobial activity of <i>Tagetes erecta</i> in terms of inhibition zone (IZ)
Gram +ve	<i>Staphylococcus aureus</i>	12.5%	22mm
		50%	25mm
		100%	29mm

Gram -ve	<i>Escherichia coli</i>	50%	23mm
		100%	26mm

Figure 11 Zone of Inhibition by *Tagetes erecta* Flower Petals Extracts



Table 7 Evaluation Parameters

Parameters	Observation
Viscosity At 20rpm, 64 no. spindle	1121 poise
pH	6.4
Colour	Yellow
Odour	Characteristics odour
Appearance	Smooth
Type of smear	Non-greasy
Dye Test	Positive; white globules appeared

Figure 12 Dye Test

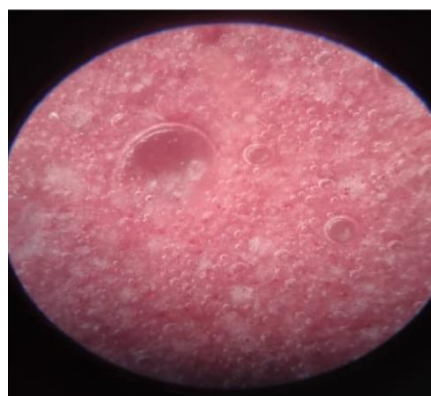


Figure 13 pH Meter



Figure 14 Brookfield Viscometer



6 CONCLUSION

The herbal anti-acne cream with extract *Tagetes erecta* (Marigold) flower petals was formulated using oil in water type emulsion method. *Tagetes erecta* is an aromatic herb which contains flavanoids which are responsible for exhibiting anti-acne property. *Tagetes erecta* extract works by reducing the oil secretions from the sebaceous glands inhibits the growth of bacteria which is a causative factor for acne. The antimicrobial activity of methanolic extract of *Tagetes erecta* in different concentrations (12.5%, 50%, 100% w/v) was investigated against *Streptococcus aureus* and *Escherichia coli* by using agar well diffusion method. The results showed that 12.5%, 50% and 100% w/v extracts of *T. erecta* exhibited good antimicrobial activity by inhibiting bacterial growth, which was confirmed by their zone of inhibition 22mm, 25mm and 100mm respectively. The research lays emphasis on flavanoids showing anti-acne effect of extracts, significantly affecting the gram positive and gram-negative bacteria. The present study concluded a successful formulation of an anti-acne cream using *Tagetes erecta* extracts which confirmed its activity to work on acne.

7 REFERENCES

1. Chandra H, Bishnoi P, Yadav A, Patni B, Mishra AP, Nautiyal AR (2017). Antimicrobial Resistance and the Alternative Resources with Special Emphasis on Plant-Based Antimicrobials - A Review. *Plants*, 6(2), pp.16.
2. Dan M, Sarmah P, Vana D, Dattatreya A (2018). Wound Healing: Concepts and Updates in Herbal Medicine. *Int J Med Res Health Sci*, 7(1), pp. 170–18.
3. Mehta D, Rastogi P, Chaudhary A. (2012). Review on Pharmacological Update: *Calendula officinalis* Linn. *Plant Activa*, (4), pp. 195-212.
4. Alsaraf K, Abbas I, Hassan E. (2019). Extraction and Clinical Application of *Calendula officinalis* L. Flowers Cream. *IOP Conference Series: Materials Science and Engineering*, (57), pp. 124-235.
5. Gupta P and Vasudeva. (2012). Marigold a Potential Ornamental Plant Drug". *Humard medicus*, 55(1), pp. 45-59.
6. Deshpande S. N. and Kadam D G. (2019). Phytochemical Analysis Extracts of *Tagetes erecta* L. And their Antibacterial Efficacy against *Streptococcus* Mutants. *Int J Pharm Biosci*, 9, pp. 70-72.

7. Sanmath B, Mehta K and Gupta A. (2016). Dispensing Pharmacy of Practical Manual. 3rd Edn, Pharmamed Press, Hyderabad, pp. 389-402.
8. R. Devika and Koilpillai J. (2012). Phytochemical Screening Studies of Bioactive Components of *Tagetes erecta*. Int J Pharm Biosci, 3(4), pp. 596-602.
9. Kumar S. R. and Dwivedi D. H. (2017). Phytochemical Screening Studies of Bioactive Compounds of African Marigold (*Tagetes erecta* L.). J Pharmacog Phytochem. 6(4), pp. 524-527.
10. Gonelimali F. D. et al. (2018). Antimicrobial Properties and Mechanism of Action of Some Plant Extracts against Food Pathogens and Spoilage Microorganisms. Frontiers in Microbiology, 1639(9), pp. 1-9.
11. Jafari B. et al. (2017). The in vitro Study of Antimicrobial Effect of Marigold (*calendula officinalis*) Extracts on Infectious Microorganisms. J Biosci, 13(4), pp. 348-352.
12. Muley B, Khadabadi S and Banarase N (2009). Phytochemical Constituents and Pharmacological Activities of *Calendula officinalis* Linn (Asteraceae): A Review. Tropical J Pharm Res, 8, pp.455-465.
13. Barethiya V, Kukde A, Badawik A. (2020). Formulation and Evaluation of Vitamin E Enriched Cold Cream with Almond Oil as an International Phase. Int J Pharm Sci Rev Res, 63(2), pp. 71-75.
14. Rabadev. S. Pawar M. and Titarmare G. (2020). Formulation and Evaluation of Polyherbal Cold Cream. Int J Pharma Res Scholars, (9), pp. 25-29.
15. Chauhan L and Gupta S. (2020). Creams: A Review on Classification, Preparation Methods, Evaluation and its Application. J Drug Delivery Therapeutics, 10(5), pp. 281-289.
16. Kamble M., Rajhatate P., and Meshram S. (2020). Formulation and Evaluation of Herbal Cold Cream using Bombaxceiba Fruit Pulp. Int J Res Scientific Innovation, 8, pp. 184-186.
17. Khandelwal KR., Vrunda S. (2018). Practical Pharmacognosy; 29th Edn; Nirali Prakashan, Pune, pp. 25.1-25.6.
18. Shinde P. et al. (2020). Formulation and Evaluation of Vanishing Herbal Cream of Crude Drugs. Asian J Pharmal Res Dev, 8(3), pp. 66-69.
19. Niyokam P. et al. (2010). Antibacterial Activity of Thai Herbal Extracts on Acne Involved Microorganism. Pharma Bio, 48(4), pp. 375-380.
20. Vora J. et al. (2018). Antibacterial and Antioxidant Strategies for Acne Treatment through Plant Extracts. Informatics in Medicine Unlocked, 49, pp. 128-132.

PCP456

EVALUATION OF THE NEUROPROTECTIVE EFFECT OF CURCUMIN-VITAMIN A-FORTIFIED YOGURT ON ALZHEIMER'S DISEASE IN RATS

AP0505

Mehta Saloni K¹

M. Parm Scholar,

Department of Pharmacology,

L. M. College of Pharmacy,

Gujarat Technological University

msaloni245@gmail.com

Abstract

Background and Objectives: The objective of the study was to formulate and development of curcumin-vitamin A fortified yogurt and to evaluate the effect of curcumin-vitamin A fortified yogurt in ICV-STZ induced Alzheimer disease in rats. **Methods:** The study was developed by inducing dementia using ICV injection of streptozotocin (STZ) (3mg/kg) afterwards, all the animal were divided into six groups namely Control, ICV-STZ (1ml/kg/day, PO), Curcumin (400mg/kg/day, PO), Vitamin A (3000mcg/kg/day, PO), Curcumin-vitamin A fortified yogurt [Curcumin (400mg/kg/day, PO), Vitamin A (3000mcg/kg/day, PO) + *L. rhamnoses* (10⁵ CFU/kg/day, PO)] and Memantine (10mg/kg/day, PO). The treatment was given for 28 days continuously for each group and the total duration of the study was 43 days. The behavioral parameters were performed under the investigation such as Y-maze, Morris water maze, passive avoidance and Novel object recognition test. Further, brains were collected, and neurochemical parameters were performed using ACHE, TNF- α , Amyloid- β 1-42, antioxidant parameters (MDA, REDUCED GLUTATHIONE) and Histopathological examinations were performed after the completion of treatment. **Results and Discussion:** All the 48 animals were used under the study had developed dementia afterwards behavioral parameters shows statistically significant ($p \leq 0.0001$) in Morris water maze, Y-maze, Passive avoidance, and Novel object recognition test which implicated, improved memory and cognitive functions. The neurochemical parameters showed statistically significant ($p \leq 0.0001$) increased in antioxidant level, Amyloid-beta and TNF- α of a curcumin-vitamin A fortified yogurt group when compared with STZ induced only. Histological examination showed less neuronal damage in combination group compared with STZ induced group. **Conclusion:** Decrease in formation of amyloid beta plaques and tau neurofibrillary tangles can be attributed to antioxidant level, Amyloid-beta and TNF- α . Thus, all these findings indicate that Curcumin in combination of Vitamin A and *L. rhamnoses* has noteworthy action on reversing Alzheimer disease.

Key words: Alzheimer disease, Curcumin, *L. rhamnoses*, Vitamin-A.

1 INTRODUCTION

Alzheimer's disease (AD), the most common cause of dementia, involves progressive declines in cognition function, and behavior, resulting primarily in difficulties remembering recent events. (Zhang et al., 2021) The term dementia refers to a cluster of symptoms manifesting in memory loss, language difficulties, behavioral changes, and impairments in day-to-day functions. (Qiu et al., 2009) AD has two distinct pathological characteristics. Often known are, Neurofibrillary tangles which are structural structures found inside neurons, whereas Beta-amyloid neurotoxic plaques which are protein aggregates outside of neurons. The primary element of Amyloid plaques is A β , and the primary element of neurofibrillary tangles is tau protein. (ERDEMCI et al., 2022) According to WHO reports, there are currently 50 million people suffering from dementia and are an estimated 4 million patients suffering from Alzheimer's

disease in India, with the expected number to grow 7.5 million by 2030. (Sathianathan & Kantipudi, 2018) US food and Drug Administration (FDA) approved 878 drugs between 1995 and 2021; a total of six of the drugs are approved for AD (four cholinesterase inhibitors [ChEIs], memantine, and aducanumab). (Cummings et al., 2022) Only few marketed products are available showing effect however there are disadvantages. Thus, there is a need for new drugs to slow or reverse the progression of AD. In our newly developed formulation, we have included the perennial herb *Curcuma Longa* Lin which contains a significant component of curcumin (diferuloylmethane) that appears to be protective of Alzheimer's disease (Patel et al., 2020) by scavenging free radicals, inhibiting the development and disaggregation of amyloid beta plaques, inhibiting tau hyperphosphorylation, enhancing tau tangle clearance, inhibiting acetylcholinesterase, reduce oxidative stress and TNF- α level, modifies insulin signalling pathway and having anti-inflammatory properties as well as metal chelation properties. (Tang et al., 2017) Because of the drawbacks of curcumin, recent years have seen many strategies and techniques used to increase the bioavailability and permeability, such as altering the solid-state through amorphous solid dispersion, reducing particle size through micronization, and creating supersaturated solutions (nanoemulsions and nanosuspensions) or encapsulating into nanoparticles. (Anand et al., 2007) These strategies increases the bioavailability of this formulation 2- to 10- fold, but the effectiveness, safety, and stability of the formulation are still major concerns. (Heger et al., 2014) The most significant method for improving the overall level of curcumin bioavailability is to slow down or inhibit the intestinal and liver metabolic pathways of a curcumin (Cas & Ghidoni, 2019) by inhibiting UGT (UDP-glucuronosyltransferase enzyme) with Vitamin A (Liu et al., 2017) and inducing the reabsorption of curcumin back into the body by increasing the amount of β -glucuronidase enzyme using *L.Rhamnosus* (Ozawa et al., 2017; Patel et al., 2020)

Hence, we have prepared a combination formulation of Curcumin-Vitamin A and *L. rhamnosus* in a form of fortified yogurt to inhibit the progression of Alzheimer's disease. It has been demonstrated in several preclinical studies that curcumin is rapidly metabolized in its metabolite after oral administration. It has been found that Nonpolar (lipophilic) drugs of all therapeutic classes are rapidly eliminated through the renal system by members of the UGT1A and 2B7 subfamilies. Curcumin is metabolized by UGT1A1, UGT1A3, UGT1A8, UGT1A10, UGT1A9, and UGT2B7 (Biology et al., 2013). Hence, we have used Vitamin A as UGT enzyme inhibitor. All tested UGT isoforms were significantly inhibited by Vitamin A, but UGT2B7 activity was strongly inhibited. (Liu et al., 2017) Vitamin A also shows effective difference in Alzheimer's disease by decreasing the aggregation of oligomerization of A β -40 and A β -42. (Ono & Yamada, 2012) The issue of rapid metabolism will be greatly accentuated and overall bioavailability impacted if β -glucuronidase, which hydrolyses curcumin again in the body, is elevated. Curcumin metabolite which is excreted into the duodenum could be hydrolysed back to the original compound by hydrolyses with the help of β -glucuronidase, and then reabsorbed through the intestinal track, and returned to the liver through the portal vein via enterohepatic circulation. (Ozawa et al., 2017) The other component we have used is a probiotic *Lactobacillus rhamnosus* (*L. rhamnosus*) confers benefits because it boosts microbiota and counters ailments by involve in gut brain axis and participate in progress of multiple disorder. (Segers & Lebeer, 2014) *L. rhamnosus* synthesizes and produces beta-glucuronidase in the gut. In this regard, we speculated that *L. rhamnosus* will improve the consequence of curcumin. Other than this *L. rhamnosus* also have a role in Alzheimer's disease. It reduces inflammatory cytokines and increases Brain-derived neurotrophic factor (BDNF) levels in hippocampus. As a results, it protects epithelial cells and reduces inflammatory markers such as interleukin-8. (Sanborn et al., 2020) The intracerebroventricular injection of streptozotocin (STZ) (3mg/kg) to model AD in rats using stereotaxic apparatus is a useful protocol to study the AD associate symptoms. (Moreira-Silva et al., 2019) STZ injection induce insulin resistance and other pathological changes associated with AD, including cognitive impairment, free radical formation, increase oxidative stress, release of proinflammatory mediators and neuronal accumulation of phosphorylated tau protein and amyloid plaques which lead to DNA damage, Neuroinflammation and neuronal cell death. (Knezovic et al., 2013) As a result, ICV-STZ

causes a disruption in spatial memory. Hence, the aim of the study was to evaluate and formulate the Curcumin-Vitamin A fortified yogurt and demonstrate the effect of the combination formulation in ICV-STZ induced AD.

2 MATERIALS AND METHODS

2.1 Probiotics, Drugs, Kits, and other chemicals:

Lactobacillus rhamnosus [Lyophilized] [UBLR-58], strength- NLT 100 billion CFU/g were obtained from UNIQUE BIOTECH Ltd, India. Curcumin was obtained from Shree Foods, Ahmedabad, India. Vitamin A were obtained from USV Pvt Ltd, Mumbai, India. Streptozotocin powder obtained from MP Biomedicals, LLC, Southern California, U.S. Memantine [Admenta-10] obtained from Sun Pharma laboratories Ltd, East Sikkim, India. TNF- α , Amyloid Beta, 1-42 peptide, Lipid peroxidase [TBARS] kits were purchased from Krishgen Biosystem [Mumbai, India]. The Lactobacillus MRS broth media was procured from HiMedia Laboratories Pvt Ltd [Mumbai, India]. All other Chemicals/reagents used in the study were of analytical grade.

2.2 Determination of viable cell in bacterial solution of Lactobacillus rhamnosus:

In order to calculate the concentration of microorganisms, serial dilutions are used. The sample is usually diluted and plated to get a reasonable number of colonies. The number of colonies on the agar plate represents the number of viable microorganisms. By measuring the dilution factor, one can find out how many microorganisms are in the samples. Approximately one colony-forming unit (CFU) represents one viable bacterial or fungal cell. (Sanders, 2012)

2.3 Animals and care:

The experiment was conducted using healthy male Wistar rats weighing between 350 and 650 grams. During the current study, the animals were bred at the L.M College of Pharmacy, Ahmedabad, India. All animals are housed in standard polypropylene cages under controlled conditions of room temperature (18°C to 25°C), humidity (30% to 70% RH), and light and dark (12 hours to 12 hours) cycles, with free access to commercially available normal pellet diet (Amrut feeds, Sangli, Maharashtra, India) and water. A week prior to the experiment, the animals were acclimated to their surroundings. Prior to carrying out the experiment **LMCP/IAEC/22/0026**, the Institutional Animal Ethics Committee (IAEC) approved the experimental protocol. The animals were taken care of according to the guidelines set by the 'Committee for the Purpose of Control and Supervision of Animal Experiments' (CPCSEA), Ministry of Fisheries, Animal Husbandry, and Dairy.

2.4 Preparation of Yogurt:

Prepare yogurt by taking milk and pasteurize it for approximately at 185°F (85°C) for 10 minutes. Homogenize the milk, which improves the consistency of the yogurt. Cool the milk and inoculate curcumin and vitamin A and kept in Sonicator for 1 hr until solution is completely clear, after that add l. rhamnosus and kept in BOD incubator at 98.6°F (38°C) for 16 hours until pH of 4.5 is achieved. A temperature of 39-44°F (4-7°C) is applied to yogurt to stop further fermentation. (Yogurt Production | MilkFacts.Info, n.d.)

2.4.1 pH determination of yogurt:

We took 9 grams of yogurt out of the prepared sample and suspended them in 100ml of distilled water. A standard Chemi line (CL-110) pH meter was used to measure the pH of the prepared yogurt. (Ilic & Ashoor, 1988)

2.4.2 %Titratable acidity of yogurt:

The amount of yogurt was determined after mixing it with 10ml of distilled water using 0.5% phenolphthalein as an indicator and titrating with 0.1 N NaOH solution until endpoint reaches to faint pink colour. (Ilic & Ashoor, 1988)

$$= (\text{Volume of Titrant} \times \text{N} \times 90 / \text{wt. of sample} \times 1000) \times 100$$

2.4.3 %Syneresis of yogurt:

With some modifications, the procedure of centrifugation was used to determine yogurt syneresis (the release of whey). A 20g of yogurt was centrifuged for 20 minutes at 4°C (640g)

and the clear supernatant was collected and weighed. Syneresis was calculated according to the following equation. (Zainoldin & Baba, 2009)

$$\text{Syneresis} = \frac{\text{Weight of supernatant (g)} \times 100\%}{\text{Weight of yogurt sample (g)}}$$

2.4.4 CFU/ml of yogurt:

Add a sample on a molten agar medium upon plating the appropriate dilution sample, colonies are uniformly distributed throughout the solid medium. Plates are kept for incubation at 37°C for 24 hours. Count the total number of colony-forming units using following equation. (Sanders, 2012)

$$\text{CFU/ml} = (\text{No. of colonies} \times \text{Total Dilution Factor}) / \text{volume of culture plated in ml}$$

2.4.5 Vitamin A analysis of yogurt:

As procedure describe in (Perez et al., 1996). Add 50ml of DCM to an accurately weighed amount of Vitamin A USP reference standard solution. Dilution with DCM of 0.5-5.0 UG of retinol results in solutions containing 0.5-5.0 UG of retinol. Prepare solution as freshly as possible. Yogurt samples (40g) were extracted with 40ml of an extractant solution (2:1, v/v, hexane solution). For two hours, this was stirred at 1000 revolutions per minute and protected from light. As a result, the organic phase was separated by centrifugation at speed of 4000rpm. The residue was subsequently evaporated in rotavapor at 50°C and treated with 6ml of methanol. Measure the absorbance at 280nm.

2.4.6 Curcumin estimation of yogurt:

Based on the results of the analysis of the samples, the curcumin contents in the samples were determined using (Maurya et al., 2020) , with a few minor modifications. An accurately weighed volumetric flask filled with mixed sample of 25ml was used to that 95% ethyl alcohol was added. To facilitate the extraction, the mixture was thoroughly mixed. Following the extraction, the mixture was centrifuged for 10 min. Collect the supernatant and filter using Whatman filter paper. The first few ml of the filtrate was discarded, measure the absorbance at 425nm using ethyl alcohol as blank.

2.5 Experimental study:

Induction of ICV injection of streptozotocin to induce Dementia and Treatment:

Animals were acclimatized for 1 week and them assigned randomly into six groups, each group bearing eight animals

- Group 1 (G1) Negative control: receives ICV-injection of artificial cerebrospinal fluid [day 1 and 3] + saline [1ml/kg/day, 28 days, p.o]
- Group 2 (G2) Disease control: receives ICV-injection of STZ [3mg/kg, day 1 and 3] + saline [1ml/kg/day, 28 days, p.o]
- Group 3 (G3) Curcumin: receives ICV-injection of STZ [3mg/kg, day 1 and 3] + Curcumin [400mg/kg/day, 28 days, p.o]
- Group 4 (G4) Vitamin A: receives ICV-injection of STZ [3mg/kg, day 1 and 3] + Vitamin A [3000mcg/kg/day, 28days, p.o]
- Group 5 (G5) Curcumin-vitamin A fortified yogurt: receives ICV-injection of STZ [3mg/kg, day 1 and 3] + Curcumin [400mg/kg/day] + Vitamin A [3000mcg/kg/day] + l. rhamnosus [10⁵ CFU/kg/day] combined yogurt for 28 days, p.o.
- Group 6 (G6) Memantine: receives ICV-injection of STZ [3mg/kg, day 1 and 3] + memantine [10mg/kg/day, 28days, p.o]

An assessment of behavioral parameters was conducted at the end of the study. After the behavioral tests were completed, rats were sacrificed with a high dose of anesthetics. Brains of 6 animals from each group were isolated and subjected to neurochemical parameter and brain of 1 animal from each group were isolated for histopathological examination.

2.6 Surgery procedure:

A total of 42 rats were anaesthetized by ketamine [90mg/kg, i.p] and xylazine [10mg/kg, i.p]. The head was fixed in an RWD life science [68528] stereotaxic apparatus. In three-dimensional coordinates, once the skull is clear, use the bregma as the point of the reference for the X-, Y-, and Z-axis. The lateral ventricle site of in the rat brain would be injected with a STZ, and according to the Rat brain in stereotaxic coordinates, (Paxinos & Watson, 1982) it is located at -1mm (ML), -0.3mm (AP), and -3.9mm (DV) with respect to bregma. 42 animals were treated with STZ on day 1 and 3, using the same hole in the skull and injection coordinates. Negative control rats [n=7] received ICV-injection of artificial cerebrospinal fluid.

2.7 Behavior Parameters

2.7.1 Assessment of spatial memory with the Morris water maze (MWM):

Morris water maze was tested for Training session on 0th day, after the ICV-STZ injection which is Induction session on 15th day and Treatment session on 39th day. MWM used a circular acrylic platform with a 12cm height surrounded by a 22cm diameter spherical maze and divided into four quadrants north east (NE), north west (NW), south east (SE), and south west (SW). There was a hidden platform positioned 1 cm below the surface of the water in NW quadrant. Training session included navigation on the hidden platform. A maximum of two minutes is set for the rats to search the hidden platform. These rats were allowed to halt on the platform for about 15 s and were recorded using Logitech webcam. Using ANY-maze software, escape latency (time to reach the platform) was measured in each trial, and animals who did not reach the platform within 60s were gently guided to the platform. The animals were subjected to four-day trials. The test session was performed on the 5th day respectively. (Zhou et al., 2013)

2.7.2 Y-maze Test:

Install the video cameras (Logitech webcam) and set up a proper tracking system (ANY-maze animal tracking software) for rats in the maze before the testing session begins. Habituate rats with the maze 1-2 days before testing session. Gently place the rats in the Y-maze, facing the center. Make the experiment feasible for an animal by stepping back from the maze. 5 minutes should be allowed for the animal to freely move in the maze. Remove the animal from the maze, place them back in their respective cage and clean the area using 70% alcohol. Calculate spontaneous alteration, the number of times a rat enters a different arm of a maze in 3 consecutive entries. The formula below calculates spontaneous alteration %. (Miedel et al., 2017)

$$\% \text{ Alternation} = \left[\frac{\text{Number of Alternations}}{\text{Total number of arm entries} - 2} \right] \times 100$$

2.7.3 Passive avoidance test:

A shock test instructs subjects to avoid environment in which they previously experienced an aversive stimulus (such as foot shock). In Passive avoidance apparatus, there is a gate that separates a lit compartment from a dark compartment. Animals were allowed to explore both the compartment on the Training session. Once animal enters into a dark compartment note the time in sec taken by animal to move from light to dark compartment. The animal was exposed to a mild foot shock of 0.3mA for 2-5 sec. After approximately 15 sec, remove the animal from the dark chamber. Next day, Testing session was performed and time in sec was noted. Calculate the latency (in sec) to enter the animal in dark compartment for both acquisition (time from first exposure to the lighted PA compartment until the rat entered into the dark compartment) and Retention (time from entry to lighted compartment until the rat entered the dark compartment after 24 hrs). (Ogren et al., 2015)

2.7.4 Novel Object recognition test:

A novel object recognition test (NOR) could be used to assess the cognitive deficits associated with Alzheimer's disease (AD). There are only three components to test: one habituation session, one training session, and a test session. A training session consist of visual exploration of two identical objects, and a test session consist of replacing a previously explored object with a novel one. The rodent's innate preference for novelty makes it more likely that it will

explore the novel object if it remembers the familiar one. (Miedel et al., 2017) The experiment was conducted using ANY-maze software and Logitech webcam. Calculate the discrimination index and time in sec for familiar and Novel object using following formula:

$$\text{Discrimination index} = \frac{T_{\text{novel}} - T_{\text{familiar}}}{T_{\text{novel}} + T_{\text{familiar}}}$$

2.8 NEUROCHEMICAL PARAMETERS

2.8.1 Preparation of brain homogenate:

Generally, hemolysis blood may affect results, so remove excess blood thoroughly by rinsing tissues with ice-cold PBS (0.01M, pH=7.4). Weigh the tissue pieces, mince them, then put them into PBS and homogenize with a glass homogenizer on ice (the volume depends on how much tissue you have. 2ml PBS for 1 gram tissue is delicate). After homogenizing, centrifuge at 5000g for 5 minutes.

2.8.2 Estimation of Acetylcholinesterase (ACHE) activity:

In this study, 0.5ml of brain homogenate were added to 0.1ml of Ellman's reagent and 2.5ml of phosphate buffer for 5 minutes, followed by the addition of 0.1ml of freshly prepared acetylcholine chloride in the buffer (pH 8). The absorbance at 412nm was measured at 1-minute intervals for 10 mins. Ache hydrolyzed per min per gram of protein is a measure of acetylcholinesterase activity. (Ellman et al., 1961)

2.8.3 Estimation of Lipid Peroxidation:

The experiment was performed using instruction provided by Rat Thiobarbituric Acid Reactive Substance, TBARS GENLISA™ ELISA kit manufactured by Krishgen BioSystem. Standard concentration of 4nmol/ml-128nmol/ml were taken.

2.8.4 Estimation of Glutathione peroxidase (GPX):

GPX were estimated by incubating 0.2ml of brain homogenate with 0.4ml of sodium azide, disodium EDTA, and hydrogen peroxide (H₂O₂) solutions, respectively, for 10 min at 37°C. In order to stop this reaction, 0.5ml of TCA solution was added. After centrifugation for ten min at 3000rpm, the resulting solution was analyzed. The supernatant was collected (0.5ml) and DTNB was added along with 4 ml of disodium hydrogen phosphate. An absorbance measurement was performed at 420nm. This measurement was expressed as microgram of GPX per milligram of tissue. (Weydert & Cullen, 2010)

2.8.5 Estimation of TNF-α activity:

The molecular analysis was done to assess the level of cytokine TNF- α by the help and instructions provided by Rat TNF-α GENLISA™ ELISA kit manufactured by Krishgen BioSystem. Calculate the concentration of unknown by taking standard concentration in a range of 31.25-2000 pg/ml.

2.8.6 Estimation of Amyloid-Beta-42:

The molecular analysis was done to assess the level of Amyloid-beta by the help and instruction provided by Rat Amyloid beta peptide 1-42, Aβ1-42 GENLISA™ ELISA kit manufactured by Krishgen BioSystem. Calculate the concentration of unknown by taking standard concentration in a range of 0-3000 pg/ml.

2.9 Histopathological examination:

The animals were sacrificed at the end of the study and the brains of animals were collected, fixed with Bovine's fixative and stored in formaldehyde for 5 days for histological studies. Cortex and hippocampus regions were cut, stained with haematoxylin and eosin and then analysed microscopically.

2.10 Statistical analysis:

All the values were expressed as Mean ± SEM (n=6), where p < 0.05 was considered statistically significant. The data obtained was statistically analyzed using GraphPad Prism version 9 software. Statistical comparison was performed using one-way as well as two - way ANOVA followed by Tukey's multiple comparison tests.

3 RESULTS:

3.1 Determination of viable cell in bacterial solution of *Lactobacillus rhamnosus*:

As shown in table 1, dilutions of three different concentrations are prepared. A number of colonies observed after 24 hours shows a concentration of 10^5 contains higher number of CFU/ml than that in 10^9 and 10^7 . This indicates *L. rhamnosus* can be used at different concentration.

Table 18: Determination of viable cells in *L. rhamnosus*.

Sr. NO.	Concentrations (cfu/ml)	No. of Colonies	Total Dilution Factor	Volume of Culture Plated in ml	CFU/ml
1	10^9	2458 2618 2956 2933	10^2	1	2.46×10^5 2.61×10^5 2.95×10^5 2.9×10^5
2	10^7	813 634 671 873	10^4	1	8.13×10^6 6.34×10^6 6.71×10^6 8.73×10^6
3	10^5	356 339 386 394	10^6	1	3.56×10^8 3.39×10^8 3.86×10^8 3.94×10^8

CFU/ml = (Number of colonies × total dilution factor)/ volume of culture plated in ml

Dilution factor (DF) = V_f/V_i , V_f = Volume of diluent + stock volume, V_i = Volume of stock transferred

3.2 pH determination of yogurt: During the four weeks of storage, pH measurement was conducted every week. The results of the experiment indicate the pH of the yogurt concentrations 10^5 and 10^7 gradually decreases, whereas the pH of the yogurt concentration of 10^9 remains stagnant. Hence, fortification of curcumin, vitamin A and *L. rhamnosus* does not pH of yogurt because it was not significantly different as shown in table 2.

Table 19: Determination of pH, %titratable acidity, and %syneresis for four weeks

	0 week			2 weeks			4 weeks		
	pH	%TA	Syneresis	pH	%TA	Syneresis	pH	%TA	Syneresis
10⁵	4.5±0.01	1.9±1.20	29.5±2.30	3.9±0.20	0.9±0.40	31.2±3.40	3.8±0.10	1.3±0.70	38.5±1.20
10⁷	4.5±0.05	0.6±0.13	23.2±0.50	4.3±0.17	0.7±0.10	28.5±1.10	3.8±0.16	1.0±0.60	32.2±2.06
10⁹	4.7±0.06	0.8±0.03	24.5±1.03	4.6±0.10	0.8±0.01	26.5±1.01	4.5±0.05	0.8±0.00	27.7±0.70

Values are expressed as Mean±SEM (n=4).

3.3 % Titratable acidity of yogurt: An analysis of % titratable acidity was performed every week for over a month. The experiment results demonstrate that a yogurt concentration of 10^9 did not increase acidity in the sample. In contrast, concentration of 10^5 and 10^7 shows significant increases in acidic content (table 2).

3.4 % Syneresis of yogurt: In the course of a month, % syneresis was analysed every week. As shown in table 2, yogurt with concentration of 10^5 and 10^7 showed significant increase in % syneresis as days increases, whereas yogurt with concentration of 10^9 no significant increase in % syneresis as shown in table 2.

3.5 CFU/ml of yogurt: After storing yogurt nearly a month, samples were collected every week to check the presence of colonies in the sample yogurt. The results of the analysis of the sample revealed that yogurt with the concentration of 10^9 displays a significantly higher number of colonies forming unit per millilitre than yogurt with concentration of 10^5 and 10^7 as shown in graph 1.

Graph 1: Analysis of CFU, %recovery of curcumin, and %recovery of vitamin A with standard calibration curve The graph represents the CFU/ml measured at different weeks for over one month of storage. The % recovery of curcumin and % recovery of vitamin A was measured using a standard calibration curve at 0,1,2,3, and 4 weeks.

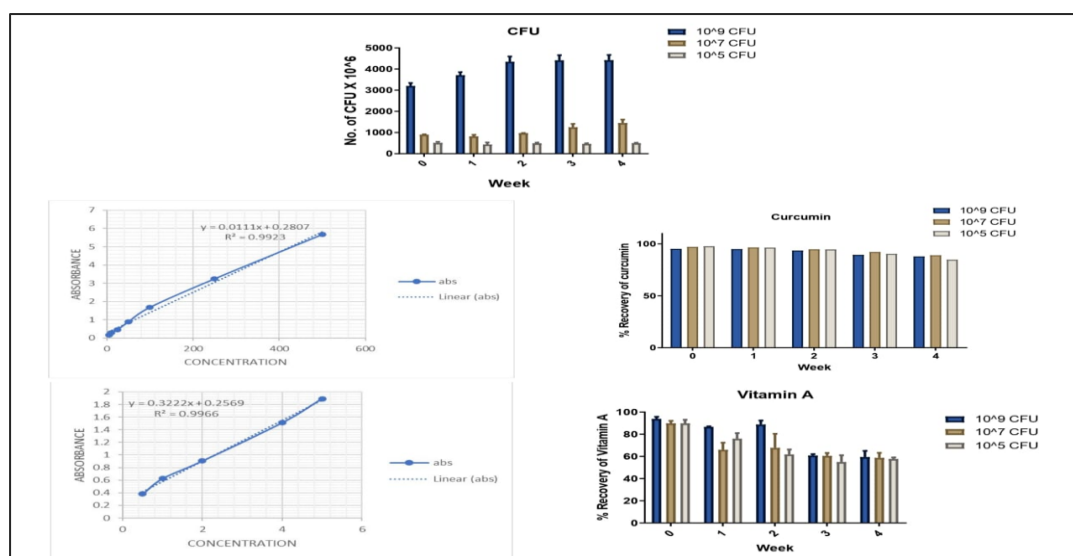
3.6 Determination of Vitamin A: After optimization of the vitamin A extraction step different yogurt samples were analysed every week for over a month. For the purpose of evaluating the recovery process of vitamin A in yogurt samples, standard solution was used to measure vitamin A levels. The study revealed that yogurt with a concentration of 10^9 showed no significant change for the first three weeks. However, measurements for the fourth and fifth weeks indicated a curtailment. Moreover, yogurt with concentration of 10^5 and 10^7 showed a gradual decline in Vitamin A content (graph 1).

3.7 Determination of Curcumin: Curcumin was extracted from the yogurt and further analysed at three different concentrations. In all three concentrations, there was a marginal change, but no significant plunge was observed in yogurt samples (graph 1).

3.8 Behaviour parameters:

3.8.1 Assessment of spatial memory with phases, the Morris water maze (MWM):

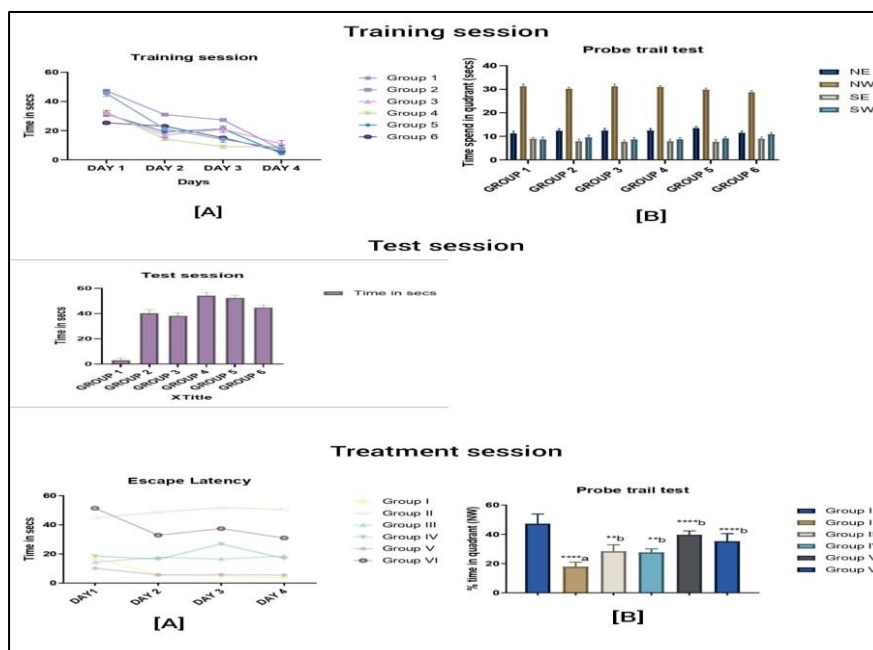
Experiments were conducted in three including training, test, and treatment sessions. We found that found that finding the hidden platform on the first day took a longer time than on days 2,3,



and 4 as shown in graph 2. Thus, we conclude that animals were trained properly. Followed by a test session after 15 days of induction with ICV-STZ. Clearly, memory impairment in rats was evident by the longer time taken to find the hidden platform except that of control group

(G1) as shown in graph 2. [A] treatment session was than conducted for 4 days, where an escape latency and probe trial test was performed (graph 2). study results indicate that rats from the control group (G1) and curcumin-vitamin A fortified groups (combination group) (G5) find hidden platform in fewer seconds ($p \leq 0.0001$) when compared to the test session, whereas rats with ICV-STZ induced (G2), curcumin (G3), and vitamin A (G4) shows no significant difference. As for the standard memantine group (G6), there was a slurp curb observed. On 5th day probe trial test were performed where curcumin-vitamin A fortified yogurt group (G5) shows significant difference ($p \leq 0.0001$) in time spent on NW quadrant when comparison was made with ICV-STZ induced group (G2) as shown in graph 2.

Graph 2: Determination of spatial memory using morris water maze.



An analysis of spatial memory using morris water maze at three sessions can be seen in the graph above. In training session [A] depicts gradual decrease in time (sec) to find hidden platform on day 4 compared to day 1, [B] while on the 5th day probe trail test showed animals spent more time in NW quadrant where hidden platform was placed, which indicates memory formation. In the test session all groups except G1 show increased time taken to find hidden platform, which indicates a loss of memory. After 28 days of treatment [A] escape latency illustrate that group G5 take less time compared to G2 which results in an increase in spatial memory.

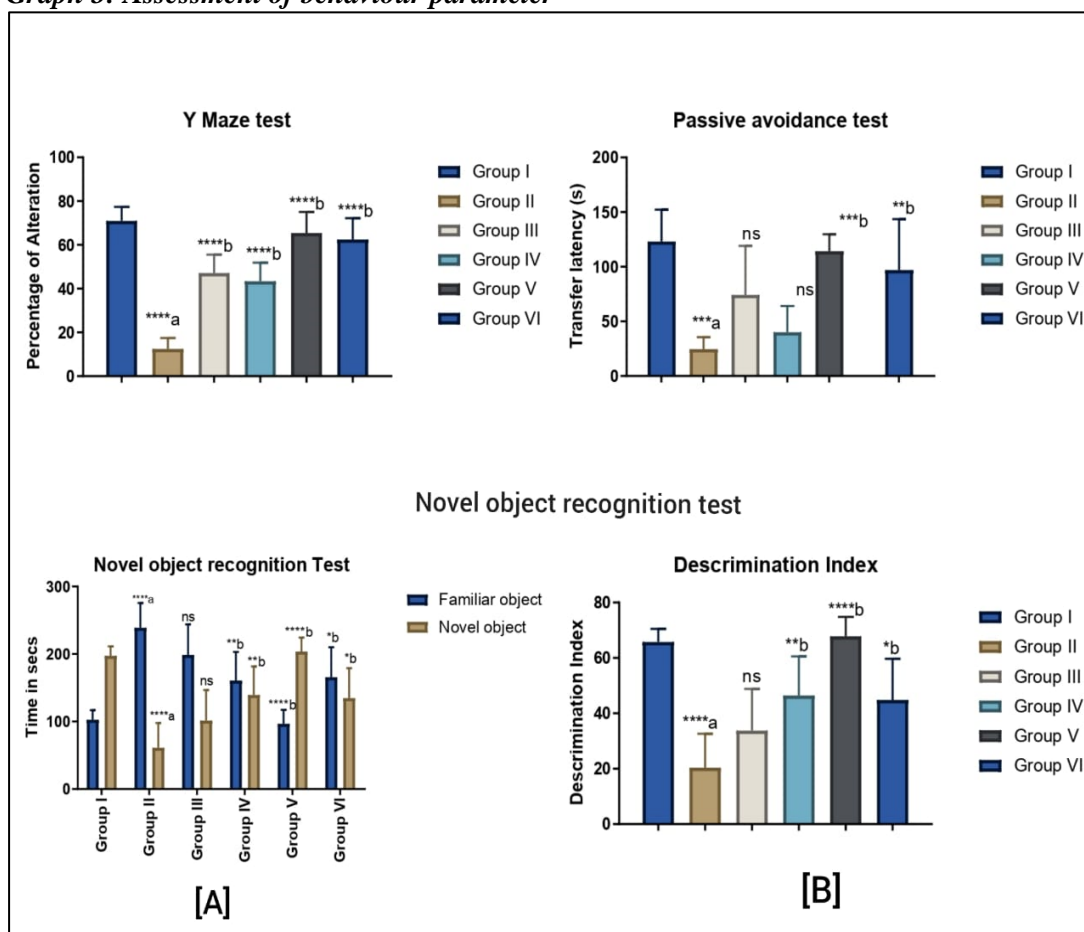
3.8.2 Post surgery evaluation:

Body weight, food intake and water intake measured after animals intracerebroventricular injection of streptozotocin using stereotaxic apparatus, the analysis of the results indicate no significant change in all groups which illustrate normal behavior of animals.

3.8.2 Y-maze test:

The rats adopt a lose-shift search strategy when placed in a Y-maze, in which each arm is explored only once for every three arm entries. The Y-maze test was conducted on the 40th day following treatment completion. When compared with STZ induced group (G2), the curcumin (G3), vitamin A (G4), curcumin-vitamin A-fortified group (G5), and memantine (G6) shows highly significant difference ($p \leq 0.0001$) as shown in graph 3.

Graph 3: Assessment of behaviour parameter



Determination of various behaviour parameters after the concurrent treatment of 28 days. Percentage of alteration measured in Y-maze test, results show a significant plunge in G2 compared to G1 indicate memory deficit, whereas G5 shows significant increase in number of alterations compared to G2. Passive avoidance test measured in transfer latency (sec); results indicate significant difference in transfer latency of G5 group when compared with G2. Novel object recognition test was performed in [A] time in sec animals spent around novel and familiar object, the analysis of result demonstrate G5 group shows animals spent more time around novel object compared to G2 group and [B] discrimination index, results shows significant difference in G5 compared to G2.

3.8.3 Passive avoidance test:

Passive avoidance test was based on transfer latencies (sec) in retention time in wistar albino rats as a function of drug treatment using shock intensities during training as indicated. A comparison between streptozotocin-induced group (G2) with curcumin-vitamin A-fortified group (G5) reveals a significant difference ($p \leq 0.001$) in transfer latency (sec). While G3 and G4 groups shows no significant (ns) difference, whereas memantine group (G6) indicate significant difference with $p \leq 0.01$ (graph 4).

3.8.4 Novel object recognition test:

Arena habituation permits measurements of spontaneous locomotion and other stereotyped behavior's relevant to a particular rat model. Here, fig A shows time spent by each group with familiar objects and novel objects. The results indicates that the curcumin-vitamin A-fortified group spent more time around a novel object with highly significant results of $p \leq 0.0001$, when compared with the ICV-STZ induced group. While curcumin shows no significant (ns) value, whereas vitamin A illustrate significant difference with $p \leq 0.01$, and memantine depicts $p \leq 0.05$.

Another parameter includes discrimination index, analysis of the results indicates curcumin-vitamin A-fortified group (G5) showed highly significant discrimination index ($p \leq 0.0001$) when compared with ICV-STZ induced group. Whereas curcumin (G3), vitamin A (G4), and memantine illustrate no significant, significant difference with $p \leq 0.01$, and significance with $p \leq 0.05$ (graph 4).

3.9 Neurochemical parameters:

3.9.1 Estimation of Acetylcholinesterase (ACHE) activity:

The activity of acetylcholinesterase increases significantly when rats are exposed to streptozotocin (5.36 ± 0.29 , $p \leq 0.0001$) compared with control group rats (1.30 ± 0.10). Curcumin in combination with vitamin A and l. rhamnosus reveals highly significant decline in acetylcholinesterase activity (1.61 ± 0.20 , $p \leq 0.0001$) when compared with G2 rats as shown in table 3.

3.9.2 Estimation of Lipid Peroxidation activity:

Exposure to rats with streptozotocin illustrate an increase in the level of MDA in brain tissue (83.16 ± 15.82 , $p \leq 0.0001$) as compared with G1 rats (33.86 ± 10.66). The concurrent administration of curcumin-vitamin A-fortified yogurt exhibits highly significant reduction in MDA levels (33.86 ± 10.66 , $p \leq 0.0001$) as compared with those treated with streptozotocin alone as shown in table 3.

Table 20: Neuro chemical Parameters

	AChE mmol/min/ gm	MDA Level nmol/g	GSH µmol/mg	TNF-α pg/ml	Amyloid β pg/ml
Group I	1.30±0.10	33.86±10.66	2.46±0.36	108.00±40.02	2.167±0.35
Group II	5.36±0.29*** * _a	83.16±15.82* *** _a	0.90±0.28 ** _a	431.75±44.84** ** _a	277.16±41.70* *** _a
Group III	3.16±0.31*** * _b	54.45±3.096* * _b	1.40±0.41 ns	234.04±41.97** *** _b	228.30±44.51 ⁿ s
Group IV	4.10±0.34*** * _b	60.27±6.72* _b	0.98±0.11 ns	261.75±60.21** * _b	211.18±48.30* b
Group V	1.61±0.20*** * _b	33.86±10.66* *** _b	2.13±0.19 ** _b	176.96±29.18** ** _b	82.39±21.25*** * _b
Group VI	5.09±0.52 ^{ns}	72.31±10.61 ^{ns}	1.66±0.36 ns	169.88±71.06** ** _b	76.48±19.36*** * _b

The values are expressed in mean ± SEM with n=6 per group

Values of $p \geq 0.05 = ns$ while p values ≤ 0.05 , ≤ 0.01 , ≤ 0.001 , and ≤ 0.0001 were expressed as *, **, *** and ****, respectively.

^a The significant level between G1 and G2 groups.

^b The significant level between G2 in comparison with G3, G4, G5, and G6 groups.

3.9.3 Estimation of Glutathione peroxidase (GPX) activity:

The enzyme activity of GPx was significantly reduced in the ICV-STZ induced group (0.90 ± 0.28 , $p \leq 0.01$) compared with the G1 group (2.46 ± 0.36). In the curcumin-vitamin A-fortified group, results showed significant elevations in enzyme activity (2.13 ± 0.19 , $p \leq 0.01$), whereas curcumin, vitamin A, and memantine groups showed insignificant change in enzyme activity (1.40 ± 0.41 , ns), (0.98 ± 0.11 , ns), (1.66 ± 0.36 , ns) when compared with the streptozotocin-induced group as shown in table 3.

3.9.4 Estimation of TNF- α activity:

Highly significant increases in TNF- α levels were observed in the streptozotocin-induced group (431.75 ± 44.84 , $p \leq 0.0001$) when compared with G1 group (108.00 ± 40.02). Significant results were obtained after 28 days of treatment in G3 (234.04 ± 41.97 , $p \leq 0.0001$), G4 (261 ± 60.21 , $p \leq 0.0001$), G5 (176.96 ± 29.18 , $p \leq 0.0001$), and G6 (169.88 ± 71.06 , $p \leq 0.0001$) as compared with the streptozotocin alone group (table 3).

3.9.5 Estimation of Amyloid-Beta-42 activity:

There was a significant increase in the level of amyloid beta as a result of streptozotocin exposure ($277.41.70 \pm 41.70$, $p \leq 0.0001$) compared to the control group (2.167 ± 0.35). The treatment with curcumin-vitamin A-fortified yogurt, it was demonstrated the highly significant curtailment in amyloid levels (82.39 ± 21.25 , $p \leq 0.0001$), whereas curcumin alone shows insignificant results (228.30 ± 44.51 , ns) when compared with G2 group as shown in table 3.

3.10 Histology study:

In histopathological examination, as shown in fig 2, the G1 group possess normal neuronal cells, where as G2 group showed neuronal damage with dark basophilic cytoplasm and dark condensed nuclei, less neuronal cells and pyknosis, and deposition of amyloid- β plaques. In G3 and G4 groups, hippocampus and cortex region shows neuronal damage. However, in the G4 group possess mild neuronal damage and cell integrity was not lost, while in G6 group cortex region shows neuronal damage.

4 DISCUSSIONS:

Disease associated with neurodegeneration contribute to morbidity, mortality, and function dependency, especially among the elderly, due to the progressive loss of neurons in central nervous system such as Alzheimer's disease (AD) (Khezri et al., 2022). AD patients report losing their memory as one of their first symptoms. As a result of AD pathology, memory formation is impaired on a molecular level as well as on a neural network level (Jahn, 2013). A pathological feature of senile plaques is the presence of intracellular neurofibrillary tangles (NFTs) as well as extracellular amyloid protein deposits. Accumulation of A β are amyloid plaques within the brain parenchyma and within brain vessels, which is termed cognophilic angiopathy or cerebral amyloid angiopathy (CAA). In NFTs, hyperphosphorylated tau proteins were paired with helical filaments. There are several distinctive lesions associated with these NFTs, such as loss of neurons and synaptic loss (Kumar Thakur et al., 2018). Originally identified as an antibiotic, streptozotocin (STZ) is composed of glucosamine and nitrosourea. It causes toxicity in beta cells of the pancreas and is transported by glucose transporter 2. It is commonly used in animal experiments to induce diabetes. The administration of STZ by intracerebroventricular or intraperitoneal injection results in impaired cognition and an increase in cerebrospinal fluid aggregated A β fragments, total tau protein, A β deposits. Additionally, there was a decreased alpha/beta ratio (phosphorylated/total) of glycogen synthase kinase-3 (GSK-3) in the brain as a result of these changes. It has been demonstrated that STZ administration results in neuroinflammation, oxidative stress, and changes in biochemistry in a rodent's brain. As a model of early pathological changes associated with neurodegenerative disease, this is considered a valid experimental approach (Kamat, 2015). Currently, there are only a few commercially available products that are effective, but they are obtain with several disadvantages. The development of novel drugs is therefore necessary in order to slow or reverse the progression of AD. Our newly designed formulation contains the perennial herb curcuma longa lin, which contains curcumin (diferuloylmethane), which has been shown to provide protection against Alzheimer's disease but it has certain drawbacks. The most significant method for improving the overall level of curcumin bioavailability is to slow down or inhibit the intestinal and liver metabolic pathways of a curcumin (Cas & Ghidoni, 2019) by inhibiting UGT (UDP- glucuronosyltransferase enzyme) with Vitamin A (Liu et al., 2017) and inducing the reabsorption of curcumin back into the body by increasing the amount of β -glucuronidase enzyme using L.Rhamnosus (Ozawa et al., 2017; Patel et al., 2020). Hence, we

have prepared a combination formulation of Curcumin-Vitamin A and L. rhamnosus in a form of fortified yogurt to inhibit the progression of Alzheimer's disease.

To ensure the structural integrity of yogurt six different parameters are measured over a period of four weeks. An analysis of pH, % titratable acidity, % syneresis, CFU/ml revealed that yogurt possesses normal texture, acidity, function and viability when measured every week for a month (Ilic & Ashoor, 1988) (Zainoldin & Baba, 2009) (Sanders, 2012)

In this study, probiotic L. rhamnosus combined with curcumin and vitamin A as fortified yogurt prevented destruction of neurons due to streptozotocin-induced memory loss in rats. In the current study, spatial memory functions were assessed by the MWM test in ICV-STZ-induced rats and curcumin treatment in combination with vitamin A and L. rhamnosus significantly and dose-dependently improved memory loss in MWM test. Y-maze test was used to measure the recognition and spontaneous memory of a rodent. A significant restoration of spontaneous alteration was observed after treatment with a curcumin-vitamin A-fortified yogurt compares to streptozotocin induced group (Kraeuter et al., 2019). To measure the learning and memory in rodents' passive avoidance test and novel object recognition test is the most appropriate parameters. Passive avoidance is a fear-aggravated test to evaluate rodent behavior, upon analysis we find that animals treated with streptozotocin tends to loss in memory as there was a significant difference when compared with control group, whereas curcumin in combination with vitamin A and L. rhamnosus shows highly significant results when compared with STZ-induced group (Shamsipour et al., 2021). Rodents' normal behavior is tending to spent more time around novel object rather than familiar object, after the 28 days of treatment, the analysis of time spent around novel and familiar object reveals that curcumin along with probiotic L. rhamnosus and vitamin A shows increased in the time taken to spend around novel object when compared with streptozotocin alone (Lueptow, 2017). Acetylcholine, a neurotransmitter found in the hippocampus, plays an important role in memory and learning through the cholinergic system. As a result of acetylcholinesterase degrading this enzyme, its pharmacological activity is diminished. As a result of acetylcholinesterase elevation, acetylcholine levels are lowered in AD. Streptozotocin significantly decreased the activity of acetylcholinesterase. Treatment of curcumin-vitamin A-fortified yogurt significantly restored acetylcholinesterase activity resulting in recovery and retaining memory processes (Patel et al., 2020). Furthermore, streptozotocin causes oxidative stress, destroys the brain's antioxidant system and results in neurodegeneration in addition to behavioral abnormalities. Curcumin along with vitamin A and L. rhamnosus- treated animals exhibits a significant rise in the rise in the antioxidant enzyme compared to STZ-induced rats. Accumulation of Amyloid beta lead to loss of neuronal structure, in our result we found that curcumin-vitamin A-fortified yogurt shows decrease in the accumulation of plaques when compared with streptozotocin induced group. In spite of its well-documented therapeutic properties, curcumin's poor oral bioavailability has hampered its development. According to studies, curcumin is metabolized in the blood after oral ingestion. In the current study, oral bioavailability of curcumin co-administered with L. rhamnosus and vitamin A is enhanced. L. rhamnosus bacteria can synthesize and release a β -d-glucuronidase enzyme and vitamin A inhibits the UGT enzyme which reverts curcumin into its active form. The study found that curcumin combined with L. rhamnosus and vitamin A enhanced memory and antioxidant enzyme levels L. rhamnosus compared with curcumin alone.

5 REFERENCES

1. Anand, P., Kunnumakkara, A. B., Newman, R. A., & Aggarwal, B. B. (2007). reviews Bioavailability of Curcumin : Problems and Promises. *Molecular Pharmaceutics*, 4(6), 807–818.
2. Biology, C., Rowland, A., Miners, J. O., & Mackenzie, P. I. (2013). The International Journal of Biochemistry The UDP-glucuronosyltransferases : Their role in drug metabolism and detoxification. *International Journal of Biochemistry and Cell Biology*, 45(6), 1121–1132. <https://doi.org/10.1016/j.biocel.2013.02.019>
3. Cas, M. D., & Ghidoni, R. (2019). Dietary curcumin: Correlation between bioavailability and health potential. *Nutrients*, 11(9), 1–14. <https://doi.org/10.3390/nu11092147>
4. Cummings, J. L., Goldman, D. P., Simmons-Stern, N. R., & Ponton, E. (2022). The costs of

- developing treatments for Alzheimer's disease: A retrospective exploration. *Alzheimer's and Dementia*, 18(3), 469–477. <https://doi.org/10.1002/alz.12450>
5. Ellman, G. L., Courtney, K. D., Andres, V., & Featherstone, R. M. (1961). A new and rapid colorimetric determination of acetylcholinesterase activity. *Biochemical Pharmacology*, 7(2), 88–95. [https://doi.org/10.1016/0006-2952\(61\)90145-9](https://doi.org/10.1016/0006-2952(61)90145-9)
 6. ERDEMCI, F., AŞIR, F., & TAŞ, F. (2022). Etiology and Histopathology of Alzheimer's Disease and Current Approaches. *Black Sea Journal of Health Science*, 322–327. <https://doi.org/10.19127/bshealthscience.1064168>
 7. Heger, M., van Golen, R. F., Broekgaarden, M., & Michel, M. C. (2014). The molecular basis for the pharmacokinetics and pharmacodynamics of curcumin and its metabolites in relation to cancers. *Pharmacological Reviews*, 66(1), 222–307. <https://doi.org/10.1124/pr.110.004044>
 8. Ilic, D. B., & Ashoor, S. H. (1988). Stability of Vitamins A and C in Fortified Yogurt. *Journal of Dairy Science*, 71(6), 1492–1498. [https://doi.org/10.3168/jds.S0022-0302\(88\)79712-X](https://doi.org/10.3168/jds.S0022-0302(88)79712-X)
 9. Jahn, H. (2013). Memory loss in alzheimer's disease. *Dialogues in Clinical Neuroscience*, 15(4), 445–454. <https://doi.org/10.31887/dcns.2013.15.4/hjahn>
 10. Kamat, P. K. (2015). Streptozotocin induced Alzheimer's disease like changes and the underlying neural degeneration and regeneration mechanism. *Neural Regeneration Research*, 10(7), 1050–1052. <https://doi.org/10.4103/1673-5374.160076>
 11. Khezri, M. R., Yousefi, K., Zolbanin, N. M., & Ghasemnejad-Berenji, M. (2022). MicroRNAs in the pathophysiology of Alzheimer's disease and Parkinson's disease: an overview. *Molecular Neurobiology*, 59(3), 1589–1603. <https://doi.org/10.1007/s12035-022-02727-4>
 12. Knezovic, M. S. A., Hoyer, S., & Riederer, P. (2013). *What have we learned from the streptozotocin-induced animal model of sporadic Alzheimer's disease, about the therapeutic strategies in Alzheimer's research*. 233–252. <https://doi.org/10.1007/s00702-012-0877-9>
 13. Kraeuter, A.-K., Guest, P. C., & Sarnyai, Z. (2019). The Y-Maze for Assessment of Spatial Working and Reference Memory in Mice. *Methods in Molecular Biology (Clifton, N.J.)*, 1916, 105–111. https://doi.org/10.1007/978-1-4939-8994-2_10
 14. Kumar Thakur, A., Kamboj, P., Goswami, K., & Ahuja, K. (2018). Pathophysiology and management of alzheimer's disease: an overview. *Journal of Analytical & Pharmaceutical Research*, 7(2), 226–235. <https://doi.org/10.15406/japlr.2018.07.00230>
 15. Liu, X., Cao, Y. F., Dong, P. P., Zhu, L. L., Zhao, Z., Wu, X., Fu, Z. W., Huang, C. T., Fang, Z. Z., & Sun, H. Z. (2017). The inhibition of UDP-glucuronosyltransferases (UGTs) by vitamin A. *Xenobiotica*, 47(5), 376–381. <https://doi.org/10.1080/00498254.2016.1198841>
 16. Lueptow, L. M. (2017). Novel object recognition test for the investigation of learning and memory in mice. *Journal of Visualized Experiments*, 2017(126), 1–9. <https://doi.org/10.3791/55718>
 17. Maurya, N., Khamrui, K., & Prasad, W. (2020). Studies on curcumin fortification in different lassi types using Tween-80 as a binding material. *Indian Journal of Dairy Science*, 73(6), 628–631. <https://doi.org/10.33785/ijds.2020.v73i06.017>
 18. Miedel, C. J., Patton, J. M., Miedel, A. N., Miedel, E. S., & Levenson, J. M. (2017). Assessment of spontaneous alternation, novel object recognition and limb clasping in transgenic mouse models of amyloid- β and tau neuropathology. *Journal of Visualized Experiments*, 2017(123), 1–8. <https://doi.org/10.3791/55523>
 19. Moreira-Silva, D., Vizin, R., Martins, T., Ferreira, T., Almeida, M., & Carrettiro, D. (2019). Intracerebral Injection of Streptozotocin to Model Alzheimer Disease in Rats. *Bio-Protocol*, 9(20), 1–12. <https://doi.org/10.21769/bioprotoc.3397>
 20. Ogren, S. O., Institutet, K., & Stiedl, O. (2015). Passive Avoidance. *Encyclopedia of Psychopharmacology*, May, 1220–1228. <https://doi.org/10.1007/978-3-642-36172-2>
 21. Ono, K., & Yamada, M. (2012). Vitamin A and Alzheimer's disease. *Geriatrics and Gerontology International*, 12(2), 180–188. <https://doi.org/10.1111/j.1447-0594.2011.00786.x>
 22. Ozawa, H., Imaizumi, A., Sumi, Y., Hashimoto, T., Kanai, M., Makino, Y., Tsuda, T., Takahashi, N., & Kakeya, H. (2017). Curcumin β -D-glucuronide plays an important role to keep high levels of free-form curcumin in the blood. *Biological and Pharmaceutical Bulletin*, 40(9), 1515–1524. <https://doi.org/10.1248/bpb.b17-00339>
 23. Patel, C., Pande, S., & Acharya, S. (2020). Potentiation of anti-Alzheimer activity of curcumin by probiotic *Lactobacillus rhamnosus* UBLR-58 against scopolamine-induced memory impairment in mice. *Naunyn-Schmiedeberg's Archives of Pharmacology*, 393(10), 1955–1962. <https://doi.org/10.1007/s00210-020-01904-3>
 24. Paxinos, G., & Watson, C. (1982). *The Rat Brain in Stereotaxic Coordinates*.
 25. Perez, A. S., Rodriguez, M. S., Perez, M. C. G., & Mendez, J. H. (1996). Determination of fat-

- soluble vitamins in yogurt by HPLC with electrochemical detection M.M. *Talanta* 43, 43(18 march 1996), 1555–1563.
26. Qiu, C., Kivipelto, M., & Von Strauss, E. (2009). Epidemiology of Alzheimer's disease: Occurrence, determinants, and strategies toward intervention. *Dialogues in Clinical Neuroscience*, 11(2), 111–128. <https://doi.org/10.31887/dcms.2009.11.2/cqiu>
 27. Sanborn, V., Azcarate-peril, M. A., Updegraff, J., Manderino, L., & Gunstad, J. (2020). *Randomized Clinical Trial Examining the Impact of Lactobacillus rhamnosus GG Probiotic Supplementation on Cognitive Functioning in Middle-aged and Older Adults*.
 28. Sanders, E. R. (2012). Aseptic laboratory techniques: Plating methods. *Journal of Visualized Experiments*, 63, 1–18. <https://doi.org/10.3791/3064>
 29. Sathianathan, R., & Kantipudi, S. (2018). The dementia epidemic: Impact, prevention, and challenges for India. *Indian Journal of Psychiatry*, 60(2), 165–167. https://doi.org/10.4103/psychiatry.IndianJPsychiatry_261_18
 30. Segers, M. E., & Lebeer, S. (2014). *Towards a better understanding of Lactobacillus rhamnosus GG - host interactions*. 13(Suppl 1), 1–16.
 31. Shamsipour, S., Sharifi, G., & Taghian, F. (2021). Impact of interval training with probiotic (*L. plantarum* / *Bifidobacterium bifidum*) on passive avoidance test, ChAT and BDNF in the hippocampus of rats with Alzheimer's disease. *Neuroscience Letters*, 756(February), 135949.
 32. Tang, M., Taghibiglou, C., & Liu, J. (2017). The Mechanisms of Action of Curcumin in Alzheimer's Disease. *Journal of Alzheimer's Disease*, 58(4), 1003–1016.
 33. Weydert, C. J., & Cullen, J. J. (2010). Measurement of superoxide dismutase, catalase and glutathione peroxidase in cultured cells and tissue. *Nature Protocols*, 5(1), 51–66.
 34. *Yogurt Production | MilkFacts.info*. (n.d.). Milkfacts. Retrieved August 24, 2022, from <http://milkfacts.info/Milk Processing/Yogurt Production.htm>
 35. Zainoldin, K. H., & Baba, A. S. (2009). The effect of *Hylocereus polyrhizus* and *Hylocereus undatus* on physicochemical, proteolysis, and antioxidant activity in yogurt. *World Academy of Science, Engineering and Technology*, 36, 904–909.
 36. Zhang, X. X., Tian, Y., Wang, Z. T., Ma, Y. H., Tan, L., & Yu, J. T. (2021). The Epidemiology of Alzheimer's Disease Modifiable Risk Factors and Prevention. *Journal of Prevention of Alzheimer's Disease*, 8(3), 313–321.
 37. Zhou, S., Yu, G., Chi, L., Zhu, J., Zhang, W., Zhang, Y., & Zhang, L. (2013). Neuroprotective effects of edaravone on cognitive deficit, oxidative stress and tau hyperphosphorylation induced by intracerebroventricular streptozotocin in rats. *NeuroToxicology*, 38, 136–145.

This Page Intentionally Left Blank

ABSTRACT

SESSION 5 – MULTIDISCIPLINARY APPROACHES IN DRUG DISCOVERY & DEVELOPMENT

PCP378

DEVELOPMENT AND VALIDATION OF QUESTIONNAIRE MEASURING QOL OF WOMEN DURING MENSTRUAL CYCLE

AP0364

Ms. Priyanka R. Parmar
Associate Professor

Shri Sarvajani Pharmacy College,
Mehsana

Research Scholar

Kadi Sarva Vishwavidhyalaya,
Gandhinagar

priyankaparmar1004@gmail.com

AP0365

Dr. Shrikalp S. Deshpande
Principal

K. B. Institute of Pharmaceutical Education
and Research, Gandhinagar

shrikalp@kbiper.ac.in

Abstract:

Introduction: Menstruation is a physiological process experienced by adolescent girls and women. Menstruation is still a taboo in India. Menstruation and premenstrual symptoms affect the Quality of Life. To develop and validate a questionnaire measuring the Quality of Life during Menstrual cycle. Methodology: It was a cross sectional and observational study. Identification was done about different aspects affecting QOL of women during menstruation from literature search. As per different QOL domains development of questionnaire was done. Menstrual Health Outcomes Questionnaire contains total 35 questions from general health, physical, economic, social, emotional, psychological and life satisfaction. Ethical consideration was obtained from independent ethics committee. Pilot study was performed, then Menstrual Health Outcomes Questionnaire was randomly self-administered by adolescent girls studying in privet college of Mehsana city, Gujarat. Results: Total 211 adolescent girls were randomly recruited in study. Questionnaire has acceptable internal consistency among constructed items showing Cronbach's Alpha 0.796. Intraclass correlation coefficient was found 0.786 which also suggested good reliability. Conclusion: The Menstrual Health Outcomes Questionnaire is scientifically sound for measuring the outcomes during menstruation.

Keywords: Menstruation, Quality of life, Menstrual Health Outcomes Questionnaire

1. INTRODUCTION:

Menstruation is a physiological process experienced by adolescent girls and women. Menstruation is still a taboo in India. Menstruation and premenstrual symptoms affect the Quality of Life. Different scales are available to measure QOL for different gynaecological problems but none scale available to measure QOL during Menstruation. WHO defines Quality of Life as an individual's perception of their position in life in the context of the culture and value systems in which they live and in relation to their goals, expectations, standards and concerns?

It is a multidimensional concept that includes domains related to physical, mental, emotional and social functioning. It goes beyond direct measure of population health, life expectancy and causes of death and focuses on the impact health status on quality of life. As India is a man dominating country, women feel hesitate to show their views or problems where problems are of Gynae. As compared to other countries Indian women have low literacy level and less awareness in different disease of reproductive system.

Some studies conducted in different parts of India suggested higher prevalence of premenstrual symptoms among adolescent girls.(Padikkal & Romate, 2018) Dysmenorrhoea is considered as physical symptoms during menstruation and it was not only affecting girls physical health but also affects their daily living and social activities. One study performed among Chinese adolescent girls in Hong Kong was reveals majority of the participants had dysmenorrhea during menstruation which limits their routine activities.(Wong, 2018) Premenstrual symptoms can be

varied in physical and psychological type. Many of them can be felt by girls during menstrual cycle like headache, backache, vomiting, mood swings, anxiety, cravings for specific food etc. Physical symptoms limits routine living practice and psychological symptoms affects mental health of the girls.

2. OBJECTIVES:

To Develop and Validate a questionnaire measuring the Quality of Life during Menstrual cycle.

3. METHODOLOGY:

3.1 Study design & study population:

It was an observational, prospective & cross-sectional study was carried out from March 2021 to June 2021. Girls studying in private college of Mehsana city were enrolled in the study as per inclusion criteria. Those respondents were attended menarche were randomly selected for the study.

3.2 Menstrual Health Outcomes Questionnaire development:

Menstrual Health Outcomes Questionnaire was prepared by authors. Literature search was done to understand different QOL scales available for different gynaecological problems. None QOL scale available which can be used during menstrual cycle. Few questions was prepared in line with Quality of life scale SF-36(Ware et al., 1994) & SF-12(Medical Outcomes Trust, 1994). The questionnaire is consisted of 35 questions of different QOL domains like physical, economic, social, emotional, psychological, life satisfaction. Physical domain has 6 questions asking about routine household, exercise and travelling activities. Economical domain is of 3 questions regarding economic criteria. Social activities like outing and social gatherings were covered by 2 questions of social domain. Six questions were asked about emotional domain about relationships and concentration in routine activities. Total 14 questions were belonging to psychological and life satisfaction domains. Last question was about to rate health status before, during and after menstruation. Questionnaire was validated by expert's opinion. Pilot study was run for further validation among 48 respondents. Minor modifications were done in questionnaire after pilot study. Questionnaire was translated in vulnerable language before initiation of final data collection.

3.3 Ethical Consideration:

Ethical consideration was obtained from the independent ethics committee of Mehsana city.

3.4 Data collection and Analysis:

Menstrual Health Outcomes Questionnaire was self-administered by the respondents after signing informed consent form. After data collection, data entry was done in IBM SPSS version 20. Cronbach alpha was determined to check internal consistency of Questionnaire. Intraclass Corelation Coefficient was obtained to check reliability of questionnaire.

4. LITERATURE REVIEW:

Followings are the literature for the development of the different scales for the assessment of the Quality of Life among women. None scale available for the QOL assessment during menstruation.

Authors	Title	Methodology	Inference
Jones, Georgina Jenkinson, Crispin	Development of the short form endometriosis health profile questionnaire: The EHP-5	Three studies were performed to establish Endometriosis Health Profile-30 core questionnaire. Pilot study was	11 items developed for core and modular questionnaire. This questionnaire is scientifically valid for further use.

<p>Kennedy, Stephen(Jones et al., 2004)</p>		<p>done. Finally, 23-item modular questionnaire was produced. It contains six dimensions which may not be applicable to every woman with endometriosis and is used to supplement the five scales on the core questionnaire when required.</p>	
<p>Cronin, L Guyatt et al.(Cronin et al., 1998)</p>	<p>Development of a health-related quality-of-life questionnaire (PCOSQ) for women with polycystic ovary syndrome (PCOS)</p>	<p>182 items was potentially relevant & used for women with PCOS through semi structured interviews. Different healthcare professionals derived information from the women with PCOD and suggested 182 items which is required to capture especially for PCOS.</p>	<p>Total 51 items are important for further identification of symptoms. The highest impact 5 domains are emotions, infertility, body hair, menstrual problems to construct a final questionnaire, the Polycystic Ovary Syndrome Questionnaire (PCOSQ) contains 26 items with 10-15 minutes self-administration time.</p>
<p>Lamping, D. L. Rowe, P. Clarke, A. Black, N. Lessof, L.(Lamping et al., 1998)</p>	<p>Development and validation of the menorrhagia outcomes questionnaire</p>	<p>Data from long research The Menorrhagia Outcomes questionnaire is a 26-item questionnaire which covers symptoms, post-operative complications, quality of life, and women's satisfaction with outcome.</p>	<p>The Menorrhagia Outcomes Questionnaire was found to be highly acceptable to women and showed excellent internal consistency, test-retest reliability, criterion and construct validity.</p>
<p>Agarwal, Anupriya Venkat, Annapoorna(Agarwal & Venkat, 2009)</p>	<p>Questionnaire Study on Menstrual Disorders in Adolescent Girls in Singapore</p>	<p>Cross-sectional study was done in Singapore with a self-administered, 27-point structured questionnaire. Data were collected from 62 schools and junior colleges in Singapore.</p>	<p>83.2% respondents reported dysmenorrhea with different severities and 24% girls reported school absenteeism due to it. 45.1% of all subjects required analgesics medications to relieve pain.</p>

<p>Chothe, Vikas Khubchandan, Jagdish Seabert, Denise Asalkar, Mahesh Rakshe, Sarika Firke, Arti Midha, Inuka Simmons, Robert(Chot he et al., 2014)</p>	<p>Students' Perceptions and Doubts About Menstruation in Developing Countries: A Case Study from India</p>	<p>84 girls from 6th grade, 117 from seventh grade, and 180 from eighth grade were enrolled in the study. The questions were about anatomy and physiology, menstrual symptoms, menstrual myths and taboos, health and beauty, menstrual abnormalities, seeking medical advice and home remedies; use of sanitary material and its disposal; diet and lifestyle; and sex education.</p>	<p>This study indicate that respondents had substantial doubts about menstruation and were influenced by societal myths and taboos in relation to menstrual practices.</p>
<p>Hyunjeong Shin, Songi Jeon, Inhae Cho(Shin et al., 2022)</p>	<p>Factors influencing health-related quality of life in adolescent girls: a path analysis using a multi-mediation model</p>	<p>This study performed at Korea reveals proportional correlation between menstrual health, social support, dietary habits, depression with Health-related quality of life.</p>	<p>The study findings are menstrual health is affected by sleep habits, food habits, psychological health and social support.</p>
<p>Kyoko Shimamoto et al.(Shimamoto et al., 2021)</p>	<p>Examining the association between menstrual symptoms and health-related quality of life among working women in Japan using the EQ-5D</p>	<p>This study investigate relation between QOL and menstrual symptoms. Self-administered questionnaire was filled by 6048 respondents. Multivariate regression analysis was carried out.</p>	<p>Menstrual symptoms were negatively affecting Health related Quality of life with different domains.</p>

5.RESULTS:

Total 211 girls with the mean age of 20.10 ± 1.68 years rated this questionnaire. Mean \pm SD were calculated for separate domain as shown in below table.

Table 1 Mean values of each question

Domain	Questions	Mean \pm SD
Health	Rate your health in general	3.04 \pm 0.91
Physical	Routine activities	2.36 \pm 0.74
	Routine exercise activities	1.68 \pm 0.74
	Sports activities	1.73 \pm 0.79
	Travelling activities	2.12 \pm 0.75
	Cut down the amount of time you spent on work	1.45 \pm 0.49
	Accomplished less than you would like	1.41 \pm 0.49
Economical	Enough money to meet expenses	2.43 \pm 0.76
	Money for leisure activities	2.32 \pm 0.74
	Living expenditure	2.47 \pm 0.74
Social	Outings	1.99 \pm 0.69
	Social gatherings	1.96 \pm 0.70
Emotional	Concentration properly in household work / study	2.27 \pm 0.72
	Personal Relationship	2.48 \pm 0.74
	Relationship with family and friends	2.67 \pm 0.62
	Support from family and friends	2.62 \pm 0.65
	Cut down the amount of time you spent on work	1.41 \pm 0.49
	Accomplished less than you would like	1.35 \pm 0.47
Psychological	Mood swings	1.88 \pm 0.69
	Anxiety or tension	1.47 \pm 0.71
	Depression or hopelessness	1.65 \pm 0.72
	Nervousness	1.54 \pm 0.65
	Lack of energy	1.89 \pm 0.72
	Get frustration easily	1.73 \pm 0.71
	Feel tiredness	2.0 \pm 0.73
Life satisfaction	Physical health	2.39 \pm 0.67
	Ability to function in daily life	2.45 \pm 0.68
	Enjoyment in life	2.52 \pm 0.67
	Overall sense of well being	2.40 \pm 0.70
	Economic status	2.48 \pm 0.69

	Daily life feeling	2.46 ± 0.67
	Sleep satisfaction	2.46 ± 0.69
Health	Before menstruation	3.83 ± 0.98
	During menstruation	3.52 ± 0.95
	After menstruation	3.47 ± 1.05

Internal Consistency among constructed items showing Cronbach Alpha 0.796. Table-2 represents the Cronbach Alpha value for separate domains of the questionnaire. The Cronbach Alpha overall health, physical, economic, social, emotional, psychological and life satisfaction were 0.61, 0.59, 0.86, 0.77, 0.60, 0.89 and 0.92 respectively.

Table 2 Cronbach Alpha

Domains	Number of Questions	Cronbach Alpha
Overall health	4	0.597
Physical	6	0.598
Economical	3	0.856
Social	2	0.769
Emotional	6	0.570
Psychological	7	0.894
Life satisfaction	7	0.919
Overall	35	0.796

The Intraclass Correlation Coefficient was determined to measure reliability of questionnaire, it was 0.786 at 95% of confidence interval as mentioned in table-3.

Table 3 Intraclass Correlation Coefficient

	Intraclass Correlation	95% Confidence Interval	
		Lower Bound	Upper Bound
Single Measures	0.095	0.076	0.119
Average Measures	0.786	0.743	0.826

6. CONCLUSION:

The Menstrual Health Outcomes Questionnaire is scientifically sound for measuring the outcomes during menstruation.

7. REFERENCES:

1. Agarwal, A., & Venkat, A. (2009). Questionnaire Study on Menstrual Disorders in Adolescent Girls in Singapore. *Journal of Pediatric and Adolescent Gynecology*. <https://doi.org/10.1016/j.jpog.2009.02.005>
2. Chothe, V., Khubchandani, J., Seabert, D., Asalkar, M., Rakshe, S., Firke, A., Midha, I., & Simmons, R. (2014). Students' Perceptions and Doubts About Menstruation in Developing Countries: A Case Study From India. *Health Promotion Practice*, 15(3), 319–326. <https://doi.org/10.1177/1524839914525175>
3. Cronin, L., Guyatt, G., Griffith, L., Wong, E., Azziz, R., Futterweit, W., Cook, D., & Dunaif, A. (1998). Development of a Health-Related Quality-of-Life Questionnaire (PCOSQ) for Women with Polycystic Ovary Syndrome (PCOS)*. In *Journal of Clinical Endocrinology and Metabolism Printed* (Vol. 83, Issue 6). <https://academic.oup.com/jcem/article-abstract/83/6/1976/2865351>

4. Jones, G., Jenkinson, C., & Kennedy, S. (2004). Development of the short form endometriosis health profile questionnaire: The EHP-5. *Quality of Life Research*, 13(3), 695–704. <https://doi.org/10.1023/B:QURE.0000021321.48041.0e>
5. Lamping, D. L., Rowe, P., Clarke, A., Black, N., & Lessof, L. (1998). Development and validation of the menorrhagia outcomes questionnaire. *British Journal of Obstetrics and Gynaecology*. <https://doi.org/10.1111/j.1471-0528.1998.tb10209.x>
6. Medical Outcomes Trust. (1994). *SF-12® Patient Questionnaire*. 1, 5–7. <https://www.hoagorthopedicinstitute.com/documents/SF12form.pdf>
7. Padikkal, T., & Romate, J. (2018). *Premenstrual Syndrome and Quality of Life of Rural Adolescent Girls in Kalaburagi District . July 2022*.
8. Shimamoto, K., Hirano, M., Wada-Hiraike, O., Goto, R., & Osuga, Y. (2021). Examining the association between menstrual symptoms and health-related quality of life among working women in Japan using the EQ-5D. *BMC Women's Health*, 21(1), 1–8. <https://doi.org/10.1186/s12905-021-01462-7>
9. Shin, H., Jeon, S., & Cho, I. (2022). Factors influencing health-related quality of life in adolescent girls: a path analysis using a multi-mediation model. *Health and Quality of Life Outcomes*, 20(1), 1–12. <https://doi.org/10.1186/s12955-022-01954-6>
10. Ware, J., Snow, K., Kosinski, M., Gandek, B., Ware Je, & Sherbourne. (1994). Medical outcomes study questionnaire short form 36 health survey (SF-36). *Med Care*, 32(306), 1–5.
11. Wong, C. L. (2018). Health-related quality of life among Chinese adolescent girls with Dysmenorrhoea. *Wong Reproductive Health*, 15:80, 1–10. <https://doi.org/10.1186/s12978-018-0540-5%0A>

PCP382

ASSESSMENT OF THE EFFECT OF METHANOLIC EXTRACT OF *VANDA TESSELLATA ROXB.* AGAINST EXPERIMENTALLY INDUCED COLITIS IN ALBINO WISTAR RATS.

AP0343	AP0370	AP0373	AP0371
Ms. Pooja Goswami	Dr. Devang B. Sheth	Ms. Dharti Ribadiya	Dr. Ravi A. Manek
Assistant Professor,	Associate Professor,	Pharmacist,	Assistant Professor,
Babaria Institute of Pharmacy, Vadodara	L. M. College of Pharmacy, Ahmedabad	Mowbray, Tasmania, Australia	B. K. Mody Govt. Pharmacy College, Rajkot
poojagoswami241@gmail.com	devangbsheth@gmail.com	ribadiyadharti210@gmail.com	ravimanek16@gmail.com

ABSTRACT:

Context: Ulcerative colitis (UC) is one of the most prevalent inflammatory bowel diseases. The *Vanda tessellate* is attaining increased importance for its proven antioxidant, anti-inflammatory, and anti-microbial activity in different extracts attributed to the presence of potentially active constituents- flavonoids, phenolics, and sterols in addition to its high safety profile. The same phytoconstituents may be considered beneficial in UC.

Objective: Present study attempted to explore the possible curative effect of methanolic extract of *Vanda tessellate* on rats to search for safe and effective treatment for UC.

Materials and Methods: Methanolic root extract was prepared and screened for phytochemicals. Albino Wistar rats were divided into five groups: normal control, disease control, standard group (Sulphasalazine-50mg/kg), and test group (VTE-200,400 mg/kg). TNBS was administered intrarectally to induce UC. Treatment commenced from the 5th day. The disease activity index (DAI) was recorded daily for 15 days. Animals were sacrificed afterward and evaluated for histopathological and biochemical examinations.

Results: Phytochemical screening confirmed the presence of flavonoids, phenolics, and sterols. Compared with disease control, the treatment group significantly reversed pathologies associated with UC including DAI, colon mucosal damage index (CMDI), level of myeloperoxidase, malondialdehyde, and nitric oxide in colon homogenate which proves the effectiveness of the drug in UC.

Discussion and conclusion: Our findings demonstrate the curative effect of *Vanda tessellate* in TNBS-induced colitis. The perspective underlying mechanisms include modification of immuno-inflammatory pathways through a reduction in MPO activity and/or NO generation and antioxidant activity.

Keywords: Ulcerative Colitis, *Vanda tessellate*, Anti-oxidant, Anti-inflammatory, Free radical scavenger.

INTRODUCTION

Ulcerative colitis is associated with recurrent uncontrolled inflammation of the colon. (Meier, 2011) It most commonly affects the colon and rectum and is characterized by abdominal pain and diarrhea with mucous, pus, and blood. (Min, 2021) (Li C. D., 2021) Another common feature of ulcerative colitis is Weight loss. (Saba, 2020) Mucosal inflammation is observed to be relapsing and remitting which starts in the rectum and extends proximally through the colon. (Du, 2020)

UC can occur anytime in life, but the peak incidence is generally observed in the second to fourth decade of life and affect both the sex equally. (Du, 2020). It annually affects 2-7/100,000

people in the USA. (Saba, 2020) Worldwide, the incidence of UC is rising with an annual incidence of 8.8 - 23.1 per 100,000 persons in North America, 0.6 - 24.3 per 100,000 persons in Europe, and 7.3 - 17.4 in Oceania. (Du, 2020) The worldwide incidence of UC is increasing in recent years. (Min, 2021) (Sasson, 2021) A longer duration and risks of disease or treatment-related complications (including infections, thromboembolic events, and malignancies) generate a burden on health facilities. (Du, 2020)

Identified factors that trigger UC includes the environment and disrupted immune system. (Li C. D., 2021) High-fat diets and westernized culture also increase the risk of UC. (Saba, 2020) Although, diet is a potentially modifiable risk factor for onset and severity of IBD. (Sasson, 2021) A higher risk of UC may also be conferred by several genes encoding proteins that modify cytokines involved in clinical outcomes of UC. (Saba, 2020)

The exact pathogenesis of UC is unclear. The development and progression of the disease is a multifactorial mechanism associated with genetic predisposition, environmental factors, microbiota, and mucosal immune dysregulation (Saba, 2020) which may culminate in progressive damage and insufficient repair of the gastrointestinal tract. (Bernstein, 2009) (Nakase, 2022) The cytokines, produced by innate and adaptive immune cells including IL-1 β , IL-6, tumor necrosis factor- α , T helper (Th) 1-, Th2-, and Th17-associated cytokines are related to the pathogenesis of UC and are expressed at relatively higher levels in the UC patients. (Saba, 2020) These cytokines provide therapeutic targets for UC treatment. (Min, 2021)

Neutrophils are the first immune cells to infiltrate and contribute to the initiation of human colitis. It stimulates epithelial barrier impairment, tissue destruction by oxidative and proteolytic damage, and perpetuates inflammation by the release of cytokines and chemokines associated with pro-inflammatory effects. (Babalola, 2022). Research evidence shows that the extensive infiltration of neutrophils in the intestinal mucosa is positively correlated with the active disease and is a hallmark of tissue damage associated with endoscopic severity and systemic inflammatory indexes in IBD. (dos Santos Ramos, 2021)

The risk of developing colorectal cancer (CRC) is high in patients with IBD. (Wijnands, 2021) The prolonged inflammation in the colon and rectum may result in the accumulation of pro-inflammatory cytokines within the colonic mucosa, which causes dysplastic lesions and increase the chances of development of colorectal cancer (CRC). Compared to the general population, UC patients have a 2.4-fold higher risk of CRC. (Min, 2021) In addition to gastrointestinal manifestations, IBD causes extraintestinal manifestations in the central and peripheral nervous system and increases the incidence of neurological complications. (Ferro, 2021)

Management of UC involves the use of drugs therapy mainly comprising corticosteroids, amino-salicylates, immunosuppressive drugs, and biological agents, which display unavoidable side effects, easy recurrence, drug resistance and high cost that hinder their clinical application. (Li C. D., 2021) Adverse reactions to these drugs include gastrointestinal discomfort, allergic reactions, obesity, water and sodium retention, and severe bone marrow suppression. (Min, 2021)

Relapse is the major factor of consideration with UC. There is a 90% chance of relapse even with the use of allopathic drugs. (Saba, 2020) Incredible advances are made in modern medicine although there are still a large number of ailments for which suitable drugs are yet to be found. The need of developing safer drugs for the treatment of various diseases still remains. Hence, the Indian traditional system of medicine is the area of interest in pharmacological evaluation. *Vanda tessellata* Roxb. belonging to Orchidaceae family is an important ayurvedic medicinal herb and has been used for a variety of disorders including; inflammations, bronchitis, rheumatism, dyspepsia, dysentery, and fever. The anti-inflammatory activity of *Vanda tessellata* methanolic extract was evaluated against carrageenan-induced edema in rodents (Chawla, 1992). The anti-oxidant activity was also studied using crude methanol extract from the roots of *Vanda tessellata* (Uddin, 2015) (Subin, 2021). Antinociceptive and cytotoxic effect of methanolic as well as aqueous extracts of *V. Tessellata* leaf was evaluated (Chowdhury, 2014). The antimicrobial activity of various solvent extracts was also evaluated (Gupta C. &., 2014) (Bhattacharjee, 2015).

OBJECTIVES

Currently used drugs (viz antibiotics, immunomodulators, corticosteroids, amino salicylates) are associated with various side effects and there is need of safe and effective alternative from herbal origin. The ultimate goal for UC treatment is complete remission; thus, whether a phytonutrient-rich plant with reported antioxidant and anti-inflammatory properties would be beneficial to UC treatment remains a progressive study that requires continual optimization. Present study attempted to explore the possible curative effect of methanolic extract of *Vanda tessellata* on rats to search for safe and effective treatment for UC.

RESEARCH METHODOLOGY

Plant material

Fresh roots of *Vanda tessellata* Roxb. were collected from Sanjivani Aushadhalay, Bhavnagar and authenticated by Department of Biology, Christ College, Rajkot.

Extraction

Powdered drug (roots) was used for extraction. Extraction was carried out with methanol using a Soxhlet apparatus.

Preliminary phytochemical screening

Methanolic extract of *Vanda tessellata* (VTE) root was used for preliminary phytochemical screening to determine the presence of Alkaloids, Flavonoids, Glycoside, Tannins, Steroid, Carbohydrates, Protein, and Amino acid (Khandelwal, 2008).

Experimental animals

Adult 30 male Albino Wistar rats (150-200g) were used. The experimental protocol was approved by Institutional Animal Ethics Committee (Protocol no. BKMGPC/IAEC17/RP13/2016) and animals were maintained under standard housing condition (12-h light/dark cycle, 24°C, 35 to 60% humidity).

Experimental design

Trinitro benzene sulfonic acid induced colitis in rats: Albino Wistar rats (150-200 gm) were divided into five groups (n=6); normal control, disease control, standard group (Sulphasalazine-50mg/kg), and test group (VTE-200,400 mg/kg). At day 1, TNBS (10mg) dissolved in 50% ethanol (total volume 0.25 ml) was given intrarectally to induce the disease. On the basis of weight loss, stool consistency and rectal bleeding, a disease activity index score was recorded daily. On the 5th day, animals were given treatment drug for next 10 days. At the end of experiment, animals were sacrificed and abdomens were opened by midline incision and evaluated for colon mucosal damage index (CMDI) and the level of myeloperoxidase (MPO), malondialdehyde (MDA), and nitric oxide (NO) in the homogenized colon tissues.

Evaluation parameters

Gross behavior

A gross behavior study was performed.

Disease Activity Index (Stevceva, 2001) (Min, 2021)

DAI is resultant of three major clinical signs including weight loss, diarrhea and rectal bleeding/hematochezia. The difference between predicted and actual body weight on a particular day was used for calculating body weight loss. A diarrhea was scored either 1 or 0 according to adherence of mucus/fecal material to anal fur. The presence or absence of rectal bleeding or diarrhea containing blood or mucus was scored either 1 or 0 respectively.

Colon Mucosal Damage Index (Patel, 2012)

Macroscopic scoring was done as follows:

1. = no mucosal damage,

2. = mild hyperaemia and mild edema, with no signs of ulcer or erosion,
3. = moderate hyperaemia and edema, mucosal surface appears with erosion,
4. = severe hyperaemia and edema, mucosal surface appears with ulcer and necrosis, ulcerative area <1 cm
5. = severe hyperaemia and edema, mucosal surface appears with ulcer and necrosis, ulcerative area >1 cm.

Histopathology (Koppikar, 2014)

The tissue samples from colon were fixed overnight in 10% neutral buffer formalin solution. A thin section (4 µm thick) was stained with haematoxylin and eosin. and observed under microscope.

Myeloperoxidase (MPO) activity (Krawisz, 1984)

Myeloperoxidase activity was determined by a method as previously described by Krawisz et al. 50 mmol/L ice-cold potassium phosphate buffer (pH 6) containing 0.5% of hexadecyl trimethyl ammonium bromide (DTAB) was used to homogenize colon tissue. The homogenate was sonicated in an ice bath for 10s and freeze-thawed thrice. It was then allowed to centrifuge at 4000 rpm for 20 min at 4°C. The supernatant (0.1 ml) was mixed with 50 mM phosphate buffer (2.9 ml), containing O- dianisidine dihydrochloride (0.167 %) and 0.0005% hydrogen peroxide. The change in absorbance was recorded at every 15-second interval for 1 minute at 460 nm wavelength using a spectrophotometer. Degradation of one micromole of peroxidase per minute at 25°C is considered as 1 unit of MPO activity which can be calculated by the following formula:

MPO activity mU/mg = $1000 \times X / \text{Weight of tissue taken (mg)}$

Where X = $10 \times \text{Change in absorption per minute Volume of supernatant taken in final reaction.}$

Malondialdehyde (MDA) measurement (Slater, 1971)

The severity of lipid peroxidation can be determined by measuring the level of malondialdehyde (MDA) in the tissue. 1 ml of supernatant was added in to 2 ml of 10% (w/v) tri- chloroacetic acid and stood in ice for 15 min. Precipitates were separated by centrifugation. 2 ml supernatant solution were added to 2 ml of aqueous 0.67% thiobarbituric acid and heated for 10 min in a boiling-water bath. The solution was cooled in ice for 5 min and absorbance was recorded at 535 nm against an appropriate blank solution. The amount of malondialdehyde (MDA), a thiobarbituric acid reactive material, was expressed as nmol of MDA/mg protein. And can be calculated using a molar extinction coefficient $1.49 \times 10^5 \text{ M}^{-1}\text{cm}^{-1}$.

Nitric oxide (NO) assessment (Alam, 2013) (Green, 1982)

The method explained by Griess in 1879 was used to determine accumulated nitrite (NO) in the homogenate. The assay was based on a diazotization reaction. The colon tissue was thawed in 0.3 ml PBS (pH 7.2 at 4°C), weighed and homogenized. The homogenate was centrifuged at 12000 rpm for 10 min. 2 ml of 10 mM sodium nitroprusside dissolved in 0.5 ml phosphate buffer saline (pH 7.4). was mixed with 0.5 ml of clear homogenate. The reaction mixture was incubated for 150 min at 25°C. 0.5 ml of Griess reagent is added to 0.5 ml of incubated solution and incubated again for 10 min at room temperature. The absorbance was recorded at 540 nm to determine NO concentration. A standard curve of sodium nitrite was used for calculation.

% Mortality

% Mortality was assessed in all groups.

Statistical Analysis

All the values were expressed as mean \pm S.E.M. Statistical significance between more than two groups was tested using one-way ANOVA followed by the Bonferroni test as appropriate using computersoftware (Prism, Graph pad 5.01.). The results were considered to be statistically significant when $p < 0.05$.

LITERATURE REVIEW

Bindiya et al studies antioxidant and antidepressant activity of chloroform and ethanol extracts of *V. tessellate* leaves. A reduction in immobility times of rats in forced swimming test (FST) and tail suspension test (TST) were observed in ethanolic extract that confirmed significant antidepressant activity may be due to the presence of polyphenol and flavonoids. (Prakash, 2018)

Anisuzzaman et al assessed the antinociceptive and cytotoxic effect of methanol and aqueous extracts of *V. tessellata* leaf by acetic acid-induced writhing test, hot plate test, and tail immersion test in mice. The result demonstrated potential antinociceptive activity with minimum cytotoxicity and significant anti-inflammatory activity. (Chowdhury, 2014)

A dose-dependent hepato-protective activity of petroleum ether extract of leaves of *Vanda tessellata* in rat was reported in the study by Anwar et al. (2013). (Anwar, 2013)

Gupta and Katewa (2014) evaluated antimicrobial activity of various root extract (petroleum ether, chloroform, ethyl acetate, acetone, methanol and hexane) of *Vanda tessellata* (Roxb.) by agar-well diffusion method. Ethyl acetate extract showed significant antibacterial activity against the human pathogens. (Gupta C. &, 2014) Another study evidenced antimicrobial activity of *Vanda tessellate*. In which chloroform and hexane extract of whole plant was evaluated and was found to be effective against bacterial species including *Bacillus subtilis*, *Escherichia coli*, *Klebsiella pneumonia*, *Staphylococcus aureus*, and *Vibrio cholerae*; and fungal species including *Aspergillus*, *Rhizopus* spp. and *Penicillium* spp. (Bhattacharjee, 2015)

Gupta et al (2016) reported that 3-ethoxy-10,17dimethyltetradecahydro-1H-cyclopenta[a]phenanthren-17(2H)-one, a new compound isolated from *Vanda tessellata*, showed antibacterial activity against *B. subtilis*, *E. coli* and *Proteus mirabilis*. (Gupta C. , 2016)

Vijaykumar et al evaluated petroleum ether extract of leaves of *Vanda tessellata* for antioxidant activity and the result showed potent 1,1-diphenyl-2-picrylhydrazyl (DPPH) and nitric oxide (NO) radicals scavenging activities. (Vijaykumar, 2013)

The antiulcer activity of petroleum ether extracts of leaves of *Vanda tessellata* was evaluated by Sailakshmi et al. (2015) in Wistar rats. The result demonstrated that the extract has preventive role in aspirin-induced gastric ulcers with minimum toxicity. (Sailakshmi, 2015.)

Sirisha et al (2014) demonstrated dose-dependent anxiolytic effects of petroleum ether extracts of *Vanda tessellata* leaves and the results were comparable to diazepam. (Sirisha, 2013)

ANALYSIS PART

Phytochemical screening:

Vanda tessellata was subjected to preliminary phytochemical analysis. The methanolic extract showed the presence of Flavonoids, Phenolic compound, Alkaloids, Tannins and Sterols.

Gross behavior:

By performing gross behavior study, changed stool consistency, bloody diarrhea, decreased body weight, decreased movements of animals were observed. A drastic drop in body weight was observed in diseased group as compare to normal group. VTE (400 mg/kg and 200 mg/kg) and standard (50 mg/kg) treated group showed less body weight reduction as compared to disease control group.

Disease Activity Index (DAI):

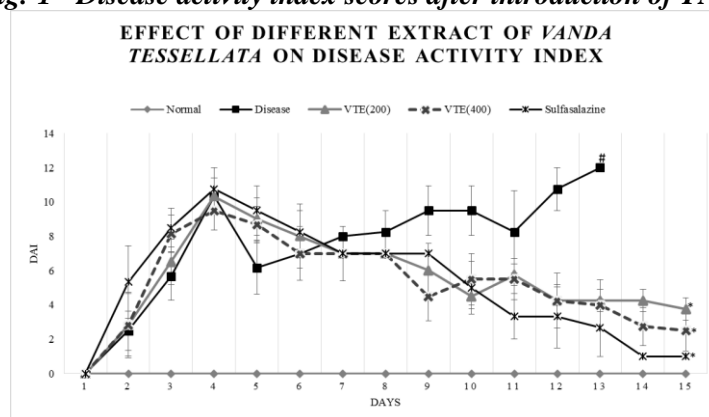
TNBS administration significantly increase DAI in all group compared to normal group. When the treatment was started it was gradually decreased in VTE as well as standard treated group compared to the disease group. (Table no.- 1; Fig no.- 1)

Table no. 1- Effect of methanolic extract of roots of *Vanda tessellata* on DAI score

DAY	DAI SCORE OF TREATMENT GROUP				
	Normal	Disease	VTE (200)	VTE (400)	Sulfasalazine
2	0	2.5 ± 1.15	2.83 ± 1.91	2.83 ± 1.82	5.33 ± 2.12
3	0	5.67 ± 1.39	6.5 ± 1.32	8.167 ± 1.08	8.5 ± 1.12

4	0	10.33 ± 1.05	10.33 ± 1.06	9.5 ± 1.12	10.75 ± 1.25
5	0	6.167 ± 1.54	9 ± 1.22	8.67 ± 1.06	9.5 ± 1.44
6	0	7 ± 1.58	8 ± 1.87	7	8.25 ± 1.25
7	0	8 ± 0.1	7	7 ± 1.59	7
8	0	8.25 ± 1.25	7	7	7
9	0	9.5 ± 1.44	6 ± 1.6	4.5 ± 1.44	7
10	0	9.5 ± 1.44	4.5 ± 0.72	5.5 ± 1.5	5 ± 1.53
11	0	8.25 ± 2.39	5.75 ± 0.62	5.5 ± 1.19	3.33 ± 1.33
12	0	10.75 ± 1.25	4.25 ± 0.8	4.25 ± 1.6	3.33 ± 1.86
13	0	12	4.25 ± 0.66	4 ± 1.47	2.67 ± 1.67
14	0	-	4.25 ± 0.66	2.75 ± 1.11	1
15	0	-	3.75 ± 0.66	2.5 ± 1.19	1

Fig.-1 - Disease activity index scores after introduction of TNBS



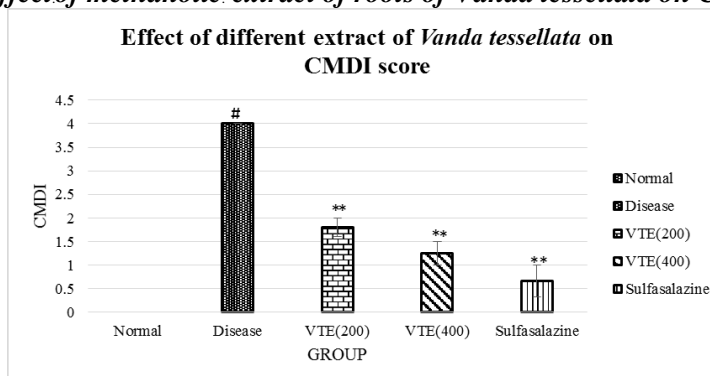
Colon Mucosal Damage Index (CMDI)

Administration of TNBS significantly increased the colon mucosal damage index score in disease control group as compare to normal control group ($P < 0.01$). Treatment with VTE and standard showed significant reduced CMDI score compared to disease control group ($P < 0.01$). (Table no.- 2; Fig no.- 2)

Table no. 2- Effect of methanolic extract of roots of Vanda tessellata on CMDI score

GROUP	CMDI SCORE
Normal	0
Disease	4 ± 0 #
VTE(200)	1.8 ± 0.2 **
VTE(400)	1.2 ± 0.25 **
Sulfasalazine	0.66 ± 0.33 **

Fig.-2- Effect of methanolic extract of roots of Vanda tessellata on CMDI score



Histopathology

Results of histopathology showed transmural inflammation with extensive necrosis, epithelial damage, ulceration, and cells infiltration in disease group. In all treatment group decreased signs of injury was found. (Fig no.- 7)

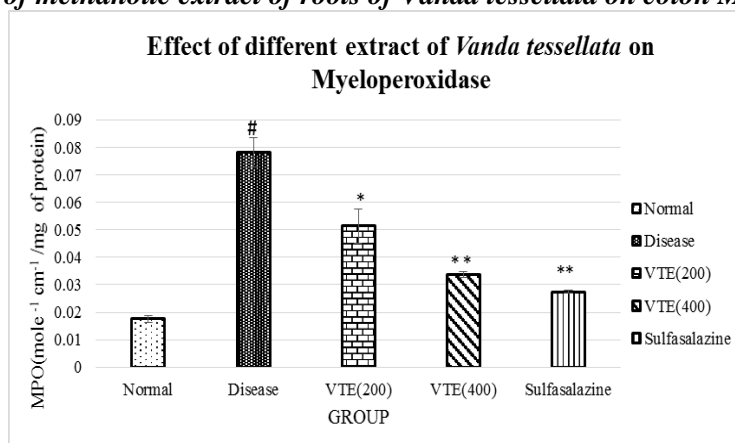
Myeloperoxidase (MPO) activity

A significant Elevation in MPO level was found in disease group as compared to normal group ($P < 0.01$). In case of treatment group, it was significantly reduced ($P < 0.05$) as compared to the disease control group. (Table no.- 3; Fig no.- 3)

Table no. 3- Effect of methanolic extract of roots of *Vanda tessellata* on colon MPO level

GROUP	MPO(mole ⁻¹ cm ⁻¹ /mg of protein)
Normal	0.018 ± 0.001
Disease	0.078 ± 0.005 #
VTE(200)	0.051 ± 0.006 *
VTE(400)	0.034 ± 0.001 **
Sulfasalazine	0.027 ± 0.001 **

Fig.-3 - Effect of methanolic extract of roots of *Vanda tessellata* on colon MPO level.



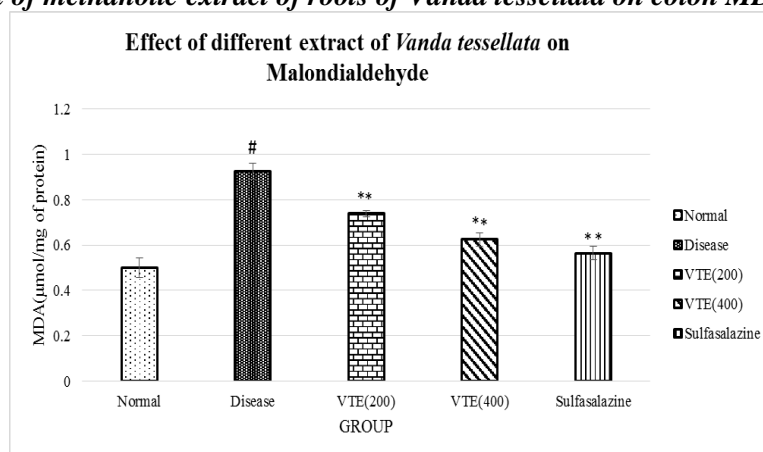
Malondialdehyde (MDA) level

Tissue MDA level was found to be high ($P < 0.01$) in disease group as compared to normal group. A significant drop was observed in drug and standard treated group as compared to the disease control group ($P < 0.01$). (Table no.- 4; Fig no.- 4)

Table no. 4- Effect of methanolic extract of roots of *Vanda tessellata* on colon MDA level.

GROUP	MDA (µmol/mg of protein)
Normal	0.5 ± 0.043
Disease	0.92 ± 0.036 #
VTE (200)	0.74 ± 0.013 **
VTE (400)	0.63 ± 0.03 **
Sulfasalazine	0.56 ± 0.029 **

Fig.-4- Effect of methanolic extract of roots of *Vanda tessellata* on colon MDA level.



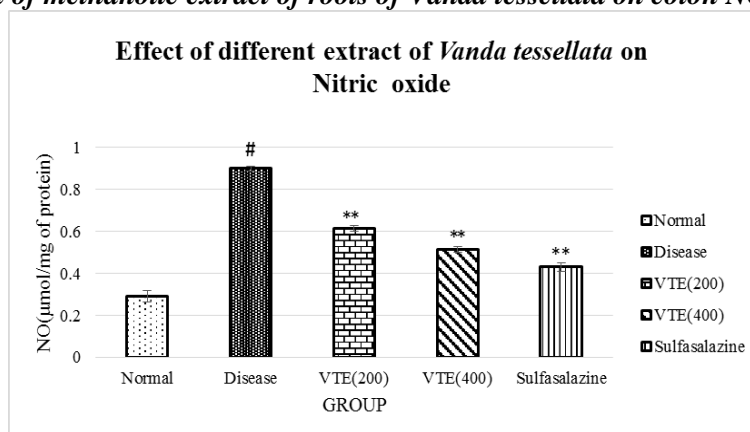
Nitric oxide (NO) assessment

Tissue NO level was found to be significantly elevated ($P < 0.01$) in disease group as compared to normal group which was significantly reduced ($P < 0.01$) in treatment group as compared to the disease control group. (Table no.- 5; Fig no.- 5)

Table no. 5- Effect of methanolic extract of roots of *Vanda tessellata* on colon NO level.

GROUP	NO(µmol/mg of protein)
Normal	0.29 ± 0.028
Disease	0.9 ± 0.013 [#]
VTE(200)	0.61 ± 0.015 ^{**}
VTE(400)	0.51 ± 0.015 ^{**}
Sulfasalazine	0.43 ± 0.021 ^{**}

Fig.-5 - Effect of methanolic extract of roots of *Vanda tessellata* on colon NO level.



% Mortality

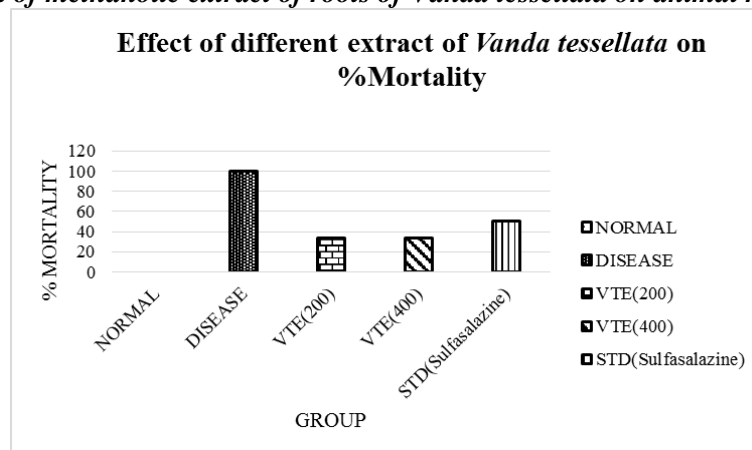
At the end of the experiment % mortality was highest in disease group. (Table no.- 6; Fig no.- 6)

Table no. 6 - Effect of methanolic extract of roots of *Vanda tessellata* on animal mortality.

GROUP	% MORTALITY
Normal	0
Disease	100

VTE (200)	33.33
VTE (400)	33.33
Sulfasalazine	50

Fig.-6 - Effect of methanolic extract of roots of *Vanda tessellata* on animal mortality.



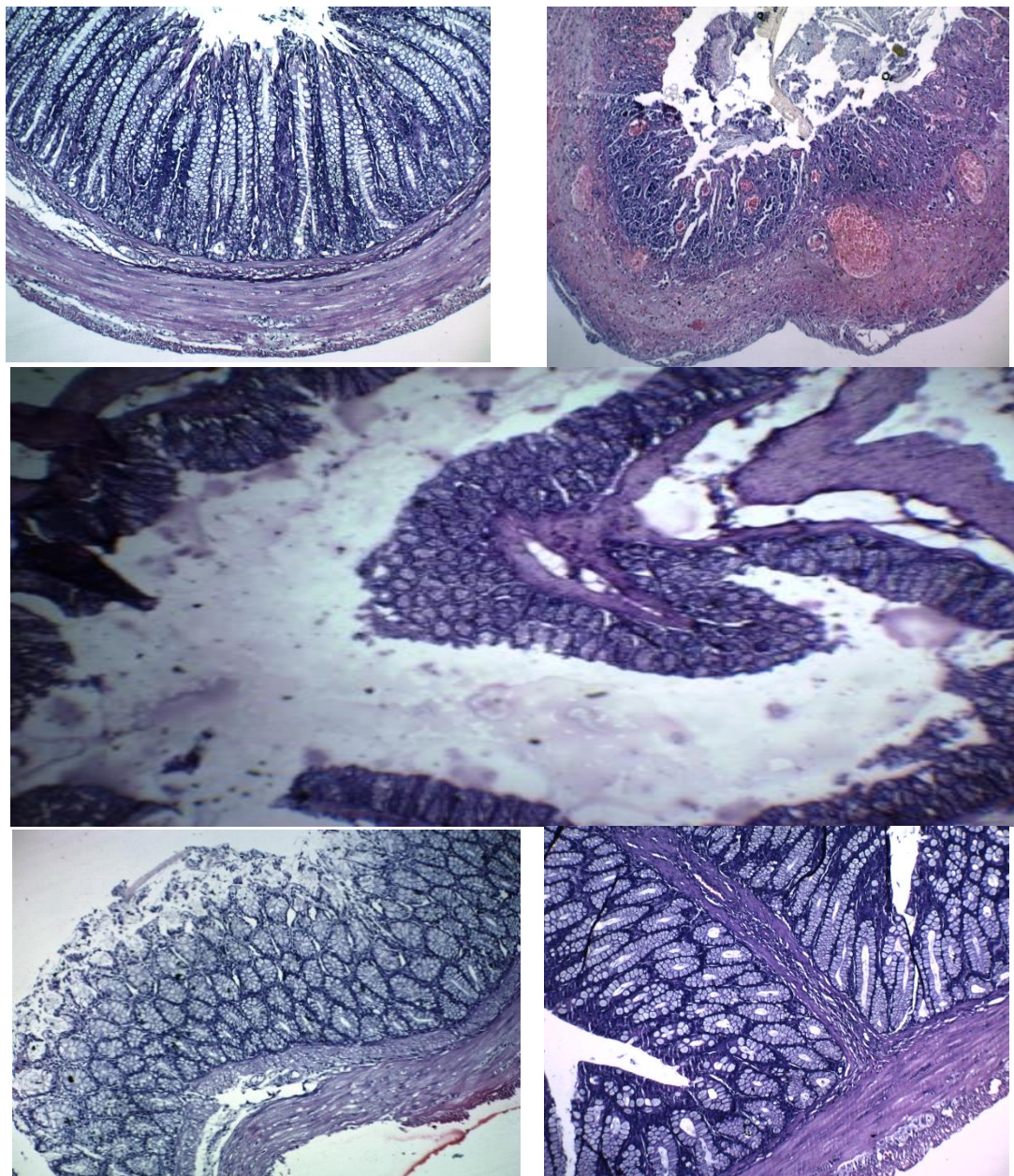
FINDINGS

In the present study, TNBS was administrated intrarectally to stimulate cell-mediated immunity in rats (Dai, 2011) (Wang, 2016). This heptane molecule produces acute and chronic colonic inflammation as well as ulceration in rats (Ko, 2005). The use of natural immunomodulatory, anti-inflammatory and anti-oxidative products provides an innovative and relatively non-toxic/less toxic alternative to modulate inflammatory disorders, including IBD and related symptoms (Dai, 2011) (Wang, 2016) (Zhou, 2006). *Vanda tessellata* had exhibited marked antioxidant (Uddin, 2015) (Prakash, 2018) and anti-inflammatory (Chawla, 1992) properties in both clinical and experimental studies. The current study demonstrates the effect of *Vanda tessellata* (400 mg/kg and 200 mg/kg) on experimental colitis. The possible correlation of *Vanda tessellata* on anti-inflammatory activity may be via presence of flavonoids and sterols and polyphenols (Dai, 2011) (Chowdhury, 2014); (Wang, 2016) and anti-oxidant activity of VTE might be due to the presence of phenolics which would be proven beneficial in the reduction of DAI and CMDI score as well as tissue injury and ulceration. The results were comparable with other studies. (Min, 2021))

The macroscopic observation confirmed that administration of TNBS resulted in mucosal lesion formation and inflammation in the distal colonic wall. The signs of hyperemia of mesenteric arteries, fibrinous adhesion and edema were observed. Clinically and histologically, UC is marked with erosion of colonic mucosa, distortion of cryptic architecture, cryptic shortening, lymphocytosis, mucin depletion and Paneth cell metaplasia in addition to severe weight loss, and bloody diarrhea. (Saba, 2020) In our results, the extract markedly recovered rats from the above-mentioned microscopic and macroscopic characteristics. The scoring system given by Geoboes et al was used to grade histopathological lesions in the colon tissue. (Saba, 2020) VTE (400 mg/kg and 200 mg/kg) treated group and standard (50 mg/kg) treated group showed reversal of mucosal damage as compared to the disease group as evidenced by less cell infiltration. The results obtained of study are similar with other studies. (Li C. D., 2021) Myeloperoxidase (MPO) is an enzyme that is found in azurophilic granules of neutrophils. It is a good marker of inflammation, tissue injury, and neutrophil infiltration in gastrointestinal tissue (Dirsch, 1998). Neutrophil infiltration into the colon mucosa is an important feature of chronic colitis and can secrete a large number of inflammatory cytokines exacerbating the inflammatory state and associated colorectal cancer. The external stimuli can lead to the accumulation of neutrophils and consequent release of myeloperoxidase (MPO) which induces

the production of proinflammatory factors that trigger inflammation and kill microorganisms in phagocytes. (Qin, 2022) In this study, the MPO-catalyzed reaction was found to be activated after TNBS administration. Treatment with VTE showed a significant decrease in polymorphonuclear infiltration confirmed by a significant reduction in MPO activity.

Fig.-7 – Histopathological study



All values represents Means \pm SEM; (n= 6), * Significantly different from normal control ($p < 0.01$), \cdot Significantly different from disease control ($p < 0.05$), $\cdot\cdot$ Significantly different from disease control ($p < 0.01$)

The presence of oxidative stress has important consequences for the pathogenesis, severity, and treatment of various inflammatory disorders due to the participation of cells in inflammation itself in the production of reactive oxygen and reactive nitrogen intermediates (Slater, 1971). MDA is an important indicator of lipid peroxidation which is found to be higher in rats treated with TNBS (Ko, 2005). Rats treated with VTE (400 mg/kg and 200mg/kg) showed a lesser extent of lipid peroxidation characterized by a significant reduced level of MDA.

In the field of inflammation research, the inducible nitric oxide synthase (iNOS) became an important pharmacological target, because of overproduction of nitric oxide after induction of this enzyme seems to be associated with numerous physiological and pathological conditions (Dirsch, 1998). Cytokine stimulation releases NO, which is a potent agent in non-specific defense mechanisms. (Camacho-Barquero, 2007) The marked reduction in NO level in the VTE treated group imitates its role in anti-inflammatory activity.

CONCLUSION

The present investigation reveals that methanolic extract of roots of *Vanda tessellata* (at the dose levels of 200 mg/kg and 400mg/kg, p.o.) is potentially benefit, as a curative agent in experimental ulcerative colitis induced by TNBS which may be attributed to flavonoids and phenolics, its antioxidant and anti-inflammatory principles. The study was conceived to find a better and safer remedy for UC than available treatment options. There was a significant reduction in DAI, CMDI and MPO activity as well as MDA and NO level in colon homogenates which proves the effectiveness of drug in ulcerative colitis. This study supports the contention that traditional medicines remain a valuable source in the potential discovery of natural product pharmaceuticals. The perspective underlying mechanisms include modification of immuno-inflammatory pathways through a reduction in MPO activity and/or NO generation and antioxidant activity. These results provide a promising step that might encourage further investigations of VTE as a protective agent in the treatment of UC.

REFERENCES

1. Alam, M. N. (2013). Review on in vivo and in vitro methods evaluation of antioxidant activity. *Saudi Pharmaceutical Journal*, 143–152.
2. Anwar, M. K. (2013). Hepatoprotective activity of pet-ether extract of *Vanda tessellata* Roxb. *Int. Ayur. Med. J.*, 1-4.
3. Babalola, W. O. (2022). Aloe vera gel attenuates acetic acid-induced ulcerative colitis in adult male Wistar rats. *Toxicology Reports*, 640–646.
4. Bernstein, C. N. (2009). *Inflammatory bowel disease: a global perspective*. World Gastroenterology Organisation *Global guidelines*. Milwaukee: World Gastroenterology Organization.
5. Bhattacharjee, B. I. (2015). Antimicrobial activity and phytochemical screening of whole plant extracts of *Vanda tessellata* (Roxb.) Hook. Ex. G. Don. *World J. Phar. Pharmace. Sci.*, 72-83.
6. Camacho-Barquero, L. V.-C.-F. (2007). Curcumin, a *Curcuma longa* constituent, acts on MAPK p38 pathway modulating COX-2 and iNOS expression in chronic experimental colitis. *International immunopharmacology*, 333-342.
7. Chawla, A. S. (1992). Chemical studies and anti inflammatory activity of *Vanda roxburghii* roots. *Indian J Pharmaceutical Sci.*, 159-61.
8. Chowdhury, M. A. (2014). Antinociceptive and cytotoxic activities of an epiphytic medicinal orchid: *Vanda tessellata* Roxb. *BMC complementary and alternative medicine*, 1-7.
9. Dai, Y. C. (2011). Influence of shenqing recipe on morphology and quantity of colonic interstitial cells of cajal in trinitrobenzene sulfonic acid induced rat colitis. *Chinese Medical Sciences Journal*, 43-48.
10. Dirsch, V. M. (1998). The Griess Assay: Suitable for a Bio-Guided Fractionation of Anti-inflammatory Plant Extracts. *Planta medica.*, 423-426.
11. dos Santos Ramos, A. G. (2021). Neutrophil extracellular traps in inflammatory bowel diseases: Implications in pathogenesis and therapeutic targets. *Pharmacological Research*, 105779.
12. Du, L. &. (2020). Epidemiology and Pathogenesis of Ulcerative. *Gastroenterology Clinics*, P643-654.
13. Ferro, J. M. (2021). Neurology of inflammatory bowel disease. *Journal of the Neurological Sciences*, 117426.
14. Green, L. C. (1982). Analysis of nitrate, nitrite, and [15N] nitrate in biological fluids. *Analytical biochemistry*, 131-138.
15. Gupta, C. &. (2014). In vitro evaluation of the antimicrobial activity of different solvent extracts of roots of *Vanda tessellata* (Roxb.) Hook. Ex. G. Don. *Indo Am J Pharm Res.*, 2386-2391.
16. Gupta, C. (2016). Isolation and characterization of new 17- ketosteroid as antimicrobial agent from *Vanda tessellata* (Roxb.) Hook. *World J. Pharm. Sci.*, 45-51.

17. Khandelwal, K. (2008). Practical book of Pharmacognosy, 19th edition. Pune: Nirali prakashan, 149-156.
18. Ko, J. K. (2005). Amelioration of experimental colitis by Astragalus membranaceus through anti-oxidation and inhibition of adhesion molecule synthesis. *World journal of gastroenterology: WJG*, 5787-5794.
19. Koppikar, S. J. (2014). Triphala, an Ayurvedic formulation improves the antioxidant status on TNBS induced IBD in rats. *European Journal of Integrative Medicine*, 646-656.
20. Krawisz, J. E. (1984). Quantitative assay for acute intestinal inflammation based on myeloperoxidase activity: assessment of inflammation in rat and hamster models. *Gastroenterology*, 1344-1350.
21. Li, C. D. (2021). Dihydroberberine, an isoquinoline alkaloid, exhibits protective effect against dextran sulfate sodium-induced ulcerative colitis in mice. *Phytomedicine*, 153631.
22. Li, L. Q. (2023). Preserved egg white alleviates DSS-induced colitis in mice through the reduction of oxidative stress, modulation of inflammatory cytokines, NF- κ B, MAPK and gut microbiota composition. *Food Science and Human Wellness*, 312-323.
23. Meier, J. &. (2011). Current treatment of ulcerative colitis. *World journal of gastroenterology: WJG*, 3204.
24. Min, X. Z. (2021). Neferine, a natural alkaloid from *Nelumbo nucifera*, ameliorates experimental chronic ulcerative colitis in mice. *Pharmacological Research - Modern Chinese Medicine*, 100022.
25. Nakase, H. S. (2022). The influence of cytokines on the complex pathology of ulcerative colitis. *Autoimmunity Reviews*, 103017.
26. Patel, S. H. (2012). Evaluation of anti-inflammatory effect of anti-platelet agent-clopidogrel in experimentally induced inflammatory bowel disease. *Indian Journal of Pharmacology*, 744.
27. Prakash, B. . (2018). Screening of antioxidant and antidepressant activity of *Vanda tessellata* leaves extract. *International Journal of Green Pharmacy*, 4.
28. Qin, W. L. (2022). *Rubia cordifolia* L. ameliorates DSS-induced ulcerative colitis in mice through dual inhibition of NLRP3 inflammasome and IL-6/JAK2/. *Heliyon*, e10314.
29. Saba, E. L. (2020). A novel herbal formulation consisting of red ginseng extract and *Epimedium koreanum* Nakai-attenuated dextran sulfate sodium-induced colitis in mice. *Journal of Ginseng Research*, 833-842.
30. Sailakshmi, K. S. (2015.). Antiulcer activity of petroleum-ether extract of *Vanda tessellata* Roxb. *Indo American J. Pharm. Res.*, 2316-2319.
31. Sasson, A. N. (2021). Diet in Treatment of Inflammatory Bowel Diseases. 425-435, 425-435.
32. Sirisha, J. S. (2013). Human red blood cell (HRBC) membrane stabilizing activity of leaves of pet-ether extract of *Vanda tessellata* Roxb. *Int. Ayur. Med. J.*, 5-8.
33. Slater, T. F. (1971). The stimulatory effects of carbon tetrachloride and other halogenoalkanes on peroxidative reactions in rat liver fractions in vitro. General features of the systems used. *Biochemical Journal*, 805-814.
34. Stevceva, L. P. (2001). Dextran sulphate sodium-induced colitis is ameliorated in interleukin 4 deficient mice. *Genes & Immunity*, 309-316.
35. Subin, R. M. (2021). Phytochemical and Pharmacological Studies of *Vanda tessellata* (Roxb.) ex. G. Don. In *The Phytochemical and Pharmacological aspects of Ethnomedicinal Plants* (pp. 427-439). Apple Academic Press.
36. Uddin, M. A. (2015). *Vanda roxburghii* chloroform extract as a potential source of polyphenols with antioxidant and cholinesterase inhibitory activities: identification of a strong phenolic antioxidant. *BMC Complementary and Alternative Medicine*, 1-9.
37. Vijaykumar, K. (2013). In vitro anti-oxidant activity of pet-ether extract of *Vanda tessellata* Roxb. *Int. Ayur. Med. J.*, 1-4.
38. Wang, S. X. (2016). Therapeutic potential of recombinant cystatin from *Schistosoma japonicum* in TNBS-induced experimental colitis of mice. *Parasites & vectors*, 1-13.
39. Wijnands, A. M. (2021). Surveillance and management of colorectal dysplasia and cancer in inflammatory bowel disease: Current practice and future perspectives. *European Journal of Internal Medicine*, 35-41.
40. Zhou, Y. H. (2006). Effects of Ginkgo biloba Extract on Inflammatory Mediators(SOD,MDA, TNF- α , NF- κ Bp65, IL-6) in TNBS-Induced Colitis in Rats. *Mediators of inflammation*, 1-9.

PCP404

**TO STUDY PHYTOPHARMACEUTICAL REGULATORY
PERSPECTIVES IN INDIA AND DEVELOPMENT OF OCIMUM
SANCTUM**

AP0417

Ms. Shital Singh Rajput Sujeet Singh
Student

GTU-Graduate School of Pharmacy
rshital2880@gmail.com

AP0413

Ms. Asmatbanu M. Pathan
Assistant Professor

GTU-Graduate School of Pharmacy
asmatbanu236@gmail.com

Abstract

Tulsi (*Ocimum Sanctum*) also known as holy basil belongs to family Lamiaceae. It is used since ancient times to treat various diseases. Tulsi is known for its several medicinal properties hence, the regulations are permitted for the development of its drug using advanced techniques for Isolation, extraction, collection, fractionation etc. Many studies such as invitro, animal and human have been carried out to authenticate Tulsi having various multiple therapeutic action such as anti-microbial, anti-inflammatory, cardio protective, immunomodulatory etc. The aim is to provide Tulsi as a medicinal product having higher therapeutic effect, lesser side effects & toxicity. During the pandemic situation of Covid 19 the consumption of natural product have been increased worldwide. They are regulated under Drug & Cosmetics Act, 1940 as a new drug in CDSCO.

Keywords: Phytopharmaceuticals regulation, Phytomedicines, PhytoPharmaceuticals, *Ocimum Sanctum*

PCP405

REVIEW ON REGULATIONS FOR GENOTOXIC IMPURITIES IN PHARMACEUTICALS

AP0416

Krupali Rangani

Student

Graduate School of Pharmacy

Gujarat Technological University

krupalirangani1@gmail.com

AP0422

Dr. Kashyap N. Thummar

Assistant Professor

Graduate School of Pharmacy

Gujarat Technological University

ap_kashyap@gtu.edu.in

Abstract:

Genotoxic impurities (GIs) are carcinogenic and mutagenic. It causes DNA damage that leads to cancer. Therefore control of GIs in pharmaceutical product is required to prevent the potential damage. Currently many products recall due to presence of carcinogenic N-nitrosamine impurities beyond its acceptable level include varenicline, accupril, valsartan, ranitidine, metformin, nizatidine, orphenadrine, propranolol. Various regulatory agencies like international council for harmonization (ICH), European Medicine Agency (EMA), United State Food & DRUG Administration (USFDA) provide guidelines framing the rules of limits the level of Genotoxic impurities in pharmaceuticals (Drug substances and drug products). In this paper we have included regulatory requirements for different agencies for the control of genotoxic impurities in pharmaceuticals. The comprehensive details of various guideline with their limits, methods available were presented in tabulated form. These details helpful for identification and control of GIs in pharmaceuticals and also helpful for risk assessment of pharmaceuticals from the Genotoxic impurities.

Keywords: Genotoxic impurities (GIs), Pharmaceuticals, USFDA, EMA, ICH

PCP407

REGENERATIVE MEDICINES: REGULATORY COMPARISON IN INDIA AND US

AP0414

Divya Sharma

Student,

Graduate School of Pharmacy,
Gujarat Technological University
divyakksharma@gmail.com

AP0421

MS. Hardi Joshi

Assistant Professor,

Graduate School of Pharmacy,
Gujarat Technological University
ap_gsp_hardijoshi@gtu.edu.in

Abstract:

Regenerative Medicine is a way for treatment of repairing, restoring, regenerating or replacing of human cells, tissues or organs that lost their function by trauma, disease, aging or congenital issues. The key components in RM are Stem cell therapy and gene therapy. RM therapies may be used to improve health with advanced therapies for organ transplant by reducing chances of rejection, organ failures, tissue repair, cardiovascular diseases, Alzheimer's, Parkinson's diseases, etc. Thus, it is required to have a defined regulatory framework for RM. In India, the RM are regulated by ICMR and DBT with alliance of CDSCO. For the development of RM products, including human cells, tissues, and cellular and tissue-based products (HCT/Ps), FDA has introduced guidance documents that are part of a comprehensive policy framework. The Office of Tissue and Advanced Therapies (OTAT) and the Office of Cellular, Tissue and Gene Therapies (OCTGT) in the CBER is responsible for cell and gene therapy products. In the US, RMs are referred as "Regenerative Medicine Advanced Therapies" (RMATs), which may be regulated as drugs, biological products, or medical devices. While in India, no standard or formal definitions for RMs are available. RMs are generally regulated as drugs in India. In India, Gene Therapy medicinal products (GTMPs), Stem cell therapy (SCT) and Tissue engineering products (TEP) are part of regenerative medicine. The focus is to review the comparative regulatory framework for Regenerative Medicine in India and US.

Keywords: Regenerative Medicine, Stem cell therapy, Gene Therapy, Tissue engineering, Regenerative Medicine Advanced Therapies

PCP412

MEDICAL FOOD: OVERVIEW OF REGULATIONS IN INDIA, US AND EUROPE

AP0418

Shivani Patel

Student

Graduate School of Pharmacy
Gujarat Technological University

AP0367

Mr. Ravisinh Solanki

Assistant Professor

Graduate School of Pharmacy
Gujarat Technological University

Abstract

Attaining an optimal health state is a wish of every individual and it lies on the shoulder of manufacturers, regulators and healthcare professionals for providing quality pharmaceuticals and food products to the consumers. Medical food is one such type of food product formulated to be administered enterally under the supervision of a physician and intended to meet the specific dietary management of a disease or condition. Its regulation varies from being flexible to strict depending on the country in which it is regulated. Medical foods' global market size was evaluated at USD 21.2 billion in 2021 and is anticipated to expand from 2022 to 2030 at a compound annual growth rate (CAGR) of 5.2%. The goal is to explain about medical food, enlisting approved products and overview of its regulatory requirements in India, US and Europe. The regulations in these countries are specified and separately defined for medical foods. US Food and Drug Administration (USFDA) regulates medical foods distinguished from the food for special dietary use. European Food Safety Authority (EFSA) and Food Safety and Standards Authority of India (FSSAI) regulates medical foods as Food for Special Medical Purposes (FSMPs).

Keywords: Medical food, US Food and Drug Administration, EFSA, FSSAI, FSMP

PCP 414

ASSESSMENT OF EFFICACY AND SAFETY OF TENELIGLIPTIN AS ADD ON THERAPY IN TYPE 2 INDIAN DIABETIC HYPERTENSIVE PATIENTS

AP0432

PARMAR VINENDRA M

Ph. D Scholar

Department of Pharmacology

L. M. College of Pharmacy, GTU

vinendra_15890@yahoo.com

AP0433

GOSWAMI SUNITA S

HOD and Associate professor

Department of Pharmacology

L. M. College of Pharmacy, GTU

Sunita.goswami@lmcp.ac.in

ABSTRACT

Background & Objectives: The objective of this study was to investigate the efficacy and safety of add-on teneligliptin, a unique and selective DPP-4 inhibitor in type 2 diabetes mellitus (T2DM) patients having hypertension. **Methods:** Study protocol was approved by Institutional Ethics Committee. Diabetic patients having hypertension were randomized to receive treatments in two groups, namely conventional antidiabetics (metformin plus glimepiride) with antihypertensive (telmisartan) therapy [treatment (A)] and add on teneligliptin 20 mg with conventional antidiabetics and telmisartan [treatment (B)] for 24 weeks. Efficacy variables included change in blood pressure, serum glycaemic, and cytokines (IL-6, TNF- α and adiponectin) levels from baseline to week 24. Treatment-emergent adverse events (TEAEs) were also assessed. **Results:** Total 120 T2DM patients having hypertension were analysed using graphpad prism. Teneligliptin, as add on treatment to conventional therapy significantly reduced serum glycaemic parameters (HbA1c, FBG, and PPBG) along with marked rise in serum adiponectin levels as compared to conventional therapy. **Interpretation & Conclusion:** It has been observed in our study that teneligliptin, as add on therapy is found well tolerated and effective in type 2 diabetic hypertensive patients that is evident from reduction in hyperglycaemia as well as improvement in adiponectin levels.

Key words: Adiponectin, Hypertension, Glycated haemoglobin (HbA1c), DPP-4 inhibitor, Teneligliptin Type 2 diabetes mellitus

1. INTRODUCTION:

Diabetes mellitus (DM) and hypertension are common comorbid conditions that are generally present together which leads to multiple vascular complications. (Grossman A., et al., 2017) Therefore, rigorous efforts have been made to lower blood glucose levels and prevent diabetic complications. (Son C., et al., 2020) Epidemiological studies have shown that hypertension and type 2 diabetes mellitus are two major global risks for disease burden and mortality in developing country. (Shen Y., et al., 2019) The number of patients with diabetes in India is likely to reach 134.2 million by 2045. (Ghosh S., et al., 2020) Study shown that tight control in hypertension appears to be more effective than glycaemic control in reducing microvascular events particularly kidney disease (Mohan V., et al., 2013)

The mechanism of hypertension in T2DM is too complex and multi-factorial, it includes enhancing sympathetic output, inappropriate activation of the renin-angiotensin-aldosterone system, oxidative stress, chronic inflammation, impaired insulin-mediated vasodilation, abnormal renal processing of sodium and obesity. (Guido L., et al., 2013 and Libianto R., et al., 2012) Treatment of hypertension in patients with T2DM is a really difficult task, as resistant hypertension is encountered more often in Indian population. (Screening of hypertension guideline, GOI, Feb 2016) The management of diabetes should go always along with the appropriate treatment of elevated blood pressure (BP), as well as the rest cardiovascular risk factors, in order to minimize micro- and macrovascular complications. (Pavlou DI., et al., 2018)

The newly released American College of Cardiology (ACC) /American Heart Association Guideline for the Prevention, Detection, Evaluation, and Management of High blood pressure in adults supports a more aggressive diagnostic and treatment approach, recommending hypertensive patients to maintain their BP < 130/80 mmHg. (Shen Y., et al., 2019)

The decision on choice of anti-diabetic therapy in T2DM patients is based on the safety, efficacy, co-morbidities and cost that were reviewed in Asian Indian context. Considering that many Indian patients do not have medical insurance and treatment needs to be continued lifelong, cost of therapy also plays a crucial role in T2DM patients from Indian and Asian subcontinent. (Chawla, R., et al., 2020) Metformin first line consideration for managing type 2 diabetes is to normalize fasting glucose levels, with weekly or monthly adjustments in the regimen. (Ripsin CM., et al., 2009) It is more efficacious in managing hyperglycaemia along with beneficial effects in reducing cardiovascular and hypoglycaemia risk, improving macrovascular outcomes, and lowering mortality rates in T2DM. (Chawla, R., et al., 2020) Incretins are a group of gastrointestinal hormones, among which the glucagon-like peptide 1 (GLP-1) and the glucose dependent insulin tropic peptide (GIP) are released in response to food and nutrient ingestion, which lead to stimulating insulin and suppressing glucagon secretion. (Chawla, R., et al., 2020) In experimental model GLP-1 seems to have some beneficial effect on pancreatic β -cells preservation. Beyond the efficacy in treatment of hyperglycaemia associated with type 2 diabetes. GLP-1 seems to exert beneficial effects on the cardiovascular system, which may be applicable in treatment of cardiovascular disease in both normal and diabetic patients. (Grieve DJ., et al., 2013) Study data suggest that DPP-4 inhibitor holds promise for vascular protection through anti-inflammatory effects, endothelial repair, and reduction of ischemic injury. (Fadini GP., et al., 2011) Some clinical data suggest the beneficial effects of DPP-4 inhibitors on hypertension, and dyslipidemia. This suggests DPP-4 inhibitors might have a potential to reduce the cardiovascular disease burden among patients with T2DM. (Schmieder R., et al., 2013 and Van Poppel PC., et al., 2011)

There is a lack of evidence that the therapeutic strategies targeting pancreatic β cell dysfunction and insulin resistance (IR) reduce the cardiovascular risk in patients with diabetes. (Duvnjak L., et al., 2016) This notion raises the need for alternative therapies that provide substantial benefits without side effects. Among emerging anti-diabetic candidates, incretin-based therapies carry a special cardiovascular protective effect. (Duvnjak L., et al., 2016) DPP-4 inhibitors are considered as a cornerstone within the management of T2DM due to their robust efficacy and favourable tolerability profile. (Duvnjak L., et al., 2016) Our previous study has demonstrated teneligliptin as add on therapy showing better glycaemic control as compared to conventional therapy in Indian patients having T2DM. (Vinendra MP, and Sunita SG., 2019) We have also study reported that teneligliptin improve in lipid profile as well as adiponectin levels in T2DM patients having dyslipidemia. (Vinendra MP, Sunita SG., 2020) However, there is no clinical literature available for the study of teneligliptin in diabetic hypertensive patients in India. Therefore, the present study is designed to evaluate efficacy, safety, and tolerability of treatment that can lead to improvement in the effectiveness of standard therapy in diabetic patients having hypertension in Indian population. Currently only few reports are available on the role of inflammatory biomarkers in type 2 diabetic patients and folks with impaired metabolic disorder in Indian population. In this manuscript, we have incorporated the role of inflammatory regulators (IL 6, TNF α and adiponectin) with respect to add on teneligliptin therapy in type 2 diabetic patients having hypertension in Indian population.

8. OBJECTIVES:

To evaluate the efficacy and safety of teneligliptin as add-on drug in patients with type 2 diabetes mellitus patients having hypertension.

9. RESEARCH METHODOLOGY:

3.1 ETHICS APPROVAL:

This study was conducted at Jivraj Mehta Hospital and Bakeri Medical Research Centre, Ahmedabad. The study protocol, informed consent form (ICF) and relevant essential documents were approved by Institutional Ethics Committee (IEC) (IEC registration No:

ECR/274/Inst/GJ/2013/RR-19); Safety, Health and welfare Ethics committee, registered under Drug Controller General of India (DCGI).

3.2 ELIGIBILITY CRITERIA:

Study protocol was clearly defined for the patients and informed consent was obtained from all the patients before participation for the study. The study included male and female patients with T2DM having hypertension, aged >18 years, HbA_{1c} levels of >7.0%, and body mass index of 20.0–35.0 kg/m² (both inclusive). Patients were excluded if they had serious disease such as kidney, liver, and cerebral stroke, history of severe heart disease or arrhythmias, history of alcohol and tobacco use, pregnant, and taking DPP-4 inhibitor other than teneligliptin, taking antihypertensive drugs other than telmisartan and on insulin therapy.

3.3 INTERVENTION:

Eligible patients were randomized in 1:1 ratio to receive either metformin plus glimepiride and telmisartan (treatment A) or metformin plus glimepiride, telmisartan, and add on teneligliptin (Treatment B). Treatment for both the groups remained stable and it included: teneligliptin 20 mg/day, metformin 500 mg/day, glimepiride 2 mg/day and telmisartan 20 mg/day for 24 weeks.

3.4 BIOCHEMICAL PARAMETERS:

Glycaemic parameters including serum glycated haemoglobin (HbA_{1c}), fasting blood glucose (FBG) and post prandial blood glucose (PPBG) levels and inflammatory cytokine levels namely IL-6, TNF- α , and adiponectin levels were measured at the baseline and at the end of 24 weeks in both the treatment groups.

3.5 MEASUREMENT OF BLOOD PRESSURE:

Both systolic (SBP) and diastolic blood pressure (DBP) were assessed twice with 2 minutes apart after a 5-minute rest in the sitting position, using an auscultatory method of measurement with a properly calibrated and validated mercury sphygmomanometer over the right brachial artery. Two measurements were made 2 minutes apart. SBP is the point at which the first of two or more sounds are heard (phase 1), and DBP is the point before the disappearance of sounds (phase 5). The mean of the two recordings were taken for analysis. Measurement of both SBP and DBP at baseline and at the end of 24 weeks in both the treatment groups

3.6 CYTOKINES ESTIMATION:

Serum was collected from each subject and stored at -80 °C until further analysis. Serum IL-6 and TNF- α levels were measured using the enzyme-linked immunosorbent assay (ELISA) according to the manufacturer's instructions (KRISHGEN Biosystems, Mumbai). The assay sensitivity ranges of KRISHGEN Biosystems kits were 3.12-200 pg/ml for IL-6 and 6.8-500 pg/ml for TNF- α in serum samples. The ELISA kits were validated with inter and intra-assay precision. Adiponectin levels were measured using the ELISA according to the manufacturer's instructions (KINESIS Dx). The assay sensitivity ranges of KINESIS Dx kit was 2-34 μ g/ml for adiponectin in serum samples. The ELISA kit was validated with inter- and intra-assay precision. The absorbance of cytokines namely IL-6, TNF- α , and adiponectin were measured at 450nm.

3.7 EFFICACY AND SAFETY END POINTS:

The primary efficacy end point was the change in glycaemic parameters from baseline to 24 weeks. Secondary efficacy endpoints include change blood pressure and inflammatory (IL-6, TNF- α , and adiponectin) cytokine levels from baseline to 24 weeks. During the clinical study period, we monitored possible adverse events (AEs), laboratory values, vital sign and physical examination results. Safety aspects were measured by recording AEs including symptomatic assessment by Naranjo causality scale for adverse events. (Naranjo CA., et al., 1981) The incidence of AEs in terms of number per patient was calculated based on the number of events, the number of patients and the total observation period.

3.8 SAMPLE SIZE AND STATISTICAL ANALYSIS:

The primary end point, difference in mean HbA_{1c} from baseline to 24 week was assumed 0.5% and also the standard deviation (SD) of 0.9% for each treatment group. Based on a power of 80% and a type I error rate of α = 0.05 (2-tailed), a sample size of at least 60 patients per group was required to detect a clinically significant difference between both the groups.

(Kadowaki T., et al., 2017) Categorical data was presented as absolute number/percentage of patients while quantitative data were presented as mean \pm SD. Within group comparison was performed using paired t-test based on the distribution of data. Unpaired t-test was used to analyse the quantitative data for between group comparisons. Correlations were investigated by Spearman's rank correlation coefficient analysis. Missing data was handled using Last observation carried forward (LOCF) method. P value of less than 0.05 was considered as statistical significant difference. Data were calculated using Graph Pad prism version 5.0.

10. RESULTS:

A flow chart is presented showing the disposition of participants throughout the study (Figure 1). Out of 178 screened patients, 134 eligible patients were randomized during this clinical study. Treatment A included 62 patients and treatment B included 61 patients. As per sample analysis plan (SAP), sixty patients in each group were analysed to detect a clinically significant difference between both the groups. A detail of both the group demographic profile and clinical characteristic parameters at baseline was mentioned in Table-1.

Blood pressure data obtained at baseline and at the end of 24 weeks. Table 2 shows baseline age wise distribution of systolic and diastolic blood pressure. According to Indian standard treatment guideline for hypertension, a systolic blood pressure > 130 mmHg or a diastolic blood pressure > 80 mmHg was defined as poor blood pressure control. Details of age wise distribution of blood pressure data with respective treatment was mentioned in table-2. The most important end point was HbA_{1c}. The list of mean changes in primary end point (glycemic parameters and blood pressure) and secondary end point (cytokines levels) were mentioned in table 3. HbA_{1c} level was found comparable in both the treatment groups at the baseline. However, there was gradual reduction in HbA_{1c} over the period of 24 weeks in both the treatment groups. Between groups comparison showed significant reduction ($p < 0.05$) in HbA_{1c} in treatment B as compared to treatment A (figure 2). There were blood glucose (FBG and PPBG) levels shown significantly reduction in treatment B as compared to treatment A after 24 weeks. However, reduction in glycaemic parameters (HbA_{1c}, FBG and PPBG) was statistically significant in treatment B as compared to treatment A after 24weeks (figure 3 &4).

Figure 1: Patient disposition chart

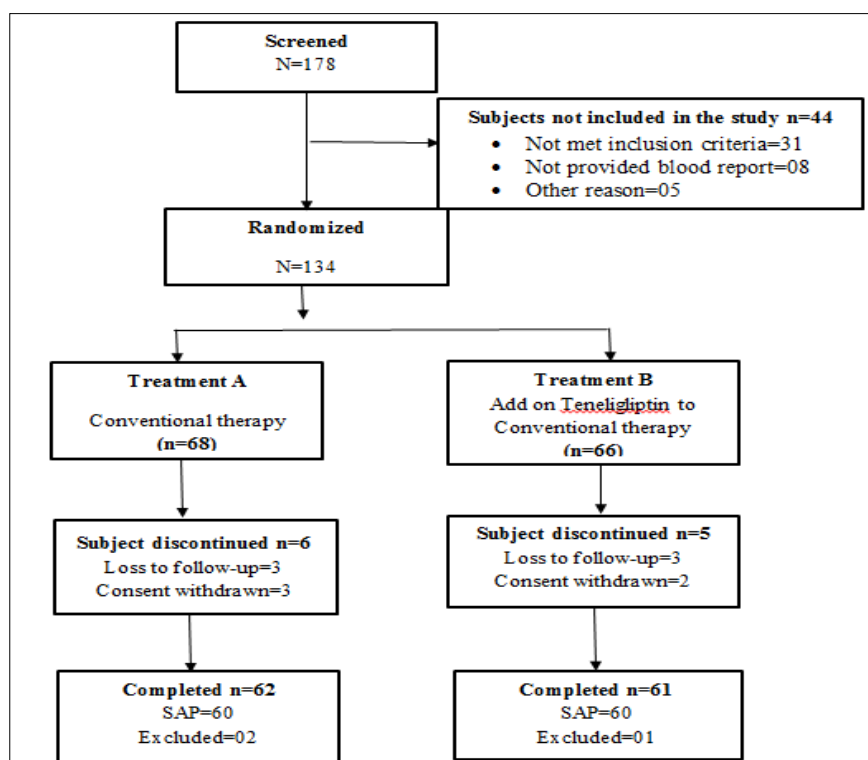


Table 1: Demographic profile and clinical characteristic

Characteristic	Treatment A (N=60)	Treatment B (N=60)
Demographic		
Gender(Male/Female)	24/36	28/32
Age (year)	48.56 ± 9.45	48.16 ± 7.64
Height (cm)	152.12 ±13.59	156.21 ± 10.69
Body Weight (kg)	68.28 ± 10.76	67.79 ±11.12
Body mass index (BMI)	26.81 ±3.78	26.24 ± 4.33
Disease duration (year)	3.54 ± 1.48	3.71 ± 2.05
Waist (cm)	91.48 ±7.03	91.68 ±7.24
Hip (cm)	96.56±8.83	96.88 ±8.32
Diet history (calories)		
• Breakfast (calories)	1452.56 ± 296.85	1445.08 ± 284.44
• Lunch (calories)	2080.33 ± 406.33	1560.21 ± 106.9
• Dinner (calories)	642.81 ± 210.74	646.14 ± 214.74
Vegetarian/ Non-vegetarian	45/15	49/11
Job/ Business	44/16	38/22
Exercise/ Yoga	47/13	47/13

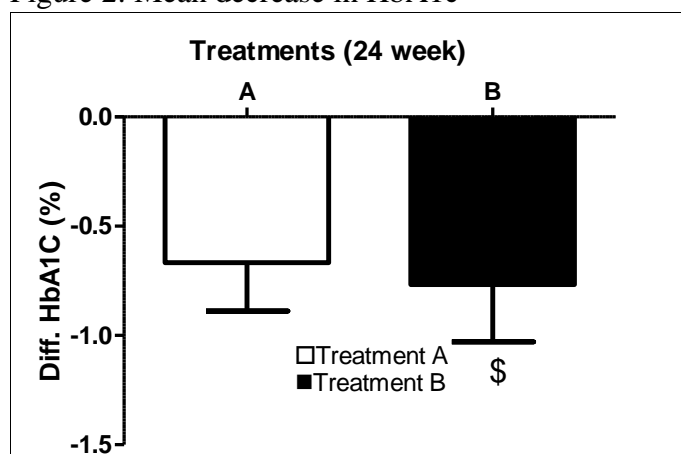
Values are expressed in terms of Mean± SD. N=number of patient, SD= standard deviation. Treatment A: Conventional treatment and Treatment B: Add on teneligliptinwith conventional treatment.

Table 2: Age wise Blood pressure distribution

Age (Year)	Treatment A (N=60)			Treatment B(N=60)		
	N	SBP (mm/Hg)	DBP (mm/Hg)	N	SBP(mm/Hg)	DBP(mm/Hg)
20-29	1	156	86	-	-	-
30-39	7	145.96 + 9.33	85.56+5.31	9	143.84+9.75	82.86+5.71
40-49	24	145.11+11.20	84.96+5.10	27	144.13+9.63	83.13+5.72
50-59	23	145.25+11.40	85.56+5.22	21	143.55+9.42	82.77+5.67
60-69	5	143.5+10.88	81.75+5.42	3	143.46+9.46	82.68+5.58

Values are expressed in terms of Mean± SD. N=number of patient, SD= standard deviation. Treatment A: Conventional treatment and Treatment B: Add on teneligliptin with conventional treatment.

Figure 2: Mean decrease in HbA1c



Data are expressed as the Mean \pm Standard deviation (n=60). \$P value<0.05 indicate mean decrease in HbA_{1c} from baseline to 24 weeks treatment using unpaired t test.

Figure 3: Mean decrease in Fasting blood glucose (FBG) level

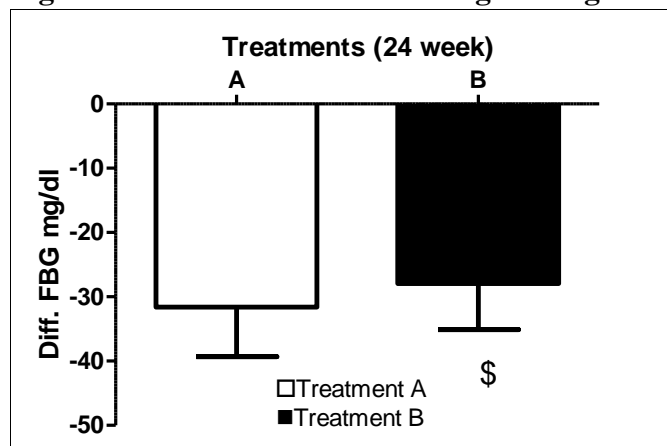
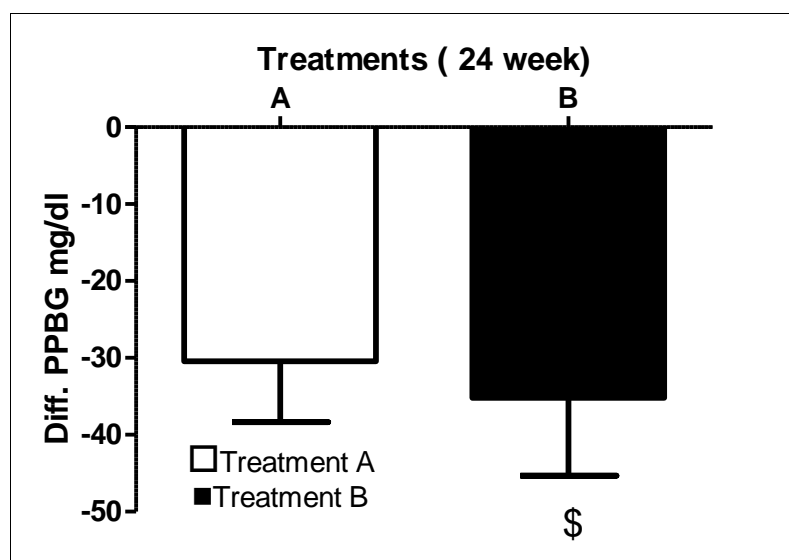


Figure 4: Mean decrease in post prandial blood glucose (PPBG) level



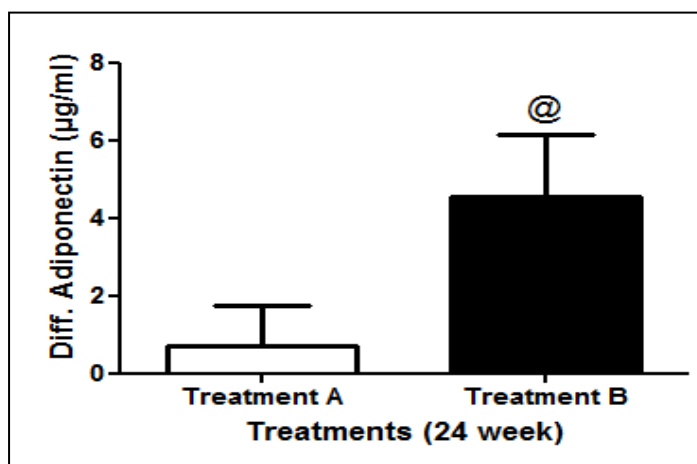
Data are expressed as the Mean \pm Standard deviation (n=60). \$ P value<0.05 indicate mean decrease in PPBG from baseline to 24 weeks treatment using unpaired t test.

Blood pressure was found comparable in both the treatment groups at the baseline. Both treatments showed significantly reduction in systolic and diastolic blood pressure at the end of 24 weeks treatments (student pair t test). Mean change in reduction of SBP in treatment A was 4.58 ± 1.93 and 5.26 ± 1.99 in treatment B. Mean change in reduction of DBP in treatment A was 4.23 ± 1.81 and 4.8 ± 1.84 in treatment B However, both treatments were not statistically significant reduction in blood pressure when it compared with between groups (unpaired t test) at the end of treatment. (Table-3)

We analyzed the changes in cytokines levels in both treatments at baseline and at the end of 24 weeks. Serum adiponectin levels at the end of 24 weeks, add on teneligliptin group (treatment B) showed tendency to increase adiponectin level. Mean change of adiponectin in treatment B was 4.776 ± 1.68 $\mu\text{g/ml}$ as compared to 0.629 ± 0.87 $\mu\text{g/ml}$ in treatment A. The mean change in adiponectin levels significantly improved in treatment B as compared to treatment A at the end of 24 week. Between groups comparison showed better improvement in adiponectin levels in treatment B as compared to treatment A (Figure 5). In addition to above, reduction in

inflammatory cytokine levels (IL 6 and TNF- α) was also observed in treatment B as compared to treatment A at the end of 24 weeks but was not found statistically significant (Table-3).

Figure 5: Mean increase in adiponectin level



Data are expressed as the Mean \pm Standard deviation (n=60). @ P value < 0.05 indicate mean increase in adiponectin from baseline to 24 weeks treatment using unpaired t test

Table 3: Mean change in glycaemic levels, blood pressure and cytokines from baseline to 24 weeks after study drug treatments

Parameters	Treatment A (N=60)	Treatment B (N=60)
Glycated haemoglobin (HbA1c)		
Baseline	8.31 \pm 0.84	8.23 \pm 0.83
End of 24 weeks	7.64 \pm 0.81*	7.47 \pm 0.72 *
Change in HbA1c	-0.66 \pm 0.21	-0.766 \pm 0.26 \$
Fasting blood glucose (FBG)		
Baseline	148.63 \pm 16.52	149.01 \pm 16.27
End of 24 weeks	120.71 \pm 13.28*	117.40 \pm 16.24*
Change in FBG	-27.91 \pm 7.13	-31.60 \pm 7.62\$
Post prandial blood glucose (PPBG)		
Baseline	226.22 \pm 20.62	221.8 \pm 27.58
End of 24 weeks	195.79 \pm 20.02*	186.92 \pm 19.87*
Change in PPBG	-30.42 \pm 7.87	-35.17 \pm 10.06\$
SBP (mm/Hg)		
Baseline	145.11 \pm 11.20	144.13 \pm 9.63
End of 24 weeks	140.53 \pm 11.08*	138.86 \pm 9.96*
Change in SBP	-4.58 \pm 1.93	-5.26 \pm 1.99
DBP (mm/Hg)		
Baseline	84.96 \pm 5.10	83.13 \pm 5.72
End of 24 weeks	80.73 \pm 4.64*	78.33 \pm 5.30*
Change in DBP	-4.23 \pm 1.81	-4.8 \pm 1.84
Cytokines levels		
IL 6 (pg/ml)		
Baseline	7.567 \pm 1.246	7.441 \pm 1.205
End of 24 weeks	7.095 \pm 1.167*	6.798 \pm 1.087*
Change in IL 6	-0.4710 \pm 0.484	-0.643 \pm 0.530
TNF-α (pg/ml)		
Baseline	16.031 \pm 1.764	15.836 \pm 1.678
End of 24 weeks	15.505 \pm 1.781 *	15.149 \pm 1.671*
Change in TNF- α	-0.526 \pm 0.402	-0.687 \pm 0.393
Adiponectin (µg/ml)		

Baseline	4.029 ± 0.639	4.352 ± 0.770
End of 24 weeks	4.773 ± 1.041*	8.895 ± 1.522 *
Change in adiponectin	+0.704 ± 1.019	+4.543 ± 1.598@

Values are expressed as Mean±SD. N=number of patient, SD= standard deviation Treatment A: Conventional treatment and Treatment B: Add on teneligliptin with conventional treatment. * p<0.05 from baseline to end of 24 weeks by using paired t test (within group comparison).

\$ p<0.05 indicate change in Glycaemic parameter (HbA1c, FBG, and PPBG) from the baseline to 24 weeks. @ p<0.05 indicate change in adiponectin level from the baseline to 24 weeks; between groups comparison was done using un-paired t test.

Detail of adverse events listed in table- IV; there were no death and no major adverse cardiovascular event (MACE) in both treatment. In treatment A total 27 (45%) and in treatment B 23 (38.3%) adverse event reported.

Table 4: Summary of adverse events

Adverse event (AE)	Treatment A N=60 (%)	Treatment B N=60 (%)	Naranjo score	Scale
Hypoglycemia	1 (1.66%)	1 (1.66%)	9	Definite
Constipation	6 (10.0%)	5 (8.33%)	9	Definite
Abdominal Pain	6 (10.00%)	6 (10.0%)	5	Probable
Acidity	5 (8.33%)	5 (8.33%)	5	Probable
Tiredness	3(5.00%)	2 (3.33%)	4	Possible
Weakness	2 (3.33%)	1 (3.33%)	4	Possible
Dry skin	1(1.66%)	1(1.66%)	0	Doubtful
Headache	2 (3.33%)	1 (1.66%)	0	Doubtful
Itching	1(1.66%)	1(1.66%)	0	Doubtful
Total	27 (45%)	23 (38.3%)		

Treatment A: Conventional treatment and Treatment B: Add on teneligliptinwith conventional treatment.

11. DISCUSSION:

Diabetes and hypertension are major global risk factor for mortality and also known to coexist in patients. (Joshi SR., et al., 2011) Diabetes confers a two-fold excess risk for a broad range of vascular diseases, which are independently from other traditional risk factors. (Sarwar N., et al., 2010) In addition, patients with hypertension often exhibit insulin resistance and are at greater risk of diabetes associated with both macrovascular (involving large arteries such as conduit vessels) and microvascular (involving small arteries and capillaries) disease. (Petrie, J. R., 2017) The prevalence of hypertension in patients with diabetes varies from about 30 to 80% across different studies. In addition to optimal glycaemic control, more efforts are required to address the comorbid conditions.(Zhang X., et al., 2016) Incretin therapies such as glucagon-like peptide 1 (GLP-1) agonists are commonly used for the treatment of type 2 diabetes mellitus. GLP-1 mimetics, besides improving glycaemic control, have been shown to influence multiple pathways regulating blood pressure. (Katout M., et al., 2014) Recent clinical trials pooled analysis suggested that there are multiple beneficial effects of GLP-1 RA including weight loss, lipid profiles improvement, BP lowering, reduction in incidence of major cardiovascular events, renal and hepatic protective effects. (Kalra S., et al., 2017) It has been reported that GLP-1 receptor agonists improve left ventricular (LV) dysfunction and clinical heart failure conditions in ischemic heart disease patients. DPP-4 inhibitors might be cardio-protective by increases in the incretin hormones levels in T2DM patients. (Hashikata T, et al., 2016)

Present work clearly demonstrated that teneligliptin addition to glimepiride and metformin concomitant therapy in stable dose significantly reduced HbA_{1c} level as compared to conventional therapy at 24 weeks from the baseline. Further, we also observed significant

reduction in blood glucose levels (FBG and PPBG) in both the treatment groups. Results of the present study are found consistent with the previous clinical reports from Japan, where efficacy of teneligliptin as add on treatment decreased HbA_{1c}, FBG and PPBG levels at 12 weeks and 52 weeks. (Kadowaki T., et al., 2017 and Kadowaki T, Kondo K., 2014) Our study suggested that, the addition of teneligliptin 20 mg to conventional therapy (metformin plus glimepiride) significantly improved the efficacy of conventional therapy. HbA_{1c} level in blood is one of key marker to know glycaemic control. Our present finding was consistent previous clinical report wherein, combination of teneligliptin with that of insulin reduced HbA_{1c} level and showed synergistic effect. (Takamiya Y., et al., 2019) In our study, teneligliptin as add on treatment significantly decreased HbA_{1c} in patients with T2DM that might be attributed to its synergistic action.

Diabetes and hypertension both considered significant risk factors for macrovascular disorders due to progression of dyslipidemia. A meta-analysis of 13 clinical studies suggested that stroke was preventable by lowering blood pressure in patients with diabetes who had a systolic blood pressure <130 mmHg and diastolic blood pressure <80 mmHg. So, there is a need to study the effect of teneligliptin on blood pressure as it should be tightly controlled in patients having diabetes complicated by hypertension to prevent cardiovascular events. (Wang B., et al., 2013) Several studies have revealed the efficacy of GLP-1 RAs in BP reduction. Liraglutide and exenatide have been associated with the reduction for SBP and DBP in patients with T2DM by 1 to 5mmHg as compared to other antidiabetic agents. (Wang B., et al., 2013) In meta-analysis reported by Zhang and Zhao, effect of DPP-4 inhibitor on blood pressure is almost neutral as compared to other antidiabetic drugs³¹. The baseline SBP in this present study was 145.11 ± 11.20 mmHg & 144.13 ± 9.63 mmHg and DBP 84.96 ± 5.10 mmHg & 83.13 ± 5.72 mmHg in the treatment A & B respectively. Many clinical studies of blood pressure interventions have shown that a reduction in SBP from 2 mmHg to 3 mmHg has been shown to reduce cardiovascular events, (Takamiya Y., et al., 2019) So a noteworthy finding of this study is that the SBP was reduced by 5 mmHg and the DBP was lowered by 4 mmHg after 24 weeks of add on treatment with teneligliptin. Thus, it is suggested from our study that add on treatment of teneligliptin helps in the control of blood pressure. A significant negative correlation was observed between the difference of HbA_{1c} and SBP in the treatment group B. Takamiya & Co-workers have reported positive correlation between HbA_{1c} and baseline HbA_{1c}, Baseline LDL-c, Baseline TG, and negative correlation with the age (Takamiya Y., et al., 2019)

There is an inverse relationship between adiponectin level and hypertension. Furthermore, hypoadiponectinemia is an independent risk factor for hypertension. (Iwashima Y., et al., 2004) As per one meta-analysis every 1 µg/ml increase in adiponectin levels is associated with 6% reduced risk of hypertension. (Kim, Dae Hyun et al., 1979) This one is note worthy finding of our study significantly improve in adiponectine level (approx. 4 µg/ml) with add on teneligliptin treatment. Adiponectin might be indirectly inhibit IL-6 and CRP expression through its ability to inhibit the production of TNF-alpha. Telmisartan, an angiotensin II receptor blocker (ARB), can act as a partial agonist of Peroxisome proliferator-activated receptor gamma (PPAR-γ). The results of meta-analysis suggest that telmisartan reduce both IL-6 and TNF alpha levels, this finding was robust in sensitivity analyses. (Takagi, H., et al., 2012)

It has been reported that adiponectin has anti-inflammatory, antiatherogenic and antidiabetic properties. The protective effects of adiponectin in the prevention of progression of IR and in cardiovascular events, and its potent influence in components of the metabolic syndrome, have made it a highly promising therapeutic target. (Yanai, H., & Yoshida, H., 2019) These markers though well understood in terms of their regulation in diabetes population are still lacking acceptance as clinical markers because of the variation of levels among various ethnic groups. Currently limited information is available on inflammatory cytokines in type 2 diabetes with hypertension. Our study has demonstrated significantly raised adiponectin levels in treatment B as compared to treatment A. In addition, an improvement in adiponectin level was found associated with reduction of inflammatory cytokines (IL-6 & TNF-α) that might help in controlling blood pressure which prevent cardiovascular complication. Clinical symptomatic

assessment was done for AE like hypoglycemia and constipation, which were considered as definite; abdominal pain, and acidity were considered as probable; weakness and tiredness considered as possible, Headache, dry skin, and itching considered as doubtful in Naranjo AE assessment scale. It is also to be noted that, the incidence of hypoglycemic symptoms was similar (1.66 %) in both the groups.

12. CONCLUSION:

It has been observed in our study that teneligliptin, as add on therapy is found well tolerated and effective in T2DM patients. Further, teneligliptin add on treatment with telmisartan has been found effective along with conventional antidiabetic therapy in reducing hyperglycaemia as well as improvement in adiponectin levels in diabetic patients with hypertension.

ACKNOWLEDGMENT: The authors acknowledge the guidance of Dr Parag Shah, Dr Krishna Shah, Dr Alka Makad, Dr Chirag Vaghela, Dr Premal Thakor and Dr Shubha Desai, without their support this work would not have been possible. We are also thankful to Dr Krishna M Shah and the staff of research department Jivraj Mehta Hospital and Bakeri medical research centre, Ahmedabad for extending required help and research facility for the present study.

CONFLICTS OF INTEREST: The author declares that they have no conflict of interest.

FINANCIAL SUPPORT & SPONSORSHIP: None

13. Reference:

1. Grossman A, Grossman E. Blood pressure control in type 2 diabetic patients. *Cardiovasc Diabetol*. 2017 Jan 6;16(1):3. doi: 10.1186/s12933-016-0485-3. PMID: 28056987; PMCID: PMC5217560.
2. Son C, Kasahara M, Tanaka T, Satoh-asahara N, Kusakabe T, Nishimura K, et al. Rationale , Design , and Methods of the Study of Comparison of Canagliflozin vs . Teneligliptin Against Basic Metabolic Risks in Patients with Type 2 Diabetes Mellitus (CANTABILE study): Protocol for a Randomized , Parallel-Group Comparison Trial. *Diabetes Ther [Internet]*. 2020;11(1):347–58. Available from: <https://doi.org/10.1007/s13300-019-00717-9>
3. Shen Y, Dai Y, Wang XQ, Zhang RY, Lu L, Ding FH, et al. Searching for optimal blood pressure targets in type 2 diabetic patients with coronary artery disease. *Cardiovasc Diabetol [Internet]*. 2019;1–13. Available from: <https://doi.org/10.1186/s12933-019-0959-1>
4. Ghosh S, Tiwaskar M, Chawla R, Jaggi S, Asirvatham A, Panikar V. Teneligliptin Real-World Effectiveness Assessment in Patients with Type 2 Diabetes Mellitus in India : A Retrospective Analysis (TREAT-INDIA 2). *Diabetes Ther [Internet]*. 2020;11(10):2257–68. Available from: <https://doi.org/10.1007/s13300-020-00880-4>
5. Mohan V, Seedat YK, Pradeepa R. The rising burden of diabetes and hypertension in southeast asian and african regions: need for effective strategies for prevention and control in primary health care settings. *Int J Hypertens*. 2013;2013:409083. doi: 10.1155/2013/409083. Epub 2013 Mar 14. PMID: 23573413; PMCID: PMC3612479.
6. Guido L., Sofia S., L. Romayne Kurukulasuriya, James R. Sowers., Type 2 diabetes mellitus and hypertension : An update. *Endocrinol Metab Clin N Am* 43 (2014) 103–122 <http://dx.doi.org/10.1016/j.ecl.2013.09.005>
7. Libianto R, Batu D, Macisaac RJ, Cooper ME, Ekinici EI. SC., Pathophysiological Links between Diabetes and Blood Pressure., *Can J Cardiol [Internet]*. 2018; Available from: <https://doi.org/10.1016/j.cjca.2018.01.010>
8. Screening, Diagnosis, Assessment, and Management of Primary Hypertension in Adults in India, Standard treatment guidelines. Published by Ministry of Health & Family Welfare Government of India., feb 2016.
9. Pavlou DI, Paschou SA, Anagnostis P, Spartalis M. Maturitas Hypertension in patients with type 2 diabetes mellitus : Targets and management. *Maturitas [Internet]*. 2018;112(February):71–7. Available from: <https://doi.org/10.1016/j.maturitas.2018.03.013>
10. Chawla, R., Madhu, S. V., Makkar, B. M., Ghosh, S., Saboo, B., Kalra, S., & RSSDI-ESI Consensus Group (2020). RSSDI-ESI Clinical Practice Recommendations for the Management of Type 2

- Diabetes Mellitus 2020. *Indian journal of endocrinology and metabolism*, 24(1), 1–122. https://doi.org/10.4103/ijem.IJEM_225_20
11. Ripsin CM, Kang H, Urban RJ. Management of blood glucose in type 2 diabetes mellitus. *Am Fam Physician*. 2009 Jan 1;79(1):29-36. PMID: 19145963.
 12. Kieffer TJ, McIntosh CH, Pederson RA. Degradation of glucose-dependent insulinotropic polypeptide and truncated glucagon-like peptide 1 in vitro and in vivo by dipeptidyl peptidase IV. *Endocrinology*. 1995 Aug;136(8):3585-96. doi: 10.1210/endo.136.8.7628397. PMID: 7628397.
 13. Grieve DJ, Cassidy RS, Green BD. Emerging cardiovascular actions of the incretin hormone glucagon-like peptide-1: potential therapeutic benefits beyond glycaemic control?. *Br J Pharmacol*. 2009;157(8):1340-1351. doi:10.1111/j.1476-5381.2009.00376.x
 14. Fadini GP, Avogaro A. Cardiovascular effects of DPP-4 inhibition : Beyond GLP-1 ☆. *Vascul Pharmacol* [Internet]. 2011;55(1–3):10–6. Available from: <http://dx.doi.org/10.1016/j.vph.2011.05.001>
 15. Schmieder R, Raff U, Schmidt S, Kistner I, Friedrich S, Bramlage P, Ottv C. Effects of the DPP-inhibitor saxagliptin on early vascular changes in the retinal and systemic circulation. doi: 10.1093/eurheartj/eh307.P607. First published online: 1 Aug 2013.
 16. van Poppel PC, Netea MG, Smits P, Tack CJ. Vildagliptin improves endothelium-dependent vasodilatation in type 2 diabetes. *Diabetes Care*. 2011 Sep;34(9):2072-7. doi: 10.2337/dc10-2421. Epub 2011 Jul 25. PMID: 21788633; PMCID: PMC3161271.
 17. Duvnjak L, Blaslov K. Dipeptidyl peptidase-4 inhibitors improve arterial stiffness, blood pressure, lipid profile and inflammation parameters in patients with type 2 diabetes mellitus. *Diabetol Metab Syndr*. 2016 Mar 22;8:26. doi: 10.1186/s13098-016-0144-6. PMID: 27006706; PMCID: PMC4802883.
 18. Vinendra MP, and Sunita SG. “efficacy and safety of teneligliptin as add-on therapy to conventional therapy in indian patients with type 2 diabetes mellitus *Asian J Pharm Clin Res*. 2019;12:12:116-120., doi:10.22159/ajpcr.2019.v12i12.35952
 19. Vinendra MP, Sunita SG (2020) Efficacy and Safety of Teneligliptin as Add on Therapy in Indian Type 2 Diabetes Mellitus Patients having Dyslipidemia. *J Diabetes Metab*. 10:844. doi: 10.35248/2155-6156.20.11.844
 20. Naranjo CA, Busto U, Sellers EM, Sandor P, Ruiz I, Roberts EA, et al. A method for estimating the probability of adverse drug reactions. *Clin Pharmacol Ther*. 1981;30:239-425.
 21. Kadowaki T, Kondo K, Sasaki N, Miyayama K, Yokota S, Terata R, et al. Efficacy and safety of teneligliptin add-on to insulin monotherapy in Japanese patients with type 2 diabetes mellitus: a 16-week, randomized, double-blind, placebo-controlled trial with an open-label period. *Expert Opin Pharmacother* [Internet]. 2017;18(13):1291–300. Available from: <https://www.tandfonline.com/doi/full/10.1080/14656566.2017.1359259>
 22. Joshi SR, Saboo B, Vadivale M, Dani SI, Mithal A, Kaul U, Badgandi M, Iyengar SS, Viswanathan V, Sivakadaksham N, Chattopadhyaya PS, Biswas AD, Jindal S, Khan IA, Sethi BK, Rao VD, Dalal JJ; SITE Investigators. Prevalence of diagnosed and undiagnosed diabetes and hypertension in India—results from the Screening India's Twin Epidemic (SITE) study. *Diabetes Technol Ther*. 2012 Jan;14(1):8-15. doi: 10.1089/dia.2011.0243. Epub 2011 Nov 3. PMID: 22050271.
 23. Emerging Risk Factors Collaboration, Sarwar N, Gao P, Seshasai SR, Gobin R, Kaptoge S, Di Angelantonio E, Ingelsson E, Lawlor DA, Selvin E, Stampfer M, Stehouwer CD, Lewington S, Pennells L, Thompson A, Sattar N, White IR, Ray KK, Danesh J. Diabetes mellitus, fasting blood glucose concentration, and risk of vascular disease: a collaborative meta-analysis of 102 prospective studies. *Lancet*. 2010 Jun 26;375(9733):2215-22. doi: 10.1016/S0140-6736(10)60484-9. Erratum in: *Lancet*. 2010 Sep 18;376(9745):958. Hillage, H L [corrected to Hillege, H L]. PMID: 20609967; PMCID: PMC2904878.
 24. Petrie, J. R., Guzik, T. J., & Touyz, R. M. (2018). Diabetes, Hypertension, and Cardiovascular Disease: Clinical Insights and Vascular Mechanisms. *The Canadian journal of cardiology*, 34(5), 575–584. <https://doi.org/10.1016/j.cjca.2017.12.005>
 25. Zhang X, Zhao Q. Effects of dipeptidyl peptidase-4 inhibitors on blood pressure in patients with type 2 diabetes: A systematic review and meta-analysis. *J Hypertens*. 2016 Feb;34(2):167-75. doi: 10.1097/HJH.0000000000000782. PMID: 26682782.
 26. Katout M, Zhu H, Rutsky J, Shah P, Brook RD, Zhong J, Rajagopalan S. Effect of GLP-1 mimetics on blood pressure and relationship to weight loss and glycemia lowering: results of a systematic meta-analysis and meta-regression. *Am J Hypertens*. 2014 Jan;27(1):130-9. doi: 10.1093/ajh/hpt196. Epub 2013 Nov 21. PMID: 24263424.

27. Kalra S, Kumar A, Rakesh D, Sahay K, Pratim M, Mangesh B. Consensus Recommendations on GLP-1 RA Use in the Management of Type 2 Diabetes Mellitus : South Asian Task Force. *Diabetes Ther* [Internet]. 2019;10(5):1645–717. Available from: <https://doi.org/10.1007/s13300-019-0669-4>
28. Hashikata T, Yamaoka-Tojo M, Kakizaki R, Nemoto T, Fujiyoshi K, Namba S, Kitasato L, Hashimoto T, Kameda R, Maekawa E, Shimohama T, Tojo T, Ako J. Tenelegliptin improves left ventricular diastolic function and endothelial function in patients with diabetes. *Heart Vessels*. 2016 Aug;31(8):1303-10. doi: 10.1007/s00380-015-0724-7. Epub 2015 Aug 13. Erratum in: *Heart Vessels*. 2016 Aug;31(8):1311-2. PMID: 26266630.
29. Kadowaki T, Kondo K, Sasaki N, Miyayama K, Yokota S, Terata R, et al. Efficacy and safety of tenelegliptin add-on to insulin monotherapy in Japanese patients with type 2 diabetes mellitus: a 16-week, randomized, double-blind, placebo-controlled trial with an open-label period. *Expert Opin Pharmacother*. 2017;18(13):1291–300.
30. Kadowaki T, Kondo K. Efficacy and safety of tenelegliptin added to glimepiride in Japanese patients with type 2 diabetes mellitus: A randomized, double-blind, placebo-controlled study with an open-label, long-term extension. *Diabetes, Obes Metab*. 2014;16(5):418–25.
31. Takamiya Y, Okamura K, Shirai K, Okuda T. Multicenter prospective observational study of tenelegliptin , a selective dipeptidyl peptidase-4 inhibitor , in patients with poorly controlled type 2 diabetes : Focus on glycemic control , hypotensive effect , and safety Chikushi Anti-Diabetes Mellitus. *Clin Exp Hypertens* [Internet]. 2019;0(0):1–8. Available from: <https://doi.org/10.1080/10641963.2019.160120>
32. Wang B, Zhong J, Lin H, Zhao Z, Yan Z, He H, Ni Y, Liu D, Zhu Z. Blood pressure-lowering effects of GLP-1 receptor agonists exenatide and liraglutide: a meta-analysis of clinical trials. *Diabetes Obes Metab*. 2013 Aug;15(8):737-49. doi: 10.1111/dom.12085. Epub 2013 Mar 20. PMID: 23433305.
33. Iwashima Y, Katsuya T, Ishikawa K, Ouchi N, Ohishi M, Sugimoto K, Fu Y, Motone M, Yamamoto K, Matsuo A, Ohashi K, Kihara S, Funahashi T, Rakugi H, Matsuzawa Y, Ogihara T. Hypoadiponectinemia is an independent risk factor for hypertension. *Hypertension*. 2004 Jun;43(6):1318-23. doi: 10.1161/01.HYP.0000129281.03801.4b. Epub 2004 May 3. PMID: 15123570.
34. Kim, Dae Hyun et al. “Adiponectin levels and the risk of hypertension: a systematic review and meta-analysis.” *Hypertension (Dallas, Tex. : 1979)* vol. 62,1 (2013): 27-32. doi:10.1161/HYPERTENSIONAHA.113.01453
35. Takagi, H., Mizuno, Y., Yamamoto, H. *et al.* Effects of telmisartan therapy on interleukin-6 and tumor necrosis factor-alpha levels: a meta-analysis of randomized controlled trials. *Hypertens Res* **36**, 368–373 (2013). <https://doi.org/10.1038/hr.2012.196>
36. Yanai, H., & Yoshida, H. (2019). Beneficial Effects of Adiponectin on Glucose and Lipid Metabolism and Atherosclerotic Progression: Mechanisms and Perspectives. *International journal of molecular sciences*, 20(5), 1190. <https://doi.org/10.3390/ijms20051190>

PCP419

NOVEL FOOD: COMPARATIVE REGULATION AND RISK ASSESSMENT

AP0447

Pooja Parmar

Student,

Graduate School of Pharmacy,
Gujarat Technological University
ppoojaabc@gmail.com

AP0380

Dr. Rajesh Patel

Associate Professor,
Graduate School of Pharmacy,
Gujarat Technological University
rajeshpatel@gtu.edu.in

Abstract

In the course of history Novel food, Food ingredients or Method of producing food have found their way to all corners of globe. Novel foods are the foods that were not used for human consumption to a significant degree. It can be innovative food or produced using new technologies that leads to significant change in the composition and structure. Regulation of novel foods represents how society has chosen to manage unknown consequences of new technologies and material. Novel food regulation can be categorized in a variety of ways for further understanding. For almost 20 years, the European Food Safety Authority (EFSA) has gained experience in the field of novel food. There are two possible ways for authorization of novel food in EU: a full application and a simplified application. The Food Safety and Standard Authority of India (FSSAI) is a principal authority that regulates food and food products under control of Food Safety and Standard Act 2006. FSSAI implement various rules and regulations for manufacture and sale of food product in India. Safety assessment is a prerequisite for assurance of human health. Substantial equivalence is a guiding principle that used to evaluate novel products. This intended to determine that the novel food or ingredient is at least safe as its traditional counterpart.

Keywords: Novel food, EFSA, FSSAI, Safety Assessment, Substantial Equivalence

PCP422

A COMPREHENSIVE REVIEW OF SARS COV-2 VACCINES IN INDIA: COVISHIELD & COVAXIN

AP0444

Nidhi Hitesh Nayi

Student,

Graduate School of Pharmacy
Gujarat Technological University
nidhinayi45@gmail.com

AP0420

Bhumika Maheriya

Assistant Professor,

Graduate School of Pharmacy
Gujarat Technological University
ra_pharmacy@gtu.edu.in

Abstract

Severe Acute Respiratory Syndrome (SARS) is a viral respiratory disease associated with coronavirus. Its outbreak was first led in December 2019 at Wuhan, China. Afterwards the story of COVID-19 pandemic continues for almost last 3 years with numerous unexpected twists and turns due to emerging waves and variants. India has also been hit badly, especially in the second wave of the pandemic. Initially, the countries which had state-of-the-art health services found it difficult to cope in preventing infections, managing cases and reducing deaths. Before discovery of vaccine FDA has authorized certain antiviral medications and monoclonal antibodies to treat mild to moderate covid-19. Vaccine development started as the number of affecting humans rised at peak, more than 25 vaccines were in various stage of development. On 13th January 2021, vaccination campaign against SARS COV-2 launched in India and started administration of two types of vaccines known to be Covaxin and Covishield under emergency use authorization. Covishield is an adenovirus vector based vaccine and Covaxin composed of adjuvant inactivated viral particles. Efficacy of vaccination depends on properties like antibodies, memory cells and cell mediated immunity. Conducting of clinical trial, Phase-3 data, Covishield showed effectiveness of nearly 90% while Covaxin about 80%. Both vaccination formulation are satisfactorily efficient against numerous variant of SARS COV-2. The efficacy of Covishield may diminished if structure of spike protein(S) changes. In such situation, Covaxin may be effective owing to its ability to produce multiple antibodies.

Keywords: - SARS COV-2, Covishield, Covaxin, Covid-19

PCP426
NUTRICOSMETICS

AP0424
Reena Makwana
Student
Graduate School of Pharmacy-GTU
reenamakwana1999@gmail.com

AP0420
Bhumika Maheriya
Assistant Professor
Graduate School of Pharmacy-GTU
ra_pharmacy@gtu.edu.in

Abstract:

Nutritional supplements are source of molecules that have nutritional and physiological benefit to human body. According to the data provided by Future Market Insights, the Nutricosmetic market is determine at USD 6.43 billion in 2022 and is expected to reach USD 12.15 billion by 2030, at a CAGR (Compound Annual Growth Rate) of 8.28%. Nutricosmetic is the latest trend in the beauty industry. This tendency rapidly gained many followers because it fits with the modern culture. Nutricosmetic are natural ingestible products that elevates the appearance of human skin, nails, and hair. It basically provides beautification and personal hygiene benefits. They contain molecules with a physiological or nutritional effect such as nutrients (minerals, vitamins, peptides, essential fatty acids, and polysaccharides) derived from food and botanical products (herbal and fruit extracts). These products are different from nutraceuticals and cosmeceuticals as they act as the convergence between the nutrition and personal care. Talking about regulation in United States Nutricosmetic market is regulated by Food and drug administration Under the Dietary Supplement Health and Education Act (1994). In European Union beauty claim of these products need to be manifested and scientifically justified.

Keywords: Nutricosmetic, Nutritional supplement, Regulation, Beauty claim

PCP427

CURRENT REGULATORY NORMS FOR CLINICAL RESEARCH IN INDIA

AP0434

Priti Modi

Student,

Graduate School of Pharmacy,
Gujarat Technological University
pritiimodi@gmail.com

AP0420

Bhumika Maheriya

Assistant Professor,

Graduate School of Pharmacy,
Gujarat Technological University
ra_pharmacy@gmail.com

Abstract

Globally, India has profound ability that can significantly contribute more to the clinical drug development process. Clinical trials are indispensable to the drug development method to confirm the effectiveness and safety of any new drug. It is known that safety of clinical trial subject should always be prioritized and backed with appropriate regulations. Considering the past scenario in India, regulatory framework for clinical trials was quite unadorned that it involved a single tier regulatory approval process followed by the review at CDSCO office. In 2012, because of a public interest litigation filed by NGO seeking justice for drug trial victims, Supreme Court directed the union government to come with a new regulatory regime for performing clinical trials in India. Therefore, in 2019, ministry of Health and Family Welfare (MoHFW) has issued New Drug and Clinical Trials Rules, which contains 13 chapters including 107 rules and 8 schedules. The new rules overrides part XA and schedule Y of medicine and cosmetics rules, 1945; applies to new drugs, investigational new drugs, orphan drugs, phytopharmaceutical drugs, clinical trials, biomedical and health research, and ethics committees. This aims to bring new and innovative medicines to Indian patients ensuring patient safety by facilitating clinical research with shorter approval duration and maintaining appropriate transparency altogether. The new rules appear comprehensive, well balanced, and certain to enhance the moral and quality standards of clinical trials in India, which can further benefit patients and industry.

Keywords: Clinical trials, New drug, CDSCO, MoHFW, New Drug and Clinical Trials Rules 2019

PCP440

Protective Effect of 2-Deoxy-D Glucose on Chemically Induced Endometrial Cancer in Mice

AP0471 Disha Patel Research Scholar Parul Institute of Pharmacy, Parul University, Vadodara, Gujarat. pateldisha0808@gmail.com	AP0473 Rishabh Malik Research Scholar Parul Institute of Pharmacy, Parul University, Vadodara, Gujarat. rishumalik2000@gmail.com	AP0472 Dr. Jitendra Vaghasiya Professor Parul Institute of Pharmacy, Parul University, Vadodara, Gujarat. j_vaghasiya@yahoo.com
---	---	--

Abstract

2-deoxy-D-Glucose is reported to inhibit Hexokinase-II activity and hence glycolysis with the result that the binding of Hexokinase-II to Voltage Dependent Anion Channel is prevented, promoting the susceptibility of malignant cells to other forms of treatment like in Neuroblastoma cells, Breast cancer, Prostate Cancer, Human Head and Neck Cancer Cells, Malignant Cell Lines, Malignant glioma, Pancreatic cancer and Colon cancer. Recent report that 2-DG promotes cancer cell apoptosis provides the basis for testing these compounds in endometrial cancer. Therefore, in present study we are investigated its effect against endometrial cancer. For carcinogenesis studies, female Swiss albino mice were randomly divided into four groups. Normal Control (NC) - Mice received vehicle only ; Disease Control (DC) - Mice received local applications of 0.1% w/v solution of 7, 12 – dimethyl benz (α) anthracene (DMBA) in triethylene glycol twice a week for 2 months; Treatment group (2-DG) - Mice were treated with daily dosing of 2-deoxy-D-Glucose (600 mg/kg, p.o.) plus DMBA application; and Standard group (5-FU) - Mice were treated with daily dosing of 5-FU (20 mg/kg, p.o) plus DMBA application. For antimutagenicity study, animals were randomly divided into three groups. NC - Mice received vehicle only; CYP - Mice injected with cyclophosphamide (50 mg/kg, i.p.); and CYP + 2-DG - Mice treated with 2-deoxy-Glucose followed by cyclophosphamide. 2-DG treated mice demonstrated significant decreased in tumor size when compared to DC. 2-DG group of mice demonstrated well preserved antioxidant profile when compared to DC group. 2-DG treatment significantly augmented RBC and hemoglobin levels which indicated minimal myelosuppressive effect, whereas WBC count was significantly reduced in 2-DG group compared with DC group. 7 days pre-treatment of 2-DG significantly reduced total % of aberrated cells and PCE/NCE ratio, moreover significantly reduced micronucleus formation when compared to CYP group. As per our finding 2-DG inhibited endometrial carcinogenesis in mice and this activity might be attributed to its anti-mutagenic and antioxidant activity.

Keywords: 2-deoxy-D-Glucose; Endometrial Cancer; Micronucleus; Antimutagenicity Study

Introduction

Cancer is one of the major causes of death in developed nations, at least one of the five of the population of Europe and America can expect to die from cancer.^[1] As per report of World Health Organisation (WHO), the number of global cancer deaths is projected to increase by 45% from 2007 to 2030 that is 7.9 million to 11.5 million. Endometrial cancer is becoming increasingly common throughout the world. Endometrial cancer is the most prevalent gynaecological cancer in the world, and represents the third commonest cancer affecting women in the Western World. Cancer is basically a disease of cells characterized by a shift in the control mechanisms that govern cell proliferation and differentiation resulting in uncontrolled cell proliferation.^[2] The extent of metastasis and deterioration in metabolic

processes, resulting from cancer, leads to eventual death of patient.^[3] Cancer is treated with chemotherapeutic agents along with radiation and surgery. The chemotherapeutic agents provide a temporary improvement of symptoms and signs of cancers and most of the therapeutic agents are given in combination with the radiation therapy and patient has to consume it for the long duration. These drugs are more toxic to the patients who further has to suffer from side effects like appetite changes, eating problems, weight loss, hair changes, immune suppression, sexual problems, skin changes, nerve and muscle problems etc. A major challenge is to design new drugs that will be more selective for cancer cells, and thus have lesser side effects.^[4,5]

Regarding chemically induced endometrial cancer, 7,12-dimethylbenz [α] anthracene (DMBA) has been widely utilized as an initiator in the chemical carcinogenesis model. As an initiator, DMBA will react with DNA to form an adduct leading to genetic mutation. In damaged genes that break away from repair the mutation will be amplified followed by abnormal growth of cells with the mutated genes. For experimental induction of endometrial cancer insertion of a sponge impregnated with DMBA is commonly used.^[6] The majority of established anticancer drugs either are non-selective or lose their efficacy because of the constant mutational changes of malignant cells. Until recently, a largely neglected target for potential anticancer agents was the mitochondrion, showing a considerable promise for future clinical applications. Mitochondria are organelles important for life and death. They are major sources of cellular energy. However, mitochondria are also central to processes resulting in the induction of apoptosis. The exact mechanism(s) by which mitochondria act is not known in detail, but there are drugs that are known to induce death of cancer cells by targeting these organelles. Such agents, called “mitocans”. Many of the agents with anti-cancer activity that act on mitochondria, mitocans, hold a substantial promise to be developed into efficient anti-cancer drugs, based on their selectivity for cancer cells.^[7,8]

A novel approach based on the molecular, cellular and systemic responses to radiation damage as well as differences in the pattern of energy metabolism between tumor and normal cells has been successfully developed for improving the therapy of cancer. Nutrient deprivation has been shown to cause cancer cell death. Glucose-deprivation can be mimicked with glucose antagonists. Glucose analogues have been found to profoundly inhibit glucose metabolism in cancer cells in vitro and in vivo. Of the many glucose analogues which have been investigated, 2-deoxy-D-glucose (2-DG), a glucose analogue and glycolytic inhibitor, which under appropriate conditions selectively enhances treatment induced damage in tumors, while protecting cells of the normal tissues.^[9]

2-deoxy-D-glucose (2DG) has proved very effective in the inhibition of glucose metabolism and ATP production.^[10] 2DG is a structural analogue of glucose differing at the second carbon atom by the substitution of hydrogen for a hydroxyl group and appears to selectively accumulate in cancer cells by metabolic trapping^[11] due to increased uptake,^[12] high intracellular levels of hexokinase or phosphorylating activity^[13] and low intracellular levels of phosphatase.^[14] Cell killing caused by 2DG has been described in several cell lines.^[15-17] Hexokinase (ATP: D-hexose 6-phosphotransferase) is a key enzyme that catalyzes the first step in the glycolysis pathway. This enzyme transfers a phosphate group from ATP to glucose to form glucose-6-phosphate. In human cells, there are four isoforms of hexokinase (I–IV). Despite their overall structural similarity, these isoforms differ in their expression patterns, subcellular localizations, and catalytic/regulatory properties. Of note, hexokinase I and II are found to be able to bind to mitochondria through their interaction with VDAC (voltage dependent anion channel), and this association appears important for the homeostasis of mitochondria. Additionally, such mitochondrial association has been reported to influence the enzyme kinetics of hexokinase. In cancer tissues, the high glycolytic activity requires an upregulation of the key glycolytic enzymes including hexokinase. Due to the frequent up-regulation of HK-II in cancer cells and its important role in glycolytic pathway, this enzyme

seems to be an attractive target for anticancer drug development.^[18] 2-deoxyD-Glucose inhibits this enzyme hexokinase-II. So far, no report is available for its activity against endometrial cancer, therefore the present work was undertaken to study the effect of 2-deoxy-D-Glucose against DMBA induced endometrial cancer in mice.

Materials & Methods

Animals

Healthy swiss albino female mice weighing about 25 - 30g were housed in polypropylene cages, maintained under standardized conditions (12 hours light/dark cycle, $24 \pm 2^{\circ}\text{C}$, 35 to 65% humidity) and provided free access to standard laboratory diet and purified drinking water *ad libitum*. All experiments described in present study were approved by the Institutional Animal Ethics Committee and carried out as per the guidelines of Committee for the Purpose of Control and Supervision of Experiments on Animals, Ministry of Social Justice and Empowerment, Government of India.

Induction of Endometrial cancer and Experimental Design

Dry powder of 2-deoxy-D-Glucose was dissolved in distilled water. 0.1% w/v solution of DMBA was prepared by dissolving DMBA in triethyleneglycol. For the intravaginal application polyurethane sponge was sliced into small cubes having size of $3 \times 3 \times 3$ mm. After 5 days of acclimatization, animals were subjected to their respective exposures. Twenty-four mice were randomly subdivided into four groups (n = 6). Group 1: Mice were daily administered with distilled water served as Normal Control (NC). Group 2: Mice were daily administered distilled water along with intra-vaginal applications of polyurethane sponge ($3 \times 3 \times 3$ mm) impregnated with 0.1% w/v solution of DMBA twice a week for 2 months. Three hours after each application sponges were taken out. This served as Disease Control (DC). Group 3: Mice were treated with daily dosing of 2-deoxy-D-Glucose (600mg/kg, p.o.) along with DMBA (0.1% w/v) application. This served as treatment group (2-DG). Group 4: Mice were treated with daily dosing of 5-FU (20 mg/kg, p.o) along with DMBA (0.1% w/v) application twice a week (5-FU). 14 weeks after the starting of the experiment, blood was collected from all animals from retro-orbital plexus into an Eppendorf tube preloaded with EDTA, which was used for the assessment of hematological parameters like Hb content, Reticulocytes, total WBC, and RBC. At the end of each experiment, animals were sacrificed with high dose of ether anaesthesia. After opening the abdominal cavity, liver tissue was excised and used for biochemical estimation. The excised tumor was used for studying physical and histopathological study.

Estimations of Physical parameters

At the end of the experiment the tissue was excised and observed for tumor size, tumor incidence, tumor inhibitory rate and median survival time (MST).

Histopathological examination

The vagina and uterus were dissected out and the tissue was washed immediately with saline and fixed in 10% buffered formalin. The fixed tissues were embedded in paraffin and serial sections (5-7 μm thick) were cut. Each section was stained with hematoxylin and eosin. The sections were examined under the trinoculour microscope (Carls Zeiss primostar) for histopathological changes.

Estimation of Hematological parameters

White Blood Cells (WBC), Red Blood Cells (RBC), Reticulocytes, Haemoglobin content by using Sahli's method.^[19]

Estimation of Biochemical parameters

The excised liver was weighed and homogenized in chilled Trisbuffer (10 mM, pH 7.4) at a concentration of 10% w/v. The homogenates were centrifuged at $10,000 \times g$ at 0°C for 20 min using Remi C-24 high speed cooling centrifuge. The clear supernatant was used for the assay of Lipid peroxidation (MDA) ^[20], Superoxide dismutase (SOD) ^[21], Catalase (CAT) ^[22], Reduced glutathione (GSH) ^[23]

Induction of Chromosomal Aberration

For chromosomal aberration cyclophosphamide (50mg/kg, i.p., in 0.9% saline) was injected in mice. 4mg/kg Colchicine was administered intra-peritoneally 2 hours before the harvest of the cells. Animals were sacrificed by high dose of ether anaesthesia and used for chromosomal aberration study. The mice were assigned to three different groups ($n = 6$). Group 1: Mice were daily administered with vehicle were served as Normal Control (NC); Group 2: Mice were daily administered with Cyclophosphamide (50mg/kg IP) served as disease control; Group 3: Mice were daily administered Cyclophosphamide (50mg/kg) along with 2-DG (600mg/kg) served as treatment group.

Animals were sacrificed by high dose of ether anaesthesia. Femurs were excised and the bone marrow were extracted in 0.56 %w/v KCl. Harvested cells were incubated at 37°C for 20 minutes and then centrifuged for 10 minutes at 1000 rpm. Fixed in Carney's fixative (Methanol: Acetic acid, 3:1), slides were stained with 5 % Giemsa solution for 15 minutes. Slides were dipped in xylene and mounted under microscope to study chromosomal aberration in 100 cells. Chromatid breaks, gaps, pulverization, stickiness, fragmentation, deletions, ring formation, and clusters were scored and expressed as % chromosomal aberrations. [24]

In-vitro Micronucleus test

Genetic effects were evaluated in the mouse bone marrow micronucleus test according to Schmid. The bone marrow cells from both femurs were flushed in the form of a fine suspension into a centrifuge tube containing Human Ab serum. This cell suspension was centrifuged at 2000 rpm for 10 minutes and pellets re-suspended in a drop of serum before being used for preparing slides. Air dried slides were stained with May Grunwald and Giemsa as described by Schmid. The smears were analyzed under oil immersion objective. For each experimental point, six mice were used and 1000 polychromatic erythrocytes scored per animal per slide to determine the frequency of micronucleated polychromatic RBC's.

Statistical analysis

All the values are expressed as mean \pm SEM. Statistical significance was tested between more than two groups using one-way ANOVA followed by the Bonferroni multiple comparisons test using a computer-based fitting program (Prism, Graphpad 5.). Differences were considered to be statistically significant when $p < 0.05$.

Result

Effect of 2-DG on Macroscopical findings

In carcinogenesis study, the macroscopical examination revealed presence of tumors in six DC mice exposed to DMBA alone whereas with compared to that tumors were observed in three mice treated with 2-DG for 8 weeks. DC group mice demonstrated an average tumor size of 1.55 mm in diameter, whereas 2-DG group of mice showed an average tumor size of 0.38 mm in diameter. Results showed a significant ($P < 0.001$) increase in tumor size in DC group which was significantly ($P < 0.001$) decreased in 2-DG group when compared to DC group. The tumor inhibitory rate observed in 2-DG group is 63.90% whereas in 5-FU showed 32.40% (Table 1).

Table-1 Macroscopic findings in uterine endometrial wall for different groups

Groups	Tumor Incidence	Tumor Size (mm)	Tumor Inhibitory Rate (%)	Median Survival Time (Days)
NC	0/0	0.00	-	99
DC	6/6	1.55 \pm 0.168*	-	99
2-DG	3/6	0.38 \pm 0.030 ⁺	63.90	99
5-FU	4/6	0.56 \pm 0.061 ⁺	32.40	99

Values of tumor size are expressed as Mean \pm SEM (n=6), analyzed by one-way ANNOVA followed by Bonferroni's Multiple Comparison's test. * Denotes P < 0.001 for chance difference vs. NC, + denotes P < 0.001 for chance difference vs. DC, where NC: Normal Control, DC: Disease Control, 2-DG: 2-deoxy D-Glucose treated mice, 5- FU: 5 - Florouracil treated mice.

Effect of 2-DG on Histopathological examination

Histopathological investigation has shown the occurrence of endometrial cancer which could not be observed nakedly. The Normal control group showed normal growth of epithelium. The groups exposed to DMBA alone, DMBA+2-DG and DMBA+ 5-FU showed appearance of endometrioid adenocarcinoma of the endometrium. Increased nuclear atypia, spindle shaped and elongated blunted nuclei are present (Fig-1). Also, the histopathological assessment of lungs tissue confirms the occurrence of malignant spread (Fig-2)

Effect of 2-DG on Haematological parameters

The Haemoglobin content, RBC count and Reticulocytes in DC group was found to be significantly (P < 0.001) lower when compared to NC group. The 2-DG group further showed significant increase in haemoglobin content, RBC count and Reticulocytes (P < 0.001) whereas 5-FU group showed insignificant (P > 0.05) change for the same when compared to DC group. The WBC count significantly (P < 0.001) increased in the DC group when compared to NC group which significantly (P < 0.001) reduced in the 2-DG group and 5-FU group (Figure 1) (Table -2).

Table -2 Effect of 2-DG on haematological parameters

Group s	Haemoglobin(gm %)	RBC's(cellsx10⁶/cm m)	Reticulocytes (%)	WBC's(cellsx10³/cm m)
NC	11.86 \pm 0.189	8.94 \pm 0.324	0.86 \pm 0.030	4.41 \pm 0.275
DC	5.73 \pm 0.809**	4.61 \pm 1.083**	0.46 \pm 0.045* *	7.73 \pm 0.563
CRN	8.95 \pm 1.109 ^{\$\$}	7.05 \pm 0.920 ^{\$\$}	0.62 \pm 0.049 ^{\$} \$	6.01 \pm 0.250
FU	6.60 \pm 0.758 ^{NS}	5.28 \pm 0.503 ^{NS}	0.51 \pm 0.050 ^N s	6.510 \pm 0.275

Values are expressed as Mean \pm SEM (n=6), analyzed by one-way ANNOVA followed by Bonferroni's Multiple Comparison's test. ** denotes P < 0.001 for chance difference vs. NC, ^{\$\$} denotes P < 0.001 for chance difference vs. DC, + denotes P < 0.05 for chance difference vs. DC, NS denotes statistically insignificant for chance difference vs. DC, where NC: Normal Control, DC: Disease Control, 2-DG: 2-deoxy-D-Glucose treated mice, 5- FU: 5 - Florouracil treated mice.

Figure-1: Haematoxylin-Eosin stained endometrioid tissue sections of: A) NC group; B) DMBA treated DC group; C) 2-DG plus DMBA treated 2-DG group; D) 5-FU plus DMBA treated 5-FU group of mice and E) Leiomyoma cells

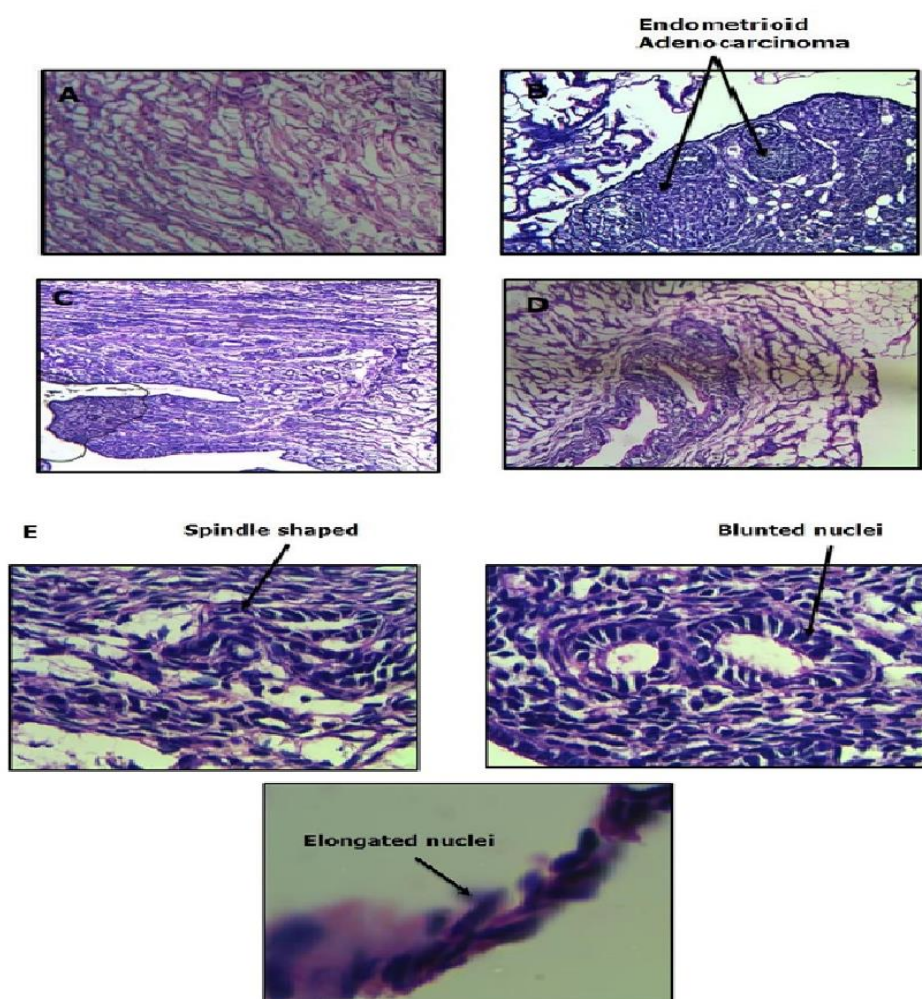
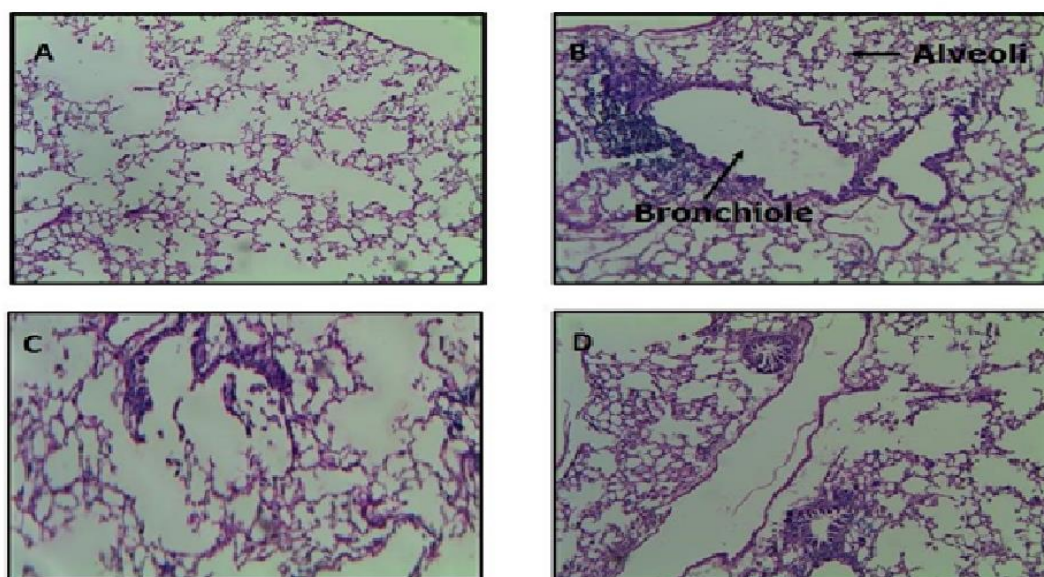


Figure- 2: Stained tissue sections of lungs of: A) NC group; B) DMBA treated DC group; C) 2-DG plus DMBA treated 2-DG group; D) 5-FU plus DMBA treated 5-FU group of mice



Effect of 2-DG on Biochemical parameters

Lipid peroxidation measured as formation of MDA which was significantly ($P < 0.001$) increased in DC group of mice whereas GSH, SOD and CAT were significantly ($P < 0.01$) decrease when compared to NC group animals. 2-DG treated group showed a significant ($P < 0.01$) decrease in the MDA levels whereas GSH, SOD and CAT were significantly ($P < 0.01$) increased when compared to DC group animals. (Table-3).

Table-3 Effect of 2-DG on Biochemical parameters

Groups	MDA (nmol/g of tissue)	GSH ($\mu\text{g/g}$ of tissue)	SOD (U/g of tissue)	CAT ($\mu\text{mol H}_2\text{O}_2$ consumed/min/g of tissue)
NC	13.91 \pm 0.988	29.10 \pm 0.901	10.65 \pm 0.791	11.67 \pm 0.904
DC	34.63 \pm 1.449**	14.07 \pm 0.905**	7.85 \pm 0.661**	7.100 \pm 0.549**
CRN	24.25 \pm 1.280 ^{\$\$}	24.63 \pm 1.071 ^{\$\$}	9.077 \pm 0.621 ^{\$\$}	9.168 \pm 0.898 ^{\$\$}
FU	29.40 \pm 1.444 ⁺	20.31 \pm 1.106 ⁺	6.192 \pm 0.584 ⁺	7.237 \pm 0.788 ⁺

Values are expressed as Mean \pm SEM (n=6), analysed by one-way ANOVA followed by Bonferroni's Multiple Comparison test. ** denotes $P < 0.001$ for chance difference vs. NC; ^{\$\$} denotes $P < 0.001$ for chance difference vs. DC and ⁺ denotes $P < 0.001$ for chance difference vs. DC, where NC; Normal Control group, DC; DMBA (0.1% w/v) treated disease control group, 2-DG; 2- deoxy-D-Glucose (600mg/kg, p.o.) treated group and 5-FU; 5-Fluorouracil (20mg/kg), p.o.) treated group.

Effects of 2-deoxy-D-Glucose on Chromosomal aberration

We observe various types of chromosomal aberrations like ring formation, deletion, fragmentation, clusters, chromatid gaps, pulverization and stickiness in the CYP treated group when compared to NC (Figure-3). Cyclophosphamide treated group of mice demonstrated a significant ($P < 0.001$) elevation in total % of aberrated cells when compared to NC. 2-deoxy-D-Glucose treated CYP+2DG group of mice showed a significant ($P < 0.001$) reduction in total % of aberrated cells when compared with CYP (Table-4).

Table-4 Effect of 2-deoxy-D-Glucose on total % chromosomal aberration

Groups	Total no. of metaphase analyzed	Total % aberrated cells
NC	500	1.33 \pm 0.516
CYP	500	17.33 \pm 2.805*
CYP+2-DG	500	13.33 \pm 0.421 ^{\$}

Data are expressed as mean \pm SEM (n = 6), analyzed by one way ANOVA followed by Bonferroni Multiple Comparison test. * denotes $P < 0.001$ for chance difference vs. NC, ^{\$} denotes $P < 0.001$ for chance difference vs. CYP, NC; Normal Control group, CYP; Cyclophosphamide group and CYP+2-DG; Cyclophosphamide plus 2-deoxy-D-Glucose treated group.

Effects of 2-deoxy-D-Glucose on Micronucleus assay

Various types of MNPCE's were observed across different groups of mice. We observed Mononucleated PCE, binucleated PC, polynucleated PCE, binucleated and polynucleated PCE and Ana-telophase stage in mice bone marrow micronucleus assay (Figure-4). Cyclophosphamide treated group of mice demonstrated a significant ($P < 0.001$) elevation in MNPCE count when compared to NC. 2-deoxy D-Glucose treated CYP+2DG group of mice showed a significant ($P < 0.001$) reduction in MNPCE count when compared with CYP (Table-

4). Cyclophosphamide treated group of mice demonstrated a significant ($P < 0.001$) elevation in PCE/NCE ratio when compared to NC. 2-deoxy-D-Glucose treated CYP+2DG group of mice showed a significant ($P < 0.001$) reduction in PCE/NCE ratio when compared with CYP (Table-5).

Figure-3: Various types of Micronucleated Polychromatic erythrocytes in mice bonemarrow micronucleus assay: A) Mononucleated PCE for Normal Control; B) Binucleated PCE; C) Polynucleated PCE; D) Binucleated and Polynucleated PCE; E) Ana-telophase stage.

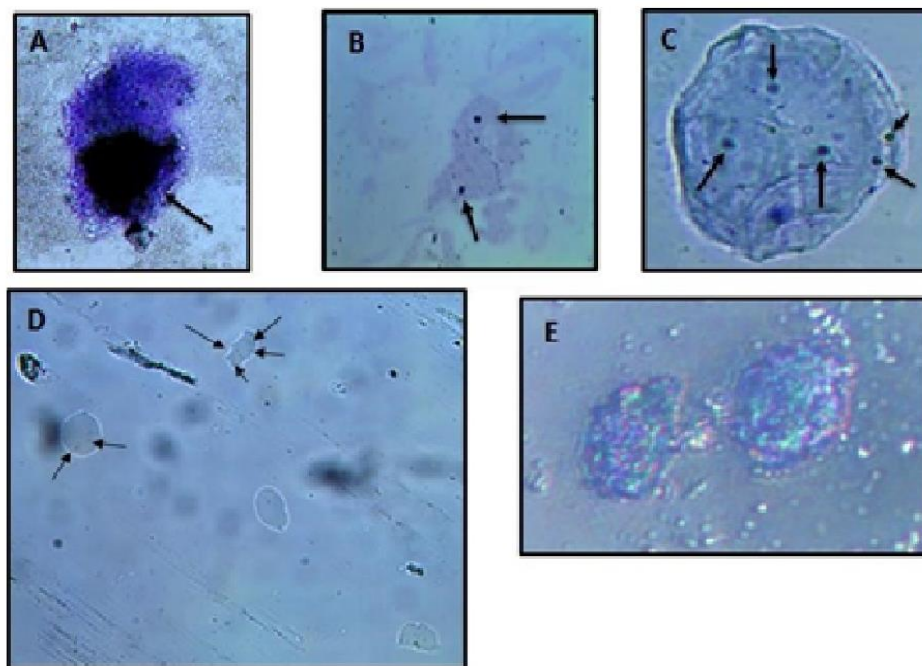
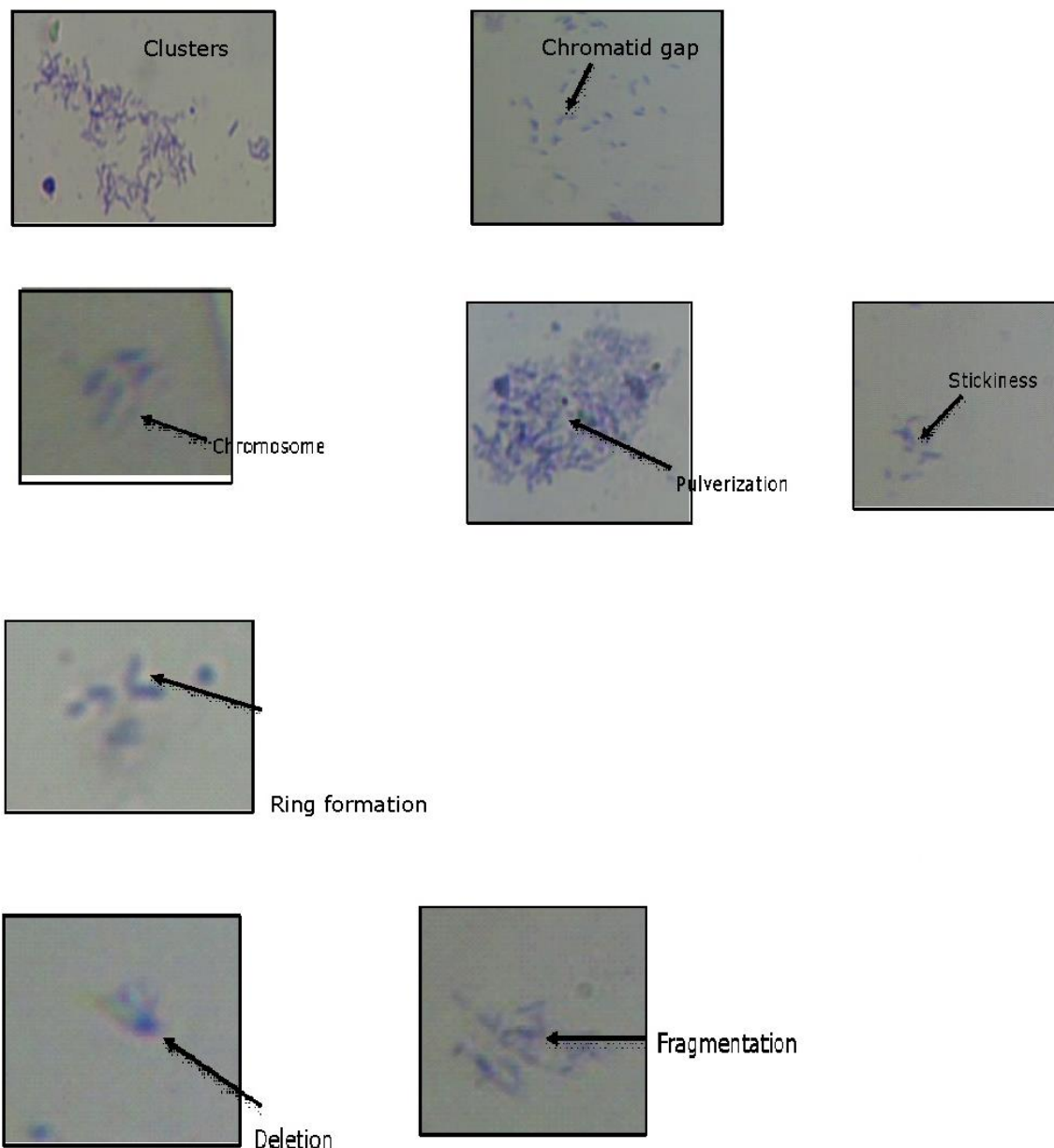


Table 5 Effect of 2-deoxy-D-Glucose on number of MNPCE cells and PCE/NCE cells ratio

Groups	PCE/NCE Ratio
NC	0.368±.033
CYP	0.61±0.045
CYP+2-DG	0.48±0.018 ^s

Data are expressed as mean \pm SEM ($n = 6$), analyzed by one way ANOVA followed by Bonferroni Multiple Comparison test. ^sdenotes $P < 0.001$ for chance difference vs. CYP, where NC; Normal Control group, CYP; Cyclophosphamide group and CYP+2-DG; Cyclophosphamide plus 2-deoxy-D-Glucose treated group.

Figure-4: Various types of Chromosomal aberrations observed: A) Normal Chromosome; B) Ring formation; C) Deletion; D) Fragmentation; E) Clusters; F) Chromatid gap; G) Pulverization and H) Stickiness



DISCUSSION

Cancer cells have been suggested to have a fundamental defect in their respiratory mechanism, which has been suggested to lead to increased generation of pro-oxidants (i.e., superoxide, hydrogen peroxide, etc.) by mitochondria.^[25,26] In addition, increased glucose metabolism and pentose phosphate cycle activity have been observed in cancer cells compared with untransformed (normal) cells.^[27,28] Because the products of glucose metabolism, pyruvate (from glycolysis) and NADPH (from the pentose cycle), are believed to function in hydroperoxide detoxification, it is hypothesized that the up regulation in glucose metabolism in cancer cells is necessary to produce more pyruvate and NADPH to compensate for the increase in intracellular pro-oxidant production. The increased dependency of cancer cells on glucose metabolism for hydroperoxide detoxification is an attractive target that may be exploited to gain a therapeutic advantage when trying to kill cancer cells while sparing normal tissues. Accordingly, glucose deprivation and treatment with 2DG have been shown to induce cytotoxicity, significant

increases in pro-oxidant production, and profound disruptions in thiol metabolism in colon, breast, cervical, and prostate cancer cells, suggesting that oxidative stress was involved with the mechanism of action.^[29] In the present study, 2DG was used to mimic the effects of glucose deprivation in the endometrial cells. 2DG is a clinically relevant analogue of glucose that competes with glucose for uptake and entry into glucose metabolic pathways.^[30] therefore 2DG can create a drug induced state of glucose deprivation, although it does not completely inhibit the regeneration of NADPH from NADP⁺ because it is a substrate for glucose-6-phosphate dehydrogenase. 2-DG is transported through plasma membrane of cancer cells with higher efficacy than in normal healthy cells and phosphorylated by mitochondria-bound Hexokinase-II to give 2-DG-6-P. In contrast to G-6-P, 2-DG-6-P is relatively stable and accumulates inside the cells inhibiting hexokinases and the glycolytic pathway.^[31] This activity has been proved in the present study which reveals its anticancer activity. The clonogenic survival assay is a commonly used approach in cancer biology for testing the efficacy of a therapy in vitro.^[32] In the study carried out here the group which received 2-DG at a concentration of 600mg/kg displayed slowed down progression of endometrial cancer. We chose the dosage of 600mg/kg of 2-DG, because it appeared empirically the best compromise with regard to previous reports that described its inhibition in-vivo. ^[33] 2-DG slowed-down the cell cycle progression, demonstrating a cytostatic effect. The histopathology normally reveals crushed endometrial glands and stroma may be extremely cellular and can cause concern. The presence of plasma cells is widely regarded as the most useful criterion for a diagnosis of endometritis, although these are often admixed with other inflammatory cells, both acute and chronic, and may be a minor component of the inflammatory cell infiltrate. The present study showed appearance of an endometrioid adenocarcinoma of the endometrium. Increased nuclear atypia, mitotic figures and elongated blunted nuclei. Also, the histopathological assessment of lungs tissue confirms the occurrence of malignant/haematologic spread. Nuclear atypia, variation in gland size, and increased mitoses are common in adenocarcinoma.

2-DG, showed an extremely significant reduction in the frequencies of micronucleated polychromatic erythrocytes (MNPCE's). It is worth noticing that the mean level of MNPCE's significantly reduced in frequency of 2-DG induced in rat bone marrow cells. Cyclophosphamide (CYP) yields clearly positive results in the micronucleus test ^[34] and therefore are used as a positive control by several investigators. The results of our bone marrow experiments induced CYP showed significant increase in the number of micronuclei as well as DNA damage.

Rather than its monotherapy as an anti-cancer moiety it has proved to act synergistically in its combination therapy with chemical entities like metformin, cisplatin and hypofractionated irradiation as already mentioned previously. Though a milestone, altogether the results from the present study in combination with the previous data provides another evidence for the beneficial effects of 2-deoxy-D-Glucose in carcinogenesis. With its lack of toxicity being a glucose analog, it can prove to be a good option for its inclusion in the main anti-cancer therapy.

Conclusion

The present experimental study suggested a beneficial role of 2-deoxy-D-Glucose in endometrial cancer. Anti-mutagenic potential and antioxidant activity might be responsible for protective effect of 2-deoxy-D-Glucose on endometrial cancer in experimental animals without affecting most of the parameters which is advantageous over available synthetic drugs.

References

- 1) Coleman M.P, Esteve J, Arsalan A and Renard H, "Trends in Cancer Incidence and Mortality", International Agency for Research on Cancer, Lyon, 2003, pp. 806
- 2) Bertran Katzung., Edward Chu; and Alan Sartorelli. Basic and clinical Pharmacology, 9th Edn, Mc Graw Hill, Singapore, 2004, pp. 848.
- 3) Sharma HL and Sharma KK. Principles of Pharmacology, 1st Edn, Paras Publishing, Hyderabad, India, 2007, pp 862.

- 4) Barbera L, Seow H and Howell D, "Symptom burden and performance status in a population-based cohort of ambulatory cancer patients" *Cancer* 2010, 116(24), pp. 5767-5776.
- 5) Frame P.S, "National Institutes of Health State-of-the-Science Conference Statement: Symptom management in cancer: pain, depression, and fatigue" July 2002. *Journal of National Cancer Institute Monograph*, 32, pp. 9-16.
- 6) Vladimir N, Zhabezhinski A, Mark A, Zaripova A, Musatov A, Andre V, Vigreux C, Godard T and Sichel F, "Inhibitory effect of melatonin on 7,12- dimethylbenz[α]anthracene induced carcinogenesis of the uterine cervix and vagina in mice and mutagenesis in vitro", *Cancer Letters*, ,2000, pp. 199-205.
- 7) Neuzil, Jiri, Dong, Lan-Feng, Rohlena, Jakub, Truksa, Jaroslav, Ralph, and Stephen J, "Classification of mitocans, anti-cancer drugs acting on mitochondria", *Mitochondrion*, 2012, pp.112.
- 8) Wallace A, Fulda Z, Ralph C, Wang, Fulda, Kroemer, Kepp, Lemarie, Grimm, Shoshan B, Ben H, "Evaluation of 2-deoxy-D-glucose as a chemotherapeutic agent: mechanism of cell death" *British Journal of Cancer*, 87, 2002, pp. 805–812.
- 9) Ball H, Wick A and Sanders C, "Influence of glucose anti-metabolites on the Walker tumor" Aug 1957, *Cancer Research* 17, pp. 235–239.
- 10) Laszlo J, Humphreys S and Goldin A, "Effects of glucose analogues (2- deoxy-D-glucose, 2-deoxy-D-galactose) on experimental tumors" *Journal of National Cancer Institute* 24, Feb 2008, pp. 267–280.
- 11) Gallagher B, Fowler J, Gutterson N, MacGregor R, Wan C and Wolf A, "Metabolic trapping as a principle of radiopharmaceutical design: some factors responsible for the biodistribution of [^{18}F] 2-deoxy-2-fluoro-D- glucose" *Journal of Nuclear Medicines*", Aug 1978, pp. 1154–1161
- 12) Waki A, Kato H, Yano R, Sadato N, Yokoyama A, Ishii Y, Yonekura Y and Fuji bayashi Y, "The importance of glucose transport activity as the rate- limiting step of 2-deoxyglucose uptake in tumor cells in vitro", *Nuclear Medecines Biologics*, Aug 1998, 25, pp. 593–597.
- 13) Segal D, Rushkin E, Polak-Charcon S and Degani H, "Glucose transporters and transport kinetics in retinoic acid differentiated T47D human breast cancer cells" *American Journal of Physiology, Endocrinology and Metabolism*", 2000, Volume 279, pp. E508– E519.
- 14) Aloj L, Caraco C, Jagoda E, Eckelman W and Neumann R, "Glut-1 and hexokinase expression: relationship with 2-fluoro-2-deoxy-D-glucose uptake in A431 and T47D cells in culture", *Cancer Research*, 1999, 59, pp. 4709–4714.
- 15) Kern K and Norton J, "Inhibition of established rat fibrosarcoma growth by the glucose antagonist 2-deoxy-D-glucose", *Surgery* 102, 1987, pp. 380–385.
- 16) Jain V, Kalia V, Sharma R, Maharajan V and Menon M, "Effects of 2-deoxy- Dglucose on glycolysis, proliferation kinetics and radiation response of human cancer cells" *International Journal of Radiation, Oncology, Biology and Physics*, 1985, Volume 11, pp. 943–950.
- 17) Ko Y, Pedersen P and Geschwind J, "Glucose catabolism in the rabbit VX2 tumor model for liver cancer: characterization and targeting hexokinase", *Cancer Letters*, 2001, Volume 173, pp. 83–91.
- 18) Wilson J.E, "Isozymes of mammalian hexokinase: structure, subcellular localization and metabolic function", *Journal of Experimental Biology*, 2003, 206, pp. 2049–2057.
- 19) Dirican A, "The effects of hematological parameters and tumor-infiltrating lymphocytes on prognosis in patients with gastric cancer", *Cancer Biomarkers*, 2013,13(1), pp. 11-20.
- 20) Slater TF and Sawyer BC, "The stimulatory effects of carbon tetrachloride and other haloalkanes or peroxidative reactions in liver fractions in vitro", *International Journal of Biochemistry*, 1971, 123, pp. 805-814.
- 21) Misra H.P and Fridovich I, "The role of superoxide anion in the autoxidation of epinephrine and a simple assay of SOD", *Journal of Biological Chemistry*,1972, 247, pp. 3170.

- 22) Aebi H, 'Oxidoreductases acting on groups other than CHOH: Catalase', *Methods in Enzymology*, London: Academic Press, 1984, 5, pp. 121.
- 23) Moran M.S, Depierre J.W and Mannervik B, "Levels of glutathione, glutathione reductase and glutathione S-transferase activities in rat lung and liver", *Biochimica et Biophysica ACTA*, 1979, 67, pp. 582.
- 24) Schmid W, "Protective effect of *Spirulina fusiformis* on chemical-induced Genotoxicity in mice", *Mutation Research*, 2008, 31, pp.9.
- 25) Lee Y.J, Galoforo S.S and Berns C.M, "Glucose deprivation-induced cytotoxicity and alterations in mitogen-activated protein kinase activation are mediated by oxidative stress in multidrug-resistant human breast carcinoma cells", *Journal of Biology and Chemistry*, 1998, 273, pp. 5294–5299.
- 26) Blackburn R.V, Spitz D.R and Liu X, "Metabolic oxidative stress activates signal transduction and gene expression during glucose deprivation in human tumor cells", *Free Radical Biology Medicine*, 1999, 26, pp. 419–430.
- 27) Warburg O, "On the origin of cancer cells" *Science*, 1956, 132, pp. 309–314.
- 28) Lehninger A.L, *Biochemistry*, New York: Worth Publishers, Inc., 1976, pp. 245–441, 467–71, 849–50.
- 29) Andringa K.K, Coleman M.C and Aykin-Burns N, "Inhibition of glutamate cysteine ligase (GCL) activity sensitizes human breast cancer cells to the toxicity of 2- deoxy-D-glucose", *Cancer Research*, 2006, 66, pp. 1605–1610.
- 30)) Shenoy M.A and Singh B.B, "Non-nitro radiation sensitizers", *International Journal of Radiation and Biology*, 1985, 48, pp. 315–326.
- 31) Li and Zhao, "Warburg Effect and Mitochondrial Metabolism in Skin Cancer", *Journal of Carcinogenes and Mutagenes*, 2012, pp. 2-5.
- 32) Spitz D.R, Malcolm R.R and Robert R.J, "Cytotoxicity and metabolism of 4- hydroxy-2-nonenol and 2-nonenol in H₂O₂-resistant cell lines. Do aldehydic byproducts of lipid peroxidation contribute to oxidative stress", *Journal of Biochemistry*, 1990, 267, pp. 453-459.
- 33) Torlińska T, Ozegowski S, Paluszak J and Hryniewiecki T, "In vivo effect of 2- deoxy-D-glucose on glucose-6-phosphate dehydrogenase activity in the cytosol of liver, heart and skeletal muscle of rats", *Nov. 1990*, 41(7), pp. 138-145
- 34) Tinwell H, Bandara L and Ashby J, "Activity of DMBA, DMH and CP in triple and single dose rodent bone marrow micronucleus assay" *Mutation Research*, 1990, 234, pp. 195-198

PCP447

A STUDY ON REGISTRATION PROCESS OF MICRO INVASIVE GLAUCOMA SURGICAL DEVICE IN USA

AP0482

Mandeep Kaur Banth

Student

GSP - GTU

mandeepbanth2@gmail.com

AP0490

Dhrastiben Bhatt

Student

GSP - GTU

Drashtibhatt015@gmail.com

AP0427

Dr.Sanjay P Chauhan

Director

GSP - GTU

prof_sanjay_chauhan@gtu.edu.in

Abstract

Glaucoma is an eye disease that damages the optic nerve. This damage is caused by abnormally high pressure in our eye. The Hydrus Microstent is a class III Medical Device according to the US Medical Device classification and was approved by the FDA in 2018. The Hydrus Microstent is an innovative micro-invasive glaucoma surgery (MIGS) device. Studies have shown promising results when Hydrus Microstent is used to target mild-to-moderate glaucoma. For registration of Hydrus microstent Class III medical Device PMA (Pre-market Approval) is required along with general and special control. PMA Submission can be carried out by eCopy submission with a PMA Cover letter to the CDRH. Medical Devices are regulated by Center for Medical Device and Radiological Health (CDRH) in the United State Food and Drug Administration (USFDA). So, here we have discussed detailed introductory information about the Class 3 medical devices along with an extensive review of regulatory guidelines for the same products with the consideration of the current market. This study provides detailed insights into similar kinds of medical devices based on regulatory approvals which can be useful to smoothly streamline the regulatory approvals.

Keywords: Glaucoma, Hydrus Microstent, Class III Medical Device, Regulatory approval.

PCP448

DIABETES MELLITUS: A REVIEW ON PATHOPHYSIOLOGY CURRENT STATUS OF ORAL MEDICATION AND FUTURE PERSPECTIVES

AP0478 Dr. D. B. Meshram Principal, PPDC, Vadodara GTU dbmeshram@ yahoo.com	AP0486 Patel Parth J. Student, Pioneer Pharmacy College, Vadodara Gujarat Technological University pjpatel021102 @gmail.com	AP0484 Dr. Vaishali Sharma Associate Professor, PPDC, Vadodara GTU vaishalisharma84 @gmail.com	AP0485 Patel Karuna A Student, PPDC, Vadodara GTU patel.karuna82 @gmail.com	AP0487 Varde Divya J Student, PPDC, Vadodara GTU divyavarde15@ gmail.com
--	--	---	--	---

ABSTRACT:

Diabetes mellitus (DM), belongs to the class of metabolite disease. The main symptom associated with this disease is the high sugar levels in blood for a long period. It can be categorized as world's major disease considering that affect large population on earth. Patients prefer oral anti-diabetic medication since they are easier to be administered and for this reason researchers focus their studies towards this direction. This work also aims to present and evaluate possible oral formulation against Diabetes. Symptoms of diabetes are sweating, blurred vision, sudden weight loss, fatigue, slow healing. Mostly patient with diabetes suffer from polydipsia, polyphagia and polyuria. In India, 77 million people suffering from Diabetes and according to healthcare organization in 2045 there will be 134 million cases occurs in India. In Gujarat, people suffering from the Diabetes nearby 1, 61,578 affected this disease. Percentage of men and women suffering from Diabetes Mellitus in Gujarat are 16.1% and 14.8%. This review is aimed to present and evaluate possible oral formulation against Diabetes mellitus.

KEYWORDS:

Diabetes mellitus, Type 1 diabetes mellitus, Type 2 diabetes mellitus, Oral medication, current medication, Epidemiology

1. INTRODUCTION:

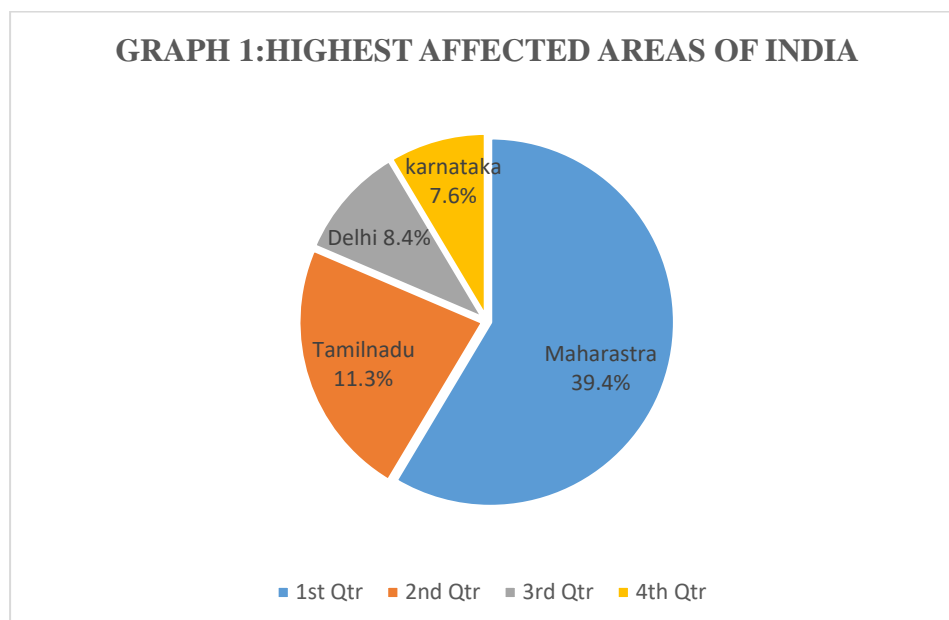
Recently, it was recorded that in 2012 atleast 1.5 million deaths induced from diabetes. The terms "Diabetes" and "Mellitus" are derived from Greek language. "Diabetes" denotes "a passer through, a siphon" and "Mellitus" means "sweet".

Diabetes mellitus (DM) is not a single disease entity, but rather a group of metabolic disorders sharing the common underlying feature of hyperglycaemia. Hyperglycaemia in diabetes results from defects in insulin secretion, insulin action, or, most commonly, both. The chronic hyperglycaemia and consequent metabolic deregulation may be associated with secondary damage in may be associated with secondary damage in multiple organ systems, especially the kidneys, eyes, nerves and blood vessels. Diabetes affects an estimated 16 million people in the united states, as many as half of whom are undiagnosed. Each year, 800,000 peoples ware

affected by this disease such a country and 54,000 death from diabetes related causes. Diabetes is a leading cause of end-stage renal disease, adult-onset blindness and non-traumatic lower extremity amputation in the United States. For especially born in the United States in 2000, the estimated lifetime risk of being diagnosed with diabetes mellitus is 1 in 3 for males and 2 in 5 for females. Universal, more than 140 million people suffer by diabetes, making this one of the most common non-communicable diseases. The number of affected individuals with diabetes is expected to double by 2025. The countries with the largest number of diabetics are India, China, and the United States.

Hyperglycemia and its associated carbohydrate, fat, and protein metabolic dysfunctions affect multiple organs of the body and disrupt their normal functioning. These disruptions progress gradually and arise mostly due to the adverse effects of hyperglycemia and its associated metabolic anomalies on the normal structure and functioning of micro- and macro vasculature, which lie at the core of organ structure, and function throughout the body. The structural and functional disruptions in organ system vasculature lead to micro- and macro vascular complications. Organ damage, dysfunction, and, ultimately, organ failure characterizes these complications and affect body organs, which include, in particular, eyes, kidneys, heart, and nerves.

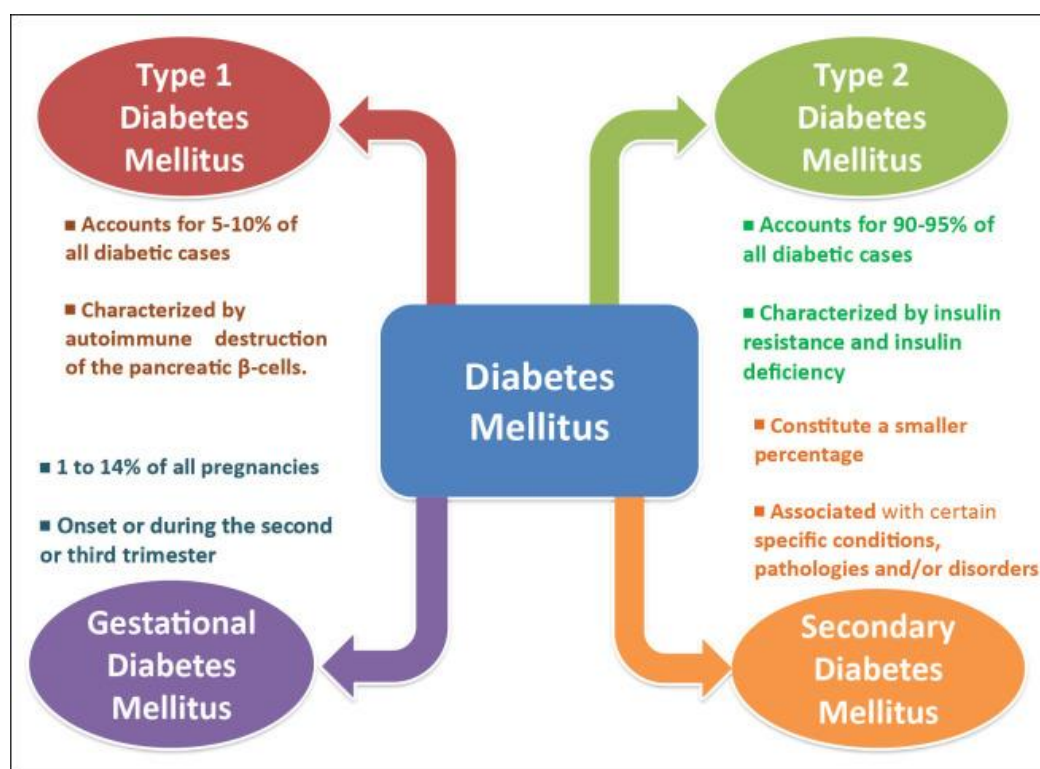
Eye-related complications result in retinopathy with progression to blindness. Kidney-associated complications lead to nephropathy and potential renal failure. Heart-related complications include hypertension and coronary heart disease. Nerve-associated complications lead to neuropathy, which can be autonomic and/or peripheral. Cardiovascular, gastrointestinal, and genitourinary (including sexual) dysfunctions are characteristic manifestations of autonomic neuropathy, whereas foot infections including ulcers requiring amputations and Charcot joint (osteoarthropathy) are often associated with long-term peripheral neuropathy. The cerebrovascular disease, peripheral arterial disease, and coronary heart disease, together termed as atherosclerotic cardiovascular disease, are of common occurrence in diabetes and constitute one of the major causes of diabetes-associated morbidity and mortality^{1, 2, 3}



1.2 CLASSIFICATION: -

DM is characterized by complex pathogenesis and varied presentation and any classification of this disorder, therefore, is arbitrary, but nevertheless useful, and is often influenced by the physiological conditions present at the time of assessment and diagnosis. The classification currently used is based on both the etiology and the pathogenesis of disease and is useful in the clinical assessment of disease and for deciding the required therapy. According to this classification, diabetes can be divided into four main types or categories: type 1 diabetes mellitus (T1DM), type 2 diabetes mellitus (T2DM), gestational diabetes mellitus (GDM), and diabetes caused or associated with certain specific conditions, pathologies, and/or disorders.

Figure 1: Types of Diabetes



1.2.1 TYPE 1 DIABETES MELLITUS (T1DM):

It also known as type 1A Diabetes Mellitus or as per the previous nomenclature as insulin-dependent diabetes mellitus (IDDM) or juvenile-onset diabetes, constitutes about 5–10% of all the cases of diabetes. It is an autoimmune disorder characterized by T-cell-mediated destruction of pancreatic β -cells, which results in insulin deficiency and ultimately hyperglycaemia. The pathogenesis of this autoimmunity, though not yet fully understood, has been found to be influenced by both genetic and environmental factors. The rate of development of this pancreatic β -cell-specific autoimmunity and the disorder itself is rapid in most of the cases as in infants and children (juvenile onset) or may be gradual as in adults (late onset).

The variability in the rate at which the immune-mediated destruction of the pancreatic β -cells occurs often defines the eventual progression of this disease. In some cases, children and adolescents, the β -cell destruction and subsequent failure occur suddenly, which can lead to diabetic ketoacidosis (DKA), often described as the first manifestation of the disease. In others, the disease progression is very slow with a mild increase in fasting blood glucose levels, which assumes a severe hyperglycaemic form with or without ketoacidosis, only in the presence of physiological stress conditions such as severe infections or onset of other disorders. In some

other cases, which include adults, β -cells may retain some degree of function to secrete only that quantity of insulin, which is only sufficient to prevent ketoacidosis for many years. However, due to progressive insulin deficiency, these individuals become insulin-dependent with the emergence of severe hyperglycaemia and subsequent ketoacidosis. Despite the variable progression of this type of diabetes, the affected individuals in the beginning or in the middle or even in the later stages of their life become severely or absolutely insulin-deficient and become dependent on insulin treatment for their survival. This severe or absolute insulin deficiency irrespective of its occurrence at any age manifests itself as low or undetectable levels of plasma C-peptide.

T1DM is an autoimmune disorder characterized by several immune markers, in particular autoantibodies. These autoantibodies are associated with the immune-mediated β -cell destruction, characteristic of this disease. The autoantibodies include glutamic acid decarboxylase autoantibodies (GADAs) such as GAD65, islet cell autoantibodies (ICAs) to β -cell cytoplasmic proteins such as autoantibodies to islet cell antigen 512 (ICA512), autoantibodies to the tyrosine phosphatases, IA-2 and IA-2 α , insulin autoantibodies (IAAs), and autoantibodies to islet-specific zinc transporter isoform 8 (ZnT8). At least one of these autoantibodies can be used for the clinical diagnosis of this disease but usually more of these immune markers have been observed in approximately 85–90% of patients with new-onset T1DM. Of these autoantibodies, GAD65 is the most important and is present in about 80% of all T1DM individuals at the time of diagnosis, followed by ICAs present in 69–90% and IA-2 α found in 54–75% of all T1DM individuals at clinical presentation.

The IAAs are important immune markers present in infants and young children who are prone to diabetes and its prevalence decreases as the age of onset of diabetes increases. The presence of IAAs in these individuals who have not been previously treated with insulin is an important indication of developing T1DM. IAAs are present in about 70% of all infants and young children at the time of diagnosis. The IAAs also play an important inhibitory role toward insulin function in patients on insulin therapy. Although not often clinically significant but nevertheless, this immune response has been observed with varying degrees of severity in at least 40% of patients on insulin treatment and therefore shows differential clinical manifestations. These autoantibodies mostly consist of polyclonal immunoglobulin G (IgG) antibodies and differ in their affinities and binding capacities toward insulin. IAAs can either be high insulin affinity/low insulin-binding capacity or low insulin affinity/high insulin-binding capacity. The low insulin affinity/high insulin-binding capacity IAAs are responsible for clinical manifestations. At high titres, the binding of these antibodies to insulin prevents or delays its action and is responsible for characteristic hyperglycaemia in the immediate postprandial period, which leads to significantly increased insulin requirements followed by unpredictable hypoglycaemic episodes (postprandial hypoglycaemia) observed later.

Latent Autoimmune Diabetes in Adults (LADA) is the most common form of adult-onset autoimmune diabetes and accounts for 2–12% of all diabetic cases in the adult population. Of the autoantibodies, GADAs are the most important and sensitive markers for LADA followed by ICAs. However, the IAAs, autoantibodies to the tyrosine phosphatases—IA-2 and IA-2 α , and autoantibodies to islet-specific zinc transporter isoform 8 (ZnT8) which are observed in patients with juvenile- or young-onset T1DM are detectable in only a small number of cases in LADA. In a study on LADA (Action LADA study), GADAs were the only diabetes-specific autoantibodies detected in 68.6% of total screened subjects whereas IA-2 α and ZnT8A represented the single-type autoantibody detections in 5% and 2.3% of all the screened study subjects. In the same study, more than one type of autoantibody was detected in 24.1% of study subjects. LADA is also sometimes referred to as T2DM with ICAs.

Besides the characteristic immune-mediated pancreatic β -cell destruction, several other autoimmune disorders including myasthenia gravis, Addison's disease (primary adrenal insufficiency), celiac sprue (celiac disease), pernicious anaemia, vitiligo, Hashimoto's

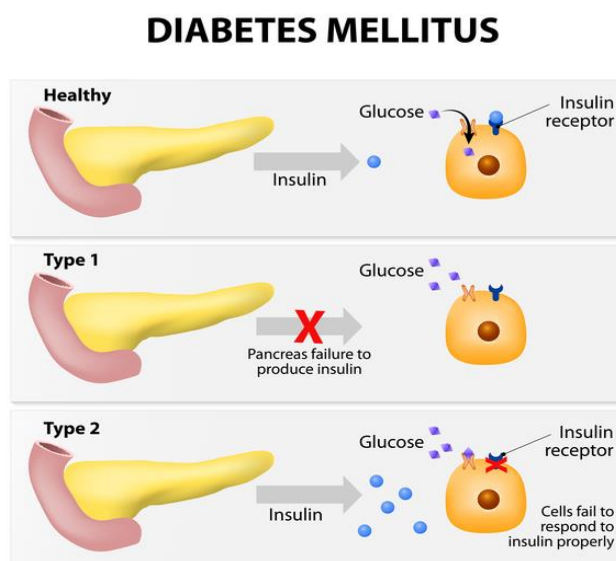
thyroiditis, Graves' disease, dermatomyositis, autoimmune gastritis, and autoimmune hepatitis have been observed with an increased incidence in patients with T1DM. The autoimmune nature of this disease and its association with other autoimmune conditions mainly stem from the strong association of this disorder with human leukocyte antigen (HLA), its linkage to the DQA and DQB genes, and its direct influence by DRB genes. All of these are hotspot gene regions associated with immune response including autoimmunity. The genome-wide association studies have shown a strong association of this disease with HLA-DR3 and HLA-DR4 haplotypes and the exclusive association of DR4-DQB1*0302 haplotype with the autoimmune destruction of the β -cells. As with other diseases, these various HLA haplotypes can increase or decrease the susceptibility toward the T1DM. However, several non-HLA genes or gene regions also influence the susceptibility to this disease. The most prominent among them is the insulin gene (INS) region, designated as IDDM2 located on chromosome 11p5.5. The variable number of tandem repeats in the promoter region of this gene region has been observed to influence the susceptibility toward this disease. Besides IDDM2, CTLA-4, PTPN-22, and CD25 are other non-HLA genes associated with the disease.] The patients with this type of diabetes can be but are rarely obese at the time of assessment and diagnosis.

1.2.1.1 IDIOPATHIC DIABETES:

Idiopathic diabetes, also referred to as ICA-negative or type 1B diabetes, includes the forms of diabetes which are similar to T1DM in presentation but characterized by variable no immune β -cell dysfunction without any observed HLA association unlike T1DM and hence, sometimes it is also described as a separate type of DM. This type of diabetes exhibits a strong pattern of inheritance and has been observed in only a minority of patients, of Asian or African-Caribbean origin. The etiology of idiopathic diabetes remains largely unknown.

The disease is characterized by severe but varying degrees of insulin deficiency (insulinopenia) which can exhibit episodic patterns concomitant with varying degrees of severity and episodic DKA. These patients, therefore, may require insulin replacement therapy initially but the need for the therapy may not be absolute and may vary in accordance with the episodic patterns of insulinopenia and ketoacidosis characteristic of these forms of T1DM.⁴⁻¹⁹

Figure 2: Insulin Binding to Its Receptor in the Normal and Diabetes Type 1 and Type 2



1.2.2 TYPE2 DIABETES MELLITUS (T2DM):-²⁰⁻²⁴

Impaired insulin secretion and insulin resistance contribute more or less jointly to the development of pathophysiological conditions. Impaired insulin secretion Impaired insulin secretion is a decrease in glucose responsiveness, which is observed before the clinical onset of disease. More specifically, impaired glucose tolerance (IGT) is induced by a decrease in glucose-responsive early-phase insulin secretion, and a decrease in additional insulin secretion after meals causes postprandial hyperglycemia. An oral glucose tolerance test (OGTT) in IGT

cases generally indicates an over-response in Western and Hispanic individuals, who have markedly high insulin resistance. On the other hand, Japanese patients often respond to this test with decreased insulin secretion. Even when an over-response is seen in persons with obesity or other factors, they show a decrease in early-phase secretory response. The decrease in early-phase secretion is an essential part of this disease, and is extremely important as a basic pathophysiological change during the onset of disease in all ethnic groups.³ Impaired insulin secretion is generally progressive, and its progression involves glucose toxicity and lipotoxicity. When untreated, these are known to cause a decrease in pancreatic cell mass in animal experiments. The progression of the impairment of pancreatic cell function greatly affects the long-term control of blood glucose. While patients in early stages after disease onset chiefly show an increase in postprandial blood glucose as a result of increased insulin resistance and decreased early-phase secretion, the progression of the deterioration of pancreatic cell function subsequently causes permanent elevation of blood glucose. Insulin resistance Insulin resistance is a condition in which insulin in the body does not exert sufficient action proportional to its blood concentration. The impairment of insulin action in major target organs such as liver and muscles is a common pathophysiological feature of type 2 diabetes. Insulin resistance develops and expands prior to disease onset. The investigation into the molecular mechanism for insulin action has clarified how insulin resistance is related to genetic factors and environmental factors (hyperglycemia, free fatty acids, inflammatory mechanism, etc.). Known genetic factors, include not only insulin receptor and insulin receptor substrate (IRS)-1 gene polymorphisms that directly affect insulin signals but also polymorphisms of thrifty genes such as the 3 adrenergic receptor gene and the uncoupling protein (UCP) gene, associated with visceral obesity and promote insulin resistance. Glucolipotoxicity and inflammatory mediators are also important as the mechanisms for impaired insulin secretion and insulin signaling impairment. Recent attention has focused on the involvement of adipocyte-derived bioactive substances (adipokines) in insulin resistance. While TNF-, leptin, resistin, and free fatty acids act to increase resistance, adiponectin improves resistance. Clinical tests to assess the extent of insulin resistance include homeostasis model assessment for insulin resistance (HOMA-IR), insulin sensitivity test (loading test), steady-state plasma glucose (SSPG), minimal model analysis, and insulin.

Type 2 diabetes mellitus is a heterogeneous disorder with varying prevalence among different ethnic groups. In the United States the populations most affected are native Americans, particularly in the desert Southwest, Hispanic-Americans, and Asian-Americans. The pathophysiology of type 2 diabetes mellitus is characterized by peripheral insulin resistance, impaired regulation of hepatic glucose production, and declining β -cell function, eventually leading to β -cell failure.

The primary events are believed to be an initial deficit in insulin secretion and, in many patients, relative insulin deficiency in association with peripheral insulin resistance.

1.2.2.1 THE β -CELL

β -Cell dysfunction is initially characterized by an impairment in the first phase of insulin secretion during glucose stimulation and may antedate the onset of glucose intolerance in type 2 diabetes.

Initiation of the insulin response depends upon the transmembranous transport of glucose and coupling of glucose to the glucose sensor. The glucose/glucose sensor complex then induces an increase in glucokinase by stabilizing the protein and impairing its degradation. The induction of glucokinase serves as the first step in linking intermediary metabolism with the insulin secretory apparatus. Glucose transport in β -cells of type 2 diabetes patients appears to be greatly reduced, thus shifting the control point for insulin secretion from glucokinase to the glucose transport system. This defect is improved by the sulfonylureas.

Later in the course of the disease, the second phase release of newly synthesized insulin is impaired, an effect that can be reversed, in part at least in some patients, by restoring strict control of glycemia. This secondary phenomenon, termed desensitization or β -cell glucotoxicity, is the result of a paradoxical inhibitory effect of glucose upon insulin release and may be attributable to the accumulation of glycogen within the β -cell as a result of sustained hyperglycemia. Other candidates that have been proposed are sorbital accumulation in the β -cell or the nonenzymatic glycation of β -cell proteins.

Other defects in β -cell function in type 2 diabetes mellitus include defective glucose potentiation in response to nonglucose insulin secretagogues, asynchronous insulin release, and a decreased conversion of proinsulin to insulin.

An impairment in first phase insulin secretion may serve as a marker of risk for type 2 diabetes mellitus in family members of individuals with type 2 diabetes mellitus and may be seen in patients with prior gestational diabetes. However, impaired first phase insulin secretion alone will not cause impaired glucose tolerance.

Autoimmune destruction of pancreatic β -cells may be a factor in a small subset of type 2 diabetic patients and has been termed the syndrome of latent autoimmune diabetes in adults. This group may represent as many as 10% of Scandinavian patients with type 2 diabetes and has been identified in the recent United Kingdom study, but has not been well characterized in other populations.

Glucokinase is absent within the β -cell in some families with maturity-onset diabetes of young. However, deficiencies of glucokinase have not been found in other forms of type 2 diabetes.

In summary, the delay in the first phase of insulin secretion, although of some diagnostic import, does not appear to act independently in the pathogenesis of type 2 diabetes. In some early-onset patients with type 2 diabetes (perhaps as many as 20%), there may be a deficiency in insulin secretion that may or may not be due to autoimmune destruction of the β -cell and is not due to a deficiency in the glucokinase gene. In the great majority of patients with type 2 diabetes ($\pm 80\%$), the delay in immediate insulin response is accompanied by a secondary hypersecretory phase of insulin release as a result of either an inherited or acquired defect within the β -cell or a compensatory response to peripheral insulin resistance. Over a prolonged period of time, perhaps years, insulin secretion gradually declines, possibly as a result of intraislet accumulation of glucose intermediary metabolites. In view of the decline in β -cell mass, sulfonylureas appear to serve a diminishing role in the long term management of type 2 diabetes. Unanswered is whether amelioration of insulin resistance with earlier detection or newer insulin-sensitizing drugs will retard the progression of β -cell failure, obviating or delaying the need for insulin therapy.

1.2.2.2 INSULIN RESISTANCE

Emanating from the prismatic demonstration by Yalow and Berson of the presence of hyperinsulinism in type 2 diabetes, insulin resistance has been considered to play an integral role in the pathogenesis of the disease. Recent critical reviews, however, have questioned the primacy, specificity, and contribution of insulin resistance to the disease state. As chronic hyperinsulinemia inhibits both insulin secretion and action, and hyperglycemia can impair both the insulin secretory response to glucose as well as cellular insulin sensitivity, the precise

relation between glucose and insulin level as a surrogate measure of insulin resistance has been questioned. Lean type 2 diabetic patients over 65 yr of age have been found to be as insulin sensitive as their age-matched nondiabetic controls . Moreover, in the majority of type 2 diabetic patients who are insulin resistant, obesity is almost invariably present . As obesity or an increase in intraabdominal adipose tissue is associated with insulin resistance in the absence of diabetes, it is believed by some that insulin resistance in type 2 diabetes is entirely due to the coexistence of increased adiposity .Additionally, insulin resistance is found in hypertension, hyperlipidemia, and ischemic heart disease, entities commonly found in association with diabetes , again raising the question as to whether insulin resistance results from different pathogenetic disease processes or is unique to the presence of type 2 diabetes.

Prospective studies have demonstrated the presence of either insulin deficiency or insulin resistance before the onset of type 2 diabetes . Two studies have reported the presence of insulin resistance in nondiabetic relatives of diabetic patients at a time when their glucose tolerance was still normal . In addition, first degree relatives of patients with type 2 diabetes have been found to have impaired insulin action upon skeletal muscle glycogen synthesis due to both decreased stimulation of tyrosine kinase activity of the insulin receptor and reduced glycogen synthase activity . Other studies in this high risk group have failed to demonstrate insulin resistance, and in the same group, impaired early phase insulin release and loss of normal oscillatory pattern of insulin release have been described . Based upon these divergent studies, it is still impossible to dissociate insulin resistance from insulin deficiency in the pathogenesis of type 2 diabetes. However, both entities unequivocally contribute to the fully established disease.

1.2.2.3 THE LIVER

The ability of insulin to suppress hepatic glucose production both in the fasting state and postprandially is normal in first degree relatives of type 2 diabetic patients . It is the increase in the rate of postprandial glucose production that heralds the evolution of IGT. Eventually, both fasting and postprandial glucose production increase as type 2 diabetes progresses. Hepatic insulin resistance is characterized by a marked decrease in glucokinase activity and a catalytic increased conversion of substrates to glucose despite the presence of insulin . Thus, the liver in type 2 diabetes is programmed to both overproduce and underuse glucose. The elevated free fatty acid levels found in type 2 diabetes may also play a role in increased hepatic glucose production . In addition, recent evidence suggests an important role for the kidney in glucose production via gluconeogenesis, which is unrestrained in the presence of type 2 diabetes.

Figure 3: Mechanism of Type 2 Diabetes

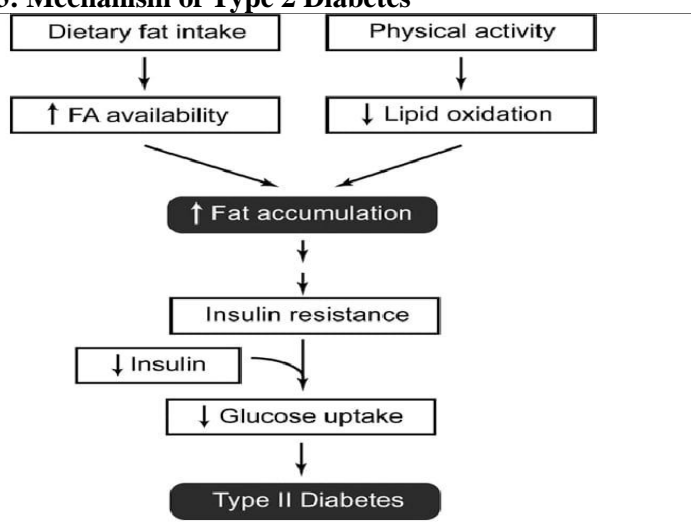
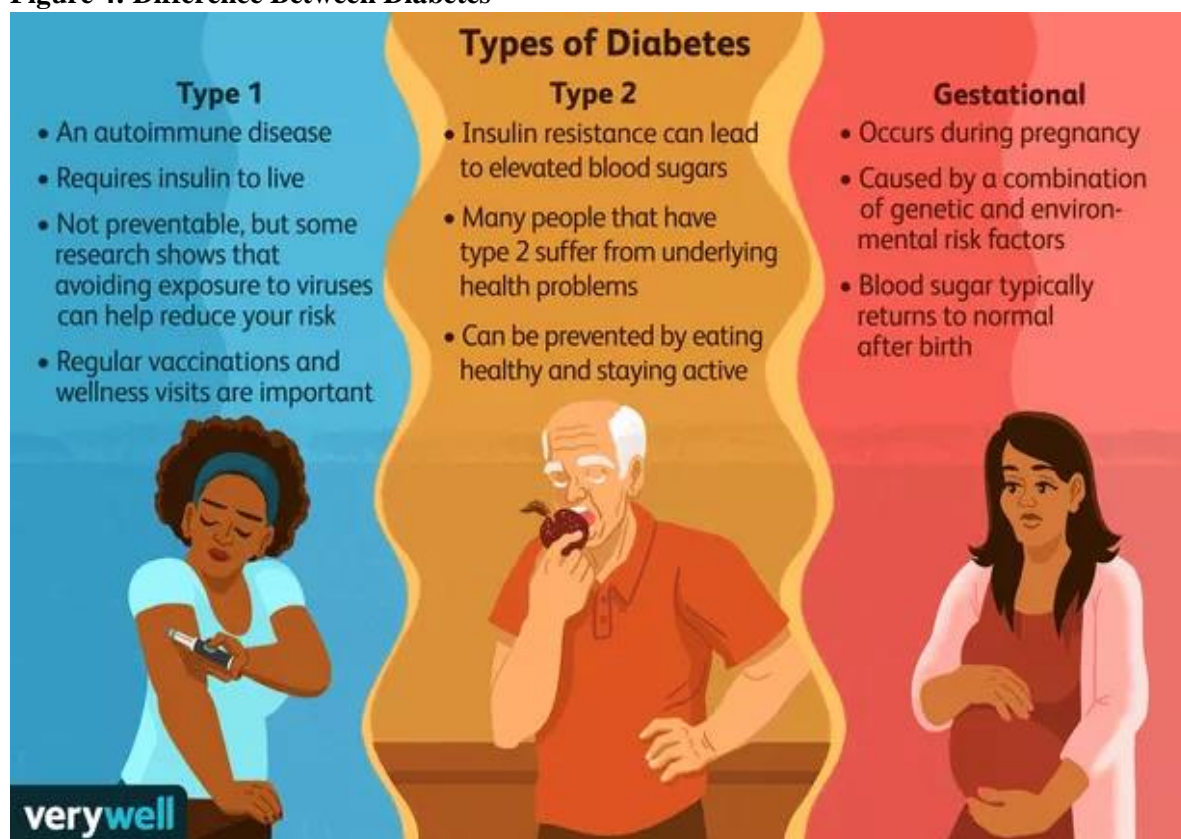


Figure 4: Difference Between Diabetes



1.3 ORAL DIABETES MEDICATIONS

1.3.1 WHAT ARE ORAL DIABETES MEDICATIONS AND HOW DO THEY WORK?

Insulin is a hormone produced by cells in the pancreas called beta cells. Insulin helps the body use blood glucose (a type of sugar) for energy. People with type 2 diabetes do not make enough insulin and/or their bodies do not respond well to it, leading to elevated blood sugar levels. Oral (non-insulin) diabetes medications bring blood sugar levels into the normal range in a variety of ways.

1.3.2 ORAL MEDICATION AFFECTED IN DIFFERENT WAYS

1.3.2.1 DRUG WHICH DECREASE THE GLUCOSE LEVEL

Biguanides- Metformin

Thiazolidinedione- Rosiglitazone, Pioglitazone

Both work by decreasing the production of glucose by the liver and by making the muscle more sensitive to insulin.

1.3.2.2 DRUGS THAT INCREASE INSULIN PRODUCTION

The earliest oral diabetes drugs were the sulfonylureas. These work by stimulating the pancreas to produce more insulin.

The oldest of these drugs still on the market is chlorpropamide (Diabinese), which has been used for more than 50 years.

The second-generation sulfonylureas are taken once or twice a day. They include glipizide (Glucotrol, Glucotrol XL), glyburide (Micronase, DiaBeta, Glynase), and glimepiride (Amaryl).

Meglitinides also stimulate the release of more insulin from beta cells.

Repaginate (Prandin) and nateglinide (Starlix) are taken before every three meals.

1.3.2.3. MEDICATIONS THAT SLOW THE BREAKDOWN OF CARBOHYDRATES

1. Alpha-glycosidase inhibitors approach the blood glucose issue in a different way. By inhibiting the breakdown of starches in the intestine, these medications slow the rise in blood sugar normally seen after a meal. Examples include acarbose (Precose) and miglitol (Glyset).

Side effect due alpha glycosidase inhibitors:

Hypoglycemia (low blood sugar), skin rash, Sensitivity to sunlight, Upset stomach, Weight gain,

2. Thiazolidinedione can increase the risk of heart failure and should not be used in patients with symptoms of heart failure. Liver enzymes should be checked regularly with use. Other side effects include weight gain, fatigue, swelling of the legs or ankles, and increased risk for fractures in female patients. Avandia may have potential increased risk for heart attack.

3. The DPP-4 inhibitor sitagliptin (Januvia) may cause serious allergic reactions, sore throat, upper respiratory infection, and headache.

4. Pramlintide (with insulin) may cause gastrointestinal problems (nausea, vomiting, abdominal pain, and anorexia), slight weight loss, headache, fatigue, dizziness, coughing, sore throat, and skin reactions at the injection site.

1.3.3 WHAT ARE THE DRUG INTERACTION WITH NON-INSULIN DIABETES MEDICATION?

Many drugs can affect your blood sugar levels, affecting in turn how well your diabetes medication works. Make sure your doctor is aware of all other drugs and supplement you are taking to ensure proper dosing of diabetes medicine.

There is much overlap of medication that may interact with oral diabetes drug. These include are not limited to some:

- Heart medication
- Decongestants
- Antibiotics
- Thiazides
- Steroid
- Thyroid drugs
- Estrogen
- Oral contraceptive
- Seizures medication

- Psychiatric medication
- Cholesterol medication

Digestive enzyme medication (such as amylase, and pancreatic) may reduce the effectiveness of alpha-glycosidase inhibitors and should not be taken at the same time.²⁵

1.3.4 ORAL DRUGS:²⁶

Oral drugs (by mouth) help to control blood sugar (Glucose) Level.

This drug is used when insulin is produced in the body. Like in T2DM

This medicine prescribed with regular exercise and changes in diet.

They may use in combinations with each other or with insulin to achieve the best glucose control.

TABLE 1: LIST OF ORAL DRUGS USED FOR DIABETES

<i>Class of drug</i>	<i>Examples</i>
Sulfonylureas	Glipizide Glyburide Tolbutamide Glibenclamide Action; causing more release of insulin from pancreas.
Thiazolidinedione's	pioglitazone Rosiglitazone Action; This medication improves the way of insulin work in the body by allowing more glucose to enter to muscle, fat, liver
Alpha – glycosidase inhibitors	Acarbose Miglitol Voglibose Action ;These are lower the blood glucose level by delayed the breakdown the carbohydrate and reduce the glucose absorption in the small intestine and block certain enzyme in order to slow down the digestion of starch
Meglitinides	repaglinide Neteglinide Action; These release the more insulin from pancreas.
Dipeptidyl peptidase 4 inhibitor	Sitagliptin Saxagliptin Linagliptin Action; help pancreas to release more insulin after meal also release the glucose by liver.
Sodium glucose co-transporter 2 inhibitor	Canagliflozin Dapagliflozin Empagliflozin Action; the drug work on kidney to remove extra sugar from the body.
Dopamine agonist	Bromocriptine(cyclone) Action; lower the release of glucose by liver.

TABLE: 2 IMPORT FEATURE OF ORAL DIABETES (SULFONYLUREA)

Drug	Preparation	Plasma $t_{1/2}$	Duration of action	Daily dose	No. of dose / day	Remarks
Tolbutamide	Rastinon ,0.5g tab.	6	6-8	0.5-3	2-3	Short acting ,Weaker ,Safe in elder
Glyburide	Daonil, Euglucon, Betanase, 2.5,5 mg tab.	2-4	24	2.5-15 mg	1-2	Potent but slow acting ,
Glipizide	Glynase , Glide , Minidiab 5 mg tab	2-5	12	5-20 mg	1-2	Fast and slower acting , weight gain is less

1.4 SULFONYLUREA (SU)

All drugs in this class have the same mechanism. Lowering blood glucose level.

1.4.1 Mode of action:

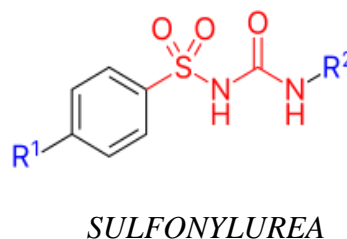
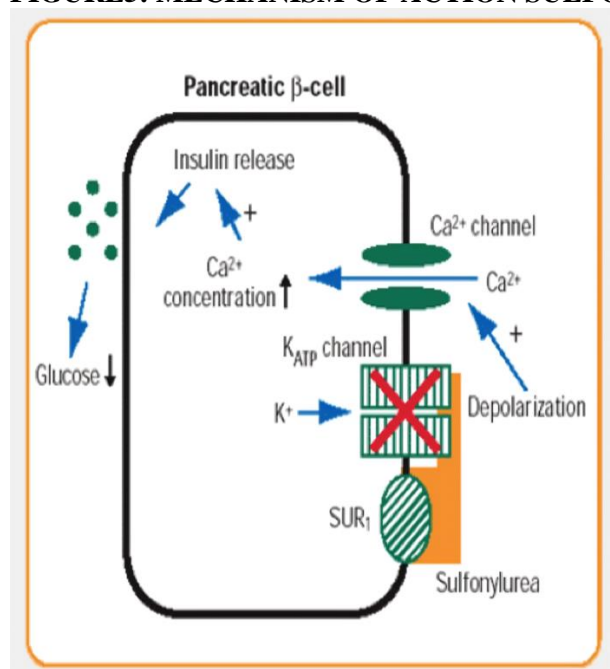
Sulfonylurea binds to a specific Sulfonylurea receptor located in pancreatic B –cell membrane and release of insulin.

The rate of insulin secretion at any glucose concentration is increased.

In T2DM the kinetic of insulin release in response to glucose or meals is delayed and subdued.

The SU primarily augment the 2nd phase insulin secretion with little effect on 1st phase. They do not cause hypoglycemia.

FIGURE5: MECHANISM OF ACTION SULFONYLUREA



1.4.2 PHARMACOKINETICS:

All SU are absorbed orally and 90% or more can bind to plasma protein. They are primarily metabolized and may produce active metabolite. The metabolites are excreted in urea.

1.4.3 INTERACTIONS:

Inhibits metabolism or excretion with ketoconazole, acute alcohol intake

Synergies with or prolong pharmacodynamics action: propranolol, sympatholytic, antihypertensive, lithium.

1.4.4 ADVERSE EFFECTS:

1. Hypoglycemia: It is commonest problem may occasionally be severe and rarely fatal. Most common in elderly, liver and kidney.

2. Nonspecific side effects: Gain body weight, Nausea, Vomiting, Flatulence, Headache.

3. Hypersensitivity: Rashes,

 Photosensitivity

 Leukopenia

 Flushing.²⁷

1.5 CHANGE IN LIFE STYLE OF DIABETIC PATIENT

Dietary intake and physical exercise are the two main determinants of energy balance and they are considered as abasicbase in the treatment of patients with diabetes. Adequate rest is also very important for maintaining energy levels and well-being, and all patients should be advised to sleep approximately 7 hour per night evidence supports an association of 6 to 9hour of sleep per night with are reduction in cardio metabolic risk factor whereas sleep deprivation aggravates insulin resistance, hypertension, hyperglycemia, and dyslipidemia.

Although the pharmacological options are each time more extensive and they offer more therapeutics possibilities especially in the T2DM, the contravention in the life style are essentials in the approach of these patients and they are needed to get the therapeutics goals.²⁸

1.6 CONCLUSION:

Anti-hyperglycemic agents have been used for the treatment of type 2 diabetes mellitus for the treatment since many years. Anti-hyperglycemic agent like Metformin and Sulfonylurea were administered for more than 50 years. After this agents other anti – hyperglycemic such as Glinides, Thiazolidines, Alpha – glycosidase inhibitors, Dipeptidyl peptidase 4 inhibitors and Sodium glucose co-transporter 2 inhibitor were introduced. Metformin used for monotherapy unless it shows contraindicated and unwanted side effect. Sulfonylurea induce hypoglycemic is losing ground to various new agents but the combination of sulfonylurea with Metformin is cheap and effective. The cardiovascular hazards of several agent need to concern with physician and legislating bodies. For the dual or triple therapy the physician need to keep in mind the health status of the patient, medication side effect, cost, and patient preference. This review addresses the merits and demerits of a range of anti-hyperglycemic agents and their application in monotherapy and combination therapy.

1.7 REFERENCES:

1. American Diabetes Association. Micro vascular complications and foot care: Standards of medical care in diabetes—2018. *Diabetes Care*. 2018; 41: S105–18.
2. American Diabetes Association. Cardiovascular disease and risk management: Standards of medical care in diabetes—2018. *Diabetes Care*. 2018; 41: S86–104.
3. Rawshani A, Franzén S, Eliasson B, Svensson AM, Miftaraj M, et al. Mortality and cardiovascular disease in type 1 and type 2 diabetes. *N Engl J Med*. 2017; 376:1407–18.]
4. American Diabetes Association. Cardiovascular disease and risk management: Standards of medical care in diabetes—2018. *Diabetes Care*. 2018; 41: S86–104.
5. Rashaan A, Rawshani A, Franzén S, Eliasson B, Svensson AM, Miftaraj M, et al. Mortality and cardiovascular disease in type 1 and type 2 diabetes. *N Engl J Med*. 2017; 376:1407–18.
6. Blas E, Koru A, editors. *Equity, Social Determinants and Public Health Programmes*. Geneva, Switzerland: World Health Organization; 2010. Diabetes: Equity and social determinants.
7. Saeedi P, Peterson I, Salpea P, Malinda B, Karuranga S, Unwin N, et al. IDF Diabetes Atlas Committee. Global and regional diabetes prevalence estimates for 2019 and projections for 2030 and 2045: Results from the international diabetes federation diabetes atlas. *Diabetes Res Clin Pract*. (9th edition) 2019; 157:107843.
8. International Diabetes Federation. *IDF Diabetes Atlas*. 9th ed. Brussels, Belgium: International Diabetes Federation; 2019.
9. American Diabetes Association. Classification and diagnosis of diabetes: Standards of medical care in diabetes—2018. *Diabetes Care*. 2018; 41: S13–27.
10. Knap M, Islander H. Autoimmune mechanisms in type 1 diabetes. *Autoimmune Rev*. 2008; 7:550–7Kahaly GJ, Hansen MP. Type 1 diabetes associated autoimmunity. *Autoimmune Rev*. 2016; 15:644–8.
11. Tallinn CE, Barker JM. Autoantibodies in type 1 diabetes. *Autoimmunity*. 2008; 41:11–8.
12. Lactea JT, Knap M, Paul R, Antonin J, Salma J. Severe antibody-mediated human insulin resistance: Successful treatment with the insulin analog lispro. A case report. *Diabetes Care*. 1997; 20:71–3.
13. Matsu Yoshi A, Shimmed S, Tsuruzoe K, Taketa K, Chirioka T, Sakamoto F, et al. A case of slowly progressive type 1 diabetes with unstable glycemic control caused by unusual insulin antibody and successfully treated with steroid therapy. *Diabetes Res Clin Pract*. 2006; 72:238–43.
14. Zimmet PZ, Tuomi T, Mackay IR, Rowley MJ, Knowles W, Cohen M, et al. Latent autoimmune diabetes mellitus in adults [LADA]: The role of antibodies to glutamic acid decarboxylase in diagnosis and prediction of insulin dependency. *Diabetes Med*. 1994; 11:299–303.
15. Naik RG, Palmer JP. Latent autoimmune diabetes in adults (LADA) *Rev Endocr Metab Disord*. 2003; 4:233–41.
16. Lampasona V, Petrone A, Tiberti C, Capizzi M, Spoletini M, di Pietro S, et al. Non-Insulin Requiring Autoimmune Diabetes (NIRAD) Study Group. Zinc transporter 8 antibodies complement GAD and IA-2 antibodies in the identification and characterization of adult-onset autoimmune diabetes: Non-insulin requiring autoimmune diabetes (NIRAD) 4. *Diabetes Care*. 2010; 33:104–8.
17. Hawa MI, Kolb H, Schloot N, Beyan H, Paschou SA, Buzzetti R, et al. Action LADA Consortium. Adult-onset autoimmune diabetes in Europe is prevalent with a broad clinical phenotype: Action LADA 7. *Diabetes Care*. 2013; 36:908–13.
18. Hughes JW, Riddlesworth TD, DiMeglio LA, Miller KM, Rickels MR, McGill JB T1D Exchange Clinic Network. Autoimmune diseases in children and adults with type 1 diabetes from the T1D exchange clinic registry. *J Clin Endocrinol Metab*. 2016; 101:4931–7
19. Tirol TM, Armstrong TK, McFann K, Yu L, Rowers MJ, Klingensmith GJ, et al. Additional autoimmune disease found in 33% of patients at type 1 diabetes onset. *Diabetes Care*. 2011; 34:1211–3.
20. Dr. Stanley L. Robbins (1915-2003) and Dr. Ramzi S. Cortan (1932-2000) ,Robbins & Cotran {7th EDITION} PATHOPHYSIOLOGY BASIS OF DISEASES
21. YALOW RS, Berson SA. 1960 Immunoassay of endogenous plasma insulin in man. *J clin invest*.
22. Kissebah A, Freedman D, Peiris A. 1989 health risk of obesity. *Med clin north Am*.
23. Charles MAE Tibet N, et al. 1997 the role of non-esterified fatty acids in the deterioration of glucose tolerance in Caucasian subjects: results of the Paris prospective study.

24. [https://www.verywellhealth.com/thmb/UjmhNb6BL2MD3xMEBM6iad9bGoo=/1500x1000/filters:no_upscale\(\):max_bytes\(150000\):strip_icc\(\)/is-diabetes-genetic-5112506_final-04c9aa844032499fbc37bc36df78b38.jpg](https://www.verywellhealth.com/thmb/UjmhNb6BL2MD3xMEBM6iad9bGoo=/1500x1000/filters:no_upscale():max_bytes(150000):strip_icc()/is-diabetes-genetic-5112506_final-04c9aa844032499fbc37bc36df78b38.jpg)
25. https://www.rxlist.com/oral_diabetes_medications/drugs-condition.htm
26. <https://www.google.com/url?sa=t&source=web&rct=j&url=https://my.clevelandclinic.org/health/articles/12070-oral-diabetes-medications&ved=2ahUKEwixwpajmPT5AhXmx4sBHbDjD38QFnoECA8QAQ&usg=AOvVaw0zWSXphjuEqQCp8FCpMVxa>
27. : Essential of pharmacology, KDT, Jaypee brother's medical publishers, Eight edition page no 294-296.
28. <https://doi.org/10.4239/wjd.v7.i17.354>

PCP453

NANOPARTICLES HOLD PROMISE IN COVID DIAGNOSIS, VACCINE DEVELOPMENT AND TREATMENT

AP0502 Ami Sureshbhai Gadhiya Gtu Student, L.M. College Of Pharmacy ami.gadhiya64@gmail.com	AP0498 Dr. Jayant B. Dave Faculty L.M. College Of Pharmacy jayant.dave@lmcp.ac.in	AP0501 Jaitri Nayanbhai Mehta Gtu Student, L.M. College Of Pharmacy jaitrimehta12@gmail.com
--	--	--

Abstract:

COVID-19 has become a major cause of global mortality and has driven massive health and economic disruptions. The pandemic also delivered a serious message to those working in the field of technology R&D to develop suitable diagnostic and therapeutic tools. Conventional technology and current advances in science were coupled to do this. Nanotechnology also opened up open up new study areas. Numerous medical applications, including drug administration via nebulized inhalation, antimicrobial and antiviral therapy utilized nanoparticles (NPs) significantly. Nanoparticle-based detection techniques have been used in an effort to build detection assays that are both sensitive and swift, as against standard methods of virus detection that takes several days to effectively confirm infection. The surface of the nanoparticle is altered with biomolecules derived from the virus. Au-NPs, which are the most nano-porous metal nanoparticles are used for coronavirus detection. Mass global vaccination has offered the most efficient pathway toward ending the pandemic. The development and deployment of COVID-19 vaccines by Pfizer and Moderna encompassing mRNA and Novavax using protein micelle NP has worked wonders. Going forward, nanoparticle-based vaccines which deliver SARS-CoV-2 antigens will play an increasing role in extending or improving vaccination outcomes against COVID-19 and other ailments. Nanoparticles are used to develop different therapeutics to check the entry and growth of viruses and to deliver antiviral drugs and drugs affecting the immune system like Tocilizumab and dexamethasone. Metal nanoparticles that can be used as antivirals include nano silver colloids, carbon nanotubes and graphene oxide. This Review paper outlines the function of NPs in detection & diagnosis, vaccine development, and treatment of COVID-19.

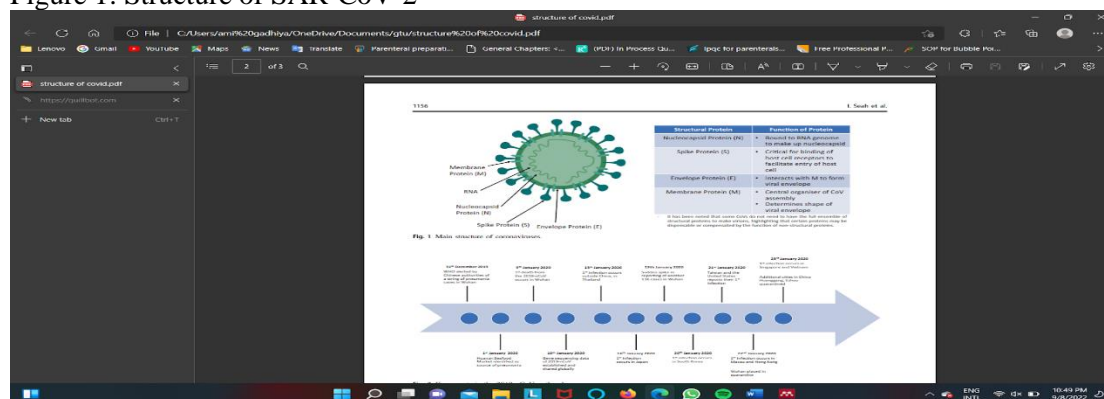
Keywords: Coronavirus, COVID-19, SARS-CoV-2, Diagnostics, Medications, vaccines, Nanoparticles, Metal/Lipid nanoparticles, Treatment.

1. INTRODUCTION:

COVID-19 epidemic has developed into one of the most serious medical emergencies that could endanger public health globally by causing thousands of hospitalizations and fatalities, raising concerns globally and necessitating extreme precaution (Mohammed & Shaaban, 2022). The four categories of the Coronavirus (CoVs) family are alpha, beta, gamma, and delta, each of which has a single-stranded positive-sense RNA genome (Dheyab et al., 2021). Transmembrane glycoprotein spike proteins adorn the membrane envelopes that house the viral DNA. When observed under a transmission electron microscope (TEM), the protein spikes on the surface coronavirus have a club-like form.

The COVID-19 pandemic's causal agent is a member of the beta class (Chauhan et al., 2020). Spike surface glycoprotein (S), small envelope protein (E), matrix protein (M), and nucleocapsid protein (N) are the four structural proteins of SARS-CoV-2 (Seah et al., 2020). The viral spike (S) protein is a key target for vaccine development because it enables viral attachment and penetration into host cells. The receptor binding domain (RBD) of S, which is present as a homo-trimer on the virion surface, allows the virus to recognize the angiotensin-converting enzyme 2 (ACE2) on the surface of the host cell.

Figure 1: Structure of SAR-CoV-2



Source:(Seah et al., 2020)

The main receptor for SARS-CoV-2 entrance into host cells is angiotensin-converting enzyme 2 (ACE2)(Chauhan et al., 2020). The primary characteristics in humans are a minor gastrointestinal or respiratory discomfort(Mohammed & Shaaban, 2022). Multiple complications can occur in vital organs such the heart, liver, kidney, gastrointestinal tract, and central nervous system.(Chauhan et al., 2020).

Nanotechnology appears as a useful tool by playing a significant role in anticipating, diagnosing, & optimizing COVID-19 preventive processes. Nanotechnology can help in targeting viral molecules on bodily fluids, including blood, nasal, and throat samples. One can adorn particular viral receptor on magnetic nanoparticles' surface. In light of the fact that viruses are nanoparticles, it is possible to build the use of virus-like entities for targeted medication delivery and gene editing.(Campos et al., 2020). Protein cargos can be effectively encapsulated and delivered using a variety of nanomaterials, including those made of inorganic, lipid, and polymer-based nanoparticles.(Yu et al., 2016).By using nanoparticle-based carriers, nanomedicine can solve issues such cargo degradation, lack of bioavailability, and quick clearance with relation to delivering medications, genes, and proteins to the patient's body.(Rashidzadeh et al., 2021)

Nanomaterials have the power to alter the pharmacokinetic characteristics of the medication that is encapsulated and, through a controlled release mechanism, can lower the necessary drug concentration. Additionally, by attaching a particular ligand to the surface of the nanoparticle holding the medicine to recognize the biomolecules of the target tissue/organ, the antiviral effects of the produced nano-drug can be enhanced. Due to their ability to produce efficient interactions between the analyte and the sensor, nanomaterials produce a significant surface-to-volume ratio that enables rapid and precise virus detection. Nanotechnology can help in vaccine development as well. The COVID19 vaccines that are now showing the most promising treatment are made of mRNA from SARS-CoV-2 surface proteins and enclosed in nanoliposomes with particular physicochemical features.(Campos et al., 2020). Lipid-based nanostructures have been suggested as a possible method for delivering mRNAs or siRNAs to produce viral proteins, administer vaccinations, or inactivate viral target genes. These unique nanoparticle preparations outperformed more conventional vaccination strategies in terms of efficacy and development speed. In contrast, the initial LNP formulation contained anti-sense RNA oligonucleotides. Longer but more fragile mRNA cargoes are now more widely used thanks to recent advancements in lipid formula, nucleic acid chemistry, and a worldwide pandemic(Huang et al., 2021). Alternatives to commonly employed chemical disinfectants with distinct antiviral activity, longevity, and efficacy at low concentrations include metal nanoparticles including silver, copper, and titanium dioxide(Sportelli et al., 2020). These photo-dynamic and photo-thermal metal nanoparticles can be employed for COVID-19. It has been proven that a number of NPs are extremely useful for coronavirus detection, inhibition, and immunization(Jeong-Eun Park, Keunsuk Kim, Yoonjae Jung, Jae-Ho Kim, 2016). In the prevention stage, we firmly believe that nanotechnology-enabled extremely effective antiviral

disinfectants and contagion-safe PPE (including respirators, medical gowns, overshoes, hair cups, etc.) can be considered the most effective means to stop viruses from spreading. This Review explains how we might improve upon the NP-based tactics employed against viruses belonging to the Coronavirus family in order to provide diagnostics, treatments, and vaccines to combat SARS-CoV-2.(Sportelli et al., 2020).

2. ROLE OF NANOTECHNOLOGY IN VIRUS DETECTION AND DIAGNOSIS:

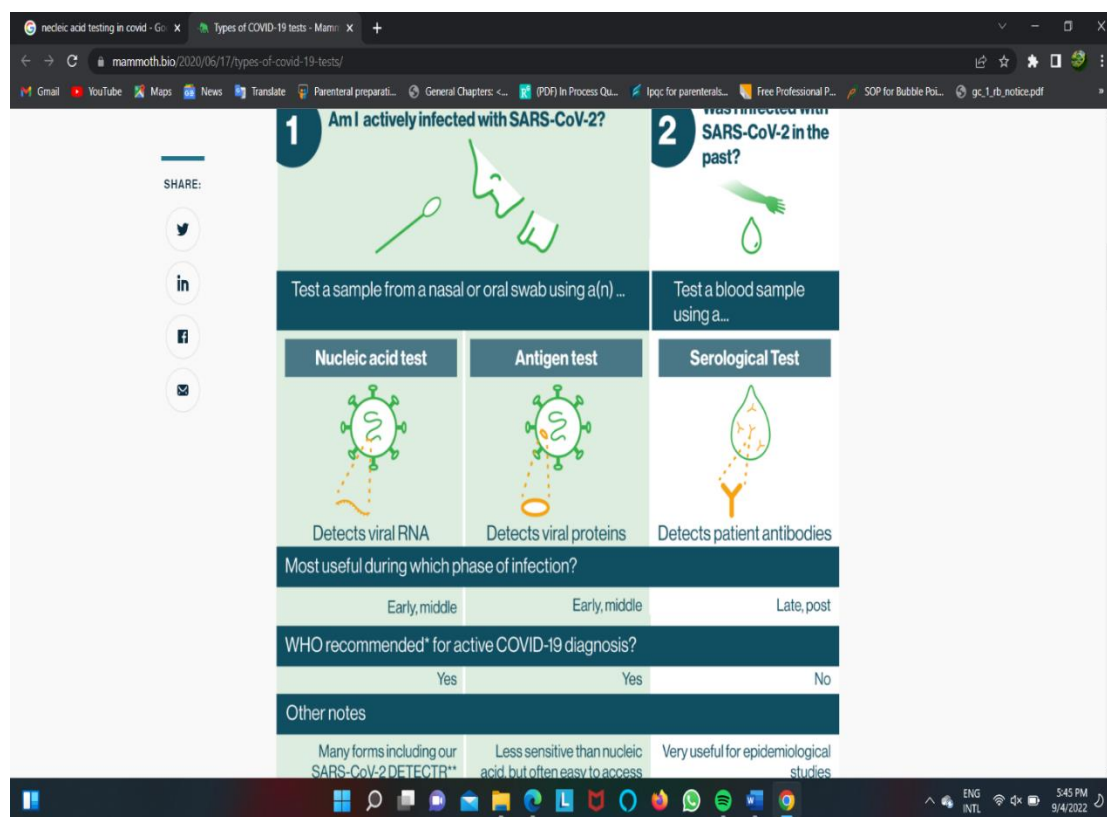
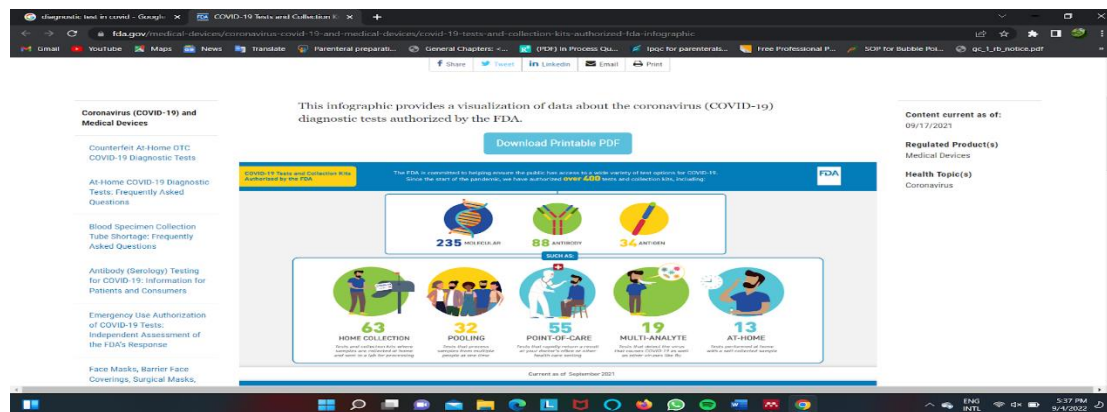
As Draz said, viruses are small, simple biological structures, with an intracellular life cycle and difficult to separate, they are frequently difficult to detect. They also cannot be seen under regular optical microscopes(Draz & Shafiee, 2018). SARS-CoV-2 requires rapid reaction tests, with consist and greater detection limits, just like other viral diseases(Campos et al., 2020). Two additional significant advancements in the history of diagnostic virology have been the discovery of different immunoassays and the polymerase chain reaction (PCR). A very broad variety of molecular and serological detection method were then developed in its wake(Draz & Shafiee, 2018). The predominant technique for detecting viruses is still serology. The most prevalent serological tests are neutralization assays, complement fixation tests, immunoprecipitation tests, hemagglutination-inhibition tests, enzyme immunoassays, radioimmunoassay, chemiluminescent immunoassays, particle agglutination tests, immunostaining, immunofluorescence assays, single radial hemolysis tests, immunoblotting assays, and immunochromatographic tests (ICT). These methods' primary method of operation is the conjugation of particular antibodies with various signal reporting tools, such as RBC, enzymes, and fluorescent materials. Additionally, unlike other direct detection techniques like cell culture and EM, they are typically not constrained by the practical issues of virus isolation and propagation(Draz & Shafiee, 2018). Molecular methods are becoming increasingly popular and have been used to detect viruses more and more frequently. New avenues in nucleic acid-based detection were opened by Mullis' groundbreaking invention of the in vitro nucleic acid amplification system, commonly known as PCR, in the early 1980s and the discovery of the genetic enzyme systems engaged in the cellular machinery of nucleic acid multiplication(Kiraz, 2015). The early development of nucleic acid testing is a result of SARS-simple CoV-2's recognition and sequencing. These tactics provide a first line of defense against an epidemic. Many different types of nanomaterials are currently being extensively researched for virus detection, including metal NPs(Au,Ag,Cu), carbon nanotubes, quantum dots, silica NPs, upconversion NPs, and polymeric Nanoparticles, magnetic NPs(Wang et al., 2009). The surface of the nanoparticle was altered with biomolecules derived from the virus, such as DNA, RNA, antibody, antigen (hemagglutinin antigen H1N1), peptide, or penta-body (avian influenza virus-pVHH3B) for the creation of these systems for virus detection(Draz & Shafiee, 2018). The contacts between the sensor and analyte are improved by the high surface-to-volume ratios of nanomaterials, resulting in a greater detection limit and shorter detection times. For the projection of virus detection tests, gold nanoparticles have stood out due to their photonic, electrical, and catalytic properties(Campos et al., 2020). Two primary methods are typically used for the colorimetric detection of viruses using AuNPs: 1) color amplification (using AuNPs as direct coloring labels with their distinctively intense red color(Draz & Shafiee, 2018); and 2). color change (using AuNPs to cause a color change from red to purple in reaction to particle aggregation).

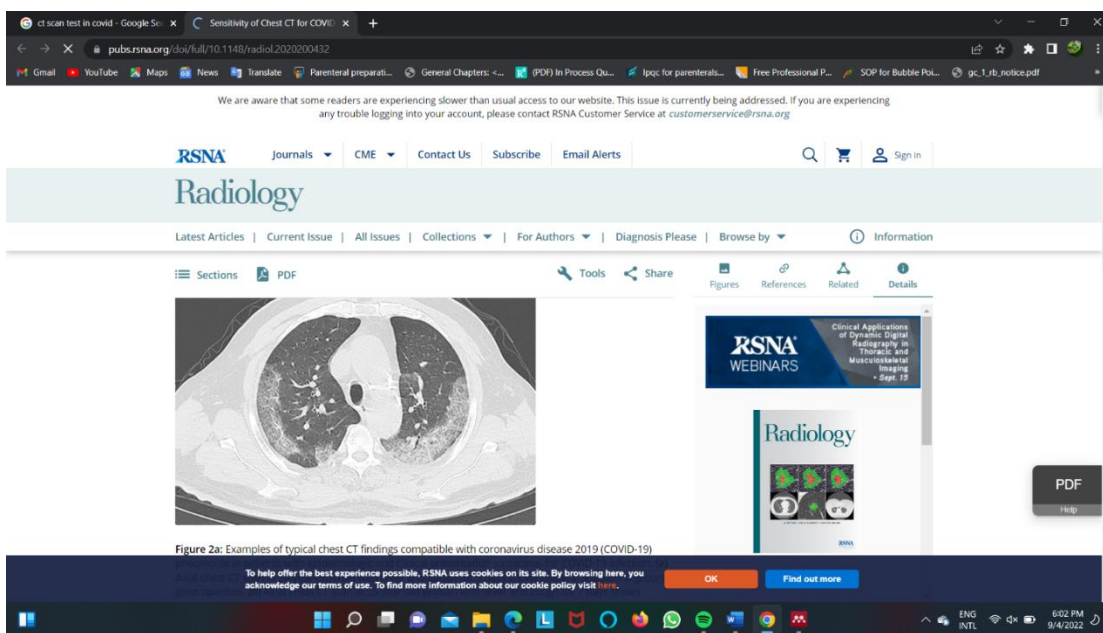
The serologic diagnostic test and RT-PCR test are currently used extensively in the detection and screening of the virus in specimens. The qSARS-CoV-2 IgG/IgM quick test, created by Cellex Inc. as a new rapid test for serological immunodetection, has just received FDA approval(Mohammed & Shaaban, 2022). Novel Cdn detectors for coronaviruses have been developed in a manner similar to how PCR tests use silica nanoparticles(Vahedifard & Chakravarthy, 2021). In a recent work, poly carboxyl-functionalized magnetic nanoparticles were used to diagnose SARS-CoV-2 on a nanoscale(Chacón-Torres et al., 2020).In PCR test routinely produces magnetic-bonded dsDNA conjugates, and it also makes it simple to detect nontargeted cDNA by reacting oligonucleotide probes using silica-encapsulated

superparamagnetic nanoparticles. When combined with poly(amino-ester) and carboxyl groups, the magneto-plasmonic nanoparticles were also used to enhance the diagnostic RT-PCR technique for SARS-Co(Dheyab et al., 2021). Other New methods are used to screen and diagnose COVID-19, such as nucleic acid tests and CT scans.

Diagnostic test: (Dheyab et al., 2021)

Figure 2: Different types of diagnostic test

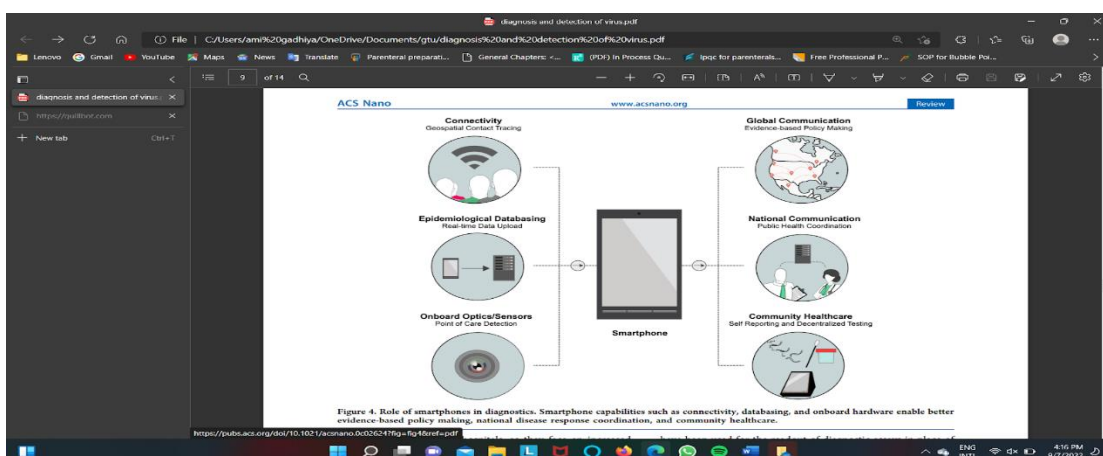




(FDA, 2021)
2020)

(FORD, 2020)

CT scan test(Fang & Pang,



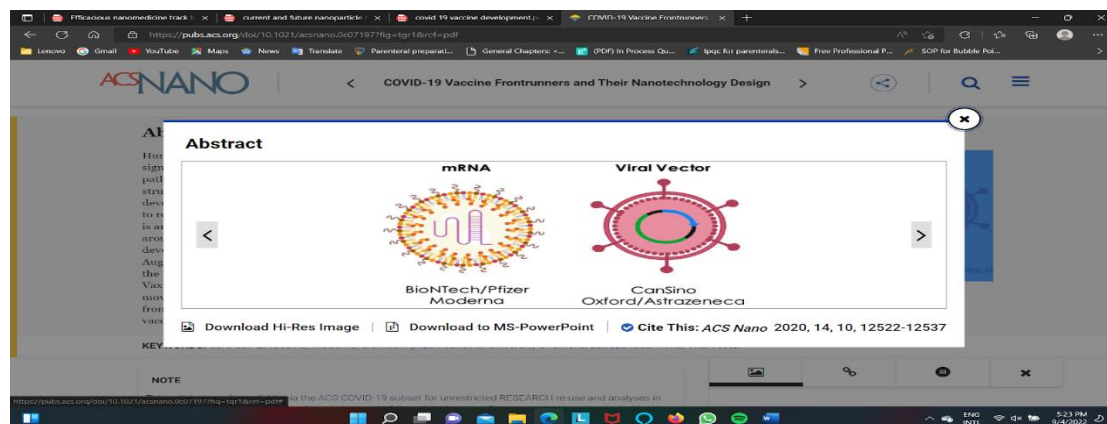
Smart phone in diagnostics(Udugama et al., 2020)

3. ROLE OF NANOTECHNOLOGY IN VACCINE DEVELOPMENT:

Since the start of the pandemic, the development of COVID-19 vaccines has progressed at an unparalleled rate. A number of them have achieved mass manufacture and market acceptance, which has enabled their widespread use throughout the world. Parallel use of two fundamentally different vaccination technologies allowed for this significant advancement. A subunit vaccine is in the final stages of approval. mRNA, adenoviral vector, and inactivated though the entire vaccines are currently widely used. They all depend on the native viral spike protein (S) of SARS-CoV-2 to cause potently neutralizing antibodies, but this important antigen is delivered to the immune system varies greatly among the various vaccine types(Heinz & Stiasny, 2021). There are 22 COVID-19 vaccines in use globally, and all of them contain S or an S-derivative with higher stability.(Mathieu et al., 2021). Several high-tech platforms, including as attenuated and inactivated viruses, replicating and nonreplicating viral vectors, DNA and mRNA, virus-like particles, and recombinant protein-based techniques, are being used to produce COVID-19 vaccine candidates(Ji et al., 2020). For protection against the virus, a number of vaccines have been made available, including those from Pfizer-BioNTech, Novavax, Moderna,

Janssen/Johnson & Johnson, Oxford-AstraZeneca(Atsa'am & Wario, 2022). Comparison between above four vaccine is given in (Table 1)

Figure 3: mRNA and Viral vaccine



Source:(Chung et al., 2020)

Nano - particle vaccines offer a unique opportunity to develop vaccine science and provide workable approaches to the current pandemic and beyond, in addition to traditional vaccine modalities (such as inactivated vaccines, recombinant protein vaccine, live attenuated vaccines, DNA and vector-based vaccines(Krammer, 2020). Viruses are tiny objects and can thus be termed natural nanomaterials. Because viruses and nanoparticles may interact at a similar length, developing vaccines and using immune-engineering techniques in nanotechnology are quite effective(Mohammed & Shaaban, 2022). Nanoparticles can be supplied through methods like oral and intranasal as well as intramuscular and subcutaneous injections to circumvent tissue barriers and it can target important locations like lymph nodes(Slütter et al., 2010)(Ballester et al., 2011). Intranasally administered vaccinations injected into the nasal passages are being developed by businesses like eTheRNA and Intravacc that may tackle such proximate lymph nodes.(B.V, 2020) At the cellular level, nanoparticles can target the innate (macrophages, monocytes, and neutrophils) and adaptive (T cells, B cells) immune systems. One of the benefits of nanoparticles in boosting the safety and efficiency of the vaccination is their capacity to transport molecular adjuvants as well as, in certain circumstances, having inherent adjuvant property for the loaded antigens.(Rashidzadeh et al., 2021). Vaccines come in a variety of forms, including protein nanoparticle, lipid nanoparticles (LNPs), virus-like particles (VLPs), micelles, etc.

Nanoparticle vaccines can be split into two categories depending on antigen loading strategies: (1) Those that encapsulate vaccine antigens or nucleic cargos within their cores, and (2) Those that present vaccine antigens on their surfaces. In contrast, nanoparticles showing vaccine antigens are capable of binding to antigen presenting cells (APCs) and/or effectively promote B cell receptor (BCR) inter, leading to potent immunogenicity. Antigen-encapsulating nanoparticle vaccines have the advantage of protecting and controlling the release of cargo after immunization(Bale et al., 2017).

Table 1: Comparing different COVID vaccine

	Pfizer-BioNTech	Moderna	Johnson & Johnson	Novavax	Oxford-AstraZeneca
Brand name	Comirnaty	Spikevax	Janssen	Nuvaxovid and Covovax	Vaxzevria(in EU)

Type	mRNA vaccine	mRNA vaccine	Carrier vaccine	Protein subunit vaccine	Carrier vaccine
Mechanism (How it works)	It functions by giving instruction to host cells in the body to create a new set of a spike protein. The immune system responds by engaging immune cells and creating antibodies as a result of our cells realizing that this protein does not belong. If you are exposed to the actual SARS CoV-2 spike protein, this will cause the body to detect and begin attacking it.	It's given instruction to the body's cells to produce a S protein which will help the immune system become used to recognizing it. The next time the immune system encounters a spike protein, it will attack it.	In contrast to mRNA vaccines, this carrier vaccine employs a novel strategy to train human cells to produce the SARS CoV-2 spike proteins. In order to transport the gene sequence on the spike protein to the cells, scientists create a harmless adenovirus as a shell. The shell cannot make you ill, but when the code is within the cells, the cells release a spike protein to instruct the immune system, which in turn produces memories and antibodies cells to guard against a real SARS-CoV-2 infection.	This vaccination uses a protein adjuvant rather than mRNA or a vector. The Novavax vaccine adopts a different strategy than existing vaccines by tricking the body's cells into producing portions of the virus which can activate the immune system. Although it is made up of nanoparticles, which are unable to spread disease, it still includes the spike protein of the coronavirus itself. The injection of the vaccine activates the immune system, causing it to create antibodies and T-cell immunological responses.	In order to transport the gene sequence on the spike protein to the cells, scientists create a safe adenovirus as a shell. When the code is within the cells, the cells release a protein called a spike to train the immune system, which then produces memory and antibodies cells to defend the body from a real SARS-CoV-2 infection.
Authorization	FDA approval WHO approval CDSCO approval	FDA approval WHO approved for emergency use CDSCO approved for restricted use in emergency situation	FDA approved for emergency use WHO approved for emergency use CDSCO approved for restricted use in emergency situation	FDA approved for emergency use WHO approval CDSCO approved for restricted use in emergency situation	Not available in U.S authorized WHO approval CDSCO approval
FDA warning	Myocarditis, pericarditis in adult after second dose	Heart inflammation in adults	Guillain-Barre syndrome (neurological)		

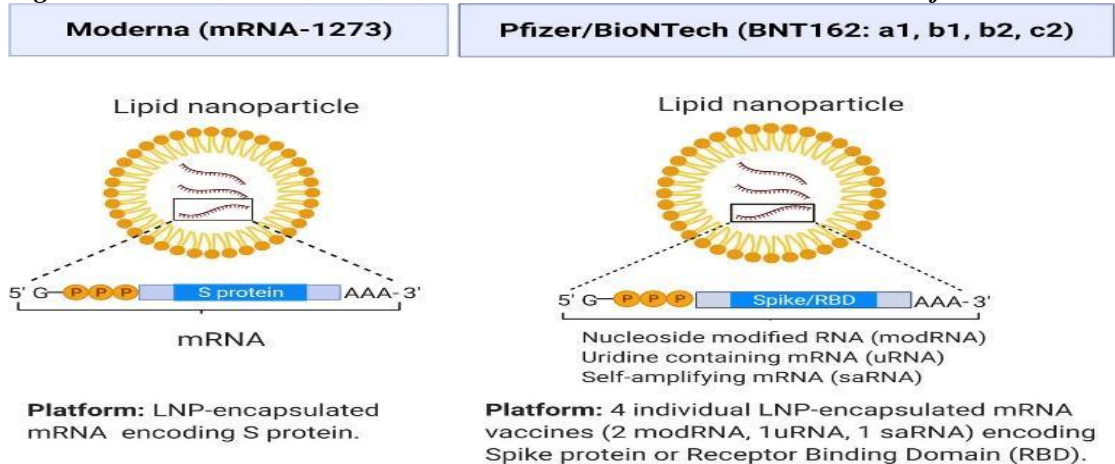
		after second dose	disorder) within 42 days. Blood clotting (thrombocytopenia syndrome) Now restricted on vaccine		
Effectiveness	91% in severe cases 100% in age 5-11	94% (with symptoms) 90% in diabetic or obesity condition	85% in severe case 66% (with symptoms)	90% in mild, medium, high case 79% in age 65 or more	76% (with symptoms) 100% in severe case 85% in age 65 or more

(Katella, 2021) ,(Pfizer-BioNTech, 2021),(FDA, 2022),(U.S. Food and Drug Administration (FDA), 2021) ,(WHO, 2022),(Central Drugs Standard Control organization, 2022)

Many vaccine manufacturers currently use lipid nanoparticles as the nanoparticles to contain the gene material, protein, and peptides of the vaccine (LNPs). For instance, LNPs are used to encapsulate COVID-19 mRNA-based vaccines produced by BioNTech/Pfizer and Moderna.(Abbott et al., 2020)(Figure:3). Both BNT162b2 & mRNA-1273 had the power to trigger the host's production of the viral spike proteins as well as an efficient and defense-enhancing immune response against SARS-CoV-2(Baden et al., 2021).

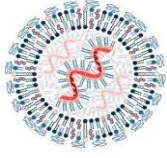
The very stable, RNase-mediated degradation-resistant mRNA vaccine enclosed in positive charge LNPs forms auto particles that can be delivered in a variety of ways(Abbott et al., 2020).

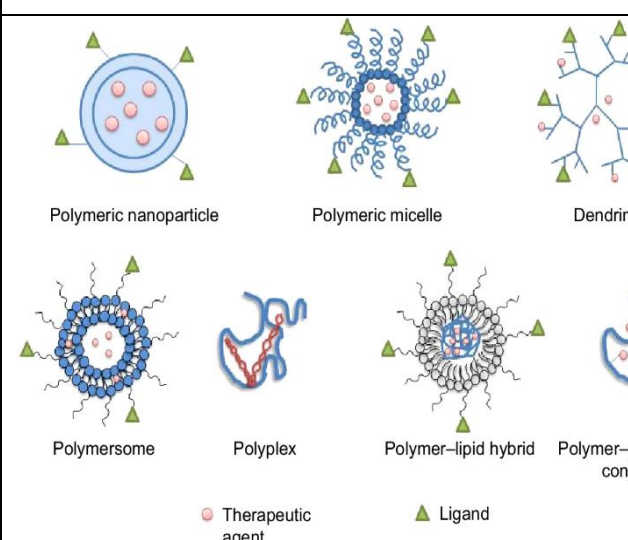
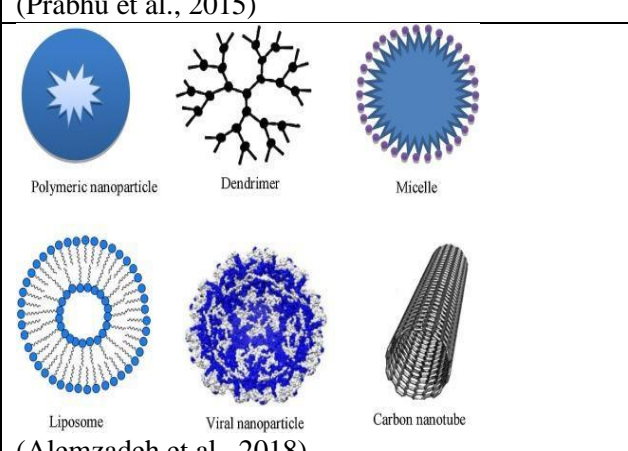
Figure 4: BNT162 and mRNA vaccine for covid

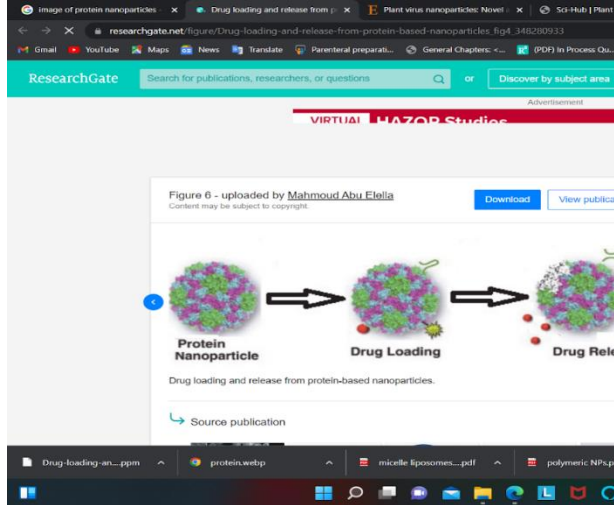
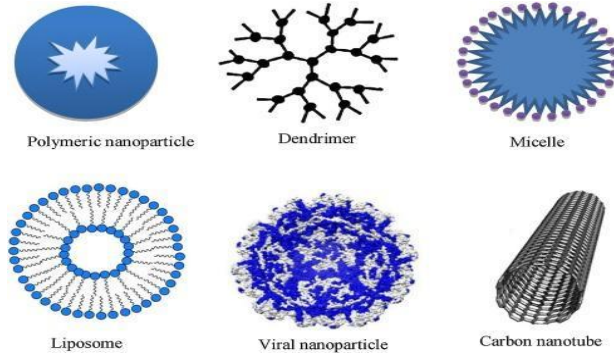
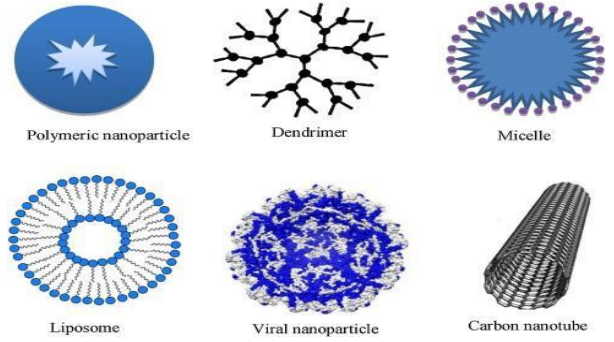


Source:(Mohammed & Shaaban, 2022)

Table 2: Nanoparticle vaccines in development as SARS-COV-2 vaccine.

Ag encapsulated in NPs core	Lipid NPs	Nucleic acid(mRNA)	Moderna, NIAID(LNPs) Pfizer/BioNTech (BNT162) CureVac AG (CVnCo	 <p>(Buschmann et al., 2021)</p>
-----------------------------	-----------	--------------------	---	---

			v mRNA vaccine)	
	Polymer NPs	RBD protein		 <p>(Prabhu et al., 2015)</p>
Ag presented onto NPs surface	Virus-like NPs	Structural protein :S,M,E	Medicago Inc. (CoVLP), VBI vaccine Inc. (Enveloped VLP of S protein), Radboud university (ABNCov2 capsid VLP (cVLP)	 <p>(Alemzadeh et al., 2018)</p>

Protein NPs	S and RBD	SK Bioscience Co., Ltd. (RBD-153-50 NPs)	 <p>(C. Ngwuluka et al., 2021)</p>
Micelle NPs	S protein	Novavax (SARS-CoV-2 Rs/Matrix M1-Adjuvant)	 <p>(Alemzadeh et al., 2018)</p>
Liposomes	S and RBD		 <p>(Alemzadeh et al., 2018)</p>

(Vu et al., 2021),(Mohammed & Shaaban, 2022)

Due to the presence of lipid in LNP composition, endosomal escape is facilitated during entrance of the LNPs-mRNA vaccine compound into the cell through endocytosis mechanism. Thereafter, it releases mRNA into the cytosol, where the mRNA is transformed into antigenic proteins that activate the immune system and cause the production of neutralizing antibodies (Chung et al., 2020). Lipid nanoparticle (LNP) formulations of messenger RNA were used in the first two SARS-CoV-2 vaccines that were authorized for use in immunization programs (mRNA)(Shapiro, 2021).

VLPs are a recent development in peptide-guided nanotechnologies that were produced from bacteriophages, mammalian, and insect viruses for novel immunotherapeutic and vaccination applications. Additionally, VLP delivery platforms serve as adjuvants for powerful stimulators and amplifiers of the immune response to certain antigen. Candidates for subunit vaccines are simplified versions of SARS-CoV-2 that, when administered alongside certain molecular adjuvants for induced immunogenicity, can generate protective immune responses. For

instance, S1/S2 subunits or formulations of the entire S protein combined with adjuvants are candidates for the SARS-CoV-2 subunit vaccine (Mohammed & Shaaban, 2022). Self-assembled protein nanoparticles and VLPs display remarkably stable and monodisperse vaccination platforms. One of the VLPs options for SARS-CoV-2, CoVLP vaccine was created by Canadian company Medicago and introduced a perfused steady nanostructure of the S proteins on the surface of self-assembling VLPs (Ward et al., 2021).

The genetic material needed to produce viral proteins in situ is delivered by nucleic acid-based vaccine (mRNA and DNA), which are an effective replacement for conventional vaccine techniques. The most effective advantage of using this type of vaccine for viral control and eradication has been the stimulation of both CD4+ and CD8+ T cell responses. Trends in nanotechnology offer amazing solutions to problems with vaccine distribution by resolving trafficking issues and delivering the vaccine to the right cellular populations and subcellular places. Although designed nanocarriers including nanomaterials and cationic liposomes have been extensively used to carry DNA vaccines across cell membranes, tailored nano-construct may further increase nuclear translocation of a plasmid DNA. (Mohammed & Shaaban, 2022)

4. ROLE OF NANOTECHNOLOGY IN TREATMENT:

A widespread loss in cell's capacity to carry out clathrin-mediated endocytosis of nano-sized particles is most likely one of the processes that account for chloroquine's effects against SARS-CoV-2 (Principi & Esposito, 2020). While chloroquine has therapeutic efficacy against SARS-CoV in cell culture, it is unable to change the levels of ACE2 on the cell surface. Furthermore, the production or glycosylation of the SARS-CoV spike glycoprotein was not significantly changed by therapeutic doses of chloroquine. Instead, the ACE2 receptor's terminal glycosylation was compromised, compromising viral binding (Vincent et al., 2005). In the beginning, there was reason to be optimistic that (hydroxy) chloroquine would have preventative and/or therapeutic benefits against COVID-19. Therefore, understanding the mechanisms governing how these medications affect SARS-CoV-2 is essential for improving and creating preventive and therapeutic approaches (Dheyab et al., 2021).

Additionally, Zachar (Zachar, 2020) developed a therapy serum and therapy for the treatment on nano-silver colloids (NAgC) to inhibit the spread both of bacteria and viruses respiratory disease. Inhalation was used to distribute the compositions. The study suggested that the exhaled portion of NAgC can be administered orally to the nasal passages by conducting nebulized inhalation or by exhaling via the nose. Additionally, the first kind of personal protection that can stop the spread of the virus is nanofiber-based facial respirators combined with highly effective antimicrobial and antiviral disinfectants that are enabled by nanotechnology. In order to treat COVID with photodynamic therapy (PDT), a nebulizer would be the most suitable device to deliver photosensitizer (PS) to the airways; specifics of this device are what we are now investigating. PDT, also known as photodynamic inactivation (PDI), outperforms traditional treatment modalities like surgery, radiation, and chemotherapy due to its non-invasive nature. Photo-inactivated viruses can boost the immune response when they operate like a vaccine. The converse should also be considered as a side effect, wherein inactivated viruses can reawaken and multiply (Dheyab et al., 2021). The treatment of PS cells revealed internalization and infecting of adenoviruses through with a photochemical internalization process, which is a further concern raised in the study.

MWCNTs, or Multi-walled carbon nanotubes, have been claimed as potent antiviral substances. Antimicrobial properties of graphene & graphene oxide sheets have also been discovered. SARS-CoV-2 infection as well as the reproduction and multiplication of the virus may be prevented using inorganic nanomaterials such graphene oxide (GO) sheets with such as AgNPs, cationic carbon dots, and Ag₂S nanoclusters (NCs). It is believed that metal NPs like Ag, Cu, and CuO NPs, which are good antiviral agents, can engage with the virus's surface proteins of the virus to prevent the SARS-CoV-2 virus from replicating. These metal NPs can therefore be utilized to disinfect surfaces as a result. It is also being investigated if photocatalytic Nano particles as Titanium dioxide and (polymer-like liposomes) and graphene-derived NPs like

graphene oxide (GO), sulfated GO, and reduced GO sheets can suppress the SARS-CoV-2 virus (Sharma, 2022). In a different investigation, riboflavin was employed to render plasma MERS-CoV inactive. The intensity of the virus was dramatically lowered below the detection threshold by riboflavin & UV light therapy. It might aid in preventing a virus from being transfused through plasma products. In the titanium photocatalytic activity section, there is a report on the utilization of photocatalytic titanium apatite filters (PTAF) for inactivating the SARS-CoV UV and non-UV.

The successful integration of the most recent developments, such as nanotechnology, can increase the efficacy of PDT toward COVID-19. Numerous strategies exist for the nanomedicine to function as antiviral medicines (Table 3). Additionally, Remdesivir was demonstrated to be a powerful antiviral drug in vitro versus COVID-19 infection (Sportelli et al., 2020). However, ribavirin monotherapy showed insufficient action against SARS-CoV, thus it is frequently combined with lopinavir, ritonavir, and HIV protease inhibitors and produces superior results. The combination of lopinavir and ritonavir was also tested (Lai et al., 2020). Additionally, there are indications that interferon (IFN) therapies are beneficial.

Table 3: Different strategies for nanomedicine as an antiviral drug

Strategies	Example
Nanoparticles that prevent viral entrance and cell attachment	Zinc, Silver, Gold, Titanium (Ti), and, Carbon dots (CDs) made from cationic curcumin (CCM-CDs), AgNPs modified with curcumin (cAgNPs), NPs in silicon (SiNPs), Mesoporous SiO ₂ (mSiO ₂), Graphene QDs, Selenium nanoparticles, and GO along with its derivatives can all prevent HIV from attaching to cells.
Nanoparticles that prevent viral reproduction and growth.	AgNPs and SeNPs, AuNPs, Ag ₂ S, and CDs made from Benzoxamine Monomer
Nanoparticles for the viricidal and inactivation of viruses	Nano discs with Decoy virus receptor functionality, Ferromagnetic Fe ₃ O ₄ , and AuNPs
Delivery of an antiviral drug	Nanoencapsulation, Polymeric nanoparticles, Virus-impersonating nanoparticles, PLGA-based nanoparticles, Cationic liposomal nanoparticles, and Polyamidoamines are some examples (PAMAMs)
Immune system targeting nanomedicine system	IL-6 antagonist tocilizumab combined with hyaluronate-gold nanoparticles, Liposomal dexamethasone, LIF nano, and Adenosine
Nanoparticles integrating various therapeutic modalities	Combining lipid-polymer hybrid nano formulation, Virosomes, virus-like particles (VLPs), and Carbon QDs (CQDs)
Additional COVID-19 nano solutions	Exosomes, Mesenchymal stem cell secretome, and regenerative nanomedicine

(Letko et al., 2020),(Vahedifard & Chakravarthy, 2021)

5. CONCLUSION:

In this review, Information on the SARS-CoV-2 virus's structural morphology has been briefly discussed, together with importance of nanomedicine in detecting, vaccine development and treatment of the disease. For the detecting of the SAR-CoV-2, different types of the detecting method are available such as serological method, nucleic acid, RT-PCR, molecular test as well as by nanomaterial. Nucleic acid tests have been developed quickly thanks to the easy recognition and sequencing of SARS-CoV-2. A first barrier against an outbreak is offered by these strategies. Serological tests are developed and used as the next stage since they are simpler to use and may support nucleic acid tests in the diagnosis of COVID-19 infection. Greater interaction and surveillance should be possible with the help of cellphones and diagnosis. diagnostics are a crucial component of the arsenal for containing epidemic.

The vaccine development and treatment has been significantly aided by the use of nanotechnology techniques. For the production of the SAR-CoV-2 vaccine, various types of platforms have been utilized. Lipid NPs are used to encapsulate both the BNT162 vaccination and the most effective vaccine, mRNA-1273. At the moment, there are only a few vaccines for prevention including Comirnaty (BNT162b2), Moderna COVID-19 Vaccine (mRNA-1273), COVID 19 Vaccine Astrazeneca (AZD1222). To evaluate various treatments, several more trials are currently under progress. Various strategies are used to develop therapeutics using nanoparticles to prevent entrance & reproduction of virus, to elicit viricidal effect and to deliver antiviral drugs and drugs affecting immune system. It is expected that significant improvements in COVID-19 diagnosis, treatment, and therapy will be made utilizing nanotechnology-based methods.

6. REFERENCES:

1. Abbott, T. R., Dhamdhare, G., Liu, Y., Lin, X., Goudy, L., Zeng, L., Chemparathy, A., Chmura, S., Heaton, N. S., Debs, R., Pande, T., Endy, D., La Russa, M. F., Lewis, D. B., & Qi, L. S. (2020). Development of CRISPR as an Antiviral Strategy to Combat SARS-CoV-2 and Influenza. *Cell*, 181(4), 865-876.e12. <https://doi.org/10.1016/j.cell.2020.04.020>
2. Alemzadeh, E., Dehshahri, A., Izadpanah, K., & Ahmadi, F. (2018). Plant virus nanoparticles: Novel and robust nanocarriers for drug delivery and imaging. *Colloids and Surfaces B: Biointerfaces*, 167, 20–27. <https://doi.org/10.1016/j.colsurfb.2018.03.026>
3. Atsa'am, D. D., & Wario, R. (2022). Association rules on the COVID-19 variants of concern to guide choices of tourism destinations. *Current Issues in Tourism*, 25(10), 1536–1540. <https://doi.org/10.1080/13683500.2021.1951182>
4. B.V, I. (2020). Intravacc Partners With Wageningen Bioveterinary Research and Utrecht University to Develop an Intranasal COVID-19 Vaccine.
5. Baden, L. R., El Sahly, H. M., Essink, B., Kotloff, K., Frey, S., Novak, R., Diemert, D., Spector, S. A., Rouphael, N., Creech, C. B., McGettigan, J., Khetan, S., Segall, N., Solis, J., Brosz, A., Fierro, C., Schwartz, H., Neuzil, K., Corey, L., ... Zaks, T. (2021). Efficacy and Safety of the mRNA-1273 SARS-CoV-2 Vaccine. *New England Journal of Medicine*, 384(5), 403–416. <https://doi.org/10.1056/nejmoa2035389>
6. Bale, S., Goebrecht, G., Stano, A., Wilson, R., Ota, T., Tran, K., Ingale, J., Zwick, M. B., & Wyatt, R. T. (2017). Covalent Linkage of HIV-1 Trimers to Synthetic Liposomes Elicits Improved B Cell and Antibody Responses. *Journal of Virology*, 91(16), 1–15. <https://doi.org/10.1128/jvi.00443-17>
7. Ballester, M., Nembrini, C., Dhar, N., de Titta, A., de Piano, C., Pasquier, M., Simeoni, E., van der Vlies, A. J., McKinney, J. D., Hubbell, J. A., & Swartz, M. A. (2011). Nanoparticle conjugation and pulmonary delivery enhance the protective efficacy of Ag85B and CpG against tuberculosis. *Vaccine*, 29(40), 6959–6966. <https://doi.org/10.1016/j.vaccine.2011.07.039>
8. Buschmann, M. D., Carrasco, M. J., Alishetty, S., Paige, M., Alameh, M. G., & Weissman, D. (2021). Nanomaterial delivery systems for mrna vaccines. *Vaccines*, 9(1), 1–30. <https://doi.org/10.3390/vaccines9010065>
9. C. Ngwuluka, N., Y. Abu-Thabit, N., J. Uwaezuoke, O., O. Erebor, J., O. Ilomuanya, M., R. Mohamed, R., M.A. Soliman, S., H. Abu Elella, M., & A.A. Ebrahim, N. (2021). Natural Polymers in Micro- and Nanoencapsulation for Therapeutic and Diagnostic Applications: Part II -

- Polysaccharides and Proteins. Nano- and Microencapsulation - Techniques and Applications, January. <https://doi.org/10.5772/intechopen.95402>
10. Campos, E. V. R., Pereira, A. E. S., De Oliveira, J. L., Carvalho, L. B., Guilger-Casagrande, M., De Lima, R., & Fraceto, L. F. (2020). How can nanotechnology help to combat COVID-19? Opportunities and urgent need. *Journal of Nanobiotechnology*, 18(1), 1–23. <https://doi.org/10.1186/s12951-020-00685-4>
 11. Central Drugs Standard Control organization. (2022). Vaccines.
 12. Chacón-Torres, J. C., Reinoso, C., Navas-León, D. G., Briceño, S., & González, G. (2020). Optimized and scalable synthesis of magnetic nanoparticles for RNA extraction in response to developing countries' needs in the detection and control of SARS-CoV-2. *Scientific Reports*, 10(1), 1–10. <https://doi.org/10.1038/s41598-020-75798-9>
 13. Chauhan, G., Madou, M. J., Kalra, S., Chopra, V., Ghosh, D., & Martinez-Chapa, S. O. (2020). Nanotechnology for COVID-19: Therapeutics and Vaccine Research. *ACS Nano*, 14(7), 7760–7782. <https://doi.org/10.1021/acsnano.0c04006>
 14. Chung, Y. H., Beiss, V., Fiering, S. N., & Steinmetz, N. F. (2020). Covid-19 vaccine frontrunners and their nanotechnology design. *ACS Nano*, 14(10), 12522–12537. <https://doi.org/10.1021/acsnano.0c07197>
 15. Dheyab, M. A., Khaniabadi, P. M., Aziz, A. A., Jameel, M. S., Mehrdel, B., Oglat, A. A., & Khaleel, H. A. (2021). Focused role of nanoparticles against COVID-19: Diagnosis and treatment. *Photodiagnosis and Photodynamic Therapy*, 34(April), 102287. <https://doi.org/10.1016/j.pdpdt.2021.102287>
 16. Draz, M. S., & Shafiee, H. (2018). Applications of gold nanoparticles in virus detection. *Theranostics*, 8(7), 1985–2017. <https://doi.org/10.7150/thno.23856>
 17. Fang, Y., & Pang, P. (2020). Senivity of Chest CT for COVID.19: Comparasion to RT.PCR. *Radiology*, 296, 15–17.
 18. FDA. (2021). COVID-19 Tests and Collection Kits Authorized by the FDA: Infographic. <https://www.fda.gov/medical-devices/coronavirus-covid-19-and-medical-devices/covid-19-tests-and-collection-kits-authorized-fda-infographic>
 19. FDA. (2022). Vaccine Information Fact Sheet for Recipients and Caregivers. 2019, 1–7.
 20. FORD, T. (2020). Types of COVID-19 tests. In *mammothbioscience*. <https://mammoth.bio/2020/06/17/types-of-covid-19-tests/>
 21. Heinz, F. X., & Stiasny, K. (2021). Distinguishing features of current COVID-19 vaccines: knowns and unknowns of antigen presentation and modes of action. *Npj Vaccines*, 6(1). <https://doi.org/10.1038/s41541-021-00369-6>
 22. Huang, J., Yuen, D., Mintern, J. D., & Johnston, A. P. R. (2021). Opportunities for innovation: Building on the success of lipid nanoparticle vaccines. *Current Opinion in Colloid and Interface Science*, 55, 101468. <https://doi.org/10.1016/j.cocis.2021.101468>
 23. Jeong-Eun Park, Keunsuk Kim, Yoonjae Jung, Jae-Ho Kim, P. J.-M. N. (2016). Metal Nanoparticles for Virus Detection. *ACS Applied Nano Materials*, 2(10).
 24. Ji, H., Yan, Y., Ding, B., Guo, W., Brunswick, M., Niethammer, A., SooHoo, W., Smith, R., Nahama, A., & Zhang, Y. (2020). Novel decoy cellular vaccine strategy utilizing transgenic antigen-expressing cells as immune presenter and adjuvant in vaccine prototype against SARS-CoV-2 virus. *Medicine in Drug Discovery*, 5, 100026. <https://doi.org/10.1016/j.medidd.2020.100026>
 25. Katella, K. (2021). Comparing the COVID-19 vaccines: How are they different? *Yale Medicine*.
 26. Kiraz, N. (2015). Molecular techniques for clinical diagnostic mycology. *Turk Hijyen ve Deneysel Biyoloji Dergisi*, 72(3), 263–272. <https://doi.org/10.5505/TurkHijyen.2015.99705>
 27. Krammer, F. (2020). SARS-CoV-2 vaccines in development. *Nature*, 586(7830), 516–527. <https://doi.org/10.1038/s41586-020-2798-3>
 28. Lai, C., Shih, T., Ko, W., Tang, H., & Hsueh, P. (2020). Since January 2020 Elsevier has created a COVID-19 resource centre with free information in English and Mandarin on the novel coronavirus COVID- 19 . The COVID-19 resource centre is hosted on Elsevier Connect , the company ' s public news and information . January.
 29. Letko, M., Marzi, A., & Munster, V. (2020). Functional assessment of cell entry and receptor usage for SARS-CoV-2 and other lineage B betacoronaviruses. *Nature Microbiology*, 5(4), 562–569. <https://doi.org/10.1038/s41564-020-0688-y>

30. Mathieu, E., Ritchie, H., Ortiz-Ospina, E., Roser, M., Hasell, J., Appel, C., Giattino, C., & Rod s-Guirao, L. (2021). A global database of COVID-19 vaccinations. *Nature Human Behaviour*, 5(7), 947–953. <https://doi.org/10.1038/s41562-021-01122-8>
31. Mohammed, S. A., & Shaaban, E. I. A. (2022). Efficient nanomedicine track toward combating COVID - 19. March 2020, 680–698.
32. Pfizer-BioNTech. (2021). Pfizer-BioNTech COVID-19 vaccine: Storage and handling summary. Centers for Disease Control and Prevention.
33. Prabhu, R. H., Patravale, V. B., & Joshi, M. D. (2015). Polymeric nanoparticles for targeted treatment in oncology: Current insights. *International Journal of Nanomedicine*, 10, 1001–1018. <https://doi.org/10.2147/IJN.S56932>
34. Principi, N., & Esposito, S. (2020). Chloroquine or hydroxychloroquine for prophylaxis of COVID-19. *The Lancet Infectious Diseases*, 20(10), 1118. [https://doi.org/10.1016/S1473-3099\(20\)30296-6](https://doi.org/10.1016/S1473-3099(20)30296-6)
35. Rashidzadeh, H., Danafar, H., Rahimi, H., Mozafari, F., Salehiabar, M., Rahmati, M. A., Rahamooz-Haghighi, S., Mousazadeh, N., Mohammadi, A., Ertas, Y. N., Ramazani, A., Huseynova, I., Khalilov, R., Davaran, S., Webster, T. J., Kavetsky, T., Eftekhari, A., Nosrati, H., & Mirsaiedi, M. (2021). Nanotechnology against the novel coronavirus (severe acute respiratory syndrome coronavirus 2): Diagnosis, treatment, therapy and future perspectives. *Nanomedicine*, 16(6), 497–516. <https://doi.org/10.2217/nmm-2020-0441>
36. Seah, I., Su, X., & Lingam, G. (2020). Revisiting the dangers of the coronavirus in the ophthalmology practice. *Eye (Basingstoke)*, 34(7), 1155–1157. <https://doi.org/10.1038/s41433-020-0790-7>
37. Shapiro, R. S. (2021). COVID-19 vaccines and nanomedicine. *International Journal of Dermatology*, 60(9), 1047–1052. <https://doi.org/10.1111/ijd.15673>
38. Sharma, S. (2022). The role of nanomedicine in COVID-19 therapeutics. *Nanomedicine*, 17(3), 133–136. <https://doi.org/10.2217/nmm-2021-0358>
39. Sl tter, B., Bal, S., Keijzer, C., Mallants, R., Hagens, N., Que, I., Kaijzel, E., van Eden, W., Augustijns, P., L wik, C., Bouwstra, J., Broere, F., & Jiskoot, W. (2010). Nasal vaccination with N-trimethyl chitosan and PLGA based nanoparticles: Nanoparticle characteristics determine quality and strength of the antibody response in mice against the encapsulated antigen. *Vaccine*, 28(38), 6282–6291. <https://doi.org/10.1016/j.vaccine.2010.06.121>
40. Sportelli, M. C., Izzi, M., Kukushkina, E. A., Hossain, S. I., Picca, R. A., Ditaranto, N., & Cioff, N. (2020). Can nanotechnology and materials science help the fight against sars-cov-2? *Nanomaterials*, 10(4), 1–12. <https://doi.org/10.3390/nano10040802>
41. U.S. Food and Drug Administration (FDA). (2021). Fact Sheet for Healthcare Providers Administering Vaccine. U.S. Food and Drug Administration (FDA), 2019, 1–13. <https://www.accessdata.fda.gov/scripts/medwatch/index.cfm?action=reporting.home>
42. Udugama, B., Kadhiresan, P., Kozłowski, H. N., Malekjahani, A., Osborne, M., Li, V. Y. C., Chen, H., Mubareka, S., Gubbay, J. B., & Chan, W. C. W. (2020). Diagnosing COVID-19: The Disease and Tools for Detection. *ACS Nano*, 14(4), 3822–3835. <https://doi.org/10.1021/acsnano.0c02624>
43. Vahedifard, F., & Chakravarthy, K. (2021). Nanomedicine for COVID-19: the role of nanotechnology in the treatment and diagnosis of COVID-19. *Emergent Materials*, 4(1), 75–99. <https://doi.org/10.1007/s42247-021-00168-8>
44. Vincent, M. J., Bergeron, E., Benjannet, S., Erickson, B. R., Rollin, P. E., Ksiazek, T. G., Seidah, N. G., & Nichol, S. T. (2005). Chloroquine is a potent inhibitor of SARS coronavirus infection and spread. *Virology Journal*, 2, 1–10. <https://doi.org/10.1186/1743-422X-2-69>
45. Vu, M. N., Kelly, H. G., Kent, S. J., & Wheatley, A. K. (2021). Current and future nanoparticle vaccines for COVID-19. *EBioMedicine*, 74, 103699. <https://doi.org/10.1016/j.ebiom.2021.103699>
46. Wang, X., Liu, L. H., Ramstr m, O., & Yan, M. (2009). Engineering nanomaterial surfaces for biomedical applications. *Experimental Biology and Medicine*, 234(10), 1128–1139. <https://doi.org/10.3181/0904-MR-134>
47. Ward, B. J., Gobeil, P., S guin, A., Atkins, J., Boulay, I., Charbonneau, P. Y., Couture, M., D’Aoust, M. A., Dhaliwall, J., Finkle, C., Hager, K., Mahmood, A., Makarkov, A., Cheng, M. P., Pillet, S., Schimke, P., St-Martin, S., Tr panier, S., & Landry, N. (2021). Phase 1 randomized trial of a plant-derived virus-like particle vaccine for COVID-19. *Nature Medicine*, 27(6), 1071–1078. <https://doi.org/10.1038/s41591-021-01370-1>

48. WHO. (2022). The Oxford/AstraZeneca (ChAdOx1-S [recombinant] vaccine) COVID-19 vaccine. <https://www.who.int/vaccine/astrazeneca>
49. Yu, M., Wu, J., Shi, J., & Farokhzad, O. C. (2016). Nanotechnology for protein delivery: Overview and perspectives. *Journal of Controlled Release*, 240, 24–37. <https://doi.org/10.1016/j.jconrel.2015.10.012>
50. Zachar, O. (2020). Formulations for COVID-19 Early Stage Treatment via Silver Nanoparticles Inhalation Delivery at Home and Hospital. *ScienceOpen Preprints*, March, 1–14. <https://doi.org/10.14293/S2199-1006.1.SOR-PPHBJEO.v1>

This Page Intentionally left Blank

ISBN : 978-81-955306-5-6



Gujarat Technological University

Visat Gandhinagar Highway, Chandkheda,
Ahmedabad, Gujarat - 382424 - India.

079-23267521/570 www.gtu.ac.in

info@gtu.ac.in /gtuoffice

GujaratTechnologicalUniversity